



EDITORIAL BOARD

Editor-in-Chief

Prof. dr P.W. Crous, Westerdijk Fungal Biodiversity Institute, P.O. Box 85167, 3508 AD Utrecht, The Netherlands. E-mail: p.crous@westerdijknstitute.nl

Senior Editors

Prof. dr U. Braun, Martin-Luther-Universität, Institut für Biologie, Geobotanik und Botanischer Garten, Herbarium, Neuwerk 21, D-06099 Halle, Germany; e-mail: uwe.braun@botanik.uni-halle.de

Dr J.Z. Groenewald, Westerdijk Fungal Biodiversity Institute, P.O. Box 85167, 3508 AD Utrecht, The Netherlands; e-mail: e.groenewald@westerdijknstitute.nl

Layout Editors

M.J. van den Hoeven-Verweij, Westerdijk Fungal Biodiversity Institute, P.O. Box 85167, 3508 AD Utrecht, The Netherlands; e-mail: m.verweij@westerdijknstitute.nl

M. Vermaas, Westerdijk Fungal Biodiversity Institute, P.O. Box 85167, 3508 AD Utrecht, The Netherlands; e-mail: m.vermaas@westerdijknstitute.nl

Associate Editors

Prof. dr A.M. Al-Sadi, Department of Crop Sciences, College of Agricultural and Marine Sciences, Sultan Qaboos University, P.O. Box 34, Al-Khod 123, Sultanate of Oman; e-mail: alsadiah@gmail.com

Prof. dr M. Arzanlou, Plant Protection Department, Agriculture Faculty, University of Tabriz, P.O. Box: 5166614766, Tabriz, Iran; e-mail: arzanlou@hotmail.com

Prof. dr T. Burgess, School of Biological Sciences and Biotechnology, Murdoch University, Perth, 6150, Australia; e-mail: tburgess@murdoch.edu.au

Prof. dr L. Cai, State Key Laboratory of Mycology, Institute of Microbiology, Chinese Academy of Sciences, No. 3 Park 1, Beichen West Road, Chaoyang District, Beijing, 100101, China; e-mail: cail@im.ac.cn

Prof. dr L. Carris, Associate Professor, Department of Plant Pathology, Washington State University, Pullman, WA 99164-6340, USA; e-mail: carris@mail.wsu.edu

Dr C. Decock, MUCL, Croix du Sud 2 bte L7.05.06, B-1348 Louvain-la-Neuve, Belgium; e-mail: cony.decock@uclouvain.be

Dr X.L. Fan, The Key Laboratory for Silviculture and Conservation of Ministry of Education, Beijing Forestry University, Beijing 100083, China; e-mail: xinleifan@bjfu.edu.cn

Dr D. Gramaje, Instituto de Ciencias de la Vid y del Vino (ICVV), Consejo Superior de Investigaciones Científicas - Universidad de La Rioja - Gobierno de La Rioja, Ctra. Mendavia-Logroño NA 134, Km. 90, 26071 Logroño, Spain; e-mail: david.gramaje@icvv.es

Dr V. Guarnaccia, Department of Agriculture, Forestry and Food Sciences (DiSAFA), University of Torino, via Paolo Braccini 2, 10095 Grugliasco, TO, Italy, Italy; e-mail: vladimiro.guarnaccia@unito.it

Dr R. Jeewon, Department of Health Sciences, Faculty of Science, University of Mauritius, Reduit, Mauritius; e-mail: r.jeewon@uom.ac.mu

Dr F. Liu, State Key Laboratory of Mycology, Institute of Microbiology, Chinese Academy of Sciences, No. 3 Park 1, Beichen West Road, Chaoyang District, Beijing, 100101, China; liufang@im.ac.cn

Dr L. Mostert, Department of Plant Pathology, University of Stellenbosch, P. Bag X1, Matieland 7602, South Africa; e-mail: lmost@sun.ac.za

Prof. dr A.J.L. Phillips, University of Lisbon, Faculty of Sciences, Biosystems and Integrative Sciences Institute (BioISI), Campo Grande, 1749-016 Lisbon, Portugal; e-mail: alan.jl.phillips@gmail.com

Dr H.D.T. Nguyen, Agriculture and Agri-Food Canada, K.W. Neatby Building, 960 Carling Ave., Ottawa, ON, Canada, K1A 0C9; e-mail: Hai.Nguyen@agr.gc.ca

Dr M. Piątek, Department of Mycology, W. Szafer Institute of Botany, Polish Academy of Sciences, Lubicz 46, PL-31-512 Kraków, Poland; e-mail: m.piatek@botany.pl

Prof. dr H.-D. Shin, Division of Environmental Science and Ecological Engineering, Korea University, Seoul 02841, Korea; e-mail: hdshin@korea.ac.kr

Prof. dr B. Summerell, Royal Botanic Gardens and Domain Trust, Mrs. Macquaries Road, Sydney, NSW 2000, Australia; e-mail: Brett.Summerell@rbgsyd.nsw.gov.au

Dr J.B. Tanney, Institut de Biologie Intégrative et des Systèmes, Charles-Eugène-Marchand Pavilion, 1030 Avenue de la Médecine, Québec City, QC G1V 0A6, Canada; e-mail: jtanney@lakeheadu.ca

Prof. dr P. Taylor, Faculty of Veterinary and Agricultural Sciences, University of Melbourne, VIC, 3010, Australia; e-mail: paulwjt@unimelb.edu.au

Prof. dr M. Thines, Goethe University Frankfurt am Main, Faculty of Biosciences, Institute of Ecology, Evolution and Diversity, Max-von-Laue-Str. 9, D-60438 Frankfurt am Main, Germany; e-mail: Marco.Thines@senckenberg.de

Dr A.D. van Diepeningen, Business Unit Biointeractions and Plant Health, Wageningen University and Research, Wageningen, the Netherlands; e-mail: anne.vandiepeningen@wur.nl

Prof. dr M.J. Wingfield, Forestry and Agricultural Research Institute (FABI), University of Pretoria, Pretoria 0002, South Africa; e-mail: mike.wingfield@fabi.up.ac.za

Prof. dr R. Zare, Agricultural Research, Education and Extension Organization, Tehrān, Iran; e-mail: simplicillium@yahoo.com

Cover: *Phlogicylindrium dunnii* (CPC 31818), Eustromatic conidioma on PDA.

SCOPE AND AIMS

SCOPE

All aspects of systematics and evolution of fungi.

AIMS

Fungal Systematics and Evolution is an international, peer-reviewed, open-access, full colour, fast-track journal. Papers will include reviews, research articles, methodology papers, taxonomic monographs, and the description of fungi. The journal strongly supports good practice policies, and requires voucher specimens to be deposited in a fungarium, cultures in long-term genetic resource collection, sequences in GenBank, alignments in TreeBASE, and taxonomic novelties in MycoBank.

ABOUT FUNGAL SYSTEMATICS AND EVOLUTION

Fungal Systematics and Evolution has an OPEN ACCESS publishing policy. All manuscripts will undergo peer review before acceptance, and will be published as quickly as possible following acceptance. There are no page charges or length restrictions, or fees for colour plates. The official journal language is English. All content submitted to Fungal Systematics and Evolution is checked for plagiarism.

Fungal Systematics and Evolution is licensed under a Creative Commons Attribution-NonCommercial-ShareAlike 4.0 International License.

PUBLISHED BY

Westerdijk Fungal Biodiversity Institute, P.O. Box 85167, 3508 AD Utrecht, The Netherlands.



WESTERDIJK
FUNGAL BIO
DIVERSITY
INSTITUTE

All articles are copyright of Westerdijk Fungal Biodiversity Institute.

FREQUENCY

Twice per year (June and December).

ISSN: 2589-3823

E-ISSN: 2589-3831

CONTENTS

Research papers

K.S. Mighell, T.W. Henkel, R.A. Koch, A. Goss, M.C. Aime. New species of <i>Amanita</i> subgen. <i>Lepidella</i> from Guyana	1
S. Uzuhashi, S. Nakagawa, H.M.A. Abdelzaher, M. Tojo. Phylogeny and morphology of new species of <i>Globisporangium</i>	13
D. Haelewaters, D.H. Pfister. Morphological species of <i>Gloeandromyces</i> (<i>Ascomycota, Laboulbeniales</i>) evaluated using single-locus species delimitation methods	19
A.T. Buaya, M. Thines. <i>Miracula moenusica</i> , a new member of the holocarpic parasitoid genus from the invasive freshwater diatom <i>Pleurosira laevis</i>	35
A. Vizzini, G. Consiglio, M. Marchetti. <i>Mythicomycetaceae</i> fam. nov. (<i>Agaricineae, Agaricales</i>) for accommodating the genera <i>Mythicomyces</i> and <i>Stagnicola</i> , and <i>Simocybe parvispora</i> reconsidered	41
P.W. Crous, R.K. Schumacher, A. Akulov, R. Thangavel, M. Hernández-Restrepo, A.J. Carnegie, R. Cheewangkoon, M.J. Wingfield, B.A. Summerell, W. Quaedvlieg, T.A. Coutinho, J. Roux, A.R. Wood, A. Giraldo, J.Z. Groenewald. New and Interesting Fungi. 2	57
L.A. Holland, D.P. Lawrence, M.T. Nouri, R. Travadon, T.C. Harrington, F.P. Trouillas. Taxonomic revision and multi-locus phylogeny of the North American clade of <i>Ceratocystis</i>	135
M. Bakhshi. Epitypification of <i>Cercospora rautensis</i> , the causal agent of leaf spot disease on <i>Securigera varia</i> , and its first report from Iran	157
P.R. Johnston, D. Park. <i>Blastocervulus metrosideri</i> sp. nov. leaf spot on <i>Metrosideros excelsa</i> in New Zealand	165
R.M. Bennett, M. Thines. Revisiting <i>Salisapiliaceae</i>	171

doi.org/10.3114/fuse.2019.03.01

New species of *Amanita* subgen. *Lepidella* from Guyana

K.S. Mighell¹, T.W. Henkel^{1*}, R.A. Koch², A. Goss¹, M.C. Aime²

¹Department of Biological Sciences, Humboldt State University, Arcata, CA 95521, USA

²Department of Botany and Plant Pathology, Purdue University, West Lafayette, IN 47907, USA

*Corresponding author: twh5@humboldt.edu

Key words:

ectomycorrhizal fungi
Guiana Shield
monodominant forests
Neotropics
new taxa
systematics
taxonomy

Abstract: New species of *Amanita* subgen. *Lepidella* are described from Guyana. *Amanita cyanochlorinosma* sp. nov., *Amanita fulvoalba* sp. nov., and *Amanita guyanensis* sp. nov. represent the latest additions to the growing body of newly described ectomycorrhizal fungi native to *Dicymbe*-dominated tropical rainforests. Macro- and micromorphological characters, habitat, and DNA sequence data for the ITS, nrLSU, *rpb2*, and *ef1-α* are provided for each taxon, and β -*tubulin* for most. Distinctive morphological features warrant the recognition of the three new species and a molecular phylogenetic analysis of taxa across *Amanita* subgen. *Lepidella* corroborates their infrageneric placements.

Effectively published online: 28 November 2018.

INTRODUCTION

Amanita (*Amanitaceae*, *Agaricomycetes*, *Basidiomycota*) is a monophyletic mushroom genus with cosmopolitan distribution (Drehmel *et al.* 1999, Tulloss 2005). It is estimated that 900–1000 *Amanita* species exist worldwide, with over 500 currently described (Tulloss 2005, Thongbai *et al.* 2016, Vargas *et al.* 2017). *Amanita* has traditionally been divided into two subgenera based on basidiospore amyloidity (e.g. Singer 1986). Subgenus *Amanita* includes those species with inamyloid basidiospores, and has traditionally been subdivided into sections *Amanita*, *Vaginatae*, and *Caesareae* based on macromorphology (e.g. Moser 1967). Molecular studies have corroborated these sections by demonstrating the monophyly of each (Weiss *et al.* 1998, Tang *et al.* 2015). Subgenus *Lepidella* includes those species with amyloid basidiospores and has been further subdivided into four sections based on velar morphology: sect. *Amidella* (marginal appendiculae and saccate volva present), sect. *Lepidella* (marginal appendiculae present, saccate volva absent), sect. *Phalloideae* (marginal appendiculae absent, saccate volva present), and sect. *Validae* (marginal appendiculae and saccate volva absent) (Corner & Bas 1962). Molecular studies have supported the monophyly of sect. *Amidella* and sect. *Validae*, whereas sect. *Lepidella* and sect. *Phalloideae* may be polyphyletic (Weiss *et al.* 1998, Drehmel *et al.* 1999, Moncalvo *et al.* 2000a, Kim *et al.* 2013, Tang *et al.* 2015, Cui *et al.* 2018).

While a few earliest diverging *Amanita* species are saprotrophic (Wolfe *et al.* 2012), the genus is otherwise considered ectomycorrhizal (ECM) and exhibits a wide range of ECM host associations (Tedersoo & Brundrett 2017). *Amanita* species are prevalent in *Fagaceae* and *Pinaceae* dominated higher latitude forests (Tulloss 2005, Truong *et al.* 2017), some with Holarctic distributions (Geml *et al.* 2006). Of the ~ 500 validly described species of *Amanita*, around 130 are known

from the tropics (Thongbai *et al.* 2016). Tropical *Amanita* species frequently occur in spatially restricted mono- or co-dominant stands of ECM host trees, and thus appear to have smaller geographic ranges. They can, however, be a major component of the local ECM fungal assemblage (Watling & Lee 1995, Henkel *et al.* 2012, Ebenye *et al.* 2017). Overall, tropical regions remain mycologically undersampled and many *Amanita* species remain to be described (Beeli 1935, Bas 1978, Mueller & Halling 1995, Halling 2001, Simmons *et al.* 2002, Zhang *et al.* 2004, Tulloss 2005, Henkel *et al.* 2012, Cui *et al.* 2018).

Around 35 species of *Amanita* have been described from lowland tropical South America. Bas (1978) mentioned several poorly documented Brazilian species described in 1937 by Johann Rick, and described eight new central Amazonian species. More recently, 25 species have been described from the South American tropics including 11 from Colombia (Tulloss *et al.* 1992, Tulloss & Franco-Molano 2008), nine from Brazil (Bas & De Meijer 1993, Menolli *et al.* 2009, Wartchow *et al.* 2009, Wartchow *et al.* 2013, Wartchow 2015, Wartchow *et al.* 2015, Wartchow 2016, Wartchow & Cortez 2016), four from Guyana (Simmons *et al.* 2002), and one from Ecuador (Wartchow & Gamboa-Trujillo 2012). An additional six species previously described from other regions have been recorded in tropical South America (Tulloss & Halling 1997, Sobestiansky 2005, Wartchow & Tulloss 2007, Lechner & Alberto 2008, Palacio *et al.* 2015). This steady accrual of new taxa suggests that many South American *Amanita* species remain to be discovered. The ectotrophic *Dicymbe* forests of Guyana provide a case in point, where 28 mostly undescribed *Amanita* species are known to occur (Henkel *et al.* 2012).

Here three new species of *Amanita* subgen. *Lepidella* are described from Guyana. *Amanita cyanochlorinosma* sp. nov. has a greyish blue pileus, saccate volva, and strong odour of chlorine. *Amanita fulvoalba* sp. nov. produces robust

basidiomata with tawny pilei, marginal appendiculae, and a saccate volva. *Amanita guyanensis* sp. nov. has a greyish brown pileus with floccose warts and a floccose volva. Each of the new species was compared to previously described *Amanita* species from the world literature, and their novelty demonstrated by comparison with morphologically similar described species. Molecular data support placement of *A. cyanochlorinosma* and *A. fulvoalba* in sect. *Lepidella*, and *A. guyanensis* in sect. *Validae*. Morphological data support these placements with the exception of *A. fulvoalba*, whose molecular-based placement in sect. *Lepidella* contrasts with its marginal appendiculae, which typically characterise sect. *Amidella*. Each of these species has been encountered repeatedly in Guyana's *Dicymbe* forests over the past 20 years (Henkel *et al.* 2012).

MATERIALS AND METHODS

Collections and morphological analyses

Collections were made in Guyana during the May–Jul. rainy seasons of 2000, 2003, 2005, 2007, 2009, 2011, 2012, and 2015 and the Dec.–Jan. rainy seasons of 2004, 2009, and 2016 from the Upper Potaro River Basin, within a 15 km radius of a permanent base camp at 5°18'04.8" N 59°54'40.4" W, 710 m a.s.l. Additional collections were made from the Upper Mazaruni River Basin during Dec. 2010 and Jun. 2012 within a 0.4 km radius of a base camp at 5°26'21.3" N and 60°04'43.1" W, 800 m a.s.l., and Jun. 2011 from the Upper Demerara River Basin at Mabura Ecological Reserve, near a field station located at 5°09'19.0"N 58°41'58.9"W, 100 m a.s.l. At the Potaro sites, basidiomata were collected from monodominant forests of ECM *Dicymbe corymbosa* (Henkel *et al.* 2012) and other stands containing ECM *Dicymbe altsonii*, *Aldina insignis* and *D. corymbosa* (Smith *et al.* 2011). At the Mazaruni site, collections were made from forests co-dominated by ECM *Pakaraimaea dipterocarpacea* and *Dicymbe jenmanii* (Smith *et al.* 2013). At the Mabura site, collections were made in monodominant stands of *D. altsonii* (Zagt 1997). Macromorphological features of fresh basidiomata were described in the field. Colours were described subjectively and coded according to Kornerup & Wanscher (1978), with colour plates noted in parentheses. Fresh collections were field-dried with silica gel.

Micromorphological features were assessed using an Olympus BX51 microscope with bright field and phase contrast optics. Rehydrated fungal tissues were mounted in H₂O, 3 % potassium hydroxide (KOH), and Melzer's solution. Twenty-five basidiospores were measured from each specimen of each species, including the types. Twenty basidia and hyphal elements of the subhymenium, hymenophoral trama, pileipellis, pileus and stipe trama, and universal veil were measured from each type specimen, and 10 from each additional specimen examined. Length/width Q values for basidiospores are reported as Q_r (range of Q values over "n" basidiospores measured) and Q_m (mean of Q values ± SD). The notation "[a/b/c]" preceding sets of basidiospore data denotes "'a' basidiospores from 'b' basidiomata from 'c' collections." Outlying measurements observed in less than 5 % of a given structure are placed in parentheses. Line drawings are freehand composites of microscopic observations. Specimens were deposited in the following herbaria: BRG, University of Guyana; HSC, Humboldt State University; PUL, Kriebel Herbarium, Purdue University.

DNA extraction, amplification, sequencing and phylogenetic analyses

DNA was extracted from dried basidioma tissue of types and additional specimens using the Wizard® Genomic DNA Purification kit (Promega Co., WI, USA). Five DNA gene fragments were sequenced, including those coding for the second-largest subunit of RNA polymerase II (*rpb2*), translation elongation factor 1-alpha (*ef1-α*) and beta-tubulin (*β-tub*), along with two non-protein coding regions, the internal transcribed spacer (ITS) and nuclear ribosomal large subunit (nrLSU). Primer pairs ITS1F/ITS4B (Gardes & Bruns 1993), LROR/LR6 (Vilgalys & Hester 1990, Moncalvo *et al.* 2000b), EF1-983F/EF1-2218R (Rehner & Buckley 2005), Am-*β-tubulin* F/Am-*β-tubulin* R (Cai *et al.* 2014) and Am-6F/Am-7R (Cai *et al.* 2014) were used to amplify ITS, nrLSU, *ef1-α*, *β-tub* and *rpb2*, respectively. Amplification reactions included 12.5 μL of Promega PCR Mastermix (Promega Co., WI, USA), 1.25 μL of each primer (at 10 μM) and approximately 100 ng of DNA. The final PCR reaction volume was 25 μL. The recommended cycling conditions for each primer pair were followed. PCR products were sequenced by GeneWiz® (South Plainfield, NJ, USA). To get readable ITS and nrLSU sequences for specimens MCA 3962 and TH 9172, these fragments were cloned using the pGem®-T Easy Vector System (Promega Co., WI, USA) following manufacturer's protocols. Ten colonies for each specimen for each locus were suspended in 30 μL of sterile water. PCR reactions were done as described above, using the original primers for each gene fragment and 10 μL of clone/sterile water mixture. All amplicons were sequenced. Sequences were edited using Sequencher v. 5.2.3 software (Gene Codes Corporation, MI, USA) and deposited in GenBank.

Initial BLAST searches with the ITS and nrLSU sequences for each new species confirmed their affinity with *Amanita* subgen. *Lepidella*. Infrageneric relationships of the three new species was assessed with phylogenetic analyses using nrLSU, *ef1-α*, *β-tub* and *rpb2* (Cai *et al.* 2014). Sequences for the final dataset were downloaded from GenBank and included exemplars from 76 specimens from all four sections of *Amanita* subgen. *Lepidella*. Eight species from *Amanita* subgen. *Amanita* were used as outgroup taxa. Table 1 gives all taxa, collection information, GenBank numbers, and references for specimens used in the phylogenetic analysis.

Sequences were aligned in MEGA v. 7 (Kumar *et al.* 2016) using the MUSCLE algorithm (Edgar 2004) with refinements to the alignment done manually. Individual gene alignments were concatenated manually after inspection for intergene conflict. Phylogenies were reconstructed using maximum likelihood (ML) and Bayesian methods. PartitionFinder v. 1.1.0 (Lanfear *et al.* 2012) was used to determine the best partitioning strategy and model of molecular evolution for each partition for both the ML and Bayesian analyses. Maximum likelihood bootstrap analysis for phylogeny and assessment of branch support by bootstrap percentages (% BS) was performed using RAxML (Stamatakis 2014). One-thousand bootstrap replicates were produced. Bayesian analyses for the reporting of Bayesian posterior probability (BPP) support for branches were conducted using the program MrBayes v. 3.2.6 (Ronquist *et al.* 2012). Four simultaneous, independent runs, each with four Markov chain Monte Carlo (MCMC) chains, were initiated and run at a temperature of 0.20 for 50 M generations, sampling trees every 1000 generations until the standard deviation of the split frequencies reached a final stop value of 0.01. The initial 20 % of trees were discarded as burn-in and a maximum

clade credibility tree from the remaining trees was produced using TreeAnnotator. The final alignment and phylogeny can be

accessed in TreeBASE (<http://purl.org/phylo/treebase/phylo/study/TB2:S23533>).

Table 1. Taxa, voucher information and GenBank accession numbers for specimens used in the phylogenetic analysis. Taxa described here and type specimens are indicated in bold.

Species	Voucher	Locality	nrLSU	rpb2	ef1-a	β -tub
<i>Amanita abrupta</i>	BW_HP_101	Massachusetts, USA	HQ539660 ^a	--	--	--
<i>Amanita asteropus</i>	RET 730-2	France	KY274804 ^b	--	--	--
<i>Amanita aurantiobrunnea</i>	MCA 4420	Guyana	MK105506 ^c	MK092931 ^c	--	MK092938 ^c
<i>Amanita ballerina</i>	OR1026	Thailand	MH157079 ^d	KY656884 ^e	--	KY656865 ^e
<i>Amanita bisporigera</i>	RET 377-9	Tennessee, USA	KJ466434 ^f	--	KJ481936 ^f	KJ466501 ^f
<i>Amanita brunneolocularis</i>	ANDES_F313 NVE57	Colombia	FJ890044 ^g	--	--	--
<i>Amanita brunnescens</i>	PBM 2429		AY631902 ^h	AY780936 ^h	AY881021 ^h	--
<i>Amanita calochroa</i>	MCA 3927	Guyana	KC155375 ⁱ	--	--	--
<i>Amanita</i> aff. <i>campinaranae</i>	MCA 5878	Guyana	MK105507 ^c	MK092934 ^c	MK092947 ^c	MK092940 ^c
<i>Amanita castanea</i>	MFLU:15-01424	Thailand	KU877539 ^j	--	--	--
<i>Amanita chlorinosma</i>	RET 328-6	New York, USA	HQ539676 ^a	--	--	--
<i>Amanita citrina</i>	ANDES_F2117_ NVE616	Colombia	KT008032 ^k	--	--	--
<i>Amanita cokeri</i>	BW_STF 090506-19	Massachusetts, USA	HQ593113 ^a	--	--	--
<i>Amanita congolensis</i>	RET 346-6	Gambia	HQ539736 ^a	--	--	--
<i>Amanita clarisquamosa</i>	HKAS29514		AF024448 ^l	--	--	--
<i>Amanita clelandii</i>	PSC 2524	Australia	HQ539680 ^a	--	--	--
<i>Amanita</i> cf. <i>cruetilemurum</i>	RET 600-3	California, USA	KP711840 ^m	--	--	--
<i>Amanita cyanochlorinosma</i>	MCA 3962	Guyana	MK105495 ^c	MK092931 ^c	MK092943 ^c	MK092936 ^c
			MK105496 ^c			
<i>Amanita cyanochlorinosma</i>	TH 9172	Guyana	MK105493 ^c	MK092933 ^c	MK092945 ^c	MK092939 ^c
			MK105494 ^c			
<i>Amanita cyanopus</i>	TH 8912	Guyana	KT339210 ⁿ	--	--	--
<i>Amanita daucipes</i>	RET 386-8	Pennsylvania, USA	HQ539688 ^a	--	--	--
<i>Amanita eriophora</i>	RET 350-4	Cambodia	HQ539672 ^a	--	--	--
<i>Amanita excelsa</i>	HKAS31510	China	AY436491 ^o	--	--	--
<i>Amanita exitialis</i>	HKAS75775	China	JX998053 ^p	KJ466592 ^f	JX998002 ^p	KJ466504 ^f
<i>Amanita farinacea</i>	PSC 2529	Australia	HQ539692 ^a	--	--	--
<i>Amanita flavipes</i>	ASIS26281		KU139456 ^q	--	--	--
<i>Amanita franchetii</i>	JM 96/27	North Carolina, USA	AF097381 ^r	--	--	--
<i>Amanita</i> aff. <i>fritillaria</i>	HKAS56832	China	KJ466479 ^f	KJ466644 ^f	KJ481979 ^f	KJ466558 ^f
<i>Amanita fuliginea</i>	HKAS75782	China	JX998049 ^p	KJ466597 ^f	JX997996 ^p	KJ466509 ^f
<i>Amanita fuligineoides</i>	HKAS52727	China	JX998047 ^p	KJ466599 ^f	--	KJ466511 ^f
<i>Amanita fulvoalba</i>	MCA 6920	Guyana	MK105498 ^c	--	--	--
	TH 8056	Guyana	MK105499 ^c	MK092925 ^c	--	--
	TH 8455	Guyana	MK105500 ^c	MK092927 ^c	--	--
	TH 9043	Guyana	MK105501 ^c	MK092928 ^c	MK092946 ^c	--
	TH 10395	Guyana	MK105497 ^c	MK092926 ^c	MK092942 ^c	--
<i>Amanita guyanensis</i>	MCA 3155	Guyana	MK105504 ^c	--	--	MK092935 ^c
	TH 9767	Guyana	MK105502 ^c	MK092929 ^c	MK092948 ^c	MK092937 ^c
	TH 9772	Guyana	MK105503 ^c	MK092930 ^c	MK092944 ^c	MK092941 ^c
<i>Amanita lanivolva</i>	TH 9190	Guyana	KT339292 ⁿ	--	--	--
<i>Amanita lavendula</i>	RET 639-7	Ontario, Canada	KR865979 ^m	--	--	--
<i>Amanita luteofusca</i>	PSC 1093b	Australia	HQ539705 ^a	--	--	--
<i>Amanita luteolovelata</i>	PSC 2187	Australia	HQ539706 ^a	--	--	--

Table 1. (Continued).

Species	Voucher	Locality	nrLSU	<i>rpb2</i>	<i>ef1-a</i>	<i>b-tub</i>
<i>Amanita manginiana</i>	HKAS56933	China	KJ466438 ^f	KJ466603 ^f	KJ481943 ^f	KJ466515 ^f
<i>Amanita modesta</i>	HKAS79688	China	KJ466440 ^f	KJ466605 ^f	KJ481944 ^f	KJ466516 ^f
<i>Amanita morrisii</i>	RET 672-6	New Jersey, USA	KR919770 ^m	--	--	--
<i>Amanita novinupta</i>	RET 60-2	Oregon, USA	KU248118 ^m	--	--	--
<i>Amanita oberwinkleriana</i>	HKAS77330	China	KJ466441 ^f	KJ466606 ^f	KJ481946 ^f	--
<i>Amanita ocreata</i>	HKAS79686	California, USA	KJ466442 ^f	KJ466607 ^f	KJ481947 ^f	KJ466518 ^f
<i>Amanita aff. odorata</i>	KM 70	Cameroon	MK105505 ^c	--	--	--
<i>Amanita orsonii</i>	RET 717-8	India	KX270345 ^b	--	--	--
<i>Amanita pallidrosea</i>	HKAS75786	China	JX998054 ^p	KJ466627 ^f	JX998011 ^p	KJ466539 ^f
<i>Amanita parvipantherina</i>	HKAS56822	China	JN941163 ^s	JQ031115 ^s	KJ482005 ^f	KJ466566 ^f
<i>Amanita peckiana</i>	RET 320-3	New York, USA	HQ539720 ^a	--	--	--
<i>Amanita phalloides</i>	HKAS75773	California, USA	JX998060 ^p	KJ466612 ^f	JX998000 ^p	KJ466523 ^f
<i>Amanita porphyria</i>	RET 370-10	Newfoundland, Canada	KP866187 ^t	--	--	--
<i>Amanita proxima</i>	RET 290-10	France	HQ539728 ^a	--	--	--
<i>Amanita pseudoporphyria</i>	HKAS56984	China	KJ466451 ^f	KJ466613 ^f	KJ481952 ^f	KJ466524 ^f
<i>Amanita rhoadsii</i>	DD97/13	North Carolina, USA	AF097391 ^r	--	--	--
<i>Amanita rhopalopus</i>	BW_RET 386-3	West Virginia, USA	HQ539733 ^a	--	--	--
<i>Amanita rimosa</i>	HKAS77335	China	KJ466455 ^f	KJ466393 ^f	KJ481957 ^f	KJ466532 ^f
<i>Amanita rubrovolvata</i>	HKAS56744	China	JN941156 ^u	JQ031117 ^s	--	--
<i>Amanita sepiacea</i>	ASIS26353		KU139443 ^q	--	--	--
	HKAS38716	China	AY436501 ^o	--	--	--
<i>Amanita sp.</i>	HKAS77321	China	KJ466481 ^f	KJ466646 ^f	--	KJ466560 ^f
	HKAS77322	Ohio, USA	KJ466470 ^f	KJ466650 ^f	KJ481984 ^f	KJ466564 ^f
	HKAS77339	South Korea	KJ466482 ^f	KJ466647 ^f	KJ481981 ^f	KJ466561 ^f
	HKAS77340	China	KJ466483 ^f	KJ466648 ^f	KJ481982 ^f	KJ466562 ^f
	HKAS77344	China	KJ466465 ^f	KJ466634 ^f	KJ481969 ^f	KJ466548 ^f
<i>Amanita sp. 12</i>	TH 9128	Guyana	JN168681 ^v	--	--	--
<i>Amanita sp. 14</i>	TH 8247	Guyana	KT339281 ⁿ	--	--	--
<i>Amanita cf. spissacea</i>	OR1214	Thailand	KY747478 ^e	KY656886 ^e	--	KY656867 ^e
<i>Amanita suballiacea</i>	RET 491-7	Michigan, USA	KJ466486 ^f	KJ466602 ^f	KJ481942 ^f	KJ466514 ^f
<i>Amanita cf. subcokeri</i>	RET 97-3	New Jersey, USA	HQ539747 ^a	--	--	--
<i>Amanita subfrostiana</i>	HKAS57042	China	JN941162 ^s	JQ031118 ^s	KJ482003 ^f	KJ466565 ^f
<i>Amanita subglobosa</i>	HKAS58837	China	JN941152 ^s	JQ031121 ^s	KJ482004 ^f	KJ466567 ^f
<i>Amanita subjunquillea</i>	HKAS77325	China	KJ466490 ^f	KJ466656 ^f	KJ481988 ^f	KJ466574 ^f
<i>Amanita cf. tephrea</i>	RET 378-9	New York, USA	HQ539751 ^a	--	--	--
<i>Amanita vestita</i>	HKAS79687	China	KJ466494 ^f	KJ466662 ^f	KJ481995 ^f	KJ466581 ^f
<i>Amanita virgineoides</i>	HKAS79691	China	KJ466495 ^f	KJ466663 ^f	KJ481996 ^f	KJ466582 ^f
<i>Amanita virosa</i>	HKAS56694	Finland	JX998058 ^p	KJ466664 ^f	JX998007 ^p	KJ466583 ^f
<i>Amanita volvata</i>	RV97/24	Virginia, USA	AF097388 ^r	--	--	--
<i>Amanita westii</i>	BW_SH26	Texas, USA	HQ539759 ^a	--	--	--
<i>Amanita xerocybe</i>	TH 8930	Guyana	KC155384 ⁱ	--	--	--
<i>Amanita zangii</i>	HKAS77331	China	KJ466500 ^f	KJ466669 ^f	KJ482001 ^f	KJ466589 ^f

^aWolfe et al. 2012, *Mycologia* **104**: 22–33; ^bTulloss et al., unpubl. data; ^cthis study; ^dRaspe, unpubl. data; ^eThongbai et al. 2017, *PLoS One* **12**: e0182131; ^fCai et al. 2014, *Mycol. Prog.* **13**: 1008; ^gVargas et al., unpubl. data; ^hMatheny et al., unpubl. data; ⁱSmith et al. 2013, *PLoS One* **8**: e55160.; ^jThongbai et al. 2016, *Phytotaxa* **286**: 211–231; ^kVargas et al., unpubl. data; ^lWeiss et al. 1998, *Canad. J. Bot.* **76**: 1170–1179; ^mTulloss et al., unpubl. data; ⁿSmith et al. 2017, *New Phytol.* **215**: 443–453; ^oZhang et al. 2004, *Fungal Diversity* **17**: 219–238; ^pCai et al. 2012, *Plant Diversity and Resources* **34**: 614–622; ^qSeok, unpubl. data; ^rDrehmel et al. 1999, *Mycologia* **91**: 610–618; ^sSchoch et al. 2012, *Proc. Nat. Acad. Sci. USA* **109**: 6241–6246; ^tHughes, unpubl. data; ^uWeiss, unpubl. data; ^vSmith et al. 2011, *New Phytol.* **192**: 699–712.

RESULTS

Nine ITS (GenBank accessions: MK064186–MK064193, MK097470), 15 nrLSU, seven *ef1-α*, ten *rpb2* and seven *β-tub* sequences were generated in this study, ranging from 444–761, 535–1075, 804–1120, 482–1174 and 289–380 bp, respectively. For specimens MCA 3962 and TH 9172, one ITS amplicon of *Amanita* origin was recovered for both specimens, while two nrLSU amplicons of *Amanita* origin were recovered from each specimen, one with a 15 bp intron relative to the other; both nrLSU sequences were used in the phylogenetic analysis. After the ends of the individual alignments were trimmed, the size of the aligned dataset was as follows: nrLSU was 941 bp, *ef1-α* was 536, *rpb2* was 669 and *β-tub* was 235. A 598 bp intron in the *rpb2* sequence that was present in specimens MCA 6920, TH 8056, TH 8455, TH 9043 and TH 10395 was removed from the alignment.

Amanita subgen. *Lepidella* was resolved as monophyletic with strong statistical support (99 % BS/0.98 BPP), along with each of the four sections in subgen. *Lepidella*: *Amidella* (100 % BS/0.99 BPP), *Lepidella* (88 % BS/0.91 BPP), *Phalloideae* (99 % BS/0.98 BPP) and *Validae* (99 % BS/0.98 BPP) (Fig. 1). Specimens MCA 3155, TH 9767 and TH 9772 were conspecific and formed a well-supported lineage (98 % BS/1.00 BPP) resolved to sect. *Validae* and represent *A. guyanensis* (Fig. 1). Specimens MCA 3962 and TH 9172 were conspecific and formed a well-supported lineage (100 % BS/0.99 BPP), representing *A. cyanochlorinosma*, and specimens MCA 6290, TH 8056, TH 8455, TH 9043 and TH 10395 were conspecific and formed another well-supported lineage (100 % BS/1.00 BPP), representing *A. fulvoalba*. The two latter species were resolved to sect. *Lepidella* (Fig. 1).

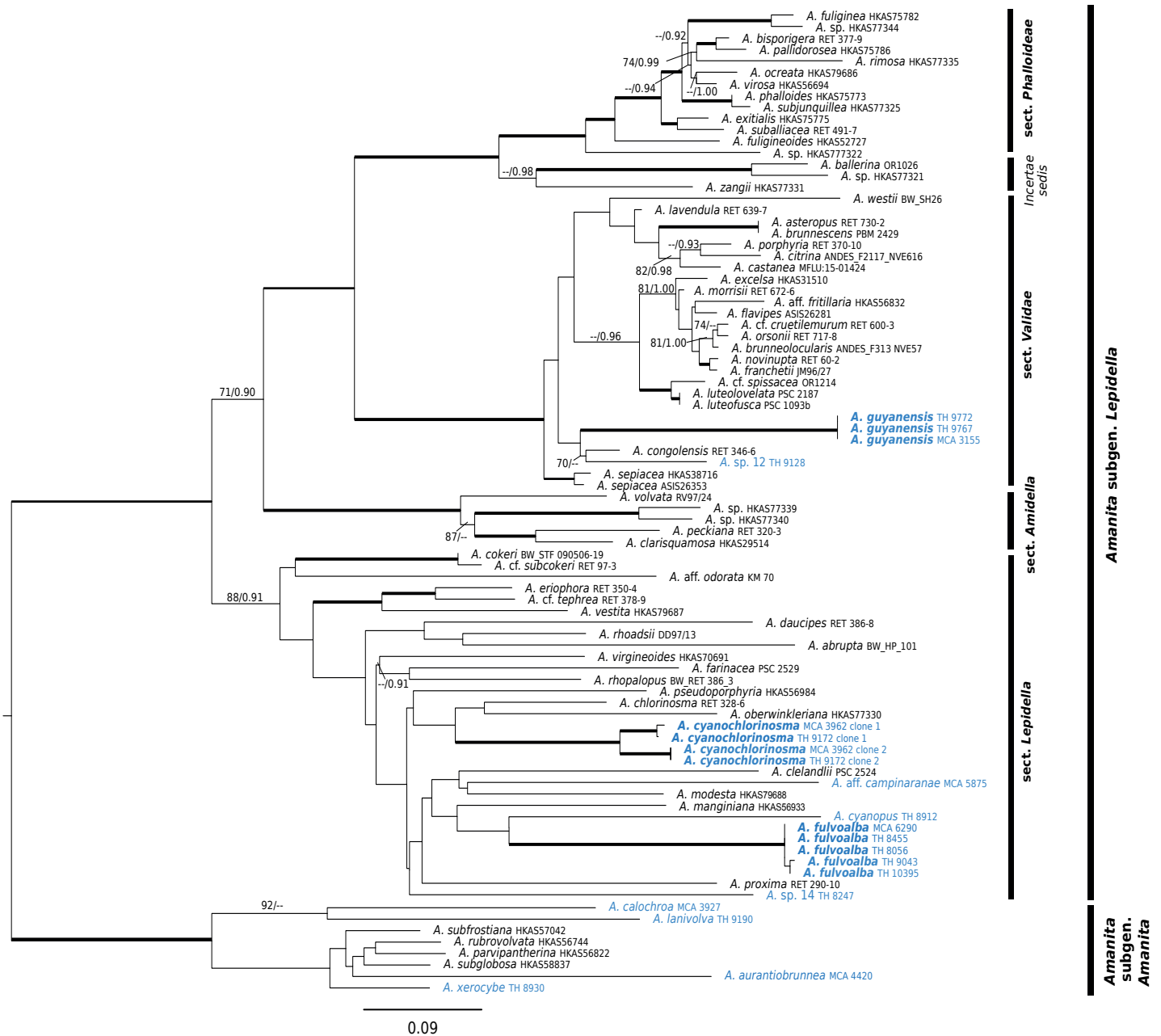


Fig. 1. Maximum-likelihood phylogeny generated from the analysis of four gene fragments (nrLSU, *ef1-α*, *β-tub* and *rpb2*) from 76 specimens in *Amanita* subgen. *Lepidella* and eight outgroup specimens in *Amanita* subgen. *Amanita*. The new species *A. cyanochlorinosma* and *A. fulvoalba* are resolved in sect. *Lepidella* and *A. guyanensis* in sect. *Validae*. Thickened black bars represent nodes with greater than 90 % BS and 0.95 BPP; support values shown above branches represent % BS/BPP; -- represents no support. New species are in bold, and all species from Guyana are in blue.

TAXONOMY

Amanita cyanochlorinosma Mighell & T.W. Henkel, *sp. nov.*
MycoBank MB827394. Figs 2, 3.

Etymology: *cyano-* (Gk. comp.) = blue; *chlorinosma*, referring to the pileus colour and chlorine odour reminiscent of *Amanita chlorinosma*.

Diagnosis: Similar to *Amanita modesta* but differs in its strong chlorine odour, larger basidiospores, and greyish blue pileus colour.

Description: *Pileus* 55–78(–114) mm broad, 3–8 mm tall, planate with slightly downturned margin, with age slightly upturned with a broad, shallow central depression, overall greyish blue (22F4), lighter concolorous (22D3) toward margin, progressively darker brownish grey (10F3–10F4, 11F3–11F4) over disc; surface subviscid, finely appressed radially fibrillose over outer 2/3, appressed matted fibrillose over disc; margin entire, under hand lens finely crenulate; volval elements absent; trama 1 mm thick at margin, 1 mm over lamellae, 3 mm at stipe, white, solid, unchanging. *Lamellae* finely and abruptly adnexed, thin, crowded, off-white to faintly pinkish cream (5A1–5A2), unchanging; edges concolorous, under hand lens very finely roughened-eroded; lamellulae numerous, usually 2–3, 2–21 mm long. *Stipe* 55–89(–136) × 6–13 mm, equal to slightly tapering upward from basal bulb, white to faint grey (10A1–10B1), subglabrous macroscopically, under hand lens finely matted fibrillose-floccose, darkening slightly with pressure; bulb 22–30 × 16–31 mm, subglobose, subabrupt apically, narrowing toward base and subradicate; trama white, solid, unchanging. *Volva* membranous, tightly adhering to bulb with 1–2 ascending limbs loosely appressed to stipe, off-white (2A1–2A2), discoloured brown from adhering soil, with white hyphal cords descending from base. *Annulus* initially superior, subsuperior with age, white to off-white (2A1–2A2 KW) throughout, thin-membranous, appressed to stipe at apex, lower margin outflaring and pendant, occasionally finely perforate. *Odour* strongly of chlorine; *taste* not obtained. *Basidiospores* white in medium deposit, [200/8/8] (6.0–)7.0–9.0(–10.0) × (4.0–)4.5–6.0(–8.0) μm, Qr = (1.0–)1.16–1.6(–1.66), Qm = 1.32, broadly ellipsoid, smooth, hyaline, amyloid; wall slightly thickened; hilar appendix truncate, up to 1 μm long; contents usually granular-guttulate. *Basidia* 23–41 × 5.5–8.0 μm, clavate, 4-sterigmate, rarely 3-sterigmate; sterigmata 1.0–5.0 μm long. *Subhymenium* up to 35 μm thick, composed of globose to ovoid, angular elements up to 44 μm wide. *Marginal tissue of lamellae* composed of abundant, easily dislodged subglobose to pyriform elements, these 16–27 × 10–19 μm. *Lamellar trama* bilateral; mediostratum 15–35 μm wide, composed of branched, interwoven, occasionally inflated hyphae, 2–17 μm wide; lateral stratum diverging obtusely from the mediostratum, composed of uninflated hyphae terminating in 1–3 inflated cylindrical to ovoid elements, these 10–49 × 8–18 μm. *Pileipellis* an ixomixtocutis with two distinct layers; suprapellis 20–115 μm thick; hyphae 2–11 μm wide, partially gelatinised, hyaline, thin-walled, loosely interwoven; subpellis 40–75 μm thick; hyphae 2–8 μm wide, non-gelatinised, hyaline, thin-walled, densely interwoven. *Pileus trama* with abundant acrophysalides, these 23–122 × 10–44 μm, ellipsoidal to clavate, usually with an abruptly tapered base; contents occasionally granular-guttulate; uninflated tramal hyphae 2–10 μm wide,



Fig. 2. *Amanita cyanochlorinosma* (Henkel 9172, type). Scale bar = 1 cm.

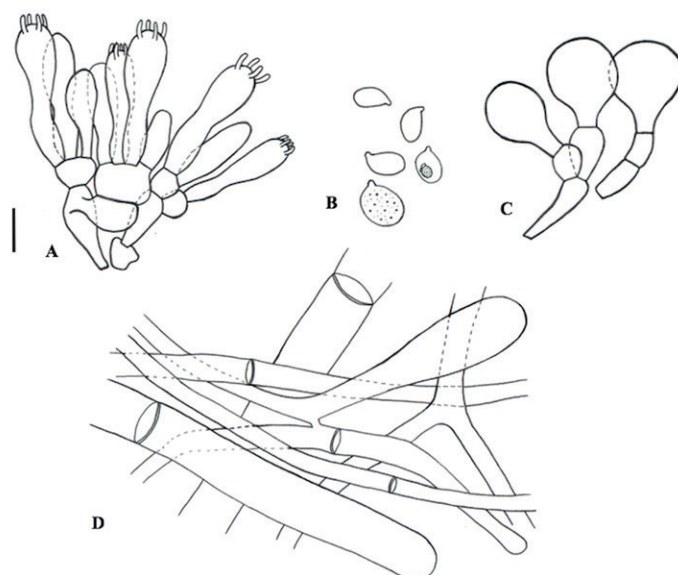


Fig. 3. *Amanita cyanochlorinosma*. A. Basidia and subhymenium. B. Basidiospores. C. Marginal tissue of lamellae. D. Slightly crushed tissue from volval limb. Scale bar = 10 μm.

frequently branching. *Stipe trama* composed of longitudinally arranged, ovoid, ellipsoid, or clavate acrophysalides, these 25–203 × 12–60 μm, occasionally with granular contents; uninflated, non-conductive tramal hyphae 2–15 μm; conductive hyphae absent to moderately frequent in localized clusters, up to 23 μm wide. *Volva at stipe base* composed of densely interwoven, often branching, uninflated hyphae 36–174 × 2–10.5 μm; terminal cells cylindrical or clavate, 25–158 × 6–43 μm. *Partial veil* composed of uninflated hyphae 1–6.5 μm wide, highly branched, thin-walled, densely interwoven; terminal cells 18–50 × 6–16 μm, mostly clavate, occasionally cylindrical or subfusiform; all elements occasionally containing diffuse or clustered granules. *Clamp connections* absent on hyphae of all tissues.

Habit, habitat and distribution: Solitary, or rarely in pairs, on humic mats of forest floor under *D. corymbosa*; also found in

stands containing *D. corymbosa*, *D. altsonii* and *A. insignis* or *P. dipterocharaceae* and *D. jenmanii*; known from the type locality in the Upper Potaro River Basin and ~25 km to the west in the Upper Mazaruni Basin.

Typus: Guyana, Region 8 Potato-Siparuni, Pakaraima Mountains, Upper Potaro River Basin, ~20 km east of Mt. Ayanganna, Tadang Base Camp 2 km south of Potaro River at 5°16'14.5"N 59°50'39.1"W, elevation 710–750 m; ~ 0.3 km ESE of base camp, on root mat in *Dicymbe corymbosa* and *Dicymbe altsonii* co-dominant forest, 30 Dec. 2009, *Henkel 9172* (**holotype** BRG 41298; **isotype** HSC G1229); GenBank accessions: ITS MK064187; nrLSU MK105493, MK105494; *rpb2* MK092933; *ef1-α* MK092956; *β-tub* MK092939.

Additional specimens examined: Guyana, Region 8 Potato-Siparuni, Pakaraima Mountains, Upper Potaro River Basin, ~15 km east of Mt. Ayanganna, Potaro base camp at 5°18'04.8"N 59°54'40.4"W, 710–750 m a.s.l.; under *D. corymbosa*, 3 km E of base camp, 7 May 2001, *Henkel 8057* (BRG 41299, HSC G1230); 3.5 km SE of base camp, 19 May 2001, *Henkel 8182* (BRG 41300, HSC G1230); 1 km SW of base camp, 25 Jun. 2001, *Henkel 8375* (BRG 41301, HSC G1231); 3 km SE of base camp, 11 Jun. 2004, *Henkel 8669* (BRG 41302, HSC G1232); 0.4 km SW of base camp near Blackwater Creek, 1 Jul. 2006, *Aime 3147* (BRG 41303, PUL F24395); 14 Jun. 2015, *Henkel 10083* (BRG 41304, HSC G1233); vicinity of base camp, 18 May 2010, *Aime 3962* (BRG 41305, PUL F24396); ~20 km east of Mt. Ayanganna, Tadang base camp at 5°16'14.5"N 59°50'39.1"W, 710–750 m a.s.l.; 100 m E of base camp, under *D. corymbosa* and *D. altsonii*, 4 Jun. 2013, *Henkel 9737* (BRG 41306, HSC G1234).

Notes: *Amanita cyanochlorinosma* is a distinctive species recognised in the field by its medium-sized, solitary basidiomata, glabrous, viscid, greyish blue pileus contrasting with the white hymenophore, stipe, and veils, strong odour of chlorine, superior annulus, and saccate-limbate volva. The species is best placed in sect. *Lepidella* due to its amyloid, broadly ellipsoid basidiospores, saccate volva, membranous annulus, chlorine odour, and gills that do not darken with desiccation (Corner & Bas 1962, Bas 1969). Although the absence of pileal appendiculae suggests placement in sect. *Phalloideae*, the strong chlorine odour, while known from a handful of sect. *Phalloideae* species, was emphasized by Bas (1969) as an important character of section *Lepidella*, occurring in about half of the known species. Additionally, the phylogenetic analysis indicated that *A. cyanochlorinosma* is nested within sect. *Lepidella* (Fig. 1).

Few other *Amanita* species resemble *A. cyanochlorinosma*. *Amanita modesta* from lowland tropical rainforests of Malaysia is similar to *A. cyanochlorinosma* in its small to medium size, membranous annulus, saccate volva, and bluish pileus lacking volval remnants (Corner & Bas 1962). *Amanita cyanochlorinosma* differs from *A. modesta* by its chlorine odour, longer basidiospores (7.0–9.0 μm versus 5.9–7.8 μm), and greyish blue as opposed to mouse grey to purplish umber pileus. *Amanita cyanochlorinosma* resembles the Japanese *A. griseoturcosa* in its similarly-sized basidiomata, greyish blue pileus, and velar structures, but differs in its chlorine odour and shorter basidiospores (7.0–9.0 μm versus 8.4–12.0 μm) (Tulloch & Yang 2018).

Amanita fulvoalba Mighell & T.W. Henkel, **sp. nov.** MycoBank MB827395. Figs 4, 5.

Etymology: *fulvo-* (L. comp.) = yellowish brown; *alba-* (L. adj. A) = white, referring to the pileus and stipe colours, respectively.

Diagnosis: Similar to *A. aurantiobrunnea* but differs in its yellowish brown pileus and gelatinised inner volva layer.

Description: Pileus 85–110 mm in broad, 11–22 mm tall, broadly convex to planate with low, broad umbo, yellowish brown (5C8) over disc, lighter concolorous (5B5) toward margin, tacky to moist, shiny and glabrous macroscopically, under hand lens finely appressed radially fibrillose, toward margin minutely rivulose; margin entire, bearing fugacious, fibrillose, irregular white appendiculae, these occasionally triangular, 1–5 mm long; volval remnants lacking; trama 0.5–2 mm thick at margin, 3 mm over lamellae, 6–8 mm over stipe, solid, white, unchanging. **Lamellae** finely adnexed to adnate, thin, subcrowded, off-white, unchanging; edges concolorous, under hand lens minutely eroded; lamellulae one, 1–40 mm long. **Stipe** 55–120 × 14–28 mm, sub-cylindrical, white, bruising light orange, longitudinally striate and floccose basally, downy-woolly centrally, finely pulverulent with short striations at apex; bulb 37–47 × 25–40 mm, subglobose to ellipsoid, subabrupt to abrupt, radicating slightly; trama white, solid, unchanging. **Volva** two layered; inner layer a white, erect to outcurved flange extending 2–3 mm above bulb apex; outer layer enclosing basal bulb, densely membranous, with 1–3 non-clasping limbs ascending 10–19 mm above bulb; exterior off-white, dry, glabrous; interior off-white, moist, shiny, glabrous. **Annulus** superior, descending with age to central, pendant, fugacious-membranous; exterior off-white, floccose; interior concolorous, striate, floccose. **Odour** mildly fruity-fungoid. **Taste** fungoid, indistinct. **Basidiospores** white in medium deposit, [250/8/8] (6.0–)7.0–9.0(–11) × (5.0–) 5.5–8.0 μm, Qr = (1.1–)1.14–1.43(–1.5), Qm = 1.29, subglobose to broadly ellipsoid, thin-walled, smooth, hyaline, opaque, amyloid; hilar appendix cylindrical to conic, truncate, up to 1 mm long; contents granular-guttulate. **Basidia** 32–53.5 × 7.75–10 μm, clavate, 4-sterigmate; sterigmata 1.5–4.5 μm long; contents granular-guttulate. **Subhymenium** 18–35 μm thick, composed of 3–4 layers of globose to elliptical, irregularly polygonal elements, these 8–42 μm wide. **Marginal tissue of lamellae** sterile, composed of easily dislodged globose to pyriform elements, these 16–25 μm wide. **Lamellar trama** bilateral; mediostratum 20–45 μm wide, composed of interwoven, frequently branched uninflated hyphae with scattered ovoid to ellipsoid inflated elements, these 26–110 × 2–15 μm; lateral stratum diverging obtusely from the mediostratum, composed of branched uninflated hyphae with clavate to ovoid, inflated elements, these 26–106 × 7–28 μm. **Pileipellis** an ixtomixtocutis with two distinct layers; suprapellis 150–260 μm thick; hyphae 1.5–8 μm wide, strongly gelatinised, periclinal, hyaline, thin-walled, loosely interwoven; subpellis 170–340 μm thick; hyphae 1.5–4 μm wide, slightly gelatinised, mostly periclinal, hyaline, thin-walled, densely interwoven. **Pileus trama** with abundant acrophysalides, these 25–244 × 11–49 μm, cylindrical, clavate, ellipsoid, or ovoid, often with irregular swollen protrusions; contents frequently granular; uninflated tramal hyphae 2–14 μm wide, branching, often swollen at branch nodes and near acrophysalides; conductive hyphae rare to moderately abundant. **Stipe trama** with abundant acrophysalides, these 19–97(–223) × 9–44 μm, longitudinally oriented, cylindrical, clavate,



Fig. 4. *Amanita fulvoalba* (Henkel 10395, type). Scale bar = 1 cm.

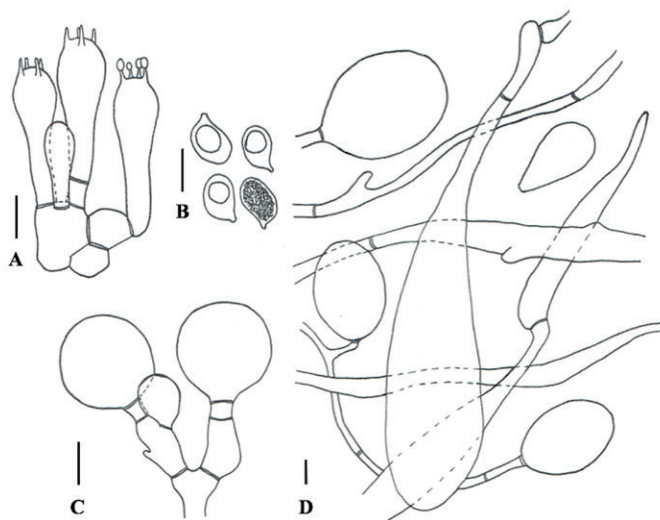


Fig. 5. *Amanita fulvoalba*. A. Basidia and subhymenium. B. Basidiospores. C. Marginal tissue of lamellae. D. Slightly crushed tissue from volval limb. Scale bars = 10 μ m.

ovoid, or ellipsoid; uninflated, non-conductive tramal hyphae 3–12 μ m wide; conductive hyphae rare, up to 25 μ m wide. *Volva at stipe base* composed of densely interwoven, uninflated, highly branched hyphae 2–10 μ m wide, and abundant inflated cells, these 24–154 \times 10–75 μ m, limoniform, clavate, globose, or ellipsoid; contents often with granular clusters; inner layer partly gelatinised. *Partial veil* composed of spherical or rarely limoniform, ellipsoid, or subclavate elements, these 8–45 μ m wide, with one or rarely two protruding lateral bulges that occasionally extend into short filaments; uninflated hyphae 2–8 μ m wide, thin-walled, attached to inflated cells or in short, detached fragments; all elements diffuse granular or with granular clusters. *Clamp connections* absent on hyphae of all tissues.

Habit, habitat, and distribution: Solitary or rarely in pairs on humic mat of forest floor under *D. corymbosa*; known only from the type locality in the Upper Potaro River Basin.

Typus: Guyana, Region 8 Potato-Siparuni, Pakaraima Mountains, Upper Potaro River Basin, ~15 km east of Mt. Ayanganna, Potaro

base camp located at 5°18'04.8"N 59°54'40.4"W, 710–750 m, 1 km SW of base camp, on root mat in *Dicymbe corymbosa* monodominant forest, 29 Dec. 2016, Henkel 10395 (holotype BRG 41307; isotype HSC G1235); GenBank accessions: ITS MK064190; nrLSU MK105497; *rpb2* MK092926; *ef1- α* MK092942.

Additional specimens examined: Guyana, Region 8 Potato-Siparuni, Pakaraima Mountains, Upper Potaro River Basin, ~15 km east of Mt. Ayanganna, Potaro base camp at 5°18'04.8"N 59°54'40.4"W, 710–750 m a.s.l., under *D. corymbosa*; vicinity of base camp, 7 May 2001, Henkel 8056 (BRG 41308, HSC G1236); 3 km SE of base camp, 10 Jun. 2002, Henkel 8455 (BRG 41309, HSC G1237); 28 Jun. 2004, Henkel 8720 (BRG 41310, HSC G1238); 1.5 km SE of base camp, 30 Jun. 2006, Henkel 8863 (BRG 43311, HSC G1239); 2 km SE of base camp, 13 July 2009, Henkel 9043 (BRG 41312, HSC G1240); 1 km SW of base camp, 25 Jun. 2016, Aime 6290 (BRG 41313, PUL F24397); 28 Dec. 2016, Henkel 10394 (BRG 41314, HSC G1241).

Notes: *Amanita fulvoalba* is recognised in the field by its medium to large, solitary or paired basidiomata, glabrous yellowish brown pileus often bearing fugacious marginal appendiculae, white hymenophore, stipe, and veils, fugacious-membranous annulus, and robust, saccate-limbate volva. *Amanita fulvoalba* is best placed in sect. *Lepidella* due to its amyloid, subglobose to broadly ellipsoid basidiospores, basal bulb, limbate volva, pileal appendiculae, and lamellae that do not darken with desiccation (Corner & Bas 1962, Bas 1969). Several features of *A. fulvoalba*, however, suggest an affinity for sect. *Amidella*, including the saccate volva, friable partial veil, and marginal appendiculae. However, given the gelatinised inner volva layer of *A. fulvoalba*, its marginal appendiculae are likely remains of the friable partial veil, not of the universal veil as in members of sect. *Amidella*. Additionally, the phylogenetic analysis shows that *A. fulvoalba* is nested within sect. *Lepidella* (Fig. 1).

Among the very few described *Amanita* species worldwide that resemble *A. fulvoalba*, the sympatric *A. aurantiobrunnea* is most similar in pileus color, its white stipe, delicate membranous annulus, saccate, two-layered volva, and similar basidiospore dimensions (Simmons *et al.* 2002). *Amanita aurantiobrunnea* can be separated from *A. fulvoalba* by its deeper orange (vs. yellowish brown) pileus and orange, friable (vs. gelatinised) inner volva layer.

The European *Amanita proxima* has a saccate volva, basal bulb, and similar basidioma dimensions as *A. fulvoalba*. However, the former has an ochraceous to reddish brown volva, whitish to ivory pileus, and a more persistent annulus than *A. fulvoalba*. *Amanita gayana*, a species known only from the description from Chile, loosely resembles *A. fulvoalba* in its orange pileus, limbate, membranous volva, and white stipe. The species is, however, much smaller than *A. fulvoalba*, with a pileus < 54 mm wide and a stipe < 13.5 mm tall, and has pale yellow as opposed to white lamellae (Tulloss & Yang 2018).

Amanita guyanensis Mighell & T.W. Henkel, *sp. nov.* MycoBank MB827396. Figs 6, 7.

Etymology: Guyana, and *-ensis* (L. adj. B), referring to the known distribution of the species across central Guyana.

Diagnosis: Similar to *A. brunnescens* but differs in its smaller, uncleft basal bulb.

Description: *Pileus* 10–94 mm broad, 4–34 mm tall, broadly convex, with age upturned, dark grey-brown or greyish brown (6F2, 7F4) throughout or darker over disc; surface dry to subviscid, glabrous macroscopically, under hand lens minutely appressed radially fibrillose, finely felted over disc; marginal fibrils separating with age revealing pale brown ground; margin entire, splitting slightly with age; volval warts with uniform, occasionally concentric arrangement, flattened to pyramidal, 1–10 mm wide, up to 1 mm tall, light grey-brown (6E3–6F3) with lighter concolourous to nearly off-white (4A1–4A2) apices, detersile; trama 0.5 mm at margin, 2 mm over lamellae, 3 mm over stipe, solid, white, unchanging. *Lamellae* finely adnexed to subfree, thin, close to crowded, white, becoming greyish or slightly orange-tinted (5C3–5C4) with age; edges concolourous, finely roughened, unchanging or browning slightly with pressure; lamellulae 1–2, 2–5 mm long. *Stipe* 35–105 × 5–14 mm, equal to slightly tapering upward from basal bulb, flaring slightly at extreme apex to 8–22 mm; apical portion above annulus usually white, occasionally grey (6D3–6D4), subscabrous; lower portion with greyish brown (6F4) appressed fibrils over white ground, these more concentrated toward base; bulb 8–20 × 11–30 mm, subglobose, subabrupt and occasionally flattened at apex, angled slightly from stipe axis, greyish over apex, lower portion progressively lighter concolourous and finely tomentose; volva of light grey-brown matted fibrillose to floccose scales adhering to bulb apex; trama white, subsolid, unchanging. *Annulus* subsuperior, 20–30 mm below stipe apex, membranous, pendant; interior white to off-white; exterior whitish marginally, grey near stipe; extreme margin an eroded band of grey, fine, floccose scales. *Odour* minimal, fungoid. *Taste* slightly sweet, occasionally with bitter overtones. *Basidiospores* white in medium deposit, [225/9/9] 5.0–9.0(–11.0) × (4.0–)5.0–9.0(–10.0) μm, Qr = (0.94–)1.0–1.27(–1.33), Qm = 1.09, subglobose to globose, thin-walled, smooth, hyaline, amyloid; hilar appendix subpyramidal, truncate, up to 1 mm long; contents usually one dark brown guttule, rarely of smaller guttules or granules. *Basidia* 22–38 × 5.5–13 μm, clavate, 4-sterigmate; contents granular or guttulate, sometimes both; sterigmata 2–5 μm long, lanceolate to slightly incurved. *Subhymenium* 16–30 μm thick, composed of 3–4 layers of subglobose to irregularly polygonal elements, these 3–19 μm wide. *Marginal tissue of lamellae* partially gelatinised, composed of easily dislodged, mostly globose, occasionally ellipsoid, fusiform or clavate elements, these 9–65 × 8–22 μm. *Lamellar trama* bilateral; mediostratum 20–40 μm wide, of interwoven, branching hyphae; inflated elements up to 17 μm wide, cylindrical or clavate; lateral stratum contiguous with mediostratum and diverging at an obtuse angle; hyphae 4–19 μm wide; conductive hyphae rare. *Volval pileal warts* composed of inflated, brownish globose cells often with a small, protruding filament. *Pileipellis* an ixtomixtocutis, two-layered with indistinct boundary; suprapellis 140–240 μm thick, hyphae heavily gelatinised, thin-walled, densely interwoven; subpellis 140–250 μm thick, hyphae brownish, densely interwoven, periclinal. *Pileus trama* with frequent acrophysalides, these cylindrical, fusiform, ellipsoid, or ovoid, 22–190 × 8–50 μm; uninflated tramal hyphae densely interwoven, highly branching, 2–6 μm; conductive hyphae not observed; contents of most elements of small (≤ 1 μm), globose, hyaline guttules and/or opaque granules, often in clusters. *Stipe trama* longitudinally oriented, with clavate or occasionally subglobose to fusiform acrophysalides, these 32–315 × 17–58 μm; uninflated hyphae highly branched, 2–6 μm wide; conductive hyphae not observed.

Volva at stipe base composed mostly of inflated, globose or rarely ellipsoid to limoniform elements, 22–49 μm wide; filamentous hyphae sparse, present as branched fragments or attached to inflated elements. *Partial veil* composed of densely interwoven, branching, highly serpentine uninflated hyphae 1–7 μm wide, most with opaque granular contents. *Clamp connections* absent on hyphae of all tissues.

Habit, habitat, and distribution: Solitary to scattered on humic mat of forest floor under *D. corymbosa*; also found in stands containing *D. corymbosa* and *D. altsonii* or *Pakaraimaea dipterocarpacea* and *Dicymbe jenmanii* on a variety of soil types; known from the type locality in the Upper Potaro River Basin, ~25 km to the west in the Upper Mazaruni Basin, and ~100 km east in the Mabura Ecological Reserve.

Typus: **Guyana**, Region 8 Potato-Siparuni, Pakaraima Mountains, Upper Potaro River Basin, ~20 km east of Mt. Ayanganna, Tadang base camp 2 km south of Potaro River at 5°16'14.5"N 59°50'39.1"W, elevation 710–750 m; 0.3 km NE of base camp in *Dicymbe corymbosa* and *Dicymbe altsonii* co-dominant forest, 7 Jun. 2013, *Henkel 9767* (**holotype** BRG 41315; **isotype** HSC); GenBank accessions: ITS MK064192; nrLSU MK105502; *rpb2* MK092929; *ef1-α* MK092948; *β-tub* MK092937.

Additional specimens examined: **Guyana**, Region 8 Potato-Siparuni, Pakaraima Mountains, Upper Potaro River Basin, ~15 km east of Mt. Ayanganna, Potaro base camp at 5°18'04.8"N 59°54'40.4"W, 710–750 m a.s.l., under *D. corymbosa*; 4 km SW of base camp, 5 May 2001, *Henkel 8034* (BRG 41316, HSC G1244); 3 km SE of base camp, 11 May 2001, *Henkel 8083* (BRG 41317, HSC G1245); 28 Jun. 2004, *Henkel 8712* (BRG 41318, HSC G1246); 0.4 km SW of base camp near Blackwater Creek, 1 Jul. 2006, *Aime 3155* (BRG 41319, PUL F24398); vicinity of base camp, 11 Jul. 2008, *Henkel 8931* (BRG 41320, HSC G1243); 4 km SW of base camp, 20 May 2010, *Aime 3991* (BRG 41321, PUL F24399); 0.5 km E of base camp, 15 Jun. 2015, *Henkel 10081* (BRG 41322, HSC G1247). ~20 km east of Mt. Ayanganna, Tadang Base Camp 2 km south of Potaro River at 5°16'14.5"N 59°50'39.1"W, 710–750 m a.s.l., under *D. corymbosa* and *D. altsonii*; 2 km SW of base camp, 8 Jun. 2013, *Henkel 9772* (BRG 41323, HSC G1248). Region 10 Upper Demerara-Berbice, Mabura Ecological Reserve, field station at 5°09'19.0"N 58°41'58.9"W, ~100 m a.s.l.; 0.4 km WNW of field station in *Dicymbe altsonii* plot #1, 1 Jun. 2011, *Henkel 9624* (BRG 41324, HSC G1249). Region 7 Cuyuni-Mazaruni, Pakaraima Mountains. Mazaruni River Basin, ~20 km NW of Mt. Ayanganna summit, base camp located at 5°26'21.3"N 60°04'43.1"W, 760 m a.s.l., in savanna fringing forest dominated by *P. dipterocarpacea* and *D. jenmanii*; ~0.4 km NW of base camp, 28 Dec. 2010, *Henkel 9563* (BRG 41325, HSC G1250); 0.2 km ESE of base camp, 4 Jun. 2012, *Henkel 9674* (BRG 41326, HSC G1251).

Notes: *Amanita guyanensis* is recognised in the field by its dark grey-brown pileus bearing off-white to greyish volval patches, white stipe, subglobose, angled basal bulb with a apical ring of grey floccose scales, and white, pendant annulus with a grey margin. *Amanita guyanensis* is best placed in sect. *Validae* due its amyloid, subglobose to globose basidiospores, deeply pigmented pileus, pulverulent volva, and the absence of marginal appendiculae (Corner & Bas 1962, Bas 1969, Cui *et al.* 2018). Additionally, the phylogenetic analysis shows that *A. guyanensis* is allied with other species in a monophyletic sect. *Validae*, including the type species of the section, *A. excelsa* (Fig. 1).



Fig. 6. *Amanita guyanensis* (Henkel 9767, type). Scale bar = 1 cm.

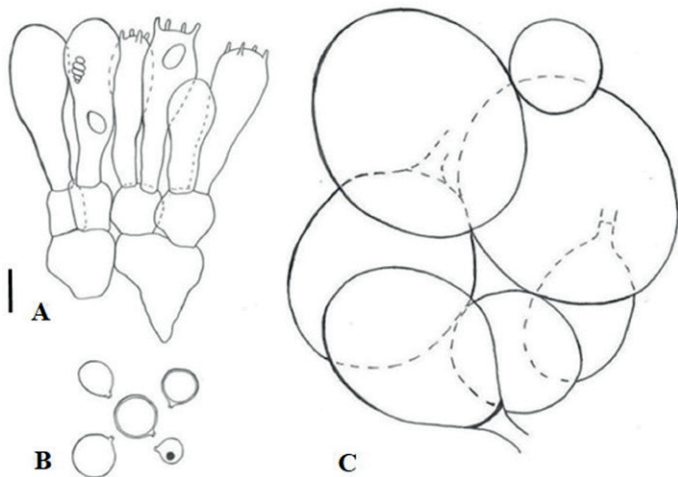


Fig. 7. *Amanita guyanensis*. A. Basidia and subhymenium. B. Basidiospores. C. Slightly crushed tissue of volval wart on pileus. Scale bars = 10 μ m.

Worldwide there are numerous species of sect. *Validae* which resemble *A. guyanensis* in stature and colour. In the Neotropics, *A. campinaranae* from the central Amazon closely resembles *A. guyanensis* in stature, pigmentation, and velar characteristics. However *A. campinaranae* differs from *A. guyanensis* in its pallid, white to greyish pileus, forked lamellae, and smaller basidiospores (5.6–6.7 \times 5.5–6.5 μ m vs. 5–9 \times 5–9 μ m) (Bas 1978). The sympatric and loosely similar *A. perphaea* can be separated by its more fragile partial veil, sulcate-striate pileus margin, distinct encrusting pigments in the pileipellis, and overall darker grey colour of the pileus, volva, and stipe (Simmons *et al.* 2002).

Among tropical African *Amanita* species *A. echinulata* is similar to *A. guyanensis* in stature and both may have a bitter taste, but *A. echinulata* can be separated by its grey annulus, dark sooty brown pileus and stipe, and smaller basidiospores (Beeli 1935; Mighell & Henkel pers. obs.). An as yet undescribed species (*Amanita* morphospecies #19) collected in Cameroon's Dja Biosphere Reserve is macroscopically very similar to *A. guyanensis* (Mighell & Henkel unpubl. data). This species exhibits similar basidioma size ranges, pigmentation, and velar

characteristics as those of *A. guyanensis*, but differs by its less defined volval remnants on the stipe and odour of raw potato.

Amanita innatifibrilla from subtropical China has a dark grey-brown pileus bearing concolorous to grey warts and floccose volval remnants at its bulb apex, but differs from *A. guyanensis* in its smaller stature, innate pileal fibrils, regularly central annulus, fusiform bulb, and smaller basidiospores (Cui *et al.* 2018). Species from Singapore described by Corner & Bas (1962) include *A. squamosa* which resembles *A. guyanensis* in its sepia-fuscos pileus, pale brownish warts, and white annulus, but differs in its spindle-shaped bulb with recurved scales and smaller basidiospores. *Amanita tristis* is similar in basidioma size, colours, and volval remnants to *A. guyanensis*, but its ellipsoid basidiospores are smaller (4.9–6.1 \times 4.3–4.6 μ m vs. 5–9 \times 5–9 μ m) than the subglobose to globose spores of *A. guyanensis*.

Among north temperate species similar to *A. guyanensis*, *A. brunnescens* and *A. sepiacea* each have similarly sized basidiomata, a dark grey to brown pileus, white, superior annulus, basal bulb with apically adhering volval remnants, and basidiospores of similar size. *Amanita brunnescens* is separated by its large, marginate, clefted basal bulb, as opposed to the smaller, unclefted bulb of *A. guyanensis*. *Amanita sepiacea* has grey squamules on the stipe base, which contrast with the longitudinal fibrils of *A. guyanensis* (Tulloss & Yang 2018). *Amanita porphyria* and *A. submaculata* loosely resemble *A. guyanensis*, but the former is differentiated by its violaceous pileus and volva, and the latter by its reddening of bruised lamella and exposed stipe trama.

Finally, *A. xanthomargaros*, *A. pausiaca*, *A. walpolei*, *A. luteolovelata*, and *A. luteofusca* all have a grey to brown pileus and similar basidioma size, but can be differentiated from *A. guyanensis* by their yellow pigments in either the universal veil, annulus, or stipe tissues.

ACKNOWLEDGEMENTS

We thank the following funding sources: National Science Foundation (NSF) DEB-0918591, DEB-1556338, National Geographic Society's Committee for Research and Exploration grants 6679-99, 7435-03 and 8481-08 to T.W.H., and NSF DEB-0732968 to M.C.A. Field assistance in Guyana was provided by M. Chin, P. Henkel, D. Husbands, J. Uehling, C. Andrew, V. Joseph, P. Joseph, F. Edmund, and L. Edmund. Research permits were granted by the Guyana Environmental Protection Agency. This paper is number 229 in the Smithsonian Institution's Biological Diversity of the Guiana Shield Program publication series.

REFERENCES

- Bas C (1969). Morphology and subdivision of *Amanita* and a monograph of its section *Lepidella*. *Persoonia* **5**: 285–573.
- Bas C (1978). Studies in *Amanita* - I: some species from Amazonia. *Persoonia* **10**: 1–22.
- Bas C, de Meijer AAR (1993). *Amanita grillipes*, a new species of *Amanita* subsection *Vittadiniae* from Southern Brazil. *Persoonia* **15**: 345–350.
- Beeli M (1935). *Flore iconographique des champignons du Congo*. Fascicle I. *Amanita*, *Amanitopsis*, *Volvaria*. Jardin botanique de l'Etat, Belgium.
- Cai Q, Tulloss RE, Tang LP, *et al.* (2014). Multi-locus phylogeny of lethal amanitas: Implications for species diversity and historical biogeography. *BMC Evolutionary Biology* **14**: 143.

- Corner EJH, Bas C (1962). The genus *Amanita* in Singapore and Malaya. *Persoonia* **2**: 241–304.
- Cui YY, Cai Q, Tang LP, *et al.* (2018). The family *Amanitaceae*: molecular phylogeny, higher-rank taxonomy and the species in China. *Fungal Diversity* **91**: 5–230.
- Drehmel D, Moncalvo JM, Vilgalys, R (1999). Molecular phylogeny of *Amanita* based on large-subunit ribosomal DNA sequences: implications for taxonomy and character evolution. *Mycologia* **91**: 610–618.
- Ebenye MCH, Taudière A, Niang N, *et al.* (2017). Ectomycorrhizal fungi are shared between seedlings and adults in a monodominant *Gilbertiodendron dewevrei* rain forest in Cameroon. *Biotropica* **49**: 256–267.
- Edgar RC (2004). MUSCLE: a multiple sequence alignment method with reduced time and space complexity. *BMC Bioinformatics* **5**: 113.
- Gardes M, Bruns TD (1993). ITS primers with enhanced specificity for basidiomycetes - application to the identification of mycorrhizae and rusts. *Molecular Ecology* **2**: 113–118.
- Geml J, Laursen GA, O'Neill K, *et al.* (2006). Beringian origins and cryptic speciation events in the fly agaric (*Amanita muscaria*). *Molecular Ecology* **15**: 225–239.
- Halling RE (2001). Ectomycorrhizae: co-evolution, significance, and biogeography. *Annals of the Missouri Botanical Garden* **88**: 5–13.
- Henkel TW, Aime MC, Chin MML, *et al.* (2012). Ectomycorrhizal fungal sporocarp diversity and discovery of new taxa in *Dicymbe* monodominant forests of the Guiana Shield. *Biodiversity and Conservation* **21**: 2195–2220.
- Kim CS, Jo JW, Kwag Y-N, *et al.* (2013). Taxonomic study of *Amanita* subgenus *Lepidella* and three unrecorded *Amanita* species in Korea. *Mycobiology* **41**: 183–190.
- Kornerup A, Wanscher JH (1978). *Methuen handbook of colour*. 3rd edn. Eyre Methuen, London.
- Kumar S, Stecher G, Tamura K (2016). MEGA7: Molecular evolutionary genetics analysis version 7.0 for bigger datasets. *Molecular Biology and Evolution* **33**: 1870–1874.
- Lanfear R, Calcott B, Ho SY, *et al.* (2012). PartitionFinder: Combined selection of partitioning schemes and substitution models for phylogenetic analysis. *Molecular Biology and Evolution* **29**: 1695–1701.
- Lechner BE, Alberto E (2008). Poisonous species of *Agaricales* found in Argentina: new record of *Amanita pantherina* and reevaluation of the edibility of *Tricholoma equestre*. *Boletín de la Sociedad Argentina de Botánica* **43**: 227–35.
- Menolli N, Capelari M, Baseia IG (2009). *Amanita viscidolutea*, a new species from Brazil with a key to Central and South American species of *Amanita* section *Amanita*. *Mycologia* **101**: 395–400.
- Moncalvo J-M, Drehmel D, Vilgalys R (2000a). Variation in modes and rates of evolution in nuclear and mitochondrial ribosomal DNA in the mushroom genus *Amanita* (*Agaricales*, *Basidiomycota*): phylogenetic implications. *Molecular Phylogenetics and Evolution* **16**: 48–63.
- Moncalvo J-M, Lutzoni FM, Rehner SA, *et al.* (2000b). Phylogenetic relationships of agaric fungi based on nuclear large subunit ribosomal DNA sequences. *Systematic Biology* **49**: 278–305.
- Moser M (1967). *Die Röhrlinge und Blätterpilze (Agaricales)*. Gustav Fischer Verlag, Germany.
- Mueller GM, Halling RE (1995). Evidence for high biodiversity of *Agaricales* (*Fungi*) in Neotropical montane *Quercus* forests. In: *Biodiversity and conservation of neotropical montane forests* (Churchill S, ed). The New York Botanical Garden, USA: 303–312.
- Palacio M, Gutierrez Y, Franco-Molano AE, *et al.* (2015). New records of macrofungi (*Basidiomycota*) for Colombia from a tropical dry forest. *Actualidades Biológicas* **37**: 79–99.
- Rehner SA, Buckley E (2005). A *Beauveria* phylogeny inferred from nuclear ITS and EF1- α sequences: evidence for cryptic diversification and links to *Cordyceps* teleomorphs. *Mycologia* **97**: 84–98.
- Ronquist F, Teslenko M, van der Mark P, *et al.* (2012). MrBayes 3.2: Efficient Bayesian phylogenetic inference and model choice across a large model space. *Systematic Biology* **61**: 539–542.
- Schoch CL, Seifert KA, Huhndorf S, *et al.* (2012). Nuclear ribosomal internal transcribed spacer (ITS) region as a universal DNA barcode marker for *Fungi*. *Proceedings of the National Academy of Sciences, USA* **109**: 6241–6246.
- Simmons C, Henkel T, Bas C (2002). The genus *Amanita* in the Pakaraima Mountains of Guyana. *Persoonia* **17**: 563–582.
- Singer R (1986). *The Agaricales in modern taxonomy*. 4th edn. Koeltz Scientific Books, Germany.
- Smith ME, Henkel TW, Aime MC, *et al.* (2011). Ectomycorrhizal fungal diversity and community structure on three co-occurring leguminous canopy tree species in a Neotropical rainforest. *New Phytologist* **192**: 699–712.
- Smith ME, Henkel TW, Uehling JK, *et al.* (2013). The ectomycorrhizal fungal community in a neotropical forest dominated by the endemic Dipterocarp *Pakaraimaea dipterocarpacea*. *PLoS One* **8**: e55160.
- Sobestiansky G (2005). Contribution to a macromycete survey of the states of Rio Grande do Sul and Santa Catarina in Brazil. *Brazilian Archives of Biology and Technology* **48**: 437–57.
- Stamatakis A (2014). RAxML version 8: a tool for phylogenetic analysis and post-analysis of large phylogenies. *Bioinformatics* **30**: 1312–1313.
- Tang LP, Cai Q, Lee SS, *et al.* (2015). Taxonomy and phylogenetic position of species of *Amanita* sect. *Vaginatae* s.l. from tropical Africa. *Mycological Progress* **14**: 39–54.
- Tedersoo L, Brundrett MC (2017). Evolution of ectomycorrhizal symbiosis in plants. In: *Biogeography of mycorrhizal symbiosis* (Tedersoo L, ed). Springer, USA: 407–467.
- Thongbai B, Tulloss RE, Miller SL, *et al.* (2016). A new species and four new records of *Amanita* (*Amanitaceae*; *Basidiomycota*) from Northern Thailand. *Phytotaxa* **286**: 211–231.
- Truong C, Sánchez-Ramírez S, Kuhar F, *et al.* (2017). The Gondwanan connection – Southern temperate *Amanita* lineages and the description of the first sequestrate species from the Americas. *Fungal Biology* **121**: 638–51.
- Tulloss RE, Ovrebo CL, Halling RE (1992). Studies on *Amanita* (*Amanitaceae*) from Andean Colombia. *Memoirs of the New York Botanical Garden* **66**: 1–46.
- Tulloss RE, Halling RE (1997). Type studies of *Amanita morenoi* and *Amanita pseudospretta* and a reinterpretation of crassosporae in *Amanita*. *Mycologia* **89**: 278–288.
- Tulloss RE (2005). *Amanita* - distribution in the Americas with comparison to eastern and southern Asia and notes on spore character variation with latitude and ecology. *Mycotaxon* **93**: 189–231.
- Tulloss RE, Franco-Molano AE (2008). Studies in *Amanita* subsection *Vittadiniae* 1 – A new species from Colombian savanna. *Mycotaxon* **105**: 317–323.
- Tulloss RE, Yang ZL (2018). Subgenus *Lepidella* in *Amanitaceae* studies. [<http://www.amanitaceae.org/?subgenus%20Lepidella>], accessed 12 April 2018.
- Vargas N, Pardo-de La Hoz CJ, Danies G, *et al.* (2017). Defining the phylogenetic position of *Amanita* species from Andean Colombia. *Mycologia* **109**: 261–76.
- Vilgalys R, Hester M (1990). Rapid genetic identification and mapping of enzymatically amplified ribosomal DNA from several *Cryptococcus* species. *Journal of Bacteriology* **172**: 4238–46.
- Wartchow F (2015). *Amanita tenacipulvis*, a new species from Amazonian campinarana. *Sydowia* **67**: 75–9.

- Wartchow F (2016). *Amanita viridissima* (Amanitaceae, Basidiomycota), a striking new species from highlands of the semiarid region of Bahia, Brazil. *Plant Ecology and Evolution* **149**: 241–248.
- Wartchow F, Cortez VG (2016). A new species of *Amanita* growing under *Eucalyptus* is discovered in South Brazil. *Mycosphere* **7**: 262–267.
- Wartchow F, Gamboa-Trujillo JP (2012). *Amanita chocoana* - a new species from Ecuador. *Mycotaxon* **121**: 405–12.
- Wartchow F, Maia LC, Cavalcanti MAQ (2013). Studies on *Amanita* (Agaricomycetidae, Amanitaceae) in Brazil: two yellow gemmatoid taxa. *Nova Hedwigia* **96**: 61–71.
- Wartchow F, Sulzbacher MA, Baseia IG (2015). *Amanita psammolimbata*, a new species from Northeastern Brazilian sand dunes. *Mycosphere* **6**: 260–5.
- Wartchow F, Tulloss RE, Cavalcanti MA (2007). The discovery of *Amanita lilloi* in Brazil. *Mycotaxon* **99**: 167–174.
- Wartchow F, Tulloss R, Cavalcanti MAQ (2009). *Amanita lippiae*: a new species from the semi-arid caatinga region of Brazil. *Mycologia* **101**: 864–870.
- Watling R, Lee LS (1995). Ectomycorrhizal fungi associated with members of the Dipterocarpaceae in peninsular Malaysia. *Journal of Tropical Forest Science* **7**: 647–669.
- Weiss M, Yang ZL, Oberwinkler F (1998). Molecular phylogenetic studies in the genus *Amanita*. *Canadian Journal of Botany* **76**: 1170–1179.
- Wolfe BE, Tulloss RE, Pringle A (2012). The irreversible loss of a decomposition pathway marks the single origin of an ectomycorrhizal symbiosis. *PLoS One* **7**: e39597.
- Zagt RJ (1997). Pre-dispersal and early post-dispersal demography, and reproductive litter production, in the tropical tree *Dicymbe altsonii* in Guyana. *Journal of Tropical Ecology* **13**: 511–526.
- Zhang LF, Yang JB, Yang ZL (2004). Molecular phylogeny of eastern Asian species of *Amanita* (Agaricales, Basidiomycota): taxonomic and biogeographic implications. *Fungal Diversity* **17**: 219–238.

doi.org/10.3114/fuse.2019.03.02

Phylogeny and morphology of new species of *Globisporangium*

S. Uzuhashi^{1,*}, S. Nakagawa², H.M.A. Abdelzaher³, M. Tojo²

¹Genetic Resources Center, National Agriculture and Food Research Organization, 2-1-2 Kannondai, Tsukuba, Ibaraki 305-8602, Japan

²Graduate School of Life and Environmental Sciences, Osaka Prefecture University, Gakuen-cho 1-1, Naka-ku, Sakai, Osaka 599-8531, Japan

³Department of Botany and Microbiology, Faculty of Science, Minia University 61519, Minia city, Egypt

*Corresponding author: uzuhashi@affrc.go.jp

Key words:

Molecular phylogeny
new taxa
pond water
Pythium
re-identification

Abstract: An isolate originally obtained from pond water in Osaka in 1992 and identified as *Pythium marsipium*, was subsequently classified as *Globisporangium marsipium*. According to molecular phylogenetic analyses based on the internal transcribed spacer regions of the nuclear ribosomal RNA and mitochondrial cytochrome c oxidase subunit 1 genes, this isolate was shown to represent a new species, described here as *G. lacustre* sp. nov. In addition, two further new combinations are introduced in *Globisporangium* as *G. camurandrum* and *G. takayamanum* based on their DNA phylogeny.

Effectively published online: 28 November 2018.

INTRODUCTION

Oomycetes are fungal-like organisms belonging to the kingdom *Straminipila*. The oomycete genus *Globisporangium* was segregated from the genus *Pythium* based on morphology and phylogeny in 2010 (Uzuhashi *et al.* 2010). Traditionally, species identification of *Pythium s. lat.*, including *Globisporangium*, was based on morphological characteristics. Because the use of DNA for species identification is well established, many new species of *Pythium s. lat* have been described based on DNA sequences in addition to their morphology (e.g. Bouket *et al.* 2015, Uzuhashi *et al.* 2015, Ueta & Tojo 2016). In particular, the internal transcribed spacer (ITS) region of the nuclear ribosomal RNA gene and the cytochrome c oxidase subunit 1 gene (*cox1*) are known as useful regions for species identification, and are recognised as DNA barcode markers for oomycetes (Robideau *et al.* 2011).

Proper identification of *Globisporangium* spp. is important not only for taxonomic studies but also biological studies, because the genus is widely distributed throughout the world, and some species have highly important ecological roles or economic impacts (e.g. Zhang & Yang 2000, Múnera & Hausbeck 2016). Additionally, taxonomic evaluation of previously collected strains is also important, especially for those that have only been identified based on morphology. One strain, MAFF 236903, stored in NARO Genebank, Microorganisms Section (MAFF), Genetic Resources Center, National Agriculture and Food Research Organization, Tsukuba, Ibaraki, Japan, was obtained from pond water in Osaka, Japan, in 1992. It was initially identified as *P. marsipium*, which is now classified as *G. marsipium*, based on its morphology (Abdelzaher *et al.* 1994). We evaluated the identification of this strain using molecular phylogenetic analyses based on the ITS and *cox1* regions. The result demonstrated that this strain is uniquely different from

G. marsipium, and it is consequently redescribed here as *Globisporangium lacustre* sp. nov. We also provide updated temperature growth profiles and phylogenetic information for this new species. Furthermore, two new combinations in *Globisporangium* are introduced based on the molecular phylogenetic analyses generated here.

MATERIALS AND METHODS

Isolates and morphology

Strain MAFF 236903 and the reference strain of *G. marsipium* (CBS 773.81) were examined. Colony patterns of the two strains were recorded on potato carrot agar plates (PCA) prepared in accordance with van der Plaats-Niterink (1981), potato dextrose agar (PDA), and V8 juice agar (V8A) plates according to Miller (1995) after incubation for 8 d at 25 °C. Morphological characteristics were examined in a grass blade water culture (van der Plaats-Niterink 1981). At least 30 measurements were taken of each structure. Hyphal growth rate was also determined on PCA, as reported previously (Uzuhashi *et al.* 2017). The isolates were incubated on PCA at 3 °C intervals from 0–40 °C for 1–3 d. Hyphal growth was evaluated by measuring the average increase in colony diameter. The experiment had two replicates and was repeated twice.

DNA extraction and phylogenetic analysis

DNA extraction from the strain was performed as reported previously (Uzuhashi *et al.* 2017). The ITS and *cox1* regions were amplified using the primer-pair ITS5/ITS4 (White *et al.* 1990) for ITS and OomCox1-Levup/OomCox1-Levlo (Robideau *et al.* 2011) for *cox1*. Amplification reactions and sequencing were conducted as reported previously (Uzuhashi *et al.* 2017).

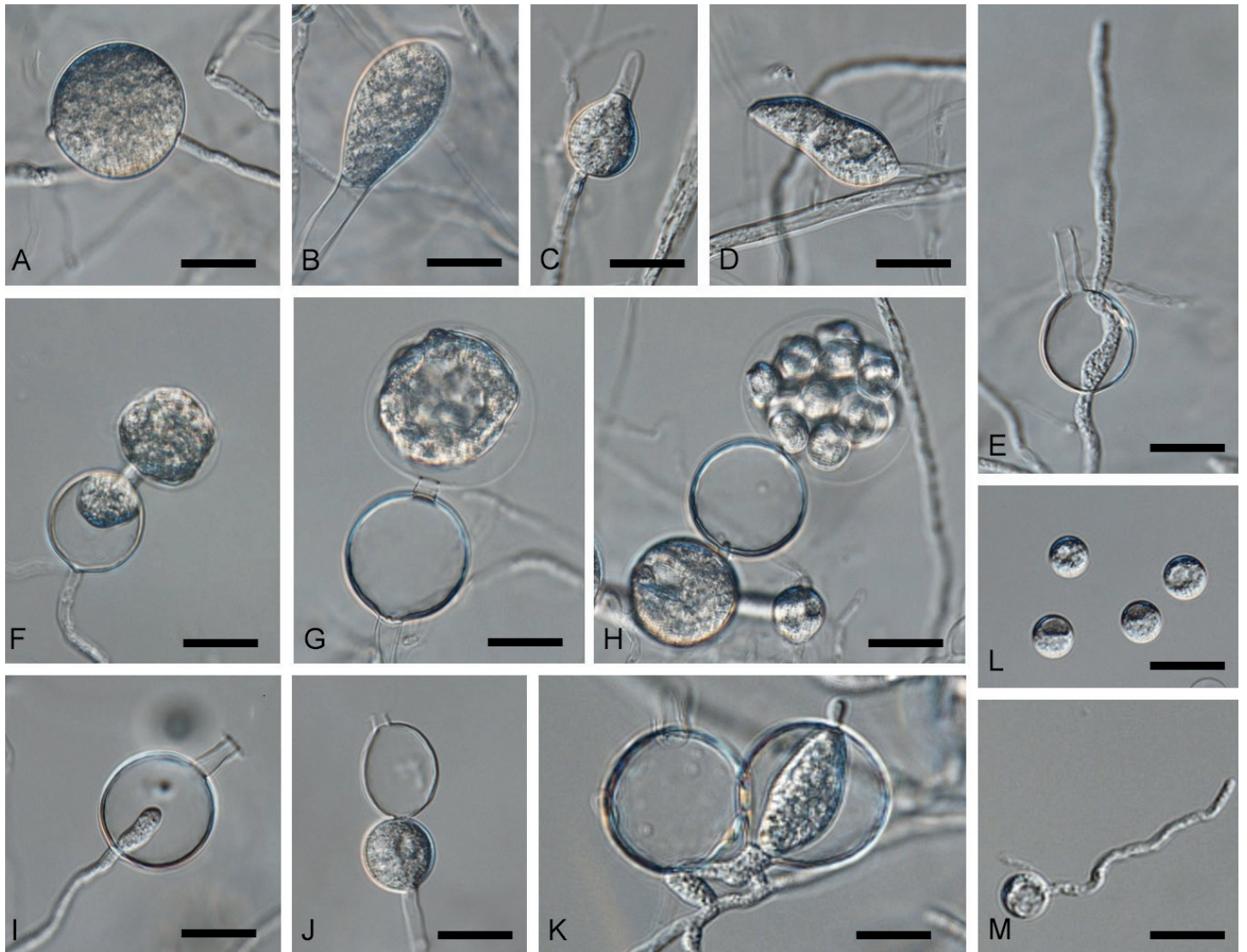


Fig. 1. Morphology of *Globisporangium lacustre*. **A–D.** Sporangia. **E.** Internally proliferation. **F.** Early stage of vesicle formation. **G, H.** Vesicle with zoospore development inside. **I.** Internal proliferation. **J.** Sporangium and empty sporangium. **K.** Empty sporangium and internal proliferation. **L.** Encysted zoospores. **M.** Germinated encysted zoospore. Scale bars = 20 μm .

The sequences of the two regions were aligned separately with relevant *Globisporangium* sequences obtained from the GenBank database using the ClustalW program included in MEGA7 (Kumar *et al.* 2016). Because *G. marsipium* is known to be located in clade E described by Lévesque & de Cock (2004) (e.g. Lévesque & de Cock 2004, Uzuhashi *et al.* 2010), sequence data of *Globisporangium* species in clade E were included for phylogenetic analyses as well as *G. splendens* and *G. intermedium* as outgroups. All alignments were submitted to TreeBASE under accession number 20573. Phylogenetic analyses based on these regions were conducted using MEGA7 with the Neighbour-Joining (NJ) and Maximum Likelihood (ML) phylogenetic methods, as reported previously (Uzuhashi *et al.* 2017). All of the positions containing gaps and missing data were eliminated. The strength of the internal branches in the trees obtained were tested by bootstrap analysis using 1 000 replications. The sequences of MAFF 236903 were deposited in DDBJ under the accession numbers LC209786 for ITS and LC209787 for *cox1*.

RESULTS

Morphology and hyphal growth

Morphological characteristics of MAFF 236903 have been described in detail previously (Abdelzaher *et al.* 1994). In this study, sexual structures such as oogonia, antheridia, and oospores were not formed in any artificial cultures, although sporangia and zoospores were abundantly produced in water culture (Fig. 1). Additionally, reference strain *G. marsipium* CBS 773.81 formed no spores in water culture as well as agar cultures. The morphological characteristics of MAFF 236903 were quite similar to those of *G. marsipium* (Table 1). The main difference was the production of yellowish oospores by MAFF 236903. Additionally, MAFF 236903 produced slightly larger oogonia and oospores and greater numbers of antheridia (Table 1).

The colony patterns of MAFF 236903 were different from those of *G. marsipium* CBS 773.81 on all three agar plates, especially on PCA and PDA (Fig. 2). Colonies of MAFF 236903 were submerged with a chrysanthemum pattern on PCA and coarse rosette pattern with aerial mycelium on PDA, but no specific pattern on V8A. On the other hand, CBS 773.81 showed

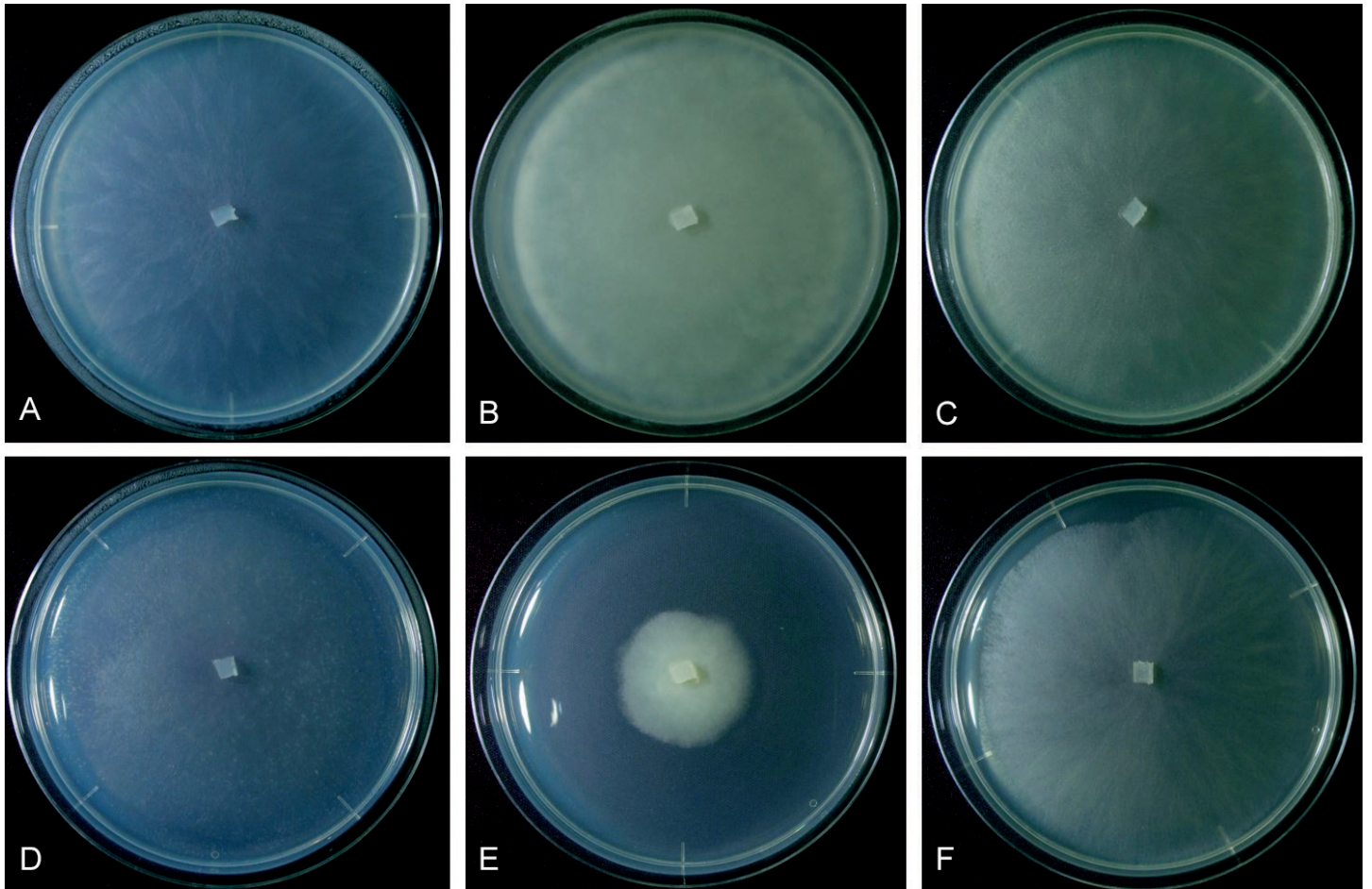


Fig. 2. Colony patterns of MAFF 236903 (*Globisporangium lacustre*) (A–C) and CBS 773.81 (*G. marsipium*) (D–F) at 25 °C on PCA (A, D), PDA (B, E), and V8A (C, F).

no specific patterns on any agar plates (Fig. 2D–F). The hyphal growth rate of MAFF 236903 determined in this study was completely different from that of CBS 773.81. In this study, MAFF 236903 grew at 10–37 °C with an optimum temperature of 31 °C. On the other hand, CBS 773.81 could be grown at 16–31 °C, also with an optimum temperature at 31 °C. Additionally, the radial growth rate of MAFF 236903 on PCA at 25 °C was 25 mm in this study, but just 5 mm in CBS 773.81 (Fig. 3).

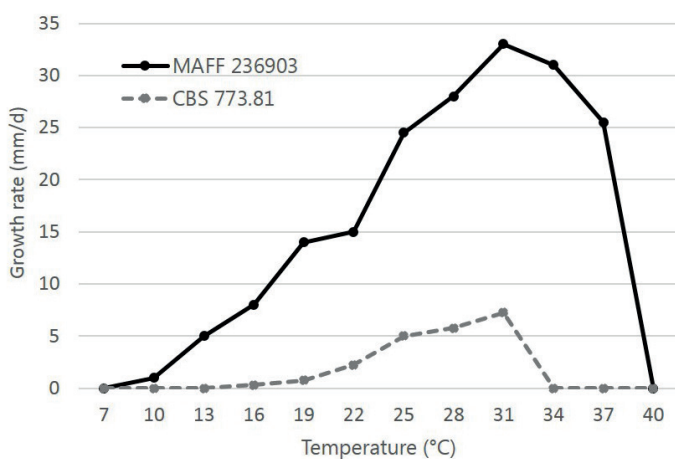


Fig. 3. Effect of temperature on the growth rate of MAFF 236903 (*Globisporangium lacustre*) and CBS 773.81 (*G. marsipium*) on PCA.

Sequencing and phylogeny

The ITS and *cox1* sequences of MAFF 236903 had 85 % and 93 % similarities with those of *G. marsipium* CBS 773.81, respectively. For both the ITS or *cox1* regions tree topologies obtained through NJ and ML analyses were similar. In phylogenetic analyses based on these two regions, MAFF 236903 was located in a sister-group position to the clade of *G. marsipium* in both trees (Figs 4, 5).

TAXONOMY

Globisporangium lacustre Uzuhashi & Tojo, *sp. nov.* MycoBank MB819698. Figs 1, 2.

Etymology: lacustre refers to the origin (pond water) of the isolate.

Colonies submerged, forming a rosette pattern on PDA, submerged, with a radiate pattern on potato-carrot agar (PCA). Daily growth at 25 °C on PCA 25 mm. *Cardinal temperatures* minimum 10 °C, optimum 31 °C, maximum 37 °C. *Main hyphae* up to 7 μm wide. *Appressoria* club-shaped. *Sporangia* terminal, occasionally intercalary, subspherical, pyriform, irregular longitudinal or often unsymmetrically utriform, papillate. Subspherical, 20–70 μm diam, pear-shaped, 16–25 × 10–15 μm diam, utriform 25–68 × 20–45 μm, internally proliferating. *Encysted zoospores*, 9–12 μm diam. *Oogonia* produced in single culture, globose, smooth-

Table 1. Morphology and hyphal growth temperature of *Globisporangium marsipium* and MAFF 236903.

	<i>G. marsipium</i> ¹	MAFF 236903 ²
Cardinal temperature for hyphal growth (°C)	16–31	10–37
Daily growth at 25 °C on PCA (mm)	5	25
Width of hyphae (µm)	Up to 7.5	Up to 7
Sporangium (Sp) production	Globose or asymmetrically utriform, papillate, beaked, often bent, transversely attached on hypha branches	Subspherical, pyriform, irregular longitudinal, often unsymmetrically utriform, papillate
Diameter of Sp (µm)	20–100 × 3–4 (terminal) 25–70 (intercalary)	20–70 (subspherical) 16–25 × 10–15 (pear-shaped) 25–68 × 20–45 (utriform)
Position of Sp	Mostly terminal, occasionally intercalary	Terminal, occasionally intercalary
Zoospore production	Produced	Produced
Oogonium diameter (µm)	(23–)27–36(–39) (av. 31)	26–39 (av. 33)
Position of oogonia	Mostly intercalary, occasionally catenulate, sometimes subterminal	Terminal or subterminal, mostly intercalary, occasionally catenulate
Oogonium ornamentation	Smooth	Smooth
Oospore diameter (µm)	(19–)23–31(–33) (av. 26)	20–35 (av. 28)
Oospore wall thickness (µm)	Up to 2.8	1.5–2.5
Plerotic or aplerotic oospores	Aplerotic	Aplerotic, usually yellowish
Number of oospores/oogonia	1	1
Number of antheridia/oogonia	1–4	1–8
Monoclinous or diclinous antheridium	Diclinous	Diclinous
Antheridia	10–20 × 8–12, making broad apical contact with the oogonium	10–27 × 8–12, apical contact with the oogonium, often persisting after fertilization

¹ van der Plaats-Niterink (1981) except for cardinal temperature for hyphal growth and daily growth at 25 °C on PCA obtained from this study.

² Abdelzاهر *et al.* (1994) except for cardinal temperature for hyphal growth and daily growth at 25 °C on PCA obtained from this study.

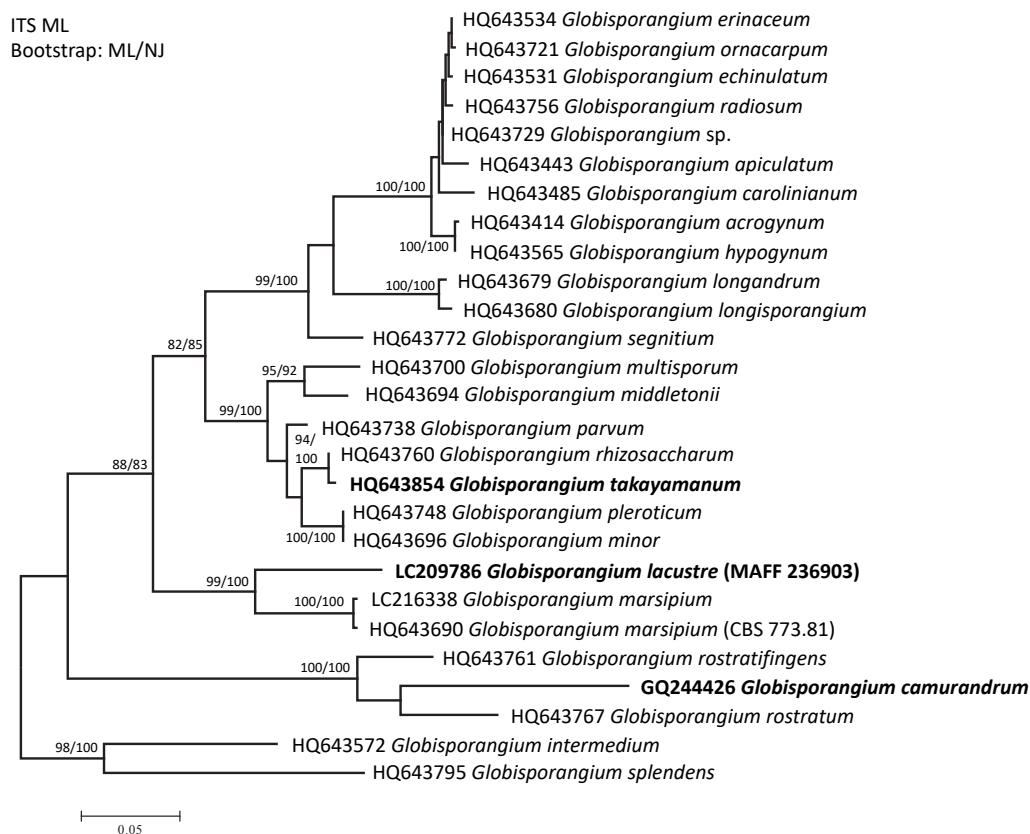


Fig. 4. Maximum Likelihood (ML) tree based on ITS sequences showing the relationship between MAFF 236903 (*Globisporangium lacustre*) and other species in clade E (Lévesque & de Cock 2004). *Globisporangium intermedium* and *G. splendens* were used as outgroups. Numbers along the nodes indicate bootstrap support values above 80 % for ML/NJ, respectively.

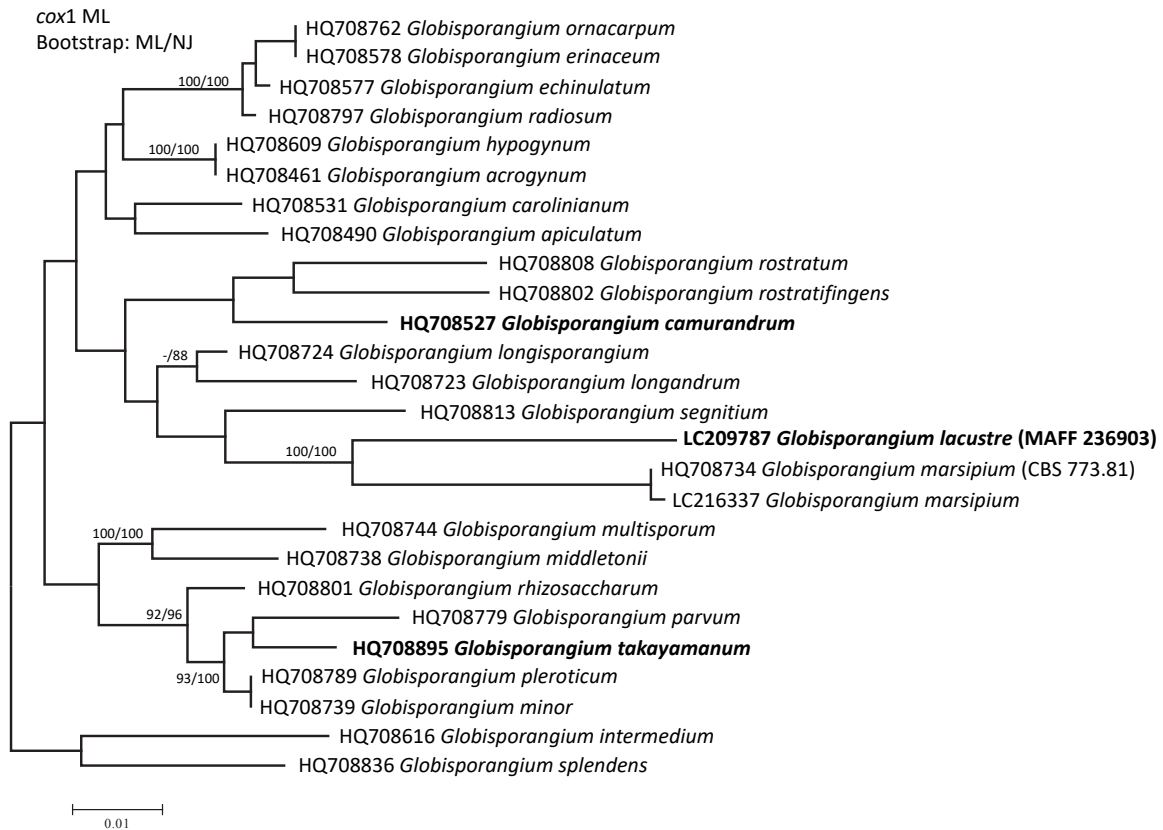


Fig. 5. Maximum Likelihood (ML) tree based on *cox1* sequences showing the relationship between MAFF 236903 (*Globisporangium lacustre*) and other species in clade E (Lévesque & de Cock 2004). *Globisporangium intermedium* and *G. splendens* were used as outgroups. Numbers along the nodes indicate bootstrap support values above 80 % for ML/NJ, respectively.

walled, terminal or subterminal, mostly intercalary, occasionally catenulate, 26–39 μm (av. 33 μm) diam. *Antheridia* ellipsoidal, cupulate or bell-shaped, declinuous, 1–8 per oogonium, antheridial stalks mostly branched, or unbranched, often persisting after fertilisation. *Oospores* aplerotic, usually yellowish, spherical to subspherical, 20–35 μm (av. 23 μm) diam, wall 1.5–2.5 μm thick.

Notes: In this study, MAFF 236903 and CBS 773.81 lost the ability to produce sexual structures, and both asexual and sexual structures in artificial conditions, respectively. Therefore, morphological comparisons are mainly conducted based on the description of MAFF 236903 by Abdelzaher *et al.* (1994) and description of *G. marsipium* by van der Plaats-Niterink (1981).

Typus: Japan, Sakai, Osaka, pond water, 12 Oct. 1992, H.M.A. Abdelzaher (**holotype**, TNS-F-53297; ex-type strain, MAFF 236903 = UOP 406).

Globisporangium camurandrum (Bala *et al.*) Uzuhashi, **comb. nov.** MycoBank MB828474.

Basionym: *Pythium camurandrum* Bala *et al.*, *Persoonia* **25**: 26. 2010.

Description and illustration: Bala *et al.* (2010).

Globisporangium takayamanum (Senda & Kageyama) Uzuhashi, **comb. nov.** MycoBank MB828473.

Basionym: *Pythium takayamanum* Senda & Kageyama, *Mycologia* **101**: 446. 2009.

Description and illustration: Senda *et al.* (2009).

DISCUSSION

Globisporangium lacustre is morphologically similar to *G. marsipium*, although colony patterns, hyphal growth speed, and its response to temperature were significantly different. Hyphal growth of *G. marsipium* has never been described previously (Drechsler 1941, van der Plaats Niterink 1981). The present result demonstrated that *G. lacustre* is also distinguished from *G. marsipium* by its wide temperature range and rapid hyphal growth. Moreover, the ITS and *cox1* sequences of *G. marsipium* were sufficiently different from those of *G. marsipium* to demonstrate that it is a different species. This was also indicated in the phylogenetic analyses (Figs 4, 5).

In culture collections, some strains are used as reference strains for studies, so it is important to maintain strains that are correctly identified. Some new techniques including molecular analyses, and new morphological or physiological characteristics, could provide new information to re-identify species. Therefore, taxonomic re-evaluation of previously collected isolates will be needed at some point. Here, we evaluated the species identification of strain MAFF 236903 in the NARO Genebank based on molecular analyses, because the strain was initially identified as *G. marsipium* by morphology alone in 1994. In this study, MAFF 236903 never formed sexual organs, and the reference strain, CBS 773.81, also lost the ability to sporulate under artificial conditions. Without morphological information, species identification or re-evaluation of species is usually difficult. However, molecular analyses could clearly indicate the difference between them. Finally, we concluded that MAFF 236903 should not be identified as *G. marsipium*, and it was re-described as *G. lacustre* sp. nov., because of differences in the molecular phylogenetic relationships

in particular, as well as hyphal growth rate and colony pattern. Most of the description of *G. lacustre* sp. nov. is based on the initial observations by Abdelzaher *et al.* (1994). Our result indicated that taxonomic re-evaluation of strains is sometimes needed even if the strain becomes sterile in culture. If there are previously published detailed morphological descriptions as in this case, re-designation of isolates should be attempted.

As shown in the phylogenetic analyses presented here, *Pythium camurandrum* and *P. takayamanum* were known to be located in the clade E in the phylogenetic trees of Bala *et al.* (2010) and Senda *et al.* (2009), respectively. Because all species of clade E were transferred to the genus *Globisporangium* by Uzuhashi *et al.* (2010), we decided to also transfer *P. camurandrum* and *P. takayamanum* to *Globisporangium*.

REFERENCES

- Abdelzaher HMA, Ichitani T, Elnaghy MA (1994). *Pythium marsipium* from pond water in Osaka. *Mycological Research* **98**: 920–922.
- Bala K, Robideau GP, Désaulniers N, *et al.* (2010). Taxonomy, DNA barcoding and phylogeny of three new species of *Pythium* from Canada. *Persoonia* **25**: 22–31.
- Bouket AC, Arzanlou M, Tojo M, *et al.* (2015). *Pythium kandovanense* sp. nov., a fungus-like eukaryotic micro-organism (*Stramenopila*, *Pythiales*) isolated from snow-covered ryegrass leaves. *International Journal of Systematic and Evolutionary Microbiology* **65**: 2500–2506.
- Drechsler C (1941). Three species of *Pythium* with proliferous sporangia. *Phytopathology* **31**: 478–507.
- Kumar S, Stecher G, Tamura K (2016). MEGA7: molecular evolutionary genetics analysis version 7.0 for bigger datasets. *Molecular Biology and Evolution* **33**: 1870–1874.
- Lévesque CA, de Cock AWAM (2004). Molecular phylogeny and taxonomy of the genus *Pythium*. *Mycological Research* **108**: 1363–1383.
- Miller PM (1995). V-8 juice agar as a general purpose medium for fungi and bacteria. *Phytopathology* **45**: 461–462.
- Múniera JDC, Hausbeck MK (2016). Characterization of *Pythium* species associated with greenhouse floriculture crops in Michigan. *Plant Disease* **100**: 569–576.
- Robideau GP, de Cock AWAM, Coffey MD *et al.* (2011). DNA barcoding of oomycetes with cytochrome c oxidase subunit I and internal transcribed spacer. *Molecular Ecology Resources* **11**: 1002–1011.
- Senda M, Kageyama K, Suga H, *et al.* (2009). Two new species of *Pythium*, *P. senticosum* and *P. takayamanum*, isolated from cool-temperate forest soil in Japan. *Mycologia* **101**: 439–448.
- Ueta S, Tojo M (2016). *Pythium barbulae* sp. nov. isolated from the moss, *Barbula unguiculata*; morphology, molecular phylogeny and pathogenicity. *Mycoscience* **57**: 11–19.
- Uzuhashi S, Hata K, Matsuura S, *et al.* (2017). *Globisporangium oryzicola* sp. nov., causing poor seedling establishment of directly seeded rice. *Antonie van Leeuwenhoek* **110**: 543–552.
- Uzuhashi S, Okada G, Ohkuma M (2015). Four new *Pythium* species from aquatic environments in Japan. *Antonie van Leeuwenhoek* **107**: 375–391.
- Uzuhashi S, Tojo M, Kakishima M (2010). Phylogeny of the genus *Pythium* and description of new genera. *Mycoscience* **51**: 337–365.
- van der Plaats-Niterink AJ (1981). Monograph of the genus *Pythium*. *Studies in Mycology* **21**: 1–242.
- White TJ, Bruns T, Lee S, *et al.* (1990). Amplification and direct sequencing of fungal ribosomal RNA gene for phylogenetics. In: PCR protocols: a guide to methods and applications (Innes MA, Gelfand DH, Sninsky JJ, White TJ, eds). USA, NY, Academic Press: 315–322.
- Zhang BQ, Yang XB (2000). Pathogenicity of *Pythium* populations from corn-soybean rotation fields. *Plant Disease* **84**: 94–99.

doi.org/10.3114/fuse.2019.03.03

Morphological species of *Gloeandromyces* (Ascomycota, Laboulbeniales) evaluated using single-locus species delimitation methods

D. Haelewaters^{1,2,3,4*}, D.H. Pfister¹

¹Department of Organismic and Evolutionary Biology & Farlow Reference Library and Herbarium of Cryptogamic Botany, Harvard University, 22 Divinity Avenue, Cambridge MA 20138, USA

²Smithsonian Tropical Research Institute, Apartado Postal 0843-03092, Balboa, Panama

³Herbario UCH, Universidad Autónoma de Chiriquí, Apartado Postal 0427, David, Panama

⁴Current affiliation: Faculty of Science, University of South Bohemia, Branišovská 31, 37005 České Budějovice, Czech Republic

*Corresponding author: danny.haelewaters@gmail.com

Key words:

ectoparasitic fungi
host specialization
phenotypic plasticity
ribosomal DNA
taxonomy

Abstract: In this paper, new species and *formae* of the genus *Gloeandromyces* (Ascomycota, Laboulbeniales) are described and illustrated. These are: *Gloeandromyces dickii* sp. nov. on *Trichobius joblingi* from Nicaragua and Panama; *G. pageanus* f. *alarum* f. nov. on *Tri. joblingi* from Panama; *G. pageanus* f. *polymorphus* f. nov. on *Tri. dugesioides* and *Tri. joblingi* from Panama and Trinidad; and *G. streblae* f. *sigmomorphus* f. nov. on *Tri. joblingi* from Panama. *Gloeandromyces pageanus* on *Tri. dugesioides* from Panama as described in *Nova Hedwigia* 105 (2017) is referred to as *G. pageanus* f. *pageanus*. Support for these descriptions of species and *formae* comes from phylogenetic reconstruction of the large subunit ribosomal DNA and from the application of species delimitation methods (ABGD, bPTP, GMYC). Host specialization results in phylogenetic segregation by host species in both *G. pageanus* and *G. streblae* and this may represent a case of incipient speciation. A second mechanism driving diversity involves position-induced morphological adaptations, leading to the peculiar morphotypes that are associated to growing on a particular position of the integument (*G. pageanus* f. *alarum*, *G. streblae* f. *sigmomorphus*).

Effectively published online: 11 January 2019.

INTRODUCTION

Laboulbeniales are microscopic fungi (Ascomycota, Laboulbeniomycetes) that live as obligate epibionts on arthropod hosts. They are developmentally and morphologically unique among fungi that often have mycelia of unlimited growth – in *Laboulbeniales* subsequent divisions of a single two-celled ascospore result in the production of a multicellular unit of determinate growth, or *thallus*. Ascospores are thought to be predominantly directly transmitted through activities of the host (De Kesel 1995), such as mating, grooming, and random physical contacts in overwintering aggregations. Most *Laboulbeniales* are host specific; they are often associated with a single host species or hosts in the same genus. De Kesel (1996) showed that *Laboulbenia slackensis*, specific to *Pogonus chalceus* in nature, can be grown on other hosts under conditions atypical for these hosts. Thus, host specificity is driven by characters of the host, but also by environmental conditions (as selected by that host). A number of species have been reported from multiple hosts. For one of these, *Hesperomyces virescens*, we recently showed using an integrative approach with morphometric, molecular phylogenetic, and ecological data, that it is a complex of several species, segregated by host (Haelewaters *et al.* 2018a). On the other hand, different arthropods can co-occur in a single microhabitat, creating

opportunities for transmission of ascospores to “atypical” hosts and host shifting, which may ultimately lead to speciation (e.g. Blum 1924, Rossi 2011, Pfliegler *et al.* 2016).

The majority of described species of *Laboulbeniales*, about 80 %, are associated with beetles (order *Coleoptera*) whereas only 10 % are associated with flies (order *Diptera*) (Weir & Hammond 1997). Four genera are known from bat flies (suborder *Hippoboscoidea*, families *Nycteribiidae* and *Streblidae*): *Arthrorhynchus* (four described species, two additional nominal species placed in synonymy), *Dimeromyces* (two described species), *Gloeandromyces* (three described species), and *Nycteromyces* (two described species) (Peyritsch 1871, 1873, Thaxter 1901, 1917, 1931, Haelewaters *et al.* 2017b, Doggoniuck *et al.* in press). Species in the genera *Arthrorhynchus*, *Gloeandromyces*, and *Nycteromyces* have been reported from bat flies exclusively. The genus *Dimeromyces*, on the other hand, is one of the largest genera of *Laboulbeniales* encompassing 115 species, of which only two are found on bat flies (Rossi *et al.* 2015, 2016, Doggoniuck *et al.* in press). In the last few years, studies on bat fly-associated *Laboulbeniales* have focused on extensive surveying, taxonomy (description of species), host specificity, tripartite association networks, phylogenetic placement of bat fly-specific genera, and morphological *versus* molecular diversity of *Gloeandromyces* (Haelewaters *et al.* 2017a, b, 2018b, Szentiványi *et al.* 2018, Walker *et al.* 2018, Doggoniuck *et al.* in press).

The genus *Gloeandromyces* was described by Thaxter (1931) to accommodate two species he had earlier described as *Stigmatomyces nycteribiidarum* and *S. streblae* (Thaxter 1917). He argued that the fan-like organization of the appendage separates the genus from *Stigmatomyces*, and described a gelatinous disorganization, which “ultimately affects the cells subtending the antheridia and even those below, so that the spreading portion of the appendage is largely obliterated” (Thaxter 1931). *Gloeandromyces nycteribiidarum* was described from a *Megistopoda aranea* bat fly [as *Pterellipsis aranea*] from Grenada; *G. streblae* from a *Strebla wiedemanni* bat fly (as *S. vespertilionis*) from Venezuela. Since their description in 1917, both species were re-collected only a century later, during the studies of D.H. Note that unidentified *Laboulbeniales* have been reported on bat flies from Brazil (Gracioli & Coelho 2001, Bertola *et al.* 2005) and Costa Rica (Fritz 1983). A third species of *Gloeandromyces* was described from *Trichobius dugesioides* bat flies (*Diptera, Streblidae, Trichobinae*) collected in Gamboa, Panama (Haelewaters *et al.* 2017b). Haelewaters *et al.* (2018b) and Walker *et al.* (2018) reported and illustrated undescribed forms of *Gloeandromyces* but refrained from morphological descriptions. In this paper, we apply sequence-based species delimitation methods to evaluate species limits in the genus *Gloeandromyces*, which thus far has only been reported from neotropical bat flies.

MATERIALS AND METHODS

Collection of bats, bat flies, and *Laboulbeniales*

Protocols to capture bats and to screen for ectoparasitic bat flies are given in the studies by Haelewaters *et al.* (2018b) and Walker *et al.* (2018). All capturing and sampling procedures were licensed and approved by the Smithsonian Tropical Research Institute (IACUC protocol: 2017-0102-2020-A5) and the Government of Panama (Ministerio de Ambiente de Panamá: SE/AH-2-16, SC/AH-117, SE/P-13-17). Specimens of bat flies preserved in 70–99 % ethanol were made available by collaborators C.W. Dick (Ecuador, Nicaragua) and J.J. Camacho (Trinidad). Field sites are shown in Fig. 1. Bat flies were screened for the presence of *Laboulbeniales* thalli using a stereomicroscope at 50× magnification. Thalli were removed from the host using Minuten Pins inserted onto wooden rods. Slide mounts were made following Benjamin (1971), with the help of Hoyer’s medium (30 g arabic gum, 200 g chloral hydrate, 16 mL glycerol, 50 mL ddH₂O) to dry-fix the thalli to the slide as described in Haelewaters *et al.* (2018a). Mounted fungal material was viewed at 400× to 1000× magnification under an Olympus BX53 compound microscope equipped with an Olympus DP73 digital camera (Waltham, Massachusetts). For detailed morphological study and descriptions, we used an Olympus BX40 microscope with XC50 camera, available at the Farlow Herbarium. Fungal specimens were identified using Thaxter (1917, 1924, 1931) and Haelewaters *et al.* (2017b). Voucher slides are deposited at Farlow Herbarium (FH; Harvard University, Cambridge, Massachusetts) and Herbario de la Universidad Autónoma de Chiriquí (UCH; David, Panamá).

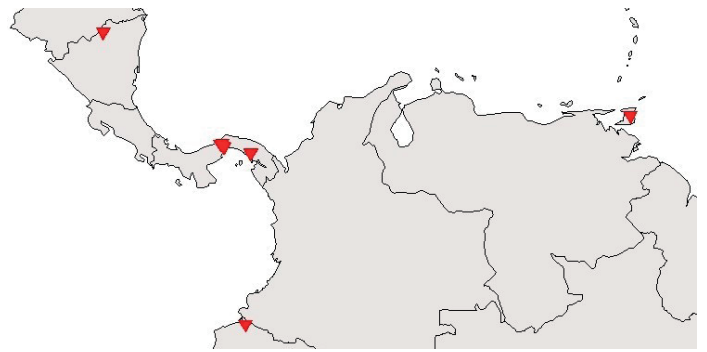


Fig. 1. Field sites where the streblid bat flies (*Diptera, Streblidae*) were collected that hosted the *Gloeandromyces* species and *formae* described in this paper. Field sites are located in Nicaragua and Panama in Central America; Ecuador in South America; and Trinidad, the southernmost island in the Caribbean.

DNA extraction, PCR amplification, sequencing

Laboulbeniales DNA was extracted from 3–12 thalli using the Extract-N-Amp Plant PCR Kit (Sigma-Aldrich, St. Louis, Missouri) (Haelewaters *et al.* 2015) or from 1–4 thalli using the REPLI-g Single Cell Kit (Qiagen, Valencia, California) (Haelewaters *et al.* 2018a). Pre-treatments employed with the Extract-N-Amp method included a prolonged incubation period at 56 °C in 20 µL Extraction Solution up to 24 h in a Shake ‘N Bake Hybridization Oven (Boekel Scientific model #136400-2, Feasterville, Pennsylvania) and mechanically crushing fungal material in a FastPrep FP120 Cell Disrupter (Thermo Fisher Scientific, Waltham, Massachusetts) at 5.5 m/s for 20 s. For about half of our extractions with the REPLI-g Single Cell Kit, we manually cut thalli in 2 or 3 parts (usually through the perithecium) using a #10 surgical blade on disposable Bard-Parker handle (Aspen Surgical, Caledonia, Michigan) to ensure successful lysis.

The nuclear large ribosomal subunit (LSU) of the ribosomal DNA (rDNA) was amplified for this study. Primer pairs were LROR (5′-ACCGCTGAAGCTTAAGC-3′) and LR5 (5′-ATCCTGAGGGAACTTC-3′) or LIC24R (5′-GAAACCAACAGGGATTG-3′) and LR3 (5′-GGTCCGTGTTTCAAGAC-3′). Amplification reactions consisted of 13.3 µL of RedExtract *Taq* polymerase (Sigma-Aldrich), 2.5 µL of each 10 µM primer, 5.7 µL of ddH₂O and 1.0 µL of template DNA. Amplifications were done in a 2720 Thermal Cycler (Applied Biosystems, Foster City, California) with initial denaturation at 94 °C for 3 min; followed by 35 cycles of denaturation at 94 °C for 1 min, annealing at 50 °C for 45 s, and extension at 72 °C for 90 s; and final extension at 72 °C for 10 min. We used the Q5 Hot Start High-Fidelity DNA Polymerase (New England BioLabs, Ipswich, Massachusetts) for difficult isolates, which had resulted in unsuccessful PCR amplification using the RedExtract *Taq*. PCR was done in 25 µL consisting of 5.0 µL of 5× Q5 Reaction Buffer, 0.5 µL of 10 mM dNTP Mix (Quantabio, Beverly, Massachusetts), 1.25 µL of each 10 µM primer, 0.25 µL of Q5 High-Fidelity DNA Polymerase, 12.75 µL of ddH₂O, and 4.0 µL of template DNA. Thermal conditions were as follows: initial denaturation at 98 °C for 30 s; followed by 35 cycles of denaturation at 98 °C for 10 s, annealing at 58 °C for 30 s (as calculated using the New England BioLabs online Tm Calculator tool, at tmcalculator.neb.com/), and extension at 72 °C for 30 + 5/cycle s; and final extension at 72 °C for 2 min.

PCR purification and sequencing steps were outsourced to Genewiz (South Plainfield, New Jersey). However, when we performed our molecular work routine locally in Panama (at the Molecular Multi-User's Lab at the Naos Marine Laboratories), we purified PCR products using the QIAquick PCR Purification Kit (Qiagen). Subsequently, we prepared 10 μ L reactions with the same primers and 3.0 μ L of purified PCR product. Sequencing reactions were performed using the BigDye[®] Terminator v. 3.1 Cycle Sequencing Kit (Life Technologies, Carlsbad, California). Generated sequences were assembled and edited in Sequencher v. 4.10.1 (Gene Codes Corporation, Ann Arbor, Michigan). All sequences are deposited in GenBank (accession numbers in Table 1).

Sequence alignment and phylogenetic analyses

We constructed an LSU rDNA dataset of newly generated sequences and sequences downloaded from NCBI GenBank to evaluate species discrimination in the genus *Gloeandromyces*. Alignments were done using MUSCLE v. 3.7 (Edgar 2004), available on the CIPRES Science Gateway v. 3.3 (Miller *et al.* 2010). Maximum likelihood (ML) analysis was run using PAUP on XSEDE 4.0b (Swofford 1991), which is available on CIPRES. The appropriate nucleotide substitution model was selected by considering the Akaike Information Criterion (AIC) in jModelTest v. 2.1 (Darriba *et al.* 2012). A transitional substitution model (TIM2) with the assumption of a gamma distribution (+G) gave the best-scoring tree ($-\ln L = 2114.8480$). ML was inferred under this model, and bootstrap (BS) values were calculated with 500 replicates. We ran Bayesian analyses using the BEAST on XSEDE tool in CIPRES with a Markov chain Monte Carlo (MCMC) coalescent approach under a strict molecular clock model, assuming a single rate of evolution across the tree. We selected the Yule speciation model (Yule 1925, Gernhard 2008) as tree prior with the TPM2uf+G nucleotide substitution model (considering the Bayesian Information Criterion, jModelTest v. 2.1). Two independent runs were performed from a random starting tree for 40 M generations, with a sampling frequency of 4 000. Resulting log files of the individual runs were imported in Tracer v. 1.6 (Rambaut *et al.* 2014) to check trace plots for convergence and effective sample size (ESS). ESS values were well ≥ 200 , and so we applied a standard burn-in of 10 % for both runs. Log files and trees files were combined in LogCombiner v. 1.8.4 (Drummond *et al.* 2012) after removal of burn-in. TreeAnnotator v. 1.8.4 was used to generate consensus trees (with 0 % burn-in) and to infer the Maximum Clade Credibility tree, presenting the highest product of individual clade posterior probabilities. Final trees with bootstrap values (BS) and posterior probabilities (pp) were visualized in FigTree v. 1.4.3 (tree.bio.ed.ac.uk/software/figtree/).

Species delimitation in *Gloeandromyces*

For species delimitation analyses within the genus *Gloeandromyces*, we used the LSU rDNA dataset. This region was put forward by our previous work as a barcode marker for species delimitation in *Laboulbeniomycetes* (Walker *et al.* 2018, Haelewaters *et al.* 2018a). We aimed to validate morphology-based species identifications by employing three species delimitation methods (SDMs): ABGD (Puillandre *et al.* 2012), PTP (Zhang *et al.* 2013), and GMYC (Pons *et al.* 2006). The Automatic Barcode

Gap Discovery method (ABGD) partitions sequence data into a maximum number of groups based on nucleotide divergence among isolates (Puillandre *et al.* 2012). We used the following parameters in the online version of ABGD (www.wabi.snv.jussieu.fr/public/abgd/abgdweb.html): $P_{min} = 0.001$, $P_{max} = 0.01$ (*sensu* Puillandre *et al.* 2012), steps = 10, and Nb bins = 20. To assess consistency in the recognition of species hypotheses by ABGD, we evaluated results for both the Jukes-Cantor (JC69) and Kimura 2-parameter (K80) distance metrics (Jukes & Cantor 1969, Kimura 1980) and for four gap width values (X): 0.1, 0.5, 1.0, and 1.5. The Poisson tree processes (PTP) model approach uses the number of nucleotide substitutions to infer speciation rate (Zhang *et al.* 2013). We used the bPTP web server (<http://species.h-its.org>) with default values for number of MCMC generations, thinning, burn-in, and seed, with the Maximum Clade Credibility tree as constructed above as input. The General Mixed Yule Coalescent (GMYC) approach models processes at the population level (coalescence) and processes at the species level (speciation) based on a fully resolved ultrametric tree (Pons *et al.* 2006). We conducted GMYC in R (R Core Team 2013) using the packages “rnc1” (Michonneau *et al.* 2015) and “SPLITS” (Ezard *et al.* 2009). Input tree was the same Maximum Clade Credibility tree generated above.

RESULTS

Nucleotide alignment dataset & phylogenetic inference

Our LSU rDNA dataset comprised 955 characters, of which 817 were constant and 110 were parsimony-informative. A total of 27 isolates were included (Table 1). These are *Stigmatomyces protrudens* (one isolate as outgroup); *Gloeandromyces dickii* (four isolates); *G. nycteribiidarum* (two isolates); *G. pageanus* (13 isolates, including three isolates of f. *pageanus*, three isolates of f. *alarum*, and seven isolates of f. *polymorphus*); and *G. streblae* (seven isolates, including one isolate of f. *sigmomorphus*). *Gloeandromyces* forms six clades in both the ML and Bayesian analyses (Fig. 2). However, the statistical support differs between both approaches. ML support was only found for *G. dickii* (BS = 100), *G. nycteribiidarum* (BS = 99), *G. streblae* clade A+B (BS = 88), *G. pageanus* clade C+D (BS = 98), and *G. pageanus* clade C (BS = 96). In comparison, Bayesian inference also supported the distinction of *G. streblae* in host-specific clades A and B (pp = 0.96 and 0.81, respectively). Clade D has no support from either ML or Bayesian inference.

Species delimitation

Results of the species delimitation methods are summarized in Fig. 2 and Tables 2 and 3. The number of putative species in *Gloeandromyces* varied from 4 to 7 with ABGD analyses, depending on the prior intraspecific divergence (Table 3). The relative gap width and used distance metrics (JC69, K80) had no influence on the results. The bPTP analysis of the LSU topology resulted in four highly supported species (the “b” in bPTP standing for Bayesian support calculated for putative species): *Gloeandromyces dickii*, *G. nycteribiidarum*, *G. pageanus* (clade C+D), and *G. streblae* (clade A+B). The GMYC model led to the same results (four species delimited), but without strong support for *G. pageanus* and *G. streblae*.

Table 1. Overview of *Laboulbeniales* sequences used in this study. For each isolate is listed: current fungal species or *forma* when applicable, host species, location, and GenBank accession number for the LSU rDNA sequence. References for sequence data: Weir & Blackwell (2001), Haelewaters *et al.* (2015, 2018b).

Isolate	Species	Host species	Location	GenBank #
AW-793	<i>Stigmatomyces protrudens</i>	<i>Ephydriidae</i> sp.	USA	AF298234
D. Haelew. 1319b	<i>Gloeandromyces nycteriidarum</i>	<i>Megistopoda aranea</i>	Panama, Chucantí	MH040566
D. Haelew. 1334c	<i>Gloeandromyces nycteriidarum</i>	<i>Megistopoda aranea</i>	Panama, Chucantí	MH040567
D. Haelew. 1312b	<i>Gloeandromyces dickii</i>	<i>Trichobius joblingi</i>	Panama, Chucantí	MH040580
D. Haelew. 1312c	<i>Gloeandromyces dickii</i>	<i>Trichobius joblingi</i>	Panama, Chucantí	MH040581
D. Haelew. 1323b	<i>Gloeandromyces dickii</i>	<i>Trichobius joblingi</i>	Panama, Chucantí	MH040582
D. Haelew. 1323c	<i>Gloeandromyces dickii</i>	<i>Trichobius joblingi</i>	Panama, Chucantí	MH040583
D. Haelew. 1090a	<i>Gloeandromyces streblae</i>	<i>Trichobius dugesioides</i>	Panama, Gamboa	MH040584
D. Haelew. 1306c	<i>Gloeandromyces streblae</i>	<i>Trichobius joblingi</i>	Panama, Chucantí	MH040585
D. Haelew. 1308b	<i>Gloeandromyces streblae</i>	<i>Trichobius dugesioides</i>	Panama, Chucantí	MH040586
D. Haelew. 1309a	<i>Gloeandromyces streblae</i>	<i>Trichobius dugesioides</i>	Panama, Chucantí	MH040587
D. Haelew. 1317a	<i>Gloeandromyces streblae</i>	<i>Trichobius joblingi</i>	Panama, Chucantí	MH040588
D. Haelew. 1335c	<i>Gloeandromyces streblae</i>	<i>Trichobius joblingi</i>	Panama, Chucantí	MH040589
D. Haelew. 1320b	<i>Gloeandromyces streblae</i> f. <i>sigmomorphus</i>	<i>Trichobius joblingi</i>	Panama, Chucantí	MH040579
D. Haelew. 1091b	<i>Gloeandromyces pageanus</i> f. <i>pageanus</i>	<i>Trichobius dugesioides</i>	Panama, Gamboa	MG906798
D. Haelew. 1367b	<i>Gloeandromyces pageanus</i> f. <i>pageanus</i>	<i>Trichobius dugesioides</i>	Panama, Parque Nacional Soberanía	MH040568
D. Haelew. 1425a	<i>Gloeandromyces pageanus</i> f. <i>pageanus</i>	<i>Trichobius dugesioides</i>	Panama, Parque Nacional Soberanía	MH040569
D. Haelew. 1306b	<i>Gloeandromyces pageanus</i> f. <i>alarum</i>	<i>Trichobius joblingi</i>	Panama, Chucantí	MH040574
D. Haelew. 1322a	<i>Gloeandromyces pageanus</i> f. <i>alarum</i>	<i>Trichobius joblingi</i>	Panama, Chucantí	MH040577
D. Haelew. 1327a	<i>Gloeandromyces pageanus</i> f. <i>alarum</i>	<i>Trichobius joblingi</i>	Panama, Chucantí	MH040578
D. Haelew. 619a	<i>Gloeandromyces pageanus</i> f. <i>polymorphus</i>	<i>Trichobius joblingi</i>	Trinidad	KT800008
D. Haelew. 1073b	<i>Gloeandromyces pageanus</i> f. <i>polymorphus</i>	<i>Trichobius joblingi</i>	Panama, Península Bohío	MH040570
D. Haelew. 1089a	<i>Gloeandromyces pageanus</i> f. <i>polymorphus</i>	<i>Trichobius dugesioides</i>	Panama, Gamboa	MH040571
D. Haelew. 1100b	<i>Gloeandromyces pageanus</i> f. <i>polymorphus</i>	<i>Trichobius joblingi</i>	Panama, Gamboa	MH040572
D. Haelew. 1272a	<i>Gloeandromyces pageanus</i> f. <i>polymorphus</i>	<i>Trichobius dugesioides</i>	Panama, Parque Nacional Soberanía	MH040573
D. Haelew. 1315a	<i>Gloeandromyces pageanus</i> f. <i>polymorphus</i>	<i>Trichobius joblingi</i>	Panama, Chucantí	MH040575
D. Haelew. 1315b	<i>Gloeandromyces pageanus</i> f. <i>polymorphus</i>	<i>Trichobius joblingi</i>	Panama, Chucantí	MH040576

Taxonomy

Gloeandromyces Thaxt., *Mem. Amer. Acad. Arts* **16**: 112. 1931.

Type species: Gloeandromyces streblae (Thaxt.) Thaxt., *Mem. Amer. Acad. Arts* **16**: 113. 1931.

Gloeandromyces dickii Haelew., *sp. nov.* MycoBank MB824616. Figs 3A–C, 6.

Etymology: Referring to Dr. Carl W. Dick, Associate Professor of Biology at Western Kentucky University, who provided 7 792 bat flies from Ecuador, Honduras, Mexico, and Nicaragua for our studies dealing with bat fly-associated *Laboulbeniales*.

Diagnosis: Different from the other species and *formae* in the genus by the single peculiar, slender outgrowth halfway at the perithecial venter and the perithecial neck bent in anterior direction. Its LSU sequence is 91.6–94.2 % similar to other species of *Gloeandromyces*, unique molecular synapomorphies at positions 71, 90, 95, 116, 150, 158, 161, 220, 311, 427, 430, 432, 450, 452 (deletion), 476, 510, 512, 515, 530, 533–535, 537,

540, 541, 544–546, 553, 555, 560, 588, 589, 593, 608, 722, 724–729.

Description: *Thallus* irregularly pale yellowish, darker at perithecial venter and neck; basal cell of appendage bright orange. *Cell I* bent or kinked towards anterior side, with parallel margins, 2.5–2.9× longer than broad, carrying cells II and VI. *Cell II* broadly rhomboidal, isodiametric or slightly longer than broad, separated from cell III by oblique septum. *Cell III* broadly trapezoidal, distally narrowing, slightly longer than broad. *Basal cell of appendage* pentagonal to dome-shaped, with margins slightly broadening distally, carrying two short (up to 32 µm) branches of dichotomously dividing cells, outer suprabasal cell always higher than inner one, final cells antheridial. *Cell VI* strongly oblique, lens-shaped or flattened between cells II and VII, posterior margin (= septum II/VI) convex. *Cell VII* next to cell VI, with convex outer margin, proximal end in contact with cell I or almost so. *Perithecium* broadly ovoid, bearing three very different outgrowths: a short but conspicuous rounded bulge at base, an elongate, finger-like protuberance halfway along venter, directed to anterior side, usually straight or slightly bent upwards, and a single

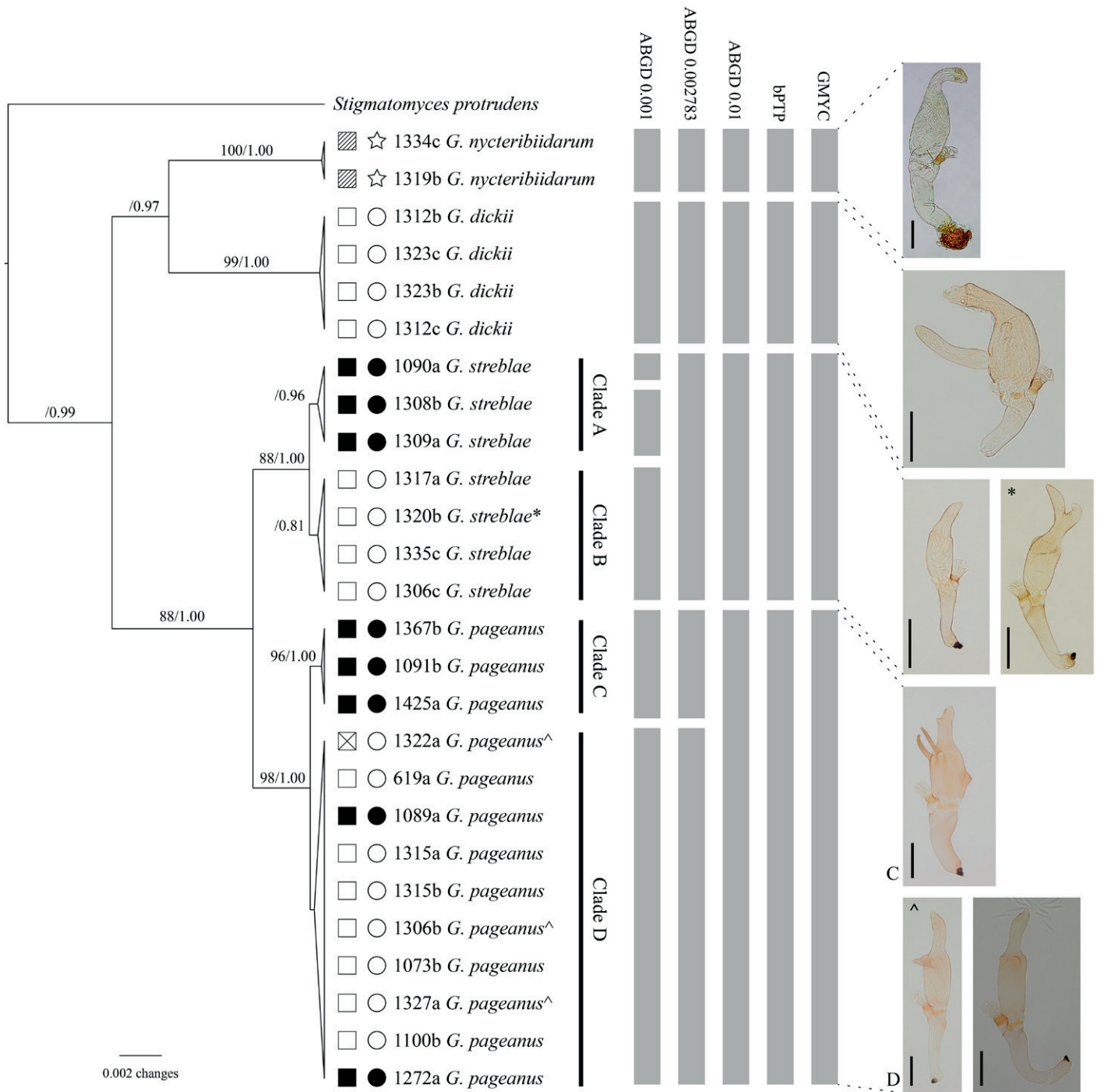


Fig. 2. Maximum clade credibility tree showing species in the genus *Gloeandromyces*, with *Stigmatomyces protrudens* as outgroup (adapted from Haelewaters *et al.* 2018b). The tree is the result of a Bayesian analysis of the LSU dataset. For each node, ML BS (≥ 70)/Bayesian pp (≥ 0.7) are presented above the branch leading to that node. Symbols indicate hosts: (bat flies) ☆ = *Megistopoda aranea*, ● = *Trichobius dugesioides*, ○ = *Tri. joblingi*; (bats) ▨ = *Artibeus jamaicensis*, ⊠ = *Carollia brevicauda*, □ = *C. perspicillata*, ■ = *Trachops cirrhosus*. Symbols behind fungus species names designate morphotypes: **Gloeandromyces streblae* f. *sigmomorphus*, ^*G. pageanus* f. *alarum*, all other isolates in clade D: *G. pageanus* f. *polymorphus*. To the right of the terminal labels of the phylogeny, SDM results are summarized, from left to right: ABGD of the aligned LSU data matrix with prior intraspecific divergence (P) = 0.001 (Pmin), ABGD with P = 0.002783, ABGD with P = 0.01 (Pmax), bPTP of the LSU topology and GMYC of the LSU ultrametric tree generated in BEAST. To the right of the SDM results, thalli of *Gloeandromyces* spp. are shown. From top to bottom: *Gloeandromyces nycteribiidarum*; *G. dickii*; *G. streblae* and **G. streblae* f. *sigmomorphus*; *G. pageanus* f. *pageanus* (clade C), and ^*G. pageanus* f. *alarum* and *G. pageanus* f. *polymorphus* (clade D).

bump (rarely two) positioned laterally at distal third of venter; neck abruptly distinguished, strongly bent, with anterior margin concave and posterior margin nearly straight, distally distinctly broader at junction with stout, tapering tip, ending with prominent rounded lips.

Measurements: *Thallus* 183–294 μm in length from foot to perithecial tip. *Cell I* 58–88 \times 21–30 μm . *Basal cell of appendage* 9–12 \times 10–16 μm . *Perithecium* 123–176 \times 40–62 μm . *Finger-like projection* up to 50–86 μm long. *Ascospores* 31–36 \times 3–5 μm (up to 10 μm wide including slime sheath).

Table 2. Summary of results of ML, Bayesian, and species delimitation analyses (ABGD, bPTP, GMYC). Explanation of symbols and values used: — indicates no support; + under ABGD represents supported clades; numbers under bPTP and GMYC are Bayesian support values for delimited species hypotheses. (+) The ABGD analysis found support for two clades within *Gloeandromyces streblae* clade A under prior maximum distance (P) = 0.001, 0.001292, 0.001668 and 0.002154.

Putative species	ML BS	pp	ABGD P 0.001	ABGD P 0.002783	ABGD P 0.01	bPTP	GMYC
<i>nycteribiidarum</i>	100	1.0	+	+	+	0.996	0.85
<i>dickii</i>	99	1.0	+	+	+	0.986	0.81
<i>streblae</i> clade A	68	1.0	(+)	+	+	0.856	0.33
<i>streblae</i> clade B	—	0.9	+				
<i>pageanus</i> clade C	96	1.0	+	+	+		
<i>pageanus</i> clade D	—	0.3	+	+		0.906	0.41

Table 3. Results of the Automatic Barcode Gap Discovery (ABGD) analyses. X, relative gap width; JC69, Jukes-Cantor substitution model; K80, Kimura 2-parameter substitution model.

Distance	Prior intraspecific divergence (P)										
	X	0.001	0.001292	0.001668	0.002154	0.002783	0.003594	0.004642	0.005995	0.007743	0.01
JC69	0.1	7	7	7	7	5	4	4	4	4	4
	0.5	7	7	7	7	5	4	4	4	4	4
	1.0	7	7	7	7	5	4	4	4	4	4
	1.5	7	7	7	7	5	4	4	4	4	4
	0.1	7	7	7	7	5	4	4	4	4	4
K80	0.5	7	7	7	7	5	4	4	4	4	4
	1.0	7	7	7	7	5	4	4	4	4	4
	1.5	7	7	7	7	5	4	4	4	4	4

Typus: **Nicaragua**, Jinotega Department, Reserva Natural Bosawás, Mayangna Sauna Bu, Amak, at fork Rio Bocay and Rio Amak, secondary growth forest, 14.2396944 N 85.148 W, 30 May 2003, M.R. Gannon, on male *Trichobius joblingi* (Diptera, Streblidae, Trichobinae) (collected from male *Carollia perspicillata*), slide D. Haelew. 1018c (FH 00313692, **holotype**, two juvenile and six mature thalli, abdominal sternae). **Panama**, Colón Province, Forest Fragment near El Giral, 9.2152675 N 79.7301492 W, 11 May 2015, T. Hiller, on *Tri. joblingi* (collected from female *C. perspicillata*), slide D. Haelew. 1069a (FH 00313696, **paratype**, one mature thallus, right-hand side abdomen); Darién Province, Reserva Natural Chucantí, field site Waterfall, young secondary succession forest, 8.7865167 N 78.4508333 W, 19 Jun. 2017, D. Haelewaters et al., on *Tri. joblingi* (collected from male *C. perspicillata*), slide D. Haelew. 1312a (FH 00313695, **paratype**, three mature thalli, right-hand side ventral abdomen); Darién Province, Reserva Natural Chucantí, field site Potrerito, old-growth broadleaf forest, 8.7909833 N 78.4510333 W, 22 Jun. 2017, D. Haelewaters et al., on *Tri. joblingi* (from male *C. perspicillata*), slide D. Haelew. 1323a (UCH, **paratype**, three mature thalli, right-hand side ventral abdomen).

Additional materials examined: **Ecuador**, Esmeraldas Province, San Francisco de Bogota, 1.0877 N 78.6915 W, 6 Aug. 2014, C.W. Dick, on female *Trichobius longipes* (Diptera, Streblidae, Trichobinae) (collected from female *Phyllostomus hastatus*), slide D. Haelew. 1042a (FH 00313693, seven mature thalli, anterior ventral abdomen); same data, slide D. Haelew. 1043a (FH 00313694, six mature thalli, right-hand side anterior ventral abdomen).

Material sequenced: **Panama**, Darién Province, Reserva Natural Chucantí, field site Waterfall, young secondary succession forest, 8.7865167 N 78.4508333 W, 19 Jun. 2017, D. Haelewaters et al., on *Tri. joblingi* (collected from male *C. perspicillata*), isolate D. Haelew. 1312b (two mature thalli, right-hand side ventral abdomen, SSU: MH040546, LSU: MH040580); same data, isolate D. Haelew. 1312c (two mature thalli, right-hand side ventral abdomen, SSU: MH040547, LSU: MH040581). **Panama**, Darién Province, Reserva Natural Chucantí, field site Potrerito, old-growth broadleaf forest, 8.7909833 N 78.4510333 W, 22 Jun. 2017, D. Haelewaters et al., on *Tri. joblingi* (from male *C. perspicillata*), isolate D. Haelew. 1323b (four mature thalli, right-hand side ventral abdomen, SSU: MG958011, LSU: MH040582); same data, isolate D. Haelew. 1323c (one juvenile & three mature thalli, right-hand side ventral abdomen, SSU: MH040548, LSU: MH040583).

Notes: The perithecia of thalli from slide FH 00313695 look different from the typical form; the venter is slenderer, in combination with a consistently shorter and tapering perithecial projection. The *G. dickii* clade in the LSU phylogeny comprises D. Haelew. 1323b and 1323c ("typical" *G. dickii*) and D. Haelew. 1312b and 1312c. This clade is strongly supported, and our SDMs support *G. dickii* as a single species. All these thalli were removed from the same bat fly host, *Tri. joblingi*. The morphological differences described here seem to represent a range of phenotypic plasticity.

In addition to the Nicaraguan and Panamanian material, we also observed specimens from Ecuador (slides FH 00313693

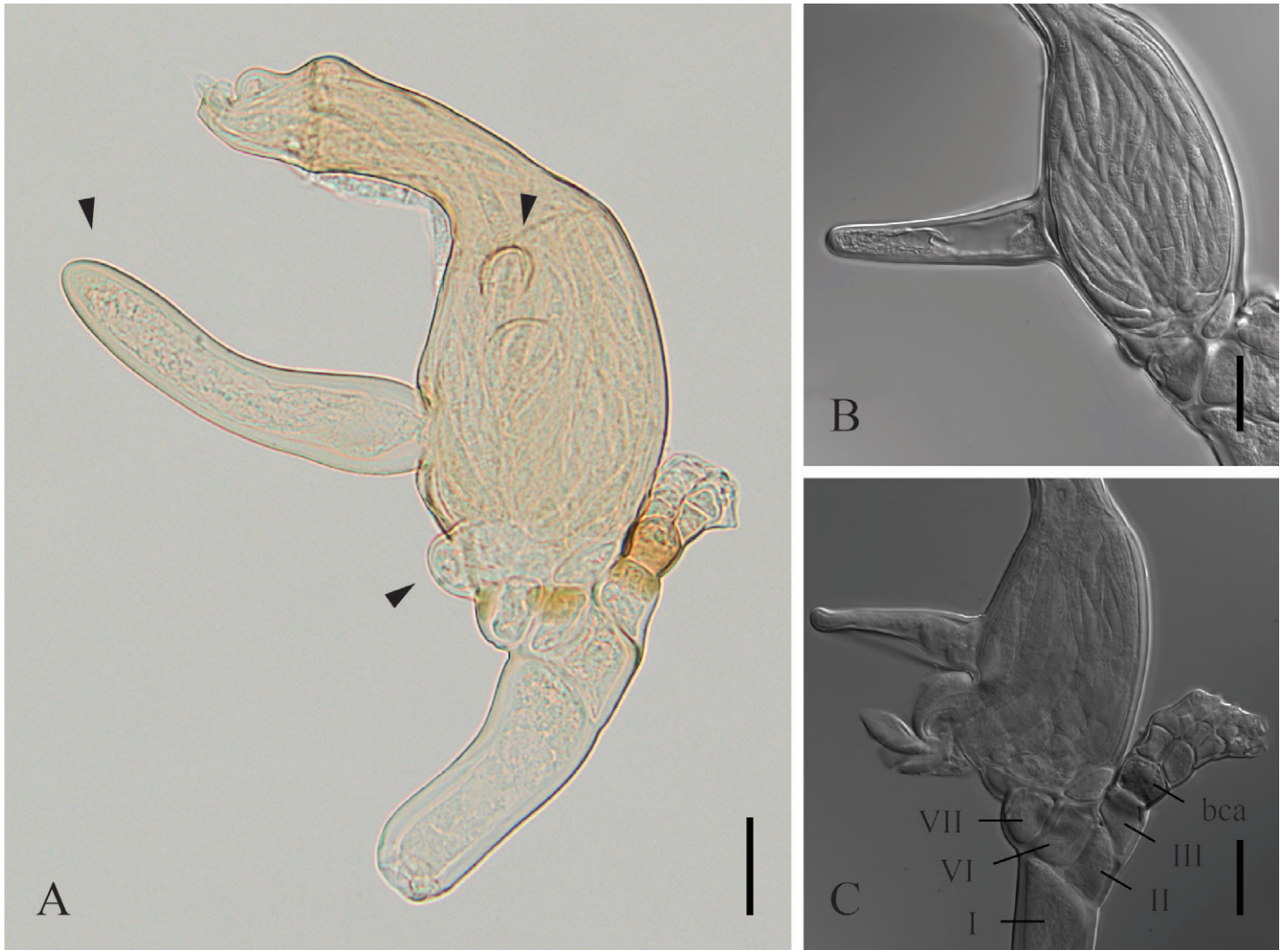


Fig. 3. Thalli of *Gloeandromyces dickii*. **A.** Mature thallus from slide FH 00313692 (holotype), with arrowheads pointing at outgrowths typical for this species. See description for details. **B.** Mature thallus from slide FH 00313694, with the perithecium less ovoidal and the anteriorly directed perithecial outgrowth halfway the venter shorter and more tapered in comparison to the type series. **C.** Mature thallus from slide FH 00313693 (with the perithecial venter ruptured anteriorly). Annotated are cells I, II, III, VI, VII, and the pentagonal-shaped basal cell of the appendage (bca). Scale bars: A = 50 μ m, B–C = 20 μ m.

and FH 00313694). We did not include them as part of the type series, because they were removed from another host species (*Tri. longipes*). We only performed DNA extractions of thalli taken from *Tri. joblingi*, and consequently, with the data in hand, we cannot rule out the possibility that there is some level of host specialization or (incipient) speciation (*sensu* Haelewaters *et al.* 2018a, b). The Ecuadorian material is also different in the following morphological characters (Fig. 3B–C): cell I can be slightly bent towards anterior side but is straight in the majority of observed thalli, the outer wall of cell VII is not convex/bulbous, the perithecial venter is less ovoidal, the bump at the base of the perithecium is less prominent and the perithecial projection halfway the venter is shorter and more tapered (like in FH 00313695). Other features are in line with those in the description of *G. dickii* above. It is clear that the Ecuadorian thalli and those from Nicaragua and Panama represent taxa that are very closely related if not the same.

Gloeandromyces pageanus Haelew., *Nova Hedwigia* **105**: 272. 2017. MycoBank MB819381. Fig. 4A–B.

Etymology: Referring to Dr. Rachel Page (Smithsonian Tropical Research Institute), mammologist, collaborator, and Principal Investigator at the Bat Lab in Gamboa.

Diagnosis: Different from the other species and *formae* in the genus by its peculiar perithecial bulbous outgrowths and finger-like projections.

Description: *Thallus* irregularly colored reddish, darker at basal cell of appendage, perithecial bulbous outgrowth and finger-like projections; upper part of cell III and cells VI and VII tinged with orange. *Cell I* curved towards anterior side, longer than broad, with divergent margins, carrying cells II and VI. *Cell II* trapezoidal, slightly broader than long. *Cell III* isodiametric, with rounded lower anterior margin. *Basal cell of appendage* pentagonal, with parallel anterior and posterior margins, carrying two very short branches of dichotomously dividing cells, final cells antheridial. *Cell VI* obliquely positioned between cells II and VII,

broadly triangular, lower margin rounded, broader than long. *Perithecium* obclavate, anterior margin bearing a short and bulbous outgrowth at lower third, and two horn-like projections obliquely directed upwards on the posterior side just below base of well-distinguished neck, bearing on upper half of posterior side two very short bulbous outgrowths, the upper one slightly smaller and darkly pigmented; tip undifferentiated, blunt.

Measurements: *Thallus* 195–257 µm in length from foot to perithecial tip. *Cell I* 45–74 × 31–44 µm (distally). *Basal cell of appendage* 7–10 × 11–13 µm. *Perithecium* 113–139 × 43–52 µm (not including bulbous outgrowth). *Perithecial projections* up to 46 µm in length. *Ascospores* 30–35 × 3–5 µm.

Typus: **Panama**, Colón Province, Gamboa, 26 Jun. 2016, R.A. Page et al., on female *Trichobius dugesioides* (collected from female *Trachops cirrhosus*), slide D. Haelew. 1093a (FH 00313699, **holotype**, six mature thalli, prescutum and scutum); Colón Province, Gamboa, 24 Jun. 2016, R.A. Page et al., on female *Tri. dugesioides* (collected from male *T. cirrhosus*), slide D. Haelew. 1091a (FH 00313697, **paratype**, one mature thallus, right-hand side thorax); same data, slide D. Haelew. 1092a (FH 00313698, **paratype**, one mature thallus, prescutum); Colón Province, Gamboa, 2 Jul. 2016, R.A. Page et al., on male *Tri. dugesioides* (collected from *T. cirrhosus*), slide D. Haelew. 1094a (FH 00313700, **paratype**, four mature thalli, right prescutum); Panamá Province, Ocelot Pond, 9.1017 N 79.685 W, 2 Jul. 2016, R.A. Page et al., on female *Tri. dugesioides* (collected from *T. cirrhosus*), slide D. Haelew. 1098a (FH 00313701, **paratype**, one mature thallus, thorax).

Additional materials examined: **Panama**, Colón Province, Gamboa, 29 Jan. 2017, R.A. Page et al., on *Tri. dugesioides* (collected from female *T. cirrhosus*), slide D. Haelew. 1280b (UCH, 2 mature thalli, left mesoprescutum); Colón Province, Parque Nacional Soberanía, Pipeline Road, Tunnel 17, 28 Jul. 2017, R.A. Page et al., on female *Tri. dugesioides* (collected from female *T. cirrhosus*), slide D. Haelew. 1367a (FH 00313702, five mature thalli, left mesoprescutum); Darién Province, Reserva Natural Chucantí, field site Potrerito, old-growth broadleaf forest, 8.7909833 N 78.4510333 W, 22 Jun. 2017, D. Haelewaters et al., on male *Tri. dugesioides* (collected from male *T. cirrhosus*), slide D. Haelew. 1329a (UCH, 1 mature thallus, left prescutum).

Material sequenced: **Panama**, Colón Province, Gamboa, 24 Jun. 2016, R.A. Page et al., on female *Tri. dugesioides* (collected from male *T. cirrhosus*), isolate D. Haelew. 1091b (six mature thalli, right-hand side thorax, SSU: MH040535, LSU: MG906798); Colón Province, Parque Nacional Soberanía, Pipeline Road, Tunnel 17, 28 Jul. 2017, R.A. Page et al., on female *Tri. dugesioides* (collected from female *T. cirrhosus*), isolate D. Haelew. 1367b (six mature thalli, left mesoprescutum, LSU: MH040568); Colón Province, Parque Nacional Soberanía, Pipeline Road, Tunnel 1,

13 Oct. 2016, I. Geipel, on *Tri. dugesioides* (collected from male *T. cirrhosus*), isolate D. Haelew. 1425a (four mature thalli, right mesoprescutum, SSU: MH040536, LSU: MH040569).

Notes: Its peculiar perithecial bulbous outgrowths and the two horn-like projections separate this species from the other species in the genus *Gloeandromyces* (Thaxter 1917, 1931, Haelewaters et al. 2017b). These characteristics are stable and have been observed in all studied specimens. *Gloeandromyces pageanus* shares with *G. streblae* a simple, blackened foot. The host for *G. pageanus*, *Tri. dugesioides*, is also reported for *G. streblae* in Panama. On most of the host specimens, we found thalli of both parasite species. *Gloeandromyces pageanus* was always found on the thorax, whereas *G. streblae* has no positional restrictions; we have observed this species on the thorax, legs, and wings. On one bat fly (D. Haelew. 1094), both species co-occurred on the right prescutum. Our phylogenetic analyses and SDMs confirm that the two taxa are separate species (Fig. 2).

Molecular synapomorphies diagnostic for clade C+D are found at positions 162, 222, 359, 450, 499, 525, 553 (deletion), 559, 567, 569, 593, 594, 689, 722, 730 (deletion). The phylogenetic reconstruction based on the LSU rDNA region shows divergence by host species into clade C (on *Tri. dugesioides*) and clade D (on *Tri. joblingi*). Because of lack of unique molecular synapomorphies in clade D, this clade is unsupported by both ML and Bayesian inferences. In addition, all SDMs but one do not recognize clades C and D as separate species. As a result, we cannot describe the specimens represented by clade D as a separate species, even though morphologically they are clearly different from the “true” *G. pageanus* (clade C). Based on the available data, we conclude that clade D represents two different morphological types, one that seems restricted to the base of the wings and a second that has no positional restrictions. To avoid confusion regarding these different morphotypes, we will refer to them as *formae*. *Gloeandromyces pageanus* as described above (clade C) will from here on be referred to as *f. pageanus*. The morphotypes from clade D will be referred to as *f. alarum* and *f. polymorphus* and are described formally below.

Gloeandromyces pageanus f. alarum Haelew., *forma nov.* MycoBank MB827804. Figs 4C–D, 6.

Etymology: From Latin, of the wings.

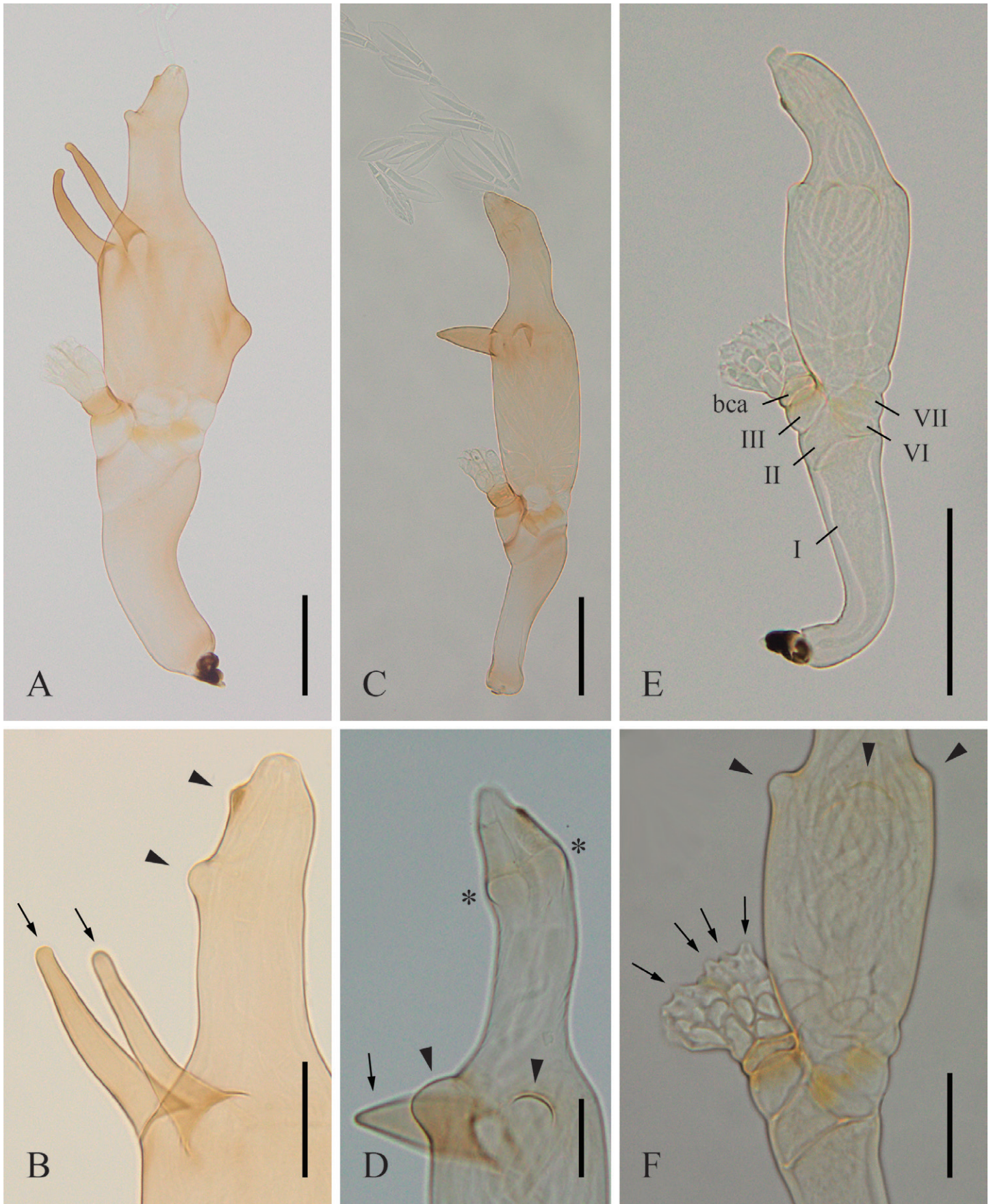
Diagnosis: Different from the other species and *formae* in the genus by its single subulate, almost horizontal projection, positioned posteriorly at the upper venter of the perithecium. Its LSU sequence is 99.7 % similar to *G. pageanus f. pageanus*, and 91.9–98.1 % similar to other species of *Gloeandromyces*.

Description: *Thallus* irregularly yellowish-light brown; septum II/III, area around septum between cell III and basal cell of

Fig. 4. Thalli of *Gloeandromyces pageanus*. **A–B.** *Gloeandromyces pageanus f. pageanus*. **A.** Mature thallus from slide FH 00313698 (paratype). **B.** Mature thallus from slide FH 00313700 (paratype), showing perithecial details on the posterior side: two horn-like projections (arrows) and two bulbous outgrowths (arrowheads). **C–D.** *Gloeandromyces pageanus f. alarum*. **C.** Mature thallus from slide FH 00313707 (paratype), releasing ascospores. **D.** Mature thallus from slide FH 00313709 (paratype), showing upper perithecial venter details: two conspicuous bumps (arrowheads) and a tapering projection directed posteriorly (arrow). Asterisks (*) highlight the two preostiole bumps at opposite sides. **E–F.** *Gloeandromyces pageanus f. polymorphus*, mature thalli from slide FH 00313706 (paratype). **E.** Mature thallus, with annotated cells I, II, III, VI, VII, and the basal cell of the appendage (bca). **F.** Detail of mature thallus, showing antheridial cells (arrows) and conspicuous bumps at the distal end of the perithecial venter (arrowheads). Scale bars: A, C, E = 50 µm; B, D, F = 20 µm.

appendage, cells VI and VII, and perithecial projection and bumps usually darker. *Cell I* straight, broadening upwards, especially at anterior side, 3.4–4.1× longer than broad, carrying cells II and VI. *Cell II* trapezoidal, slightly broader than long, obliquely positioned. *Cell III* broadly triangular, slightly longer than broad.

Basal cell of appendage pentagonal, with parallel anterior and posterior margins, carrying two short (up to 25 µm) branches of dichotomously dividing cells, outer suprabasal cell always higher than inner one, final cells antheridial. *Cell VI* broader than long, obliquely positioned, broadly lens-shaped or flattened between



cells II and VII. *Perithecium* with nearly straight, parallel or very slightly diverging margins; venter ending in one to three conspicuous bumps and a subulate, almost horizontal projection directed to posterior side, up to 36 μm in length; venter passing without abrupt transition into neck; the latter with subparallel margins, somewhat curving towards posterior side, tapering to conical tip, with two minute preostiolar bumps at opposite sides.

Measurements: *Thallus* 183–294 μm in length from foot to perithecial tip. *Cell I* 58–102 \times 15–26 μm (distally). *Basal cell of appendage* 8–11 \times 10–12 μm . *Perithecium* 130–163 \times 28–45 μm . *Ascospores* 33–43 \times 4–6 μm (with slime sheath up to 12 μm wide).

Typus: **Panama**, Darién Province, Reserva Natural Chucantí, field site Waterfall, young secondary succession forest, 8.7865167 N 78.4508333 W, 18 Jun. 2017, *D. Haelewaters et al.*, on *Tri. joblingi* (collected from female *C. perspicillata*), slide D. Haelew. 1306a (FH 00313708, **holotype**, three mature thalli, base of right wing); Colón Province, Gamboa, Harding Avenue past Building 183, 9.115876 N 79.696784 W, 17 Jul. 2016, *D. Haelewaters*, on *Trichobius joblingi* (collected from female *Carollia perspicillata*), slide D. Haelew. 1100a (FH 00313707, **paratype**, one mature thallus, base of left wing); Darién Province, Reserva Natural Chucantí, field site Potrerito, old-growth broadleaf forest, 8.7909833 N 78.4510333 W, 20 Jun. 2017, *D. Haelewaters et al.*, on *Tri. joblingi* (collected from female *C. perspicillata*), slide D. Haelew. 1316a (FH 00313709, **paratype**, 1 mature thallus, base of right wing).

Material sequenced: **Panama**, Darién Province, Reserva Natural Chucantí, field site Waterfall, young secondary succession forest, 8.7865167 N 78.4508333 W, 18 Jun. 2017, *D. Haelewaters et al.*, on *Tri. joblingi* (collected from female *C. perspicillata*), isolate 1306b (two mature thalli, base of right wing, SSU: MH040541, LSU: MH040574); Darién Province, Reserva Natural Chucantí, field site Camp Site, 8.7996833 N 78.45355 W, 21 Jun. 2017, *D. Haelewaters et al.*, on *Tri. joblingi* (collected from female *Carollia brevicauda*), isolate 1322a (one mature thallus, base of right wing R1 vein, SSU: MH040543, LSU: MH040577); Darién Province, Reserva Natural Chucantí, field site Potrerito, old-growth broadleaf forest, 8.7909833 N 78.4510333 W, 22 Jun. 2017, *D. Haelewaters et al.*, on male *Tri. joblingi* (collected from male *C. perspicillata*), isolate D. Haelew. 1327a (one mature thallus, base of right wing, SSU: MH040544, LSU: MH040578).

Gloeandromyces pageanus* f. *polymorphus Haelew., **forma nov.** MycoBank MB827805. Fig. 4E–F.

Etymology: From Greek (*poly* + *morphus*), existing in multiple forms.

Diagnosis: Recognized by its morphology, with the perithecial venter ending in four conspicuous bumps, in combination with its LSU sequence, which is 100 % similar to *G. pageanus* f. *alarum*, 99.7 % similar to *G. pageanus* f. *pageanus*, and 91.9–98.1 % similar to other species of *Gloeandromyces*.

Description: *Thallus* faintly yellowish, with distinctly darker upper half of cell III, basal cell of appendage, and upper portions of cells VI and VII. *Cell I* 3.3–3.8 \times longer than broad, curved towards posterior side, broadening upwards, carrying cells II and VI. *Cell II* irregularly trapezoidal, slightly broader than long,

septum II/III very oblique. *Cell III* broader than long, usually with convex outer margins. *Basal cell of appendage* pentagonal, with parallel anterior and posterior margins, carrying two short (up to 20 μm) branches of dichotomously dividing cells, final cells antheridial. *Cell VI* broader than long, obliquely positioned between cells II and VII, allantoid to broadly triangular, with rounded lower margin. *Perithecial venter* with slightly diverging margins, anterior nearly straight, posterior slightly convex, ending in four conspicuous bumps; neck abruptly distinguished, with subparallel margins, slightly curving towards anterior side, distinctly inflated at junction with tapering, subconical tip; ending with blunt apex directed upwards.

Measurements: *Thallus* 183–189(–311) μm in length from foot to perithecial tip. *Cell I* 66–69(–120) \times 18–26 μm (distally). *Basal cell of appendage* 5–7(–12) \times 11–12(–15) μm . *Perithecium* 89–96(–152) \times 31–35 μm .

Typus: **Panama**, Colón Province, Península Bohío, 9.2045036 N 79.8299767 W, 3 Jul. 2015, *T. Hiller*, on male *Trichobius joblingi* (collected from female *Carollia perspicillata*), slide D. Haelew. 1073a (FH 00313705, **holotype**, two mature thalli, left-hand side abdomen); Colón Province, Parque Nacional Soberanía, Pipeline Road, Tunnel 10, 2 Jun. 2017, *D. Haelewaters & L.A. Meckler*, on *Tri. dugesioides* (collected from *T. cirrhosus*), slide D. Haelew. 1272b (FH 00313706, **paratype**, three mature thalli, right metatibia).

Material sequenced: **Panama**, Colón Province, Península Bohío, 9.2045036 N 79.8299767 W, 3 Jul. 2015, *T. Hiller*, on male *Trichobius joblingi* (collected from female *Carollia perspicillata*), isolate D. Haelew. 1073b (three mature thalli, left-hand side abdomen, SSU: MH040538, LSU: MH040570); Colón Province, Gamboa, 25 Apr. 2016, *R.A. Page et al.*, on *Trichobius dugesioides* (collected from female *Trachops cirrhosus*), isolate D. Haelew. 1089a (four mature thalli, left-hand side abdomen, SSU: MH040539, LSU: MH040571); Colón Province, Gamboa, Harding Avenue past Building 183, 9.115876 N 79.696784 W, 17 Jul. 2016, *D. Haelewaters*, on *Trichobius joblingi* (collected from female *Carollia perspicillata*), isolate D. Haelew. 1100b (two submature & five mature thalli, right profemur & protibia, SSU: MH040307, LSU: MH040572); Colón Province, Parque Nacional Soberanía, Pipeline Road, Tunnel 10, 2 Jun. 2017, *D. Haelewaters & L.A. Meckler*, on *Tri. dugesioides* (collected from *T. cirrhosus*), isolate D. Haelew. 1272a (two mature thalli, left metafemur, SSU: MH040540, LSU: MH040573); Darién Province, Reserva Natural Chucantí, field site Waterfall, young secondary succession forest, 8.7865167 N 78.4508333 W, 19 Jun. 2017, *D. Haelewaters et al.*, on *Tri. joblingi* (collected from male *C. perspicillata*), isolate D. Haelew. 1315a (one mature thallus, right sternopleuron, LSU: MH040575); same data, isolate D. Haelew. 1315b (two mature thalli, right profemur, SSU: MH040542, LSU: MH040576). **Trinidad and Tobago**, Trinidad, Sangre Grande Regional Corporation, 10.4671389 N 61.2025833 W, 9 May 2014, *J.J. Camacho*, on *Tri. joblingi* (collected from female *C. perspicillata*), isolate D. Haelew. 619a (12 mature thalli, different body parts, SSU: MH040537, LSU: KT800008), erroneously identified as *G. nycteribiidarum* in Haelewaters *et al.* (2015).

Notes: The thalli from Península Bohío are slenderer and somewhat darker colored compared to those from Soberanía. This is due to phenotypic plasticity because the DNA of the isolates from these localities is identical. The thalli from slide

D. Haelew. 1308a were preliminarily thought to be identical to those described here, under f. *polymorphus*. Also these thalli show four conspicuous bumps at the distal end of the perithecial venter. However, isolate D. Haelew. 1308b is placed in the A clade, as *G. streblae*. In addition, the host species are different: the bat fly host for *G. streblae* clade A is *Tri. dugesioides*, whereas the (main) host species for *G. pageanus* f. *polymorphus* is *Tri. joblingi*. This might be a case of cryptic diversity in the *Laboulbeniales*. However, it is likely that this form falls under the phenotypic plasticity exhibited by *G. streblae* (see Discussion).

Gloeandromyces streblae (Thaxt.) Thaxt., *Mem. Amer. Acad. Arts* 16: 113. 1931.

Basionym: *Stigmatomyces streblae* Thaxt., *Proc. Amer. Acad. Arts* 52: 700. 1917.

Notes: This species was described based on material from a single bat fly *Strebla wiedemanni* [as *S. vespertilionis*] (*Diptera*, *Streblidae*, *Streblinae*) from Venezuela. This poses a problem; our material of *G. streblae* was collected from *Tri. dugesioides* and *Tri. joblingi*. Although not recognized as separate species by our SDMs, we found evidence for two clades within *G. streblae* (clades A and B), both clades correlating with isolates from a

single host species. This points to divergence by host species, and because we do not have isolates available of thalli from *S. wiedemanni*, we do not know the “true” *G. streblae*. As a result, we refrain from formally re-describing or emending the description for this species. Molecular synapomorphies diagnostic for clade A+B are found at positions 52, 224, 360, 380, 447 (deletion), 450 (deletion), 518, 557, 566, 594, 725–727 (deletions), 730.

Based on our molecular data, it is evident that the thalli that we had initially identified as a new species based on morphology (*Gloeandromyces* sp. nov. 2 *sensu* Walker *et al.* 2018), are part of the B clade, together with thalli of “typical” *G. streblae*. As is the case with *G. pageanus* f. *alarum*, this morphotype seems restricted to a precise position of the host’s integument. We have only observed thalli of this morphotype at the last sternite/tergite. Again, to avoid confusion when referring to these thalli, we will describe them as *G. streblae* f. *sigmomorphus*.

Gloeandromyces streblae* f. *sigmomorphus Haelew., *forma nov.* MycoBank MB827806. Figs 5, 6.

Etymology: Referring to the general habitus of the fungus, which is curved like the letter s (sigma in Greek).

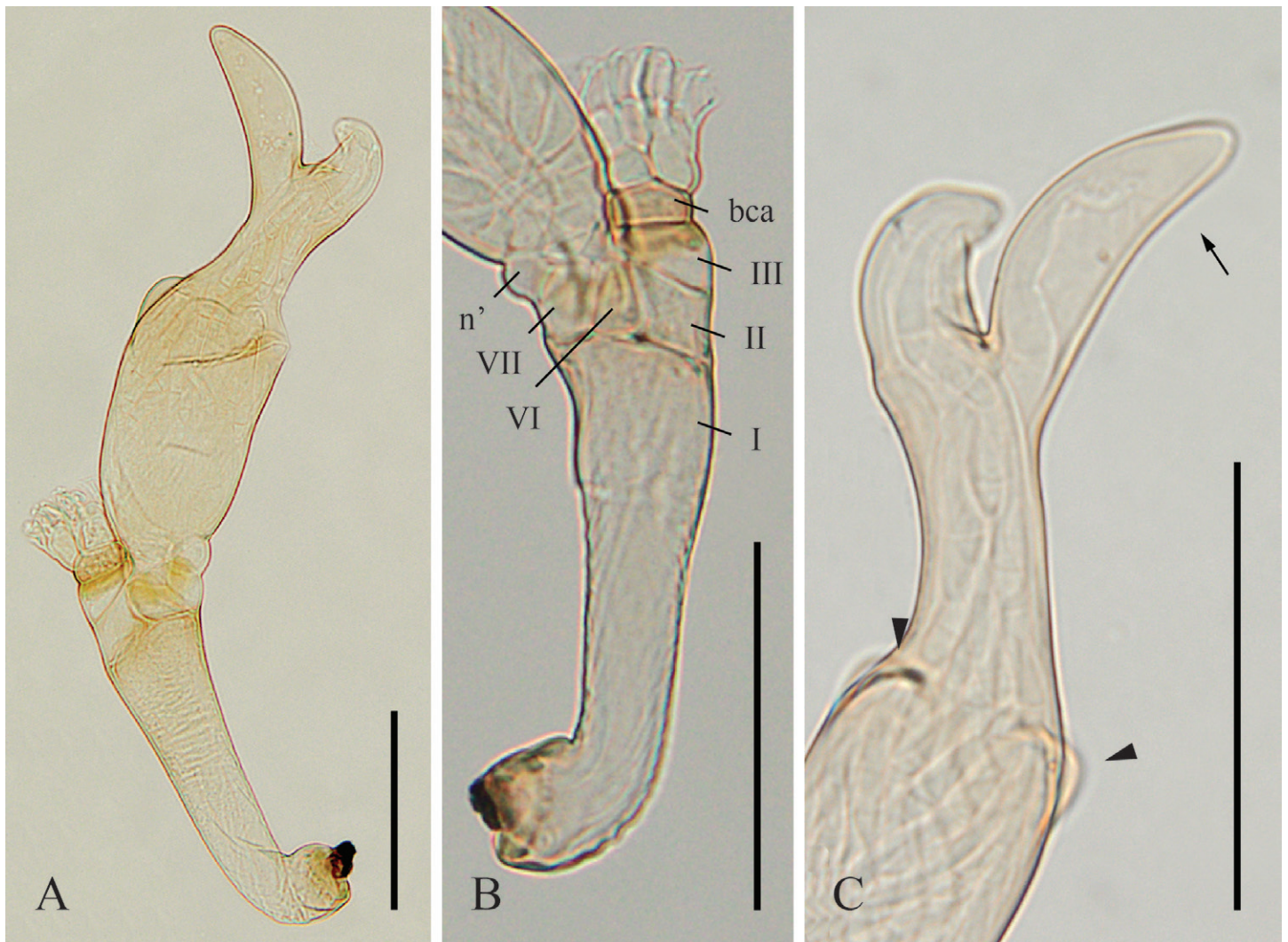


Fig. 5. Thalli of *Gloeandromyces streblae* f. *sigmomorphus*. **A.** Mature thallus from slide FH 00313703 (paratype). **B–C.** Details of mature thallus from slide FH 00313704 (holotype). **B.** Details of receptacle, appendage, and perithecial base, with annotated cells I, II, III, VI, VII, n', and the basal cell of the appendage (bca). **C.** Details of upper perithecial venter, with conspicuous rounded bumps at the distal end of the perithecial venter (arrowheads) and the very large preapical outgrowth (arrow). Scale bars = 50 µm.

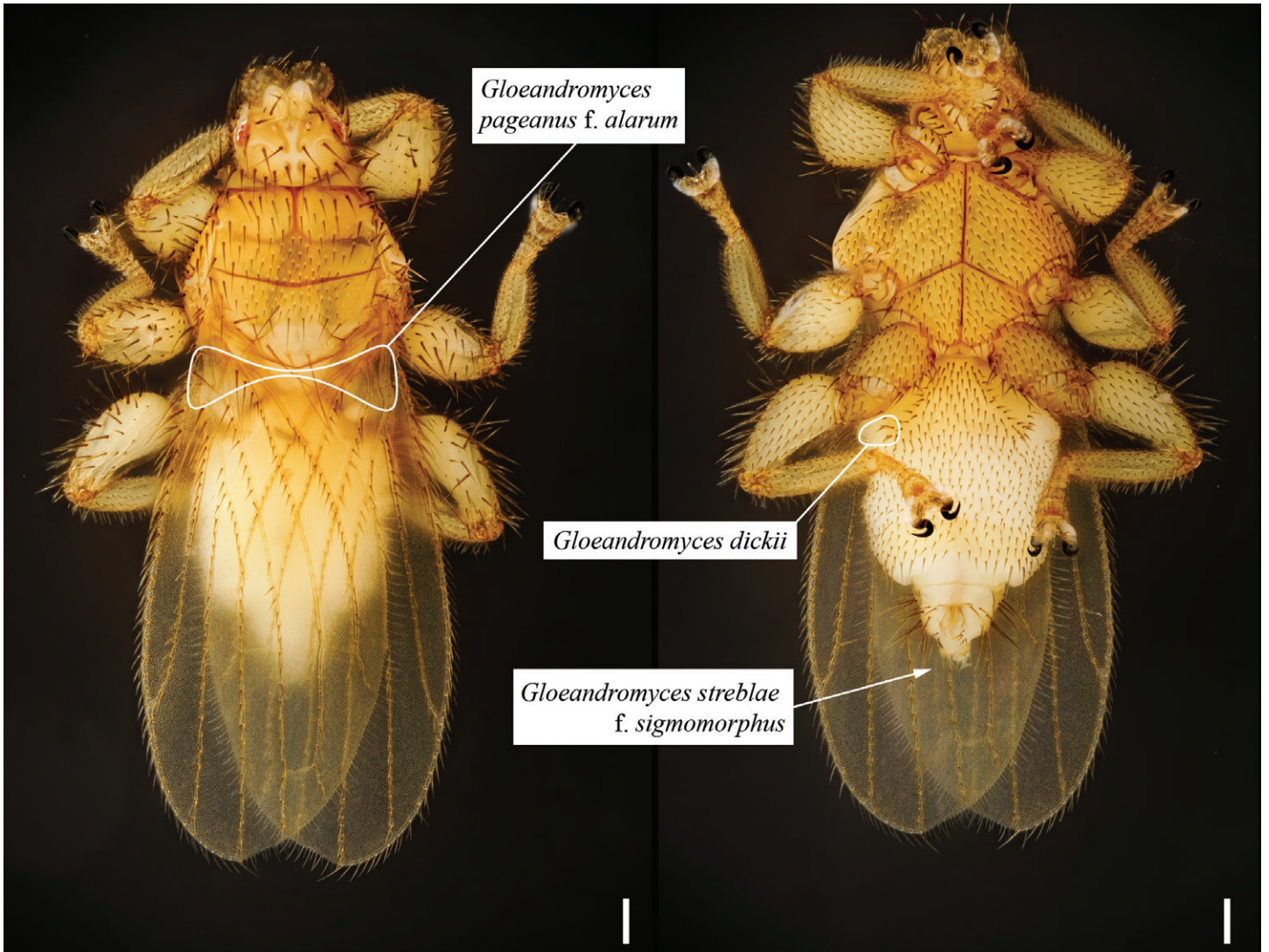


Fig. 6. A specimen of a *Trichobius* bat fly, photographed *in situ* dorsally (left) and ventrally (right). Annotated (encircled or with arrow) are the positions of the bat fly cuticle at which some (morpho-)species of *Gloeandromyces* seem to be restricted to: *G. dickii* on the abdomen, ventrally, at the right side; *G. pageanus* f. *alarum* at the base of both wings; and *G. streblae* f. *sigmomorphus* at the last tergite/sternite. Scale bars = 100 μ m. Images provided by André De Kesel.

Diagnosis: Different from the other species and *formae* in the genus by its sigmoid habitus. The LSU sequence is 97.6–98.1 % similar to other species of *Gloeandromyces*.

Description: *Thallus* pale yellowish, upper portion of cell III and basal cell of appendage tinged with darker yellow. *Cell I* 3.0–4.1 \times longer than broad, basally curved towards anterior side, otherwise straight, gradually broadening upwards, with outer wall longitudinally or radially striped, carrying cells II, VI, and VII. *Cell II* rhomboidal, slightly broader than long, separated from cell III by oblique septum. *Cell III* triangular and broader than long. *Basal cell of appendage* broader than long, pentagonal, with parallel anterior and posterior margins, carrying two short (up to 19 μ m) branches of dichotomously dividing cells, outer suprabasal cell always higher than inner one, final cells antheridial. *Cell VI* between cells II and VII, ovoidal to broadly triangular. *Cell VII* similar to cell VI. *Cell n'* inflated, outer margin rounded, protruding between cell VII and lower end of perithecium. *Perithecial venter* with margins slightly diverging upwards to conspicuous rounded prominences of wall cells; neck with broad base, short and stout; apex blunt, distinctly

bent towards posterior side, subtended by a very large, sickle-shaped outgrowth at posterior side.

Measurements: *Thallus* 201–243 μ m in length from foot to perithecial tip. *Cell I* 65–85 \times 19–22 μ m (distally). *Basal cell of appendage* 6–8 \times 11–12 μ m. *Perithecium* 115–126 \times 27–30 μ m. *Horn-like perithecial appendage* 36–44 μ m in length.

Typus: Panama, Darién Province, Reserva Natural Chucantí, field site Potrerito, old-growth broadleaf forest, 8.7909833 N 78.4510333 W, 20 Jun. 2017, D. Haelewaters et al., on *Tri. joblingi* (collected from female *C. perspicillata*), slide D. Haelew. 1320a (FH 00313704, **holotype**, one juvenile & one mature thallus, last sternite/tergite), referred to as *Gloeandromyces* sp. nov. 2 in Walker et al. (2018); Colón Province, Gamboa, Harding Avenue past Building 183, 9.115876 N 79.696784 W, 17 Jul. 2016, D. Haelewaters, on *Trichobius joblingi* (collected from female *Carollia perspicillata*), slide D. Haelew. 1099b (FH 00313703, **paratype**, five mature thalli, tip of last sternite), referred to as *Gloeandromyces* sp. nov. 2 in Walker et al. (2018).

Material sequenced: Panama, Darién Province, Reserva Natural Chucantí, field site Potrerito, old-growth broadleaf forest, 8.7909833 N 78.4510333 W, 20 Jun. 2017, D. Haelewaters *et al.*, on *Tri. joblingi* (collected from female *C. perspicillata*), isolate D. Haelew. 1320b (one mature thallus, last sternite/tergite, SSU: MH040545, LSU: MH040579).

DISCUSSION

GMYC recognizes *G. streblae* (clade A+B) and *G. pageanus* (clade C+D) as species, but the Bayesian support values are low (pp = 0.33 and 0.41, respectively). De Kesel (1997) argued that populations of *Laboulbeniales*-parasitized insects are similar to islands in the model of island biogeography (MacArthur & Wilson 1967). Divergence of host populations and subsequent speciation will lead to population divergence of the ectoparasites by isolation of gene pools. With regard to bat fly hosts, *Tri. dugesioides* can be exchanged between several bat species and thus co-occur with *Tri. joblingi* (see further). This might lead to intermittent gene flow between *Gloeandromyces* populations, complicating branching rates of gene trees. In addition, Esselstyn *et al.* (2012) mentioned that any given GMYC analysis can accurately estimate the number of species, even though it may not correctly assign individuals to species when taxonomically defined species are not monophyletic, which is the case for *G. pageanus*. The monophyly of clade D is unsupported, causing it to collapse. In other words, the node that describes *G. pageanus* is an unresolved polytomy between the highly supported clade C and the isolates that form clade D.

The ABGD analysis gives different numbers of putative species depending on P, the prior intraspecific divergence. If this parameter is set too high, the entire dataset will be seen as a single species; if set too low, only identical sequences will be retrieved as species (Puillandre *et al.* 2012). These authors also proposed to use P = 0.01 as this setting provided highest congruence with previous studies (meaning that under this setting, ABGD results matched the number of species found by previous studies using other approaches). Indeed, when P = 0.01, the ABGD results in four species of *Gloeandromyces*, congruent with bPTP and GMYC results. These congruent estimates of species diversity within the LSU rDNA dataset provide confidence in our understanding of *Gloeandromyces*, based on the currently available data.

We identified seven “morphospecies” (or morphotypes) of *Gloeandromyces* on the basis of morphological characters but this morphological diversity is not reflected in phylogenetic inference by LSU rDNA barcode sequences. Using SDMs resulted in four species only: *Gloeandromyces dickii*, *G. nycteribiidarum*, *G. pageanus*, and *G. streblae*. In *G. pageanus*, thalli from *Tri. dugesioides* are in line with the original description of the species by Haelewaters *et al.* (2017b). However, thalli on *Tri. joblingi* showed two distinct morphologies. One morphotype, *G. pageanus* f. *alarum*, was restricted to the base of the wings (Fig. 6), whereas the other, *G. pageanus* f. *polymorphus*, was not restricted to a particular position on the host. In *G. pageanus*, two mechanisms drive diversity: 1) host specialization, resulting in the two clades segregating by host species (*sensu* Haelewaters *et al.* 2018a), and 2) position-induced morphological adaptations, resulting in the wing-restricted f. *alarum* (*sensu* Goldmann & Weir 2012, Goldmann *et al.* 2013).

In their study of species in the genus *Coreomyces* on water boatmen (*Hemiptera*, *Corixidae*), Sundberg *et al.* (2018) found that different species can occupy the same position on the host, without strict position specificity. Each of the four considered species occurs in two or three positions, with one position much more preferred over the others. The authors also pointed out that the considered species did not show strict host specificity. For example, thalli of *C. corixae* (green clade in Sundberg *et al.* 2018) were removed from species in the genera *Callicorixa*, *Hesperocorixa*, and *Sigara* (Sundberg 2018). In other words, contrary to *Hesperomyces* and *Gloeandromyces* in which specialization on different hosts drives divergent evolution (Haelewaters *et al.* 2018a, b, this study), host species does not seem to be a major factor in species delimitation within *Coreomyces*.

Two *G. pageanus* isolates seem aberrant, D. Haelew. 1089a and 1272a; these isolates were removed from *Tri. dugesioides* but are present in clade D, which includes *Tri. joblingi* isolates. We think we can explain this by bat fly behavior and interactions. Bat flies are usually strictly host specific, with non-primary associations being defined as host species with less than 5 % of the total individuals of a parasite species (Dick 2007). When Wenzel *et al.* (1966) described *Tri. dugesioides*, they reported it from *Trachops cirrhosus*, *Chrotopterus auratus*, and *Carollia perspicillata*, all bats in the family *Phyllostomidae*. The main hosts are *T. cirrhosus* and *C. auratus*. Because *C. perspicillata* bats make use of the same roost environments, *Tri. dugesioides* can be “exchanged” between these bat species. Apparently, dynamics are different for *Tri. joblingi*, which is strictly restricted to *Carollia* species.

Finally, even though SDMs only recognize four species of *Gloeandromyces*, it is evident that in *G. pageanus* and *G. streblae*, there is phylogenetic divergence by host species (Haelewaters *et al.* 2018b). This host specialization may represent an important first step in a potential radiation process; our results suggest a case of sympatric speciation into two incipient species, both in *G. pageanus* and *G. streblae*. Rosenblum *et al.* (2012) proposed the “ephemeral speciation model,” in which they postulated that speciation is common and rapid, but the new species produced almost never persist. This could be due to extinction or changes in conditions that maintain reproductive isolation.

ACKNOWLEDGEMENTS

Unknowingly, Jasmin Camacho (Harvard University) presented the first author with a silly little bat fly back in 2014. It was infected with *Gloeandromyces* and this single fly has turned into a collaborative project during which we now have looked at close to 10 000 bat flies. A thank you is in place. We would like to express our gratitude to the following researchers, without whom this manuscript would have been a lot scantier: Guido C. Berguido (Asociación Adopta el Bosque Panamá) generously assisted with logistics during fieldwork; André De Kesel (Botanic Garden Meise, Belgium) provided excellent *in situ* photographs of bat flies; Carl W. Dick (Western Kentucky University) provided bat fly specimens for this project; Edilma Gomez (Molecular Multi-User’s Lab, Panama) facilitated molecular work in Panama; Thomas Hiller (University of Ulm, Germany) identified the majority of our bat fly collections and has been a great collaborator and friend along the road; W. Owen McMillan (Smithsonian Tropical Research Institute, Panama) allowed usage of his lab facilities in Gamboa, Panama; Rachel A. Page (Smithsonian Tropical Research Institute, Panama) has been a wonderful

collaborator throughout this project, facilitating fieldwork and sharing knowledge and information; Walter Rossi (University of L'Aquila, Italy) provided feedback on drafted morphological descriptions. Funding for fieldwork (to D.H.) came from the following sources and institutions: David Rockefeller Center for Latin American Studies (Summer Research Travel Grant), Harvard University Herbaria (Fernald Fund), Mycological Society of America (Graduate Fellowship, Robert W. Lichtwardt Student Research Award), and Smithsonian Tropical Research Institute (Short-Term Research Fellowship). Pedro Crous (Westerdijk Fungal Biodiversity Institute, The Netherlands), Henrik Enghoff (Natural History Museum of Denmark), and an anonymous reviewer are thanked for critically reviewing the manuscript.

REFERENCES

- Benjamin RK (1971). Introduction and supplement to Roland Thaxter's contribution towards a monograph of the *Laboulbeniaceae*. *Bibliotheca Mycologica* **30**: 1–155.
- Bertola PB, Aires CC, Favorito SE, *et al.* (2005). Bat flies (*Diptera: Streblidae, Nycteribiidae*) parasitic on bats (*Mammalia: Chiroptera*) at Parque Estadual da Cantareira, São Paulo, Brazil: parasitism rates and host-parasite associations. *Memórias do Instituto Oswaldo Cruz* **100**: 25–32.
- Blum G (1924). Zwei neue *Laboulbenien* aus Brasilien. *Centralblatt für Bakteriologie, Parasitenkunde und Infektionskrankheiten, Zweite Abteilung* **62**: 300–302.
- Darriba D, Taboada GL, Doallo R, *et al.* (2012). jModelTest 2: more models, new heuristics and parallel computing. *Nature Methods* **9**: 772.
- De Kesel A (1995). Relative importance of direct and indirect infection in the transmission of *Laboulbenia slackensis* (*Ascomycetes, Laboulbeniales*). *Belgian Journal of Botany* **128**: 124–130.
- De Kesel A (1996). Host specificity and habitat preference of *Laboulbenia slackensis*. *Mycologia* **88**: 565–573.
- De Kesel A (1997). *Contribution towards the study of the specificity of Laboulbeniales (Fungi, Ascomycetes), with particular reference to the transmission, habitat preference and host-range of Laboulbenia slackensis*. Ph.D. dissertation. Department of Biology, University of Antwerp, Belgium.
- Dick CW (2007). High host specificity of obligate ectoparasites. *Ecological Entomology* **32**: 446–450.
- Dogonniuck AE, Squires TJ, Weir A. Studies on *Dimorphomycetaceae* I. New species of *Nycteromyces* and *Dimeromyces* (*Laboulbeniales*) on bat flies (*Streblidae*). *Mycologia*: In press.
- Drummond AJ, Suchard MA, Xie D, *et al.* (2012). Bayesian phylogenetics with BEAUti and the BEAST 1.7. *Molecular Biology and Evolution* **29**: 1969–1973.
- Edgar RC (2004). MUSCLE: multiple sequence alignment with high accuracy and high throughput. *Nucleic Acids Research* **32**: 1792–1797.
- Esselstyn JA, Evans BJ, Sedlock JL, *et al.* (2012). Single-locus species delimitation: a test of the mixed Yule–coalescent model, with an empirical application to Philippine round-leaf bats. *Proceedings of the Royal Society of London B: Biological Sciences* **279**: 3678–3686.
- Ezard T, Fujisawa T, Barraclough TG (2009). splits: SPecies' Limits by Threshold Statistics. R package version 1.0-14/r31. <http://R-Forge.R-project.org/projects/splits/> (<http://R-Forge.R-project.org/projects/splits/>).
- Fritz GN (1983). Biology and ecology of bat flies (*Diptera: Streblidae*) on bats in the genus *Carollia*. *Journal of Medical Entomology* **20**: 1–10.
- Gernhard T (2008). The conditioned reconstructed process. *Journal of Theoretical Biology* **253**: 769–778.
- Goldmann L, Weir A (2012). Position specificity in *Chitonomyces* (*Ascomycota, Laboulbeniomycetes*) on *Laccophilus* (*Coleoptera, Dytiscidae*): a molecular approach resolves a century-old debate. *Mycologia* **104**: 1143–1158.
- Goldmann L, Weir A, Rossi W (2013). Molecular analysis reveals two new dimorphic species of *Hesperomyces* (*Ascomycota, Laboulbeniomycetes*) parasitic on the ladybird *Coleomegilla maculata* (*Coleoptera, Coccinellidae*). *Fungal Biology* **117**: 807–813.
- Gracioli G, Coelho DC (2001). *Streblidae* (*Diptera, Hippoboscoidea*) sobre morcegos filomídeos (*Chiroptera, Phyllostomidae*) em cavernas do Distrito Federal Brasil. *Revista Brasileira de Zoologia* **18**: 965–970.
- Haelewaters D, De Kesel A, Pfister DH. 2018a. Integrative taxonomy reveals hidden species within a common fungal parasite of ladybirds. *Scientific Reports* **8**: 15966.
- Haelewaters D, Gorczak M, Pfliegler WP, *et al.* (2015). Bringing *Laboulbeniales* into the 21st century: enhanced techniques for extraction and PCR amplification of DNA from minute ectoparasitic fungi. *IMA Fungus* **6**: 363–372.
- Haelewaters D, Page RA, Pfister DH (2018b). *Laboulbeniales* hyperparasites (*Fungi, Ascomycota*) of bat flies: Independent origins and host associations. *Ecology and Evolution* **8**: 8396–8418.
- Haelewaters D, Pfliegler WP, Szentiványi T, *et al.* (2017a). Parasites of parasites of bats: *Laboulbeniales* (*Fungi: Ascomycota*) on bat flies (*Diptera: Nycteribiidae*) in Central Europe. *Parasites & Vectors* **10**: 96.
- Haelewaters D, Verhaeghen SJC, Ríos Gonzáles TA, *et al.* (2017b). New and interesting *Laboulbeniales* from Panama and neighboring areas. *Nova Hedwigia* **105**: 267–299.
- Jukes TH, Cantor CR (1969). Evolution of protein molecules. In: *Mammalian protein metabolism* (Munro NH, ed). Academic Press, New York: 21–132.
- Kimura M (1980). A simple method for estimating evolutionary rates of base substitutions through comparative studies of nucleotide sequences. *Journal of Molecular Evolution* **16**: 111–120.
- MacArthur RH, Wilson EO (1967). *The theory of island biogeography*. Princeton University Press, Princeton, New Jersey.
- Michonneau F, Bolker B, Holder M, *et al.* (2015) rnc1: an interface to the nexus class library. R package version 0.6.0. <http://CRAN.R-project.org/package=rnc1> (<http://CRAN.R-project.org/package=rnc1>).
- Miller MA, Pfeiffer W, Schwartz T (2010). Creating the CIPRES Science Gateway for inference of large phylogenetic trees. *Proceedings of the Gateway Computing Environments Workshop* 14 Nov. 2010: 1–8. New Orleans, Louisiana.
- Peyritsch J (1871). Über einige Pilze aus der Familie der *Laboulbenien*. *Sitzungsberichte der Kaiserlichen Akademie der Wissenschaften. Mathematisch-naturwissenschaftliche Classe* **64**: 441–458.
- Peyritsch J (1873). Beiträge zur Kenntniss der *Laboulbenien*. *Sitzungsberichte der Kaiserlichen Akademie der Wissenschaften. Mathematisch-naturwissenschaftliche Classe* **68**: 227–254.
- Pfliegler WP, Báthori F, Haelewaters D, Tartally A (2016). Studies of *Laboulbeniales* on *Myrmica* ants (III): myrmecophilous arthropods as alternative hosts of *Rickia wasmannii*. *Parasite* **23**: 50.
- Pons J, Barraclough TG, Gomez-Zurita J, *et al.* (2006). Sequence-based species delimitation for the DNA taxonomy of undescribed insects. *Systematic Biology* **55**: 595–609.
- Puillandre N, Lambert A, Brouillet S, *et al.* (2012) ABGD, Automatic Barcode Gap Discovery for primary species delimitation. *Molecular Ecology* **21**: 1864–1877.
- R Core Team (2013). R: a language and environment for statistical computing. Vienna, Austria: R Foundation for Statistical Computing. <http://www.R-project.org> (<http://www.R-project.org>).

- Rambaut A, Suchard MA, Xie D, *et al.* (2014). Tracer v1.6. <http://tree.bio.ed.ac.uk/software/tracer/> (<http://tree.bio.ed.ac.uk/software/tracer/>).
- Rosenblum EB, Sarver BAJ, Brown JW, *et al.* (2012). Goldilocks meets Santa Rosalia: an ephemeral speciation model explains patterns of diversification across time scales. *Evolutionary Biology* **39**: 255–261.
- Rossi W (2011). New species of *Laboulbenia* from Ecuador, with evidence for host switch in the *Laboulbeniales*. *Mycologia* **103**: 184–194.
- Rossi W, Bernardi M, Torres JA (2015). New species of *Dimeromyces* from Ecuador. *Mycological Progress* **14**: 5.
- Rossi W, Máca J, Preisler J (2016). A new parasitic fungus on the cleptoparasite of bees *Braula coeca* (Insecta, Diptera): *Dimeromyces braulae* (Ascomycota, Laboulbeniales). *Nova Hedwigia* **102**: 271–274.
- Sundberg H (2018). *Contributions to the understanding of diversity and evolution in the genus Coreomyces*. Ph.D. dissertation. Department of Organismal Biology, Uppsala University, Sweden.
- Sundberg H, Krusys Å, Bergsten J, Ekman S (2018). Position specificity in the genus *Coreomyces* (Laboulbeniomycetes, Ascomycota). *Fungal Systematics and Evolution* **1**: 217–228.
- Swofford DL (1991). *PAUP: Phylogenetic Analysis Using Parsimony, Version 3.1*. Computer program distributed by the Illinois Natural History Survey, Champaign, Illinois.
- Szentiványi T, Haelewaters D, Pfliegler WP, *et al.* (2018). *Laboulbeniales* (Fungi: Ascomycota) infection of bat flies (Diptera: Nycteribiidae) from *Miniopterus schreibersii* across Europe. *Parasites & Vectors* **11**: 395.
- Thaxter R (1901). Preliminary diagnosis of new species of *Laboulbeniaceae*. III. *Proceedings of the American Academy of Arts and Sciences* **36**: 397–414.
- Thaxter R (1917). New *Laboulbeniales*, chiefly dipterophilous American species. *Proceedings of the American Academy of Arts and Sciences* **52**: 649–721.
- Thaxter R (1924). Contribution toward a monograph of the *Laboulbeniaceae* III. *Memoirs of the American Academy of Arts and Sciences* **14**: 309–426, Pl. I–XII.
- Thaxter R (1931). Contribution toward a monograph of the *Laboulbeniaceae* V. *Memoirs of the American Academy of Arts and Sciences* **16**: 1–435, Pl. I–LX.
- Walker MJ, Dorrestein A, Camacho JJ, *et al.* (2018). A tripartite survey of hyperparasitic fungi associated with ectoparasitic flies on bats (Mammalia: Chiroptera) in a neotropical cloud forest in Panama. *Parasite* **25**: 19.
- Weir A, Blackwell M (2001). Extraction and PCR amplification of DNA from minute ectoparasitic fungi. *Mycologia* **93**: 802–806.
- Weir A, Hammond PM (1997). *Laboulbeniales* on beetles: Host utilization patterns and species richness of the parasites. *Biodiversity and Conservation* **6**: 701–719.
- Wenzel RL, Tipton VJ, Kiewlicz A (1966). The streblid batflies of Panama (Diptera Calypterae: Streblidae). In: *Ectoparasites of Panama* (Wenzel RL, Tipton VJ, eds). Field Museum of Natural History, Chicago: 405–676.
- Yule GU (1925). A mathematical theory of evolution based on the conclusions of Dr. J. C. Willis. *Philosophical Transactions of the Royal Society B* **213**: 21–87.
- Zhang J, Kapli P, Pavlidis P, *et al.* (2013) A general species delimitation method with applications to phylogenetic placements. *Bioinformatics* **29**: 2869–2876.

doi.org/10.3114/fuse.2019.03.04

Miracula moenusica, a new member of the holocarpic parasitoid genus from the invasive freshwater diatom *Pleurosira laevis*

A.T. Buaya^{1,2}, M. Thines^{1,2*}

¹Goethe University, Department of Biological Sciences, Institute of Ecology, Evolution and Diversity, Max-von-Laue-Str. 13, D-60486 Frankfurt am Main, Germany

²Senckenberg Biodiversity and Climate Research Centre, Senckenberg Gesellschaft für Naturforschung, Senckenberganlage 25, D-60325 Frankfurt am Main, Germany

Key words:

diatom parasites
holocarpic oomycetes
life-cycle
phylogeny
taxonomy

*Corresponding author: m.thines@thines-lab.eu

Abstract: Holocarpic oomycetes are poorly known but widespread parasites in freshwater and marine ecosystems. Most of the holocarpic species seem to belong to clades that diverge before the two crown lineages of the oomycetes, the *Saprolegniomycetes* and the *Peronosporomycetes*. Recently, the genus *Miracula* was described to accommodate *Miracula helgolandica*, a holocarpic parasitoid of *Pseudo-nitzschia* diatoms, which received varying support for its placement as the earliest-diverging oomycete lineage. In the same phylogenetic reconstruction, *Miracula helgolandica* was grouped with some somewhat divergent sequences derived from environmental sequencing, indicating that *Miracula* would not remain monotypic. Here, a second species of *Miracula* is reported, which was found as a parasitoid in the limnic centric diatom *Pleurosira laevis*. Its life-cycle stages are described and depicted in this study and its phylogenetic placement in the genus *Miracula* revealed. As a consequence, the newly discovered species is introduced as *Miracula moenusica*.

Effectively published online: 14 January 2019.

INTRODUCTION

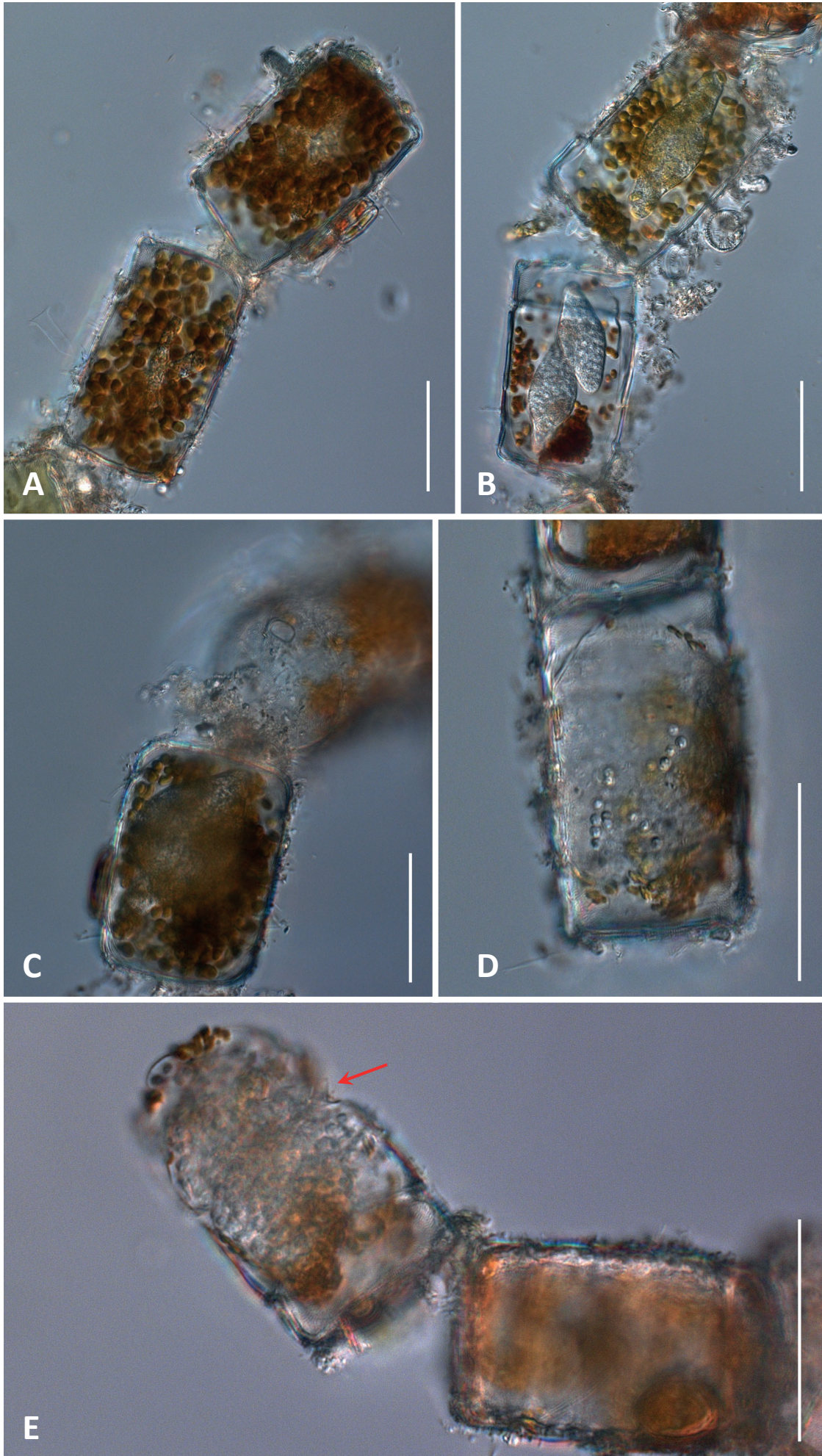
Despite their global distribution in various habitats, including streams, lakes, and oceans, holocarpic oomycetes are still poorly known (Scholz *et al.* 2016). However, these organisms play a pivotal role in the breakdown of plankton blooms, as parasitoids of multicellular and unicellular algae (Scholz *et al.* 2016, Raghukumar 2017, Buaya *et al.* 2017). Most work on diatom parasitoids has been published in the late 19th and early 20th century, with the monographic treatments of Karling (1942) and Sparrow (1960) pretty much reflecting the current knowledge of this group. Only recently, research interest in oomycete parasitoids of diatoms has increased again, leading to the phylogenetic characterisation of *Lagenisma coscinodisci*, a pathogen of centric diatoms of the genus *Coscinodiscus* (Thines *et al.* 2015a), and the description of two new diatom parasitoids, *Olpidiopsis drebesii* in *Rhizosolenia* spp. and *Miracula helgolandica* in species of the genus *Pseudo-nitzschia* (Buaya *et al.* 2017). While *L. coscinodisci* was found to belong to the early-diverging members of one of the two crown oomycete lineages, the *Saprolegniomycetes*, the other two parasitoids were branching below the *Peronosporomycetes*/*Saprolegniomycetes* split. *Olpidiopsis drebesii* grouped loosely with other *Olpidiopsis* species on red algae, while *Miracula helgolandica* was inferred to likely be the most early-divergent oomycete lineage (Buaya *et al.* 2017). Both new species were grouped with several somewhat divergent environmental sequences, suggesting a widespread nature and the presence

of additional, still undiscovered species. While screening for diatom-infecting oomycetes in water and sediment samples from the river Main, a tributary to the central to western European stream Rhine, an unusual parasitoid was found in *Pleurosira laevis*, an invasive species (Litchman 2010) which had not been reported as host for holocarpic oomycetes before. It was the aim of this study to characterise this pathogen in terms of phylogenetic relationships and life cycle and to clarify its taxonomic assignment.

MATERIALS AND METHODS

Diatom sampling

In September 2018, sediment surface samples were taken from the banks of the river Main in Frankfurt am Main Germany, by scraping biofilms into 1 L plastic bottles, which were subsequently filled half with water from the river. Samples were brought to the laboratory and screened by pouring sediment suspension into 9-cm-diam Petri dishes and observing them at 50–100 × magnification on an inverted microscope (AE31, Motic, China). Infected diatom cells were transferred to droplets of tap water and observed at 400 × using a Zeiss Imager equipped with DIC and an AxioCam (Zeiss, Oberkochen, Germany). For phylogenetic investigations, around 20 infected filaments were collected in a 2 mL vial containing 1 mL of Ambion RNA Later™ solution (Sigma-Aldrich, Munich, Germany).



DNA extraction, PCR, and sequencing

For DNA extraction, the tube was centrifuged in a table centrifuge at 19 000 *g* for 2 min and the RNA Later was removed by pipetting. Subsequently, samples were disrupted, and DNA was extracted using the innuprep plant DNA extraction kit (analyticjena, Jena, Germany), as described earlier (Buaya *et al.* 2017). PCR for the amplification of partial small ribosomal subunit (18S nrDNA) and sequencing were performed as described in Buaya *et al.* (2017). Sequencing was done by the Laboratory Centre of the Senckenberg Biodiversity and Climate Research Centre, with the primers Euk573 and Euk1422 (Wang *et al.* 2014), which were also used in PCR. The consensus sequence of the parasite of *Pleurosira laevis* was deposited in GenBank under the accession number MK239934.

Phylogenetic inference

Sequences were added to the dataset of Buaya *et al.* 2017 and aligned using MUSCLE with standard settings in MEGA v. 5 (Tamura *et al.* 2011), except for using a gap opening penalty of -200 and a gap extension penalty of -4. Phylogenetic inference was done using RAxML v. 8 (Stamatakis 2014) with the GTRGAMMA model and running 1 000 bootstrap replicates for Maximum Likelihood analysis, and using MEGA v. 5 (Tamura *et al.* 2011) with the Tamura-Nei model and running 1 000 bootstrap replicates for Minimum Evolution analysis.

RESULTS

Life-cycle observation

Filaments infected with oomycete parasitoids were observed from September 2018 to November 2018, usually at low abundance (less than 5 % of filaments infested). The parasitoid becomes first visible near the central nucleus, rod-shaped, elongating towards the periphery. Subsequently the central part enlarges, giving the thalli a lemon-shaped appearance. Parasitoids remain at this shape for some time, steadily increasing in volume. Towards the end of this stage, chloroplasts degrade into irregular shapes and assume a reddish-brown colouration. Subsequently, a large, central vacuole is forming, the thallus again increasing in size, until almost filling the diatom cells. Within the cytoplasm, the formation of refractive structures can be observed, and zoospores start to mature. When compartmentation is almost concluded, tubular exit tubes with a slightly thickened base develop at or close to the girdle region and push between the valves. Zoospores begin moving within the mature thallus, and then the discharge tube ruptures at the apex, releasing roundish, biflagellate zoospores into the surrounding medium, which swim away from the host cell. After a few minutes, zoospores come to rest. If they assume movement again has not been seen. Frequently, a few zoospores come to rest within the empty thallus and take a globose shape. If they develop further into meioszoospores or if they start moving again has not been observed. The different stages of the life-cycle are illustrated in Fig. 1.

Phylogenetic inference

In the phylogenetic trees based on partial small ribosomal subunit sequences of the parasitoid of *Pleurosira laevis* grouped together with *Miracula helgolandica* and two sequences derived from environmental sequencing with maximum support in all analyses (Fig. 2). Collectively, they formed the earliest-diverging oomycete lineage, but without strong support. The parasitoid from the river Main was sister to all remaining lineages in *Miracula*, which were grouped together with maximum support in all analyses. Apart from *Lagenisma coscinodisci*, which grouped with other early diverging members of the *Saprolegniomycetes*, all other holocarpic parasitoids of algae and diatoms branched before the split of *Peronosporomycetes* and *Saprolegniomycetes*. These crown oomycete classes were grouped together with moderate to strong support. While the *Peronosporomycetes* and the crown *Saprolegniomycetes* were each grouped together with strong support, the sister-group relationship of the crown *Saprolegniomycetes* and the early-diverging lineages was only weakly supported. The branching order of the early-diverging subclades was not well resolved, but some of the groups received moderate (*Haptoglossa* and *Eurychasma*; *Haliphthoros*, *Halocrusticia*, and *Halodaphnea*), to strong support (phaeophyte parasitoids – *Anisolpidium ectocarpus*, *Olpidiopsis drebesii*, and three sequences derived from environmental sequencing). The parasitoids of red algae did not form a monophyletic assemblage, however, without support.

Taxonomy

Due to its unique development, diatom host and phylogenetic placement, a new species of *Miracula* is introduced here.

Miracula moenusica A. Buaya & Thines, *sp. nov.* MycoBank MB829271. Fig. 1.

Etymology: From *moenus*, the Latin name of the river Main.

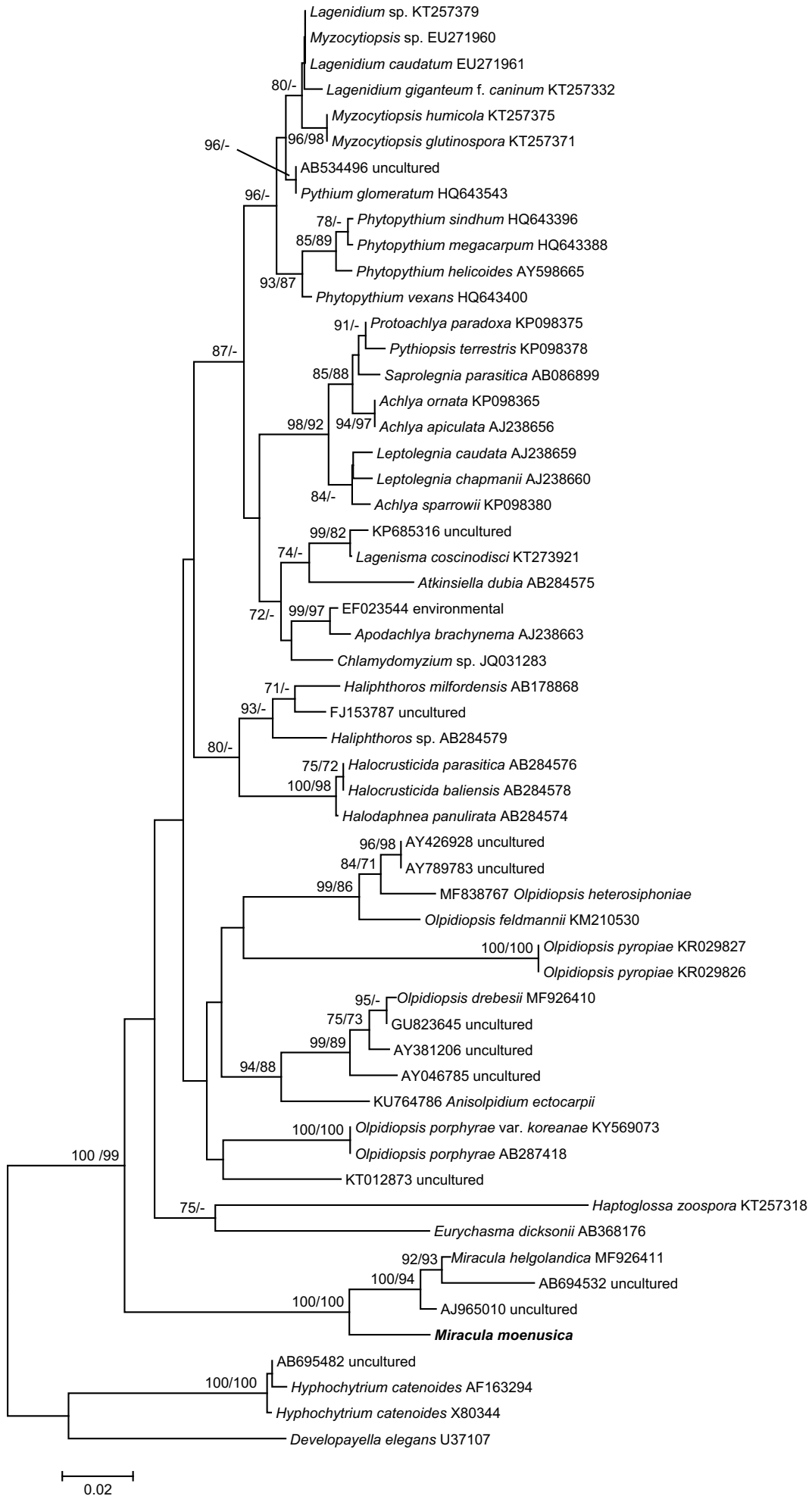
Diagnosis: Differs from *Miracula helgolandica* by its lemon-shaped maturing thallus, its more elongated discharge tube, its host in *Coscinodiscophyceae*, and its occurrence in a freshwater habitat.

Description: *Thallus* hyaline, normally one, rarely two to three, endobiotic in *Pleurosira laevis*, rod shaped when young, lemon-shaped during maturation, expanding until large parts of the host cell are filled, up to 100 µm long; *wall* thin, smooth, colourless; *zoospore cleavage* from a large central vacuole; *zoospores* roundish to grape-seed-shaped, 2–3 µm in diameter, beginning movement within the thallus; *exit tube* single, with a somewhat thickened base, 4–6 µm wide, 4–8 µm long.

Typus: **Germany**, Hessen, Frankfurt, northern bank, in *Coscinodiscophyceae* in freshwater, *leg. A. Buaya*, Sep. 2018 (**holotype** specimen in the Herbarium Senckenbergianum under the accession number FR0046007). Ex-type sequence deposited in GenBank under the accession number MK239934.

Known distribution: Germany, river Main.

Fig. 1. Micrographs (DIC) of various developmental stages of *Miracula moenusica*. **A.** Young, elongate thalli. **B.** Early limoniform stage. **C.** Late limoniform stage with intermediate thallus expansion. **D.** Fully expanded and empty thallus with several encysted zoospores that failed to escape inside. **E.** Discharge tube (arrow) developing from a thallus with maturing zoospores. Scale bars: 50 µm.



DISCUSSION

While the past two decades have seen huge advances towards a natural system of the crown oomycetes, in particular for both obligate biotrophic plant pathogens (Constantinescu 1998, Constantinescu & Fatehi 2002, Göker *et al.* 2003, Voglmayr *et al.* 2004, Constantinescu *et al.* 2005, Thines & Spring 2005, Thines *et al.* 2006, 2007, 2015b, Voglmayr & Constantinescu 2008, Telle & Thines 2011) and cultivable *Peronosporomycetes* (Bala *et al.* 2010, Hulvey *et al.* 2010, Uzuhashi *et al.* 2010, Li *et al.* 2016, Bennett *et al.* 2017, Jung *et al.* 2017), many genera of the *Saprolegniomycetes* and even more that were assumed to belong to the early-diverging oomycetes have not been revised, so far (Beakes & Sekimoto 2009, Beakes *et al.* 2014, Beakes & Thines 2017). However, the finding that some oomycete lineages diverged before the two major classes (Hudspeth *et al.* 2003), has spurred some interest in holocarpic oomycetes and has revealed the genera *Haptoglossa* and *Eurychasma* as the earliest-diverging lineages (e.g. Sekimoto *et al.* 2008, 2009, Gachon *et al.* 2017), a placement that only recently has been contested by the holocarpic diatom parasitoid *Miracula helgolandica* (Buaya *et al.* 2017). *Miracula helgolandica* parasitises the filamentous diatoms of the genus *Pseudo-nitzschia* (Hanic *et al.* 2009, Buaya *et al.* 2017) and could not be assigned to any of the five holocarpic genera known to parasitize diatoms (*Aphanomycoopsis*, *Ectrogella*, *Lagenidium*, *Lagenisma*, and *Olpidiopsis*), which was the reason the new genus *Miracula* had been introduced. Overall, the evolutionary diversity of oomycetes parasitising diatoms seems to be very high, as witnessed by the relatively many descriptions of such organisms in the second half of the 19th and the first half of the 20th century (Zopf 1884, Karling 1942, Sparrow 1960, Drebes 1968, and references therein). So far, sequence data are available only from *Lagenisma*, *Miracula*, and *Olpidiopsis* diatom parasitoids. For all these genera, sequences from environmental sequencing exist, suggesting the presence of additional species that await their discovery. The finding of a second member of the genus *Miracula* in this study supports this notion. That *Miracula moenusica* was found in a freshwater environment is another example of the wide ecological amplitude of water-borne oomycetes, in which the border between marine and freshwater environments has been crossed several times, e.g. in *Haptoglossa* (Beakes & Sekimoto 2009), *Phytophthium* (Thines 2014), and *Halophytophthora* (Yang & Hong 2014). *Miracula moenusica* bears some similarity to *Ectrogella monostoma* (Scherffel 1925, Sparrow 1960), in the central swellings of the thallus. However, the behaviour or the zoospores is rather olpidioid in the former species, as they swim away from the host after emergence, rather than encysting directly at the orifice for the formation of secondary zoospores in the latter species. As in addition to these differences, the host species, *Pleurosira leavis*, has not been reported as a host of oomycete parasitoids, it seems that the species has not been observed previously. The unexpected observation of a second species of *Miracula* in a freshwater diatom, as well as the recent finding of a marine *Olpidiopsis* species in *Rhizosolenia* diatoms highlights that the diversity of holocarpic oomycetes is largely uncharted and promises to hold additional surprises for the future.

ACKNOWLEDGEMENTS

We are grateful to Sebastian Ploch for laboratory support and KAAD for funding. Author contributions – ATB and MT conceived the study, ATB planned and conducted PCR experiments as well as sequencing and performed light microscopy, ATB and MT analysed the sequence data, MT wrote the manuscript with contributions from ATB.

REFERENCES

- Bala K, Robideau GP, Lévesque CA, *et al.* (2010). *Phytophthium* Abad, de Cock, Bala, Robideau, Lodhi & Lévesque, gen. nov. and *Phytophthium sindhum* Lodhi, Shahzad & Lévesque, sp. nov. *Fungal Planet* 49. *Persoonia* **24**: 136–137.
- Beakes GW, Sekimoto S (2009). The evolutionary phylogeny of *Oomycetes*—insights gained from studies of holocarpic parasites of algae and invertebrates. In: *Oomycete genetics and genomics: Diversity, interactions, and research tools* (Lamour K, Kamoun S, eds). John Wiley & Sons, USA: 1–24.
- Beakes GW, Honda D, Thines M (2014). Systematics of the Straminipila: *Labyrinthulomycota*, *Hyphochytriomycota*, and *Oomycota*. In: *The Mycota, Vol. VIIA. Fungal Taxonomy and Systematics* (McLaughlin DJ, Spatafora J, eds). Springer Verlag, Germany: 39–97.
- Beakes GW, Thines M (2017). *Hyphochytriomycota* and *Oomycota*. In: *Handbook of the Protists* (Archibald JM, Simpson AGB, Slamovits CH, eds). Springer Verlag, Germany: 435–505.
- Bennett RM, de Cock AWAM, Lévesque CA, *et al.* (2017). *Calycofera* gen. nov., an estuarine sister taxon to *Phytophthium*, *Peronosporaceae*. *Mycological Progress* **16**: 947–954.
- Buaya AT, Ploch S, Hanic L, *et al.* (2017). Phylogeny of *Miracula helgolandica* gen. et sp. nov. and *Olpidiopsis drebesii* sp. nov., two basal oomycete parasitoids of marine diatoms, with notes on the taxonomy of *Ectrogella*-like species. *Mycological Progress* **16**: 1041–1050.
- Constantinescu O (1998). A revision of *Basidiophora* (*Chromista*, *Peronosporales*). *Nova Hedwigia* **66**: 251–265.
- Constantinescu O, Fatehi J (2002). *Peronospora*-like fungi (*Chromista*, *Peronosporales*) parasitic on *Brassicaceae* and related hosts. *Nova Hedwigia* **74**: 291–338.
- Constantinescu O, Voglmayr H, Fatehi J, *et al.* (2005). *Plasmoverna* gen. nov., and the nomenclature and taxonomy of *Plasmopara* (*Chromista*, *Peronosporales*). *Taxon* **54**: 813–821.
- Drebes G (1968). *Lagenisma coscinodisci* gen. nov., spec. nov., ein Vertreter der *Lagenidiales* in der marinen Diatomee *Coscinodiscus*. *Veröffentlichungen des Instituts für Meeresforschung in Bremerhaven, Sonderband* **3**: 67–70.
- Gachon CM, Strittmatter M, Badis Y, *et al.* (2017). Pathogens of brown algae: culture studies of *Anisolpidium ectocarpii* and *A. rosenvingei* reveal that the *Anisolpidiales* are unflagellated oomycetes. *European Journal of Phycology* **52**: 133–148.
- Göker M, Voglmayr H, Riethmüller A, *et al.* (2003). Taxonomic aspects of *Peronosporaceae* inferred from Bayesian molecular phylogenetics. *Canadian Journal of Botany* **81**: 672–683.
- Hanic LA, Sekimoto S, Bates SS (2009). Oomycete and chytrid infections of the marine diatom *Pseudo-nitzschia pungens* (*Bacillariophyceae*) from Prince Edward Island, Canada. *Canadian Journal of Botany* **87**: 1096–1105.

Fig. 2. Minimum Evolution (ME) phylogenetic reconstruction. Numbers at branches are bootstrap support values in ME and Maximum Likelihood analyses, respectively. A minus sign denotes support values below 70 % for the presented node or a conflicting topology. The scales bar indicates the number of substitutions per site. The new species introduced in this study is highlighted in bold.

- Hudspeth DS, Stenger D, Hudspeth ME (2003). A *cox2* phylogenetic hypothesis for the downy mildews and white rusts. *Fungal Diversity* **13**: 47–57.
- Hulvey J, Telle S, Nigrelli L, et al. (2010). *Salisapiliaceae* - A new family of oomycetes from marsh grass litter of southeastern North America. *Persoonia* **25**: 109–116.
- Jung T, Scanu B, Bakonyi J, et al. (2017). *Nothophytophthora* gen. nov., a new sister genus of *Phytophthora* from natural and semi-natural ecosystems. *Persoonia* **39**: 143–174.
- Karling JS (1942). *The simple holocarpic biflagellate Phycomycetes*. JS Karling, USA.
- Li GJ, Hyde KD, Zhao RL, et al. (2016). Fungal diversity notes 253–366: taxonomic and phylogenetic contributions to fungal taxa. *Fungal Diversity* **78**: 1–237.
- Litchman E (2010). Invisible invaders: non-pathogenic invasive microbes in aquatic and terrestrial ecosystems. *Ecology Letters* **13**: 1560–1572.
- Marano AV, Jesus AL, de Souza JI, et al. (2016). Ecological roles of saprotrophic *Peronosporales* (Oomycetes, *Straminipila*) in natural environments. *Fungal Ecology* **19**: 77–88.
- Raghukumar S (2017). The Pelagic Ecosystem. In: *Fungi in Coastal and Oceanic Marine Ecosystems* (Raghukumar S, ed). Springer Verlag, Heidelberg: 173–205.
- Scherffel A (1925). Endophytische Phycomyceten-Parasiten der *Bacillariaceen* und einige neue *Monadinen*. Ein Beitrag zur Phylogenie der Oomyceten (Schröter). *Archiv für Protistenkunde* **52**: 1–141.
- Scholz B, Guillou L, Marano AV, et al. (2016). Zoospore parasitism infecting marine diatoms—a black box that needs to be opened. *Fungal Ecology* **19**: 59–76.
- Sekimoto S, Beakes GW, Gachon CM, et al. (2008a). The development, ultrastructural cytology, and molecular phylogeny of the basal oomycete *Eurychasma dicksonii*, infecting the filamentous phaeophyte algae *Ectocarpus siliculosus* and *Pylaiella littoralis*. *Protist* **159**: 401–412.
- Sekimoto S, Klochkova TA, West JA, et al. (2009). *Olpidiopsis bostrychia* sp. nov.: an endoparasitic oomycete that infects *Bostrychia* and other red algae (*Rhodophyta*). *Phycologia* **48**: 460–471.
- Sparrow FK (1960). *Aquatic Phycomycetes*. 2nd ed. The University of Michigan Press, USA.
- Stamatakis A (2014). RAxML version 8: a tool for phylogenetic analysis and post-analysis of large phylogenies. *Bioinformatics* **30**: 1312–1313.
- Tamura K, Peterson D, Peterson N, et al. (2011). MEGA5: molecular evolutionary genetics analysis using maximum likelihood, evolutionary distance, and maximum parsimony methods. *Molecular Biology and Evolution* **28**: 2731–2739.
- Telle S, Thines M (2012). Reclassification of an enigmatic downy mildew species on lovegrass (*Eragrostis*) to the new genus *Eraphthora* with a key to the genera of the *Peronosporaceae*. *Mycological Progress* **11**: 121–129.
- Thines M, Spring O (2005). A revision of *Albugo* (*Chromista*, *Peronosporomycetes*). *Mycotaxon* **92**: 443–458.
- Thines M, Göker M, Spring O, et al. (2006). A revision of *Bremia graminicola*. *Mycological Research* **110**: 646–656.
- Thines M, Göker M, Oberwinkler F, et al. (2007). A revision of *Plasmopara penniseti*, with implications for the host range of the downy mildews with pyriform haustoria. *Mycological Research* **111**: 1377–1385.
- Thines M (2014). Phylogeny and evolution of plant pathogenic oomycetes – a global overview. *European Journal of Plant Pathology* **138**: 431–447.
- Thines M, Nam B, Nigrelli L, et al. (2015a). The diatom parasite *Lagenisma coscinodisci* (*Lagenismatales*, *Oomycota*) is an early diverging lineage of the *Saprolegniomycetes*. *Mycological Progress* **14**: 1–7.
- Thines M, Telle S, Choi Y-J, et al. (2015b). *Baobabopsis*, a new genus of graminicolous downy mildews from tropical Australia, with an updated key to the genera of downy mildews. *IMA Fungus* **6**: 483–491.
- Uzuhashi S, Kakishima M, Tojo M (2010). Phylogeny of the genus *Pythium* and description of new genera. *Mycoscience* **51**: 337–365.
- Voglmayr H, Riethmüller A, Göker M, et al. (2004). Phylogenetic relationships of *Plasmopara*, *Bremia* and other genera of downy mildews with pyriform haustoria based on Bayesian analysis of partial LSU rDNA sequence data. *Mycological Research* **108**: 1011–1024.
- Voglmayr H, Constantinescu O (2008). Revision and reclassification of three *Plasmopara* species based on morphological and molecular phylogenetic data. *Mycological Research* **112**: 487–501.
- Wang Y, Tian RM, Gao ZM, et al. (2014). Optimal eukaryotic 18S and universal 16S/18S ribosomal RNA primers and their application in a study of symbiosis. *PLoS ONE* **9**: e90053.
- Yang X, Hong C (2014). *Halophytophthora fluviatilis* sp. nov. from freshwater in Virginia. *FEMS Microbiology Letters* **352**: 230–237.
- Zopf W (1884). Zur Kenntniss der *Phycomyceten*. I. Zur Morphologie und Biologie der *Ancylisteen* und *Chytridiaceen*, zugleich ein Beitrag zur Phytopathologie. *Abhandlungen der Kaiserlichen Leopoldinisch-Carolinischen Deutschen Akademie der Naturforscher* **47**: 141–236.

doi.org/10.3114/fuse.2019.03.05

Mythicomycetaceae fam. nov. (*Agaricineae*, *Agaricales*) for accommodating the genera *Mythicomyces* and *Stagnicola*, and *Simocybe parvispora* reconsidered

A. Vizzini^{1*}, G. Consiglio², M. Marchetti³

¹Department of Life Sciences and Systems Biology, University of Torino, Viale P.A. Mattioli 25, I-10125 Torino, Italy

²Via Ronzani 61, I-40033 Casalecchio di Reno (Bologna), Italy

³Via Molise 8, I-56123 Pisa, Italy

Key words:

Agaricomycetes
Basidiomycetes
molecular systematics
new taxa
Phaeocollybia
Psathyrellaceae
taxonomy

*Corresponding author: alfredo.vizzini@unito.it

Abstract: The analysis of a combined dataset including 5.8S (ITS) rDNA, 18S rDNA, 28S rDNA, and *rpb2* data from species of the *Agaricineae* (Agaricoid clade) supports a shared monophyletic origin of the monotypic genera *Mythicomyces* and *Stagnicola*. The new family *Mythicomycetaceae*, sister to *Psathyrellaceae*, is here proposed to name this clade, which is characterised, within the dark-spored agarics, by basidiomata with a mycenoid to phaeocollybioid habit, absence of veils, a cartilaginous-horny, often tapering stipe, which discolours dark brown towards the base, a greyish brown, pale hazel brown spore deposit, smooth or minutely punctate-verruculose spores without a germ pore, cheilocystidia always present, as metuloids (thick-walled inocybe-like elements) or as thin-walled elements, pleurocystidia, when present, as metuloids, pileipellis as a thin ixocutis without cystidioid elements, clamp-connections present everywhere, and growth on wood debris in wet habitats of boreal, subalpine to montane coniferous forests. *Simocybe parvispora* from Spain (two collections, including the holotype), which clusters with all the sequenced collections of *Stagnicola perplexa* from Canada, USA, France and Sweden, must be regarded as a later synonym of the latter.

Effectively published online: 25 January 2019.

INTRODUCTION

The *Agaricineae emend.* Aime *et al.* represents one of the seven suborders recently recognised in the *Agaricales* by Dentinger *et al.* (2016) using a phylogenomic approach. This corresponds to a previously recognised “Agaricoid” clade, which has been consistently recovered as monophyletic in recent studies (Matheny *et al.* 2006, 2015, Garnica *et al.* 2007, Binder *et al.* 2010, Kohler *et al.* 2015). Many species in this suborder show pigmented and thick-walled spores (Matheny *et al.* 2006, 2015, Garnica *et al.* 2007). Although species producing dark-pigmented spores (dark-pigmented agarics) are present in a few other lineages (e.g. *Melanomphalia*, Aime *et al.* 2005 or *Ripartites*, Walther *et al.* 2005, Garnica *et al.* 2007), the overwhelming majority of these have evolved within *Agaricineae*. The presence of spores with a thickened, dark-pigmented wall is perhaps indicative of adaptations to specialised environments (e.g. dung, burnt sites) (Garnica *et al.* 2007, Halbwachs *et al.* 2015).

Within the dark (brown)-spored agarics, the monotypic genera *Mythicomyces* and *Stagnicola* were established by Redhead & Smith (1986) based on the two morphologically similar species *Agaricus corneipes* and *Phaeocollybia perplexa*, respectively. The two taxa occupy a rather isolated position within the brown-spored agarics and share a complex of characters that make it difficult to place them at the family level: a mycenoid to phaeocollybia-like appearance (i.e. a widely acute umbonate pileus and a dark brown, cartilaginous-horny,

tapering stipe with a tawny strigosity at base), a pallid spore deposit, greyish brown, pale hazel brown to milk coffee brown with light purple tones, spores without a germ-pore and almost hyaline or faintly brownish under light microscope, a pileipellis as a thin ixocutis, growth on wood debris, presence of clamp-connections. *Mythicomyces* differs from *Stagnicola* mainly by minutely verruculose spores, thick-walled hymenial cystidia and a spore deposit with purple hues. Redhead & Smith (1986) tentatively placed the two genera in the *Strophariaceae* s. Kuhnner (1984) and the *Cortinariaceae* s. l., respectively, mainly based on spore-print colour. In subsequent years, such family placements were debated and questioned. On morphological basis only, Watling & Gregory (1993) suggested *S. perplexa* to be probably better placed in *Inocybeae* within *Cortinariaceae*. Horak (2005) recognised both in *Cortinariaceae* and Gulden (2008a, b) in *Crepidotaceae* (family which includes also *Inocybaceae* according to the author). Extensive phylogenetic studies based on large datasets by Moncalvo *et al.* (2002), Matheny *et al.* (2006, 2015), Padamsee *et al.* (2008), Nagy *et al.* (2011) and Zhao *et al.* (2017) resolved either one or both of these genera in a clade sister to the *Psathyrellaceae* (*Agaricineae*, formerly Agaricoid clade s. Matheny *et al.* 2006, 2015, Garnica *et al.* 2007, Binder *et al.* 2010). The molecular work by Matheny & Griffith (2010) based on a dataset limited to *Squamanita* and allied taxa, indicated *M. corneipes* as sister (with low support) to a superclade formed by *Psathyrellaceae*, *Cystodermateae* and *Nidulariaceae*. In the phylogenetic analysis by Gulden *et al.* (2005) based on a dataset

of only brown-spored agarics, *Stagnicola* occupied an *incertae sedis* position, while *Mythicomyces* clustered in *Strophariaceae* s. l. In Broussal & Dumesny (2015), *Mythicomyces* and *Stagnicola* were sister to each other (with low support) and were part of a superclade, consisting of *Cortinariaceae*, *Bolbitiaceae*, *Tubariaceae*, *Strophariaceae* and *Hymenogastraceae*, which was sister to *Psathyrellaceae*.

However, in molecular studies where both *Mythicomyces* and *Stagnicola* were taken into account at the same time, they were represented at most by two collections each with only 28S rDNA sequences (Moncalvo *et al.* 2002, Gulden *et al.* 2005, Padamsee *et al.* 2008, Broussal & Dumesny 2015).

In accordance with all these molecular studies indicating a sisterhood relationship of the two genera to *Psathyrellaceae*, *Mythicomyces* and *Stagnicola* have recently been classified within the *Psathyrellaceae* by Gulden (2012a, b), Strittmatter & Obenauer (2013) and Prydiuk (2015, 2018). Inexplicably, and probably because they were unaware of the results of the previous molecular studies, the two most frequently used online registries, *Index Fungorum* (<http://www.indexfungorum.org>), *Mycobank* (<http://www.mycobank.org/>), and Begerow *et al.* (2018) assigned the two genera to two different families, namely *Mythicomyces* to the *Psathyrellaceae* and *Stagnicola* to the *Strophariaceae*.

Currently, whereas at least one collection of *Mythicomyces corneipes* (AFTOL-ID 972) is represented by multiple markers in GenBank (<https://www.ncbi.nlm.nih.gov/genbank/>), only a few collections of *Stagnicola perplexa* are present and only with ribosomal (ITS and 28S) sequences. The aim of the present paper was to provide *Stagnicola* with a sound phylogenetic placement within the *Agaricineae* by increasing its taxon sampling and the number of molecular markers. The study of the type collections of *Simocybe parvispora*, which is part of a research project in progress on the European species of the genus *Simocybe*, has revealed its conspecificity with *Stagnicola perplexa*. Morphological and molecular data of these collections were also included because they are central to the main focus of the present work.

MATERIALS AND METHODS

Morphological examination

The microscopic structures were examined from dried material, in different mountants: water, L4 [7.2 g KOH, 160 mL glycerine, 840 mL dH₂O, 7.6 g NaCl and 5 mL Invadin (Ciba-Geigy), Cléménçon 1972], Melzer's reagent, ammoniacal Congo red, Phloxine, Cresyl blue and Cotton blue. Cresyl blue and Cotton blue were utilised to highlight the ortho-/metachromatic reactions in the spores. Dried fragments were rehydrated in water and mounted in L4. All microscopic measurements were carried out under oil immersion at $\times 1\,000$ with Nikon Eclipse 80i microscope.

Spore measurements were made by photographing all the spores (taken from lamellar squashes of exsiccate material of mature specimens) occurring in the visual field of the microscope using the Mycomètre software (Fannechère 2011). Spore dimensions do not include the hilar appendix, and are reported as follows: average minus standard deviation – average plus standard deviation of length \times average minus standard deviation – average plus standard deviation of width; Q = average minus standard deviation – average plus standard deviation of ratio

length/width; Q_m = average \pm standard deviation of ratio length/width; V = average minus standard deviation – average plus standard deviation of the volume [μm^3]; V_m = average \pm standard deviation of the volume [μm^3]. The approximate spore volume was calculated as that of an ellipsoid (Gross 1972, Meerts 1999). The notation “n/m/p” indicates that measurements were made on “n” randomly selected spores from “m” basidiomes of “p” collections. The width of the basidia was measured at the widest part, and the length was measured from the apex (sterigmata excluded) to the basal septum. Microscopic pictures were taken using a Nikon DS 5M digital connected to a Nikon Eclipse 80i microscope with both brightfield and interferential contrast optics.

DNA extraction, amplification and sequencing

Total DNA was extracted from eight dry specimens (Table 1) employing a modified protocol based on Murray & Thompson (1980). PCR amplification was performed with the primers ITS1F and ITS4 (White *et al.* 1990, Gardes & Bruns 1993) for the ITS rDNA region, while LR0R and LR5 (Vilgalys & Hester 1990, Cubeta *et al.* 1991) were used to amplify the 28S (LSU) rDNA region, NS19b and NS41 for the 18S (SSU) rDNA ribosomal region (Hibbett 1996), and bRPB2-6F and bRPB2-7R2 for the RNA polymerase II second largest subunit (*rpb2*) gene (Liu *et al.* 1999, Matheny *et al.* 2007a). PCR reactions were performed under a program consisting of a hot start at 95 °C for 5 min, followed by 35 cycles at 94 °C, 54 °C and 72 °C (45, 30 and 45 s respectively) and a final 72 °C step for 10 min. PCR products were checked in 1 % agarose gels, and positive reactions were sequenced with one or both PCR primers. Chromatograms were checked searching for putative reading errors, and these were corrected. The sequences were submitted to GenBank (<http://www.ncbi.nlm.nih.gov/genbank/>) and their accession numbers are reported in Table 1.

Phylogenetic analysis

BLAST (Altschul *et al.* 1997) was used to select the most closely related sequences from INSD public databases (www.insd.org). Two distinct alignments were built. 1) A multigenic alignment including 5.8S rDNA, 28S (LSU) rDNA, 18S (SSU) rDNA and *rpb2* sequences from representative species of the major lineages in the *Agaricineae* based mainly on Matheny *et al.* (2015). Two species of *Tricholoma* (*T. myomyces*, *T. palustre*) (*Tricholomatineae*), were used as outgroups to root the tree, because of their phylogenetic position external to the *Agaricineae* (Matheny *et al.* 2015, Dentinger *et al.* 2016). 2) A ITS rDNA data alignment of *Mythicomyces* and *Stagnicola* sequences, using *Psathyrella candolleana* as outgroup taxon. Sequences were aligned in MEGA v. 6.0 (Tamura *et al.* 2013) software with its Muscle application and then corrected manually. GTR+G models were chosen for both the alignments. The datasets were analysed using Bayesian inference (BI) and Maximum likelihood (ML) criteria. The Bayesian analysis was performed through the CIPRES Science Gateway platform (Miller *et al.* 2010) by using the MrBayes v. 3.2.6 algorithm with 28S rDNA-18S rDNA-5.8S rDNA-*rpb2* data partitioned, two simultaneous runs, four chains, temperature fixed at 0.2 and sampling every 1 000 generations until reaching the convergence parameters (standard deviation less than 0.01) after about 5 M generations. The first 25 % trees were discarded

Table 1. Samples used for the present phylogenetic studies. Newly sequenced collections are in **bold**.

Taxon	Voucher	Country	GenBank acc. numbers			
			ITS	28S	18S	<i>rpb2</i>
<i>Agaricaceae</i> sp.	RC_Mart06_016	Martinique	HQ839742	HQ839743	HQ839744	HQ839745
<i>Agaricus</i> aff. <i>campestris</i>	PBM 2580	Massachusetts, USA	DQ486682	DQ110871	DQ113914	—
<i>Agaricus bisporus</i>	AFTOL-ID 448/strain OMF	Denmark/USA	DQ404388	AY635775	AY787216	AF107785
<i>Agaricus sylvaticus</i>	JFM-AS	Taiwan	—	AJ244523	AJ012405	—
<i>Agrocybe pediades</i>	AFTOL-ID 1493	California, USA	DQ484057	DQ110872	DQ113915	—
<i>Agrocybe praecox</i>	AFTOL-ID 728	Washington, USA	AY818348	AY646101	AY705956	DQ385876
<i>Agrocybe rivulosa</i>	strain CCB160	Tennessee, USA	KF830098	KF830090	KF830078	KF830069
<i>Agrocybe smithii</i>	AFTOL-ID 1494	Washington, USA	DQ484058	DQ110873	DQ115779	—
<i>Bogbodia uda</i> (“ <i>Nematoloma longisporum</i> ”)	AFTOL-ID 1893	Massachusetts, USA	DQ490634	DQ457681	DQ444863	—
<i>Bolbitius viscosus</i>	PBM 3032	Tennessee, USA	HQ840656	HQ840657	KJ137269	HQ840658
<i>Bolbitius vitellinus</i>	AFTOL-ID 1730	Washington, USA	DQ200920	AY691807	AY705955	DQ385878
<i>Chlorophyllum agaricoides</i>	AFTOL-ID 440	Greece	DQ200928	AY700187	AY657010	—
<i>Conocybe lactea</i>	PBM 2706	Massachusetts, USA	DQ486693	DQ457660	DQ437683	DQ470834
<i>Conocybe smithii</i>	CCB 185	Oregon, USA	KF830097	KF830088	—	KF830068
<i>Coprinellus disseminatus</i>	SFSU MRK18/strain 24.3/ strain C345.1	Various	AY461838	AF056456	—	DQ056143
<i>Coprinopsis atramentaria</i>	PBM 992	Washington, USA	DQ486694	DQ457661	DQ115781	—
<i>Coprinopsis cinerea</i>	KACC49356/C13/okayama 7#130	Various	AF345819	AF041494	M92991	XM_001829088
<i>Coprinus comatus</i>	AFTOL-ID 626	California, USA	AY854066	AY635772	AY665772	AY780934
<i>Cortinarius aurilicis</i>	TSJ1998-101	France	DQ083772	AY684152	AY705957	DQ083880
<i>Cortinarius bolaris</i>	IB19990199 /strain REG MB 96-086/	Germany	AF389169	AY293173	AY293125	—
<i>Cortinarius iodes</i>	IB19850061/AFTOL-ID 285	Massachusetts, USA	AF389133	AY702013	AY771605	AY536285
<i>Cortinarius sodagnitus</i>	TF2001-094/AFTOL-ID 811	Denmark	DQ083812	AY684151	AY752975	DQ083920
<i>Cortinarius violaceus</i>	MTS 4854/AFTOL-ID 814	Washington, USA	DQ486695	DQ457662	AY705950	DQ470835
<i>Crassisporium funariophyllum</i> (“ <i>Pachylepyrium carbonicola</i> ”)	TENN 028784/AHS44809	Idaho, USA	HQ222013	HQ832460	HQ832427	—
	TENN 028785/AHS65056	Idaho, USA	HQ222014	HQ222015	HQ832428	—
	PBM 2293/PBM1411	Washington, USA	—	DQ986294	—	HQ832438
	strain Moser 49/22	Austria	KF830095	KF830085	—	—
	strain Moser 49/8	Austria	KF830096	KF830086	—	—
<i>Crepidotus</i> cf. <i>applanatus</i>	PBM717 (WTU)	Washington, USA	DQ202273	AY380406	AY705951	AY333311
<i>Crepidotus</i> sp.	PBM3463	Western Australia, AU	HQ728537	HQ728538	HQ728539	HQ728540
<i>Crepidotus variabilis</i>	REG JE 5.3	Unknown	—	AY293174	AY293126	—
<i>Crucibulum laeve</i>	REG Crul1/DSH 96-02	Unknown	DQ486696	AF336246	AF026624	DQ470836
<i>Cyathus striatus</i>	DSH 96-028/Cyst1/DSH 96-001	Unknown	DQ486697	AF336247	AF026617	DQ472711
<i>Cystoderma amianthinum</i>	TENN063549/AFTOL-ID 1553	Wales, UK	GU296098	DQ154108	GU296097	—
<i>Descolea maculata</i>	AFTOL-ID 1521	Western Australia, AU	DQ192181	DQ457664	DQ440633	—
<i>Descolea phlebophora</i>	TENN 063626/PBM 3108	New Zealand	HQ728543	HQ728544	KJ137258	HQ728545
<i>Descolea recedens</i>	TENN 063870/PBM 3211	Tasmania, AU	HQ728546	HQ827174	—	HQ827175
<i>Descolea tenuipes</i>	TENN 063871/PBM 3212	Tasmania, AU	HQ832453	HQ832466	HQ832432	HQ832443
<i>Flammula alnicola</i>	PBM 2608/AFTOL-ID 1501	Tennessee, USA	DQ486703	DQ457666	DQ113916	DQ472714
<i>Flammulaster</i> sp.	PBM 1871	Washington, USA	—	AY380408	—	AY333315
	PBM 3449	Tasmania, AU	HQ827176	HQ827177	HQ827178	—
<i>Galerina atkinsoniana</i>	PBM 2719/AFTOL-ID 1760	Colorado, USA	DQ486705	DQ457668	DQ440634	—

Table 1. (Continued).

Taxon	Voucher	Country	GenBank acc. numbers			
			ITS	28S	18S	rpb2
<i>Galerina clavus</i>	Contu_15122007	Italy	—	HQ832461	HQ832429	—
<i>Galerina marginata</i>	AFTOL-ID 465	Massachusetts, USA	DQ192182	DQ457669	DQ440635	—
<i>Galerina semilanceata</i>	PBM 1398/AFTOL-ID 1497	Washington, USA	DQ486706	AY038309	DQ440639	AY337357
<i>Galerina</i> sp.	PR 6574	USA, Puerto Rico	HQ827182	HQ827183	HQ827184	HQ839737
<i>Hebeloma affine</i>	NI 270904	Ontario, Canada	FJ436320	EF561632	HQ832422	FJ436321
<i>Hebeloma angustilamellatum</i> ("Anamika angustilamellata")	AFTOL-ID 543	China	AY575919	AY575919	DQ092918	—
<i>Hebeloma olympianum</i>	BK 21-Nov-98-20	Washington, USA	—	AY038310	—	AY337359
<i>Hebeloma velutipes</i>	AFTOL-ID 980 PBM2277	California, USA	AY818351	AY745703	AY752972	DQ472718
<i>Hydnangium carneum</i>	TENN 063868/PBM 3209	Tasmania, AU	HQ832445	HQ832455	HQ832423	HQ832433
<i>Hymenagaricus taiwanensis</i>	AFTOL-ID 1383	Taiwan	DQ490633	DQ457680	DQ089016	—
<i>Hypholoma australianum</i> ("Hypholoma australe")	PBM 3481	Western Australia, AU	HQ832446	HQ832456	KJ137259	HQ832434
<i>Hypholoma fasciculare</i>	PBM 1844	Washington, USA	—	AY380409	—	AY337413
<i>Hypholoma sublateritium</i>	AFTOL-ID 597	Massachusetts, USA	AY818349	AY635774	AY787215	—
<i>Hypholoma subviride</i>	TENN 062712/TJB10226	Tennessee, USA/Belize	HQ222020	HQ832457	HQ832424	HQ832435
<i>Inocybe aff. asterospora</i>	PBM 2014/PBM 2453	New York, USA	DQ404390	AY702015	AY654889	—
<i>Inocybe mutata</i>	PBM 2953/PBM 2542/ AFTOL-ID 1632	Tennessee/ Massachusetts, USA	JQ801410	AY732212	DQ457623	DQ472729
<i>Inocybe myriadophylla</i>	AFTOL-ID 482	Finland	DQ221106	AY700196	AY657016	AY803751
<i>Inocybe pallidicremea</i>	PBM2448 /PBM2039	Washington, USA	HQ201357	AY380385	—	AY337388
<i>Inocybe rimosoides</i>	AFTOL-ID 520	New York, USA	DQ404391	AY702014	AY752967	DQ385884
<i>Inocybe unicolor</i>	PBM 2589/ PBM1841/DUKE RV7/4	Tennessee/Missouri, USA	EU523554	AY380403	AF287836	AY337409
<i>Laccaria amethystina</i>	DSH s.n.	Unknown	—	AF393062	AF287837	—
<i>Laccaria bicolor</i>	TWO 752 (MONT)/Cham3/ S238N-H82	Montana, USA/France	DQ149869	AF042588	—	XM_001873347
<i>Laccaria ochropurpurea</i>	AFTOL-ID 1477	France/New York, USA	AF006598	AY700200	AY654886	DQ472731
<i>Laccaria pumila</i>	DSH s.n.	Unknown	—	AF287869	AF287838	—
<i>Lacrymaria velutina</i>	AFTOL-ID 478	Massachusetts, USA	DQ490639	AY700198	AY654885	DQ472733
<i>Langermannia gigantea</i>	DSH96-032	Unknown	—	AF518603	AF026622	—
<i>Lepiota cristata</i>	ECV2449/AFTOL-ID 1625	Michigan, USA	AF391041	DQ457685	DQ457627	—
<i>Lepiota maculans</i>	JMB 080509_18	Tennessee, USA	HM222939	HQ832458	HQ832425	HQ832436
<i>Leucoagaricus barssii</i>	AFTOL-ID 1899	California, USA	DQ911600	DQ911601	GU187658	DQ911602
<i>Lycoperdon pyriforme</i>	AFTOL-ID 480/DSH96-054	Unknown	AY854075	AF287873	AF026619	AY218495
<i>Macrolepiota dolichaula</i>	AFTOL-ID 481/AFTOL-ID 529	China	DQ221111	DQ411537	AY771602	DQ385886
<i>Macrolepiota procera</i>	18-X-1990, R.P.J. de Kok/ DSH 96-038	Netherlands	AY243589	AF518628	—	—
<i>Mycocalia denudata</i>	AFTOL-ID 2018/CBS 494.85	Canada	DQ911596	DQ911597	DQ911598	KJ137274
<i>Mythicomyces corneipes</i>	AFTOL-ID 972	Washington, USA	DQ404393	AY745707	DQ092917	DQ408110
	DAOM 178138	Canada	—	AF261381	—	—
	strain KB51	Pakistan	KY648897	—	—	—
	ES11.10.2.A	Germany	KC964108	—	—	—
<i>Naucoria escharioides</i>	PAM03/99/PBM 1719	France/Washington, USA	AY900086	AY380405	—	AY337411
<i>Nidula niveotomentosa</i>	AFTOL-ID 1945/CBS250.84	Canada	DQ917654	DQ986295	GU296099	KJ137275
<i>Phaeocollybia festiva</i>	AFTOL-ID 1489/PBM 2366	Norway	DQ494682	AY509119	DQ462516	AY509118
<i>Phaeomarasmius fulvidulus</i>	Okada 170163	Argentina	KF830092	KF830087	—	—
	T 1495	Argentina	KF830091	KF830080	KF830072	KF830063

Table 1. (Continued).

Taxon	Voucher	Country	GenBank acc. numbers			
			ITS	28S	18S	rpb2
<i>Phaeomarasmium proximans</i>	AFTOL-ID 979/PBM1936 (WTU)	Vermont, USA	DQ404381	AY380410	AY752970	AY333314
<i>Phaeomyces dubiosus</i>	strain PAM06110301	France	KF830099	KF830089	KF830077	KF830070
<i>Pholiota aff. astragalina</i>	PBM 2975	Tennessee, USA	HQ832448	HQ832462	KJ137263/ KJ137264	HQ832439
<i>Pholiota multicingulata</i>	TENN 063875	New Zealand	HQ832449	HQ832463	HQ832430	HQ832440
<i>Pholiota nubigena</i> ("Nivatogastrium nubigenum")	AFTOL-ID 1500	California, USA	DQ494679	DQ470815	DQ459373	—
<i>Pholiota squarrosa</i>	AFTOL-ID 1627	Colorado, USA	DQ494683	DQ470818	DQ465337	—
<i>Pholiotina filaris</i>	AFTOL-ID 1498	Massachusetts, USA	DQ494684	DQ470819	DQ465338	—
<i>Pleuroflammula flammea</i>	AFTOL-ID 1381/MCA 339	Unknown	DQ494685	AF367962	DQ089021	DQ474124
<i>Pleuroflammula praestans</i>	PBM3461	Western Australia, AU	HQ832450	HQ832464	HQ832431	HQ832441
<i>Pleuroflammula tuberculosa</i>	PAM 02072903	France	HQ832452	HQ832465	KJ137265	HQ832442
<i>Psathyroma catervatim</i>	PBM 3420	Tasmania, AU	HQ840663	HQ840664	HQ840665	HQ840666
<i>Psathyroma leucocarpum</i>	PBM 3116	New Zealand	HQ840659	HQ840660	HQ840661	HQ840662
<i>Psathyrella candolleana</i>	AFTOL-ID 1507	Massachusetts, USA	DQ494689	DQ110874	DQ465339	—
<i>Psathyrella gracilis</i>	J 130	Unknown	—	AF041533	DQ851582	—
<i>Psathyrella rhodospora</i>	AFTOL-ID 723 MP133 (MIN)	Minnesota, USA	DQ267129	AY645058	DQ089018	—
<i>Psathyrella spadicea</i>	AFTOL-ID 1628	Colorado, USA	DQ494690	DQ470822	DQ465340	—
<i>Psilocybe caerulipes</i>	T SAT09-216-06	Tennessee, USA	KC669282	KF830084	KF830075	KF830067
<i>Psilocybe cubensis</i>	strain DNA2052	Unknown	KF830094	KF830083	KF830074	KF830066
<i>Psilocybe cyanescens</i>	PSMICSY-200	Unknown	KJ137276	KJ137277	KJ137266	KJ137278
<i>Psilocybe</i> sp. ("Pachylepyrium funariophilum")	strain TENN 6030	Washington, USA	—	AF261513	—	—
<i>Psilocybe stuntzii</i>	VT1263	Unknown	—	AF042567	DQ851584	—
<i>Psilocybe subaeruginosa</i>	PBM 3218 TENN065481	Tasmania, AU	KC669278	KF830079	KF830071	KF830062
<i>Romagnesiella clavus</i>	AMB 15091	Italy	—	MK353795	MK353799	MK359092
<i>Romagnesiella clavus</i> ("Tubaria minima")	PAM 06090110	France	EF051060	EF051055	—	—
<i>Simocybe serrulata</i>	AFTOL-ID 970	Massachusetts, USA	DQ494696	AY745706	DQ465343	DQ484053
<i>Simocybe</i> sp.	PBM 3031	Tennessee, USA	GQ893023	GQ892979	KJ137267	HQ832444
<i>Squamanita paradoxa</i>	TENN 063549/GG_BM05B	Wales, UK	GU296096	EF535266	GU296095	—
<i>Stagnicola perplexa</i>	DAOM 191293	British Columbia, Canada	—	AF261509	—	—
<i>Stagnicola perplexa</i>	Broussal 20160928_909MB	France	MK351604	MK353788	MK353797	MK359087
	DAOM 191292	British Columbia, Canada	MK351605	MK353789	—	MK359088
	DAOM 191296	Newfoundland Labrador, Canada	MK351606	MK353790	—	MK359089
	DAOM 191295	British Columbia, Canada	MK351607	MK353791	—	—
	SFSU F-032462	California, USA	MK351608	MK353792	MK353798	MK359090
<i>Stagnicola perplexa</i> ("Simocybe parvispora")	AH 25260 holotype	Spain	MK351609	MK353793	—	MK359091
	AH 25282 paratype	Spain	MK351610	MK353794	—	—
	KS-BR126	Sweden	MK045203	—	—	—
<i>Stropharia ambigua</i>	AFTOL-ID 726	Washington, USA	AY818350	AY646102	DQ092924	DQ484054
<i>Stropharia rugosoannulata</i>	Hopple D258	Unknown	DQ494697	AF518654	AF026635	—
<i>Tricholoma myomyces</i>	KMS 589	Unknown	DQ825428	U76459	DQ367422	DQ367436
<i>Tricholoma palustre</i>	AFTOL-ID 1497	Massachusetts, USA	DQ494699	AY700197	AY757267	DQ484055

Table 1. (Continued).

Taxon	Voucher	Country	GenBank acc. numbers			
			ITS	28S	18S	<i>rpb2</i>
<i>Tubaria confragosa</i>	AFTOL-ID 498	Washington, USA	DQ267126	AY700190	AY665776	DQ408113
<i>Tubaria furfuracea</i>	MCA 391	California, USA	—	AF205710	DQ851587	—
<i>Tubaria serrulata</i>	AFTOL-ID 1528	Western Australia, AU	DQ182507	DQ156128	DQ462517	—
<i>Tubaria</i> sp.	PBM 3355	Tasmania, AU	HQ839739	HQ839740	HQ839741	—
	BM378_17	Washington, USA	HQ832454	HQ832467	KJ137268	HQ839738
<i>Tubaria vinicolor</i>	AFTOL-ID 499	Washington, USA	DQ536417	DQ536415	DQ536416	DQ536418
<i>Tulostoma macrocephala</i>	strain Long 10111	Unknown	—	AF518663	AF026625	—
<i>Verrucospora flavofusca</i>	AFTOL-ID 655	China	DQ241779	DQ470825	AY665783	—

as burn-in. Finally, a full search for the best-scoring Maximum Likelihood tree was performed in RAxML v.7.0.4 (Stamatakis 2006) using the standard search algorithm (data partitioned, GTRMIX model, 2 000 bootstrap replications). Significance threshold was set above 0.95 for posterior probability (BPP) and 70 % for bootstrap proportions (MLBP).

RESULTS

Phylogenetic analyses

The final multigenic alignment is composed of 129 OTU and contained 4 100 total sites: 1 443 sites from 28S, 1 800 sites from 18S, 158 sites from 5.8S and 699 sites from *rpb2*. The ITS alignment consisted of 12 collections and contained 664 sites.

As both Bayesian and Maximum likelihood analyses produced similar topologies, only the Bayesian trees with both BPP and MLBP values are shown (Figs 1, 2). The concatenated analysis (Fig. 1) supported the existence of at least 14 major lineages (families) within the *Agaricineae*. Nine of these (*Agaricaceae*, *Bolbitiaceae*, *Cortinariaceae*, *Crassisporiaceae*, *Hydnangiaceae*, *Inocybaceae*, *Mythicomycetaceae*, *Psathyrellaceae* and *Tubariaceae*) received strong statistical support (BPP \geq 0.95 and MLBP \geq 70 %); *Crepidotaceae*, *Nidulariaceae*, *Squamanitaceae* and *Strophariaceae* showed high BPP values (\geq 0.95) but only poor maximum likelihood bootstrap support (< 70 %). For the first time a significant sister relationship (BPP = 0.96) was obtained between *Crassisporiaceae* and *Cortinariaceae* based on Bayesian inference. *Mythicomycetes* and *Stagnicola* clustered as sister (BPP = 100 and MLBP = 100 %) in a strongly supported clade (BPP = 100 and MLBP = 100 %), the *Mythicomycetaceae*. The family is sister with strong statistical support (BPP = 100 and MLBP = 100 %) to the *Psathyrellaceae*.

The ITS analysis (Fig. 2) highlighted the presence of three subclades in *Stagnicola perplexa* which would seem to be quite related to a different geographic origin (North America vs. Europe, but see below the notes about the species).

Taxonomy

Mythicomycetaceae Vizzini, Consiglio & M. Marchetti, *fam. nov.*
MycoBank MB829479.

Habit mycenoid to phaeocollybioid (phaeocollybia-like). *Veils* absent (gymnocarpic development). *Pileus* 5–30 mm, hemispherical-conical, obtusely to acutely conical, bell-shaped, umbonate or papillate. *Lamellae* adnexed to narrowly adnate. *Stipe* 15–70 \times 0.5–2 mm, cylindrical, often tapering towards the base (but without pseudorhiza), typically cartilaginous-elastic, tough, corneous (horny) (marasmius cohaerens-like), shiny, gradually darkening (reddish-brown to blackish) from base upwards, with tawny basal strigosity. *Spore deposit* greyish-brown, pale hazel brown to milky coffee brown with light purple hues. *Spores* ovoid to ellipsoid, often somewhat inequilateral, smooth or minutely punctate-verruculose, without a germ pore, thin- to thick-walled, almost hyaline or faintly brownish under light microscope, binucleate, walls cyanophilous, inamyloid or dextrinoid. *Basidia* clavate, usually 4-spored. *Cheilocystidia* present, thick-walled, inocybe-like, often with hyaline crystals at apex and slightly amyloid at apex, or thin-walled and inamyloid. *Pleurocystidia* absent, if present then only as thick-walled elements. *Hymenophoral trama* regular, consisting of parallel hyphae. *Pileipellis* a thin ixocutis with parietal pigment. *Clamp-connections* present.

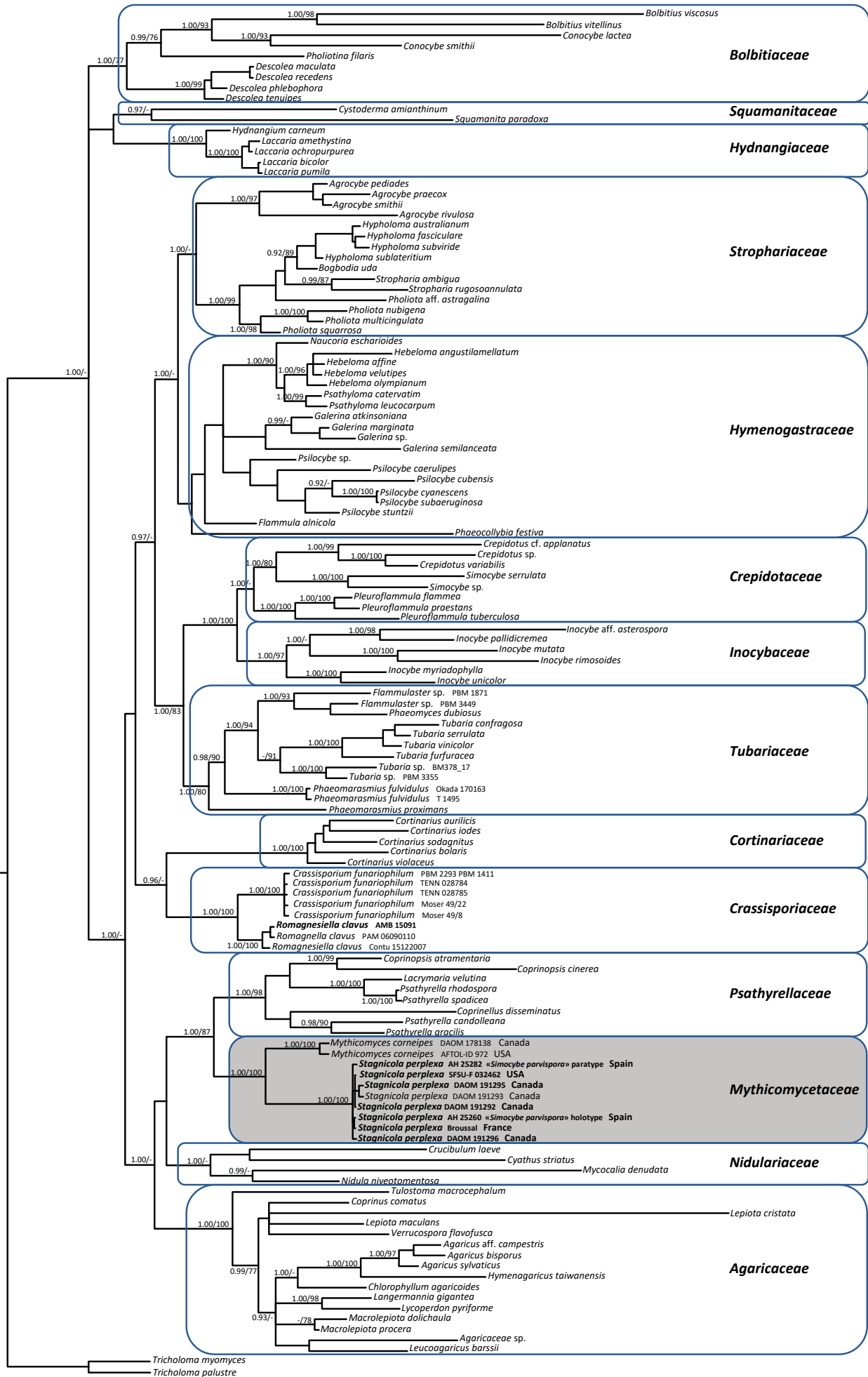
Type genus: *Mythicomycetes* Redhead & A.H. Sm., *Canad. J. Bot.* **64**: 643. 1986.

Habit: Saprotrophic on wood debris, Northern Hemisphere, mostly temperate to boreal.

Genera included: *Mythicomycetes* and *Stagnicola*.

Notes: The genus *Mythicomycetes* and not the genus *Stagnicola* was chosen as type of the family because *Stagnicola* Jeffreys (1830) is also a genus of snails (aquatic pulmonate gastropod mollusks) and there is a larger body of literature on *Stagnicola* Jeffreys (e.g. searches in GenBank[®], Scopus[®], Biosis[®]) than there is on *Stagnicola* Redhead & Smith, which can cause confusion.

Fig. 1. Phylogeny of the *Agaricineae* based on Bayesian Inference and Maximum Likelihood analysis of a dataset of four nuclear gene regions (5.8S-rDNA, 28S-rDNA, 18S-rDNA and *rpb2*). *Tricholoma myomyces* and *T. palustre* were used as outgroup taxa. Only BPP \geq 0.95 and \geq MLBP 70 % are indicated above branches. The newly sequenced collections are in **bold**. Clade nomenclature follows mainly Matheny et al. (2015).



0.06

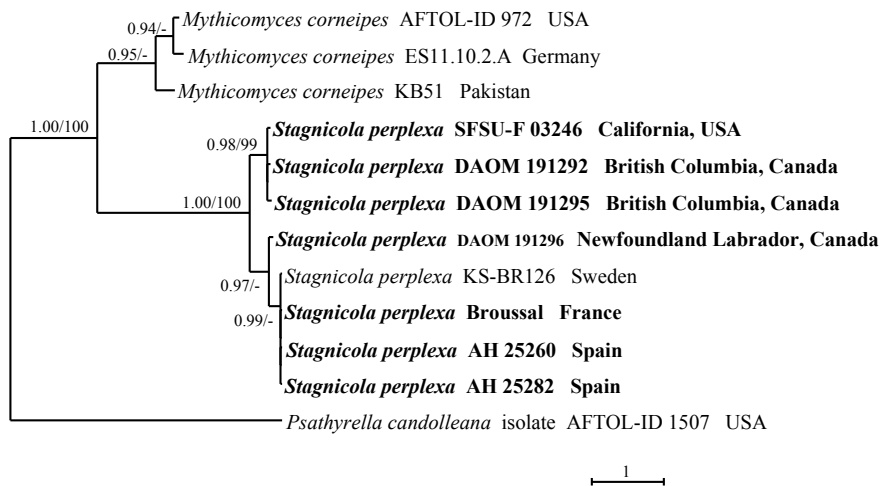


Fig. 2. Phylogeny of the *Mythicomycetaceae* based on Bayesian Inference and Maximum likelihood analysis of ITS rDNA sequences with *Psathyrella candolleana* as outgroup taxon. Only BPP ≥ 0.95 and \geq MLBP 70 % are indicated above branches. The newly sequenced collections are in **bold**.

Mythicomycetes Redhead & A.H. Sm., *Canad. J. Bot.* **64**: 643. 1986.

Etymology: from Greek mythikòs = mythical and mykes = fungus.

Development gymnocarpic. *Habit* mycenoid/collybioid to phaeocollybia-like. *Pileus* obtusely conical later convex, with a broad umbo, up to 4/5-striate, hygrophorous, greasy-shiny, slightly viscid, smooth, reddish brown, orange brown, at margin yellowish brown. *Lamellae* adnate to narrowly adnate, crowded, straw yellow, then cinnamon to greyish-brown. *Stipe* central, smooth, cartilaginous, rigid, glossy, shiny, flexuous, red brown at apex, darker and discolouring brown to blackish towards the base, with a tawny basal mycelial tomentum. Smell indistinct, taste indistinct or slightly bitterish. *Spore print* greyish brown to yellowish brown, pale purplish brown. *Spores* ovoid to ellipsoid, often somewhat inequilateral, minutely roughened, punctate-verruculose, with a small plage, lacking a germ-pore, thick-walled; pale greyish to yellowish brown in water (practically hyaline) under the microscope, cyanophilous, dextrinoid, inamyloid, slightly metachromatic in Cresyl blue, binucleate. *Basidia* usually 4-spored. *Cheilocystidia* and *Pleurocystidia* metuloid (thick-walled), thin-walled at the pedicel, abundant, ventricose, utriform to lageniform or fusiform, someones with hyaline crystals at apex, moderately amyloid in the apical part. *Pileipellis* a thin ixocutis. *Caulocystidia* present. *Clamp-connections* present. *Tissues* non-sarcodimitic.

Type species: *Mythicomycetes corneipes* (Fr.) Redhead & A.H. Sm.

Ecology and distribution: Saprotrophic on plant debris, mainly wood, in wet, mossy areas, usually hemiboreal to boreal, Europe, North America and Asia.

Mythicomycetes corneipes (Fr.) Redhead & A.H. Sm., *Mycotaxon* **118**: 456. 2011.

Basionym: *Agaricus corneipes* Fr., *Öfvers. K. Vetensk Akad. Förh.* **18**: 25. 1861.

Synonyms: *Psilocybe corneipes* (Fr.) P. Karst., *Bidr. Känn. Finl. Nat. Folk* **32**: 504. 1879.

Geophila corneipes (Fr.) Quélet., *Enchiridion Fungorum in Europa media et praesertim in Gallia Vigentium*: 114. 1886.

Mythicomycetes corneipes (Fr.) Redhead & A.H. Sm., *Canad. J. Bot.* **64**: 643. 1986 (*Nom. inval.*, Art. 33.5, 33.7, 33.8).

Gruber P-88 (neotype, MICH).

Selected descriptions: Smith (1938: 26, fig. 2b, d, f, as *Psilocybe corneipes*); (Smith (1949: 518–520, as *Psilocybe corneipes*); Redhead & Smith (1986: 643–645); Moser & Jülich (1987: III *Mythicomycetes* 1); Huhtinen & Vauras (1992: 7–10); Ståhlberg (1991: 64–67); Ludwig (2001a: 397–398, 2001b: plate 107, 51.1); Strittmatter & Obenhauer (2013: 338–340); Prydiuk (2015: 56–58).

Ecology and distribution: Rare. Gregarious, in autumn, saprotrophic on plant debris, among mosses in moist habitats, such as edges of bogs, brook ravines, or under conifers or birch in soil wet from spring flooding. Found throughout the Northern Hemisphere, Europe (mainly northern part), North America (most common in the Pacific Northwest region) and Asia (Pakistan). So far known from Finland, Norway, Sweden (Fries 1861, Ståhlberg 1991, Huhtinen & Vauras 1992, Gulden 2008a, 2012a), Estonia (see locked ITS sequence UDB024379 in UNITE, <https://unite.ut.ee>, specimen TU109530, 11.09.2015, Valga maakond, Otepää vald, leg. I. Kytövuori), Spain (*Mythicomycetes* sp. environmental 18S sequence DQ304712T4B-S13. L. Laiz et al.), Germany (Gminder & Saar 2012, Strittmatter & Obenhauer 2013), Russia (Palamarchuk 2009), Ukraine (Prydiuk 2015, 2018), USA, Canada (Morgan 1917, Smith 1938, 1975, Redhead & Smith 1986, Castellano et al. 2003), and Pakistan (ITS sequence KY648897, strain KB51, 06.09.2013, leg. A.N. Khalid & K. Bakht).

Notes: The species was originally named *Agaricus corneipes* by Fries (1861), who described it from collections made in a fir forest near Alsike, Sweden, as mainly characterised by a glossy, shiny, very rigid horny stipe darkening towards the base and similar to that of *Agaricus cohaerens*. The species was placed in *Psilocybe* by Karsten (1879) and in *Geophila* by Quélet (1886). It was subsequently recorded in North America (northwestern USA) by Morgan (1907, as *Psilocybe corneipes*), who again underlined its resemblance to *Marasmius cohaerens* and by Smith (1938, 1975, as *Psilocybe corneipes*), who also provided photos. These last two authors described the spores as smooth and with a hyaline germ-pore.

Subsequently, in his monographic treatment of the genus *Psilocybe* worldwide, Guzmán (1983), after examining Smith's collections, excluded the taxon from *Psilocybe*, because of its roughened spores lacking a germ pore, presence of metuloids, a pale spore print, stipe texture, and the tawny basal mycelium. Guzmán suggested that probably the best placement for the species would be in *Galerina*.

Redhead & Smith (1986) pointed out that some of the features of the species did not fully fit *Galerina*, in particular the colour of the spore in mass (not ochre to rusty brown), the spores lacking a plage, presence of metuloids, stipe texture and tawny basal mycelium, and established *Mythicomycetes* for accommodate this puzzling species.

Redhead & Smith (1986) proposed the genus *Mythicomycetes* citing as type "*Mythicomycetes corneipes* (Fries) comb. nov." and listing Fries (1863) (and not the earlier Fries 1861) for the basionym *Agaricus corneipes*. They listed also as obligate synonym the validly published name *Psilocybe corneipes* (Fr.) P. Karst. (Karsten 1879: 504). While the indication of the type fulfilled the requirements for a valid publication of the generic name (Art. 37.2), the incorrect citation of the basionym did not meet the requirements for a valid publication of the binomial. Therefore, they published the correct, valid combination later (Redhead *et al.* 2010).

Redhead & Smith (1986) placed the genus provisionally in the *Strophariaceae*, mainly because the habit of the basidiomes and spore print colour fit the broad concept of that family as circumscribed by Kühner (1980, 1984), which included all the non-ectomycorrhizal taxa with a cinnamon-brown, rusty-brown to lilac-brown spore deposit. They noted, however, that the genus did not fit a more restricted concept of *Strophariaceae* (Singer 1986) due to the lack of a germ-pore and the roughened spore wall.

Later, Huhtinen & Vauras 1992, after studying several collections from Fennoscandia, Canada and USA, discovered features never reported by previous authors. In particular, an amyloid reaction in cystidial walls, the dextrinoid reaction of the spores and the presence of a small plage (visible in light microscopy). The latter spore character, detected by scanning electron microscopy also by Prydiuk (2015) in Ukrainian collections, is typical of most *Galerina* species (Smith 1964, Bon 1992, Wood 2001, Gulden *et al.* 2005, Haan & Walley 2009, Gulden 2012c). Subsequent molecular works demonstrated, however, that *Galerina* is phylogenetically unrelated to *Mythicomycetes* and had to be placed in the family *Hymenogastraceae* (Matheny *et al.* 2006, 2015).

Stagnicola Redhead & A.H. Sm., *Canad. J. Bot.* **64**: 645. 1986.

Development gymnocarpic. *Habit* mycenoid/collybioid to phaeocollybia-like. *Pileus* conical to convex, umbonate, hygrophanous, smooth, lubricous-viscid to greasy, striate, tawny, fulvous to sienna, orange yellowish at margin. *Lamellae* adnexed-ventricose, crowded with olivaceous tints and concolorous edge. *Stipe* central, smooth, bay or purplish reddish, dark brown to blackish towards the base, horny, cartilaginous, shiny, often deeply tapering towards base, marasmius cohaerens-like, xeromphalina-like (but without forming a true pseudorhiza), with a saffron to ochre basal mycelial tomentum. *Smell* and *taste* indistinct or astringent, bitterish. *Spore print* deep olive buff to pale hazel brown. *Spores* ellipsoid to amygdaliform-reniform, smooth, without a germ-pore, pale hazel, yellowish brown in water (practically hyaline) under the microscope, non-dextrinoid, inamyloid, cyanophilous, non-metachromatic, binucleate. *Basidia* usually 4-spored, rarely 1–2-spored. *Cheilocystidia* thin-walled, cylindrical to fusiform. *Pleurocystidia* absent. *Hymenophoral trama* regular, consisting of parallel hyphae. *Pileipellis* a thin ixocutis of encrusted hyphae with yellow brown parietal pigment. *Caulocystidia* present. *Clamp-connections* present. *Tissues* non-sarcodimitic.

Habit: Saprotrophic, usually on rotten plant debris (buried needles, leaves, twigs), in damp places, in moist to wet sites, coniferous forests, acid soils, often among *Sphagnum*, montane-boreal, Europe and North America.

Type species: *Stagnicola perplexa* (P.D. Orton) Redhead & A.H. Sm.

Stagnicola perplexa (P.D. Orton) Redhead & A.H. Sm., *Canad. J. Bot.* **64**: 645. 1986.

Basionym: *Phaeocollybia perplexa* P.D. Orton, *Kew Bull.* **31**: 713. 1977.

Synonyms: *Agaricus cidaris* var. *minor* Fr., *Icon. select. Hymenomyc. t.* **123**: 2. 1878.

Naucoria cidaris var. *minor* (Fr.) Sacc., *Syll. Fung.* **5**: 831. 1887.

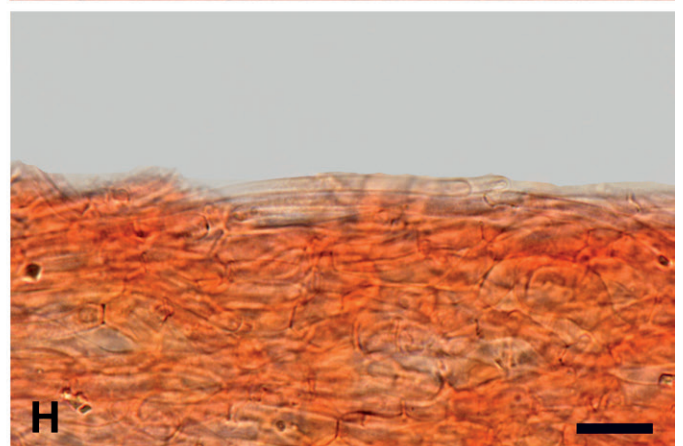
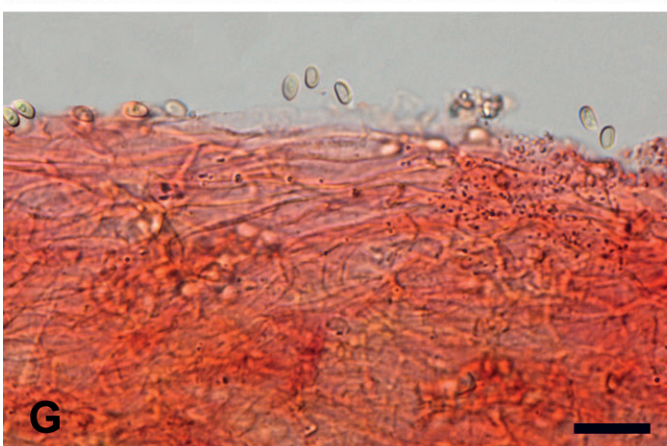
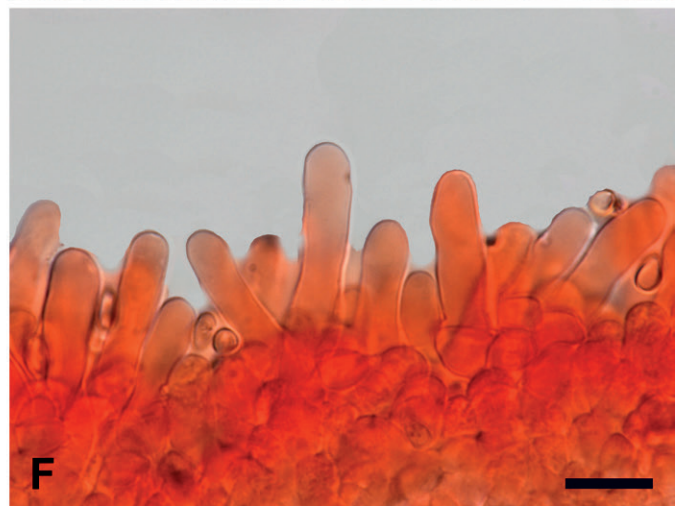
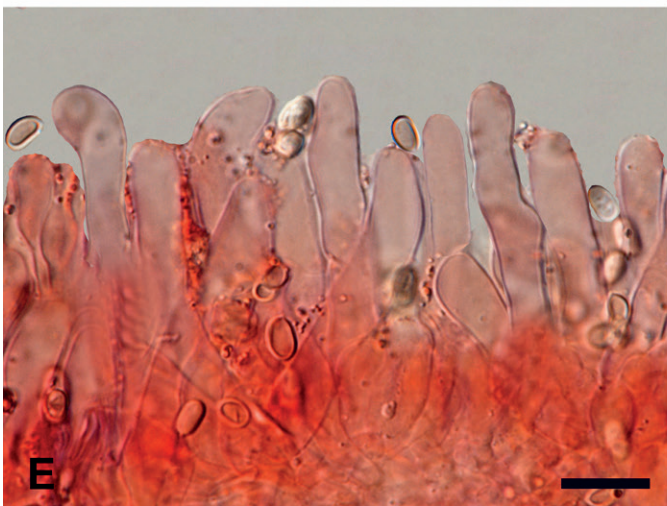
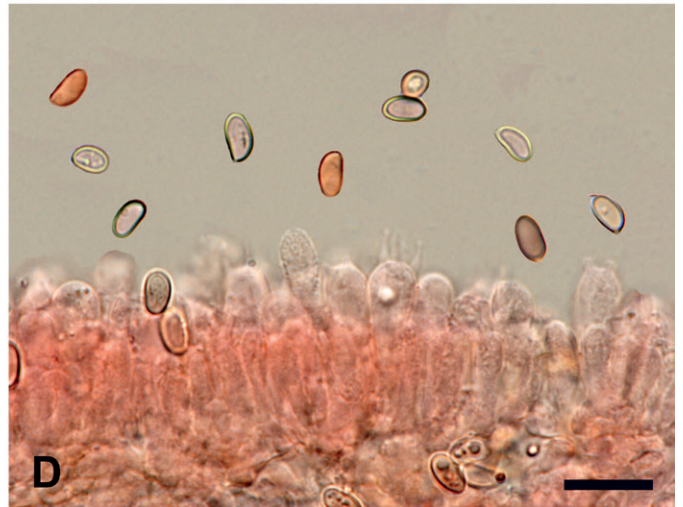
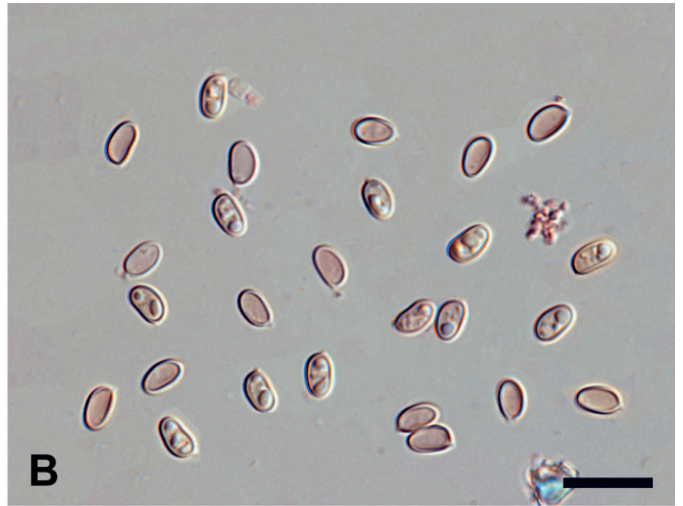
Simocybe parvispora Bandala *et al.*, *Sydowia* **60**: 183. 2008.

Selected descriptions: Orton (1977: 713, as *Phaeocollybia perplexa*); Redhead & Smith (1986: 645, 646); Laber & Marklund (1992: 54–56); Watling & Gregory (1993: 93–95; figs 136–138, p. 128, 129); Ludwig (2001a: 659, 660, 2001b: plate 173, 82.1); Bandala *et al.* (2008: 183–185, fig. 1 p. 188, fig. 2 p. 189; as *Simocybe parvispora*); Broussal & Dumesny (2015: 238–240).

Microscopy (based mainly on Broussal 20160928_909MB, SFSU-F-032462 and DAOM 191295). Fig. 3.

Spores 5.1–6.1 × 3.0–3.5 μm (145/3/3) (on average 5.6 × 3.3 μm), Q = 1.57–1.85 (Q_m 1.71), V = 24.3–38.8 μm³ (V_m = 31.5 μm³), subellipsoid with a flat to depressed adaxial side in lateral view, mainly ellipsoid in front view, hilar appendix visible, smooth, wall up to 0.3–0.5 μm thick, pale yellowish in water, slightly darker at wall level, often mono- to multiguttulate, cyanophilic, inamyloid, non-dextrinoid, non-metachromatic in Cresyl blue. *Basidia* 18–28 × 5–8 μm, mainly tetra-spored, subcylindrical to clavate, even subcapitate, with up to 6 μm long sterigmata, content mostly smooth, at times guttulate. *Hymenophoral trama* regular, consisting of thin-walled, hyaline to yellowish cylindrical hyphae, 4–8 μm wide, having a parallel arrangement. Occasionally, it was observed the occurrence of crystalline particles either free or sticking to the hyphal walls. *Subhymenium* hardly differentiated. *Cheilocystidia* 25–40(–45) × 4.5–7(–8) μm, thin-walled, subcylindrical, at times flexuous or slightly ventricose or clavate, with a rounded, occasionally subgival or lobate apex, other times with a tapered base; edge heteromorphous. *Pleurocystidia* not found. *Pileipellis* a regular thin ixocutis, consisting of cylindrical, yellowish, thin-walled hyphae, 3–8(–10) μm wide, smooth but with occasional crystalline deposits, at times with clavate terminal elements; subcutis well differentiated, composed of short articles, 16–12(–15) μm wide, subvesicular or allantoid. *Pileocystidia* not found. *Stipe hyphae* 2–8(–10) μm wide, mostly cylindraceous, at times fusiform, parallel, often short-celled, hyaline to yellowish, thin-walled, occasionally it can be noted the presence of polymorphous, refractive, small-sized crystalline deposits. *Caulocystidia* present in the apical portion of the stipe, similar to the hymenial ones but more irregular in shape. *Clamp-connections* common everywhere. *Tissues* non-sarcodimitic.

Specimens examined: **France**: Haute-Auvergne: Condat, Cantal, Maubert et Gaulis forest, alt. 872 m, coniferous forest (*Picea abies*, *Abies alba*), on debris in mossy area, 28 Sep. 2016, H. Dumesny [det. M. Broussal] (Broussal 20160928_909MB). **Canada**: *British*



Columbia: Queen Charlotte Is., Graham I., Kliki Damen Cr. mouth, in a drying temporary pool amongst *Carex*, 16 Sep. 1982, S.A. Redhead (DAOM 191292); Queen Charlotte Is., Graham I., Yakoun R. near Port Clements, on reed bed, along river, 15 Sep. 1982, S.A. Redhead (DAOM 191295). *Newfoundland-Labrador*: Gros Morne Natl. Park, on debris in wet depression by alders, Bakers Brook Pond trail, 19 Sep. 1983, S.A. Redhead (DAOM 191296). **USA**: *California*: Siskiyou County, Shasta-Trinity National Forest, alt. 485 m, *Abies magnifica* litter with an understory of *Symphoricarpos* sp., 8 Nov. 2012, C. Schwarz [det. S. Davison] (SFSU-F-032462).

Microscopy (based on *Simocybe parvispora* AH 25282 (paratype). Fig. 4.

Spores 5.2–6 × 3–3.5 µm (44/1/1) (av. 5.6 × 3.2 µm), Q = 1.57–1.90 (Q_m 1,74), V = 25.2–36.6 µm³ (V_m = 30.9 µm³), ellipsoid in side-view, often with an almost flat adaxial side, occasionally with central constriction, mostly ellipsoid in front-view, smooth. Lacking a germ pore, wall up to 0.3–0.5 µm thick, hilar appendix visible, pale yellowish in water, often mono- or multi-guttulate, cyanophilic, iodine-negative, non-metachromatic in Cresyl blue. *Basidia* 18–28 × 5–7 µm, tetrasporic, sterigmata up to 6 µm long, often even monosporic with a sterigm up to 10 µm long, subcylindrical to clavate or even subcapitate, content mostly smooth, at times guttulate. *Hymenophoral trama* regular, made up by cylindrical, hyaline to yellowish, thin-walled hyphae, 4–8 µm wide, occasionally it is possible to observe minute crystalline formations. *Subhymenium* hardly differentiated. *Cheilocystidia* 25–55(–60) × 4.5–7(–8) µm, thin-walled, hyaline, subcylindrical, often flexuous or slightly ventricose or clavate, with rounded or ogival apex, plentiful to scarce, at times completely absent. *Pleurocystidia* not found. *Pileipellis* a regular thin ixocutis, with long to short hyphae, at times with clavate terminal elements, 3–7 µm wide, thin-walled, yellowish, with occasional crystalline deposits; subcutis and underlying layer well differentiated, consisting of short hyphae, 8–20 µm wide, subvesicular or allantoid. *Pileocystidia* not found. *Stipe hyphae* 2–8(–10) µm wide, mostly cylindrical, at times fusiform, parallel, often short-celled, with yellowish content, thin-walled, refractive polymorphous crystalline deposits present. *Caulocystidia* numerous in the apical portion, tufted, at times multi-septate, subcylindrical-clavate or utricular, even lageniform, 20–40 × 3–8 µm. *Clamp-connections* common everywhere. *Tissues* non-sarcodimitic.

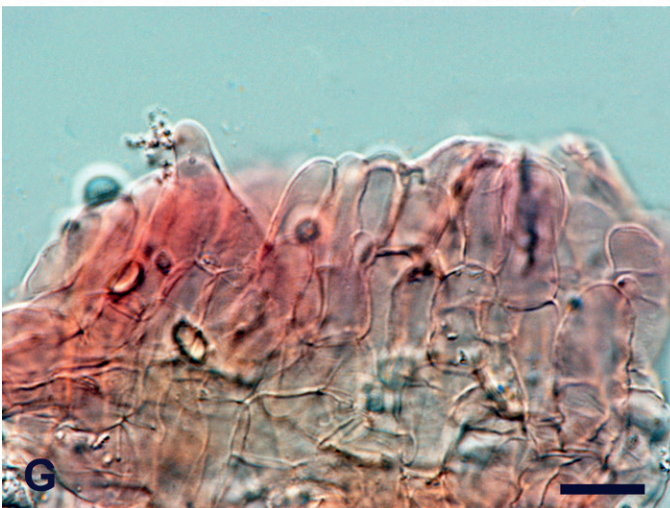
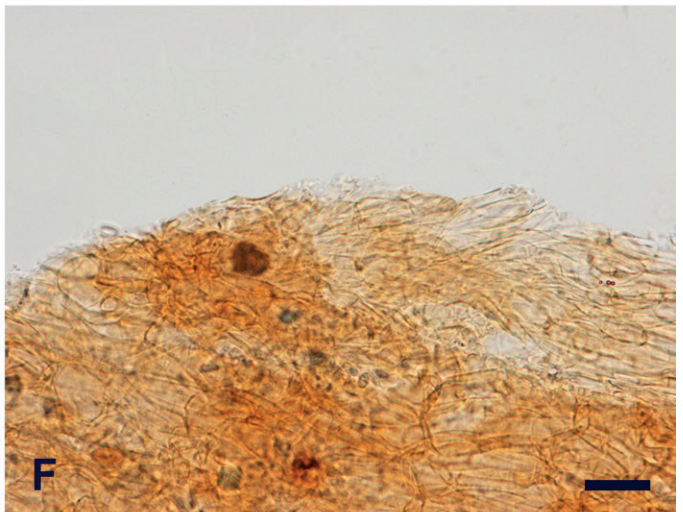
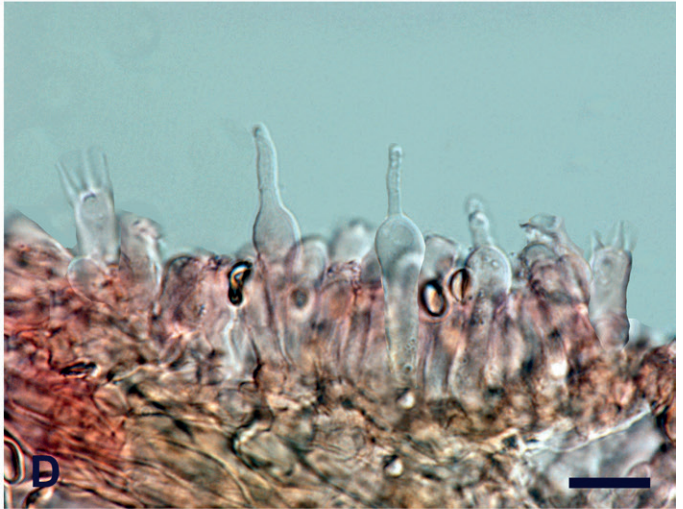
Ecology and distribution: Rare. Gregarious, in autumn, saprotrophic on plant debris, in moist to wet areas, usually in acid coniferous forests among mosses. Found throughout the Northern Hemisphere (Europe and North America) and so far known from Sweden and Finland (Fries 1878 as *Agaricus cidaris* var. *minor*, Stridvall & Stridvall 1996, Gulden 2008b, 2012b), Great Britain (Scotland, Orton 1977 as *Phaeocollybia perplexa*; Watling & Gregory 1993), Germany (Laber & Marklund 1992), France (Broussal & Dumesny 2015, Spain (Bandala *et al.* 2008 as *Simocybe parvispora*), Moldova (Manic 2015), USA and Canada (Smith 1937, Redhead & Smith 1986). In Index Fungorum and

MycoBank, *Panaeolus sphinctrinus* var. *minor*, described by Singer (1960, 1969) based on Mexican and Argentine collections, is (mistakenly) considered as a posterior synonym of *A. corneipes* and consequently Niveiro & Albertó (2012), Coimbra (2015) and Begerow *et al.* (2018) reported in their checklists *S. perplexa* (= *P. sphinctrinus* var. *minor*) as present in Argentine. In comparison with *M. corneipes*, however, *P. sphinctrinus* var. *minor* has a non-corneous stipe, lacks a tawny mycelial tomentum at stipe base and its spores are darker, hexagonal to citriform in shape, have a with germ-pore and measure 12–13.3 × 9–9.3 µm (Singer 1960, Guzmán & Pérez-Patracá 1972, Gerhardt 1996).

Specimens examined: **Spain**: *Castilla-La Mancha*: Guadalajara, road from Aldeanueva de Atienza to Condemios de Arriba, river Pelagallinas, on decaying branches of *Pinus sylvestris*, alt. 1380 m, 2 Oct. 1999, Villarreal *et coll.* (AH 25282-paratype/topotype).

Notes: The species was clearly first reported from Sweden by Fries (1878) as *Agaricus (Naucoria) cidaris* var. *minor* (plate 123, fig. 2). Fries differentiated the variety from the type (to date considered a true *Phaeocollybia*), mainly on the lack of a rooting stipe. Saccardo (1887) then combined this variety in *Naucoria*. Smith (1937) signalled it from North America, providing also a photo (plate 23, fig. c). When the species was collected for the first time by Orton (1977), the English mycologist, unaware of Fries's taxon, was not able, at first, to place it in a known genus (hence the specific epithet of "*perplexa*", i.e. puzzled). Subsequently, after additional collections, in spite of the smooth, pale-coloured spores and the pileus not strongly viscid, he became convinced that the new taxon had to be placed in the genus *Phaeocollybia* [traditionally included in *Cortinariaceae* due to the presence of a viscid pileus surface, a pseudorhiza, rusty-brown, ornamented spores, and the absence of a veil (Heim 1931, Horak 1977, Laber 1982, 1991)]. It was accommodated near *P. jennyae*, since other features such as the conical umbonate pileus, horny cartilaginous rooting stipe, absence of veils, absence of pleurocystidia, bitter astringent taste and yellowish olive lamellae fitted neatly into the genus. Horak (1977) considered the inclusion of the species in *Phaeocollybia* doubtful and questionable. Redhead & Smith (1986) removed *P. perplexa* from *Phaeocollybia* mainly because of its pale smooth spores, a not truly rooting stipe and presence of a tawny tomentum at stipe base, transferring it to the monotypic genus *Stagnicola*. Subsequent accurate morpho-ecological works by Redhead & Malloch (1986), Norvell (1998a, b, 2000, 2004) and Norvell & Exeter (2008) allowed a better circumscription of *Phaeocollybia*, which, when additional distinguishing features were discovered, led to a better delimitation of *P. stagnicola* and the other brown-spored agarics. Noteworthy among the new features are the (pileo)stipitocarpic-monovelangiocarpic development revealed by the presence of a thin pellicular veil (primordial envelope sheath) sheathing the subterranean primordium, but tearing during basidiome elongation and easily overlooked in mature basidiomes (where velar remnants are only observable as fibrillose patches on the aerial stipe); the presence of a rhizomorphic pseudorhiza (a pseudorhiza forming several thread-like myceliar cords that

Fig. 3. Macro- and micromorphological features of *Stagnicola perplexa*. **A.** Basidiomata in the field (Broussal 20160928_909MB). **B.** Spores (Broussal 20160928_909MB). **C.** Spores (DAOM 191295). **D.** Spores and hymenium (SFSU-F-032462). **E.** Cheilocystidia (DAOM 191295). **F.** Cheilocystidia (SFSU-F-032462). **G.** Pileipellis (DAOM 191295). **H.** Pileipellis (SFSU-F-032462). B–H in ammoniacal Congo red. Scale bars: A = 10 mm; B–H = 10 µm. Photographs: A, H  l  ne Dumesny; B–H, Mauro Marchetti.



make contact with the plant root tips); tibiiform diverticula on the hyphae of the mycelium, a pellicular veil and sarcodimitic pseudotissues in the pseudorhizal trama, often present also in the stipittrama, pileitrama, and hymenophoral trama. Last but not least, evidence that *Phaeocollybia* is an ectomycorrhizal genus (trophic lifestyle confirmed also by the stable isotopes analysis by Trudell *et al.* 2004), even though some species are possibly parasitic. Molecular phylogeny placed *Phaeocollybia* in *Hymenogastraceae* (Matheny *et al.* 2006, 2015).

As first suggested by Redhead & Smith (1985), species of the genus *Tubaria* (*Tubariaceae*) may resemble *S. perplexa*, but they possess a non-umbonate pileus, veils, broadly attached, adnate to subdecurrent lamellae, a non-tapering stipe which is fibrous and fleshy and with white basal mycelium, and thin-walled easily collapsing spores (Singer 1986, Bon 1992, Volders 2002, Matheny *et al.* 2007b).

Stagnicola perplexa could be confused with the central-stemmed species of *Simocybe* (e.g. *S. centunculus*, *S. sumptuosa*) (*Crepidotaceae*), but the latter differ in having olivaceous tinges on pileus surface, more pigmented, distinctly ovoid-reniform spores and a trichodermic-hymenidermic pileipellis with well-developed pileocystidia (Romagnesi 1962, Senn-Irlet 1995, Aime *et al.* 2005, Horak & Ronikier 2011). The morphological affinities between *Stagnicola* and *Simocybe* are such that, according to our phylogenetic analyses (Figs 1, 2), the recently described *Simocybe parvispora* from Spain (Bandala *et al.* 2008) is to be regarded as identical to *S. perplexa*. Moreover, also the morphological study of the two sequenced *Simocybe parvispora* collections (holotype and paratype) showed characters that, based on the descriptions in the literature (Orton 1977, Redhead & Smith 1986, Laber & Marklund 1992, Watling & Gregory 1993, Broussal & Dumesny 2015) and our personal observations, match perfectly those of *S. perplexa*.

Finally, also the two recently described sister genera *Crassisporium* and *Romagnesiella* (*Crassisporiaceae*) have some characters in common with *Stagnicola*. In particular, they share a collybioid habit, a filamentous pileipellis, pale-coloured, smooth spores and presence of clamp-connections. Nonetheless, they differ in the non-umbonate pileus, fleshy, non-rooting stipe, which does not progressively darken towards the base and lacks a tawny basal tomentum and the non-dextrinoid spores with walls becoming rusty brown to reddish brown or reddish cinnamon in KOH. Additionally, *Crassisporium*, typified by *Pholiotina funariophila*, a taxon traditionally placed in the polyphyletic genus *Pachylepirium* (Matheny *et al.* 2015), is distinguished by a fugacious veil on pileus and stipe surface, thick-walled spores (> 0.5 µm thick) with a broad and conspicuous germ pore (often > 0.5 µm wide) and carbonicolous habitat (Matheny *et al.* 2015), while *Romagnesiella*, typified by *Galerina clavus*, may be differentiated by a dry, non-hygrophanous pileus (Matheny *et al.* 2015).

The phylogenetic analysis based on ITS sequences (Fig. 2) showed that *Stagnicola perplexa* collections from Europe and from North America form slightly different subclades, but, in the multigene analysis (Fig. 1), these small differences are no longer perceptible.

DISCUSSION

In the field, *Mythicomyces corneipes* and *Stagnicola perplexa* can be easily confused due to a series of shared characters such as a similar habit, absence of veils, pale-coloured lamellae, pale spore deposit, a tapering corneus-rigid stipe, gradually blackening from base upward and with a tawny basal mycelium and occurrence in the same habitats. Microscopically, however, *Mythicomyces* can be easily distinguished by the minutely roughened, verrucose spores and the presence of thick-walled, encrusted hymenial cystidia.

The presence in both *Agaricus corneipes* and *Phaeocollybia perplexa* of this unusual combination of characters, which is anomalous in dark-spored agarics, caused uncertainty as to their intergeneric relationships and family placement, which remained controversial and debated (Redhead & Smith 1986, Huhtinen & Vauras 1992) until the application of molecular techniques. However, while the molecular works provided a definitive answer regarding both the validity and independence of these two genera within the dark-spored agarics (Gulden *et al.* 2005) and their sister relationships (Moncalvo *et al.* 2002, Padamsee *et al.* 2008, Broussal & Dumesny 2015), the data on their definitive family placement have remained inconclusive, because of the poor taxon sampling and the few sequences available for these two taxa, for *S. perplexa* in particular.

Our analysis, which includes seven new *Stagnicola* collections with four molecular markers, clearly indicates that, in agreement with previous works (Moncalvo *et al.* 2002, Padamsee *et al.* 2008, Broussal & Dumesny 2015), the two genera are sister (with high support, BPP = 1, MLBP = 87%) to the *Psathyrellaceae*. The family *Psathyrellaceae* includes all the taxa formerly treated under the name *Coprinaceae*, but with the exclusion of *Coprinus comatus* (type of the genus) and allied species, which were found to be more closely related to *Agaricaceae* (Redhead *et al.* 2001). They have a saprotrophic nutritional mode or, rarely, parasite other agarics (e.g. *Psathyrella epimyces*) and are characterized by a dark brown, purplish brown to black spore deposit, non-cyanophilous thick-walled spores, usually with a distinct germ-pore and, in the psathyrelloid taxa, with pigment in the walls bleaching in concentrated sulfuric acid, without iodine reactions, hymenial cystidia often present, sterile pseudoparaphyses surrounding the basidia present in the coprinoid taxa, a non-radicating, fleshy, fibrous, non-corneous stipe, lamellae deliquescing in the coprinoid genera [ability to digest themselves by means of autodigestive chitinases (Kües 2000)], pileipellis a cutis or more commonly an epitelium/hymeniderm, often covered with velar structures (Singer 1986, as *Coprinaceae*, Redhead *et al.* 2001, Noordeloos 2005, as *Coprinaceae partim*; Knudsen & Vesterholt 2012).

There is an evident morphological hiatus between *Mythicomyces/Stagnicola* with their pale-coloured spores without germ-pore, corneous, tapering stipe and absence of veils, pileipellis as a thin ixocutis, and the members of the *Psathyrellaceae*. No genus within the coprinoid taxa *Coprinellus*, *Coprinopsis*, *Parasola* (Redhead *et al.* 2001, Nagy *et al.* 2009, 2010, 2011, 2012, 2013a, b) as well as in the polyphyletic

Fig. 4. Macro- and micromorphological features of *Simocybe parvispora*. **A.** Basidiomata in the field (AH 25260, holotype). **B.** Basidiomata in the field (AH 25282, paratype). **C.** Spores (AH 25282). **D.** Mono- and tetrasporic basidia (AH 25282). **E.** Cheilocystidia (AH 25282). **F.** Pileipellis (AH 25282). **G.** Caulocystidia (AH 25282). **H.** Caulocystidia (AH 25282). C–H in ammoniacal Congo red. Scale bars: A, B = 10 mm; C–H = 10 µm. Photographs: A, B, Fernando Esteve-Raventós; C–H, Mauro Marchetti.

Psathyrella s.l. (Kits van Waveren 1985), including the recently segregated genera *Homophron*, *Kauffmania*, *Typhrasa* (Örstadius & Knudsen 2012, Örstadius et al. 2015), shows clear morphological affinities with *Mythicomyces* and *Stagnicola*.

It stands to reason that forcing the two genera into *Psathyrellaceae s.l.*, as proposed by Gulden 2012a, b, Strittmatter & Obenauer 2013, Prydiuk 2015, 2018), makes this family heterogeneous and non-natural, hence the necessity to establish the new family, *Mythicomycetaceae* proposed in this paper.

ACKNOWLEDGEMENTS

The authors are grateful to staff at Herbaria AH (F. Javier Rejos), AMB (Gianfranco Medardi), and DAOM (Jennifer Wilkinson) for loan of collections. Gabriele Cacialli (Livorno, Italy) is acknowledged for his bibliographic expertise. Micheline Broussal (Cournonsec, France), Fernando Esteve-Raventós (Madrid, Spain), Brandon Matheny (Knoxville, USA), Gabriel Moreno (Madrid, Spain), Mark Miller (San Diego, USA), and Scott Redhead (Ottawa, Canada) are also acknowledged for their valuable collaboration.

REFERENCES

- Aime MC, Vilgalys R, Miller OK (2005). The *Crepidotaceae* (Basidiomycota, Agaricales): phylogeny and taxonomy of the genera and revision of the family based on molecular evidence. *American Journal of Botany* **92**: 74–82.
- Altschul SF, Gish W, Miller W, et al. (1990). Basic local alignment search tool. *Journal of Molecular Biology* **215**: 403–410.
- Bandala VM, Esteve-Raventós F, Montoya L (2008). Two remarkable brown-spored agarics from Spain: *Simocybe parvispora* sp. nov. and *Crepidotus ibericus* comb. nov. *Sydowia* **60**: 181–196.
- Begerow D, McTaggart A, Agerer R (2018). *Syllabus of Plant Families. Part 1/3. Basidiomycota and Entorrhizomycota*. Borntraeger Science Publishers, Stuttgart, Germany.
- Binder M, Larsson KH, Matheny PB, et al. (2010). *Amylocorticiales* ord. nov. and *Jaapiales* ord. nov.: early diverging clades of agaricomycetidae dominated by corticioid forms. *Mycologia* **201**: 865–888.
- Bon M (1992). Clé monographique des espèces galéro-naucorioides. *Documents Mycologiques* **21**: 1–89.
- Broussal M, Dumesny E (2015). Une récolte française de *Stagnicola perplexa*. *Bulletin de la Société Mycologique de France* **131**: 237–243.
- Castellano MA, Cázares E, Fondrick B, et al. (2003). *Handbook to Additional Fungal Species of Special Concern in the Northwest Forest Plan. General Technical Report PNW-GTR-572. Part 7: Species Gyromitra montana to Phaeocollybia fallax* (PDF) (Report). United States Department of Agriculture, Forest Service: S3–81.
- Cléménçon H (1972). Zwei verbesserte Präparierlösungen für die mikroskopische Untersuchung von Pilze. *Zeitschrift für Pilzkunde* **38**: 49–53.
- Coimbra VRM (2015). Checklist of Central and South American Agaricales (Basidiomycota) II: *Strophariaceae*. *Mycosphere* **6**: 441–458.
- Cubeta MA, Echandi E, Abernethy T, et al. (1991). Characterization of anastomosis groups of binucleate *Rhizoctonia* species using restriction analysis of an amplified ribosomal RNA gene. *Phytopathology* **81**: 1395–1400.
- de Haan A, Walleyn R (2009). Studies in *Galerina*. *Galerinae Flandriae* (3). *Fungi non Delineati* **46**: 1–84.
- Dentinger BTM, Gaya E, O'Brien H, et al. (2016). Tales from the crypt: genome mining from fungarium specimens improves resolution of the mushroom tree of life. *Biological Journal of the Linnean Society* **117**: 11–32.
- Fannechére G (2011). *Mycomètre, logiciel d'aide à la mesure et de traitement statistique*. http://mycolim.free.fr/DOC_SML/mycm202/Charg_Mycm202.htm
- Fries EM (1861). Hymenomycetes novi vel minus cogniti, in Suecia 1852–1860 observati. *Öfversigt af Kongliga Vetenskaps-Akademiens förhandlingar* **18**: 19–34.
- Fries EM (1863). *Monographia Hymenomycetum Sueciae* 2: [147]–355. CA Leffler, Uppsala, Sweden.
- Fries EM (1878). *Icones selectae Hymenomycetum nondum delineatorum / sub auspiciis Regiae Academiae Scientiarum Holmiensis editae ab Elia Fries; Volumen secundum, Fasc. II-III*. Typographia centralis & Ed. Berling, Holmiae et Upsaliae, Sweden.
- Gardes M, Bruns TD (1993). ITS primers with enhanced specificity for *Basidiomycetes*—application to the identification of mycorrhizae and rusts. *Molecular Ecology* **2**: 113–118.
- Garnica S, Weiss M, Walther G, et al. (2007). Reconstructing the evolution of agarics from nuclear gene sequences and basidiospore ultrastructure. *Mycological Research* **9**: 1019–1029.
- Gerhardt E (1996). Taxonomische revision der Gattungen *Panaeolus* und *Panaeolina* (Fungi, Agaricales, Coprinaceae). *Bibliotheca Botanica* **147**: 1–150.
- Gminder A, Saar G (2012). Ergänzungen zur Großpilzflora von Baden-Württemberg. *Andrias* **19**: 185–223.
- Gross G (1972). Kernzahl und sporenvolumen bei einigen Hymenogasterarten. *Zeitschrift für Pilzkunde* **38**: 109–158.
- Gulden G, Stensrud O, Shalchian-Tabrizi K, et al. (2005). *Galerina* Earle: A polyphyletic genus in the consortium of dark-spored agarics. *Mycologia* **97**(4): 823–837.
- Gulden G (2008a). *Mythicomyces* Redhead & A.H. Sm. In: *Funga Nordica. Agaricoid, boletoid and cyphelloid genera* (Knudsen H, Vesterholt J, eds). Nordsvamp, Copenhagen, Denmark: 907.
- Gulden G (2008b). *Stagnicola* Redhead & A.H. Sm. In: *Funga Nordica. Agaricoid, boletoid and cyphelloid genera* (Knudsen H, Vesterholt J, eds). Nordsvamp, Copenhagen, Denmark: 910.
- Gulden G (2012a). *Mythicomyces* Redhead & A.H. Sm. In: *Funga Nordica. Agaricoid, boletoid, clavarioid, cyphelloid and gastroid genera* (Knudsen H, Vesterholt J, eds). 2nd edn. Nordsvamp, Copenhagen, Denmark: 688.
- Gulden G (2012b). *Stagnicola* Redhead & A.H. Sm. In: *Funga Nordica. Agaricoid, boletoid, clavarioid, cyphelloid and gastroid genera* (Knudsen H, Vesterholt J, eds). 2nd edn. Nordsvamp, Copenhagen, Denmark: 728.
- Gulden G (2012c). *Galerina* Earle. In: *Funga Nordica. Agaricoid, boletoid, clavarioid, cyphelloid and gastroid genera* (Knudsen H, Vesterholt J, eds). 2nd edn. Nordsvamp, Copenhagen, Denmark: 886–903.
- Guzmán G, Pérez-Patracá AM (1972). Las especies conocidas del género *Panaeolus* en México. *Boletín de la Sociedad Mexicana de Micología* **6**: 17–53.
- Guzmán G (1983). The genus *Psilocybe*. A systematic revision of the known species including the history, distribution and chemistry of the hallucinogenic species. *Beihefte Nova Hedwigia* **74**: 1–439.
- Jeffreys JG (1830). A synopsis on the testaceous pneumonobranchous Mollusca of Great Britain. *Transactions of the Linnean Society of London* **16**: 323–392.
- Halbwachs H, Brandl R, Bässler C (2015). Spore wall traits of ectomycorrhizal and saprotrophic agarics may mirror their distinct lifestyles. *Fungal Ecology* **17**: 197–204.

- Heim R (1931). *Le genre Inocybe: Précédé d'une introduction générale à l'étude des agarics ochrosporés*. Paul Lechevalier & Fils, Paris, France.
- Hibbett DS (1996). Phylogenetic evidence for horizontal transmission of group I introns in the nuclear ribosomal DNA of mushroom-forming fungi. *Molecular Biology and Evolution* **13**: 903–917.
- Horak E (1977). Further additions towards a monograph of *Phaeocollybia*. *Sydowia* **29**: 28–70.
- Horak E (2005). *Röhrlinge und Blätterpilze in Europa*. Elsevier GmbH, Spectrum Akademischer Verlag, München, Germany.
- Horak E, Ronikier A (2011). *Simocybe montana* (Crepidotaceae, Agaricales), a new species from the alpine belt in the Swiss Alps and the Romanian Carpathians. *Mycological Progress* **10**: 439–443.
- Huhtinen S, Vauras J (1992). *Mythicomycetes corneipes*, a rare agaric, in Fennoscandia. *Karstenia* **32**: 7–12.
- Karsten PA (1879). Rysslands, Finlands och den Skandinaviska halföns Hattsvampar. Förra Delen: Skifsvampar. *Bidrag till Kännedom av Finlands Natur och Folk* **32**: 1–571.
- Kits van Waveren E (1985). The Dutch, French and British species of *Psathyrella*. *Persoonia* Suppl. **2**: 1–300.
- Knudsen H, Vesterholt J (eds) (2012). *Psathyrellaceae* Redhead, Vilgalys & Hopple. In: *Funga Nordica. Agaricoid, boletoid, clavarioid, cyphelloid and gastroid genera*. 2nd edn. Nordsvamp, Copenhagen, Denmark: 661–728.
- Kohler A, Kuo A, Nagy LG, et al. (2015). Convergent losses of decay mechanisms and rapid turnover of symbiosis genes in mycorrhizal mutualists. *Nature Genetics* **47**: 410–415.
- Kües U (2000). Life history and developmental processes in the basidiomycete *Coprinus cinereus*. *Microbiology and Molecular Biology Reviews* **64**: 316–353.
- Kühner R (1980). Les Hyménomycètes agaricoïdes (*Agaricales*, *Tricholomatales*, *Pluteales*, *Russulales*). Etude générale et classification. *Bulletin mensuel de la Société linnéenne de Lyon* **49** Numero special: 1–1027.
- Kühner R (1984). Some mainlines of classification in the gill fungi. *Mycologia* **76**: 1059–1074.
- Laber D (1982). Die europäischen Arten der Gattung *Phaeocollybia* (Wurzelschnitzlinge) und ihr Vorkommen in südliches Schwarzwald. *Zeitschrift für Mykologie* **48**: 89–98.
- Laber D (1991). Ergänzung zu 'Die europäischen Arten der Gattung *Phaeocollybia* und ihr Vorkommen in südliches Schwarzwald.' *Zeitschrift für Mykologie* **57**: 109–116.
- Laber D, Marklund H (1992). *Stagnicola perplexa* (Orton) Redhead & Smith = *Agaricus cidaris* var. *minor* Fries, eine sehr seltene Art in Europa? *Zeitschrift für Mykologie* **58**: 53–56.
- Liu YJ, Whelen S, Hall BD (1999). Phylogenetic relationships among *Ascomycetes*: evidence from an RNA Polymerase II Subunit. *Molecular Biology and Evolution* **16**: 1799–1808.
- Ludwig E (2001a). *Pilzkompedium Band 1: Beschreibungen*. IHW Verlag, Eching, Germany.
- Ludwig E (2001b). *Pilzkompedium Band 1: Abbildungen*. IHW Verlag, Eching, Germany.
- Manic S (2015). *Macromicetele din ecosistemele Republicii Moldova (taxonomie, bioecologie, corologie)*. PhD Dissertation, Biological Sciences, Academia de Științe a Moldovei Grădina Botanică (Institut), Chișinău, Moldova.
- Matheny PB, Curtis JM, Hofstetter V, et al. (2006). Major clades of *Agaricales*: a multilocus phylogenetic overview. *Mycologia* **98**: 982–995.
- Matheny PB, Griffith JW (2010). Mycoparasitism between *Squamanita paradoxa* and *Cystoderma amianthinum* (*Cystodermateae*, *Agaricales*). *Mycoscience* **51**: 456–461.
- Matheny PB, Wang Z, Binder M, et al. (2007a). Contributions of *rpb2* and *tefl1* to the phylogeny of mushrooms and allies (*Basidiomycota*, Fungi). *Molecular Phylogenetics and Evolution* **43**: 430–451.
- Matheny P B, Vellinga EC, Bougher N, et al. (2007b). Taxonomy of displaced species of *Tubaria*. *Mycologia* **99**: 569–585.
- Matheny PB, Moreau PA, Vizzini A, et al. (2015). *Crassisporium* and *Romagnesiella*: two new genera of dark-spored *Agaricales*. *Systematics and Biodiversity* **13**: 28–41.
- Meerts P (1999). The evolution of spores in agarics: do big mushrooms have big spores? *Journal of Evolutionary Biology* **12**: 161–165.
- Miller MA, Pfeiffer W, Schwartz T (2010). Creating the CIPRES Science Gateway for inference of large phylogenetic trees. In: *Proceedings of the Gateway Computing Environments Workshop (GCE)*, 14 November 2010, New Orleans, LA: 1–8.
- Moncalvo JM, Vilgalys R, Redhead SA, et al. (2002). One hundred and seventeen clades of euagarics. *Molecular Phylogenetics and Evolution* **23**: 357–400.
- Morgan AP (1907). North American species of *Agaricaceae*. *The Journal of Mycology* **13**: 246–255.
- Moser M, Jülich W (1987). *Farbatlas der Basidiomyceten*. 3. Gustav Fischer, Stuttgart, Germany.
- Murray HG, Thompson WF (1980). Rapid isolation of high molecular weight DNA. *Nucleic Acids Research* **8**: 4321–4325.
- Nagy LG, Kocsubé S, Papp T, et al. (2009). Phylogeny and character evolution of the coprinoid mushroom genus *Parasola* as inferred from LSU and ITS nrDNA sequence data. *Persoonia* **22**: 28–37.
- Nagy GL, Urban A, Örstadius L, et al. (2010). The evolution of autodigestion in the mushroom family *Psathyrellaceae* (*Agaricales*) inferred from Maximum Likelihood and Bayesian methods. *Molecular Phylogenetics and Evolution* **57**: 1037–1048.
- Nagy GL, Walther G, Házi J, et al. (2011). Understanding the evolutionary processes of fungal fruiting bodies: correlated evolution and divergence times in the *Psathyrellaceae*. *Systematic Biology* **60**: 303–331.
- Nagy LG, Házi J, Vágvölgyi C, et al. (2012). Phylogeny and species delimitation in the genus *Coprinellus* with special emphasis on the haired species. *Mycologia* **104**: 254–275.
- Nagy LG, Desjardin ED, Vágvölgyi C, et al. (2013a). Phylogenetic analyses of *Coprinopsis* section *Lanatulii* and *Atramentarii* identify multiple species within morphologically defined taxa. *Mycologia* **105**: 112–114.
- Nagy LG, Vágvölgyi C, Papp T (2013b). Morphological characterization of clades of the *Psathyrellaceae* (*Agaricales*) inferred from a multigene phylogeny. *Mycological Progress* **12**: 505–517.
- Niveiro N, Albertó EO (2012). Checklist of the Argentine *Agaricales* 2. *Coprinaceae* and *Strophariaceae*. *Mycotaxon* **120**: 505, <http://dx.doi.org/10.5248/119.505>.
- Noordeloos ME (2005). *Coprinaceae* Overeem. In: *Flora Agaricina Neerlandica 6* (Noordeloos ME, Kuyper THW, Vellinga EC, eds). CRC Press, Taylor & Francis Group, Boca Raton, USA: 21.
- Norvell LL (1998a). *The biology and taxonomy of Pacific Northwest species of Phaeocollybia Heim (Agaricales, Cortinariaceae)*. Ph.D. dissertation (Dept. Botany), University of Washington, Seattle, USA.
- Norvell LL (1998b). Observations on development, morphology and biology in *Phaeocollybia*. *Mycological Research* **102**: 615–630.
- Norvell LL (2000). *Phaeocollybia* in Western North America 1: The *Phaeocollybia kauffmanii* complex. *Canadian Journal of Botany* **78**: 1055–1076.
- Norvell LL (2004). *Phaeocollybia* in western North America 4: Two new species with tibiiform cheilocystidia and section *Versicolores* reconsidered. *Mycotaxon* **90**: 241–260.

- Norvell LL, Exeter RL (2008). *Phaeocollybia of Pacific Northwest North America*. United States Department of Interior Bureau of Land Management Salem District, Salem, USA.
- Örstadius L, Knudsen H (2012). *Psathyrella* (Fr.) Quél. In: *Funga Nordica. Agaricoid, boletoid, cyphelloid and gasteroid genera* (Knudsen H, Vesterholt J, eds). 2nd edn. Nordsvamp, Copenhagen, Denmark: 692–728.
- Örstadius L, Ryberg M, Larsson E (2015). Molecular phylogenetics and taxonomy in *Psathyrellaceae* (Agaricales) with focus on psathyrelloid species: introduction of three new genera and 18 new species. *Mycological Progress* **14**: 25.
- Orton PD (1977). Notes on British Agarics: V. *Kew Bulletin* **31**: 709–721.
- Padamsee M, Matheny PB, Dentinger BT, et al. (2008). The mushroom family *Psathyrellaceae*: evidence for large-scale polyphyly of the genus *Psathyrella*. *Molecular Phylogenetics and Evolution* **46**: 415–429.
- Palamarchuk MA (2009). The xylotrophic agaricoid *Basidiomycetes* of Pechoro-Ilych reserve (North Urals). *Conifers of the Boreal Area* **26**: 67–72. (in Russian)
- Prydiuk MP (2015). *Mythicomyces* (*Psathyrellaceae*), a new for Ukraine genus of mushrooms. *Ukrainian Botanical Journal* **72**: 55–60.
- Prydiuk MP (2018). *Mushrooms of the families Bolbitiaceae and Psathyrellaceae of Ukraine: species composition, distribution, evolution*. Ph.D. dissertation for Doctor of Science degree in Biology (Dr. Sci. Biol.), specialty 03.00.21 – Mycology. M.G. Kholodny Institute of Botany of National Academy of Sciences of Ukraine, Kyiv, Ukraine.
- Quélet L (1886). *Enchiridion fungorum in Europa media et praesertim in Gallia vigentium*. O. Doin, Paris, France.
- Redhead SA, Malloch DW (1986). The genus *Phaeocollybia* (Agaricales) in eastern Canada and its biological status. *Canadian Journal of Botany* **64**: 1249–1254.
- Redhead SA, Smith AH (1986). Two new genera of agarics based on *Psilocybe comeipes* and *Phaeocollybia perplexa*. *Canadian Journal of Botany* **64**: 643–647.
- Redhead SA, Vilgalys R, Moncalvo JM, et al. (2001). *Coprinus* Persoon and the disposition of *Coprinus* species *sensu lato*. *Taxon* **50**: 203–241.
- Redhead SA, Ammirati JF, Norvell LL, et al. (2011). Validation of combinations with basionyms published by Fries in 1861. *Mycotaxon* **118**: 455–458.
- Romagnesi H (1962). Les *Naucoria* du groupe *Centunculus* (*Ramicola* Velen.). *Bulletin Trimestriel de la Société Mycologique de France* **78**: 337–358.
- Saccardo PA (1887). *Sylloge Hymenomycetum*, Vol. I. *Agaricineae. Sylloge Fungorum* **5**: 1–1146.
- Senn-Irlet B (1995). Die Gattung *Simocybe* Karsten in Europa. *Mycologia Helvetica* **7**: 27–61.
- Singer R (1960). Sobre algunas especies de hongos presumiblemente psicotropicos. *Lilloa* **30**: 117–127.
- Singer R (1969). Mycoflora australis. *Beihefte zur Nova Hedwigia* **29**: 1–405.
- Singer R (1986). *The Agaricales in modern taxonomy*, 4th ed. Koeltz Scientific Books, Koenigstein, Germany.
- Smith AH (1937). Unusual agarics from Michigan. IV. *Papers from the Michigan Academy of Science, Arts and Letters* **22**: 215–223.
- Smith AH (1938). New and unusual Agarics from North America: I. *Mycologia* **30**: 20–41.
- Smith AH (1949). *Mushrooms in their natural habitats*. Sawyer's Inc, Portland, USA.
- Smith AH (1975). *A field guide to Western Mushrooms*. Univ. Mich. Press, Ann Arbor, USA.
- Smith AH, Singer R (1964). *A Monograph of the Genus Galerina Earle*. Hafner Publishing, New York, USA.
- Stålberg J (1991). *Mythicomyces corneipes* (Fr.) Redhead & Smith. Mystisk skivling identifierad. *Jordstjärnan* **12**: 64–67.
- Stamatakis A (2006). RAxML-VI-HPC: maximum likelihood based phylogenetic analyses with thousands of taxa and mixed models. *Bioinformatics* **22**: 2688–2690.
- Stridvall A, Stridvall L (1996). Fynd av två för Sverige nya skivlingar *Russula rutila* Romagn. och *Stagnicola perplexa* (Orton) Redhead & Smith. *Jordstjärnan* **17**: 11–16.
- Strittmatter E, Obenauer H (2013). Ein Fund des Hornstieligen Scheinschwefelkopfes *Mythicomyces corneipes* (Fr.) Redhead & A. H. Sm. in Südwestdeutschland. *Zeitschrift für Mykologie* **79**: 337–349.
- Tamura K, Stecher G, Peterson D, et al. (2013). MEGA6: Molecular evolutionary genetics analysis version 6.0. *Molecular Biology and Evolution* **30**: 2725–2729.
- Trudell SA, Rygielwicz PT, Edmonds RL (2004). Patterns of nitrogen and carbon stable isotope ratios in macrofungi, plants and soils in two old-growth conifer forests. *New Phytologist* **164**: 317–335.
- Vilgalys R, Hester M (1990). Rapid genetic identification and mapping of enzymatically amplified ribosomal DNA from several *Cryptococcus* species. *Journal of Bacteriology* **172**: 4238–4246.
- Volders J (2002). Het genus *Tubaria* in Vlaanderen en het Brussels Gewest. *Sterbeeckia* **21–22**: 3–28.
- Watling R, Gregory NM (1993). *British Fungus Flora 7. Cortinariaceae pp.* Royal Botanic Garden, Edinburgh, UK.
- Walther G, Garnica S, Weiss M (2005). The systematic relevance of conidiogenesis modes in the gilled *Agaricales*. *Mycological Research* **109**: 525–544.
- White TJ, Bruns TD, Lee S, et al. (1990). Amplification and direct sequencing of fungal ribosomal RNA genes for phylogenetics. In: *PCR protocols: a guide to methods and applications* (Innis MA, Gelfand DH, Sninsky J, White TJ, eds). Academic Press, San Diego, USA: 315–322.
- Wood AE (2001). Studies in the genus *Galerina* (Agaricales) in Australia. *Australian Systematic Botany* **14**: 615–676.
- Zhao R-L, Li G-J, Sánchez-Ramírez S, et al. (2017). A six-gene phylogenetic overview of *Basidiomycota* and allied phyla with estimated divergence times of higher taxa and a phyloproteomics perspective. *Fungal Diversity* **84**: 43–74.

doi.org/10.3114/fuse.2019.03.06

New and Interesting Fungi. 2

P.W. Crous^{1,2,3*}, R.K. Schumacher⁴, A. Akulov⁵, R. Thangavel⁶, M. Hernández-Restrepo¹, A.J. Carnegie⁷, R. Cheewangkoon⁸, M.J. Wingfield⁹, B.A. Summerell¹⁰, W. Quaedvlieg¹, T.A. Coutinho², J. Roux¹¹, A.R. Wood¹², A. Giraldo^{1,13}, J.Z. Groenewald¹

¹Westerdijk Fungal Biodiversity Institute, P.O. Box 85167, 3508 AD Utrecht, The Netherlands

²Department of Genetics, Biochemistry and Microbiology, Forestry and Agricultural Biotechnology Institute (FABI), University of Pretoria, Pretoria, 0002, South Africa

³Microbiology, Department of Biology, Utrecht University, Padualaan 8, 3584 CH Utrecht, The Netherlands

⁴Hölderlinstraße 25, 15517 Fürstenwalde / Spree, Germany

⁵Department of Mycology and Plant Resistance, V. N. Karazin Kharkiv National University, Maidan Svobody 4, 61022 Kharkiv, Ukraine

⁶Plant Health and Environment Laboratory, Ministry for Primary Industries, P.O. Box 2095, Auckland 1140, New Zealand

⁷Forest Health & Biosecurity, NSW Department of Primary Industries - Forestry, Level 12, 10 Valentine Ave, Parramatta NSW 2150, NSW 2124, Australia

⁸Department of Plant Pathology, Faculty of Agriculture, Chiang Mai University, Chiang Mai 50200, Thailand

⁹Forestry and Agricultural Biotechnology Institute (FABI), University of Pretoria, Pretoria, 0002, South Africa

¹⁰Royal Botanic Gardens and Domain Trust, Mrs Macquaries Rd, Sydney, NSW 2000, Australia

¹¹Department of Plant and Soil Sciences, Faculty of Natural and Agricultural Sciences, Forestry and Agricultural Biotechnology Institute (FABI), University of Pretoria, Pretoria, 0002, South Africa

¹²ARC – Plant Protection Research Institute, P. Bag X5017, Stellenbosch 7599, South Africa

¹³Faculty of Natural and Agricultural Sciences, Department of Plant Sciences, University of the Free State, P.O. Box 339, Bloemfontein 9300, South Africa

Key words:

biodiversity
ITS barcodes
multi-gene phylogeny
new taxa
systematics
typification

*Corresponding author: p.crous@westerdijkinstituut.nl

Abstract: One order, seven families, 28 new genera, 72 new species, 13 new combinations, four epitypes, and 21 interesting new host and / or geographical records are introduced in this study. *Pseudorobillardaceae* is introduced for *Pseudorobillarda* (based on *P. phragmitis*). New genera include: *Jeremyomyces* (based on *J. labinae*) on twigs of *Salix alba* (Germany); *Neodothidotthia* (based on *N. negundinicola*) on *Acer negundo* (Ukraine); *Neomedicopsis* (based on *N. prunicola*) on fallen twigs of *Prunus padus* (Ukraine); *Neophaeoappendicospora* (based on *N. leucaena*) on *Leucaena leucocephala* (France) (incl. *Phaeoappendicosporaceae*); *Paradevriesia* (incl. *Paradevriesiaceae*) (based on *P. americana*) from air (USA); *Phaeoseptoriella* (based on *P. zaeae*) on leaves of *Zea mays* (South Africa); *Piniphoma* (based on *P. wesendahlina*) on wood debris of *Pinus sylvestris* (Germany); *Pseudoconiothyrium* (based on *P. broussonetiae*) on branch of *Broussonetia papyrifera* (Italy); *Sodiomyces* (based on *S. alkalinus*) from soil (Mongolia), and *Turquoiseomyces* (incl. *Turquoiseomycetales* and *Turquoiseomycetaceae*) (based on *T. eucalypti*) on leaves of *Eucalyptus leptophylla* (Australia); *Typhicola* (based on *T. typharum*) on leaves of *Typha* sp. (Germany); *Xenodevriesia* (incl. *Xenodevriesiaceae*) (based on *X. strelitzicola*) on leaves of *Strelitzia* sp. (South Africa). New species include: *Bacillicladium clematidis* on branch of *Clematis vitalba* (Austria); *Cercospora gomphrenigena* on leaves of *Gomphrena globosa* (South Africa); *Cyphellophora clematidis* on *Clematis vitalba* (Austria); *Exophiala abietophila* on bark of *Abies alba* (Norway); *Exophiala lignicola* on fallen decorticated trunk of *Quercus* sp. (Ukraine); *Fuscostagonospora banksiae* on *Banksia* sp. (Australia); *Gaeumannomycella caricicola* on dead leaf of *Carex remota* (Germany); *Hansfordia pruni* on *Prunus persica* twig (Italy) (incl. *Hansfordiaceae*); *Microdochium rhopalostylidis* on *Rhopalostylis sapida* (New Zealand); *Neocordana malayensis* on leaves of *Musa* sp. (Malaysia); *Neocucurbitaria prunicola* on fallen twigs of *Prunus padus* (Ukraine); *Neocucurbitaria salicis-albae* on *Salix alba* twig (Ukraine); *Neohelicomyces deschampsiae* on culm base of dead leaf sheath of *Deschampsia cespitosa* (Germany); *Pararoussoella juglandicola* on twig of *Juglans regia* (Germany); *Pezicula eucalyptigena* on leaves of *Eucalyptus* sp. (South Africa); *Phlogicylindrium dunnii* on leaves of *Eucalyptus dunnii* (Australia); *Phyllosticta hagahagaensis* on leaf litter of *Carissa bispinosa* (South Africa); *Phyllosticta austroafricana* on leaf spots of unidentified deciduous tree host (South Africa); *Pseudosigmoidea alnicola* on *Alnus glutinosa* leaf litter (Germany); *Pseudoteratosphaeria africana* on leaf spot on unidentified host (Angola); *Porodiplodia vitis* on canes of *Vitis vinifera* (USA); *Sodiomyces alkalinus* from soil (Mongolia), *Sodiomyces magadiensis* and *Sodiomyces tronii* from soil (Kenya), *Sympodiella quercina* on fallen leaf of *Quercus robur* (Germany) and *Zasmidium hakeicola* on leaves of *Hakea corymbosa* (Australia). Epitypes are designated for: *Cryptostictis falcata* on leaves of *E. alligatrix* (Australia), *Hendersonia phormii* on leaves of *Phormium tenax* (New Zealand), *Sympodiella acicola* on needles of *Pinus sylvestris* (Netherlands), and *Sphaeria scirpicola* var. *typharum* on leaf of *Typha* sp. (Germany). Several taxa originally described from rocks are validated in this study. New taxa include: *Extremaceae* fam. nov., and new genera, *Arthrocatena*, *Catenulomyces*, *Constantinomyces*, *Extremus*, *Hyphoconis*, *Incertomyces*, *Lapidomyces*, *Lithophila*,

Monticola, *Meristemomyces*, *Oleoguttula*, *Perusta*, *Petrophila*, *Ramimonilia*, *Saxophila* and *Vermiconidia*. New species include: *Arthrocatena tenebrosa*, *Catenulomyces convolutus*, *Constantinomyces virgultus*, *C. macerans*, *C. minimus*, *C. nebulosus*, *C. virgultus*, *Exophiala bonariae*, *Extremus adstrictus*, *E. antarcticus*, *Hyphoconis sterilis*, *Incertomyces perditus*, *Knufia karalitana*, *K. marmoricola*, *K. mediterranea*, *Lapidomyces hispanicus*, *Lithophila guttulata*, *Monticola elongata*, *Meristemomyces frigidus*, *M. arctostaphyli*, *Neodevriesia bulbilosa*, *N. modesta*, *N. sardiniae*, *N. simplex*, *Oleoguttula mirabilis*, *Paradevriesia compacta*, *Perusta inaequalis*, *Petrophila incerta*, *Rachicladosporium alpinum*, *R. inconspicuum*, *R. mcmurdoi*, *R. monterosanum*, *R. paucitum*, *Ramimonilia apicalis*, *Saxophila tyrrhenica*, *Vermiconidia antarctica*, *V. calcicola*, *V. foris*, and *V. flagrans*.

Effectively published online: 5 February 2019.

INTRODUCTION

This paper represents the second contribution to the New and Interesting Fungi (NIF) series, aimed at expanding the body of knowledge of fungal biodiversity and fungal conservation. The series focuses on new records, new sexual-asexual connections, consolidation of sexual and asexual genera following the abandonment of dual nomenclature for fungi (Hawksworth *et al.* 2011, Wingfield *et al.* 2012), and the description of fungal taxa, or notes relating to interesting observations (Crous *et al.* 2018c). The series represents a regular feature of the journal Fungal Systematics and Evolution (www.FUSE-journal.org). It is hoped that it will provide an attractive resource for mycologists to publish single new species or to highlight the relevance of important fungi. Mycologists and other researchers wishing to contribute to future issues of NIF are encouraged to contact the Editor-in-Chief (p.crous@westerdijkinstitut.nl).

MATERIALS AND METHODS

Isolates

Samples were placed in damp chambers and incubated at room temperature for 1–3 d. Single conidial colonies were grown from sporulating conidiomata in Petri dishes containing 2 % malt extract agar (MEA) as described by Crous *et al.* (1991). Leaf and stem tissues bearing ascomata were soaked in water for approximately 2 h, after which they were attached to the undersides of the lids of Petri dishes containing MEA. After ascospores had been ejected onto the MEA surface, germination patterns were determined after 24 h, and single ascospore or conidial cultures were established following the method described by (Crous 1998). Colonies were sub-cultured on 2 % potato-dextrose agar (PDA), oatmeal agar (OA), MEA (Crous *et al.* 2009c), autoclaved pine needles on 2 % tap water agar (PNA) (Smith *et al.* 1996), or autoclaved banana leaves (BLA), and incubated at 25 °C under continuous near-ultraviolet light to promote sporulation. Reference strains and specimens of the studied fungi are maintained in the CBS culture collection (CBS) of the Westerdijk Fungal Biodiversity Institute (WI), Utrecht, the Netherlands.

DNA extraction, amplification (PCR) and phylogeny

Fungal mycelium (Table 1) was scraped from the agar surface of cultures with a sterile scalpel and the genomic DNA was isolated using the Wizard® Genomic DNA Purification Kit (Promega Corporation, WI, USA) following the manufacturers' protocols. Nine loci were amplified following previously published

protocols. First, the 28S nrRNA gene (LSU) and internal transcribed spacer regions with intervening 5.8S nrRNA gene (ITS) of the nrDNA operon were sequenced for all the isolates included in this study (for amplification conditions, see Fan *et al.* 2018). Other loci were sequenced for various species or genera using primers and conditions specific for those groups of fungi (Table 1). Amplification of the partial DNA-directed RNA polymerase II second largest subunit gene (*rpb2*), the partial translation elongation factor 1-alpha gene (*tef1*) and the partial beta-tubulin gene (*tub2*) followed Braun *et al.* (2018), while the amplification of the partial actin gene (*act*), the partial calmodulin gene (*cmdA*), the partial glyceraldehyde-3-phosphate dehydrogenase gene (*gapdh*) and the partial histone H3 gene (*his3*) followed Videira *et al.* (2016). The resulting fragments were sequenced in both directions using the respective PCR primers and the BigDye Terminator Cycle Sequencing Kit v. 3.1 (Applied Biosystems Life Technologies, Carlsbad, CA, USA); DNA sequencing amplicons were purified through Sephadex G-50 Superfine columns (Sigma-Aldrich, St. Louis, MO) in MultiScreen HV plates (Millipore, Billerica, MA). Purified sequence reactions were analysed on an Applied Biosystems 3730xl DNA Analyzer (Life Technologies, Carlsbad, CA, USA). The DNA sequences were analysed and consensus sequences were computed using SeqMan Pro v. 13 (DNASTAR, Madison, WI, USA).

The sequences for each gene region were subjected to megablast searches (Zhang *et al.* 2000) to identify closely related sequences in the NCBI's GenBank nucleotide database. The results are provided as part of the species notes or as selected phylogenetic trees. Phylogenetic trees were generated using Bayesian analyses performed with MrBayes v. 3.2.6 (Ronquist *et al.* 2012) for the overview trees and Maximum Parsimony analyses performed with PAUP v. 4.0b10 (Swofford 2003) as explained in Braun *et al.* (2018) for the genus and species trees. All resulting trees were printed with Geneious v. 11.0.3 (<http://www.geneious.com>, Kearse *et al.* 2012) and the layout of the trees was done in Adobe Illustrator v. CC 2017. Statistical measures calculated included tree length (TL), consistency index (CI), retention index (RI) and rescaled consistency index (RC).

Morphology

Slide preparations were mounted in lactic acid, Shear's mounting fluid or water, from colonies sporulating on MEA, PDA, PNA, BLA or OA. Sections through conidiomata were made by hand. Observations were made with a Nikon SMZ25 dissection-microscope, and with a Zeiss Axio Imager 2 light microscope using differential interference contrast (DIC) illumination and images recorded on a Nikon DS-Ri2 camera with associated software. Colony characters and pigment production were noted after 2–4 wk of growth on MEA, PDA and OA (Crous *et al.* 2009c).

Table 1. Collection details and GenBank accession numbers of isolates considered in this study.

Species	Locality	Substrate	Culture accession number(s) ¹	GenBank accession number ²		
				ITS, LSU, act	cmdA, gapdh, his3	rpb2, tef1, tub2
<i>Allelochaeta falcata</i>	Australia	<i>Eucalyptus alligatrix</i>	CPC 13578 = CBS 131117, ex-epitype	JN871204.1, JN871213.1, –	–, –, –	–, –, –
<i>Amycosphaerella africana</i>	New Zealand	<i>Metrosideros excelsa</i>	CPC 32782 = CBS 144635 = T16_03926C	MK442569.1, MK442511.1, –	–, –, –	–, MK442688.1, MK442725.1
<i>Bacillicladium clematidis</i> , sp. nov.	Austria	<i>Clematis vitalba</i>	CPC 33882 = CBS 145035, ex-type	MK442570.1, MK442512.1, –	–, –, –	–, –, MK442726.1
<i>Beltrania rhombica</i>	Chile	<i>Eucalyptus urophylla</i>	CPC 31775 = CBS 144521	MK442571.1, MK442513.1, –	–, –, –	–, –, –
<i>Brevistachys lateralis</i>	Thailand	<i>Musa</i> sp.	CPC 33958 = CBS 145062	MK442572.1, MK442514.1, –	MK442649.1, –, –	MK442661.1, MK442689.1, MK442727.1
<i>Cercospora gomphrenigena</i> , sp. nov.	South Africa	<i>Gomphrena globosa</i>	CPC 32470 = CBS 144613, ex-type	MK442573.1, MK442515.1, –	MK442650.1, –, MK442658.1	–, MK442690.1, MK442728.1
<i>Cladoriella xanthorrhoeae</i>	Australia	<i>Xanthorrhoea</i> sp.	CPC 32609 = CBS 144523	MK442574.1, MK442516.1, –	–, –, –	–, –, –
<i>Creosphaeria sassafras</i>	Spain	<i>Laurus nobilis</i>	CPC 33410 = CBS 144984	MK442575.1, MK442517.1, –	–, –, –	–, –, –
<i>Cylindrocladiella peruviana</i>	South Africa	<i>Pelargonium</i> sp.	CPC 33527 = CBS 145053 = SPXX	MK442576.1, MK442518.1, –	–, –, MK442659.1	MK442662.1, MK442691.1, MK442729.1
<i>Cyphellophora clematidis</i> , sp. nov.	Austria	<i>Clematis vitalba</i>	CPC 33880 = CBS 144983, ex-type	MK442577.1, MK442519.1, –	–, –, –	–, –, MK442730.1
<i>Diaporthe anacardii</i>	South Africa	Unidentified leaf litter	CPC 33074 = CBS 144610	MK442578.1, MK442520.1, –	MK442651.1, –, –	–, MK442692.1, –
<i>Diaporthe eres</i>	Netherlands	<i>Lactuca sativa</i>	CPC 34055 = CBS 145040	MK442579.1, MK442521.1, MK442634.1	MK442652.1, –, –	MK442663.1, MK442693.1, MK442731.1
<i>Dichotomophthora basellae</i>	Thailand	Unidentified host plant	CPC 33044 = CBS 145050	MK442580.1, MK442522.1, –	–, –, –	MK442664.1, –, –
<i>Exophiala abietophila</i> , sp. nov.	Norway	<i>Abies alba</i>	CPC 34580 = CBS 145038, ex-type	MK442581.1, MK442523.1, –	–, –, –	–, –, –
<i>Exophiala lignicola</i> , sp. nov.	Ukraine	cf. <i>Quercus</i> sp.	CPC 32464 = CBS 144622, ex-type	MK442582.1, MK442524.1, –	MK442653.1, –, –	–, MK442694.1, –
<i>Fuscostagonospora banksiae</i> , sp. nov.	Australia	<i>Banksia</i> sp.	CPC 31724 = CBS 144621, ex-type	MK442583.1, MK442525.1, –	–, –, –	–, –, –
<i>Gaeumannomyces caricicola</i> , sp. nov.	Germany	<i>Carex remota</i>	CPC 33925 = CBS 145041, ex-type	MK442584.1, MK442526.1, –	–, –, MK442660.1	–, –, MK442732.1
<i>Hansfordia pruni</i> , sp. nov.	Italy	<i>Prunus persica</i>	CBS 194.56 = IMI 146912, ex-type	MK442585.1, MH869122.1, KU760903.1	–, –, –	KU684307.1, –, –
<i>Hansfordia pulvinata</i>	Italy	<i>Cercospora unamunoi</i> on <i>Capsicum annuum</i>	CBS 134.62 = IMI 146913	MK442586.1, MH869699.1, –	–, –, –	–, –, –
<i>Hypothecha maxima</i> , comb. nov.	Australia	<i>Macrozamia miquelii</i>	CPC 32119 = CBS 144422	MK442587.1, MK442527.1, –	–, –, –	–, –, –
<i>Hypothecha nigra</i> , comb. nov.	Brazil	<i>Niphidium crassifolium</i>	CPC 24674 = COAD 1983, ex-epitype	KX891229.1, KX891228.1, –	–, –, –	–, –, –
<i>Hypothecha pleomorpha</i> , comb. nov.	Spain	Epiphytic lichens growing on bark of holm oak	MA 18191	–, KP144011.1, –	–, –, –	–, –, –
<i>Hypothecha pleomorpha</i> , comb. nov.	Australia	<i>Eucalyptus piperita</i>	CPC 32144 = CBS 144636	MK442588.1, MK442528.1, –	–, –, –	–, –, –
<i>Jeremyomyces labinae</i> , gen. et sp. nov.	Germany	<i>Salix alba</i>	CPC 33154 = CBS 144617, ex-type	MK442589.1, MK442529.1, –	MK442654.1, –, –	MK442665.1, MK442695.1, MK442733.1
<i>Macgarvieomyces luzulae</i>	Ukraine	<i>Luzula sylvatica</i>	CPC 34292 = CBS 145042	MK442591.1, MK442531.1, MK442635.1	–, –, –	–, –, –
<i>Microdochium rhopalostylidis</i> , sp. nov.	New Zealand	<i>Rhopalostylis sapida</i>	CPC 34449 = CBS 145125, ex-type	MK442592.1, MK442532.1, MK442636.1	MK442655.1, –, –	MK442667.1, –, MK442735.1

Table 1. (Continued).

Species	Locality	Substrate	Culture accession number(s) ¹	GenBank accession number ²			
				ITS, LSU, act	cmdA, gapdh, his3	rpb2, tef1, tub2	
<i>Neocardana malayensis</i> , sp. nov.	Malaysia	<i>Musa</i> sp.	CPC 32837 = CBS 144604, ex-type	MK442593.1, MK442533.1, MK442637.1	–, –, –	–, –, MK442736.1	
<i>Neocucurbitaria prunicola</i> , sp. nov.	Ukraine	<i>Prunus padus</i>	CPC 33709 = CBS 145033, ex-type	MK442594.1, MK442534.1, –	–, –, –	MK442668.1, –, MK442737.1	
<i>Neocucurbitaria salicis-albae</i> , sp. nov.	Germany	<i>Salix alba</i>	CPC 33162 = CBS 144611, ex-type	MK442595.1, MK442535.1, –	–, –, –	MK442669.1, –, MK442738.1	
<i>Neodevriesia metrosideri</i>	New Zealand	<i>Metrosideros excelsa</i>	CPC 32786 = CBS 144638	MK442596.1, MK442536.1, MK442638.1	–, –, –	–, –, MK442739.1	
<i>Neodotthidia negundinicola</i> , gen. et sp. nov.	Ukraine	<i>Acer negundo</i>	CPC 34071 = CBS 145039, ex-type	MK442597.1, MK442537.1, –	–, –, –	–, MK442697.1, –	
<i>Neodotthidotthia negundinis</i> , comb. nov.	USA	<i>Fendlera rupicola</i>	CPC 12928 = CBS 119686	MK442598.1, EU673272.1, –	–, –, –	–, –, –	
	USA	<i>Euonymus alatus</i>	CPC 12930 = CBS 119688	MK442599.1, EU673274.1, –	–, –, –	–, –, –	
	USA	<i>Acer negundo</i>	CPC 12932 = CBS 119690	MK442600.1, EU673275.1, –	–, –, –	–, –, –	
	USA	<i>Acer negundo</i>	CPC 12933 = CBS 119691	MK442601.1, EU673276.1, –	–, –, –	–, –, –	
<i>Neohelicomyces deschampsiae</i> , sp. nov.	Germany	<i>Deschampsia cespitosa</i>	CPC 33686 = CBS 145029, ex-type	MK442602.1, MK442538.1, –	–, –, –	–, –, –	
<i>Neomedicopsis prunicola</i> , gen. et sp. nov.	Ukraine	<i>Prunus padus</i>	CPC 33711 = CBS 145031, ex-type	MK442603.1, MK442539.1, –	–, –, –	MK442670.1, –, –	
<i>Neophaeoappendicospora leucaenae</i> , gen. et sp. nov.	La Réunion	<i>Leucaena leucocephala</i>	CPC 27240, ex-type	MK442604.1, MK442540.1, –	–, –, –	–, –, –	
<i>Ochroconis musae</i>	Thailand	<i>Persea americana</i>	CPC 33947 = CBS 145061	MK442605.1, MK442541.1, MK442639.1	–, –, –	–, MK442698.1, –	
<i>Paradevriesia americana</i> , gen. et comb. nov.	USA	Air	CBS 117726 = CPC 5121 = ATCC 96545, ex-type	MH863026.1, EU040227.1, –	–, –, –	–, –, –	
<i>Paradevriesia compacta</i> , sp. nov.	Mallorca	Rock	CBS 118294 = TRN 111 = dH 14587, ex-type	GU323967.1, GU323967.1, –	–, –, –	KF310095.1, –, KF546761.1	
<i>Paradevriesia pseudoamericana</i> , comb. nov.	Germany	<i>Malus domestica</i>	CPC 16174 = CBS 126270, ex-type	GU570527.1, GU570544.1, –	–, –, –	–, HM177416.1, –	
<i>Pararamichloridium livistonae</i>	Australia	<i>Livistona australis</i>	CPC 32152 = CBS 144522, ex-type	MK442606.1, MK442542.1, –	–, –, –	–, –, –	
<i>Pararousoella juglandicola</i> , sp. nov.	Germany	<i>Juglans regia</i>	CPC 33400 = CBS 145037, ex-type	MK442607.1, MK442543.1, –	–, –, –	MK442671.1, MK442699.1, –	
<i>Pararousoella mukdahanensis</i> , comb. nov.	Thailand	Bamboo, dead culms	MFLUCC 11-0201, ex-type	KU940129.1, KU863118.1, –	–, –, –	–, –, –	
<i>Petriella sordida</i>	Ukraine	<i>Luzula</i> sp.	CPC 32460 = CBS 144612	MK442608.1, MK442544.1, –	MK442656.1, –, –	–, MK442700.1, MK442740.1	
<i>Pezizula eucalyptigena</i> , sp. nov.	Ukraine	<i>Luzula</i> sp.	CPC 32461 = CBS 145121	MK442609.1, MK442545.1, –	–, –, –	MK442672.1, MK442701.1, –	
<i>Phaeoseptoriella zaeae</i> , gen. et sp. nov.	South Africa	<i>Eucalyptus</i> sp.	CPC 32129 = CBS 144637, ex-type	MK442610.1, MK442546.1, –	–, –, –	MK442673.1, –, –	
	South Africa	<i>Zea mays</i>	CPC 33064 = CBS 144614, ex-type	MK442611.1, MK442547.1, –	–, –, –	MK442674.1, MK442702.1, MK442741.1	
<i>Phlogicylindrium dunnii</i> , sp. nov.	Australia	<i>Eucalyptus dunnii</i>	CPC 31818 = CBS 144620, ex-type	MK442612.1, MK442548.1, –	–, –, –	MK442675.1, MK442703.1, –	

Table 1. (Continued).

Species	Locality	Substrate	Culture accession number(s) ¹	GenBank accession number ²			
				ITS, LSU, act	cmdA, gapdh, his3	rpb2, tef1, tub2	
<i>Phyllosticta austroafricana</i> , sp. nov.	South Africa	Leaf spots of unidentified deciduous tree host	CPC 31920 = CBS 144593, ex-type	MK442613.1, MK442549.1, MK442640.1	-	-	MK442704.1, -
<i>Phyllosticta hagahagaensis</i> , sp. nov.	South Africa	<i>Carrisa bispinosa</i>	CPC 32799 = CBS 144592, ex-type	MK442614.1, MK442550.1, MK442641.1	-	MK442657.1, -	-
<i>Piniphoma wesendahlina</i> , gen. et sp. nov.	Germany	<i>Pinus sylvestris</i>	CPC 33693 = CBS 145032, ex-type	MK442615.1, MK442551.1, -	-	-	MK442676.1, MK442706.1, MK442742.1
<i>Parodiopodia vitis</i> , sp. nov.	USA	<i>Vitis vinifera</i>	CPC 31642 = CBS 144634, ex-type	MK442616.1, MK442552.1, -	-	-	-
<i>Pseudoanungitea variabilis</i>	Spain	Leaf litter	CBS 132716 = FMR 11934, ex-type	KY853424.1, KY853484.1, -	-	-	MK442678.1, MK442710.1, -
<i>Pseudocercospora hakeae</i>	Australia	<i>Hakea</i> sp.	CPC 32100 = CBS 144520	MK442617.1, MK442553.1, MK442642.1	-	-	MK442677.1, MK442708.1, MK442743.1
<i>Pseudoconiothyrium broussonetiae</i> , gen. et sp. nov.	Italy	<i>Broussonetia papyrifera</i>	CPC 33570 = CBS 145036, ex-type	MK442618.1, MK442554.1, -	-	-	-
<i>Pseudophaeocephalospora phormii</i> , comb. nov.	New Zealand	<i>Phormium tenax</i>	CPC 32742 = CBS 144606 = T16_03297D, ex-epitype	MK442619.1, MK442555.1, MK442643.1	-	-	-
<i>Pseudosigmaidea alnicola</i> , sp. nov.	Germany	<i>Alnus glutinosa</i>	CPC 33776 = CBS 145034, ex-type	MK442620.1, MK442556.1, -	-	-	-
<i>Pseudoteratosphaeria africana</i> , sp. nov.	Angola	Leaf spot on unidentified host	CPC 33072 = CBS 144597	MK442621.1, MK442557.1, MK442644.1	-	-	-
	Angola	Leaf spot on unidentified host	CPC 33144 = CBS 144595, ex-type	MK442622.1, MK442558.1, MK442645.1	-	-	-
	Angola	Leaf spot on unidentified host	CPC 33145 = CBS 144596	MK442623.1, MK442559.1, MK442646.1	-	-	-
<i>Selenodiella fertilis</i>	Australia	<i>Eucalyptus</i> sp.	CPC 32663 = CBS 144589	MK442624.1, MK442560.1, -	-	-	-
<i>Septonema crispulum</i>	Italy	<i>Pinus pinea</i>	CBS 735.96, ex-isotype	MH862607.1, MH874232.1, -	-	-	MK442679.1, -
<i>Stagonospora pseudoperfecta</i>	Germany	<i>Typha</i> sp.	CPC 33138 = CBS 144607	MK442625.1, MK442561.1, -	-	-	-
<i>Symptodiella acicola</i>	Netherlands	<i>Pinus sylvestris</i>	CBS 425.76	KY853467.1, KY853529.1, -	-	-	MK442680.1, MK442716.1, -
	Netherlands	<i>Pinus sylvestris</i>	CBS 487.82, ex-epitype	KY853468.1, KY853530.1, -	-	-	MK442681.1, MK442717.1, -
<i>Symptodiella alternata</i> , comb. nov.	Japan	<i>Pinus densifolia</i>	IFO 8933 = CBS 326.69, ex-type	MK442626.1, MH871053.1, -	-	-	MK442682.1, MK442718.1, -
	-	-	HKUCC 10828 = NIN43193	-	-	-	DQ435078.1, -
<i>Symptodiella goidanichii</i> , comb. nov.	Italy	<i>Fagus sylvatica</i>	CBS 136.58, ex-type	MH857722.1, MH869262.1, -	-	-	-
<i>Symptodiella quercina</i> , sp. nov.	UK	<i>Betula</i> sp.	CBS 987.70	MH860019.1, MH871803.1, -	-	-	MK442683.1, MK442720.1, -
	Germany	<i>Quercus robur</i>	CPC 33903 = CBS 145028, ex-type	MK442627.1, MK442562.1, -	-	-	MK442684.1, MK442721.1, -

Table 1. (Continued).

Species	Locality	Substrate	Culture accession number(s) ¹	GenBank accession number ²			
				ITS, LSU, act	<i>cmdA</i> , <i>gapdh</i> , <i>his3</i>	<i>rpb2</i> , <i>tef1</i> , <i>tub2</i>	
<i>Sympoventuria regnans</i>	Australia	<i>Eucalyptus pauciflora</i>	CPC 31820 = CBS 144605	MK442628.1, MK442563.1, –	–, –, –	–, MK442722.1, MK442748.1	
<i>Tubakia suttoniana</i>	New Zealand	<i>Quercus</i> sp.	CPC 32745 = CBS 144591 = T16_01981A	MK442629.1, MK442564.1, –	–, –, –	MK442685.1, MK442723.1, MK442749.1	
<i>Turquoiseomyces eucalypti</i> , gen. et sp. nov.	Australia	<i>Eucalyptus leptophylla</i>	CPC 34399 = CBS 145126, ex-type	MK442630.1, MK442565.1, –	–, –, –	MK442686.1, –, MK442750.1	
<i>Typhicola typharum</i> , gen. et comb. nov.	Germany	<i>Typha</i> sp.	CPC 33271 = CBS 145043, ex-neotype	MK442590.1, MK442530.1, –	–, –, –	MK442666.1, MK442696.1, MK442734.1	
<i>Wojnowiciella dactylidis</i>	New Zealand	<i>Dypsis</i> sp. (Arecaceae)	CPC 32741 = CBS 145077 = T16_03296B	MK442631.1, MK442566.1, –	–, –, –	–, MK442724.1, MK442751.1	
<i>Xenodevriesia strelitzicola</i> , gen. et comb. nov.	South Africa	<i>Strelitzia</i> sp.	CBS 122480 = X1045, ex-type	GU214635.1, GU214417.1, –	–, –, –	–, –, –	
<i>Zasmidium hakeicola</i> , sp. nov.	Australia	<i>Hakea corymbosa</i>	CPC 32703 = CBS 144590, ex-type	MK442632.1, MK442567.1, MK442647.1	–, –, –	MK442687.1, –, MK442752.1	
<i>Zygosporium pseudogibbum</i>	Australia	<i>Macrozamia miquelii</i>	CPC 32120 = CBS 144442	MK442633.1, MK442568.1, MK442648.1	–, –, –	–, –, MK442753.1	

¹ ATCC: American Type Culture Collection, Virginia, USA; CBS: Westerdijk Fungal Biodiversity Institute, Utrecht, The Netherlands; CPC: Culture collection of Pedro Crous, housed at CBS; dH: Culture collection of Sybren de Hoog, housed at CBS; IFO: Institute for Fermentation, Osaka, Yodogawa-ku, Osaka, Japan (collection transferred to NBRC); IMI: International Mycological Institute, CABI-Bioscience, Egham, Bakenham Lane, United Kingdom; MFLUCC: Mae Fah Luang University Culture Collection, Chiang Rai, Thailand.

² ITS: internal transcribed spacers and intervening 5.8S rDNA; LSU: large subunit (28S) of the rRNA gene operon; *act*: partial actin gene; *cmdA*: partial calmodulin gene; *gapdh*: partial glyceraldehyde-3-phosphate dehydrogenase gene; *his3*: partial histone H3 gene; *rpb2*: partial DNA-directed RNA polymerase II second largest subunit gene; *tef1*: partial translation elongation factor 1- α gene; *tub2*: partial beta-tubulin gene.

incubated at 25 °C. Colony colours (surface and reverse) were scored using the colour charts of Rayner (1970). Sequences derived in this study were deposited in GenBank (Table 1), the alignment in TreeBASE (www.treebase.org; study number S23853), and taxonomic novelties in MycoBank (www.MycoBank.org; Crous et al. 2004).

RESULTS

Phylogeny

Dothideomycetes LSU phylogeny (Fig. 1): The alignment contained 254 isolates and *Helotium subcorticale* (CBS 248.62, GenBank MH869740.1) was used as outgroup. The final alignment contained a total of 809 characters used for the phylogenetic analyses, including alignment gaps. The alignment contained a total of 392 unique site patterns. Based on the results of MrModelTest, dirichlet base frequencies and the GTR+I+G model was used for the Bayesian analysis. The Bayesian analyses generated 133 802 trees from which 100 352 were discarded as burn-in. The posterior probability values (PP) higher than 0.84 are plotted on the tree (Fig. 1).

Eurotiomycetes LSU phylogeny (Fig. 2): The alignment contained 71 isolates and *Saccharata proteae* (CBS 119218, GenBank EU552145.1) was used as outgroup. The final alignment contained a total of 772 characters used for the phylogenetic analyses, including alignment gaps. The alignment contained a total of 265 unique site patterns. Based on the results of MrModelTest, dirichlet base frequencies and the GTR+I+G model was used for the Bayesian analysis. The Bayesian analyses generated 30 502 trees from which 22 878 were discarded as burn-in. The posterior probability values (PP) higher than 0.84 are plotted on the tree (Fig. 2).

Lecanoromycetes and *Leotiomyces* LSU phylogeny (Fig. 3): The alignment contained 42 isolates and *Saccharata proteae* (CBS 119218, GenBank EU552145.1) was used as outgroup. The final alignment contained a total of 838 characters used for the phylogenetic analyses, including alignment gaps. The alignment contained a total of 222 unique site patterns. Based on the results of MrModelTest, dirichlet base frequencies and the GTR+I+G model was used for the Bayesian analysis. The Bayesian analyses generated 9 102 trees from which 6 828 were discarded as burn-in. The posterior probability values (PP) higher than 0.84 are plotted on the tree (Fig. 3).

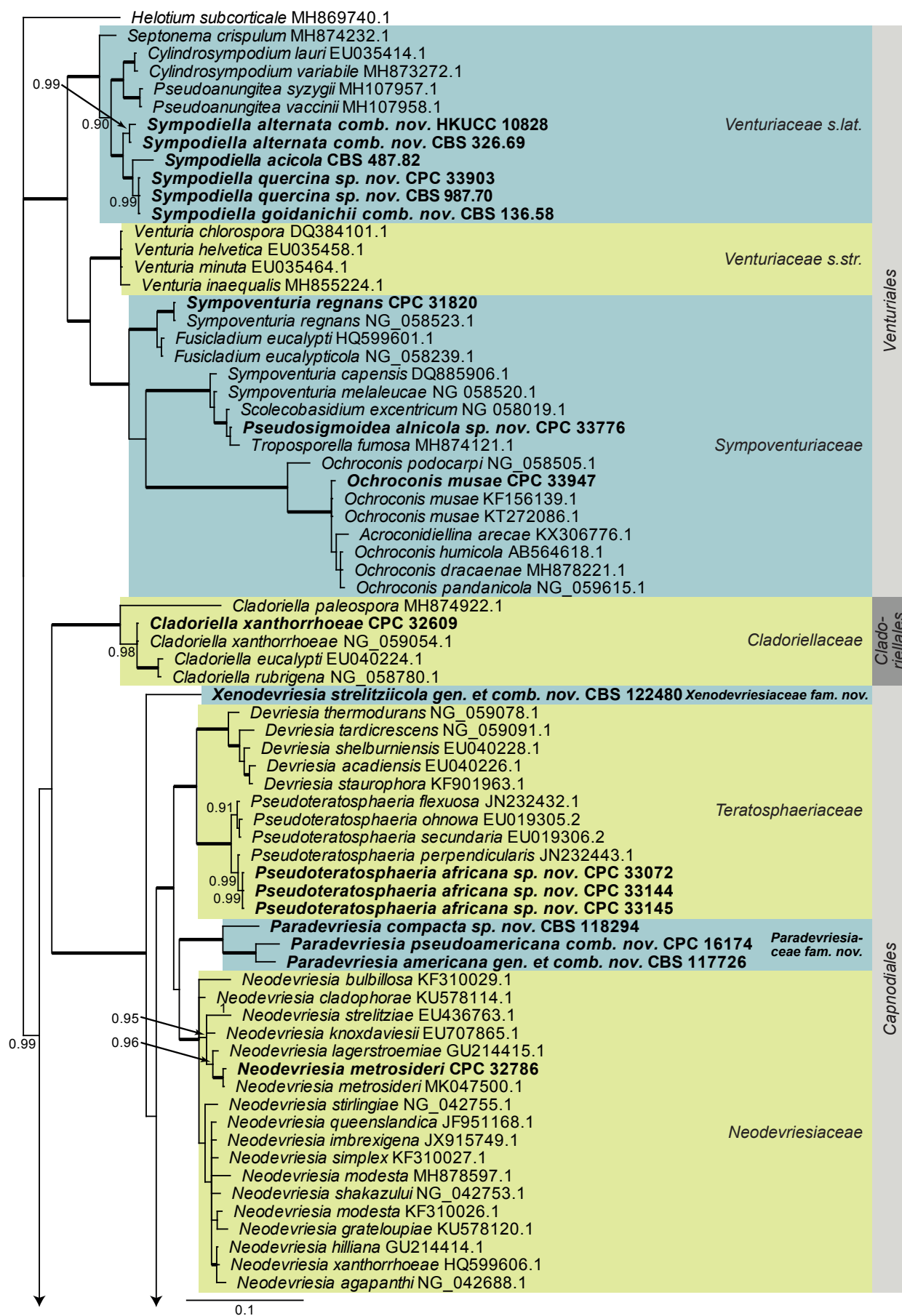


Fig. 1. Consensus phylogram (50% majority rule) obtained from a Bayesian analysis of the *Dothideomycetes* alignment. Bayesian posterior probabilities (PP) >0.84 are shown at the nodes and thickened lines represent nodes with PP = 1.00. The scale bar represents the expected changes per site. Families and orders are indicated with coloured blocks to the right of the tree. GenBank accession and/or culture accession numbers are indicated behind the species names. The tree was rooted to *Helotium subcorticale* (GenBank MH869740.1) and the novelties treated in the Taxonomy section are indicated in bold face.

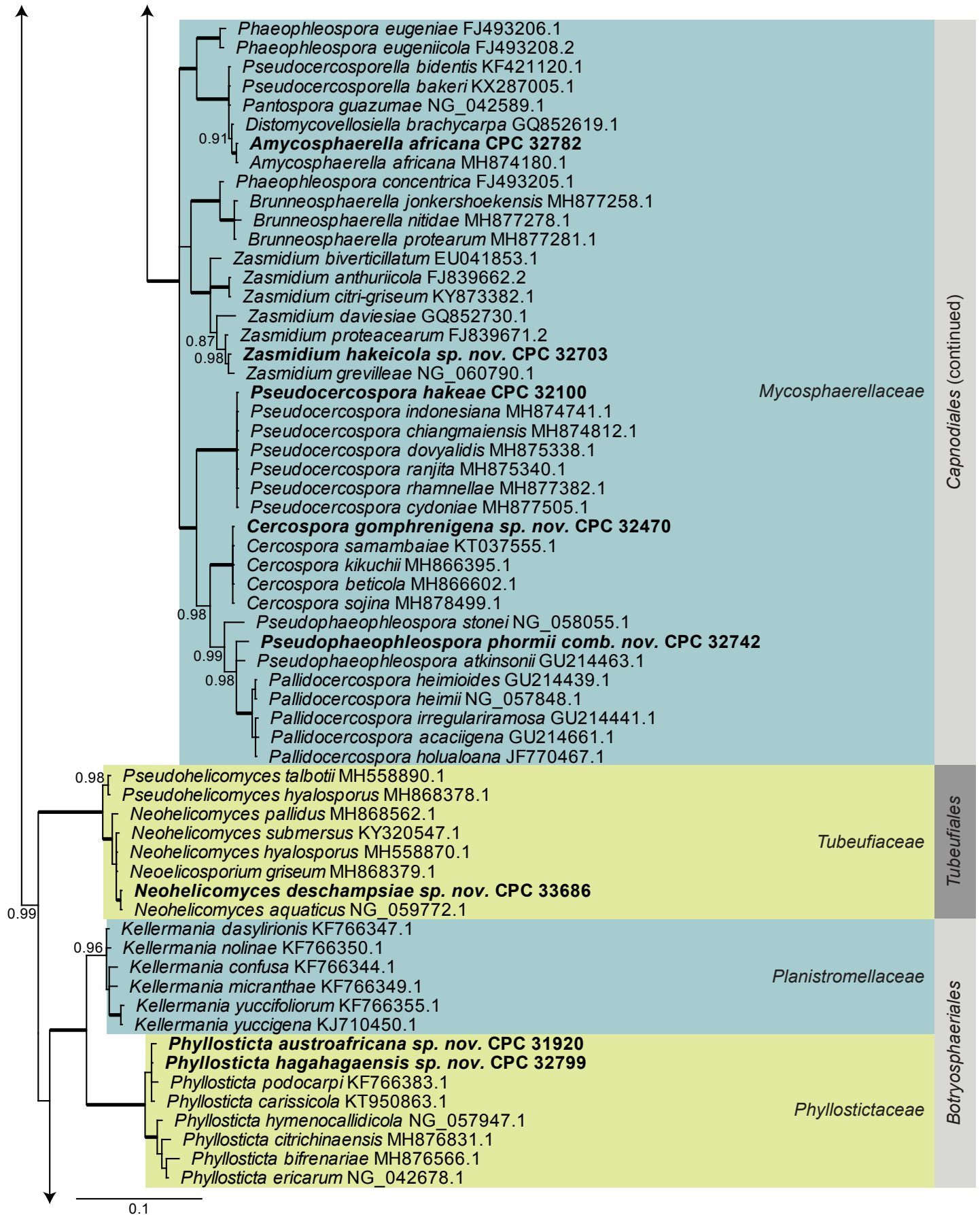


Fig. 1. (Continued).

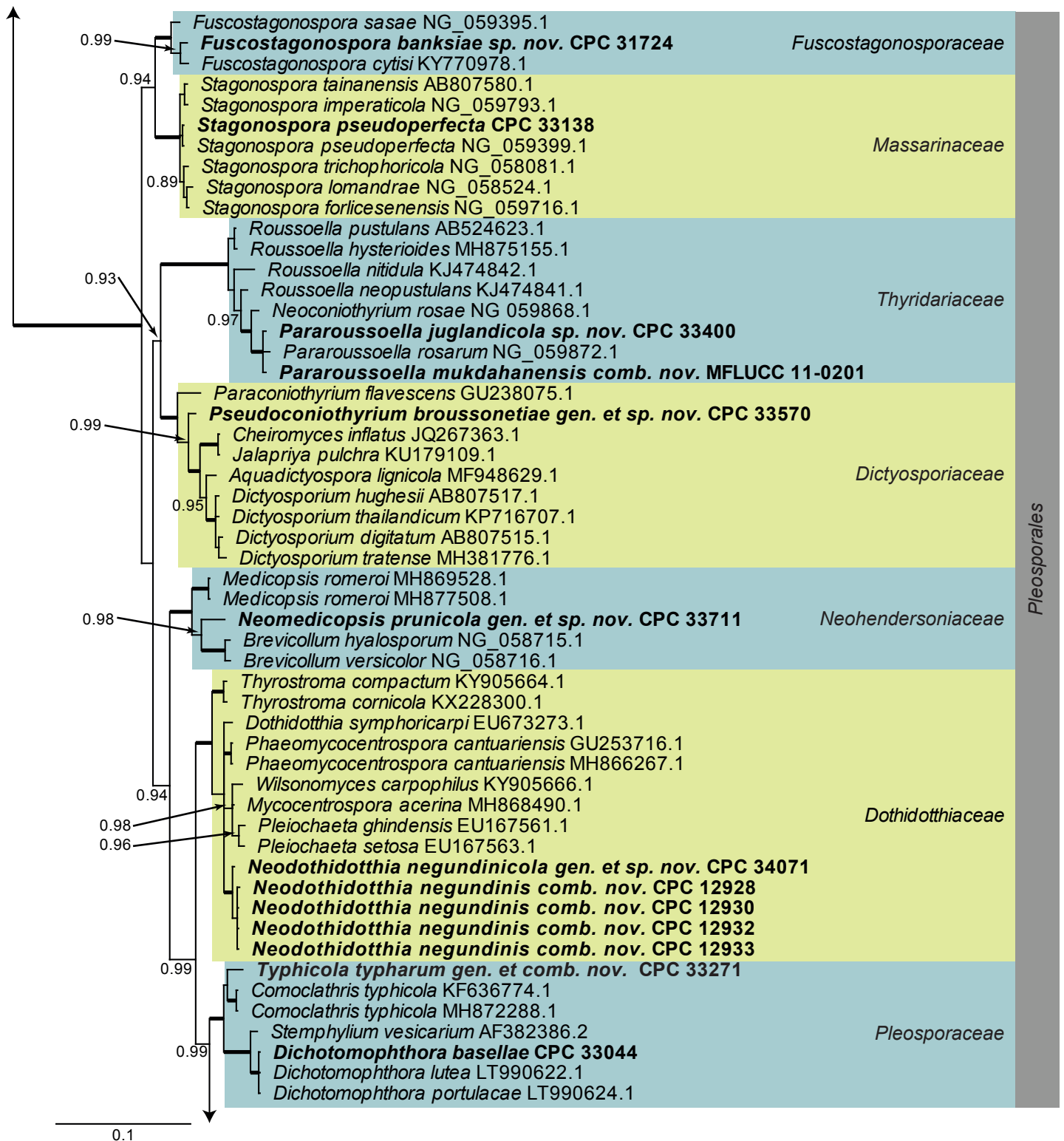


Fig. 1. (Continued).

Sordariomycetes LSU phylogeny (Fig. 4): The alignment contained 174 isolates and *Saccharata proteae* (CBS 119218, GenBank EU552145.1) was used as outgroup. The final alignment contained a total of 778 characters used for the phylogenetic analyses, including alignment gaps. The alignment contained a total of 334 unique site patterns. Based on the results of MrModelTest, dirichlet base frequencies and the GTR+I+G model was used for the Bayesian analysis. The Bayesian analyses

generated 161 202 trees from which 120 902 were sampled after 25 % of the trees were discarded as burn-in. The posterior probability values (PP) higher than 0.84 are plotted on the tree (Fig. 4).

Species phylogenies: Specific phylogenetic analyses were run for selected species and the resulting phylogenies are discussed in the species notes where applicable. Statistics associated with those phylogenies are provided in the figure legends.

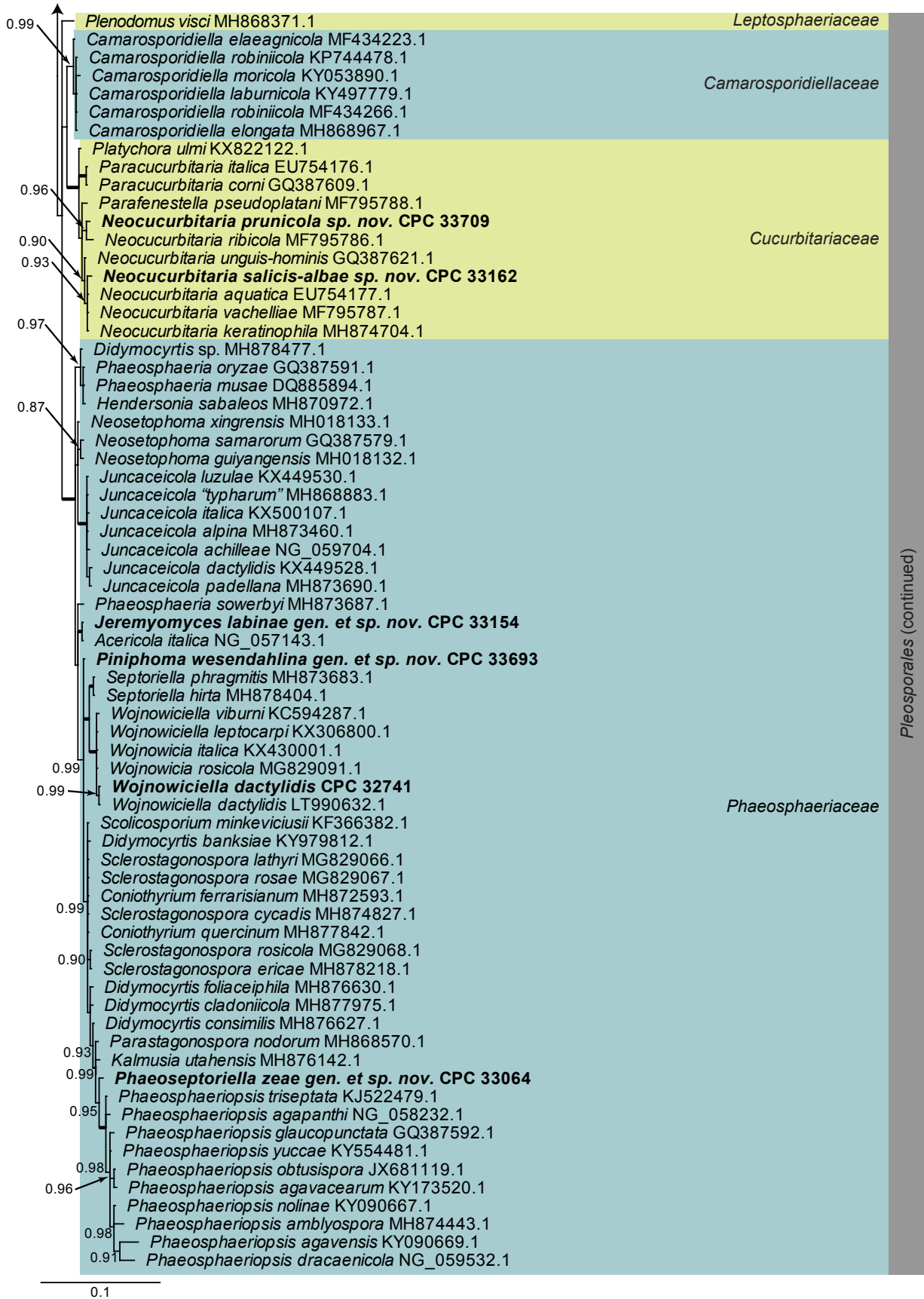


Fig. 1. (Continued).

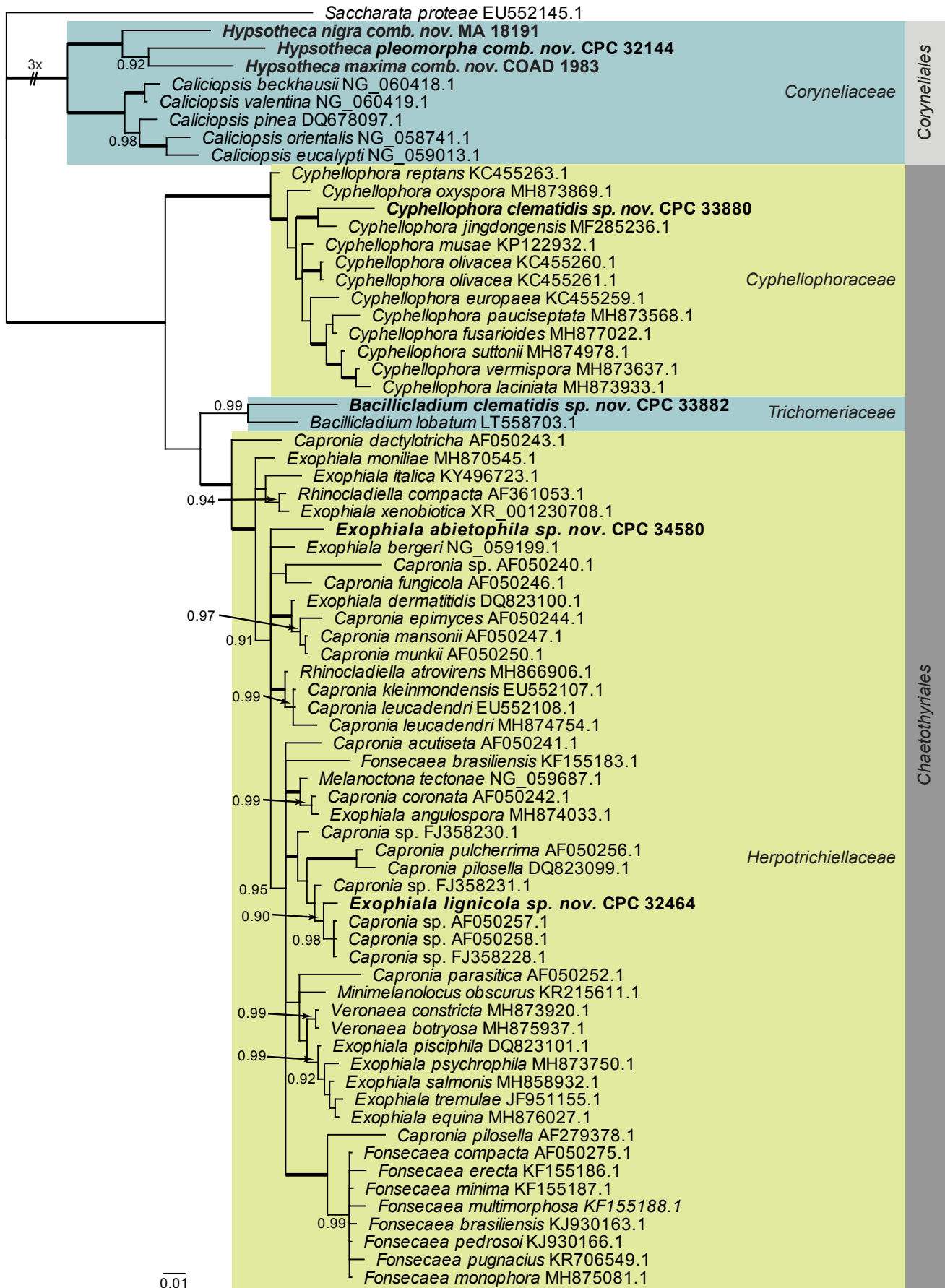


Fig. 2. Consensus phylogram (50 % majority rule) obtained from a Bayesian analysis of the *Eurotiomycetes* alignment. Bayesian posterior probabilities (PP) >0.84 are shown at the nodes and thickened lines represent nodes with PP = 1.00. The scale bar represents the expected changes per site. Families and orders are indicated with coloured blocks to the right of the tree. GenBank accession and/or culture accession numbers are indicated behind the species names. The tree was rooted to *Saccharata proteae* (GenBank EU552145.1) and the novelties treated in the Taxonomy section are indicated in bold face.

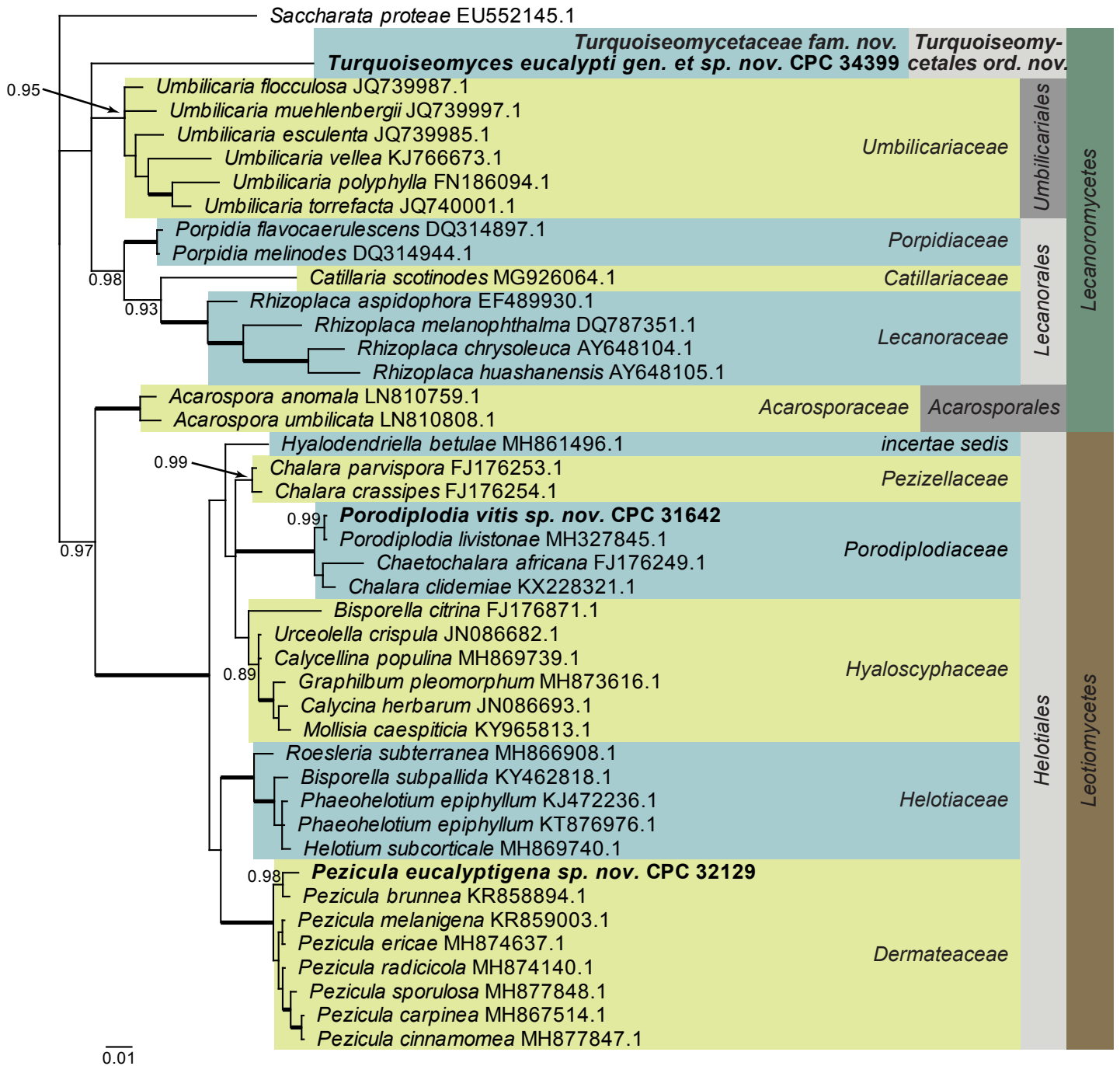


Fig. 3. Consensus phylogram (50 % majority rule) obtained from a Bayesian analysis of the *Lecanoromycetes* and *Leotiomyces* alignment. Bayesian posterior probabilities (PP) >0.84 are shown at the nodes and thickened lines represent nodes with PP = 1.00. The scale bar represents the expected changes per site. Families, orders and classes are indicated with coloured blocks to the right of the tree. GenBank accession and/or culture accession numbers are indicated behind the species names. The tree was rooted to *Saccharata proteae* (GenBank EU552145.1) and the novelties treated in the Taxonomy section are indicated in bold face.

Taxonomy

Amycosphaerella africana (Crous & M.J. Wingf.) Quaedvl. & Crous, *Persoonia* **33**: 23. 2014. Fig. 5.
Basionym: *Mycosphaerella africana* Crous & M.J. Wingf., *Mycologia* **88**: 450. 1996.

In vitro. Ascomata pseudothecial, erumpent to superficial on agar, black, globose, 70–90 µm diam; apical ostiole; wall of 2–4 layers of medium brown *textura angularis*. Asci paraphysate, fasciculate, bitunicate, narrowly ellipsoid to subcylindrical, straight to incurved, 8-spored, 28–37 × 6–7 µm. Ascospores

multiseriate, overlapping, hyaline, guttulate, thin-walled, straight to slightly curved, fusoid-ellipsoid with obtuse ends, widest in middle of the apical cell, medianly 1-septate, not to slightly constricted at septum, tapering toward both ends, 10–12 × (2–)2.5 µm.

Culture characteristics: Colonies erumpent, spreading, with moderate aerial mycelium, and smooth, lobate margins, covering dish in 2 wk. On MEA surface pale olivaceous grey to olivaceous grey, reverse iron-grey; on PDA surface olivaceous grey with patches of pale olivaceous grey, reverse iron-grey; on OA surface olivaceous grey with patches of dirty white.

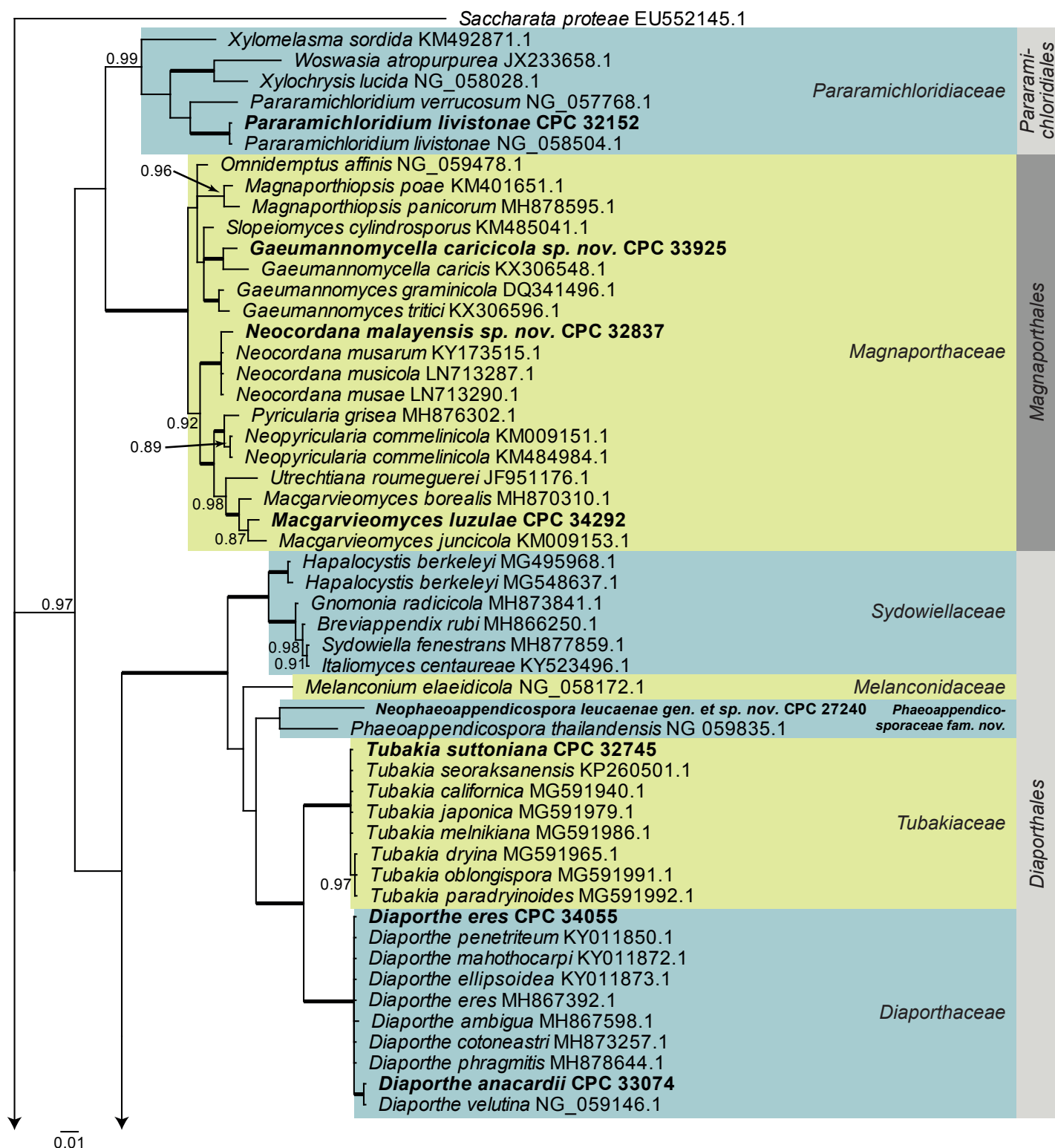


Fig. 4. Consensus phylogram (50% majority rule) obtained from a Bayesian analysis of the *Sordariomycetes* alignment. Bayesian posterior probabilities (PP) >0.84 are shown at the nodes and thickened lines represent nodes with PP = 1.00. The scale bar represents the expected changes per site. Families and orders are indicated with coloured blocks to the right of the tree. GenBank accession and/or culture accession numbers are indicated behind the species names. The tree was rooted to *Saccharata proteae* (GenBank EU552145.1) and the novelties treated in the Taxonomy section are indicated in bold face.

Material examined: New Zealand, Auckland, Bucklands Beach, 22 Wells Road, on leaves of *Metrosideros excelsa* (Myrtaceae), 2015, R. Thangavel, T16_03926C = CBS H-23809, culture CBS 144635 = CPC 32782.

Notes: *Amycosphaerella africana*, which is the oldest name for this taxon, is known from Australia (*Buckinghamia* sp., *Eucalyptus grandis*, *E. globulus*), Colombia (*E. grandis*), New Zealand (*Dracaena draco*), Portugal (*E. globulus*), South Africa (*E. cladocalyx*, *E. deanei*, *E. grandis*, *E. radiata*, *E. smithii*, *E. viminalis*), and Zambia (*E. globulus*) (Videira et al. 2017).

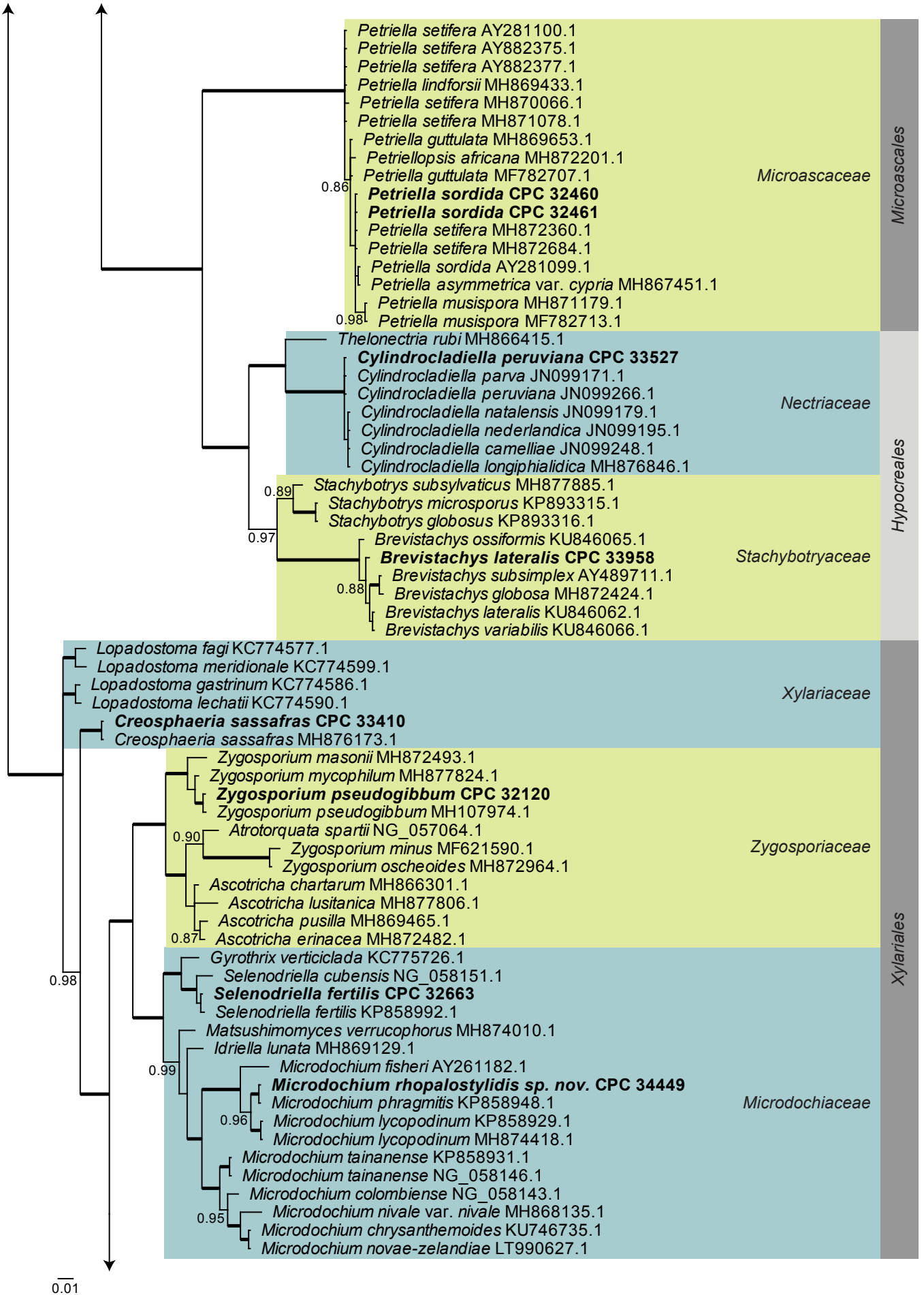


Fig. 4. (Continued).

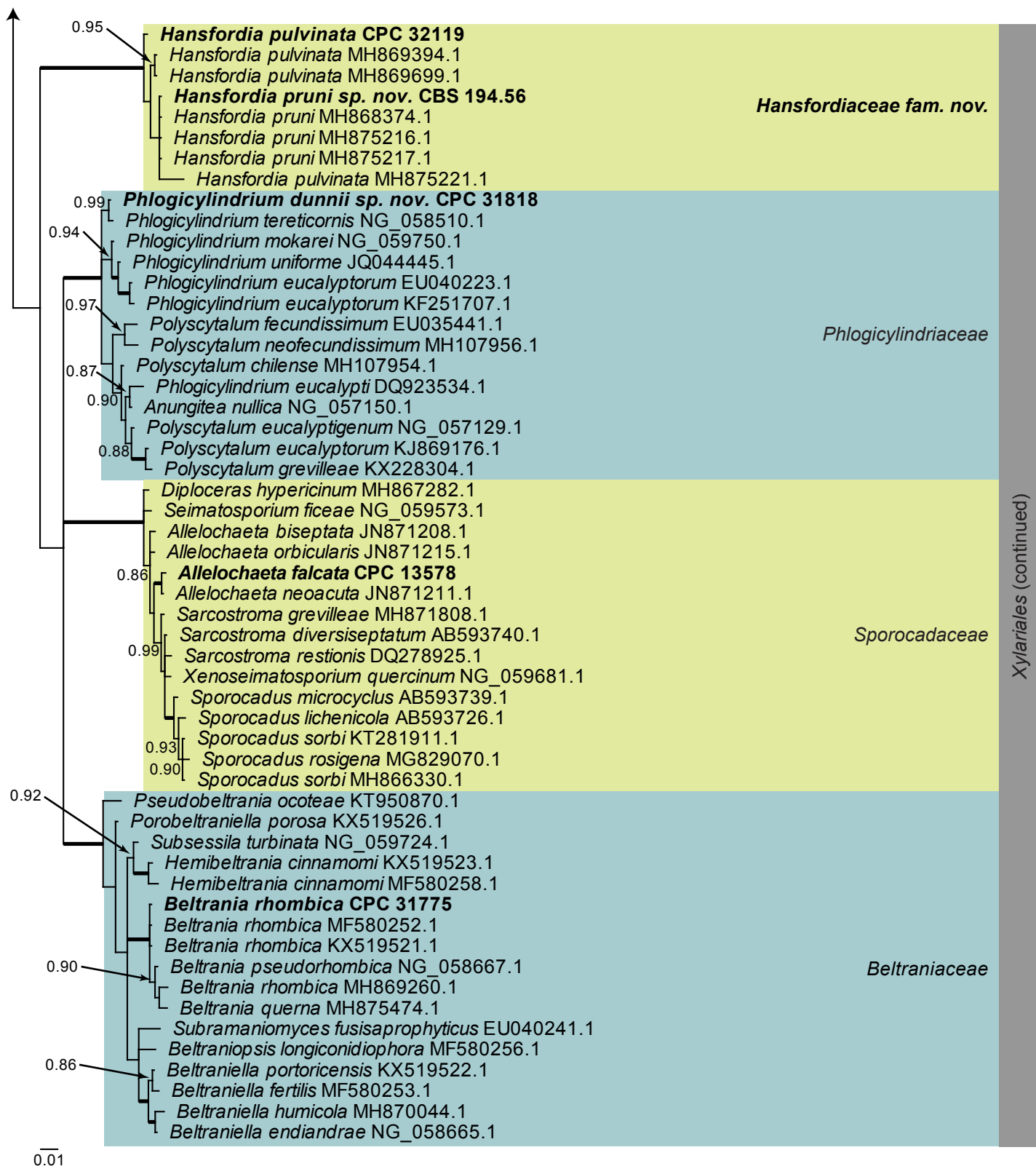


Fig. 4. (Continued).

Based on a megablast search of NCBI's GenBank nucleotide database, the ITS sequence was identical to *Mycosphaerella buckinghamiae* (GenBank EU707856.2; Identities = 523/523 (100 %)), *Amycosphaerella africana* (as *Mycosphaerella africana*, GenBank AY626981.1; Identities = 523/523 (100 %)), and related to *Pantospora guazumae* (GenBank NR_119971.1; Identities = 521/523 (99 %), no gaps). Closest hits using the LSU sequence are *Amycosphaerella africana* (GenBank

MH874180.1; Identities = 785/785 (100 %)), *Mycosphaerella buckinghamiae* (GenBank EU707856.2; Identities = 785/785 (100 %)), and *Distomycovellosiella brachycarpa* (as *Passalora brachycarpa*, GenBank GU214664.1; Identities = 782/785 (99 %), 2 gaps (0 %)). The *tef1* sequence was identical to numerous sequences of *Amycosphaerella africana* (e.g. as *Mycosphaerella ellipsoidea*, GenBank JX901653.1; Identities = 394/394 (100 %)). Closest hits using the *tub2*

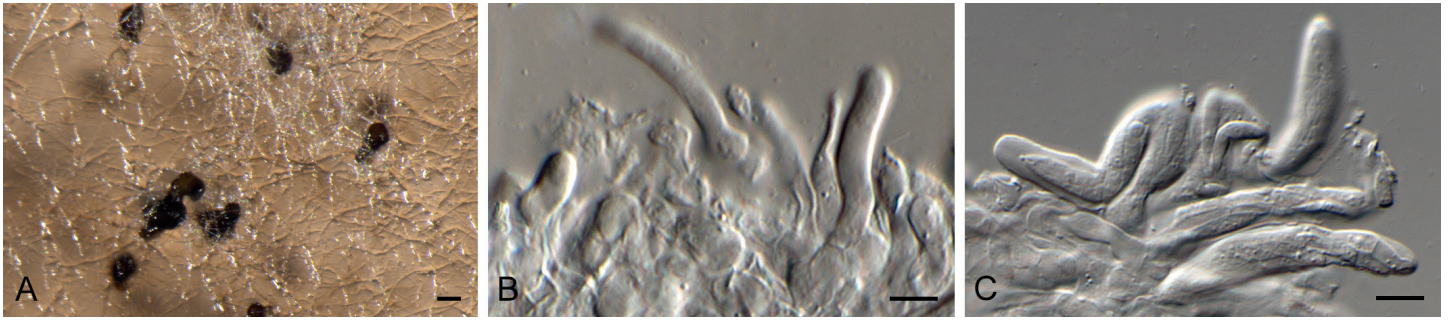


Fig. 5. *Amycosphaerella africana* (CPC 32782). A. Ascomata forming on SNA. B, C. Asci and ascospores. Scale bars: A = 90 μ m, B, C = 10 μ m.

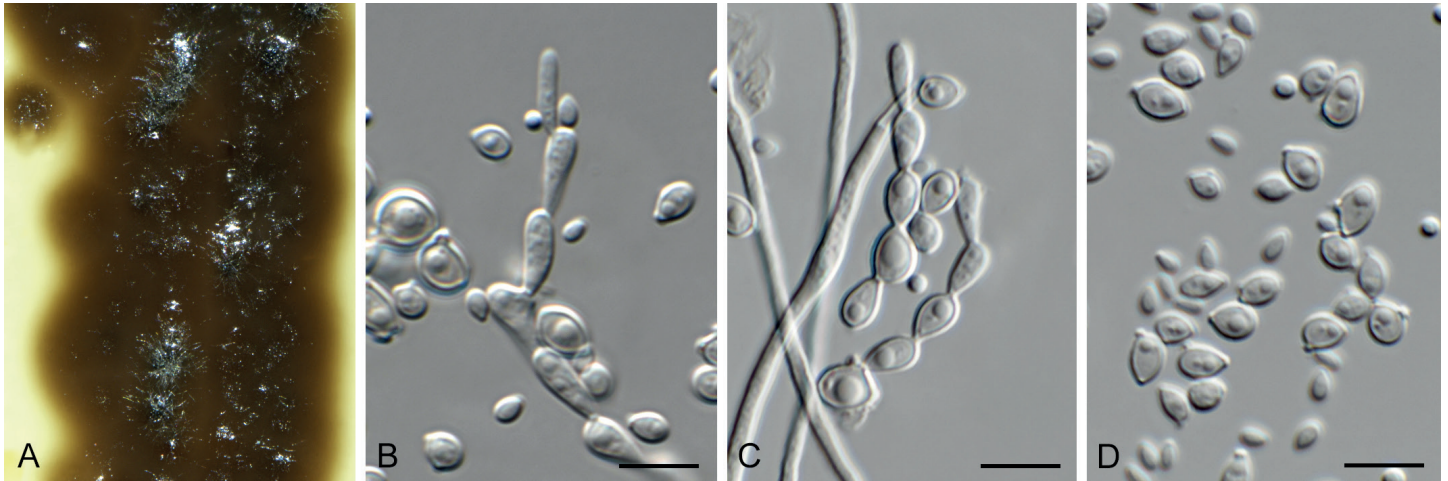


Fig. 6. *Bacillicladium clematidis* (CPC 33882). A. Colony on OA. B, C. Conidiogenous cells giving rise to conidia. D. Budding conidia. Scale bars = 10 μ m.

sequence had highest similarity to *Amycosphaerella africana* (GenBank LC121222.1; Identities = 571/572 (99 %), no gaps), *Pseudocercospora fijiensis* (GenBank XM_007921924.1; Identities = 566/616 (92 %), no gaps), and *Zymoseptoria tritici* (GenBank XM_003856727.1; Identities = 552/616 (90 %), no gaps).

Bacillicladium clematidis Crous & R.K. Schumach., *sp. nov.* MycoBank MB829299. Fig. 6.

Etymology: Name reflects the host genus *Clematis* from which it was isolated.

Mycelium consisting of pale brown, smooth, branched, 1.5–2 μ m diam hyphae that become swollen and constricted at septa in the conidiogenous region, where individual cells become more ellipsoid and clavate to globose, up to 5 μ m diam. **Conidiophores** reduced to conidiogenous cells on hyphae, pale brown, smooth, phialidic, 0.5–1 \times 1 μ m, with inconspicuous collarette, not flared. **Conidia** solitary, ellipsoid, pale brown, smooth, guttulate, aseptate, apex obtuse, basal locus truncate, 0.5 μ m diam; older conidia undergoing microcyclic conidiation, (3–)4–4.5(–5) \times (1.5–)2.5–3(–5) μ m.

Culture characteristics: Colonies flat, spreading, lacking aerial mycelium and even, lobate margin, reaching 6 mm diam after 2 wk at 25 °C. On MEA, PDA and OA surface and reverse umber.

Typus: Austria, Gaaden, branch of *Clematis vitalbae* (*Ranunculaceae*), 21 Apr. 2017, M. Mann & R.K. Schumacher,

HPC 2101, RKS 102 (**holotype** CBS H-23828, culture ex-type CPC 33882 = CBS 145035).

Notes: *Bacillicladium clematidis* is phylogenetically allied to the genus *Bacillicladium*, based on *B. lobatum*. *Bacillicladium lobatum*, which grows on bare granite walls, has three different growth habits *in vitro*, dependent on cultivation medium, temperature and colony age. But morphologically, *B. clematidis* provides an appropriate fit for the genus, sharing the black yeast-like growth in culture (Réblová *et al.* 2016).

Based on a megablast search of NCBI's GenBank nucleotide database, the closest hits using the **ITS** sequence had highest similarity to *Camptophora hylomeconis* (GenBank NR_132881.1; Identities = 352/402 (88 %), 20 gaps (5 %)), *Aphanophora eugeniae* (GenBank NR_132829.1; Identities = 394/466 (85 %), 24 gaps (5 %)), and *Ceratomyrium thailandicum* (GenBank NR_137768.1; Identities = 346/415 (83 %), 36 gaps (8 %)). Closest hits using the **LSU** sequence are *Bacillicladium lobatum* (GenBank LT558703.1; Identities = 822/863 (95 %), 2 gaps (0 %)), *Veronaea botryosa* (GenBank MH875937.1; Identities = 818/869 (94 %), 5 gaps (0 %)), and *Veronaea constricta* (GenBank MH873920.1; Identities = 811/862 (94 %), 5 gaps (0 %)). No significant hits were obtained when the **tub2** sequence was used in blastn and megablast searches.

Beltrania rhombica Penz., *Michelia* 2(8): 474. 1882. Fig. 7.

Setae rarely observed, erect, dark brown, thick-walled, 7–10-septate, straight to flexuous, tapering to an acute apex, 200–300 \times 4–5 μ m, with lobed basal cell, 6–8 μ m diam.

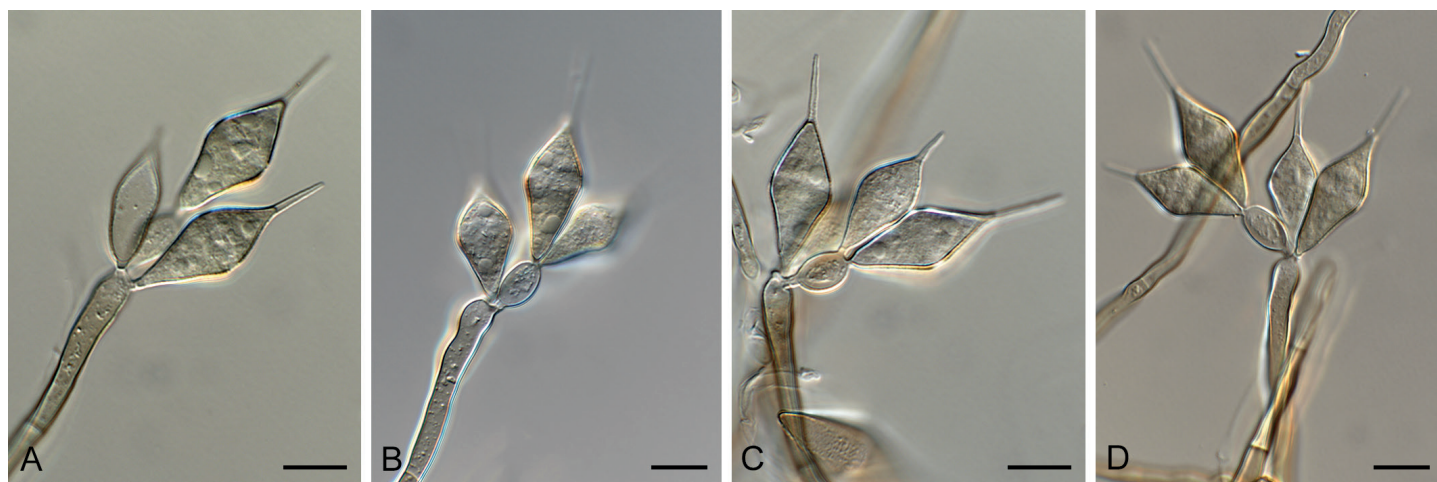


Fig. 7. *Beltrania rhombica* (CPC 31775). A–D. Conidiophores, separating cells and conidia. Scale bars = 10 μm .

Conidiophores erect, unbranched, medium brown, smooth, multi-septate, $50\text{--}300 \times 4\text{--}7 \mu\text{m}$. *Conidiogenous cells* terminal, pale brown, smooth, $15\text{--}30 \times 4\text{--}6 \mu\text{m}$, polyblastic with several flat-tipped denticles, $1.5\text{--}2 \mu\text{m}$. *Separating cells* pale brown, finely roughened, $7\text{--}13 \times 5\text{--}7 \mu\text{m}$, with several apical, flat-tipped denticles, $1\text{--}2 \mu\text{m}$ diam. *Conidia* solitary, biconic, pale brown, aseptate, with a distinct median transverse band of paler pigment, $(22\text{--})24\text{--}27(\text{--}29) \times (9\text{--})10\text{--}11 \mu\text{m}$; apical appendage $(10\text{--})12\text{--}14(\text{--}15) \times 1 \mu\text{m}$, tapering to an acutely rounded tip.

Culture characteristics: Colonies spreading, with moderate aerial mycelium, covering dish after 2 wk at 25°C . On MEA surface dark brick, reverse fawn; on PDA surface and reverse umber; on OA surface umber.

Material examined: Chile, Llanos, on leaves of *Eucalyptus urophylla* (Myrtaceae), Jul. 2010, M.J. Wingfield, HPC 1412, CBS H-23264, culture CPC 31775 = CBS 144521.

Notes: *Beltrania pseudorhombica* was described from needles of *Pinus tabulaeformis* collected in Beijing, China (Crous *et al.* 2014), and distinguished from *B. rhombica*, which has longer setae (can be up to $330 \mu\text{m}$ long, and wider conidia $15\text{--}30 \times 7\text{--}14 \mu\text{m}$; Ellis 1971). There is no ex-type strain for *B. rhombica*, and it needs to be recollected on *Citrus limon* in Italy to clarify its taxonomy.

Based on a megablast search of NCBI's GenBank nucleotide database, the closest hits using the **ITS** sequence had highest similarity to *Beltrania rhombica* (GenBank MH857718.1; Identities = 574/577 (99%), no gaps), *Beltrania pseudorhombica* (GenBank NR_148074.1; Identities = 574/577 (99%), no gaps), and *Beltrania querna* (GenBank MH856775.1; Identities = 530/538 (99%), no gaps). Closest hits using the **LSU** sequence are *Beltrania rhombica* (GenBank MF580252.1; Identities = 823/823 (100%), no gaps), *Beltrania pseudorhombica* (GenBank NG_058667.1; Identities = 810/812 (99%), no gaps), and *Beltrania querna* (GenBank MH875474.1; Identities = 859/866 (99%), 2 gaps (0 %)).

Brevistachys lateralis L. Lombard & Crous, *Persoonia* **36**: 183. 2016. Fig. 8.

Mycelium consisting of hyaline, branched, septate, smooth, $2.5\text{--}3 \mu\text{m}$ diam hyphae (hyphae thick-walled and brown in

conidiogenous region). *Conidiophores* erect, simple, single, rarely in groups, mostly unbranched, straight to slightly flexuous, 2–3-septate, thick-walled on PDA, thin-walled on OA, olivaceous brown, verruculose, $80\text{--}100 \times 2.5\text{--}3.5 \mu\text{m}$, with bulbous apex, $6\text{--}7 \mu\text{m}$ diam, bearing a whorl of 10–12 conidiogenous cells. *Conidiogenous cells* terminal, elongate, doliiform to subcylindrical, pale brown, smooth, $9\text{--}12 \times 4\text{--}4.5 \mu\text{m}$, with conspicuous collarettes. *Conidia* aggregating in slimy mass with brown exudate on PDA, but in long unbranched dry chains on OA (without exudate), dimorphic, conidia globose, becoming dark brown and verruculose, $(4\text{--})5(\text{--}6) \mu\text{m}$ diam, or ellipsoid, pale brown, verruculose, $9\text{--}10 \times 4\text{--}5 \mu\text{m}$.

Culture characteristics: Colonies flat, spreading, with sparse to moderate aerial mycelium and smooth, lobate margin, reaching 30 mm diam after 2 wk at 25°C . On MEA surface olivaceous grey, reverse umber in middle, sienna in outer region; on PDA surface ochreous with diffuse saffron pigment, reverse vinaceous; on OA surface saffron.

Material examined: Thailand, Rachaburi Province, Bangkok, on leaves of *Musa* sp. (Musaceae), 2008, P.W. Crous, HPC 2156, CBS H-23831, culture CPC 33958 = CBS 145062.

Notes: *Brevistachys lateralis* was described from leaves of *Musa* sp. collected in Queensland, Australia (Lombard *et al.* 2016). This is the first record of the fungus from Thailand where it also occurs on *Musa* leaves.

Based on a megablast search of NCBI's GenBank nucleotide database, the closest hits using the **ITS** sequence had highest similarity to *Brevistachys variabilis* (GenBank NR_153620.1; Identities = 531/542 (98%), 6 gaps (1 %)), *Brevistachys globosa* (GenBank NR_145070.1; Identities = 555/569 (98%), 4 gaps (0 %)), and *Brevistachys subsimplex* (as *Stachybotrys subsimplex*, GenBank AF205439.1; Identities = 558/573 (97%), 2 gaps (0 %)). Closest hits using the **LSU** sequence are *Brevistachys lateralis* (GenBank KU846062.1; Identities = 823/825 (99%), 1 gap (0 %)), *Brevistachys variabilis* (GenBank KU846066.1; Identities = 822/825 (99%), 1 gap (0 %)), and *Brevistachys subsimplex* (as *Stachybotrys subsimplex*, GenBank AY489711.1; Identities = 829/833 (99%), no gaps). Closest hits using the **cmdA** sequence had highest similarity to *Brevistachys lateralis* (GenBank KU846027.1; Identities = 360/360 (100%), no gaps), *Brevistachys variabilis* (GenBank KU846030.1; Identities = 360/360 (100%), no

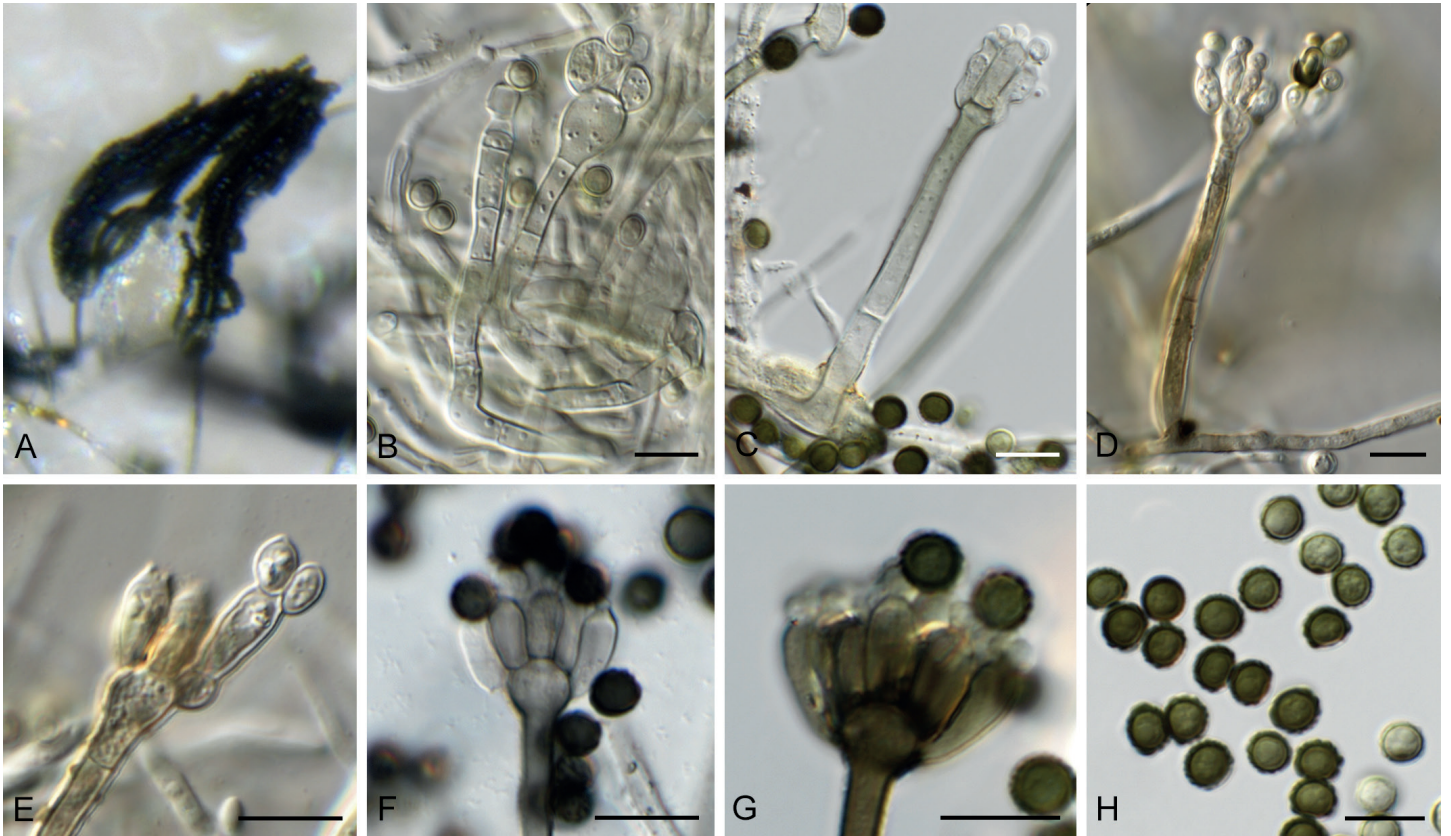


Fig. 8. *Brevistachys lateralis* (CPC 33958). **A–G.** Conidiophores with phialides, forming chains of conidia. **H.** Conidia. Scale bars = 10 µm.

gaps), *Brevistachys globosa* (GenBank KU846023.1; Identities = 315/326 (97%), 1 gap (0%)) and *Brevistachys ossiformis* (GenBank KU846028.1; Identities = 307/326 (94%), 1 gap (0%)), and distant hits with *Stachybotrys chlorohalonata* (GenBank AY180255.1; Identities = 125/133 (94%), no gaps), *Stachybotrys chartarum* (GenBank KM231452.1; Identities = 124/133 (93%), no gaps), and *Xenoacremonium recifei* (GenBank KM231420.1; Identities = 122/131 (93%), no gaps). Closest hits using the *rpb2* sequence had highest similarity to *Brevistachys lateralis* (GenBank KU846074.1; Identities = 760/760 (100%), no gaps), *Brevistachys subsimplex* (as *Stachybotrys subsimplex*, GenBank EF692519.1; Identities = 762/785 (97%), no gaps), and *Brevistachys ossiformis* (GenBank KU846075.1; Identities = 738/760 (97%), no gaps). Closest hits using the *tef1* sequence had highest similarity to *Brevistachys lateralis* (GenBank KU846090.1; Identities = 439/442 (99%), no gaps), *Brevistachys globosa* (GenBank KU846085.1; Identities = 423/442 (96%), 4 gaps (0%)), and *Brevistachys ossiformis* (GenBank KU846091.1; Identities = 412/443 (93%), 10 gaps (2%)). Closest hits using the *tub2* sequence had highest similarity to *Brevistachys lateralis* (GenBank KU846106.1; Identities = 361/361 (100%), no gaps), *Brevistachys variabilis* (GenBank KU846110.1; Identities = 359/361 (99%), no gaps), and *Brevistachys globosa* (GenBank KU846101.1; Identities = 351/362 (97%), 1 gap (0%)).

Cercospora gomphrenigena Crous, *sp. nov.* MycoBank MB829300. Fig. 9.

Etymology: Name refers to the host genus *Gomphrena* from which it was isolated.

Leaf spots circular, 1–4 mm diam, medium brown, with broad purple-red border. **Fascicles** only developing in moist chambers.

Conidiophores solitary, arising from weakly developed stroma of a few brown globoid cells, subcylindrical, medium brown, smooth, flexuous, multiseptate, up to 800 µm tall, 3–6 µm diam. **Conidiogenous cells** subcylindrical, brown, smooth, terminal and intercalary, 30–160 × 4–5 µm; scars thickened, darkened and refractive, 3–4 µm diam. **Conidia** solitary, acicular, hyaline, smooth, flexuous, multiseptate, apex subobtuse, base truncate, 150–300 × 4–5 µm; hila thickened, darkened and refractive, 3–4 µm diam.

Culture characteristics: Colonies flat, spreading, with moderate aerial mycelium and even, lobate margin, reaching 50 mm diam after 2 wk at 25 °C. On MEA surface smoke grey, reverse scarlet with diffuse scarlet pigment; on PDA surface smoke grey, reverse olivaceous grey; on OA surface olivaceous grey with patches of dirty white, with diffuse scarlet pigment.

Typus: **South Africa**, Gauteng Province, Gauteng, on leaves of *Gomphrena globosa* (*Amaranthaceae*), 2010, P.W. Crous, HPC 1516 (**holotype** CBS H-23803, culture ex-type CPC 32470 = CBS 144613).

Notes: A DNA phylogeny for most common species of *Cercospora* known from culture was presented by Groenewald *et al.* (2013), with secondary barcode genes treated by Bakhshi *et al.* (2018). *Cercospora gomphrenigena* was collected from leaves of *Gomphrena globosa* in South Africa in an attempt to resolve the identity of *Cercospora pretoriensis* that occurs on this host (conidia narrowly cylindrical to subacicular, 15–90 × 2–4.5 µm; Braun *et al.* 2015), from which *C. gomphrenigena* is morphologically distinct, having much longer and wider conidia. It is morphologically closer to *C. gomphrenae* [conidiophores in

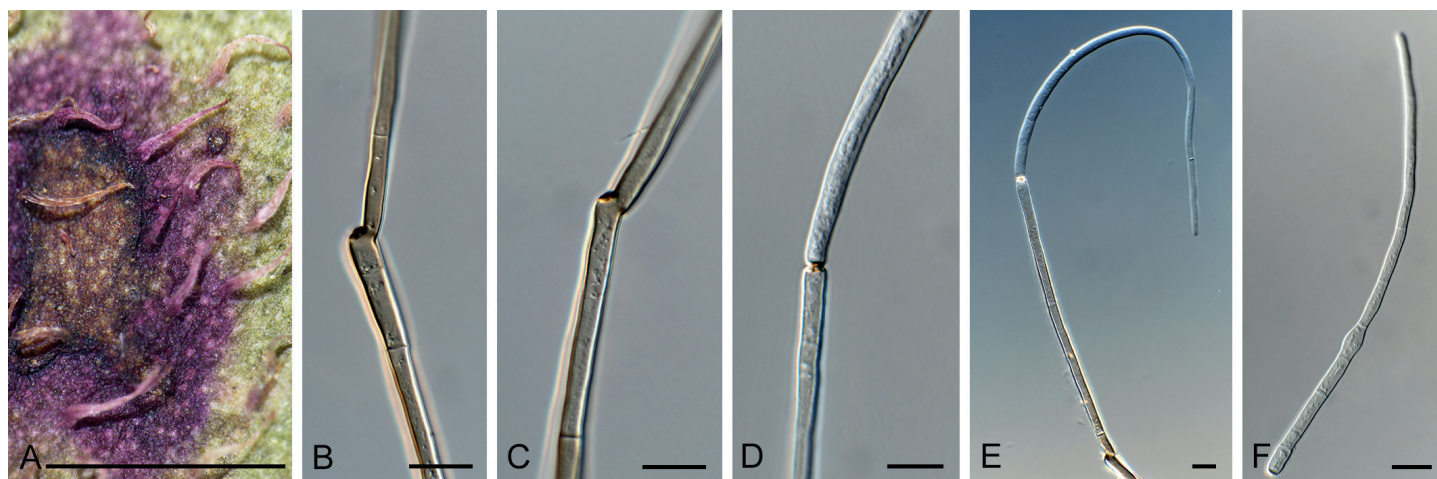


Fig. 9. *Cercospora gomphrenigena* (CPC 32470). **A.** Leaf spot. **B–E.** Conidiophores with conidial loci. **F.** Conidium. Scale bars: A = 4 mm, B–F = 10 μ m.

small, divergent fascicles, 30–300 \times 3–7 μ m, conidiogenous cells 10–30 μ m long, conidia 30–300(–450) \times 2–5 μ m, 3–20-septate; Braun *et al.* 2015], but is distinct in having longer conidiophores and conidiogenous cells, wider scars, and wider conidia.

Based on a megablast search of NCBI's GenBank nucleotide database, the **ITS** sequence was identical to *Cercospora dichondrae* (GenBank MK039698.1; Identities = 525/525 (100 %)), *Cercospora beticola* (GenBank MH424448.1; Identities = 525/525 (100 %)), and *Cercospora malayensis* (GenBank MH129519.1; Identities = 525/525 (100 %)). The **LSU** sequence is identical to those of numerous *Cercospora* species, e.g. *Cercospora sesami* (GenBank MK029365.1; Identities = 783/783 (100 %)). Closest hits using the **cmdA** sequence had highest similarity to *Cercospora samambaiiae* (GenBank KT037463.1; Identities = 448/448 (100 %)), *Cercospora* sp. G NV-2018 (GenBank MF681410.1; Identities = 443/444 (99 %), no gaps), and *Cercospora cyperina* (GenBank KT193729.1; Identities = 444/448 (99 %), no gaps). Closest hits using the **his3** sequence had highest similarity to *Cercospora* sp. 3 LO-2017 (GenBank KX522813.1; Identities = 375/375 (100 %)), *Cercospora kikuchii* (GenBank KP825147.1; Identities = 375/375 (100 %)), and *Cercospora* cf. *physalidis* (GenBank JX142654.1; Identities = 380/381 (99 %), no gaps). Closest hits using the **tef1** sequence had highest similarity to *Cercospora* sp. 3 LO-2017 (GenBank KX522847.1; Identities = 280/280 (100 %)), *Cercospora* cf. *alchemillicola* (GenBank KR733109.1; Identities = 279/279 (100 %)), and *Cercospora samambaiiae* (GenBank KT037468.1; Identities = 487/488 (99 %), no gaps). Closest hits using the **tub2** sequence had highest similarity to *Cercospora kikuchii* (GenBank AB240222.1; Identities = 581/581 (100 %)), *Cercospora beticola* (GenBank XM_023592737.1; Identities = 754/784 (96 %), no gaps), and *Cercospora* sp. Q (GenBank JX142482.1; Identities = 1016/1054 (96 %), 4 gaps (0 %)).

Cladoriella xanthorrhoeae Crous, *Persoonia* **39**: 417. 2017. Fig. 10.

Mycelium consisting of pale brown, smooth, septate, branched, 2.5–3 μ m diam hyphae. *Conidiophores* solitary, erect, flexuous, medium brown, smooth, subcylindrical, unbranched, 1–4-septate, 20–40 \times 2.5–3 μ m; at times conidiophores can be reduced to conidiogenous cells arising from hyphae, 5–8 \times 2.5–3 μ m. *Conidiogenous cells* terminal, integrated, medium brown, smooth to finely roughened, subcylindrical, with 1–2 flat-tipped

loci, 2–2.5 μ m diam, darkened, somewhat thickened, 7–12 \times 3.5–4 μ m. *Ramoconidia* medium brown, finely verruculose, 1(–2)-septate, subcylindrical to somewhat fusoid-ellipsoid, 12–19 \times 3.5–4 μ m; loci thickened, darkened, 1.5–2 μ m diam. *Conidia* in short (2–6), branched chains, medium brown, verruculose, fusoid-ellipsoid, 1-septate; hila truncate, thickened, darkened, 1.5–2 μ m diam, (9–)12–15(–17) \times (3.5–)4 μ m; hila thickened, somewhat darkened, 1.5–2 μ m diam.

Culture characteristics: Colonies erumpent, spreading, with sparse aerial mycelium and feathery margin, reaching 7 mm diam after 2 wk at 25 °C. On MEA, PDA and OA surface iron-grey; diffuse red pigment visible in agar on PDA and OA.

Material examined: **Australia**, New South Wales, Nullica State Forest, on leaves of *Xanthorrhoea* sp. (*Asphodelaceae*), Nov. 2016, P.W. Crous, HPC 1830, CBS H-23804, culture CPC 32609 = CBS 144523.

Notes: *Cladoriella xanthorrhoeae* was recently described on *Xanthorrhoea* sp. from Australia (Crous *et al.* 2017), and CPC 32609 represents the second collection of this fungus from the type locality, where it appears to be well established on *Xanthorrhoea*.

Based on a megablast search of NCBI's GenBank nucleotide database, the **ITS** sequence was identical to *Cladoriella xanthorrhoeae* (GenBank NR_156392.1; Identities = 602/602 (100 %)); and related to *Cladoriella rubrigena* (GenBank NR_156219.1; Identities = 498/552 (90 %), 15 gaps (2 %)) and *Cladoriella eucalypti* (GenBank EU040224.1; Identities = 589/641 (92 %), 15 gaps (2 %)). Closest hits using the **LSU** sequence are *Cladoriella rubrigena* (GenBank NG_058780.1; Identities = 867/881 (98 %), 2 gaps (0 %)), *Cladoriella eucalypti* (GenBank EU040224.1; Identities = 861/876 (98 %), 2 gaps (0 %)), and *Cladoriella paleospora* (GenBank MH874922.1; Identities = 823/880 (94 %), 3 gaps (0 %)).

Creosphaeria sassafras (Schwein.) Y.M. Ju *et al.*, *Mycotaxon* **47**: 223. 1993. Fig. 11.

Basionym: *Sphaeria sassafras* Schwein., *Schr. naturf. Ges. Leipzig* **1**: 36 (10 of repr.). 1822.

In vitro: *Mycelium* consisting of hyaline to brown, smooth to warty, 1.5–3 μ m diam hyphae. *Conidiophores* reduced to

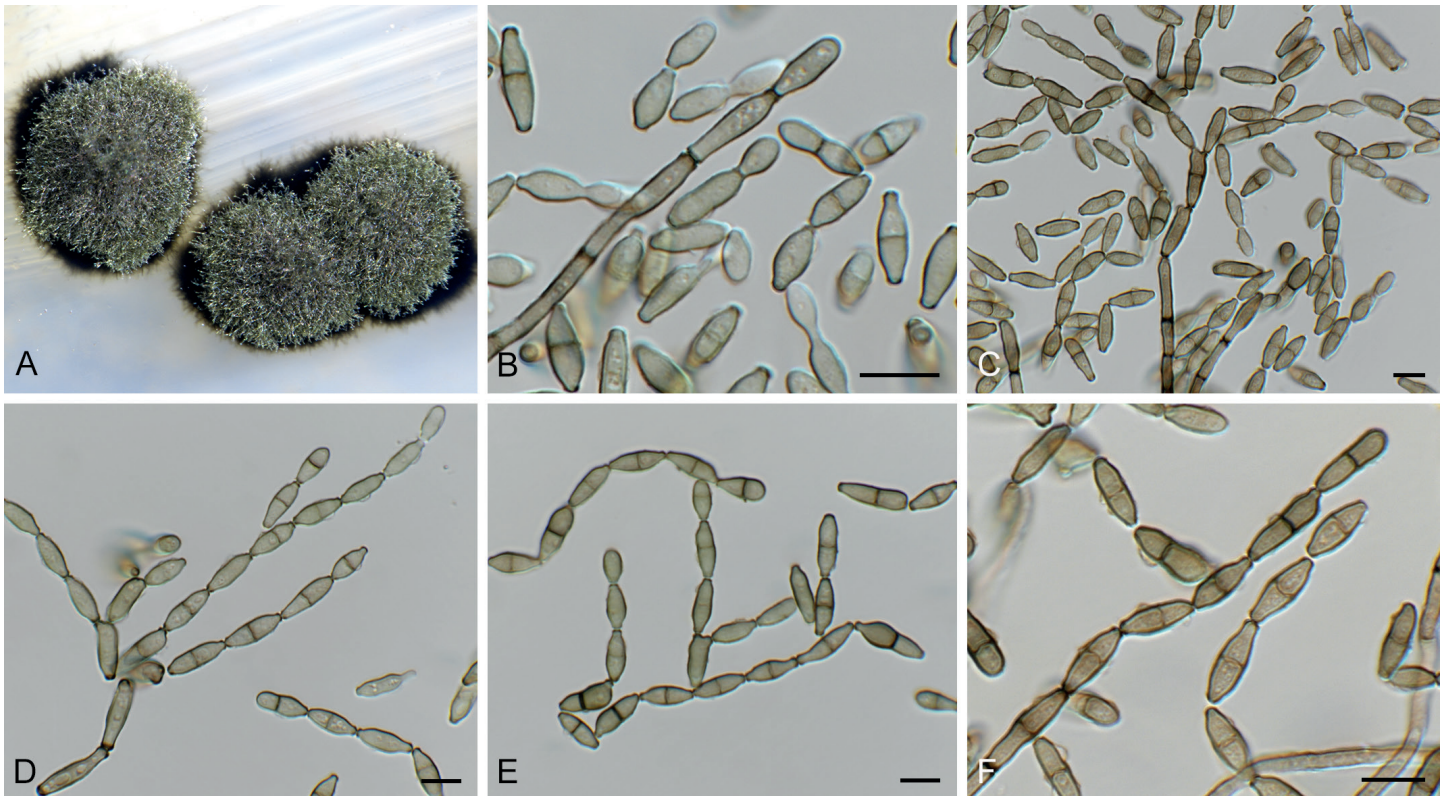


Fig. 10. *Cladoriella xanthorrhoeae* (CPC 32609). **A.** Colonies on SNA. **B–F.** Conidiophores giving rise to branched conidial chains. Scale bars = 10 μ m.

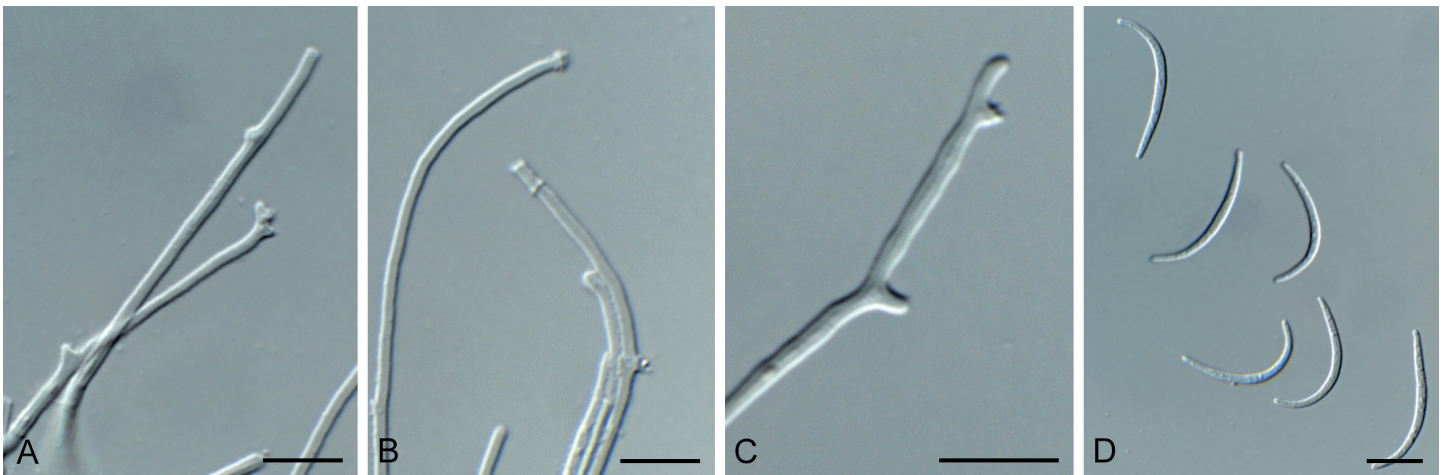


Fig. 11. *Creosphaeria sassafras* (CPC 33410). **A–C.** Conidiophores with conidial loci. **D.** Conidia. Scale bars = 10 μ m.

conidiogenous cells occurring on narrower hyphae (1.5–2 μ m diam), solitary, erect, pale brown to hyaline, smooth, nodes 1–3 \times 1–1.5 μ m. *Conidia* hyaline, smooth, aseptate, curved, spindle-shaped, apex subobtuse, base truncate, 20–30 \times 2 μ m.

Culture characteristics: Colonies flat, spreading, with moderate aerial mycelium and smooth, lobate margin, covering dish after 2 wk at 25 $^{\circ}$ C. On MEA surface hazel, reverse sepia in inner region, orange in outer zone; on PDA surface hazel, reverse brown vinaceous; on OA surface hazel.

Material examined: Spain, Barcelona, dead branch of *Laurus nobilis* (Lauraceae), Mar. 2017, M. Vera Inrago & R.K. Schumacher, HPC 2043, RKS 90, culture CPC 33410 = CBS 144984.

Notes: Bills & Peláez (1996) reported conidia of the asexual morph to be 16–22 \times 1.2–1.8 μ m. Based on a megablast search of NCBI's GenBank nucleotide database, the closest hits using the ITS sequence had the greatest similarity to several sequences of *Creosphaeria sassafras* (e.g. GenBank HQ660446.1; Identities = 515/516 (99%), no gaps). Closest hits using the LSU sequence are *Creosphaeria sassafras* (GenBank MH876173.1; Identities = 854/854 (100%), no gaps), *Lopadostoma lechatii* (GenBank KC774590.1; Identities = 833/854 (98%), no gaps), and *Lopadostoma meridionale* (GenBank KC774599.1; Identities = 833/855 (97%), 3 gaps (0 %)).

Cylindrocladiella peruviana (Bat. et al.) Boesew., *Canad. J. Bot.* **60**: 2289. 1982. Fig. 12.

Basionym: *Cylindrocladium peruvianum* Bat. et al., *Atas Inst. Micol. Univ. Recife* **2**: 386. 1965.



Fig. 12. *Cylindrocladiella peruviana* (CPC 33527). A. Subverticillate conidiophore. B, C. Penicillate conidiophores. D. Conidia. Scale bars = 10 μ m.

Conidiophores dimorphic, penicillate and subverticillate, mononematous and hyaline, comprising a stipe, a penicillate arrangement of fertile branches, a stipe extension and a terminal vesicle; *stipe extension* aseptate, straight, 50–70 \times 2–3 μ m, thick-walled with one basal septum, terminating in thin-walled, ellipsoid to lanceolate vesicles, 3–4 μ m wide. *Penicillate conidiogenous apparatus* with primary branches 0–1-septate, 15–25 \times 3–4 μ m, secondary branches aseptate, 8–15 \times 2.5–3 μ m, each terminal branch producing 2–4 phialides; *phialides* cylindrical, doliiform to reniform to cymbiform, hyaline, aseptate, 9–12 \times 2.5–3 μ m, apex with minute periclinal thickening and collarette. *Subverticillate conidiophores* comprising of a septate stipe and rarely primary branches terminating in 2–4 phialides; *phialides* cymbiform to cylindrical, hyaline, aseptate, 20–30 \times 2–2.5 μ m, apex with minute periclinal thickening and collarette. *Conidia* cylindrical, rounded at both ends, straight, (0–)1-septate, (9–)10–12(–13) \times 2(–2.5) μ m, held in asymmetrical clusters by colourless slime. *Sexual morph* unknown.

Culture characteristics: Colonies flat, spreading, with fluffy, moderate aerial mycelium, covering dish after 2 wk at 25 °C. On MEA, PDA and OA surface sienna with patches of ochreous, reverse umber to sienna.

Material examined: South Africa, Western Cape Province, Stellenbosch, *Pelargonium* sp. (*Geraniaceae*), 1 Feb. 2010, P.W. Crous, CBS H-23821, culture CPC 33527 = CBS 145053.

Notes: *Cylindrocladiella peruviana* is known to occur in South Africa (van Coller *et al.* 2005), and has been confirmed from hosts such as *Acacia mearnsii*, *Eucalyptus* spp., and *Vitis vinifera*, but this is the first record from *Pelargonium*.

Based on a megablast search of NCBI's GenBank nucleotide database, the ITS sequence was identical to *Cylindrocladiella peruviana* (GenBank KU896173.1; Identities = 550/550), *Cylindrocladiella parvispora* (GenBank MH017028.1; Identities = 546/546), and *Cylindrocladiella malesiana* (GenBank MH017019.1; Identities = 546/546). Closest hits using the LSU sequence are *Cylindrocladiella peruviana* (GenBank JN099266.1; Identities = 841/841 (100 %), no gaps), *Cylindrocladiella longiphialidica* (GenBank MH876846.1; Identities = 840/841 (99 %), no gaps), and *Cylindrocladiella camelliae* (GenBank

JN099248.1; Identities = 840/841 (99 %), no gaps). Closest hits using the *his3* sequence had highest similarity to *Cylindrocladiella peruviana* (GenBank MH017011.1; Identities = 480/480 (100 %), no gaps), *Cylindrocladiella microcylindrica* (as *Nectricladiella camelliae*, GenBank AY793523.1; Identities = 442/457 (97 %), 5 gaps (1 %)), and *Cylindrocladiella solicola* (GenBank MH017002.1; Identities = 469/485 (97 %), 5 gaps (1 %)). Closest hits using the *rpb2* sequence had highest similarity to *Cylindrocladiella camelliae* (GenBank KM232304.1; Identities = 819/837 (98 %), no gaps), *Cylindrocladiella lageniformis* (GenBank KM232303.1; Identities = 648/722 (90 %), no gaps), and *Calonectria brevistipitata* (GenBank KY653367.1; Identities = 744/861 (86 %), 2 gaps (0 %)). Closest hits using the *tef1* sequence had highest similarity to *Cylindrocladiella peruviana* (GenBank JN099007.1; Identities = 482/483 (99 %), 1 gap (0 %)), *Cylindrocladiella obpyriformis* (GenBank MH016985.1; Identities = 475/489 (97 %), 7 gaps (1 %)), and *Cylindrocladiella arbusta* (GenBank MH016978.1; Identities = 475/489 (97 %), 7 gaps (1 %)). Closest hits using the *tub2* sequence had highest similarity to *Cylindrocladiella peruviana* (GenBank JN098801.1; Identities = 618/618 (100 %), no gaps), *Cylindrocladiella terrestris* (GenBank MF444930.1; Identities = 482/493 (98 %), no gaps), and *Cylindrocladiella camelliae* (GenBank JN098749.1; Identities = 604/618 (98 %), no gaps).

Cyphellophora clematidis Crous & R.K. Schumach., *sp. nov.* MycoBank MB829301. Fig. 13.

Etymology: Name reflects the host genus *Clematis* from which it was isolated.

Mycelium consisting of pale brown, smooth, septate, branched, (1.5–)2–3 μ m diam hyphae. *Conidiomata* sporodochial, round, erumpent, olivaceous, 30–120 μ m diam, consisting of a basal stroma of globose to ellipsoid, olivaceous, smooth-walled cells, 2–4 μ m diam, giving rise to aggregated conidiogenous cells. *Conidiogenous cells* ellipsoid to ampulliform, olivaceous brown, smooth, 4–6(–10) \times 2.5–4 μ m, phialidic with darker brown, flared collarette, 1.5–2 μ m diam. *Conidia* aseptate, aggregated in mucoid mass, olivaceous, smooth, guttulate, ellipsoid, apex obtuse, tapering toward a truncate base, 0.5 μ m diam, (3–)4–5(–6.5) \times (1.5–)2(–2.5) μ m.

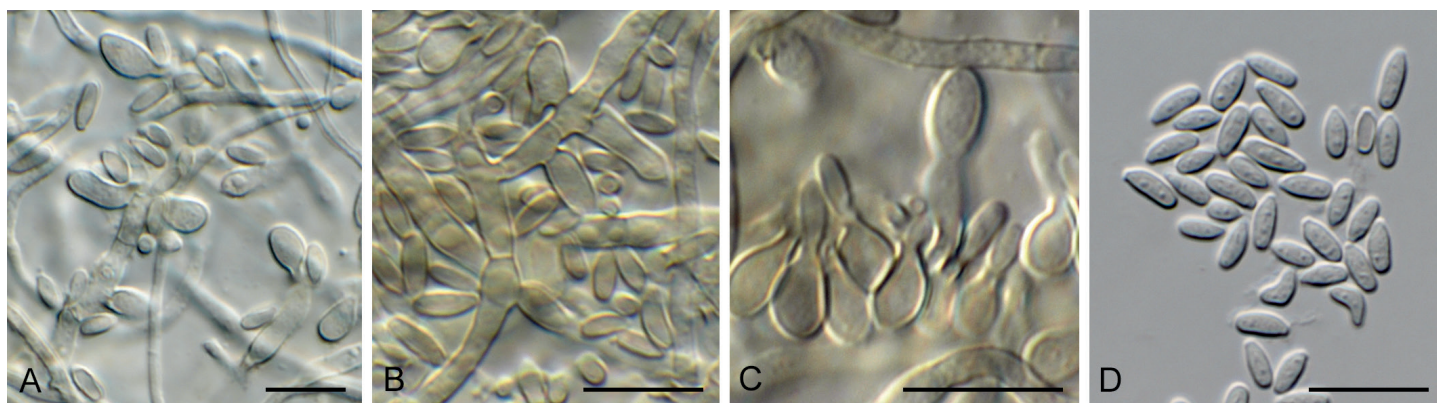


Fig. 13. *Cyphellophora clematidis* (CPC 33880). A–C. Hyphae with clusters of conidiogenous cells. D. Conidia. Scale bars = 10 µm.

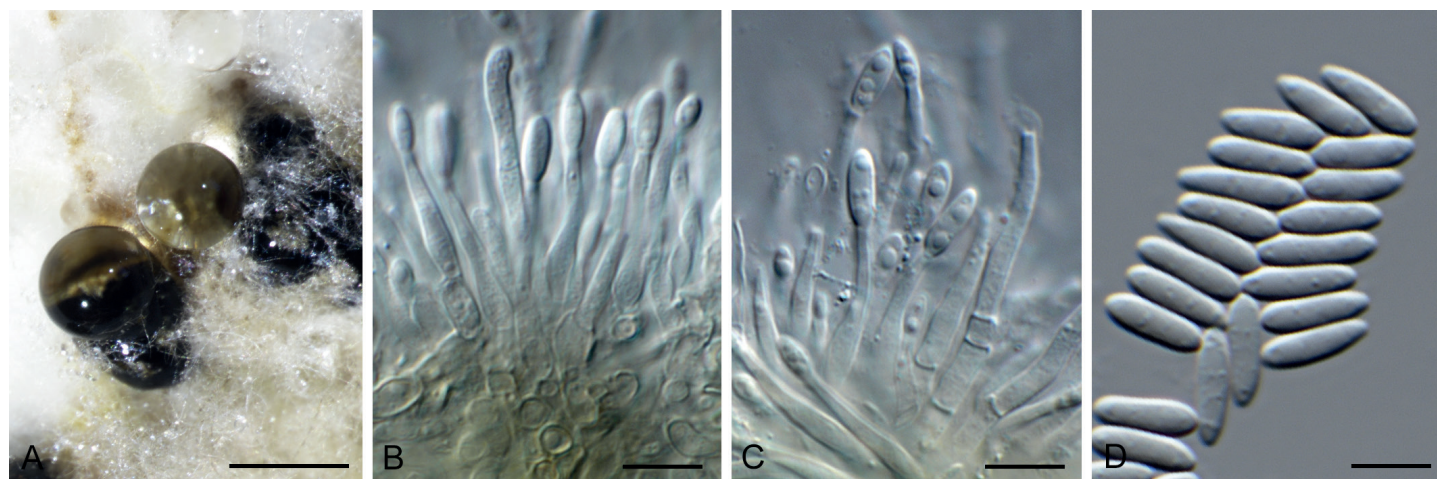


Fig. 14. *Diaporthe anacardii* (CPC 33074). A. Conidiomata on PDA. B, C. Conidiogenous cells. D. Conidia. Scale bars: A = 250 µm, B–D = 10 µm.

Culture characteristics: Colonies flat, spreading with sparse to moderate aerial mycelium, and smooth, lobate margin, reaching 40 mm diam after 2 wk at 25 °C. On MEA surface umber, reverse chestnut; on PDA surface hazel, reverse iron-grey; on OA surface olivaceous grey.

Typus: Austria, lower Austria, Gaaden, on *Clematis vitalba* (*Ranunculaceae*), 21 Apr. 2017, M. Mann & R.K. Schumacher, HPC 2101 = RKS 102 (**holotype** CBS H-23827, culture ex-type CPC 33880 = CBS 144983).

Notes: Although *Cyphellophora clematidis* was isolated from *Clematis vitalba*, *Cyphellophora* also contains species that are associated with human and animal skin and nails (Gao *et al.* 2015). *Cyphellophora clematidis* is phylogenetically distinct from other species presently known based on their DNA sequences, and is introduced here as new, being morphologically distinct in that it has predominantly aseptate conidia.

Based on a megablast search of NCBI's GenBank nucleotide database, the closest hits using the **ITS** sequence had highest similarity to *Anthopsis deltoidea* (GenBank NR_153555.1; Identities = 492/557 (88 %), 40 gaps (7 %)), *Cyphellophora pluriseptata* (GenBank MH063042.1; Identities = 481/562 (86 %), 24 gaps (4 %)), and *Cyphellophora eucalypti* (GenBank GQ303274.1; Identities = 530/633 (84 %), 48 gaps (7 %)). Closest hits using the **LSU** sequence are *Cyphellophora fusarioides* (GenBank MH877022.1; Identities = 836/861 (97 %), 4 gaps (0 %)), *Cyphellophora musae* (GenBank KP122932.1; Identities

= 835/861 (97 %), 3 gaps (0 %)), and *Cyphellophora suttonii* (GenBank MH874978.1; Identities = 834/861 (97 %), 4 gaps (0 %)). No significant hits were obtained when the **tub2** sequence was used in blastn and megablast searches.

Diaporthe anacardii (Early & Punith.) R.R. Gomes *et al.*, *Persoonia* **31**: 15. 2013. Fig. 14.

Basionym: *Phomopsis anacardii* Early & Punith., *Trans. Brit. Mycol. Soc.* **59**: 345. 1972.

Conidiomata black, globose, erumpent, 250–350 µm diam, exuding a creamy conidial mass. **Conidiophores** hyaline, smooth, branched, 2–3-septate, subcylindrical, 25–50 × 2.5–3.5 µm. **Conidiogenous cells** subcylindrical, smooth, terminal, intercalary, 15–35 × 2–2.5 µm, apex 1.5 µm diam, mostly without collarette. **Conidia** solitary, aseptate, hyaline, smooth, guttulate, fusoid-ellipsoid, straight, apex subobtuse, base truncate, 1 µm diam, (7–)8–10(–11) × (2.5–)3 µm.

Culture characteristics: Colonies flat, spreading, with moderate aerial mycelium, covering dish after 2 wk at 25 °C. On MEA, PDA and OA surface buff with patches of pale olivaceous grey, reverse cinnamon.

Material examined: South Africa, Western Cape Province, Stellenbosch, on unidentified leaf litter, 2010, P.W. Crous, HPC 1692, culture CPC 33074 = CBS 144610.

Notes: This collection is closely related to *Diaporthe anacardii* (from *Anacardi occidentalis* in Kenya, and also recorded from Nigeria, Guinea and Cuba; Gomes *et al.* 2013), and *Diaporthe velutina* (from leaves of *Neolitsea* sp., *Callerya cinerea* and *Camellia sinensis* collected in China; Gao *et al.* 2017). Based on the *cmdA* and *tef1* sequence data, this isolate is identified as *Diaporthe anacardii*, which represents the first record from South Africa.

Based on a megablast search of NCBI's GenBank nucleotide database, the closest hits using the **ITS** sequence had highest similarity to *Diaporthe velutina* (GenBank NR_152470.1; Identities = 561/563 (99 %), 2 gaps (0 %)), *Diaporthe foeniculina* (GenBank KP050598.1; Identities = 534/538 (99 %), 2 gaps (0 %)), and *Diaporthe inconspicua* (GenBank KC343125.1; Identities = 556/561 (99 %), no gaps). Closest hits using the **LSU** sequence are *Diaporthe velutina* (GenBank NG_059146.1; Identities = 788/788 (100 %)), *Diaporthe phragmitis* (GenBank MH878644.1; Identities = 785/788 (99 %), no gaps), and *Diaporthe cotoneastri* (GenBank MH873257.1; Identities = 785/788 (99 %), no gaps). Closest hits using the **cmdA** sequence had highest similarity to *Diaporthe anacardii* (GenBank KC343266.1; Identities = 681/682 (99 %), no gaps), *Diaporthe portugallica* (as *Diaporthe* sp. VG-2018, GenBank MH063893.1; Identities = 469/486 (97 %), no gaps), and *Diaporthe velutina* (GenBank KX999286.1; Identities = 444/461 (96 %), no gaps). Closest hits using the **tef1** sequence had highest similarity to *Diaporthe anacardii* (GenBank KC343750.1; Identities = 335/341 (98 %), 2 gaps (0 %)), *Diaporthe portugallica* (as *Diaporthe* sp. VG-2018, GenBank MH063911.1; Identities = 324/339 (96 %), no gaps), and *Diaporthe velutina* (GenBank KX999178.1; Identities = 324/339 (96 %), 2 gaps (0 %)).

Diaporthe eres Nitschke, *Pyrenomyc. Germ.* 2: 245. 1870. Fig. 15.

Conidiomata pycnidial, globose, erumpent, brown, up to 400 µm diam; creamy conidial droplets exude from ostiole; walls of 3–6 layers of brown *textura angularis*. *Conidiophores* lining the inner cavity, hyaline, smooth, 1–3-septate, branched, densely aggregated, subcylindrical, straight to sinuous, 15–35 × 3–4 µm. *Conidiogenous cells* 6–20 × 2–2.5 µm, phialidic, subcylindrical, terminal and intercalary, with slight apical taper towards apex, 0.5 µm diam with visible periclinal thickening; collarette inconspicuous. *Conidia* aseptate, hyaline, smooth, fusoid,

tapering towards both ends, straight, apex subobtusate, base truncate, (7–)8–9(–10) × (2–)2.5(–3) µm.

Culture characteristics: Colonies flat, spreading, with sparse to moderate aerial mycelium and smooth, lobate margin, covering dish after 2 wk at 25 °C. On MEA, PDA and OA surface isabelline with patches of sepia and honey, reverse brown vinaceous with patches of hazel and ochreous.

Material examined: Netherlands, on *Lactuca sativa* (Asteraceae), Jun. 2017, W. Quaadvlieg, NAK Tuinbouw INS-17-08263A, culture CPC 34055 = CBS 145040.

Notes: *Diaporthe* includes important plant pathogens, saprobes, and endophytes on a wide range of plant hosts (Guarnaccia & Crous 2017). *Diaporthe eres*, the type species of *Diaporthe*, was circumscribed by Udayanga *et al.* (2014). The present collection from *Lactuca sativa* in the Netherlands fits within the broad concept of *D. eres*.

Based on a megablast search of NCBI's GenBank nucleotide database, the **ITS** sequence was identical to *Diaporthe eres* (GenBank MG281122.1; Identities = 576/576 (100 %)) and *Diaporthe cotoneastri* (GenBank KC145903.1; Identities = 576/576 (100 %)). Closest hits using the **LSU** sequence are *Diaporthe eres* (GenBank MH867392.1; Identities = 893/893 (100 %), no gaps), *Diaporthe cotoneastri* (GenBank MH873257.1; Identities = 891/891 (100 %), no gaps), and *Diaporthe ambigua* (GenBank MH867598.1; Identities = 892/893 (99 %), no gaps). Closest hits using the **actA** sequence had highest similarity to *Diaporthe eres* (GenBank KJ420750.1; Identities = 234/234 (100 %)), *Diaporthe cotoneastri* (GenBank KC843231.1; Identities = 273/275 (99 %), no gaps), and *Phomopsis fukushii* (GenBank JN230379.1; Identities = 265/268 (99 %), no gaps). Closest hits using the **cmdA** sequence had highest similarity to *Diaporthe* cf. *nobilis* (GenBank KC343391.1; Identities = 409/409 (100 %), no gaps), *Diaporthe eres* (GenBank KC343331.1; Identities = 409/409 (100 %), no gaps), and *Diaporthe cotoneastri* (GenBank KC763137.1; Identities = 403/409 (99 %), 4 gaps (0 %)). Closest hits using the **rpb2** sequence had highest similarity to *Diaporthe ampelina* (as *Phomopsis viticola*, GenBank HQ446836.1; Identities = 632/683 (93 %), no gaps), *Diaporthe limonicola* (GenBank MH797629.1; Identities = 622/683 (91 %), no gaps), and *Diaporthe foeniculina* (GenBank MG922553.1; Identities = 619/680 (91 %), no gaps). Closest hits using the **tef1**

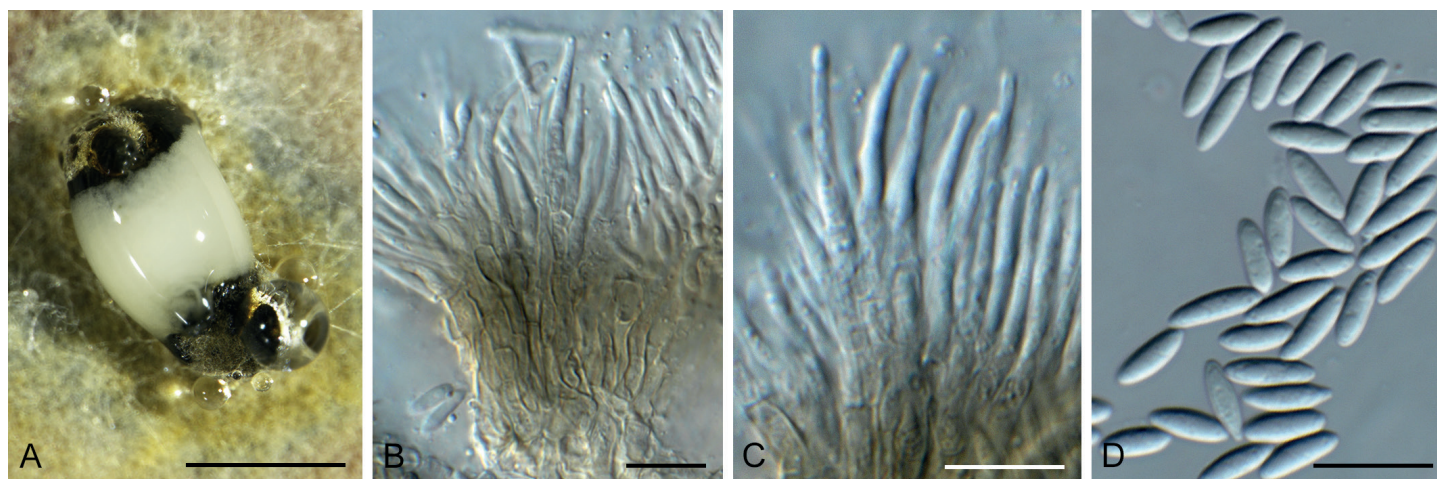


Fig. 15. *Diaporthe eres* (CPC 34055). **A.** Conidioma on OA. **B, C.** Conidiophores with conidiogenous cells. **D.** Conidia. Scale bars: A = 400 µm, B–D = 10 µm.

sequence had highest similarity to *Diaporthe eres* (GenBank MG281568.1; Identities = 610/610 (100 %), no gaps), *Diaporthe* cf. *nobilis* (GenBank KC343875.1; Identities = 346/347 (99 %), no gaps), and *Diaporthe phaseolorum* (GenBank HQ445915.1; Identities = 355/359 (99 %), no gaps). Closest hits using the **tub2** sequence had highest similarity to *Diaporthe hungariae* (GenBank MG281303.1; Identities = 317/317 (100 %), no gaps), *Diaporthe rosicola* (GenBank MG843877.1; Identities = 311/313 (99 %), no gaps), and *Diaporthe betulae* (GenBank KT733021.1; Identities = 429/439 (98 %), no gaps).

Dichotomophthora basellae Hern.-Restr. *et al.*, *Stud. Mycol.* **92**: 69. 2018. Fig. 16.

Hyphae hyaline to brown, septate, smooth to verruculose, 6–8 µm wide. *Conidiophores* macronematous, unbranched or irregularly branched, lobed at the apex, forming a stipe and head; *stipe* pale brown, smooth, 500–2000 × 9–17 µm; head 30–60 µm diam, pale brown. *Conidiogenous cells* polytretic, integrated and terminal, lobed, cicatrized, individual lobes 15–25 × 9–20 µm. *Conidia* (50–)80–95(–105) × (9–)12–14(–15), solitary, dry, subcylindrical, rounded at the ends, pale yellow-brown, 3–5-distoseptate, at times forking at apex, giving rise to bifurcate appearance, two apical branches 0–2-septate, 7–30 µm long. *Microconidia* obovoid to ellipsoid, 0–2-distoseptate, 10–30 × 10–11 µm. *Sclerotia* and *sexual morph* unknown.

Culture characteristics: Colonies spreading, with sparse to moderate aerial mycelium and smooth, even margin, reaching 50 mm diam after 2 wk at 25 °C. On MEA surface and reverse umber, with diffuse apricot pigment; on PDA surface and reverse orange, with patches of umber, and orange pigment; on OA surface orange, with patches of umber, apricot to orange pigment.

Material examined: **Thailand**, Chiang Mai Province, Chiang Mai, on unidentified host plant, 2008, *R. Cheewangkoon*, CBS H-23813, culture CPC 33044 = CBS 145050.

Notes: The genus *Dichotomophthora* was recently revised by Marin-Felix *et al.* (2019), who accepted four species associated with leafspots on various host plants. *Dichotomophthora basellae* was described as having conidia that are 32–86 × 10–18 µm, ellipsoid to cylindrical rounded at ends, and 2–5-distoseptate. The present isolate is morphologically atypical, as its conidia are frequently forking at the apex. Phylogenetically however, it is identical to *D. basellae*, and was collected at the same locality.

Based on a megablast search of NCBI's GenBank nucleotide database, the closest hits using the **ITS** sequence had highest similarity to *Dichotomophthora basellae* (GenBank NR_158422.1; Identities = 595/595 (100 %), no gaps) and *Dichotomophthora lutea* (GenBank NR_158420.1; Identities = 590/596 (99 %), 1 gap (0 %)). Closest hits using the **LSU** sequence of CPC 33044 are *Dichotomophthora portulacae* (GenBank LT990624.1; Identities = 833/833 (100 %), no gaps), *Dichotomophthora lutea* (GenBank LT990622.1; Identities = 810/810 (100 %), no gaps), *Curvularia papendorffii* (GenBank MH875471.1; Identities = 855/855 (100 %), no gaps), *Bipolaris cactivora* (GenBank LT715590.1; Identities = 855/855 (100 %), no gaps), and *Drechslera helianthi* (GenBank MH876194.1; Identities = 854/855 (99 %), no gaps). There are no LSU sequences of *Dichotomophthora basellae* available on GenBank. Closest hits using the **rpb2** sequence had highest similarity to *Dichotomophthora basellae* (GenBank LT990640.1; Identities = 860/860 (100 %), no gaps), *Dichotomophthora lutea* (GenBank LT990636.1; Identities = 906/911 (99 %), no gaps), and *Bipolaris cactivora* (GenBank LT715726.1; Identities = 718/739 (97 %), no gaps).

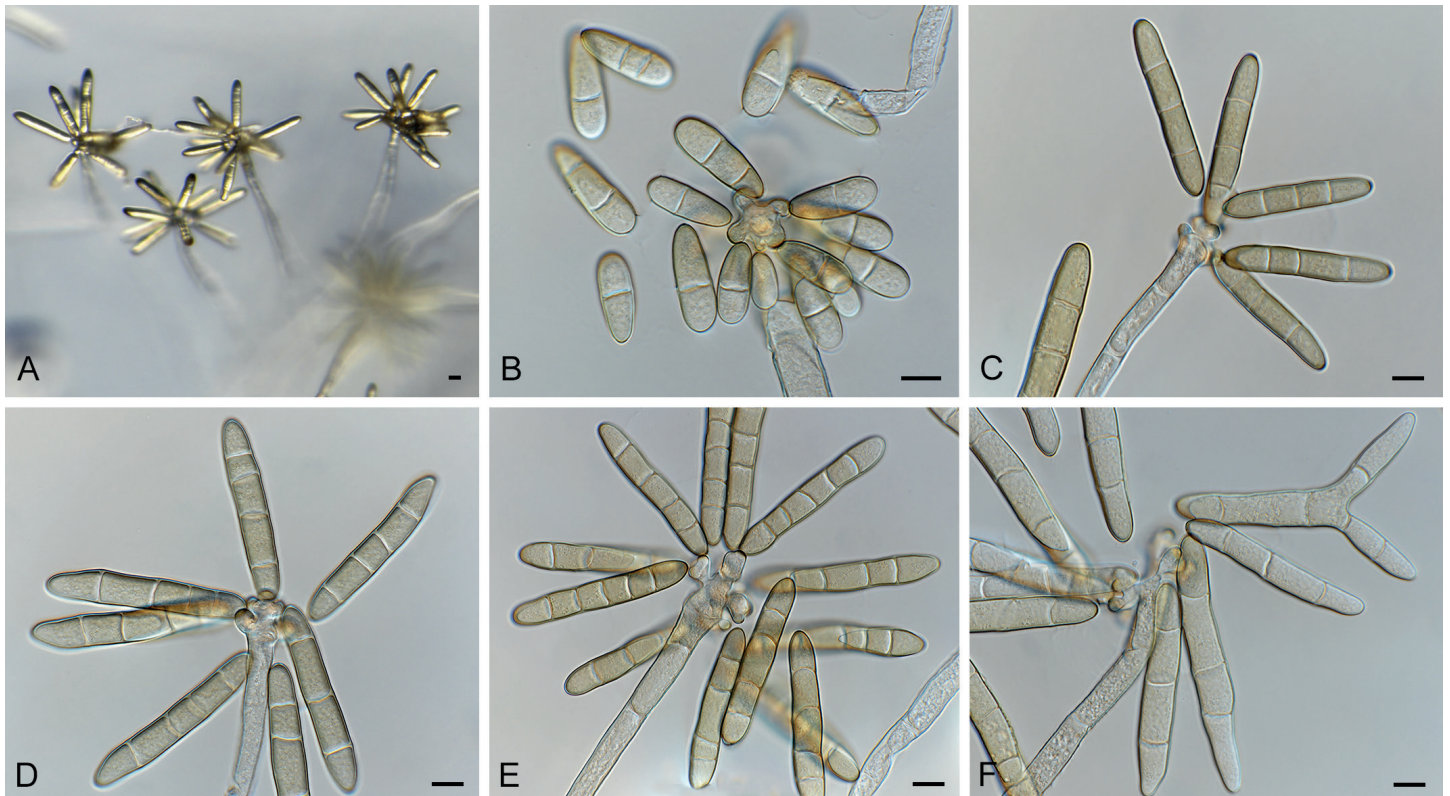


Fig. 16. *Dichotomophthora basellae* (CPC 33044). **A.** Conidiophores on SNA. **B.** Microconidia. **C–F.** Macroconidia. Scale bars = 10 µm.

Exophiala abietophila Crous & R.K. Schumach., *sp. nov.* MycoBank MB829302. Fig. 17.

Etymology: Name refers to the host genus *Abies* from which it was isolated.

Mycelium consisting of smooth, septate, brown, branched, 2–3 μm diam hyphae. **Conidiophores** reduced to conidiogenous cells or with a supporting cell. **Conidiogenous cells** pale brown, smooth, reduced to conidiogenous loci, 0.5 μm diam, or ampulliform to doliiform, 4–6 \times 2.5–3 μm . **Conidia** aseptate, (2.5–)3(–3.5) \times 1.5–2 μm , ellipsoid, hyaline, smooth-walled, guttulate, apex obtuse, tapering to a truncate base, 0.5 μm diam.

Culture characteristics: Colonies flat, spreading, with folded surface, sparse aerial mycelium and smooth, lobate margin, reaching 10 mm diam after 2 wk at 25 °C. On MEA, PDA and OA surface and reverse umber.

Typus: Norway, Oppland, Vestre Sildre, on bark of *Abies alba* (*Pinaceae*), 29 Jul. 2017, F. Sanchez *et al.*, HPC 2230 (**holotype** CBS H-23836, culture ex-type CPC 34580 = CBS 145038).

Notes: *Exophiala* includes several species of dematiaceous hyphomycetes that are clinically relevant (de Hoog 1977).

Species of *Exophiala* are however commonly isolated from plant litter and soil. Phylogenetically *E. abietophila* is distinct from all species presently known from their DNA sequence data.

Based on a megablast search of NCBI's GenBank nucleotide database, the closest hits using the **ITS** sequence had highest similarity to *Exophiala moniliae* (GenBank HE605213.1; Identities = 567/643 (88 %), 34 gaps (5 %)), *Exophiala bergeri* (GenBank MH857080.1; Identities = 484/544 (89 %), 25 gaps (4 %)), and *Atrokylandriopsis setulosa* (GenBank KP337330.1; Identities = 516/576 (90 %), 19 gaps (3 %)). Closest hits using the **LSU** sequence are *Exophiala dermatitidis* (GenBank DQ823100.1; Identities = 1112/1194 (93 %), 24 gaps (2 %)), *Exophiala bergeri* (GenBank NG_059199.1; Identities = 1099/1184 (93 %), 27 gaps (2 %)), and *Capronia pilosella* (GenBank DQ823099.1; Identities = 1106/1199 (92 %), 27 gaps (2 %)).

Exophiala lignicola Crous & Akulov, *sp. nov.* MycoBank MB829303. Fig. 18.

Etymology: Name refers to rotten wood from which it was isolated.

Mycelium consisting of smooth, pale brown, septate, branched, 2–3 μm diam hyphae. **Conidiophores** penicillate with conidia in apical slimy mass, or reduced to solitary conidiogenous cells

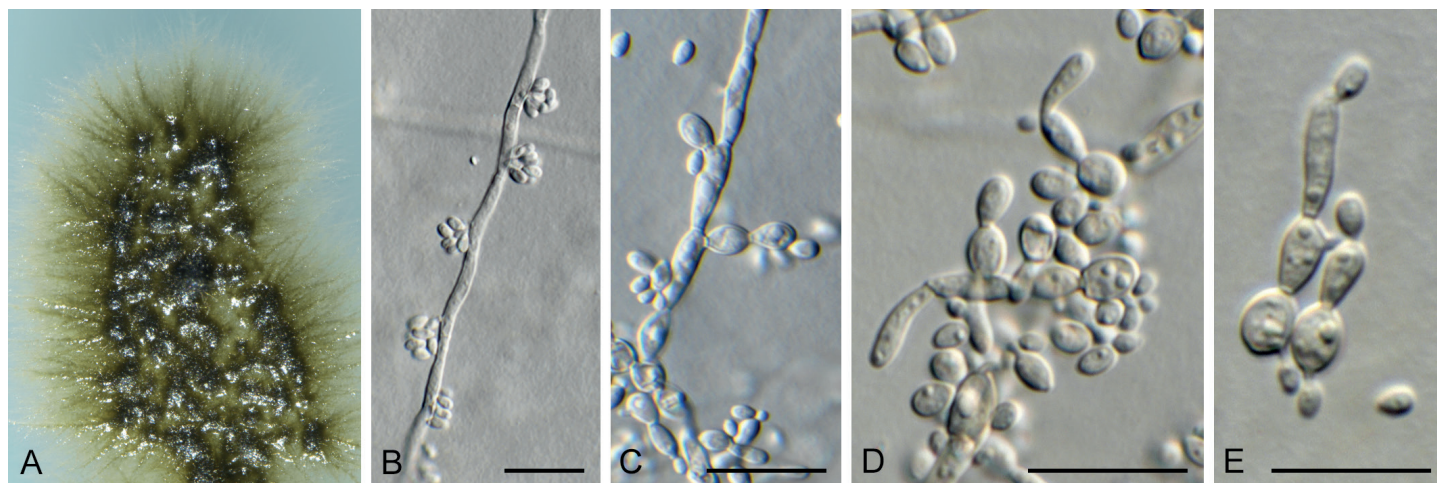


Fig. 17. *Exophiala abietophila* (CPC 34580). A. Colony on SNA. B, C. Conidiogenous loci on hyphae. D, E. Budding conidia. Scale bars = 10 μm .

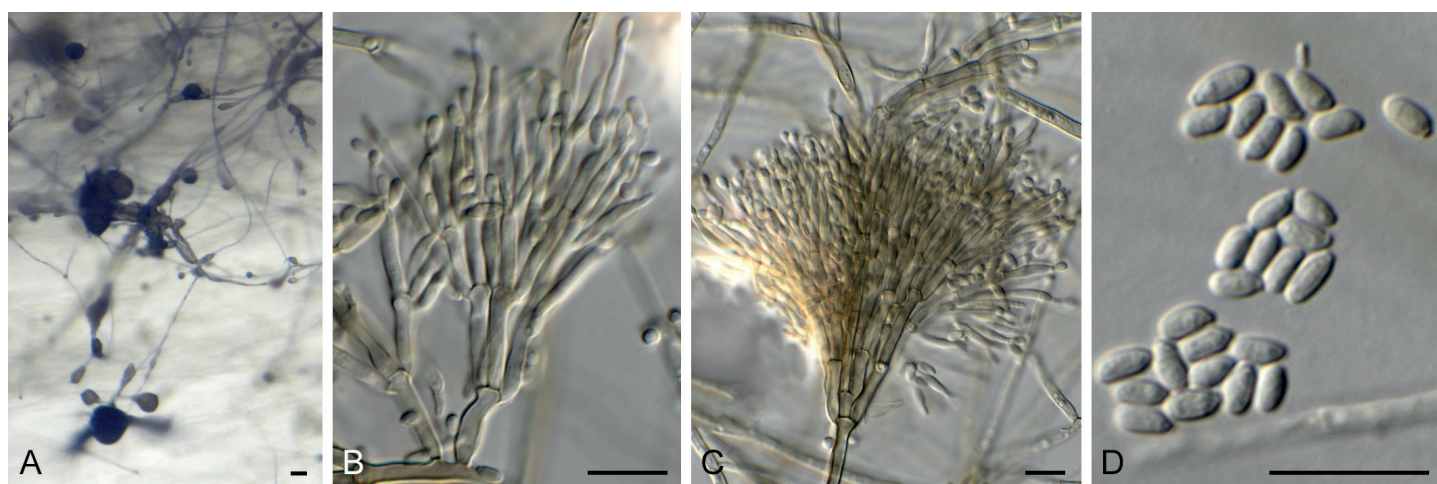


Fig. 18. *Exophiala lignicola* (CPC 32464). A. Conidiophores on SNA. B, C. Penicillate conidiophores. D. Conidia. Scale bars: A = 20 μm , B–D = 10 μm .

or loci on hyphae; conidiophores erect, arising from superficial hyphae, pale to medium brown, smooth, subcylindrical, flexuous, branched or not, stipe 10–20 × 2–3 µm, with apical and lateral penicillate conidiophores; primary branches aseptate, medium brown, smooth, 5–15 × 2–2.5 µm; secondary and tertiary branches subcylindrical, medium brown, smooth, aseptate, 8–12 × 1.5–2 µm, giving rise to 1–4 phialides, pale brown, smooth, subcylindrical to fusoid-ellipsoid, with prominent taper at apex to form a narrow cylindrical channel with percurrent proliferations, (1–)8–16 × (1.5–)2 µm. *Conidia* solitary, aseptate, pale brown, smooth, fusoid-ellipsoid, apex obtuse, base truncate, slightly reflective, (3.5–)4(–5.5) × 2(–3) µm.

Culture characteristics: Colonies erumpent, spreading, with sparse aerial mycelium and smooth, lobate margin, reaching 12 mm diam after 2 wk at 25 °C. On MEA, PDA and OA surface and reverse olivaceous grey.

Typus: **Ukraine**, Kharkiv, Forest park, on fallen decorticated trunk of cf. *Quercus* sp. (*Fagaceae*) in a native oak-maple-ash forest, 28 Oct. 2016, A. Akulov, CWU (MYC) AS 6112 = HPC 1509 (**holotype** CBS H-23802, culture ex-type CPC 32464 = CBS 144622).

Notes: *Exophiala* (*Herpotrichiellaceae*) is commonly isolated from decaying wood, soil, and plant litter. This genus of dematiaceous hyphomycetes, commonly referred to as black yeasts, is morphologically variable, with conidiophores ranging from well-defined penicillate structures as in *E. lignicola*, or solitary loci on hyphae. The genus presently contains approximately 60 epithets, several of which have *Capronia* sexual morphs (Untereiner 1997). Numerous species of *Exophiala* / *Capronia* are known as host-specific fungicolous or lichenicolous fungi (Halici *et al.*, 2010; Friebe, 2012). Phylogenetically, *E. lignicola* is distinct from those species known from their DNA sequences, and based on its unique conidiophores, it is treated as a unique taxon.

Based on a megablast search of NCBI's GenBank nucleotide database, the closest hits using the **ITS** sequence had highest similarity to *Rhinocladiella coryli* (GenBank NR_155727.1; Identities = 542/612 (89 %), 18 gaps (2 %)), *Exophiala eucalypticola* (GenBank NR_158438.1; Identities = 518/589 (88 %), 21 gaps (3 %)), and *Rhinocladiella aquaspersa* (GenBank MH374866.1; Identities = 539/619 (87 %), 32 gaps (5 %)). Closest hits using the **LSU** sequence are *Exophiala angulospora* (GenBank MH874033.1; Identities = 875/885 (99 %), no gaps), *Capronia coronata* (GenBank AF050242.1; Identities = 875/885 (99 %), no gaps), and *Fonsecaea pedrosoi* (GenBank AF050276.1; Identities = 872/887 (98 %), 2 gaps (0 %)). No significant hits were obtained when the **cmdA** sequence was used in blastn and megablast searches. Closest hits using the **tef1** sequence had highest similarity to *Exophiala dermatitidis* (GenBank DQ840566.1; Identities = 186/192 (97 %), no gaps), *Capronia munkii* (GenBank EF413607.1; Identities = 184/193 (95 %), no gaps), and *Capronia coronata* (GenBank XM_007726769.1; Identities = 187/198 (94 %), 2 gaps (1 %)).

Fuscostagonospora banksiae Crous & Carnegie, *sp. nov.* MycoBank MB829304. Fig. 19.

Etymology: Name reflects the host genus *Banksia* from which it was isolated.

Conidiomata solitary, pycnidial, globose, brown, 180–200 µm diam, exuding a milky white conidial mass. *Conidiophores* lining the inner cavity, reduced to conidiogenous cells or with a supporting cell, branched at base or not, 5–12 × 3–4 µm. *Conidiogenous cells* ampulliform to doliiform, hyaline, smooth, 5–7 × 3–4 µm; proliferating indistinctly percurrently at apex. *Conidia* solitary, aseptate, hyaline, smooth, guttulate, ellipsoid, apex obtuse, base bluntly rounded, (3–)4(–5) × (2–)2.5(–3) µm.

Culture characteristics: Colonies flat, spreading, with moderate aerial mycelium and lobed, feathery margin, reaching 40 mm diam after 2 wk at 25 °C. On MEA surface ochreous to dirty white with chestnut sectors, reverse ochreous with chestnut; on PDA surface umber with sections of dirty white and scarlet, reverse chestnut with sectors of scarlet and umber; on OA surface umber to pale luteous.

Typus: **Australia**, New South Wales, Riamukka State Forest, 31.376993S 151.693569E, on *Banksia* sp. (*Proteaceae*), 2015, A.J. Carnegie, HPC 1445 (**holotype** CBS H-23796, culture ex-type CPC 31724 = CBS 144621).

Notes: *Fuscostagonospora* was introduced for a sexual species occurring on bamboo (Tanaka *et al.* 2015). The present collection represents an asexual morph, and is thus difficult to compare with the known sexual species in the genus, but it is placed in *Fuscostagonospora* based on its phylogeny.

Based on a megablast search of NCBI's GenBank nucleotide database, the closest hits using the **ITS** sequence had highest similarity to *Periconia pseudobyssoides* (GenBank KY364628.1; Identities = 426/464 (92 %), 10 gaps (2 %)), *Periconia byssoides* (GenBank KY364620.1; Identities = 426/464 (92 %), 10 gaps (2 %)), and *Fuscostagonospora sasae* (GenBank NR_153964.1; Identities = 425/468 (91 %), 16 gaps (3 %)). Closest hits using the **LSU** sequence are *Fuscostagonospora cytisi* (GenBank KY770978.1; Identities = 839/846 (99 %), no gaps), *Fuscostagonospora sasae* (GenBank AB807548.1; Identities = 838/850 (99 %), no gaps), and *Corynespora olivacea* (GenBank JQ044448.1; Identities = 858/879 (98 %), 5 gaps (0 %)).

Gaeumannomycella caricicola Hern.-Restr., Crous & R.K. Schumach., *sp. nov.* MycoBank MB829305. Fig. 20.

Etymology: Name refers to the host genus *Carex* from which it was isolated.

In vivo. *Ascomata* perithecial, immersed or semi-immersed on the substrate, globose, subglobose to elliptical, pale brown, 275–390 × 135–235 µm, with a lateral, central cylindrical neck, 108–167 × 57–97 µm; *ascomatal wall texture intricata* to *epidermoidea*. *Paraphyses* sparse, basally moniliform, upwards filiform, unbranched, multi-celled, hyaline, thin-walled and smooth, evanescent. *Asci* numerous, unitunicate, cylindrical to elongated clavate, stalked, 8-spored, 73–210 × 9–18 µm. *Ascospores* cylindrical, to slightly curved at one or both ends, widest in the middle, tapering to the base, ends rounded, multi-guttulate, 0–3-septate, septa often indistinct, hyaline, 32–45 × 3–3.5 µm. *Hyphopodia* brown, lobed (few hyphopodia were observed close to the perithecial neck).

Culture characteristics: Colonies flat, spreading, with folded surface, sparse to moderate aerial mycelium and smooth,

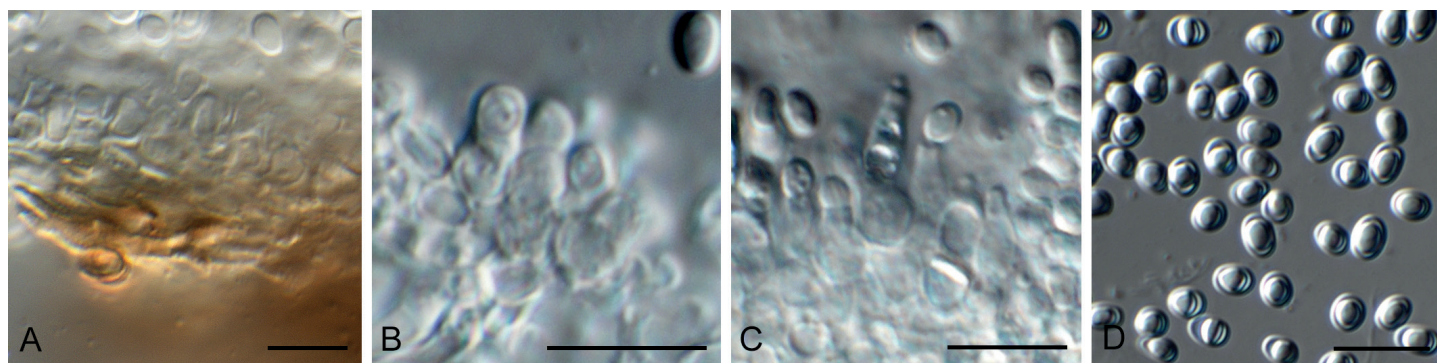


Fig. 19. *Fuscostagonospora banksiae* (CPC 31724). **A.** Conidiomatal wall giving rise to conidiogenous cells. **B, C.** Conidiogenous cells. **D.** Conidia. Scale bars = 10 μ m.

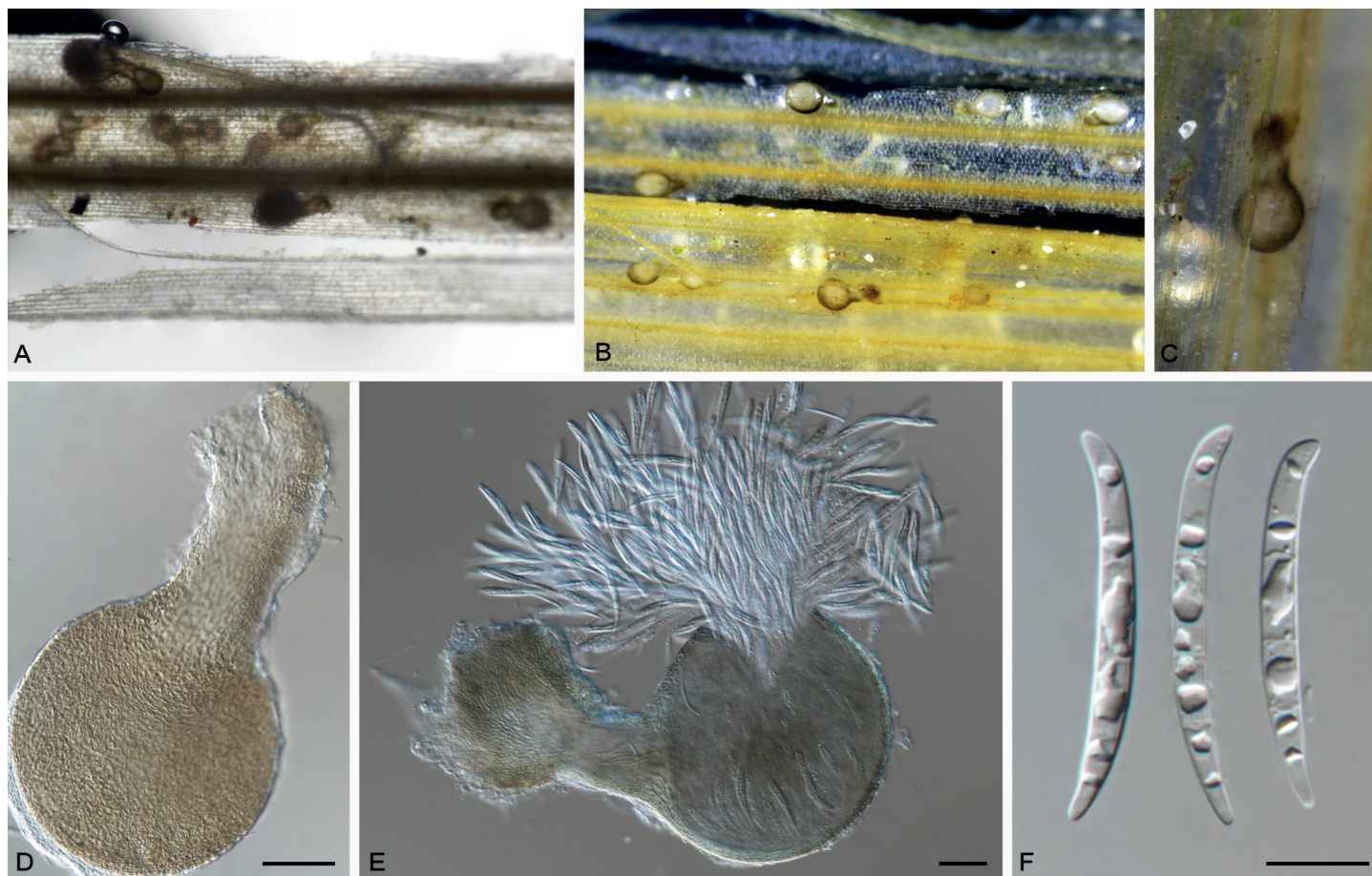


Fig. 20. *Gaeumannomyces caricicola* (CPC 33925). **A–C.** Perithecial ascomata embedded on the substrate (grass leaves). **D.** Perithecia. **E.** Perithecia with asci. **F.** Ascospores. Scale bars. **A–E** = 50 μ m, **F** = 10 μ m.

lobate margin, covering dish after 2 wk at 25 °C. On MEA surface pale olivaceous, reverse luteous; on PDA surface and reverse olivaceous grey; on OA surface olivaceous grey.

Typus: **Germany**, near Berlin, on dead leaf of *Carex remota* (Cyperaceae), 2 Jun. 2017, R.K. Schumacher, HPC 2136 = RKS 122 (**holotype** CBS H-23793, culture ex-type CPC 33925 = CBS 145041).

Notes: *Gaeumannomyces* was introduced by Hernández-Restrepo *et al.* (2016) for a genus of fungi morphologically similar to *Gaeumannomyces*, and associated with a disease on Cyperaceae. *Gaeumannomyces caricicola* is phylogenetically distinct from *Gaeumannomyces caricis*, the only other species

presently known in the genus. Of interest is the fact that both species occur on *Carex*.

Based on a megablast search of NCBI's GenBank nucleotide database, the closest hits using the **ITS** sequence had highest similarity to *Slopeiomyces cylindrosporus* (as *Gaeumannomyces cylindrosporus*, GenBank JF508361.1; Identities = 506/519 (97%), 3 gaps (0%)), *Gaeumannomyces caricis* (GenBank KX306478.1; Identities = 523/553 (95%), 10 gaps (1%)), and *Nakataea oryzae* (GenBank FJ746639.1; Identities = 511/550 (93%), 9 gaps (1%)). Closest hits using the **LSU** sequence are *Slopeiomyces cylindrosporus* (GenBank KM009159.1; Identities = 835/848 (98%), no gaps), *Omnidemtus affinis* (GenBank NG_059478.1; Identities = 832/848 (98%), no gaps), and *Gaeumannomyces graminicola* (GenBank DQ341496.1; Identities = 832/848 (98%

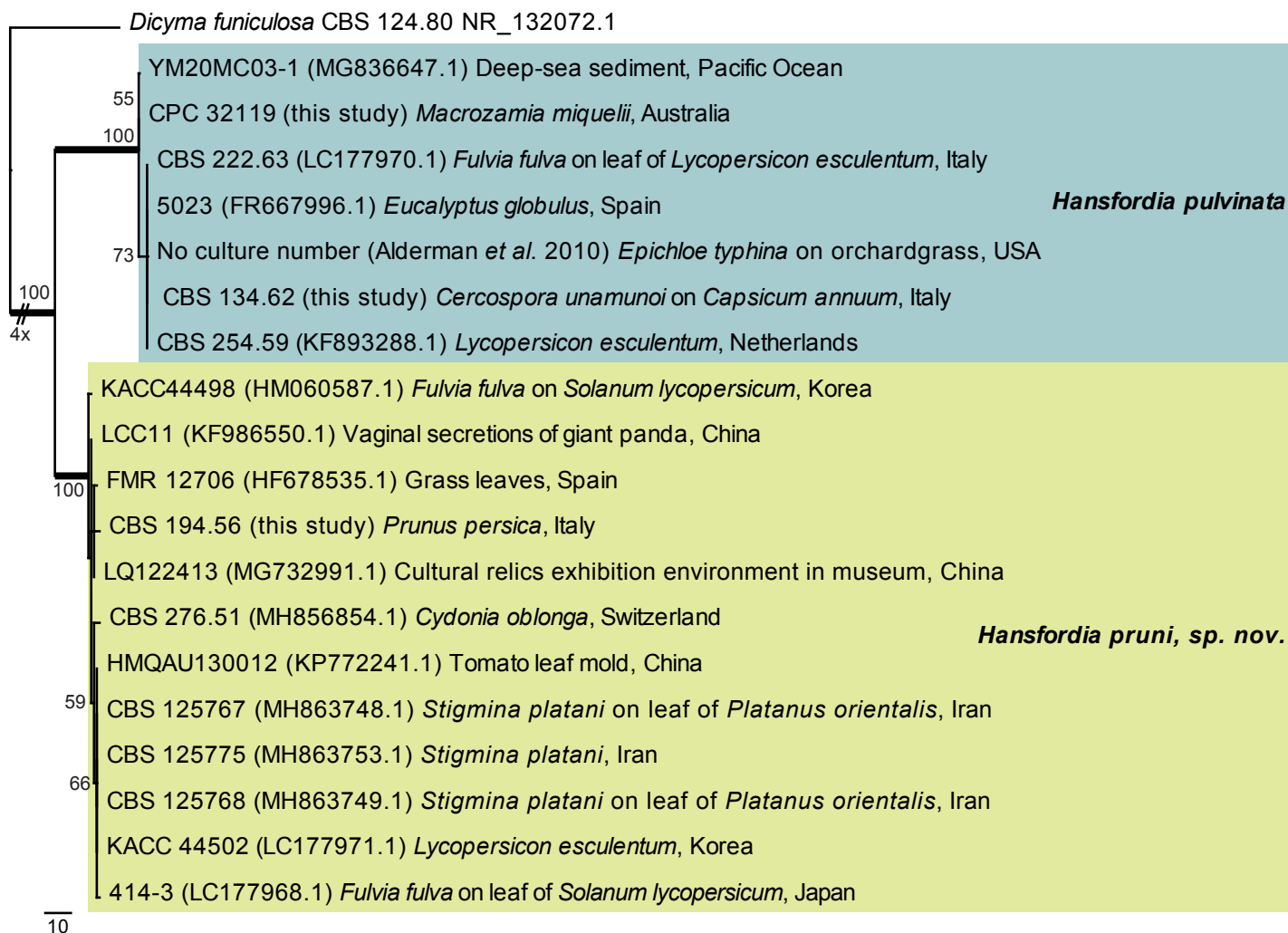


Fig. 21. The first of five equally most parsimonious trees obtained from a phylogenetic analysis of the *Hansfordia* ITS alignment (20 strains including the outgroup; 477 characters analysed: 337 constant, 93 variable and parsimony-uninformative and 47 parsimony-informative). The tree was rooted to *Dicyma funiculosa* (GenBank NR_132072.1) and the scale bar indicates the number of changes. Bootstrap support values higher than 49 % are shown at the nodes and the species clades are highlighted with coloured boxes. Species names are indicated to the right of the tree. Strain numbers, followed by the sources between round brackets, substrate/source and country of origin are indicated for each sequence. Branches present in the strict consensus tree are thickened. The length of the most basal branch was shortened to facilitate layout. Tree statistics: TL = 159, CI = 0.975, RI = 0.986, RC = 0.961.

%), no gaps). Distant hits using the *his3* sequence had highest similarity to *Colletotrichum arxii* (GenBank KF687846.1; Identities = 173/183 (95 %), no gaps), *Verticillium albo-atrum* (GenBank DQ266200.1; Identities = 173/184 (94 %), no gaps), and *Colletotrichum vietnamense* (GenBank KF687854.1; Identities = 172/183 (94 %), no gaps). Distant hits using the *tub2* sequence had highest similarity to *Gibellina cerealis* (GenBank KT377187.1; Identities = 334/409 (82 %), 28 gaps (6 %)), *Slopeiomyces cylindrosporus* (*Gaeumannomyces cylindrosporus* as, GenBank AY435448.1; Identities = 333/425 (78 %), 32 gaps (7 %)), and *Magnaportheopsis maydis* (as *Cephalosporium maydis*, GenBank AY435435.1; Identities = 265/351 (75 %), 27 gaps (7 %)).

Hansfordiaceae Crous, *fam. nov.* MycoBank MB829455.

Mycelium superficial to immersed. *Conidiophores* solitary, erect, straight to flexuous, branched, medium brown, smooth, arising from superficial mycelium, at times setiform, multi-septate with lateral branches, each giving rise to several smaller, pale brown branches that form *conidiogenous cells*,

subhyaline, subcylindrical or clavate; subdenticulate apical loci with rhexolytic conidiogenesis. *Conidia* aseptate, solitary, dry, globose to ellipsoid to fusoid, hyaline to pale brown, smooth or finely roughened, with minute basal frill derived from the apex of the separating cell.

Type genus: *Hansfordia* S. Hughes.

Type species: *H. ovalispora* S. Hughes.

Hansfordia pruni Crous, *sp. nov.* MycoBank MB829306. Figs 21, 22.

Etymology: Name refers to the genus *Prunus* from which it was isolated.

Conidiophores solitary, erect, straight to flexuous, branched, medium brown, smooth, arising from superficial mycelium, 100–1000 × 2.5–3 μm, multi-septate with lateral branches in upper half, each giving rise to several smaller, pale brown branches that form 1–2 *conidiogenous cells*, subhyaline, subcylindrical with

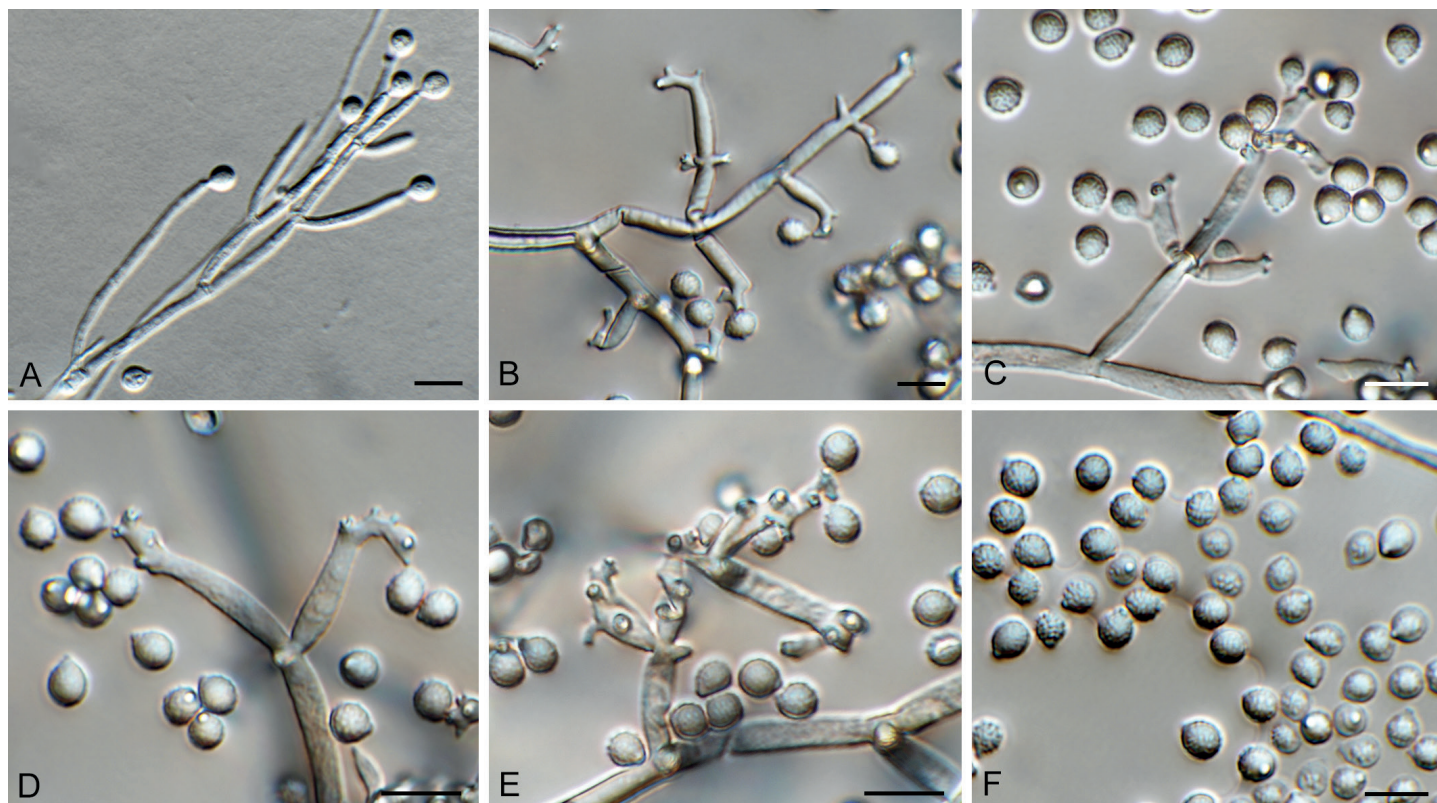


Fig. 22. *Hansfordia pruni* (CBS 194.56). A–E. Conidiophores with conidiogenous cells. F. Conidia. Scale bars = 10 µm.

apical taper, $5\text{--}20 \times 2.5\text{--}3$ µm, with 2–6 subdenticulate apical loci with rhexolytic conidiogenesis. *Conidia* aseptate, solitary, dry, globose to subglobose, subhyaline, finely roughened, (4–)5(–6) \times 4 µm diam, with minute basal frill derived from the apex of the separating cell.

Culture characteristics: Colonies erumpent, spreading, with moderate aerial mycelium and feathery, lobate margins, reaching 35 mm diam after 2 wk. On MEA fawn, reverse cinnamon; on PDA isabelline, reverse brown vinaceous; on OA vinaceous buff.

Typus: **Italy**, on twig of *Prunus persica* (*Rosaceae*), deposited in 1956, *M. Ribaldi* (**holotype** CBS H-23837, culture ex-type IMI 146912 = CBS 194.56).

Notes: *Hansfordia pulvinata* has many proposed synonyms (Deighton 1972), which based on morphology, appear similar to the type. However, *H. pruni* differs in that it has longer conidiophores, more aggregated sub-denticulate loci on its conidiogenous cells, and smaller conidia.

Based on a megablast search of NCBI's GenBank nucleotide database, the **ITS** sequence was identical to *Hansfordia pulvinata* (GenBank KU683763.1; Identities = 1040/1040 (100 %)); other closest hits included *Entosordaria quercina* (GenBank MF488994.1; Identities = 842/915 (92 %), 20 gaps (2 %)), and *Entosordaria perfidiosa* (GenBank MF488993.1; Identities = 840/914 (92 %), 18 gaps (1 %)).

Hansfordia pulvinata (Berk. & M.A. Curtis) S. Hughes, *Canad. J. Bot.* **36**: 771. 1958. Fig. 21, 23.

Basionym: *Polyactis pulvinata* Berk. & M.A. Curtis, *Grevillea* **3**(27): 110. 1875.

Conidiophores solitary, erect, flexuous, branched, medium brown, smooth, arising from superficial mycelium, $200\text{--}600 \times 3\text{--}4$ µm, multi-septate with lateral branches in upper half, each giving rise to several smaller, pale brown branches that form 1–2 *conidiogenous cells*, subhyaline, subcylindrical with apical taper, $10\text{--}17 \times 3\text{--}3.5$ µm, with 1–2 subdenticulate apical loci with rhexolytic conidiogenesis. *Conidia* solitary, dry, globose, subhyaline, finely roughened, (5–)6(–7) µm diam, with minute basal frill derived from apex of the separating cell.

Culture characteristics: Colonies erumpent, spreading, with moderate aerial mycelium and feathery, lobate margin, reaching 25 mm diam after 2 wk at 25 °C. On MEA surface olivaceous grey in centre, smoke grey in outer region, luteous in reverse; on PDA surface olivaceous grey in centre, smoke grey in outer region, reverse olivaceous grey in centre, luteous in outer region; on OA surface pale olivaceous grey, outer region pale luteous.

Material examined: **Australia**, New South Wales, Australian Botanical Garden Mount Annan, on leaves of *Macrozamia miquelii* (*Zamiaceae*), 25 Nov. 2016, *P.W. Crous*, HPC 1734, CBS H-23581, culture CPC 32119 = CBS 144422.

Notes: *Hansfordia pulvinata* (a mycoparasite on other fungi, including *Fulvia fulva* on tomatoes; Peresse & le Picard 1980) was originally described from branches of *Alnus* sp. collected in North America. It needs to be recollected in the USA to fix the application of the name. Morphologically however, the culture considered in this study applies best to the current concept for this taxon (Ellis 1971, 1976, Deighton 1972). *Hansfordia pulvinata* has been suggested as possible biological control agent for plant pathogenic fungi (Mitchell & Taber 1986, Alderman *et al.* 2010).

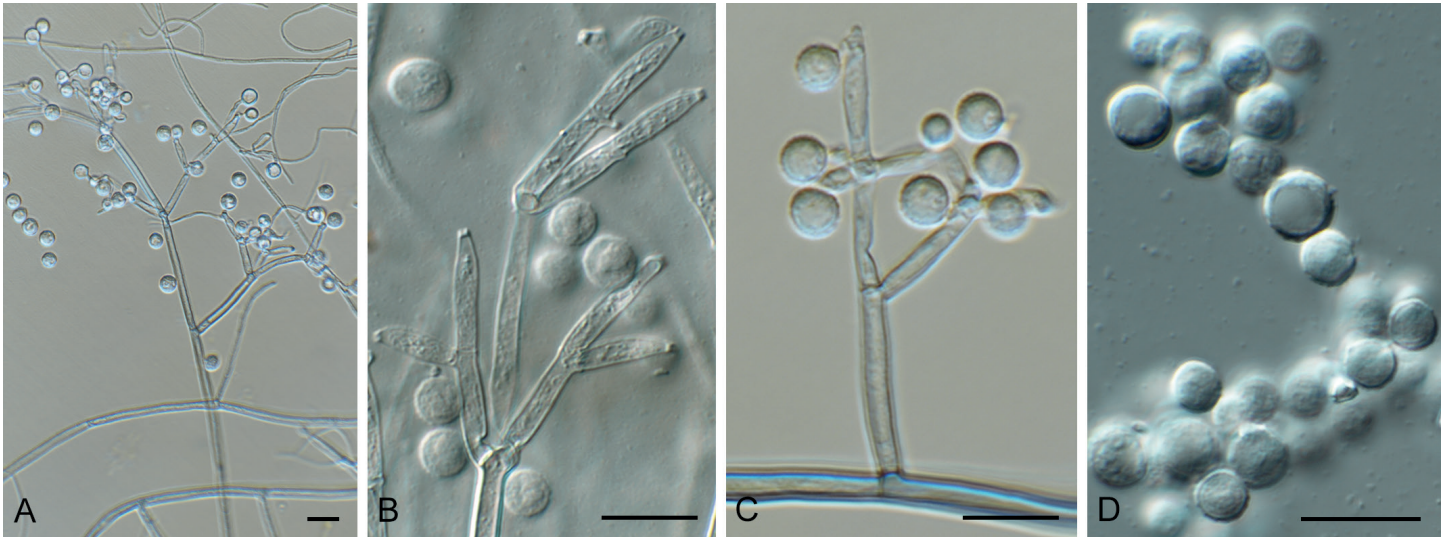


Fig. 23. *Hansfordia pulvinata* (CPC 32119). A. Conidiophore. B, C. Conidiogenous cells. D. Conidia. Scale bars = 10 μ m.

Based on a megablast search of NCBI's GenBank nucleotide database, the closest hits using the ITS sequence had highest similarity to *Hansfordia pulvinata* (GenBank LC177970.1; Identities = 468/471 (99 %), no gaps), *Hansfordia pulvinata* (GenBank MH863749.1; Identities = 510/546 (93 %), 11 gaps (2 %)), *Gyrothrix verticiclada* (GenBank KC775750.1; Identities = 407/463 (88 %), 17 gaps (3 %)), *Selenodriella fertilis* (GenBank KP859055.1; Identities = 473/544 (87 %), 24 gaps (4 %)), and *Daldinia bambusicola* (GenBank KY610385.1; Identities = 474/553 (86 %), 22 gaps (3 %)). Closest hits using the LSU sequence are *Gyrothrix circinata* (GenBank KJ476964.1; Identities = 793/830 (96 %), 5 gaps (0 %)), *Circinotrichum maculiforme* (GenBank KR611896.1; Identities = 805/844 (95 %), 5 gaps (0 %)), and *Oxydothis garethjonesii* (GenBank KY206762.1; Identities = 799/842 (95 %), 2 gaps (0 %)).

Hypsotheca Ellis & Everh., *J. Mycol.* **1**: 128. 1885.

Synonyms: *Capnodiella* (Sacc.) Sacc. & D. Sacc., *Syll. fung.* (Abellini) **17**: 621. 1905. [based on *Capnodium maximum*] *Sorica* Giesenh., *Ber. dt. bot. Ges.* **22**: 195. 1904. [based on *Sorica dusenii*]

Ascomata separate or loosely grouped, not arising from a visible stroma, dark brown to black, ventricose, straight or curved, elongate with a submedian to suprabaasal swollen ascigerous locule. Ascomatal wall of *textura porrecta* to *textura intricata*. *Asci* 8-spored, elongating at maturity and extending up the ascoma neck to the apex before deliquescing to release ascospores at or below the ostiole; discharged ascospores accumulating in a dry reddish brown mass at the ostiole. *Ascospores* golden brown, thick-walled, smooth, depressed globose to subellipsoid. Pycnidial and hyphomycetous morphs produced. *Pycnidial conidiomata* solitary, dark brown to black, globose or depressed globose, or short stipitate, with a prominent papillate ostiole, wall of *textura angulata* to *textura intricata*. *Conidiophores* hyaline, arising from the inner cells of the pycnidial wall, simple ampulliform or elongate, septate. *Conidiogenous cells* phialidic with an inconspicuous collarette. *Conidia* hyaline, asymmetrical, oblong to allantoid or fusoid, aseptate, smooth. *Hyphomycetous morph* with mucoid heads of conidia scattered on short lateral phialodes,

phaeoacremonium-like, sub-hyaline to pale brown, smooth or rough. *Conidiogenous cells* lageniform, the collarettes usually inconspicuous or flared (phialophora-like). *Conidia* aseptate, ellipsoid-ovoid, smooth.

Type species: *Hypsotheca subcorticalis* [Basionym: *Sphaeronema subcorticale*, perithecia occurring inside the bark of *Quercus*, New Jersey, USA, type at K].

Hypsotheca nigra (Schrad. ex DC.) Crous, *comb. nov.* MycoBank MB829445.

Basionym: *Stilbum nigrum* Schrad. ex DC., *Flore française* **2**: 593. 1805.

Synonyms: *Lagenula nigra* (Schrad. ex DC.) G. Arnaud, *Annls Épiphyt.* **16**: 267. 1930.

Caliciopsis nigra (Schrad. ex DC) Fitzp., *Mycologia* **34**: 501. 1942.

Hypsotheca maxima (Berk. & M.A. Curtis) Crous, *comb. nov.* MycoBank MB829446.

Basionym: *Capnodium maximum* Berk. & M.A. Curtis, *J. Linn. Soc., Bot.* **10**: 391. 1868 (1869).

Polychaeton maximum (Berk. & M.A. Curtis) Kuntze, *Revis. gen. pl.* (Leipzig) **1**: 13. 1891.

Sorica maxima (Berk. & M.A. Curtis) Giesenh., *Ber. dt. bot. Ges.* **22**: 358. 1904.

Capnodiella maxima (Berk. & M.A. Curtis) Sacc. & D. Sacc., *Syll. fung.* (Abellini) **17**: 621. 1905.

Caliciopsis maxima (Berk. & M.A. Curtis) Höhn., *Sitzungsber. Akad. Wiss. Wien, Math.-Naturwiss. Kl., Abt. 1*, **128**: 84. 1919.

Typus: **Cuba**, on fronds of *Niphidium* sp. (*Polypodiaceae*) (originally identified as *Polypodium* sp.), 1941, Wright (*holotype* CUP-029913). **Brazil**, Rio de Janeiro, Nova Friburgo, on fronds of *Niphidium crassifolium* (*Polypodiaceae*), 5 Nov. 2011, R.W. Barreto (*epitype* VIC 42568, culture ex-epitype COAD 1983 = CPC 24674).

Material examined: **Brazil**, Rio de Janeiro, Nova Friburgo, on fronds of *Microgramma squamulosa* (*Polypodiaceae*), 10 Oct. 2013, R.W. Barreto, VIC 42602.

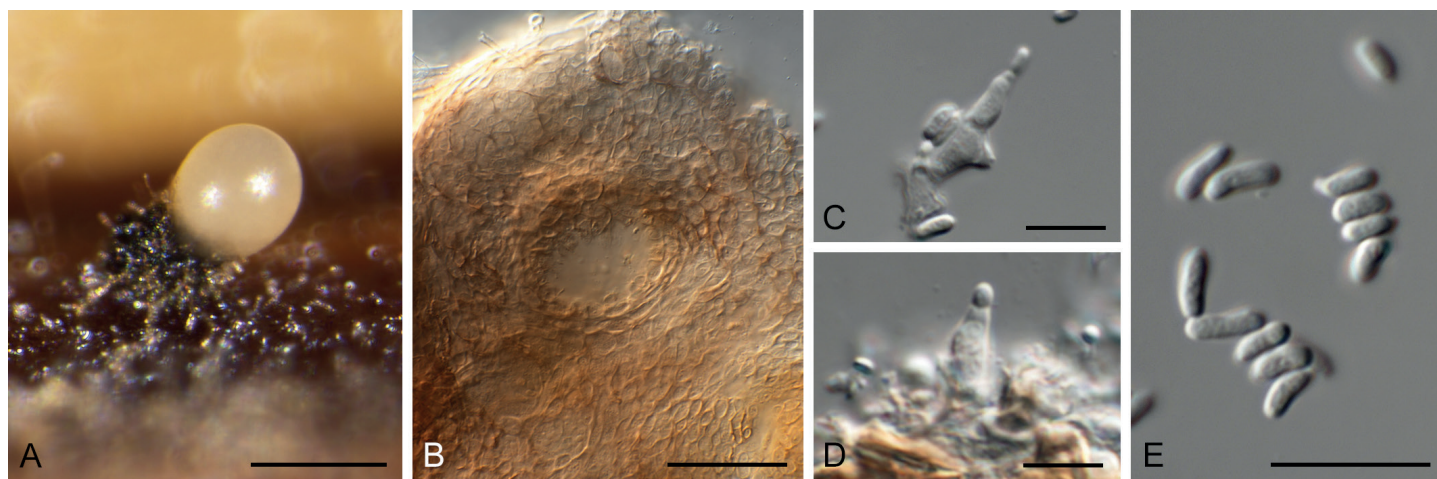


Fig. 24. *Hypsotheca pleomorpha* (CPC 32144). **A.** Conidioma forming on PDA. **B.** Conidioma with ostiole. **C, D.** Conidiogenous cells. **E.** Conidia. Scale bars: A = 200 µm, B = 50 µm, C–E = 10 µm.

Hypsotheca pleomorpha (Patricia McGee & I. Pascoe) Crous, **comb. nov.** MycoBank MB829312. Fig. 24.

Basionym: *Caliciopsis pleomorpha* Patricia McGee & I. Pascoe, *Fungal Syst. Evol.* **2**: 50. 2018.

Conidiomata pycnidial, globose, ostiolate, brown, 50–200 µm diam, separate (on PNA), or aggregated in a brown stroma (on PDA, MEA). **Conidiophores** arising from inner layer, hyaline, smooth, subcylindrical, branched, 1–4-septate, 5–20 × 3–4 µm. **Conidiogenous cells** subcylindrical to doliiform, hyaline, smooth, terminal and intercalary, phialidic with prominent periclinal thickening, 3–6 × 2–4 µm. **Conidia** solitary, aseptate, hyaline, smooth, granular, fusoid-ellipsoid, mostly somewhat curved, apex obtuse, tapered towards base, truncate, 0.5 µm diam, (3–) 4–5(–6) × 1.5(–2) µm.

Culture characteristics: Colonies spreading, surface folded, with sparse to moderate aerial mycelium and smooth, lobate margins, reaching 50 mm diam after 2 wk. On MEA, PDA and OA surface and reverse chestnut.

Material examined: **Australia**, New South Wales, on leaves of *Eucalyptus piperita* (Myrtaceae), 2014, P.W. Crous, HPC 1762, culture CBS 144636 = CPC 32144.

Notes: The genus *Caliciopsis* (based on *C. pinea*) represents two phylogenetically distinct, well-supported clades, one of which is ascribed here to the former generic synonym, *Hypsotheca*, which appears to be the oldest name available for this clade. *Hypsotheca* (based on *Hypsotheca subcorticalis*; globose ascospores) was formerly distinguished from *Caliciopsis* (*Caliciopsis pinea*; ellipsoid ascospores) based on ascospore shape, although Fitzpatrick (1942) did not consider this character to be significant at generic level. Morphologically there are few differences between these genera, except that species of *Hypsotheca* known from culture also form a phaeoacremonium-like synasexual morph in culture, which has not yet been observed for species of *Caliciopsis* s.str. *Hypsotheca pleomorpha* was recently described as the causal agent of a canker disease of *Eucalyptus* spp. in Australia (Pascoe et al. 2018), and is reported here from leaves of *Eucalyptus piperita*, although its possible role as foliar pathogen remains unknown.

Based on a megablast search of NCBI's GenBank nucleotide database, the **ITS** sequence was identical to *Caliciopsis pleomorpha* (GenBank MG641785.1; Identities = 523/523 (100 %)), and related to *Corynelia uberata* (GenBank KU204606.1; Identities = 511/526 (97 %), 5 gaps (0 %)) and *Caliciopsis maxima* (GenBank KX891229.1; Identities = 467/533 (88 %), 20 gaps (3 %)). Closest hits using the **LSU** sequence are *Caliciopsis nigra* (GenBank KP144011.1; Identities = 769/826 (93 %), 9 gaps (1 %)), *Caliciopsis pinea* (GenBank DQ678097.1; Identities = 781/843 (93 %), 8 gaps (0 %)), and *Caliciopsis beckhausii* (GenBank NG_060418.1; Identities = 789/855 (92 %), 5 gaps (0 %)).

Jeremyomyces Crous & R.K. Schumach., **gen. nov.** MycoBank MB829307.

Etymology: Name refers to Jeremy, a young man who due to social circumstances has to live in a children's home in Germany. Despite these difficult circumstances, he has proven to be an attentive observer with a special interest in fungi.

Ascomata pseudothecial, intracorticolous, singly, gregarious, unilocular, sphaerical, black; ostiole indistinct. **Peridium** few-layered, consisting of a *textura angularis* with thick-walled, smooth, and eguttulate cells, inner layers hyaline, outer layers red brown. **Paraphysoids** numerous, distinctly longer than the asci, basally moniliform, upwards tapered and filiform, end cells gnarled, multi-celled, hyaline, thin-walled, smooth, eguttulate, branched, with anastomoses. **Asci** 8-spored, clavate, apically rounded with an ocular chamber, pedicel short and furcate, thick-walled, bitunicate, fissitunicate, apical chamber well-defined, clavate to subcylindrical, spores oblique biseriate overlapped. **Ascospores** hyaline, smooth, guttulate, 1-septate (3-septate with age), fusoid, widest above septum, prominently constricted with well-defined mucoid sheath; basal cell somewhat longer and apical cell. **Conidiomata** developing in culture, pycnidial, brown, globose with central ostiole. **Conidiophores** reduced to conidiogenous cells, lining the inner cavity, ampulliform to doliiform, hyaline, smooth, phialidic. **Conidia** solitary, aseptate, hyaline, smooth, subcylindrical with obtuse ends.

Type species: *Jeremyomyces labinae* Crous & R.K. Schumach.

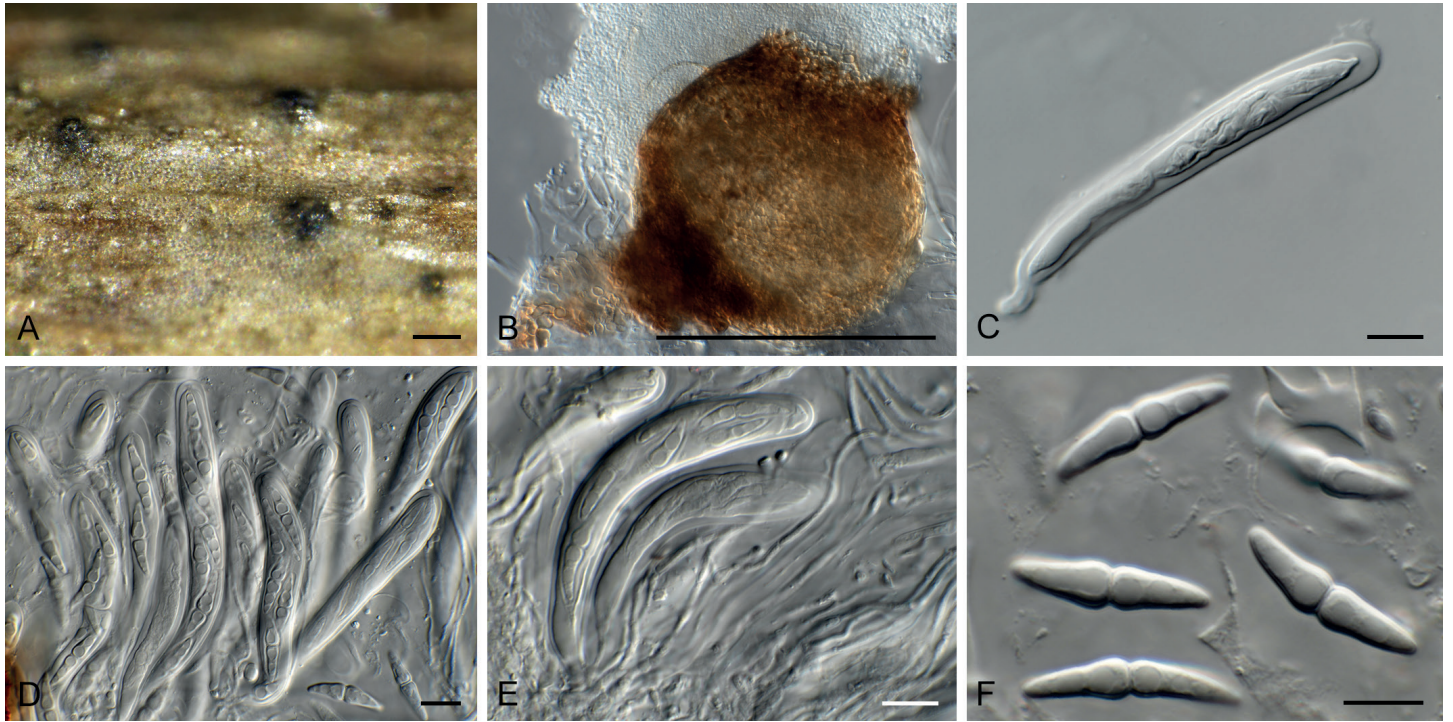


Fig. 25. *Jeremyomyces labinae* (CPC 33154). **A.** Ascomata on host tissue. **B.** Conidioma in culture. **C–E.** Asci. **F.** Ascospores with sheath. Scale bars: A, B = 200 μ m, C–F = 10 μ m.

Jeremyomyces labinae Crous & R.K. Schumach., *sp. nov.*
Mycobank MB829309. Fig. 25.

Etymology: Name refers to Mrs. Elena Labina, a Russian colleague who has dedicated much of her personal time to collaborating with the authorities of this species in fungal research.

Ascomata pseudothecial, intracorticolous, singly, gregarious, unilocular, sphaerical, black, soft, +/-thin, ostiole indistinct, basally with a few short and red brown hyphae, up to 200 μ m diam. **Peridium** few-layered, consisting of a *textura angularis* with thick-walled, smooth, and eguttulate cells, inner layers hyaline, outer layers red brown. **Paraphysoids** numerous, distinctly longer than the asci, basally moniliform, upwards tapered and filiform, end cells gnarled, multi-celled, 2–3 μ m diam, hyaline, thin-walled, smooth, eguttulate, branched, with anastomoses. **Asci** 8-spored, clavate, apically rounded with an ocular chamber, pedicel short and furcate, thick-walled, bitunicate, fissitunicate, 75–115 \times 10–13 μ m, apical chamber well-defined, 2 μ m diam, clavate to subcylindrical, spores oblique biseriate overlapped. **Ascospores** hyaline, smooth, guttulate (at least 2 guttules per cell), 1-septate (3-septate with age), fusoid, widest above septum, prominently constricted with well-defined mucoid sheath, 5 μ m diam; basal cell somewhat longer and apical cell, (19–)22–24(–26) \times (4–)5(–6) μ m. In culture: **Conidiomata** developing in culture, pycnidial, brown, globose with central ostiole, 150–180 μ m diam. **Conidiophores** reduced to conidiogenous cells, lining the inner cavity, ampulliform to doliiform, hyaline, smooth, phialidic, 3–4 \times 3–5 μ m. **Conidia** solitary, aseptate, hyaline, smooth, subcylindrical with obtuse ends, (3–)4–5 \times 2 μ m.

Culture characteristics: Colonies spreading, with moderate aerial mycelium and smooth, lobate margin, reaching 35 mm diam after 2 wk at 25 $^{\circ}$ C. On MEA surface pale olivaceous

grey, reverse olivaceous grey; on PDA surface olivaceous grey in centre, scarlet in outer region, reverse scarlet with diffuse scarlet pigment; on OA surface olivaceous grey with patches of scarlet and diffuse scarlet pigment.

Typus: Germany, near Berlin, on twig of *Salix alba* (*Salicaceae*), 21 Jan. 2017, R.K. Schumacher, HPC 1956 (**holotype** CBS H-23817, culture ex-type CPC 33154 = CBS 144617).

Notes: Morphologically *Jeremyomyces* is similar to *Angustimassarina* (Thambugala *et al.* 2015), except that it has a coelomycetous asexual morph. Strangely, the LSU sequence clusters with the type sequence of *Acericola italica*, a fungus that is morphologically quite distinct, having brown, three-septate ascospores. This suggests that the GenBank sequence of *Acericola* is incorrect. Based on this sequence however, this fungus was placed in a new genus, *Acericola*, rather than *Setomelanomma*, which is probably where it belongs.

Based on a megablast search of NCBI's GenBank nucleotide database, the closest hits using the **ITS** sequence had highest similarity to *Acericola italica* (GenBank NR_156344.1; Identities = 523/534 (98 %), 3 gaps (0 %)), *Xenophoma punctelliae* (as *Phoma* sp. JDL-2012a, GenBank JQ238617.1; Identities = 553/578 (96 %), 9 gaps (1 %)), and *Phaeosphaeria caricis* (GenBank KY090633.1; Identities = 536/583 (92 %), 13 gaps (2 %)). Closest hits using the **LSU** sequence are *Acericola italica* (GenBank MF167429.1; Identities = 883/883 (100 %), no gaps), *Phaeosphaeria sowerbyi* (GenBank MH873687.1; Identities = 891/896 (99 %), no gaps), and *Phaeosphaeria herpotrichoides* (GenBank MH873664.1; Identities = 891/896 (99 %), no gaps). No significant hits were obtained when the **cmdA** sequence was used in blastn and megablast searches. Distant hits using the **rpb2** sequence had highest similarity to *Phaeosphaeriopsis triseptata* (GenBank KJ522486.1; Identities = 877/1003 (87 %), 2 gaps (0 %)), *Hawksworthiana alliariae* (as *Dematiopleospora*

alliariae, GenBank KX507261.1; Identities = 846/1008 (84 %), 1 gap (0 %)), and *Dematiopleospora salsolae* (GenBank MG829254.1; Identities = 830/1005 (83 %), 2 gaps (0 %)). Distant hits using the **tef1** sequence had highest similarity to *Didymocyrtis cladoniicola* (as *Diederichomyces cladoniicola*, GenBank KP170668.1; Identities = 435/521 (83 %), 16 gaps (3 %)), *Phaeosphaeria ammophilae* (GenBank MF795877.1; Identities = 411/495 (83 %), 30 gaps (6 %)), and *Chaetosphaeronema hispidulum* (GenBank KF253108.1; Identities = 394/472 (83 %), 23 gaps (4 %)). Distant hits using the **tub2** sequence had highest similarity to *Xenophoma puncteliae* (GenBank KP170711.1; Identities = 249/278 (90 %), 1 gap (0 %)), *Didymocyrtis banksiae* (GenBank KY979923.1; Identities = 245/279 (88 %), 9 gaps (3 %)), and *Phoma haematocycla* (GenBank KT309405.1; Identities = 239/272 (88 %), 3 gaps (1 %)).

Macgarvieomyces luzulae (Ondřej) Y. Marín *et al.*, Stud. Mycol. 92: 84. 2018 (2019). Fig. 26.

Basionym: *Pyricularia luzulae* Ondřej, Česká Mykol. 42: 81. 1988.

Conidiophores solitary, erect, straight to flexuous, subcylindrical, unbranched, thick-walled, brown, smooth-walled, 1–3-septate, arising from hyphae looking lacking a swollen base, 60–120 × 5–6 µm. **Conidiogenous cells** integrated, terminal, pale brown, smooth-walled, subcylindrical with apical taper towards a rachis of sympodially arranged denticles, 1–2 × 1–1.5 µm. **Conidia** solitary, pale brown, finely roughened, guttulate, fusoid, apex appendiculate, base tapering to protruding hilum, 1–1.5 µm diam, somewhat darkened, (21–)22–23(–25) × (5.5–)6–7(–8) µm with a single supramedian transverse septum; when sporulating on PNA, germinating conidia form appressoria that are brown, irregularly lobed, 5–10 µm diam, with a hyaline central infection pore, 1 µm diam.

Culture characteristics: Colonies flat, spreading, with sparse aerial mycelium and smooth, lobate margin, covering dish after 2 wk at 25 °C. On MEA surface and reverse saffron; on PDA and OA surface and reverse pale luteous.

Material examined: **Ukraine**, Rakhiv district, Transcarpathian region, Sidlovyana stow, Petros mountains, on *Luzula sylvatica* (*Juncaceae*), 9 Aug. 2017, A. Akulov, CWU (MYC) AS 6437 = HPC 2197, CBS H-23833, culture CPC 34292 = CBS 145042.

Notes: *Macgarvieomyces* was introduced by Klaubauf *et al.* (2014) for a genus of fungi resembling *Pyricularia* in general morphology, but which was distinct from the latter genus in having fusoid, 1-septate conidia, and occurring on *Juncaceae*. *Macgarvieomyces luzulae* was recently treated by Marín-Felix *et al.* (2019), and this is the second collection from *Luzula sylvatica*.

Based on a megablast search of NCBI's GenBank nucleotide database, the closest hits using the **ITS** sequence had highest similarity to *Macgarvieomyces luzulae* (GenBank MG934442.1; Identities = 548/548 (100 %)), *Macgarvieomyces borealis* (GenBank NR_145384.1; Identities = 485/517 (94 %), 10 gaps (1 %)), and *Macgarvieomyces juncicola* (GenBank KM009165.1; Identities = 462/494 (94 %), 11 gaps (2 %)). Closest hits using the **LSU** sequence are *Macgarvieomyces juncicola* (GenBank KM009153.1; Identities = 854/864 (99 %), 1 gap (0 %)), *Macgarvieomyces borealis* (GenBank NG_058088.1; Identities = 853/863 (99 %), no gaps), and *Deightoniella roumeguerii* (as *Utrechtiana cibiessia*, GenBank JF951176.1; Identities = 877/895 (98 %), no gaps). Closest hits using the **actA** sequence had highest similarity to *Macgarvieomyces luzulae* (GenBank MG934464.1; Identities = 348/350 (99 %), no gaps), *Macgarvieomyces borealis* (GenBank KM485170.1; Identities = 221/251 (88 %), 9 gaps (3 %)), and *Macgarvieomyces juncicola* (GenBank KM485171.1; Identities = 252/318 (79 %), 29 gaps (9 %)).

Microdochium rhopalostylidis Crous & Thangavel, *sp. nov.* MycoBank MB829310. Fig. 27.

Etymology: Name refers to the genus *Rhopalostylis* from which it was isolated.

Mycelium immersed and superficial, consisting of hyaline, smooth, branched, septate, 2–3 µm diam hyphae. **Sporodochia** slimy, hyaline, becoming pale brown with age. **Conidiophores** tightly aggregated, irregularly branched, hyaline, smooth, 0–4-septate, 5–25 × 2.5–3.5 µm. **Conidiogenous cells** smooth, hyaline, ampulliform, terminal and lateral with sympodial proliferation and inconspicuous flat-tipped loci, 4–10 × 3–3.5 µm. **Conidia** solitary, aggregating in mucoid packets, hyaline, smooth-walled, guttulate, fusoid, curved, apex subobtuse, base truncate, 1–3-septate, (13–)16–20(–23) × (2.5–)3(–4) µm.

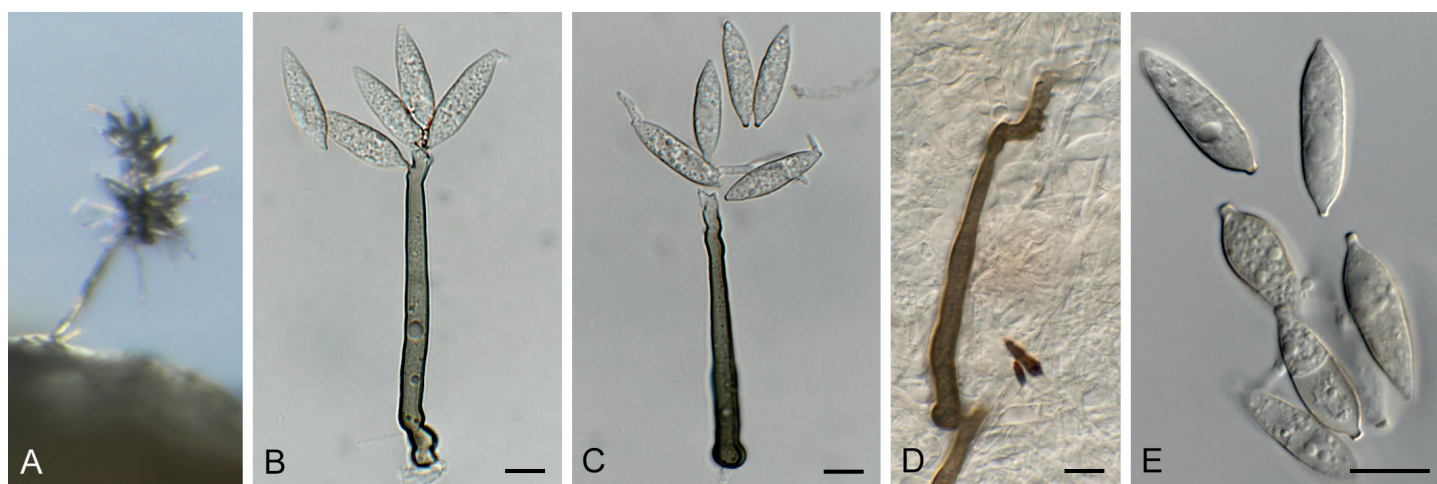


Fig. 26. *Macgarvieomyces luzulae* (CPC 34292). **A.** Conidiophore on PNA. **B–D.** Conidiophores. **E.** conidia. Scale bars = 10 µm.

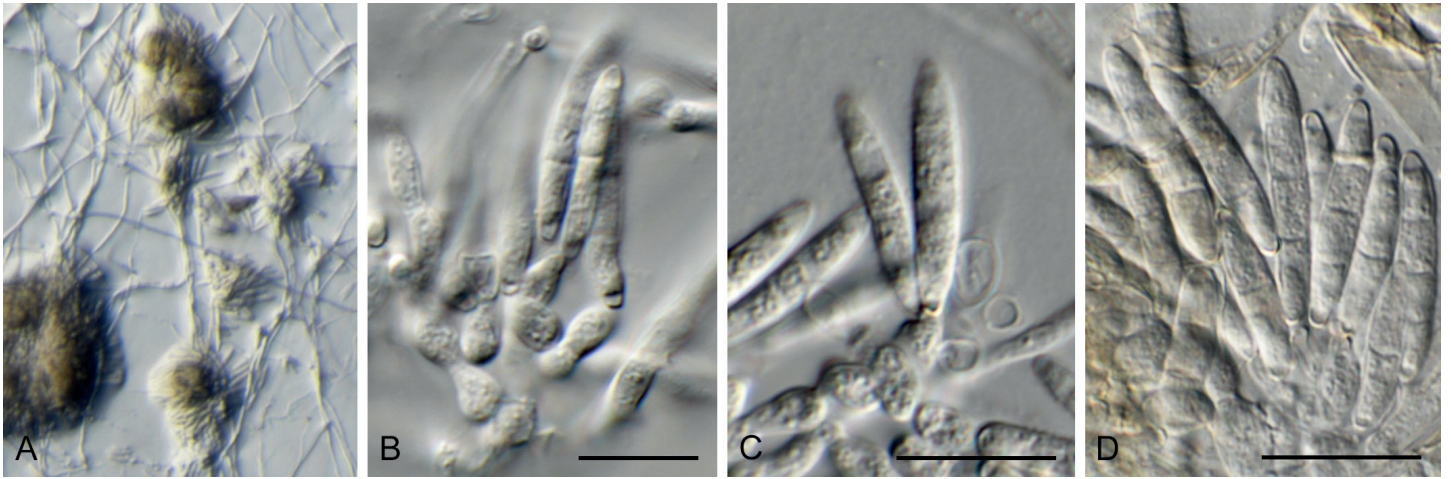


Fig. 27. *Microdochium rhopalostylidis* (CPC 34449). **A.** Sporodochia on SNA. **B–D.** Conidiogenous cells giving rise to conidia. Scale bars = 10 µm.

Culture characteristics: Colonies flat, spreading, with moderate aerial mycelium and smooth, lobate margin, covering dish after 2 wk at 25 °C. On MEA and PDA surface saffron to luteous, reverse sienna; on OA surface umber to saffron.

Typus: **New Zealand**, Auckland, Auckland Botanical Garden, on leaves of *Rhopalostylis sapida* (*Arecaceae*), 2017, *R. Thangavel*, T17_03052B (**holotype** CBS H-23835, culture ex-type CPC 34449 = CBS 145125).

Note: *Microdochium* and allied genera were revised by Hernández-Restrepo *et al.* (2016). Based on a megablast search of NCBI's GenBank nucleotide database, the closest hits using the **ITS** sequence had highest similarity to *Pseudofusarium fusarioideum* (GenBank MH860033.1; Identities = 537/551 (97 %), 7 gaps (1 %)), *Microdochium phragmitis* (GenBank NR_132916.1; Identities = 529/544 (97 %), 7 gaps (1 %)), and *Microdochium lycopodium* (GenBank KP859005.1; Identities = 529/544 (97 %), 8 gaps (1 %)). Closest hits using the **LSU** sequence are *Microdochium phragmitis* (GenBank KP858948.1; Identities = 893/893 (100 %), no gaps), *Microdochium lycopodium* (GenBank KP858929.1; Identities = 847/855 (99 %), no gaps), and *Microdochium fisheri* (GenBank KP858951.1; Identities = 825/844 (98 %), 2 gaps (0 %)). Distant hits using the **actA** sequence had highest similarity to *Penicillifer pulcher* (GenBank KM231107.1; Identities = 406/420 (97 %), no gaps), *Penicillifer bipapillatus* (GenBank KM231105.1; Identities = 404/420 (96 %), no gaps), and *Gliocephalotrichum longibrachium* (GenBank KM231117.1; Identities = 403/419 (96 %), no gaps). Only very distant hits were obtained using the **cmdA** sequence, for example with *Penicillium johnkrugii* (GenBank JN686399.1; Identities = 135/142 (95 %), no gaps), *Penicillium exsudans* (GenBank KX885052.1; Identities = 133/139 (96 %), no gaps), and *Penicillium austrosinicum* (GenBank KX885051.1; Identities = 133/139 (96 %), no gaps). Closest hits using the **rpb2** sequence had highest similarity to *Microdochium phragmitis* (GenBank KP859122.1; Identities = 798/849 (94 %), no gaps), *Microdochium lycopodium* (GenBank KP859102.1; Identities = 789/837 (94 %), no gaps), and *Microdochium fisheri* (GenBank KP859124.1; Identities = 750/841 (89 %), 2 gaps (0 %)). The best hit using the **tub2** sequence had highest similarity to *Microdochium musae* (GenBank MH108044.1; Identities = 115/135 (85 %), 5 gaps (3 %)).

Neocordana malayensis Crous, *sp. nov.* MycoBank MB829313. Fig. 28.

Etymology: Name refers to Malaysia where it was isolated.

Mycelium consisting of pale brown, smooth, branched, septate, 2–3 µm diam hyphae. **Conidiophores** subcylindrical, flexuous, erect, medium brown, smooth, multiseptate, 200–500 × 7–9 µm. **Conidiogenous cells** polyblastic, terminal and intercalary, 10–40 × 6–8 µm, denticulate; denticles up to 1 µm long, 0.5–1 µm wide. **Conidia** oblong to obovoid, (12–)14–18(–20) × (8–)10 µm, 1-septate, thick-walled, brown with truncate hilum, 1 µm diam.

Culture characteristics: Colonies flat, spreading, with moderate aerial mycelium and feathery margin, reaching 65 mm diam after 2 wk at 25 °C. On MEA, PDA and OA surface dirty white with patches of pale olivaceous grey or pale luteous.

Typus: **Malaysia**, on leaves of *Musa* sp. (*Musaceae*), Feb. 2010, *P.W. Crous*, HPC 1595 (**holotype** CBS H-23812, culture ex-type CPC 32837 = CBS 144604).

Notes: *Neocordana* was introduced by Hernández-Restrepo *et al.* (2015) to accommodate several species of hyphomycetes causing a foliar disease on *Canna* and *Musa*. The morphological characteristics of *N. malayensis* overlap with those of *N. musae* and *N. musicola* in conidial dimensions, but are distinct from them in having very long, flexuous conidiophores. Phylogenetically, it also clusters apart from *N. musae* and *N. musicola*.

Based on a megablast search of NCBI's GenBank nucleotide database, the closest hits using the **ITS** sequence had highest similarity to *Neocordana musigena* (GenBank KY979749.1; Identities = 553/575 (96 %), 15 gaps (2 %)), *Neocordana musarum* (GenBank KY173425.1; Identities = 553/575 (96 %), 15 gaps (2 %)), and *Neocordana musae* (GenBank LN713276.1; Identities = 553/575 (96 %), 15 gaps (2 %)). Closest hits using the **LSU** sequence are *Neocordana musicola* (GenBank LN713287.1; Identities = 843/847 (99 %), no gaps), *Neocordana musarum* (GenBank KY173515.1; Identities = 820/824 (99 %), no gaps), and *Neocordana musae* (GenBank LN713290.1; Identities = 873/878 (99 %), 1 gap (0 %)). Closest hits using the **actA** sequence had highest similarity to *Neocordana musigena* (GenBank



Fig. 28. *Neocordana malayensis* (CPC 32837). A. Conidiophores on PNA. B–E. Conidiophores with conidiogenous loci. F. Conidia. Scale bars = 10 μ m.

KY979854.1; Identities = 746/746 (100 %), no gaps), *Neocordana musarum* (GenBank KY173568.1; Identities = 357/358(99%), no gaps), and *Gaeumannomyces tritici* (GenBank XM_009225830.1; Identities = 386/414 (93 %), no gaps). Closest hits using the **tub2** sequence had highest similarity to *Neocordana musigena* (GenBank KY979915.1; Identities = 553/559 (99 %), 1 gap (0 %)), *Hyphoxylon calileguense* (GenBank KU604578.1; Identities = 714/797 (90 %), 1 gap (0 %)), and *Chaetomium globosum* (GenBank XM_001226965.1; Identities = 654/735 (89 %), 2 gaps (0 %)).

Neocucurbitaria prunicola Crous & Akulov, *sp. nov.* MycoBank MB829314. Fig. 29.

Etymology: Name refers to the host genus *Prunus* from which it was isolated.

Conidiomata pycnidial, solitary to aggregated, globose, medium brown, 100–200 μ m diam, with central ostiole, 20–40 μ m diam, surrounded with erect, unbranched, brown, smooth, 1–2-septate, thick-walled setae, 20–40(–70) \times 3–4 μ m, with obtuse ends; conidiomatal wall of 3–4 layers of flattened, brown *textura angularis*. **Conidiophores** lining the inner cavity, hyaline, smooth, subcylindrical, branched, 1–3-septate, 10–20 \times 2–3 μ m. **Conidiogenous cells** hyaline, smooth, subcylindrical to doliiform, phialidic, terminal and intercalary, 3–10 \times 2–3 μ m. **Conidia** hyaline, smooth, aseptate, guttulate, subcylindrical with obtuse ends, (2–)3–3.5(–4) \times 1.5(–2) μ m.

Culture characteristics: Colonies flat, spreading, with moderate aerial mycelium and smooth, lobate margin, reaching 40 mm diam after 2 wk at 25 $^{\circ}$ C. On MEA, PDA and OA surface and reverse grey olivaceous.

Typus: Ukraine, Ternopil region, Dniester Canyon N.P., forest, fallen twigs of *Prunus padus* (= *Padus avium*) (*Rosaceae*), 6

Oct. 2016, A. Akulov, CWU AS 6209 = HPC 2045 (**holotype** CBS H-23824, culture ex-type CPC 33709 = CBS 145033).

Notes: *Neocucurbitaria* was treated by Jaklitsch *et al.* (2018), and shown to have phoma-like asexual morphs. *Neocucurbitaria prunicola* is phylogenetically distinct from other species presently known in the genus.

Based on a megablast search of NCBI's GenBank nucleotide database, the closest hits using the **ITS** sequence had highest similarity to *Neocucurbitaria rhamnii* (GenBank MF795778.1; Identities = 446/483 (92 %), 5 gaps (1 %)), *Neocucurbitaria rhamnoides* (GenBank MF795784.1; Identities = 447/486 (92 %), 7 gaps (1 %)), and *Astragalicola vasilyevae* (GenBank NR_157504.1; Identities = 453/494 (92 %), 13 gaps (2 %)). Closest hits using the **LSU** sequence are *Neocucurbitaria unguis-hominis* (GenBank GQ387621.1; Identities = 850/854 (99%), no gaps), *Neocucurbitaria keratinophila* (GenBank MH874704.1; Identities = 849/854 (99%), no gaps), and *Neocucurbitaria quercina* (GenBank GQ387620.1; Identities = 849/854 (99 %), no gaps). Closest hits using the **rpb2** sequence had highest similarity to *Neocucurbitaria unguis-hominis* (as *Pyrenochaeta unguis-hominis*, GenBank LT717682.1; Identities = 760/866 (88 %), 2 gaps (0 %)), *Cucurbitaria berberidis* (GenBank LT854936.1; Identities = 768/876 (88 %), 7 gaps (0 %)), and *Neocucurbitaria cava* (as *Pyrenochaeta cava*, GenBank LT717681.1; Identities = 744/856 (87 %), 2 gaps (0 %)). Distant hits using the **tub2** sequence had highest similarity to *Neocucurbitaria juglandicola* (GenBank MF795901.1; Identities = 452/495 (91 %), 2 gaps (0 %)), *Neocucurbitaria populi* (GenBank MF795902.1; Identities = 451/495 (91 %), 2 gaps (0 %)), *Neocucurbitaria rhamnoides* (GenBank MF795908.1; Identities = 448/493 (91 %), 7 gaps (1 %)), *Leptosphaeria biglobosa* (as *Leptosphaeria maculans*, GenBank FO906902.1; Identities = 887/999 (89 %), 11 gaps (1 %)), *Leptosphaeria biglobosa* (GenBank FO905876.1; Identities = 877/987 (89 %), 10 gaps (1 %)), and *Helminthosporium solani* (GenBank AF461130.1; Identities = 702/803 (87 %), 10 gaps (1 %)).

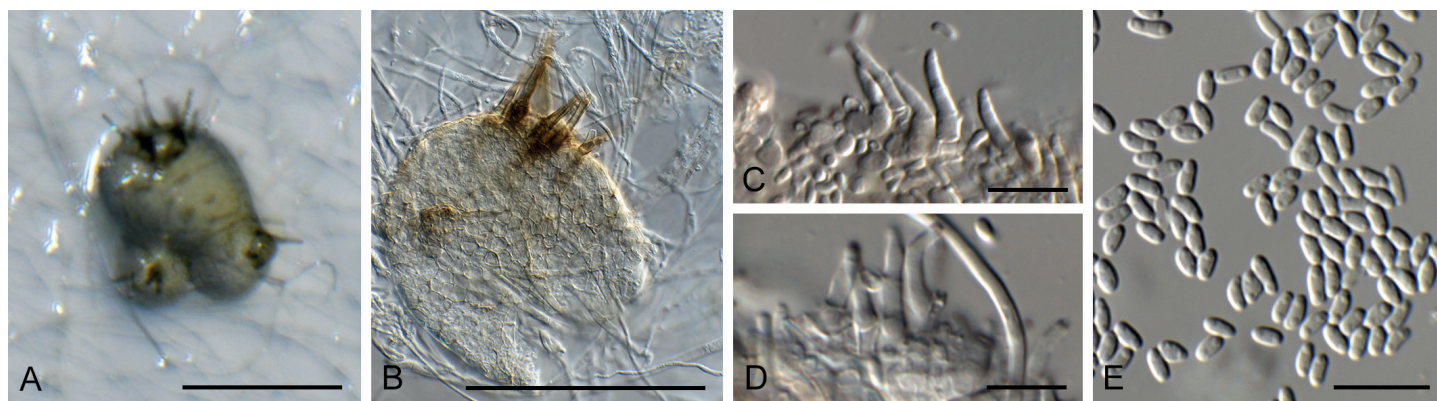


Fig. 29. *Neocucurbitaria prunicola* (CPC 33709). **A, B.** Conidiomata on SNA. **C, D.** Conidiogenous cells. **E.** Conidia. Scale bars: A, B = 200 μ m, C–E = 10 μ m.

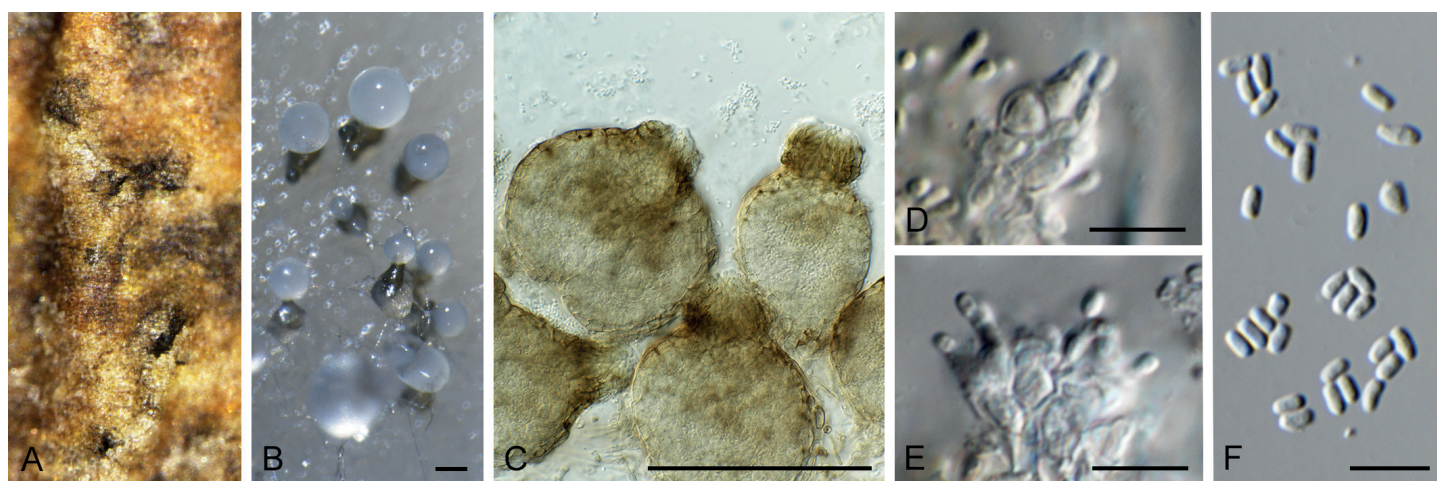


Fig. 30. *Neocucurbitaria salicis-albae* (CPC 33162). **A.** Immersed conidiomata on host tissue. **B, C.** Conidiomata in culture. **D, E.** Conidiogenous cells. **F.** Conidia. Scale bars: B, C = 120 μ m, C–F = 10 μ m.

Neocucurbitaria salicis-albae Crous & R.K. Schumach., *sp. nov.*
Mycobank MB829315. Fig. 30.

Etymology: Name refers to *Salix alba* from which it was isolated.

Conidiomata pycnidial, solitary or aggregated, brown, globose, 70–120 μ m diam, with prominent papillate darker brown central ostiole 1(–3), 20–30 μ m diam; wall of 3–6 layers of pale brown *textura angularis*. **Conidiophores** lining the inner cavity, hyaline, smooth, reduced to conidiogenous cells, ampulliform, phialidic, 5–7 \times 2.5–4 μ m. **Conidia** solitary, aseptate, hyaline, smooth, prominently guttulate, thin-walled, subcylindrical to fusoid-ellipsoid, (2.5–)3–3.5(–4) \times 2 μ m.

Culture characteristics: Colonies erumpent, spreading, with moderate aerial mycelium and smooth, lobate margin, reaching 17–30 mm diam after 2 wk at 25 $^{\circ}$ C. On MEA, PDA and OA surface and reverse olivaceous grey.

Typus: **Germany**, near Berlin, on *Salix alba* twig, 21 Jan. 2017, R.K. Schumacher, HPC 1963 (**holotype** CBS H-23818, culture ex-type CPC 33162 = CBS 144611).

Notes: *Pyrenochaeta* (= *Cucurbitaria*) was resurrected as discrete genus by De Gruyter *et al.* (2010). *Neocucurbitaria* was established by Wanasinghe *et al.* (2017) for a sister genus with pyrenochaeta-like asexual morphs, and cucurbitaria-like

sexual morphs. *Neocucurbitaria* and several pyrenochaeta-like genera and their respective families were clarified further by Valenzuela-Lopez *et al.* (2018). *Neocucurbitaria salicis-albae* is a new species from *Salix*.

Based on a megablast search of NCBI's GenBank nucleotide database, the closest hits using the **ITS** sequence had highest similarity to *Neocucurbitaria quercina* (as *Pyrenochaeta quercina*, GenBank LT623220.1; Identities = 519/533 (97 %), no gaps), *Neocucurbitaria acanthocladae* (GenBank MF795766.1; Identities = 515/535 (96 %), 2 gaps (0 %)), and *Neocucurbitaria unguis-hominis* (as *Pyrenochaeta unguis-hominis*, GenBank KP794081.1; Identities = 472/490 (96 %), 7 gaps (1 %)). The ITS sequence is identical to "*Cucurbitariaceae* sp. MUT 4403" (GenBank KC339238.1; Identities = 491/491 (100 %)), isolated from *Posidonia oceanica* in the Punta Manara-Riva Trigoso Bay, Italy. Closest hits using the **LSU** sequence are *Neocucurbitaria keratinophila* (GenBank MH874704.1; Identities = 859/861 (99 %), no gaps), *Neocucurbitaria quercina* (GenBank GQ387620.1; Identities = 859/861 (99 %), no gaps), and *Neocucurbitaria aquatica* (GenBank EU754177.1; Identities = 859/861 (99 %), no gaps). Closest hits using the **rpb2** sequence had highest similarity to *Neocucurbitaria quercina* (as *Pyrenochaeta quercina*, GenBank LT623277.1; Identities = 919/956 (96 %), no gaps), *Neocucurbitaria unguis-hominis* (as *Pyrenochaeta unguis-hominis*, GenBank LT623279.1; Identities = 872/952 (92 %), no gaps), and *Neocucurbitaria aetnensis* (GenBank MF795811.1; Identities = 832/900 (92 %), no gaps). Closest hits using the

tub2 sequence had highest similarity to *Neocucurbitaria acanthocladae* (GenBank MF795894.1; Identities = 440/457 (96 %), 1 gap (0 %)), *Neocucurbitaria cinerea* (GenBank MF795899.1; Identities = 438/457 (96 %), 1 gap (0 %)), *Neocucurbitaria ribicola* (GenBank MF795912.1; Identities = 432/457 (95 %), 2 gaps (0 %)), *Leptosphaeria biglobosa* (GenBank FO905876.1; Identities = 932/1036 (90 %), 6 gaps (0 %)), *Westerdykella cylindrica* (GenBank JX235707.1; Identities = 689/777 (89 %), 10 gaps (1 %)), and *Helminthosporium solani* (GenBank AF461130.1; Identities = 745/861 (87 %), 12 gaps (1 %)).

Neodevriesia metrosideri Crous, *Persoonia* **41**: 303. 2018. Fig. 31.

Etymology: Name refers to the host genus *Metrosideros* from which it was isolated.

Mycelium consisting of branched, septate, brown, smooth, 3(–5) μm diam hyphae. **Conidiophores** erect, solitary, arising directly from superficial hyphae, subcylindrical, straight to somewhat curved, smooth, brown, 0–2-septate, 10–30 \times 2–3 μm . **Conidiogenous cells** terminal, integrated, subcylindrical, brown, smooth, 5–10 \times 2–3 μm ; hila truncate, 2–3 μm diam, not darkened nor thickened. **Conidia** occurring in branched chains (–15), medium brown, smooth, subcylindrical to fusoid-ellipsoid, 0–1(–2)-septate, (10–)13–15(–20) \times 2–3(–4) μm ; hila unthickened, not darkened, 1.5–2 μm diam.

Culture characteristics: Colonies erumpent, with moderate aerial mycelium, and smooth, lobate margins, reaching 20 mm diam after 2 wk. On MEA, PDA and OA surface and reverse iron-grey.

Material examined: **New Zealand**, Auckland, Bucklands Beach, 22 Wells Road, on leaves of *Metrosideros excelsa* (Myrtaceae), 2015, R. Thangavel, T16_03926G, CBS H-23810, culture CBS 144638 = CPC 32786.

Notes: *Neodevriesia metrosideri* was recently described from *Metrosideros* sp. on the Great Barrier Island in New Zealand (Crous *et al.* 2018b), and this is the second collection of this taxon from this country.

Based on a megablast search of NCBI's GenBank nucleotide database, the closest hits using the **ITS** sequence had highest similarity to *Neodevriesia lagerstroemiae* (GenBank GU214634.1; Identities = 518/533 (97 %), 4 gaps (0 %)), *Neodevriesia fraseriae* (as *Devriesia fraseriae*, GenBank NR_144961.1; Identities = 508/535 (95 %), 9 gaps (1 %)), and *Devriesia sardiniae* (GenBank KP791766.1; Identities = 504/531 (95 %), 4 gaps (0 %)). Closest hits using the **LSU** sequence are *Neodevriesia lagerstroemiae* (GenBank KF902149.1; Identities = 732/741 (99 %), no gaps), *Neodevriesia knoxdavesii* (as *Teratosphaeria knoxdavesii*, GenBank EU707865.1; Identities = 801/814 (98 %), 2 gaps (0 %)), and *Neodevriesia cladophorae* (as *Devriesia* sp. MW-2016a, GenBank KU578114.1; Identities = 798/813 (98 %), no gaps). No **actA** sequences of *Neodevriesia* or *Devriesia* are currently available for comparison on GenBank. No significant hits were obtained when the **tub2** sequence was used in blastn and megablast searches.

Neodothidotthia Crous, *gen. nov.* MycoBank MB829317.

Etymology: Name reflects its morphological similarity to the genus *Dothidotthia*.

Sporodochia dark brown, punctiform. **Stromata** immersed to superficial, brown. **Conidiophores** brown, finely roughened, subcylindrical, septate. **Conidiogenous cells** brown, subcylindrical, finely roughened, proliferating percurrently at apex. **Conidia** fusoid to ellipsoid, medium brown, transversely septate, apex obtuse, base truncate.

Type species: *Neodothidotthia negundinicola* Crous & Akulov.

Neodothidotthia negundinicola Crous & Akulov, *sp. nov.* MycoBank MB829318. Fig. 32.

Etymology: Name refers to *Acer negundo* from which it was isolated.

Sporodochia dark brown, punctiform, 100–300 μm diam. **Stromata** immersed to superficial, brown, 80–150 μm diam. **Conidiophores** brown, finely roughened, subcylindrical, 4–6-septate, 60–150 \times 7–12 μm . **Conidiogenous cells** brown, subcylindrical, finely roughened, 8–15 \times 5–7 μm , proliferating

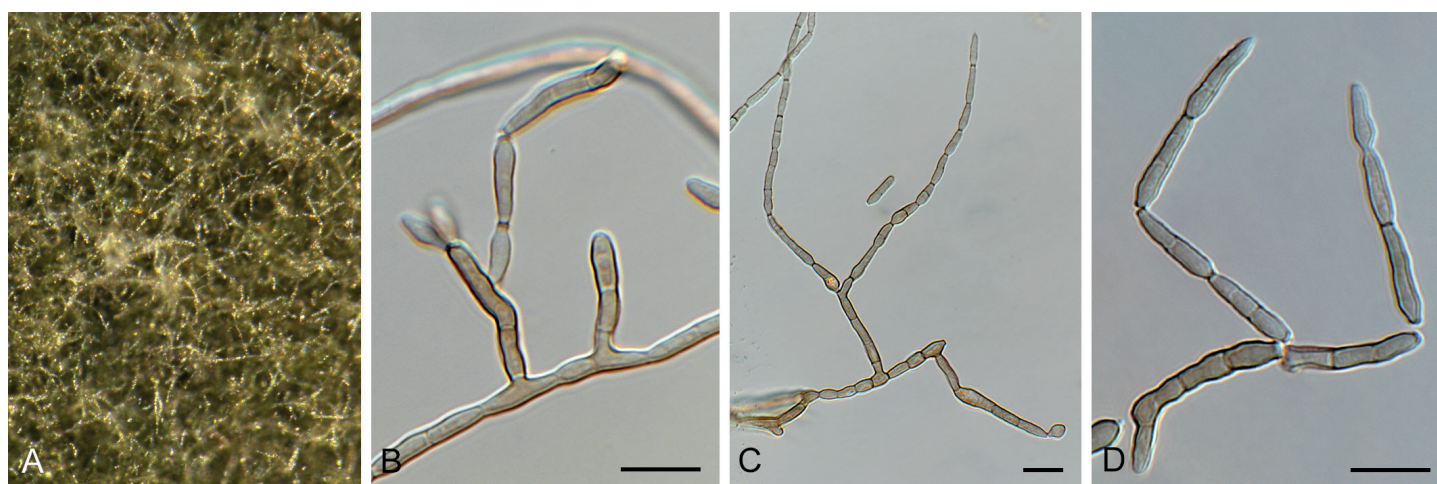


Fig. 31. *Neodevriesia metrosideri* (CPC 32786). **A.** Colony on PDA. **B–D.** Conidiophores giving rise to branched conidial chains. Scale bars = 10 μm .

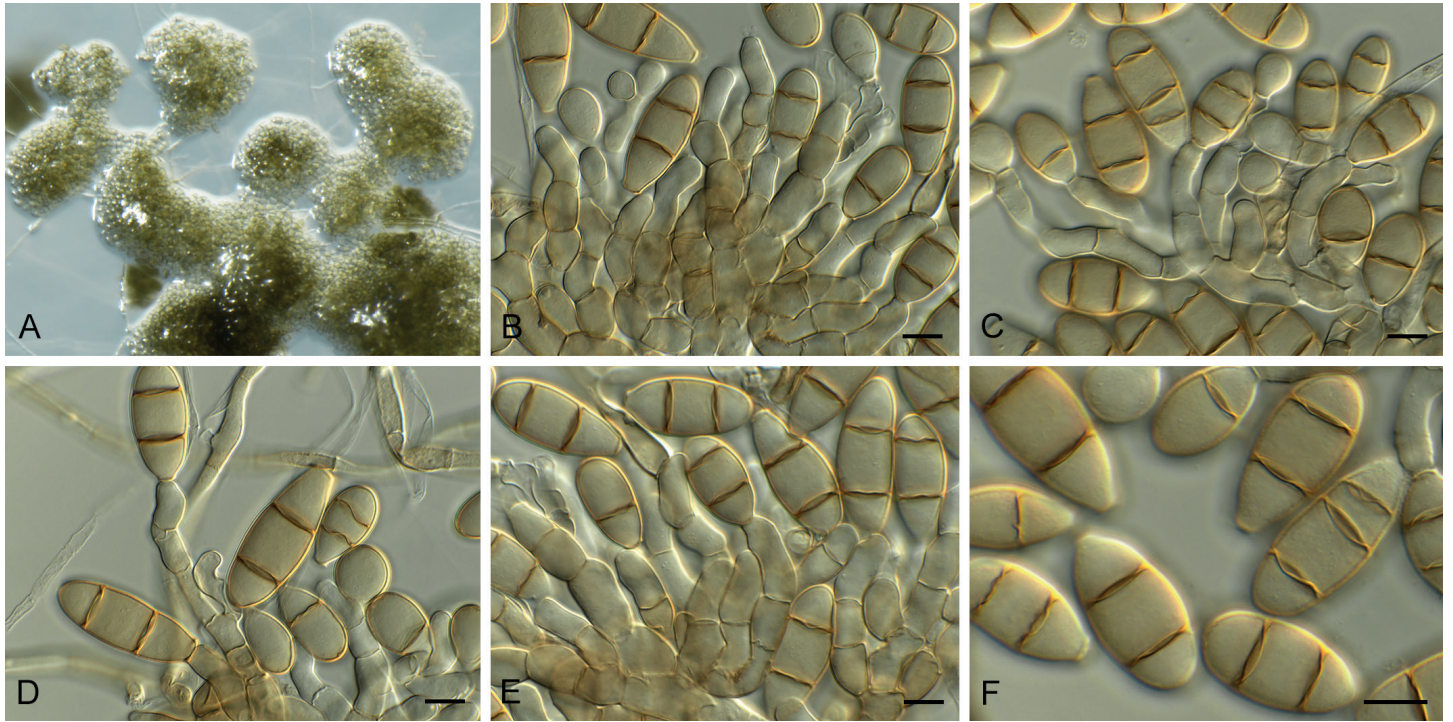


Fig. 32. *Neodothidotthia negundinicola* (CPC 34071). **A.** Sporodochia on SNA. **B–E.** Conidiogenous cells giving rise to conidia. **F.** Conidia. Scale bars = 10 μ m.

percurrently at apex. *Conidia* fusoid to ellipsoid, medium brown, transversely (1–)2-septate, apex obtuse, base truncate, 4–5 μ m diam, (25–)30–35(–37) \times (12–)13–15(–16) μ m.

Culture characteristics: Colonies flat, spreading, with moderate aerial mycelium and smooth to feathery, lobate margin, covering dish after 2 wk at 25 $^{\circ}$ C. On MEA, PDA and OA surface and reverse olivaceous grey.

Typus: **Ukraine**, Kharkiv region, Zolochiv district, on the dead branches of *Acer negundo* (*Sapindaceae*) still attached to the tree, 28 May 2017, A. Akulov & R.K. Schumacher, CWU AS 6293 = HPC 2127 = RKS 116 (**holotype** CBS H-23832, culture ex-type CPC 34071 = CBS 145039).

Neodothidotthia negundinis (Berk. & M.A. Curtis) Crous, **comb. nov.** MycoBank MB829319.

Basionym: *Coryneum negundinis* Berk. & M.A. Curtis, *Grevillea* **2**(22): 153. 1874.

Synonym: *Thyrostroma negundinis* (Berk. & M.A. Curtis) A.W. Ramaley, *Mycotaxon* **94**: 131. 2006 (2005).

Illustration: See Phillips *et al.* (2008).

Material examined: **USA**, Colorado, Durango, 7 Animas Place, dead twigs of *Euonymus alatus*, 29 Jun. 2004, A.W. Ramaley 0411, BPI 871820, culture CPC 12930 = CBS 119688; Colorado, Durango, between Animas Place and Animas River, dead twigs of *Acer negundo*, 8 Jul. 2004, A.W. Ramaley 0414, BPI 871819, asexual morph culture CPC 12933 = CBS 119691, sexual morph CPC 12932 = CBS 119690; Colorado, La Plata Co, ca. 1.75 mile up Carbon Junction Trail, dead twigs of *Fendlera rupicola*, 11 May 2004, A.W. Ramaley 0403, BPI 871821, culture CPC 12928 = CBS 119686.

Notes: *Thyrostroma negundinis* (as *Stigmina negundinis*, on twigs of *Acer negundo*, North America) has conidia that are

ellipsoid, 2-septate, 25–38 \times 12–18 μ m, base 4–5 μ m diam (Ellis 1971), thus closely fitting with the present collection, although they are phylogenetically distinct. Ramaley (2005) found conidia on the type specimen of *Amphisphaeria aspera* to be much smaller, namely (10–)12–15 \times 6–7 μ m, suggesting that the latter collection represents a different species in this complex.

Ramaley (2005) and Phillips *et al.* (2008) showed that *Dothidotthia* (based on *D. symphoricarpi* from the USA; CBS 119687) has a *Thyrostroma* (based on *T. compactum*, reference strain CBS 335.37) asexual morph, which they ascribed to *Thyrostroma negundinis*. The link between the two genera has however, not been confirmed in culture. It has thus been proposed to continue using both names until this question has been resolved (Wijayawardene *et al.* 2014, Rossman *et al.* 2015). As we show here, *Thyrostroma* is closely allied, but not congeneric with *Dothidotthia*, thus both generic names should be retained. Furthermore, the European collection of “*Thyrostroma negundinis*” is allied to *D. symphoricarpi*, but is phylogenetically distinct, and therefore described here as a new genus, *Neodothidotthia*.

Based on a megablast search of NCBI’s GenBank nucleotide database, the closest hits using the **ITS** sequence had highest similarity to *Thyrostroma cornicola* (GenBank NR_154514.1; Identities = 517/540 (96 %), 6 gaps (1 %)), *Thyrostroma compactum* (GenBank MH859911.1; Identities = 516/540 (96 %), 6 gaps (1 %)), and *Phaeomycoentrospora cantuariensis* (GenBank MH866055.1; Identities = 515/539 (96 %), 6 gaps (1 %)). Closest hits using the **LSU** sequence are *Phaeomycoentrospora cantuariensis* (GenBank GU253716.1; Identities = 866/877 (99 %), 2 gaps (0 %)), *Pleiochaeta setosa* (GenBank EU167563.1; Identities = 847/859 (99 %), 3 gaps (0 %)), and *Pleiochaeta ghindensis* (GenBank EU167561.1; Identities = 845/858 (98 %), 2 gaps (0 %)). Closest hits using the **tef1** sequence had highest similarity to *Phaeomycoentrospora cantuariensis* (GenBank GU384382.1; Identities = 265/308 (86 %), 9 gaps (2 %)), *Thyrostroma cornicola*

(GenBank KX228372.1; Identities = 312/372 (84 %), 12 gaps (3 %)), and *Pyrenophora biseptata* (as *Drechslera biseptata*, GenBank JN712588.1; Identities = 321/402 (80 %), 30 gaps (7 %)).

Neohelicomyces deschampsiae Crous & R.K. Schumach., *sp. nov.* MycoBank MB829320. Fig. 33.

Etymology: Name refers to the host genus *Deschampsia* from which it was isolated.

Conidiophores erect, flexuous, mostly unbranched, subcylindrical with slight apical taper, 10–15-septate, 150–220 × 3–4 µm, brown, smooth-walled, tapering toward subobtuse apex. **Conidiogenous cells** intercalary, consisting of short, lateral, cylindrical pegs, pale brown, monoblastic, rarely polyblastic, 2–5 × 1.5–2.5 µm. **Conidia** solitary, coiled 2–3 times, multiseptate, coils 19–22 µm diam, cells 2–2.5 µm diam.

Culture characteristics: Colonies erumpent, spreading, with folded surface and feathery lobate margin, reaching 20 mm diam after 2 wk at 25 °C. On MEA surface umber, reverse sienna; on PDA surface umber, reverse ochreous; on OA surface umber.

Typus: **Germany**, near Berlin, culm base of dead leaf sheath of *Deschampsia cespitosa* (*Poaceae*), 3 May 2017, R.K. Schumacher, HPC 2109 = RKS 101 (**holotype** CBS H-23590, culture ex-type CPC 33686 = CBS 145029).

Notes: *Neohelicomyces* differs from *Tubeufia* and allied genera, especially from *Helicomyces*, in having elongate, erect, conspicuous conidiophores, and differs from *Helicosporium* based on conidial morphology (Tsui *et al.* 2006). Based on the species known from their DNA, *N. deschampsiae* appears to represent a new species, being phylogenetically distinct from *T. helicomyces* and *T. paludosa*, which have also been reported from this host (Ellis & Ellis 1997).

Based on a megablast search of NCBI's GenBank nucleotide database, the closest hits using the **ITS** sequence had highest similarity to *Tubeufia helicomyces* (GenBank MH857031.1; Identities = 556/591 (94 %), 18 gaps (3 %)), *Helicosporium lumbricoides* (GenBank MH856861.1; Identities = 554/590 (94 %), 16 gaps (2 %)), *Helicosporium pallidum* (GenBank AY916462.1; Identities = 550/586 (94 %), 16 gaps (2 %)), and *Neohelicomyces*

aquaticus (as *Tubeufiaceae* sp. ZL-2017b, GenBank KY320528.1; Identities = 422/452 (93 %), 20 gaps (4 %)). Closest hits using the **LSU** sequence are *Neohelicomyces aquaticus* (as *Tubeufiaceae* sp. ZL-2017b, GenBank KY320545.1; Identities = 849/849 (100 %), no gaps), *Neohelicomyces hyalosporus* (as *Neohelicomyces* sp. YZL-2018a, GenBank MH558870.1; Identities = 841/843 (99 %), no gaps), *Neohelicomyces submersus* (as *Tubeufiaceae* sp. ZL-2017c, GenBank KY320547.1; Identities = 827/830 (99 %), no gaps), and *Tubeufia helicomyces* (GenBank MH868562.1; Identities = 854/860 (99 %), no gaps).

Neomedicopsis Crous & Akulov, *gen. nov.* MycoBank MB829321.

Etymology: Name refers to the genus *Medicopsis*, which is phylogenetically allied to it.

Conidiomata pycnidial, globose, erumpent with central ostiole; wall of 6–12 layers of brown *textura angularis*. **Conidiophores** reduced to conidiogenous cells, hyaline, smooth, ampulliform with long cylindrical neck, proliferating percurrently. **Conidia** solitary, globose to subglobose, initially pale brown, becoming dark brown, thick-walled, guttulate, granular, apex obtuse, base truncate.

Type species: *Neomedicopsis prunicola* Crous & Akulov.

Neomedicopsis prunicola Crous & Akulov, *sp. nov.* MycoBank MB829322. Fig. 34.

Etymology: Name refers to the host genus *Prunus* from which it was isolated.

Conidiomata pycnidial, globose, 200–300 µm diam, erumpent with central ostiole; wall of 6–12 layers of brown *textura angularis*. **Conidiophores** reduced to conidiogenous cells, hyaline, smooth, ampulliform with long cylindrical neck, 10–30 × 3–6 µm, proliferating percurrently. **Conidia** solitary, globose to subglobose, initially pale brown, becoming dark brown, thick-walled, guttulate, granular, apex obtuse, base truncate, 3–4 µm diam, (12–)17–20(–22) × (12–)14–16(–17) µm.

Culture characteristics: Colonies flat, spreading, with moderate aerial mycelium and smooth, lobate margin, reaching 25 mm



Fig. 33. *Neohelicomyces deschampsiae* (CPC 33686). **A.** Conidiophores on SNA. **B, C.** Conidiophores giving rise to conidia. **D.** Conidia. Scale bars: A = 20 µm, B–D = 10 µm.



Fig. 34. *Neomedicopsis prunicola* (CPC 33711). **A.** Conidiomata on OA. **B, C.** Conidiogenous cells. **D, E.** Conidia. Scale bars: A = 300 μ m, B–E = 10 μ m.

diam after 2 wk at 25 °C. On MEA surface pale olivaceous grey, reverse olivaceous grey; on PDA surface and reverse olivaceous grey; on OA surface olivaceous grey.

Typus: **Ukraine**, Ternopil region, Dniester Canyon N.P., forest, fallen twigs of *Prunus padus* (= *Padus avium*) (*Rosaceae*), 6 Oct. 2016, A. Akulov, HPC 2045 = CWU AS 6209 (**holotype** CBS H-23825, culture ex-type CPC 33711 = CBS 145031).

Notes: de Gruyter *et al.* (2013) introduced the genus *Medicopsis* to accommodate *P. romeroi*, a pathogen associated with mycetoma in humans (Ahmed *et al.* 2014). *Medicopsis* is phoma-like in morphology, and *Neomedicopsis* is distinct in having globose, dark brown, thick-walled conidia that arise from long cylindrical conidiogenous cells that proliferate percurrently. *Neomedicopsis* is somewhat reminiscent of *Lasmeniella*, except that it lacks multilocular conidiomata.

Based on a megablast search of NCBI's GenBank nucleotide database, the closest hits using the **ITS** sequence had highest similarity to *Medicopsis romeroi* (GenBank JX088727.1; Identities = 506/557 (91 %), 13 gaps (2 %)), *Pleomassaria acericola* (GenBank MH863515.1; Identities = 490/555 (88 %), 22 gaps (3 %)), and *Neohendersonia kickxii* (GenBank KX820257.1; Identities = 483/555 (87 %), 21 gaps (3 %)). Closest hits using the **LSU** sequence are *Medicopsis romeroi* (GenBank MH869528.1; Identities = 837/861 (97 %), 1 gap (0 %)), *Lentithecium aquaticum* (GenBank MH874800.1; Identities = 837/867 (97 %), 12 gaps (1 %)), and *Murilenthicium clematidis* (GenBank KM408758.1; Identities = 834/864 (97 %), 7 gaps (0 %)). Closest hits using the **rpb2** sequence had highest similarity to *Medicopsis romeroi* (GenBank LT797035.1; Identities = 584/706 (83 %), 4 gaps (0 %)), *Crassiparies quadrisporus* (GenBank LC271252.1; Identities = 578/718 (81 %), 4 gaps (0 %)), and *Farasanispora avicenniae* (GenBank MG973031.1; Identities = 576/726 (79 %), 12 gaps (1 %)).

Phaeoappendicosporaceae Crous & M.J. Wingf., **fam. nov.** MycoBank MB829458.

Pseudostroma immersed, becoming erumpent; ectostroma pale brown to grey, containing periphyses; ostioles cylindrical. *Perithecia* globose to lenticular, dark brown, wall of *textura angularis*. *Paraphyses* hyaline, septate, unbranched, hypha-like. *Asci* ellipsoid to fusoid, 8-spored, without a refractive

canal at apex. *Ascospores* ellipsoid-fusoid, brown, 1-euseptate, with gelatinous appendage at each truncate end. *Conidiomata* pycnidial, multilocular, forming a long neck. *Paraphyses* hyaline, cylindrical, septate, unbranched, hypha-like. *Conidiophores* subcylindrical, hyaline to pale brown, septate, unbranched. *Conidiogenous cells* cylindrical, hyaline to pale brown, proliferating percurrently at apex. *Conidia* ellipsoid to oblong, straight to slightly curved, thick-walled, transversely euseptate with oblique septa.

Type genus: *Phaeoappendicospora* Senan., Q.R. Li & K.D. Hyde

Neophaeoappendicospora Crous & M.J. Wingf., **gen. nov.** MycoBank MB829323.

Etymology: Name reflects its morphological similarity to *Phaeoappendicospora*.

Pseudostroma immersed, becoming erumpent, causing fissures; ectostroma pale brown to grey, containing tightly packed periphyses; ostioles cylindrical, inconspicuous with brown walls, not projecting; entostroma confined to a network of pale brown hyphae, enclosing a circular group of tightly packed perithecial ascomata with convergent ostioles. *Perithecia* globose to lenticular, dark brown, wall of *textura angularis*. *Paraphyses* intermingled among asci, hyaline, septate, unbranched, constricted at septa, hypha-like. *Asci* ellipsoid to fusoid, with 8 biseriolate ascospores, without a refractive canal at apex (Melzer's reagent). *Ascospores* ellipsoid-fusoid, brown, 1-euseptate, thick-walled, with gelatinous appendage at each truncate end, smooth, becoming verruculose with age, granular to guttulate, with truncate apices and central apiculus. *Conidiomata* immersed in bark, pycnidial, multilocular, forming a long neck. *Paraphyses* hyaline, cylindrical, septate, unbranched, hypha-like. *Conidiophores* subcylindrical, hyaline to pale brown, septate, unbranched. *Conidiogenous cells* cylindrical, hyaline to pale brown, proliferating percurrently with numerous percurrent proliferations at apex. *Conidia* ellipsoid to oblong, straight to slightly curved, thick-walled, guttulate, transversely euseptate with oblique septa.

Type species: *Neophaeoappendicospora leucaenae* Crous & M.J. Wingf.



Fig. 35. *Neophaeoappendicospora leucaenae* (CPC 27240). **A.** Conidiomata on MEA. **B, C.** Conidiogenous cells giving rise to conidia. **D.** Conidia. **E.** Ascomata on host tissue. **F.** Pseudoparaphyses. **G, H.** Asci. **I.** Ascospores. Scale bars = 10 µm.

Neophaeoappendicospora leucaenae Crous & M.J. Wingf., *sp. nov.* MycoBank MB829324. Fig. 35.

Etymology: Name refers to the host genus *Leucaena* from which it was isolated.

Pseudostroma immersed in bark, up to 2 mm diam, becoming erumpent, causing fissures; ectostroma pale brown to grey, containing tightly packed periphyses; ostioles cylindrical, inconspicuous with brown walls, not projecting; entostroma confined to a network of pale brown hyphae, enclosing a circular group of up to 12 tightly packed perithecial ascomata with convergent ostioles. *Perithecia* globose to lenticular, dark brown, wall of *textura angularis*. *Paraphyses* intermingled among asci, hyaline, septate, unbranched, constricted at septa, hypha-like, 5–6 µm diam. *Asci* ellipsoid to fusoid, with 8 biseriate ascospores, without a refractive canal at apex (Melzer's reagent), 130–180 × 17–25 µm. *Ascospores* ellipsoid-fusoid, brown, 1-euseptate, thick-walled, with gelatinous appendage at each truncate end, smooth, becoming verruculose with age, granular to guttulate, (34–)36–42(–47) × (9–)10(–11) µm; at times slightly swollen at septum (wall appearing thickened), and truncate apices with central apiculus. *Conidiomata* immersed in bark, pycnidial, up to 800 µm diam, multilocular, forming a long neck on host, up to 1 mm tall. *Paraphyses* hyaline, cylindrical, septate, unbranched, hypha-like, 3–4 µm diam. *Conidiophores* subcylindrical, hyaline to pale brown, 0–2-septate, unbranched, 15–50 × 4–6 µm. *Conidiogenous cells* cylindrical, hyaline to pale brown, proliferating percurrently with numerous percurrent proliferations at apex, 15–30 × 4–6 µm. *Conidia* ellipsoid to oblong, straight to slightly curved, thick-

walled, guttulate, 3-transversely euseptate with 1–3 oblique septa, apex obtuse, base truncate, 3–4 µm diam, (24–)26–29(–34) × (11–)12(–13) µm.

Culture characteristics: Colonies erumpent, with sparse aerial mycelium, slow-growing, with lobate margins. On MEA surface umber with patches of dirty white, reverse chestnut. On PDA surface umber, reverse umber with patches of diffuse sienna pigment. On OA surface isabelline.

Typus: France, La Réunion, stems of *Leucaena leucocephala* (*Fabaceae*), 13 Mar. 2014, M.J. Wingfield, HPC 309 (**holotype** CBS H-23794, culture ex-type CPC 27240).

Notes: *Neophaeoappendicospora* is morphologically similar to *Phaeoappendicospora*, which was established as monotypic genus by Senanayake *et al.* (2017) for a fungus occurring on dead twigs of *Quercus* in Thailand. *Neophaeoappendicospora leucaenae* is distinct from *P. thailandensis* (ascospores 26–34.5 × 11–13 µm) by its larger ascospores, and the fact that *Neophaeoappendicospora* readily forms an asexual morph in culture, which is absent in *Phaeoappendicospora*. *Phaeoappendicospora* and *Neophaeoappendicospora* represent genera in a new family, introduced here as *Phaeoappendicosporaceae*.

Based on a megablast search of NCBI's GenBank nucleotide database, the closest hits using the **ITS** sequence had highest similarity to *Diaporthe australafricana* (GenBank KR534731.1; Identities = 395/458 (86 %), 22 gaps (4 %)), *Diaporthe phaseolorum* (GenBank LC171670.1; Identities = 505/615 (82 %), 55 gaps (8 %)), and *Diaporthe helianthi* (GenBank MF033502.1;

Identities = 505/615 (82 %), 55 gaps (8 %)). Closest hits using the **LSU** sequence are *Pachytrype rimosa* (GenBank FJ532381.1; Identities = 806/851 (95 %), 8 gaps (0 %)), *Hapalocystis berkeleyi* (GenBank MG548637.1; Identities = 797/844 (94 %), 6 gaps (0 %)), and *Melanconium elaeidicola* (GenBank NG_058172.1; Identities = 803/851 (94 %), 5 gaps (0 %)).

Ochroconis musae (G.Y. Sun & Lu Hao) Samerp. & de Hoog, *Mycol. Progr.* **14** (no. 6): 8. 2015. Fig. 36.

Basionym: *Scolecobasidium musae* G.Y. Sun & Lu Hao, *Mycol. Progr.* **12**: 492. 2012 (2013).

Synonym: *Ochroconis mirabilis* Samerp. & de Hoog, *Fungal Divers.* **65**: 110. 2013 (2014).

Mycelium consisting of pale brown, smooth, branched, septate, 1.5–2 µm diam hyphae. *Conidiophores* erect to flexuous, arising from vegetative hyphae, subcylindrical, 1–3-septate, 7–40 × 2.5–3 µm, branched or not, brown, smooth-walled, proliferating sympodially with several denticles that are 1–2 × 1 µm; conidiogenous cells 7–12 × 1.5–3 µm. *Conidia* subcylindrical, (8–)11–13(–16) × (2.5–)3(–4) µm, smooth-walled, pale brown, 1(–3)-septate, becoming verruculose and constricted at septa with age, apex obtuse, tapering to truncate hilum, 1 µm diam.

Culture characteristics: Colonies erumpent, spreading, with moderate aerial mycelium and smooth, lobate margin, reaching 25 mm diam after 2 wk at 25 °C. On MEA surface umber with diffuse sienna pigment, reverse chestnut; on PDA surface and reverse umber; on OA surface umber.

Material examined: **Thailand**, Chiang Mai, on leaf trichomes of *Persea americana* (*Lauraceae*), 2008, P.W. Crous, CBS H-23830, culture CPC 33947 = CBS 145061.

Notes: *Ochroconis* has pigmented conidiophores, and sympodial conidiogenesis with denticles that give rise to septate, pigmented, verruculose conidia (Giraldo *et al.* 2014, Crous *et al.* 2017). The present collection is closely related to *O. musae* (Samerpitak *et al.* 2015).

Based on a megablast search of NCBI's GenBank nucleotide database, the closest hits using the **ITS** sequence had highest similarity to *Ochroconis musae* (GenBank KT272078.1; Identities = 581/588 (99 %), no gaps), *Acroconidiellina arecae* (GenBank KX306747.1; Identities = 663/672 (99 %), 2 gaps (0 %)), and *Ochroconis musae* (as *Ochroconis mirabilis*, GenBank KF156028.1; Identities = 580/589 (98 %), 1 gap

(0 %)). Closest hits using the **LSU** sequence are *Ochroconis musae* (as *Ochroconis mirabilis*, GenBank KF156139.1; Identities = 791/793 (99 %), no gaps), *Ochroconis musae* (GenBank KT272086.1; Identities = 815/818 (99 %), 2 gaps (0 %)), and *Ochroconis dracaenae* (GenBank MH878221.1; Identities = 808/813 (99 %), no gaps). Closest hits using the **actA** sequence had highest similarity to *Ochroconis mirabilis* (GenBank HQ916972.1; Identities = 263/264 (99 %), no gaps), *Ochroconis constricta* (GenBank KF155942.1; Identities = 263/264 (99 %), no gaps), and *Ochroconis musae* (as *Ochroconis mirabilis*, GenBank KT272055.1; Identities = 263/264 (99 %), no gaps). Closest hits using the **tef1** sequence had highest similarity to *Ochroconis humicola* (GenBank AB564640.1; Identities = 430/433 (99 %), no gaps), *Ochroconis dracaenae* (GenBank KX228377.1; Identities = 492/510 (96 %), 1 gap (0 %)), and *Ochroconis musae* (GenBank KF156002.1; Identities = 367/370 (99 %), no gaps).

Paradevriesiaceae Crous, *fam. nov.* MycoBank MB829459.

Paradevriesia Crous, *gen. nov.* MycoBank MB829325.

Etymology: Name reflects the fact that it is phylogenetically allied to *Devriesia s.str.*

Mycelium consisting of branched, septate, hyphae, irregular in width, smooth to verruculose, at times forming hyphal strands and hyphal coils; hyphae frequently forming dark brown, thick-walled, intercalary, muriformly septate chlamydospores in culture. *Conidiophores* macro- and micronematous subcylindrical, medium brown, straight to irregularly curved, septate, or reduced to conidiogenous cells. *Conidiogenous cells* terminal or lateral on hyphae, medium brown, smooth, guttulate, subcylindrical, mono- to polyblastic; scars somewhat darkened and thickened, but not refractive. *Conidia* medium brown, guttulate, smooth, in mostly unbranched chains, subcylindrical to narrowly ellipsoidal, septate; hila darkened, somewhat thickened, not refractive.

Type species: *Paradevriesia americana* (Arzanlou & Crous) Crous.

Paradevriesia americana (Crous & Dugan) Crous, *comb. nov.* MycoBank MB829326.

Basionym: *Devriesia americana* Crous & Dugan, *Stud. Mycol.* **58**: 42. 2007.



Fig. 36. *Ochroconis musae* (CPC 33947). **A–D.** Conidiophores giving rise to conidia. Scale bars = 10 µm.

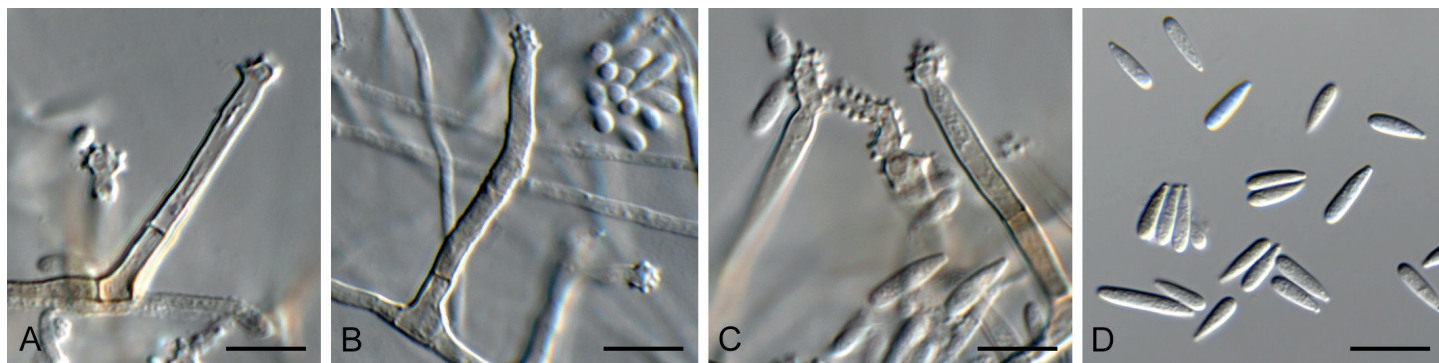


Fig. 37. *Pararamichloridium livistonae* (CPC 32152). A–C. Conidiophores. D. Conidia. Scale bars = 10 μ m.

Paradevriesia pseudoamericana (J. Frank *et al.*) Crous, **comb. nov.** MycoBank MB829328.

Basionym: *Devriesia pseudoamericana* J. Frank *et al.*, *Persoonia* **24**: 97. 2010.

Notes: Although morphologically similar, members of *Paradevriesia* have a different ecology to members of *Devriesia* s. str. (Seifert *et al.* 2004), which usually occur in soil, and are thermotolerant. Species of *Paradevriesia* are presently known from plant and rock surfaces, and do not grow at high temperatures. Phylogenetically, *Paradevriesia* also represents a distinct family in *Capnodiales*.

Pararamichloridium livistonae Crous, *Persoonia* **39**: 357. 2017. Fig. 37.

Mycelium consisting of hyaline, smooth, branched, septate, 2–3 μ m diam hyphae. *Conidiophores* solitary, cylindrical, erect, straight to flexuous, arising from superficial hyphae, pale brown, smooth, 2–6-septate, 25–65 \times 2.5–3 μ m. *Conidiogenous cells* terminal, integrated, cylindrical, pale brown, smooth, 14–20 \times 2.5–3 μ m, with terminal rachis of aggregated, short denticles, 1 \times 1 μ m, flat-tipped, not darkened nor thickened. *Conidia* aseptate, solitary, hyaline, smooth-walled, fusoid-ellipsoid to clavate, apex obtuse, tapering from middle to truncate hilum, 0.5 μ m diam, slightly reflective, 7–8 \times 2–2.5 μ m.

Culture characteristics: Colonies erumpent, spreading, with moderate aerial mycelium and smooth, lobate margin, reaching 15 mm diam after 2 wk at 25 $^{\circ}$ C. On MEA surface and reverse sienna with diffuse sienna pigment; on PDA surface pale luteous, reverse sienna with diffuse sienna pigment; on OA surface pale luteous.

Material examined: **Australia**, New South Wales, Murramarang National Park, on leaves of *Livistona australis* (*Arecaceae*), Nov. 2016, P.W. Crous, CBS H-23800, culture CPC 32152 = CBS 144522.

Notes: *Pararamichloridium livistonae* was described from leaves of *Livistona australis* collected in Australia (Crous *et al.* 2017), and isolate CPC 32152 represents the second collection of this fungus from the type locality.

Based on a megablast search of NCBI's GenBank nucleotide database, the closest hits using the **ITS** sequence had highest similarity to *Pararamichloridium livistonae* (GenBank NR_156652.1; Identities = 616/617 (99%), no gaps), *Pararamichloridium verrucosum* (GenBank NR_156653.1; Identities = 380/447 (85%), 22 gaps (4%)), and *Paramicrothyrium chinense* (GenBank KM246198.1; Identities = 507/632 (80%), 63 gaps (9%)). Closest hits using the **LSU** sequence are *Pararamichloridium livistonae* (GenBank NG_058504.1; Identities = 834/835 (99%), 1 gap (0%)), *Pararamichloridium verrucosum* (GenBank MH873621.1; Identities = 844/877 (96%), 2 gaps (0%)), and *Magnaportheopsis poae* (GenBank KM401651.1; Identities = 824/870 (95%), 3 gaps (0%)).

Pararousoella juglandicola Crous & R.K. Schumach., **sp. nov.** MycoBank MB829329. Fig. 38.

Etymology: Name refers to the host genus *Juglans* from which it was isolated.

Conidiomata erumpent, globose, brown, pycnidial, 150–300 μ m diam with central ostiole, exuding a black conidial mass. *Conidiophores* reduced to conidiogenous cells lining the inner cavity, hyaline, smooth, ampulliform to doliiform, phialidic with periclinal thickening at apex, 5–7 \times 4–5 μ m. *Conidia* aseptate,



Fig. 38. *Pararousoella juglandicola* (CPC 33400). A. Conidioma on SNA. B. Conidiogenous cells. C. Conidia. Scale bars: A = 300 μ m, B, C = 10 μ m.

solitary, subcylindrical, guttulate, apex bluntly rounded, base truncate, hyaline becoming brown, smooth, (5–)6(–7) × (2.5–)3 µm.

Culture characteristics: Colonies flat, spreading, with moderate aerial mycelium and feathery, lobate margin, reaching 60 mm diam after 2 wk at 25 °C. On MEA, PDA and OA surface and reverse olivaceous grey.

Typus: **Germany**, near Berlin, on twig of *Juglans regia* (*Juglandaceae*), 21 Jan. 2017, *R.K. Schumacher*, HPC 1953 = RKS 12 (**holotype** CBS H-23820, culture ex-type CPC 33400 = CBS 145037).

Pararousoella mukdahanensis (Phook. *et al.*) Crous, **comb. nov.** MycoBank MB829330.

Basionym: *Rousoella mukdahanensis* Phook. *et al.*, *Fungal Diversity* **82**: 32. 2016 (2017).

Notes: Species of *Thyridariaceae* are commonly isolated from various plant substrates. The family was recently treated by Wanasinghe *et al.* (2018), in which the genus *Pararousoella* was established based on its distinct phylogenetic relationship to *Rousoella*. *Pararousoella juglandicola* represents a new member of the genus, which is phylogenetically distinct from other species, including *Rousoella mukdahanensis*, for which a new combination is required.

Based on a megablast search of NCBI's GenBank nucleotide database, the closest hits using the **ITS** sequence had highest similarity to *Rousoella mukdahanensis* (GenBank NR_155722.1; Identities = 488/497 (98 %), 1 gap (0 %)), *Pararousoella rosarum* (GenBank NR_157529.1; Identities = 492/505 (97 %), 4 gaps (0 %)), and *Aaosphaeria arxii* (GenBank MH872962.1; Identities = 541/587 (92 %), 7 gaps (1 %)). Closest hits using the **LSU** sequence are *Rousoella neopustulans* (GenBank KJ474841.1; Identities = 824/837 (98 %), no gaps), *Arthopyrenia salicis* (GenBank KP671722.1; Identities = 852/866 (98 %), no gaps), and *Rousoella pustulans* (GenBank AB524623.1; Identities = 820/834 (98 %), no gaps). Distant hits using the **rpb2** sequence had highest similarity to *Rousoella percutanea* (GenBank KF366453.1; Identities = 575/710 (81 %), 10 gaps (1 %)), *Parathyridaria percutanea* (GenBank LT797063.1; Identities = 730/905 (81 %), 6 gaps (0 %)) and *Flammeoscoma lignicola* (GenBank KT324586.1; Identities = 696/898 (78 %), 8 gaps

(0 %)). Very distant hits using the **tef1** sequence had highest similarity to *Rousoella scabriscpora* (GenBank KX650537.1; Identities = 130/140 (93 %), no gaps), *Thyrostroma franseriae* (GenBank KY905680.1; Identities = 203/235 (86 %), 3 gaps (1 %)), *Stachybotrys limonisporea* (GenBank KU847058.1; Identities = 131/136 (96 %), no gaps), and *Trichoderma applanatum* (GenBank KJ634759.1; Identities = 141/150 (94 %), 3 gaps (2 %)).

Petriella sordida (Zukal) G.L. Barron & J.C. Gilman, *Canad. J. Bot.* **39**: 839. 1961. Fig. 39.

Basionym: *Microascus sordidus* Zukal, *Ber. dt. bot. Ges.* **8**: 297. 1890.

Conidiophores synnematal, erect, flexuous, olivaceous brown, smooth, arising from a reduced basal stroma, consisting of numerous (30–100) individual conidiophores, septate (septa 10–30 µm apart), 250–350 µm long, stipe (7–)15–30(–90) µm diam, with flaring conidiogenous head, containing an olivaceous brown, mucoid conidial mass. **Conidiogenous cells** subcylindrical, olivaceous, smooth, 10–25 × 2–2.5 µm, proliferating inconspicuously percurrently at apex. **Conidia** solitary, aseptate, guttulate, smooth, subcylindrical, apex obtuse, slightly constricted in middle, base truncate, 2 µm diam, slightly darkened, (7–)9–10(–12) × (3–)3.5(–4) µm.

Culture characteristics: Colonies flat, spreading, with moderate aerial mycelium and smooth, lobate margin, reaching 25 mm diam after 2 wk at 25 °C. On MEA surface saffron, reverse ochreous; on PDA surface pale luteous, reverse buff, on OA surface buff.

Material examined: **Ukraine**, Rakhiv district, Transcarpathian region, on leaves of *Luzula* sp. (*Juncaceae*), Nov. 2016, *A. Akulov*, HPC 1497, CBS H-23801, culture CBS 144612 = CPC 32460).

Notes: Species of *Petriella* are commonly isolated from soil and dung (Lackner & de Hoog 2011), and thus it is assumed that the isolate in the present study was probably an opportunist on leaves of *Luzula* sp. *Petriella sordida* was described to have synnemata with conidia being (5–)6.5–11.5(–14) × 2.5–5.5 µm (Corlett & MacLachy 1987).

Based on a megablast search of NCBI's GenBank nucleotide database, the closest hits using the **ITS** sequence of CPC 32460



Fig. 39. *Petriella sordida* (CPC 32460). **A.** Synnemata on OA. **B, C.** Conidiophores with conidiogenous cells. **D.** Conidia. Scale bars = 10 µm.

had highest similarity to *Petriella sordida* (GenBank MH863637.1; Identities = 564/565 (99 %), no gaps), *Melanospora asymmetrica* (GenBank KY628677.1; Identities = 554/556 (99 %), no gaps), and *Petriella guttulata* (GenBank MF782707.1; Identities = 558/565 (99 %), 1 gap (0 %)). The ITS sequence was identical to that of "*Petriella* sp. Vega423" (GenBank EU002908.1, 565/565) isolated as root endophyte of *Coffea arabica* in Colombia. The ITS sequences of CPC 32460 and 32461 are identical. Closest hits using the **LSU** sequence of CPC 32460 are *Petriella setifera* (GenBank MH872684.1; Identities = 794/794 (100 %)), *Petriella sordida* (GenBank MH875102.1; Identities = 793/794 (99 %), no gaps), and *Petriella asymmetrica* var. *cypria* (GenBank MH867451.1; Identities = 793/794 (99 %), no gaps). The LSU sequences of CPC 32460 and 32461 are identical. The **cmdA** sequence of CPC 32460 was identical to that of *Petriella sordida* (strain UTHSC 03-394, GenBank AM409103.1; Identities = 449/449 (100 %)). Closest hits using the **rpb2** sequence of CPC 32461 had highest similarity to *Petriella setifera* (GenBank DQ368640.1; Identities = 701/702 (99 %), no gaps), *Scedosporium boydii* (GenBank KP981186.1; Identities = 510/600 (85 %), no gaps), and *Pseudallescheria fusioidea* (GenBank KP981195.1; Identities = 509/600 (85 %), no gaps). No **tef1** sequences of *Petriella* which cover the same region amplified here are available for comparison in GenBank; distant hits include *Scedosporium aurantiacum* (GenBank KJ784086.1; Identities = 278/334 (83 %), 8 gaps (2 %)), *Scopulariopsis brevicaulis* (GenBank KP009002.1; Identities = 148/159 (93 %), no gaps), and *Thyronectria rhodochlora* (GenBank KM225694.1; Identities = 144/154 (94 %), no gaps). The **tef1** sequences of CPC 32460 and 32461 are identical. The **tub2** sequence of CPC 32460 was identical to both *Petriella setifera* (GenBank EU977491.1; Identities = 488/488 (100 %)) and *Petriella sordida* (GenBank AM409104.1; Identities = 399/399 (100 %)).

Pezizula eucalyptigena Crous, *sp. nov.* MycoBank MB829331. Fig. 40.

Etymology: Name refers to the host genus *Eucalyptus* from which it was isolated.

In vitro. Conidiomata sporodochial, forming superficially on agar, scattered, dark brown, 100–250 μm diam, exuding a creamy conidial mass. *Macroconidiophores* hyaline, smooth,

subcylindrical, branched, 1–4-septate, 40–90 \times 3–4 μm . *Macroconidiogenous cells* integrated, terminal and intercalary, subcylindrical, hyaline, smooth, phialidic with indistinct percurrent proliferations, 10–25 \times 3.5–4 μm . *Macroconidia* aseptate, hyaline, smooth, guttulate, ellipsoid-clavate, straight to slightly curved, with prominently protruding truncate hilum, 2 μm diam, (23–)24–27(–30) \times (6–)7(–8) μm . *Microconidiophores* hyaline, smooth, subcylindrical, branched, 6–12-septate, 60–130 \times 2.5–3.5 μm . *Microconidiogenous cells* integrated, terminal and intercalary, subcylindrical, hyaline, smooth, phialidic, 10–20 \times 2.5–3 μm . *Microconidia* hyaline, smooth, aseptate, subcylindrical, apex obtuse, base truncate, straight to irregularly curved, (7–)10–12(–15) \times 2(–2.5) μm .

Culture characteristics: Colonies spreading with moderate aerial mycelium, covering dish in 2 wk. On MEA surface honey to hazel, reverse hazel; on PDA surface buff, reverse isabelline; on OA surface honey.

Typus: South Africa, Western Cape Province, Malmesbury, on leaves of *Eucalyptus* sp. (*Myrtaceae*), 2006, P.W. Crous (**holotype** CBS H-23799, culture ex-type CBS 144637 = CPC 32129).

Notes: The *Pezizula* generic complex was recently revised by Chen *et al.* (2016). Species from this complex known to occur on *Eucalyptus* include *Parafabraea caliginosa*, *Parafabraea eucalypti*, and *Pezizula californiae* (from *Eucalyptus* leaves in California, USA). *Pezizula eucalyptigena* is phylogenetically closely related to *P. californiae* (conidia 12.5–27.5 \times 4.2–5.8 μm), but morphologically distinct in that it has larger conidia (Cheewangkoon *et al.* 2010, Chen *et al.* 2016).

Based on a megablast search of NCBI's GenBank nucleotide database, the closest hits using the **ITS** sequence had highest similarity to *Pezizula cinnamomea* (GenBank KR859109.1; Identities = 498/524 (95 %), 5 gaps (0 %)), *Pezizula sporulosa* (GenBank JN693514.1; Identities = 495/519 (95%), 4 gaps (0 %)), and *Pezizula californiae* (GenBank JX144747.1; Identities = 495/519 (95 %), 4 gaps (0 %)). Closest hits using the **LSU** sequence are *Pezizula brunnea* (GenBank KR858894.1; Identities = 842/848 (99 %), no gaps), *Pezizula ericae* (GenBank MH874637.1; Identities = 876/883 (99 %), no gaps), and *Pezizula melanigena* (GenBank KR859003.1; Identities = 838/845 (99 %), no gaps). Closest hits using the **rpb2** sequence had highest similarity to *Pezizula eucrita*

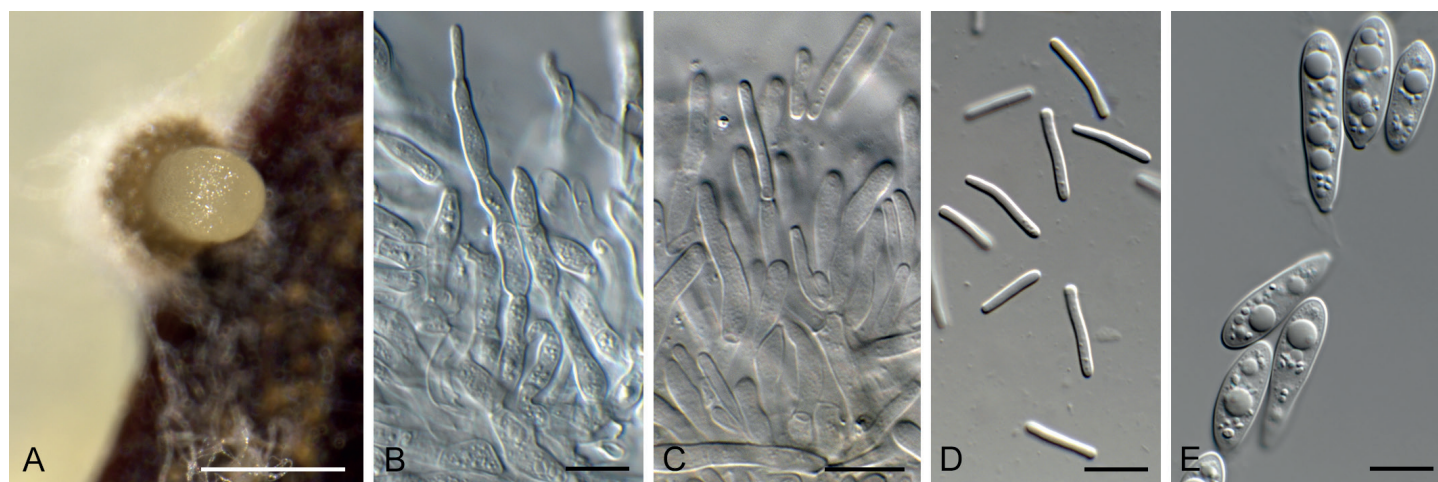


Fig. 40. *Pezizula eucalyptigena* (CPC 32129). **A.** Conidioma on PNA. **B, C.** Conidiogenous cells. **D.** Microconidia. **E.** Macroconidia. Scale bars: A = 250 μm , B–E = 10 μm .

(GenBank KF376205.1; Identities = 866/915 (95 %), no gaps), *Pezicula neoheterochroma* (GenBank KR859338.1; Identities = 850/899 (95 %), no gaps), and *Pezicula* aff. *cinnamomea* (GenBank KF376209.1; Identities = 864/915 (94 %), no gaps).

Phaeoseptoriella Crous, *gen. nov.* MycoBank MB829332.

Etymology: Name refers to its morphological similarity to small species of *Phaeoseptoria*.

Associated with leaf spots. *Conidiomata* solitary, globose, brown with central ostiole. *Conidiophores* reduced to conidiogenous cells lining the inner cavity. *Conidiogenous cells* ampulliform to doliiform, pale brown, smooth, proliferating percurrently at apex. *Conidia* solitary, pale brown, finely roughened, straight to slightly curved, fusoid-ellipsoid, septate, apex subobtuse, base truncate.

Type species: *Phaeoseptoriella zeae* Crous.

Phaeoseptoriella zeae Crous, *sp. nov.* MycoBank MB829333. Fig. 41.

Etymology: Name refers to the host *Zea mays* from which it was isolated.

Associated with small, subcircular, pale brown, amphigenous leaf spots, 2–6 mm diam. *Conidiomata* solitary, globose, 200–250 µm diam, brown with central ostiole. *Conidiophores* reduced to conidiogenous cells lining the inner cavity. *Conidiogenous cells* ampulliform to doliiform, pale brown, smooth, proliferating percurrently at apex, 4–6 × 4–6 µm. *Conidia* solitary, pale brown, finely roughened, straight to slightly curved, fusoid-ellipsoid, apex subobtuse, base truncate, 1.5–2 µm diam, (1–)3-septate, (14–)17–20(–23) × (3–)4 µm.

Culture characteristics: Colonies flat, spreading, with moderate aerial mycelium and smooth, lobate margin, covering dish after 2 wk at 25 °C. On MEA surface dirty white, reverse cinnamon; on PDA surface dirty white, reverse rosy buff; on OA surface rosy vinaceous.

Typus: **South Africa**, Gauteng Province, Gauteng, on leaves of *Zea mays* (*Poaceae*), 12 Apr. 2010, T.A. Coutinho, HPC 2038

(**holotype** CBS H-23814, culture ex-type CPC 33064 = CBS 144614).

Notes: *Phaeosphaeria* leaf spot (PLS) has previously been attributed to *Phaeosphaeria maydis* (described from leaves of *Zea mays* in Sao Paulo, Brazil), which has been linked to various asexual morphs including a *Phyllosticta* sp. (= *Guignardia* sexual morph), and *Phoma maydis*. Amaral *et al.* (2005) reported a phoma-like asexual morph associated with PLS as similar in culture to colonies of *Phaeosphaeria maydis*, and postulated that several fungal species were involved in causing PLS. However, in a recent study, Gonçalves *et al.* (2013) showed that a bacterium, *Pantoea ananatis*, was the primary disease-causing agent, and that the fungi isolated from these lesions, were secondary colonist of the diseased tissue, stating also that the disease symptoms shown by Amaral *et al.* (2005) were atypical for PLS. In South Africa, prominent tan-coloured subcircular leaf spots were found on *Z. mays* to be associated with a new genus, described here as *Phaeoseptoriella zeae*. Further studies are now required to determine the relative importance of this fungus, and confirm its role as maize pathogen.

Based on a megablast search of NCBI's GenBank nucleotide database, the closest hits using the **ITS** sequence had highest similarity to *Parastagonospora avenae* (as *Phaeosphaeria avenaria*, GenBank FJ605258.1; Identities = 526/546 (96 %), 6 gaps (1 %)), *Camarosporioides phragmitis* (GenBank NR_153925.1; Identities = 425/474 (90 %), 15 gaps (3 %)), and *Coniothyrium ferrarisianum* (GenBank MH860854.1; Identities = 424/474 (89 %), 15 gaps (3 %)). Closest hits using the **LSU** sequence are *Didymocyrtis consimilis* (GenBank MH876627.1; Identities = 878/882 (99 %), no gaps), *Parastagonospora nodorum* (GenBank MH868570.1; Identities = 878/882 (99 %), no gaps), and *Kalmusia utahensis* (GenBank MH876142.1; Identities = 877/882 (99 %), no gaps). Closest hits using the **rpb2** sequence had highest similarity to *Didymocyrtis banksiae* (GenBank KY979850.1; Identities = 759/902 (84 %), 2 gaps (0 %)), *Parastagonospora nodorum* (as *Phaeosphaeria nodorum*, GenBank DQ499803.1; Identities = 757/903 (84 %), 2 gaps (0 %)), and *Parastagonospora avenaria* f. sp. *tritici* (as *Phaeosphaeria avenaria* f. sp. *triticae*, GenBank DQ499799.1; Identities = 757/905 (84 %), 6 gaps (0 %)). Closest hits using the **tef1** sequence had highest similarity to *Sclerostagonospora ericae* (GenBank KX228375.1; Identities = 417/515 (81 %), 28 gaps (5 %)), *Didymocyrtis cladoniicola* (as

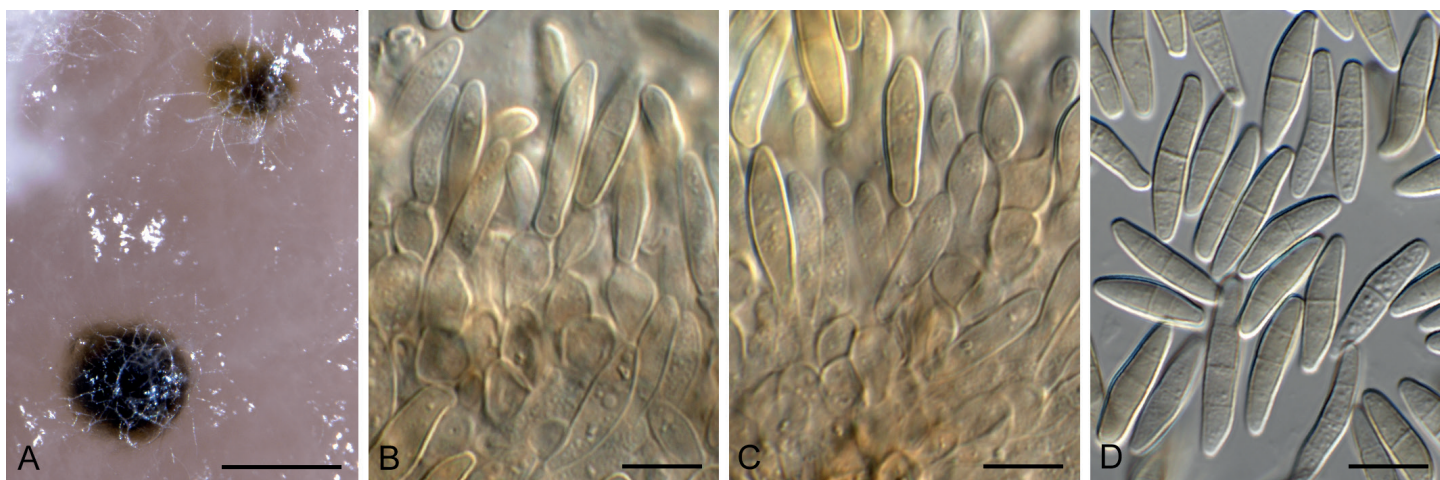


Fig. 41. *Phaeoseptoriella zeae* (CPC 33064). **A.** Conidiomata on OA. **B, C.** Conidiogenous cells. **D.** Conidia. Scale bars: A = 250 µm, B–D = 10 µm.

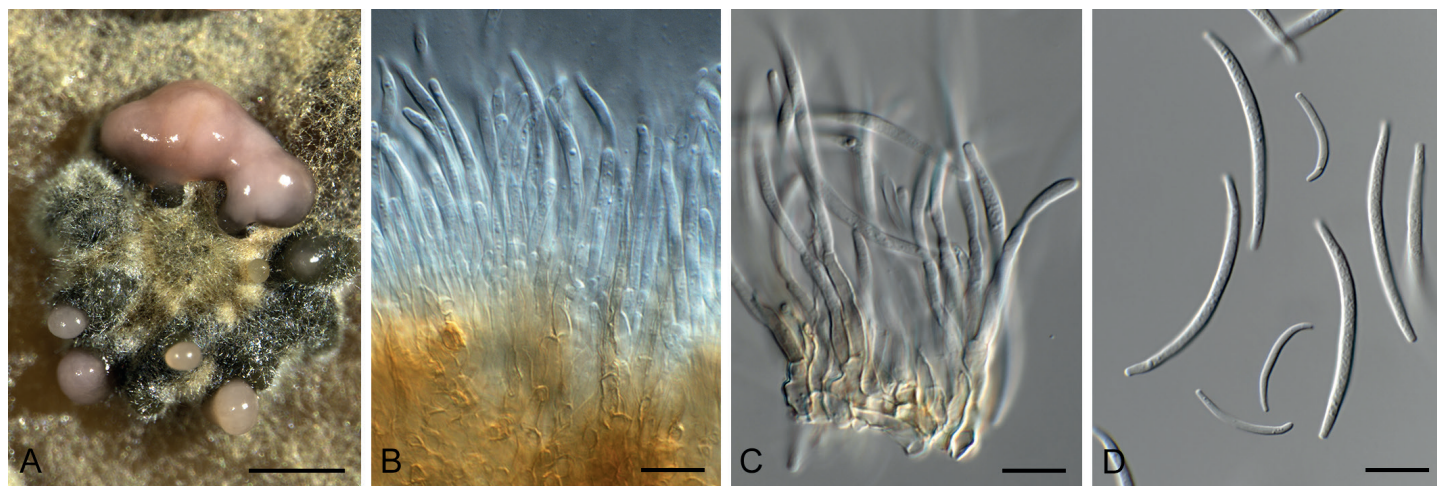


Fig. 42. *Phlogicylindrium dunnii* (CPC 31818). **A.** Eustromatic conidioma on PDA. **B, C.** Conidiophores. **D.** Micro- and macroconidia. Scale bars: A = 200 μm , B–D = 10 μm .

Diederichomyces cladoniicola, GenBank KP170668.1; Identities = 409/516 (79 %), 10 gaps (1 %), and *Septoria oudemansii* (GenBank KF253436.1; Identities = 333/409 (81 %), 8 gaps (1 %)). Closest hits using the **tub2** sequence had highest similarity to *Sclerostagonospora ericae* (GenBank KX228383.1; Identities = 263/287 (92 %), 4 gaps (1 %)), *Diederichomyces ficuzzae* (GenBank KP170697.1; Identities = 262/290 (90 %), 6 gaps (2 %)), and *Didymocytis foliaceiphila* (as *Diederichomyces foliaceiphila*, GenBank KP170698.1; Identities = 260/288 (90 %), 3 gaps (1 %)).

Phlogicylindrium dunnii Crous, *sp. nov.* MycoBank MB829334. Fig. 42.

Etymology: Name refers to *Eucalyptus dunnii* from which it was isolated.

Conidiomata eustromatic, multilocular, locules 100–200 μm diam, occurring solitary on leaves, but in clusters on agar, exuding a slimy pink conidial mass. **Conidiophores** arising from a brown stroma of 3–6 layers of *textura angularis*, subcylindrical, branched, 1–3-septate, brown, smooth, 30–70 \times 3–4 μm . **Conidiogenous cells** pale brown, smooth, subcylindrical, 15–30 \times 2.5–3 μm , proliferating sympodially and percurrently near apex. **Macroconidia** hyaline, smooth, narrowly fusoid to widest in the middle with slight taper towards ends, subcylindrical, 1-septate, apex subobtuse, base truncate, curved, (32–)35–42(–47) \times (2–) 2.5(–3) μm . **Microconidia** hyaline, smooth, aseptate, cylindrical, curved, apex obtuse, base truncate, 15–18 \times 1.5 μm , forming in same conidioma as macroconidia.

Culture characteristics: Colonies flat, spreading, with moderate aerial mycelium and folded surface and smooth, lobate margin, reaching 10 mm diam after 2 wk at 25 $^{\circ}\text{C}$. On MEA surface ochreous, reverse umber; on PDA surface ochreous, reverse salmon to ochreous; on OA surface smoke grey.

Typus: **Australia**, New South Wales, Tooloom State Forest, on leaves of *Eucalyptus dunnii* (*Myrtaceae*), 20 Jan. 2016, A.J. Carnegie, HPC 1447 (**holotype** CBS H-23264, culture ex-type CPC 31818 = CBS 144620).

Notes: *Phlogicylindrium* was established by Summerell *et al.* (2006) to accommodate a genus with erect, flame-like

conidiomatal tufts to sporodochial conidiomata, and cylindrical, hyaline conidia forming on brown, percurrently proliferating conidiogenous cells. *Phlogicylindrium dunnii* is rather atypical in the fact that it has eustromatic, multilocular conidiomata, that with age appear sporodochial as they age.

Based on a megablast search of NCBI's GenBank nucleotide database, the closest hits using the **ITS** sequence had highest similarity to *Phlogicylindrium tereticornis* (GenBank NR_156660.1; Identities = 550/566 (97 %), 3 gaps (0 %)), *Phlogicylindrium eucalyptorum* (GenBank EU040223.1; Identities = 411/432 (95 %), 3 gaps (0 %)), and *Phlogicylindrium mokareii* (GenBank KY173431.1; Identities = 409/432 (95 %), 3 gaps (0 %)). Closest hits using the **LSU** sequence are *Phlogicylindrium tereticornis* (GenBank NG_058510.1; Identities = 788/789 (99 %), no gaps), *Phlogicylindrium mokareii* (GenBank NG_059750.1; Identities = 782/789 (99 %), no gaps), and *Phlogicylindrium uniforme* (GenBank JQ044445.1; Identities = 780/789 (99 %), no gaps). The best hit using the **rpb2** sequence was with *Phlogicylindrium tereticornis* (GenBank MG386142.1; Identities = 861/871 (99 %), no gaps). The best hit using the **tef1** sequence was with *Phlogicylindrium tereticornis* (GenBank MG386151.1; Identities = 396/402 (99 %), no gaps).

Phyllosticta austroafricana Crous, *sp. nov.* MycoBank MB829336. Fig. 43.

Etymology: Name refers to the continent Africa where it was collected.

Associated with leaf spots on leaf litter of unidentified deciduous tree host. **Conidiomata** pycnidial, solitary, black, erumpent, globose, exuding hyaline conidial masses; pycnidia up to 200 μm diam; wall of several layers of brown *textura angularis*. **Ostiole** central, up to 20 μm diam. **Conidiophores** subcylindrical, with 1–2 supporting cells, at times branched at base, 20–30 \times 3–5 μm . **Conidiogenous cells** terminal, subcylindrical, hyaline, smooth, coated in a mucoid layer, 10–15 \times 3–4 μm , proliferating several times percurrently near apex. **Conidia** (11–)14–17(–23) \times (6–)8–10(–11) μm , solitary, hyaline, aseptate, thin- and smooth-walled, coarsely guttulate, ellipsoid to obovoid, tapering towards a truncate base, 2–3 μm diam, enclosed in a mucoid sheath, 2–3 μm thick, and bearing a hyaline apical mucoid appendage, (5–) 7–8(–10) \times 1.5(–2) μm , tapering towards an acutely rounded tip.

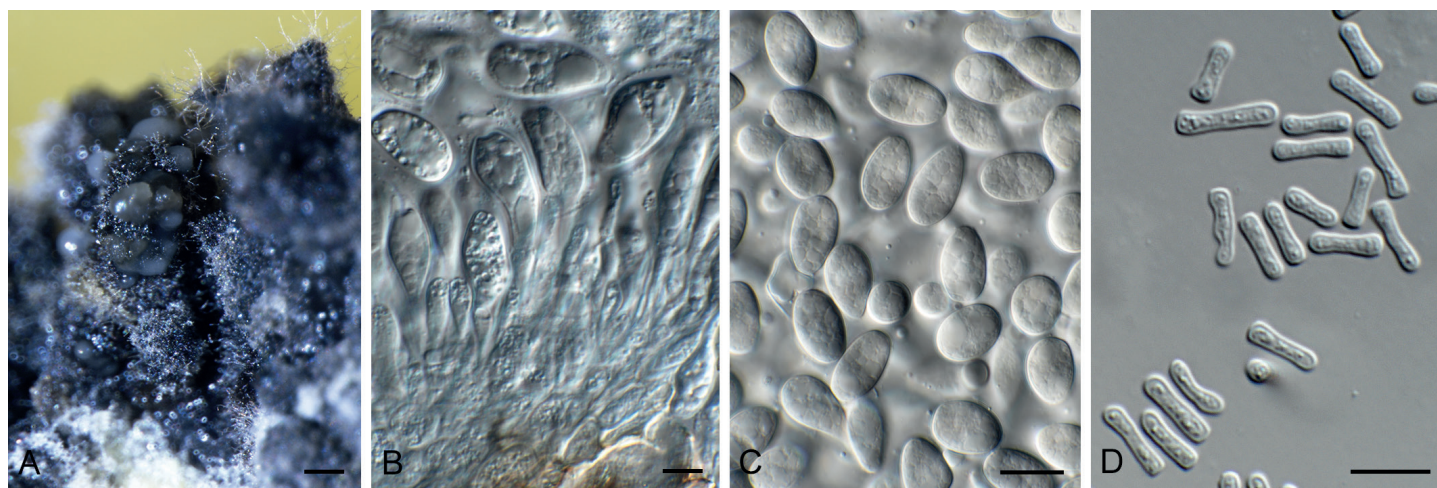


Fig. 43. *Phyllosticta austroafricana* (CPC 31920). **A.** Conidiomata on MEA. **B.** Conidiogenous cells. **C.** Conidia. **D.** Spermatia. Scale bars: A = 200 μm , B–D = 10 μm .

Spermatia bacilliform, hyaline, smooth, guttulate, 6–8 \times 2–3 μm .

Culture characteristics: Colonies erumpent, spreading, with sparse aerial mycelium and uneven surface and lobed margin, reaching 5 mm diam after 2 wk at 25 $^{\circ}\text{C}$. On MEA, PDA and OA surface iron-grey, and reverse iron-grey, with diffuse yellow pigment on OA.

Typus: **South Africa**, Western Cape Province, on leaf spots of unidentified deciduous tree host, 2010, *P.W. Crous* (**holotype** CBS H-23797, culture ex-type CPC 31920 = CBS 144593).

Notes: *Phyllosticta* includes several important plant pathogens causing leaf and fruit spot diseases. Important species are *P. ampellicida* causing black rot disease on grapevines (Zhou et al. 2015), species in the *P. musarum* species complex causing banana freckle disease (Wong et al. 2012), and *P. citricarpa* causing citrus black spot (Guarnaccia et al. 2017). *Phyllosticta austroafricana* is a phylogenetically distinct species, associated with leaf spots on an unidentified tree host.

Based on a megablast search of NCBI's GenBank nucleotide database, the closest hits using the **ITS** sequence had highest similarity to *Phyllosticta pseudotsugae* (GenBank KF154277.1; Identities = 539/573 (94 %), 5 gaps (0 %)), *Phyllosticta carissicola* (GenBank NR_147363.1; Identities = 574/613 (94 %), 4 gaps (0 %)), and *Phyllosticta podocarpi* (GenBank KF154276.1; Identities = 535/572 (94 %), 3 gaps (0 %)). Closest hits using the **LSU** sequence are *Phyllosticta carissicola* (GenBank KT950863.1; Identities = 848/851 (99 %), no gaps), *Phyllosticta podocarpi* (GenBank KF766383.1; Identities = 835/840 (99 %), no gaps), and *Phyllosticta hymenocallidicola* (GenBank NG_057947.1; Identities = 869/882 (99 %), no gaps). Closest hits using the **actA** sequence had highest similarity to *Phyllosticta acaciigena* (GenBank KY173570.1; Identities = 517/562 (92 %), 5 gaps (0 %)), *Exserohilum khartoumense* (as *Setosphaeria khartoumensis*, GenBank LT837600.1; Identities = 474/526 (90 %), 11 gaps (2 %)), *Exserohilum rostratum* (as *Setosphaeria rostrata*, GenBank LT837683.1; Identities = 473/526 (90 %), 11 gaps (2 %)), and *Exserohilum prolatum* (GenBank LT837660.1; Identities = 473/526 (90 %), 11 gaps (2 %)). Closest hits using the **tef1** sequence had highest similarity to *Phyllosticta ericarum* (GenBank KR025452.1; Identities = 303/331 (92 %), 5 gaps (1 %)), *Phyllosticta carissicola* (GenBank KT950879.1; Identities =

367/403 (91 %), 19 gaps (4 %)), and *Phyllosticta catimbauensis* (GenBank MF466155.1; Identities = 299/331 (90 %), 4 gaps (1 %)).

Phyllosticta hagahagaensis Crous & M.J. Wingf., *sp. nov.* MycoBank MB829335. Fig. 44.

Etymology: Name reflects Haga Haga in the Eastern Cape Province of South Africa where it was collected.

Conidiomata pycnidial, solitary, black, erumpent, globose, exuding hyaline conidial masses; pycnidia 250–350 μm diam; wall of several layers of brown *textura angularis*. **Ostiole** central, up to 20 μm diam. **Conidiophores** subcylindrical, unbranched or branched below, 0–2-septate, 15–30 \times 4–5 μm . **Conidiogenous cells** terminal and intercalary, subcylindrical, hyaline, smooth, coated in a mucoïd layer, 7–16 \times 3.5–4 μm , proliferating several times percurrently near apex. **Conidia** (11–)13–14(–15) \times (7–) 8(–9) μm , solitary, hyaline, aseptate, thin- and smooth-walled, guttulate, granular, ellipsoid to obovoid, tapering towards a truncate base, 3–3.5 μm diam, enclosed in a mucoïd sheath, 2.5–5 μm thick, and bearing a hyaline apical mucoïd appendage, 5–15 \times 1.5–2 μm , tapering towards an acutely rounded tip.

Culture characteristics: Colonies erumpent, spreading, with sparse to moderate aerial mycelium and uneven surface and margin, reaching 18 mm diam after 2 wk at 25 $^{\circ}\text{C}$. On MEA surface smoke grey to grey olivaceous, reverse olivaceous grey; on PDA surface and reverse olivaceous grey; on OA surface olivaceous grey to grey olivaceous.

Typus: **South Africa**, Eastern Cape Province, Haga Haga, on leaf litter of *Carissa bispinosa* (*Apocynaceae*), 23 Dec. 2010, *M.J. Wingfield*, HPC 1545 (**holotype** CBS H-23811, culture ex-type CPC 32799 = CBS 144592).

Notes: *Phyllosticta carissicola* [conidia (11–)12–14(–15) \times (9–) 10(–11) μm , sheath 2–3 μm thick apical mucoïd appendage, (10–)12–17(–25) \times 1.5(–2) μm] was described from leaves of *Carissa macrocarpa* (CPC 25665) in South Africa by Crous et al. (2015). *Phyllosticta hagahagaensis* differs morphologically from *P. carissicola* in having wider conidia, a wider mucoïd sheath, and shorter appendages.



Fig. 44. *Phyllosticta hagahagaensis* (CPC 32799). **A.** Conidioma on OA. **B, C.** Conidiogenous cells. **D.** Conidia. Scale bars: A = 300 µm, B–D = 10 µm.

Based on a megablast search of NCBI's GenBank nucleotide database, the closest hits using the **ITS** sequence had highest similarity to *Phyllosticta podocarpi* (GenBank KF766217.1; Identities = 591/603 (98 %), 1 gap (0 %)), *Phyllosticta pseudotsugae* (GenBank KF154277.1; Identities = 559/572 (98 %), 1 gap (0 %)), and *Phyllosticta owaniana* (GenBank JF261462.1; Identities = 569/588 (97 %), no gaps). Closest hits using the **LSU** sequence are *Phyllosticta carissicola* (GenBank KT950863.1; Identities = 855/856 (99 %), no gaps), *Phyllosticta podocarpi* (GenBank KF766383.1; Identities = 837/840 (99 %), no gaps), and *Phyllosticta hymenocallidicola* (GenBank NG_057947.1; Identities = 876/887 (99 %), no gaps). Closest hits using the **actA** sequence had highest similarity to *Phyllosticta acaciigena* (GenBank KY173570.1; Identities = 521/560 (93 %), 1 gap (0 %)), *Phyllosticta carissicola* (GenBank KT950872.1; Identities = 233/243 (96 %), no gaps), *Cladosporium velox* (GenBank KT600654.1; Identities = 459/510 (90 %), 3 gaps (0 %)), and *Alternaria frumenti* (GenBank JQ671649.1; Identities = 467/523 (89 %), 9 gaps (1 %)). Closest hits using the **gapdh** sequence had highest similarity to *Phyllosticta owaniana* (GenBank JF343766.1; Identities = 299/300 (99 %), no gaps), *Phyllosticta podocarpi* (GenBank KF289168.1; Identities = 298/300 (99 %), no gaps), and *Phyllosticta carissicola* (GenBank KT950876.1; Identities = 501/510 (98 %), 1 gap (0 %)). Closest hits using the **tef1** sequence had highest similarity to *Phyllosticta carissicola* (GenBank KT950879.1; Identities = 379/389 (97 %), 2 gaps (0 %)), *Phyllosticta hakeicola* (GenBank MH108025.1; Identities = 328/353 (93 %), 10 gaps (2 %)), and *Phyllosticta yuccae* (GenBank JX227948.1; Identities = 355/398 (89 %), 14 gaps (3 %)).

Piniphoma Crous & R.K. Schumach., **gen. nov.** MycoBank MB829337.

Etymology: Name combined the name of the host genus *Pinus*, and the fungal genus *Phoma*.

Conidiomata solitary, pycnidial, globose with central ostiole, pale brown, exuding a creamy conidial mass. **Conidiophores** reduced to conidiogenous cells lining inner cavity, ampulliform, hyaline, smooth, phialidic. **Conidia** solitary, aseptate, smooth, hyaline, straight, guttulate, subcylindrical with obtuse ends.

Type species: *Piniphoma wesendahlina* Crous & R.K. Schumach.

Piniphoma wesendahlina Crous & R.K. Schumach., **sp. nov.** MycoBank MB829338. Fig. 45.

Etymology: Name reflects to the city of Berlin where it was collected.

Conidiomata solitary, pycnidial, 80–120 µm diam, globose with central ostiole, pale brown, only observed on PNA, exuding a creamy conidial mass. **Conidiophores** reduced to conidiogenous cells lining inner cavity, ampulliform, hyaline, smooth, phialidic, 4–5 × 3–4 µm. **Conidia** solitary, aseptate, smooth, hyaline, straight, guttulate, subcylindrical with obtuse ends, (3–)4(–5) × 2 µm.

Culture characteristics: Colonies flat, spreading, with moderate aerial mycelium and smooth, lobate margin, reaching 45 mm

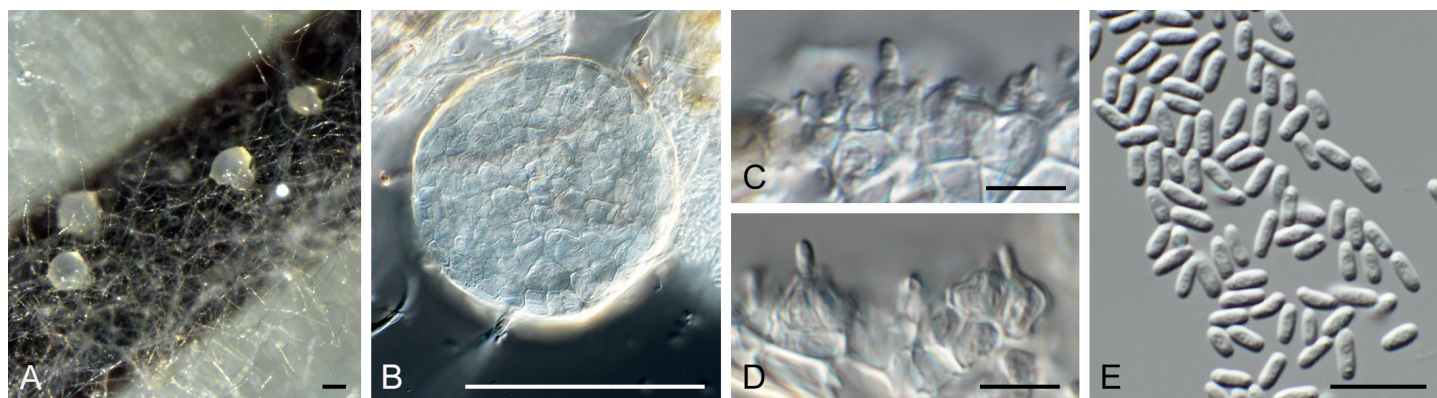


Fig. 45. *Piniphoma wesendahlina* (CPC 33693). **A.** Conidiomata on PNA. **B.** Conidioma. **C, D.** Conidiogenous cells. **E.** Conidia. Scale bars: A, B = 100 µm, C–E = 10 µm.

diam after 2 wk at 25 °C. On MEA, PDA and OA surface and reverse olivaceous grey.

Typus: Germany, Berlin, wood debris of *Pinus sylvestris* (*Pinaceae*), 1 May 2017, H. Schreiber & R.K. Schumacher, HPC 2114 = RKS 106 (**holotype** CBS H-23823, culture ex-type CPC 33693 = CBS 145032).

Notes: *Piniphoma wesendahlina* is a phoma-like genus occurring on *Pinus sylvestris* wood debris collected in Berlin, Germany. Phylogenetically, it appears distinct from other phoma-like genera presently known (Chen *et al.* 2015, Valenzuela-Lopez *et al.* 2018), and is thus introduced as new.

Based on a megablast search of NCBI's GenBank nucleotide database, the closest hits using the **ITS** sequence had highest similarity to *Setophoma vernoniae* (GenBank KJ869141.1; Identities = 445/486 (92 %), 8 gaps (1 %)) and *Shiraia bambusicola* (GenBank MF062656.1; Identities = 451/491 (92 %), 11 gaps (2 %)). It was identical to several unidentified sequences, e.g. GenBank GU566235.1 from the rhizosphere of *Phalaris arundinacea* in Czech Republic, GenBank FN394707.1 from a fungal endophyte of *Holcus lanatus* in Spain and GenBank MH063650.1 from surface-sterilised, asymptomatic roots of *Arrhenatherum elatius* in France. Closest hits using the **LSU** sequence are *Coniothyrium quercinum* (GenBank MH877842.1; Identities = 858/860 (99 %), no gaps), *Sclerostagonospora cycadis* (GenBank MH874827.1; Identities = 858/860 (99 %), no gaps), and *Coniothyrium ferrarianum* (GenBank MH872593.1; Identities = 858/860 (99 %), no gaps). Distant hits using the **rpb2** sequence had highest similarity to *Exserohilum fusiforme* (GenBank LT852483.1; Identities = 732/899 (81 %), 22 gaps (2 %)), *Exserohilum oryzicola* (GenBank LT715748.1; Identities = 717/883 (81 %), 19 gaps (2 %)), and *Bipolaris maydis* (GenBank XM_014222497.1; Identities = 740/918 (81 %), 17 gaps (1 %)). Very distant hits using the **tef1** sequence had highest similarity to *Dendryphion penicillatum* (GenBank AY375376.1; Identities = 207/234 (88 %), 4 gaps (1 %)), *Libertasomyces quercus* (GenBank KY929197.1; Identities = 208/235 (89 %), 8 gaps (3 %)), and *Alternaria alternariae* (as *Ulocladium alternariae*, GenBank AY375370.1; Identities = 207/234 (88 %), 6 gaps (2 %)). Distant hits using the **tub2** sequence had highest similarity to *Sclerostagonospora ericae* (GenBank KX228383.1; Identities = 467/551 (85 %), 26 gaps (4 %)), *Parastagonospora avenae* f. sp. *avenae* (as *Phaeosphaeria avenaria* f. sp. *avenaria*, GenBank

AY870404.1; Identities = 468/557 (84 %), 31 gaps (5 %)), and *Seltsamia ulmi* (GenBank MF795918.1; Identities = 409/487 (84 %), 17 gaps (3 %)).

Pseudocercospora hakeae (U. Braun & Crous) U. Braun & Crous, *Stud. Mycol.* **75**: 88. 2012 (2013). Fig. 46.

Basionym: *Cercostigmina protearum* var. *hakeae* U. Braun & Crous, *Sydowia* **46**: 206. 1994.

Leaf spots amphigenous, elongated, confined by leaf veins, 2–3 mm diam, medium brown with raised, dark brown border. **Caespituli** olivaceous brown, amphigenous, developing on a well-defined brown stroma up to 250 µm diam. **Conidiophores** densely aggregated, subcylindrical, branched or not, geniculous-sinuous, 3–7-septate, medium brown, thick-walled, finely verruculose, 30–70 × 6–8 µm. **Conidiogenous cells** subcylindrical, medium brown, finely verruculose, thick-walled, terminal and intercalary, proliferating percurrently and or sympodially, 12–20 × 5–7 µm; loci truncate, unthickened, not darkened, 2–3 µm diam. **Conidia** solitary, subcylindrical, medium brown, finely verruculose, apex obtuse, base truncate, 2(–2.5) µm diam, straight to geniculous-sinuous, (1–)3–6(–7)-septate, (15–)30–50(–65) × 4(–5) µm.

Culture characteristics: Colonies erumpent, spreading, with moderate aerial mycelium and smooth, lobate margin, reaching 7 mm diam after 2 wk at 25 °C. On MEA, PDA and OA surface olivaceous grey, and reverse iron-grey.

Material examined: Australia, New South Wales, Fitzroy Falls, Morton National Park, on leaves of *Hakea* sp. (*Proteaceae*), 26 Nov. 2016, P.W. Crous, HPC 1756 = CBS H-23798, culture CPC 32100 = CBS 144520).

Notes: *Pseudocercospora hakeae* (as *Cercostigmina protearum* var. *hakeae*) was described from leaves on *Hakea saligna* collected in the Limpopo Province of South Africa (Crous & Braun 1994). The culture linked to this species (CBS 112226), was, however, collected on *Grevillea* sp. in Australia (Crous *et al.* 2013). The present collection provided the first culture from a *Hakea* sp., also collected in Australia.

Based on a megablast search of NCBI's GenBank nucleotide database, the closest hits using the **ITS** sequence had highest similarity to *Pseudocercospora fuligena* (GenBank GU214675.1; Identities = 533/535 (99 %), 1 gap (0 %)), *Pseudocercospora*



Fig. 46. *Pseudocercospora hakeae* (CPC 32100). **A.** Leaf spot. **B.** Stroma. **C.** Conidiogenous cells. **D.** Conidia. Scale bars = 10 µm.

chengtuensis (GenBank GU214672.1; Identities = 533/535 (99 %), 1 gap (0 %)), and *Pseudocercospora atomarginalis* (GenBank GU214671.1; Identities = 533/535 (99 %), 1 gap (0 %)). Closest hits using the **LSU** sequence are *Pseudocercospora cydoniae* (GenBank MH877505.1; Identities = 852/852 (100 %), no gaps), *Pseudocercospora rhamnellae* (GenBank MH877382.1; Identities = 852/852 (100 %), no gaps), and *Pseudocercospora ranjita* (GenBank MH875340.1; Identities = 852/852 (100 %), no gaps). Closest hits using the **actA** sequence had highest similarity to *Pseudocercospora hakeae* (GenBank JQ325017.1; Identities = 587/588 (99 %), no gaps), *Pseudocercospora cruenta* (GenBank JQ325012.1; Identities = 574/590 (97 %), 2 gaps (0 %)), and *Pseudocercospora neriicola* (GenBank KJ869231.1; Identities = 573/589 (97 %), no gaps). Closest hits using the **rpb2** sequence had highest similarity to *Pseudocercospora prunicola* (GenBank MF951621.1; Identities = 851/893 (95 %), no gaps), *Pseudocercospora nymphaeacea* (GenBank LC199939.1; Identities = 813/860 (95 %), no gaps), and *Pseudocercospora flavomarginata* (GenBank MF951619.1; Identities = 841/893 (94 %), no gaps). Closest hits using the **tef1** sequence had highest similarity to *Pseudocercospora hakeae* (GenBank GU384495.1; Identities = 314/315 (99 %), no gaps), *Pseudocercospora basiramifera* (GenBank DQ211677.2; Identities = 458/510 (90 %), 9 gaps (1 %)), and *Pseudocercospora pallida* (GenBank GU384469.1; Identities = 280/315 (89 %), 3 gaps (0 %)). Closest hits using the **tub2** sequence had highest similarity to *Pseudocercospora atomarginalis* (GenBank KM452894.1; Identities = 226/235 (96 %), no gaps), *Pseudocercospora pyracanthigena* (GenBank JX902271.1; Identities = 225/235 (96 %), no gaps), and *Pseudocercospora tereticornis* (GenBank JX902280.1; Identities = 224/235 (95 %), no gaps).

Pseudoconiothyrium Crous & R.K. Schumach., **gen. nov.** MycoBank MB829339.

Etymology: Name refers to its morphological similarity to the genus *Coniothyrium*, from which it is phylogenetically distinct.

Conidiomata eustromatica, pycnidial, aggregated, globose with central opening; wall of 6–10 layers of brown *textura angularis*. *Conidiophores* reduced to conidiogenous cells lining inner cavity, hyaline, smooth, doliiform to ampulliform, phialidic with periclinal thickening, and at times with percurrent proliferation. *Conidia* solitary, aseptate, subcylindrical to ellipsoid to subglobose, apex obtuse, base truncate to bluntly rounded, medium brown, verruculose.

Type species: *Pseudoconiothyrium broussonetiae* Crous & R.K. Schumach.

Pseudoconiothyrium broussonetiae Crous & R.K. Schumach., **sp. nov.** MycoBank MB829340. Fig. 47.

Etymology: Name refers to the host genus *Broussonetia* from which it was isolated.

Conidiomata eustromatica, pycnidial, aggregated, 250–400 µm diam, globose with central opening; wall of 6–10 layers of brown *textura angularis*. *Conidiophores* reduced to conidiogenous cells lining inner cavity, hyaline, smooth, doliiform to ampulliform, phialidic with periclinal thickening, and at times with percurrent proliferation, 5–10 × 4–6 µm. *Conidia* solitary, aseptate, subcylindrical to ellipsoid to subglobose, apex obtuse, base truncate to bluntly rounded, medium brown, verruculose, (5–) 6–7(–8) × (4.5–)5(–6) µm.

Culture characteristics: Colonies spreading, with folded surface, moderate aerial mycelium and smooth, lobate margin, reaching 30 mm diam after 2 wk at 25 °C. On MEA surface dirty white to ochreous, reverse ochreous; on PDA surface pale luteous to ochreous, reverse ochreous; on OA surface ochreous with diffuse ochreous pigment.

Typus: Italy, Firenze, Plaza della indipendenza, branch of *Broussonetia papyrifera* (*Moraceae*), 16 Feb. 2017, G. Bonari & R.K. Schumacher, HPC 2009 = RKS 68 (**holotype** CBS H-23822, culture ex-type CPC 33570 = CBS 145036).

Notes: *Pseudoconiothyrium* is allied to *Paraconiothyrium* in the phylogenetic tree, but it is phylogenetically distinct from the latter genus. Based on a megablast search of NCBI's GenBank nucleotide database, the closest hits using the **ITS** sequence had highest similarity to *Pseudocoleophoma typhicola* (GenBank NR_154350.1; Identities = 508/563 (90 %), 13 gaps (2 %)), *Coniothyrium crepinianum* (GenBank MH860873.1; Identities = 507/574 (88 %), 25 gaps (4 %)), and *Pseudocoleophoma polygonicola* (GenBank NR_154274.1; Identities = 429/470 (91 %), 11 gaps (2 %)). Closest hits using the **LSU** sequence are *Aquadictyospora lignicola* (as *Pleosporales* sp. ZLL-2017a, GenBank MF948629.1; Identities = 774/789 (98 %), 1 gap (0 %)), *Dictyosporium tratense* (as *Dictyocheirospora* sp. YJ-2018b, GenBank MH381776.1; Identities = 814/831 (98 %), 4 gaps (0 %)), and *Cheiromyces inflatus* (GenBank JQ267363.1; Identities = 802/819 (98 %), 1 gap (0 %)). Very distant hits



Fig. 47. *Pseudoconiothyrium broussonetiae* (CPC 33570). **A.** Conidiomata on PDA. **B, C.** Conidiogenous cells. **D.** Conidia. Scale bars: A = 300 µm, B–D = 10 µm.

using the *tef1* sequence had highest similarity to *Xenophoma puncteliae* (GenBank KP170686.1; Identities = 265/321 (83 %), 18 gaps (5 %)) and *Pseudochaetosphaeronema ginkgonis* (as *Pseudochaetosphaeronema* sp. XYD-2016a, GenBank KU365984.1; Identities = 278/345 (81 %), 18 gaps (5 %)).

Pseudophaeophleospora phormii (Naito) Crous, **comb. nov.** MycoBank MB829341. Fig. 48.

Basionym: *Hendersonia phormii* Naito, *Science Rep. Kagoshima Univ.* 1: 77. 1952.

Synonyms: *Kirramyces phormii* (Naito) M.E. Palm, *Mycol. Res.* 100: 374. 1996.

Phaeophleospora phormii (Naito) Crous *et al.*, *S. Afr. J. Bot.* 63: 115. 1997.

Leaf spots brown, elliptical to elongate, surrounded by a dark red-purple border. **Conidiomata** pycnidial, immersed, solitary, globose to subglobose, up to 200 µm diam; wall of 3–6 layers of brown *textura angularis*. **Conidiophores** reduced to conidiogenous cells lining the inner cavity. **Conidiogenous cells** cylindrical to lageniform, medium brown, finely roughened, 10–15 × 4–5 µm, proliferating percurrently near apex. **Conidia** solitary, medium brown, verruculose, aggregating in mucoid mass, cylindrical, apex obtuse, base truncate, 2–3 µm diam, with marginal frill, 3(–6)-septate, (30–)38–55(–60) × (3–)3.5(–4) µm.

Culture characteristics: Colonies erumpent, spreading, with moderate aerial mycelium, folded surface and smooth, lobate margin, reaching 7 mm diam after 2 wk at 25 °C. On MEA surface grey olivaceous, reverse olivaceous grey; on PDA surface dirty white, reverse olivaceous grey; on OA surface dirty white with diffuse red pigment.

Typus: **New Zealand**, Levin, Earl St, on *Phormium tenax*, 12 Dec. 1971, G. Laudon, PDD 39822 (**neotype** designated by Palm 1996); Auckland, Grey Lynn Park, on *Phormium tenax* (*Asphodelaceae*), 5 Oct. 2016, R. Thangavel T16_03297D (**epitype designated here** CBS H-23264, MBT385290, culture ex-epitype CPC 32742 = CBS 144606).

Notes: *Pseudophaeophleospora* was established by Videira *et al.* (2017) to accommodate a phaeophleospora-like genus occurring on *Eucalyptus*. The two genera are morphologically similar, and best distinguished based on their DNA sequences.

The present collection closely matches the morphology of the neotype of *Hendersonia phormii*, described by Palm (1996).

Unfortunately, the culture used in the latter paper is no longer viable, and could thus not be deposited. The culture from the present collection is thus herewith designated as epitype, to fix the phylogenetic application of the name.

Based on a megablast search of NCBI's GenBank nucleotide database, the closest hits using the **ITS** sequence had highest similarity to *Pseudophaeophleospora atkinsonii* (as *Phaeophleospora atkinsonii*, GenBank GU214643.1; Identities = 480/505 (95 %), no gaps), *Pallidocercospora acaciigena* (GenBank MH862893.1; Identities = 478/520 (92 %), 5 gaps (0 %)), and *Pallidocercospora heimii* (as *Mycosphaerella heimii*, GenBank GQ852745.1; Identities = 479/521 (92 %), 7 gaps (1 %)). Closest hits using the **LSU** sequence are *Pseudophaeophleospora atkinsonii* (as *Phaeophleospora atkinsonii*, GenBank GU214463.1; Identities = 839/849 (99 %), no gaps), *Pallidocercospora irregulariramosa* (GenBank GU214441.1; Identities = 878/892 (98 %), 1 gap (0 %)), and *Pallidocercospora holualoana* (as *Mycosphaerella holualoana*, GenBank JF770467.1; Identities = 877/892 (98 %), 1 gap (0 %)). No **actA** sequences of *Pseudophaeophleospora* are available for comparison on GenBank; distant hits include *Pseudocercospora udagawana* (GenBank GU320527.1; Identities = 544/604 (90 %), 12 gaps (1 %)), *Parapallidocercospora thailandica* (as *Pallidocercospora thailandica*, GenBank EU514333.1; Identities = 496/535 (93 %), 7 gaps (1 %)), and *Pallidocercospora heimii* (GenBank KF903399.1; Identities = 487/525 (93 %), 6 gaps (1 %)). No **tef1** sequences of *Pseudophaeophleospora* are available for comparison on GenBank; distant hits include *Pallidocercospora crystallina* (GenBank MF135483.1; Identities = 376/463 (81 %), 27 gaps (5 %)), *Parapallidocercospora thailandica* (as *Mycosphaerella thailandica*, GenBank AY840477.2; Identities = 329/399 (82 %), 24 gaps (6 %)), and *Neoceratosperma cyatheae* (GenBank KT037504.1; Identities = 184/196 (94 %), no gaps).

Pseudorobillardaceae Crous, **fam. nov.** MycoBank MB829342.

Etymology: Name refers to the genus *Pseudorobillarda*.

Conidiomata immersed, globose, unilocular, with central ostiole; wall of 3–6 layers of thin-walled, flattened *textura angularis*; conidiomata giving rise to both micro- and macroconidia. **Macroconidiophores** lining the inner cavity, reduced to conidiogenous cells, hyaline, smooth, doliiform, phialidic with periclinal thickening and flared collarete, or proliferating percurrently when older. **Paraphyses** numerous, hyphae-like, intermingled among conidiophores, aseptate, flexuous.

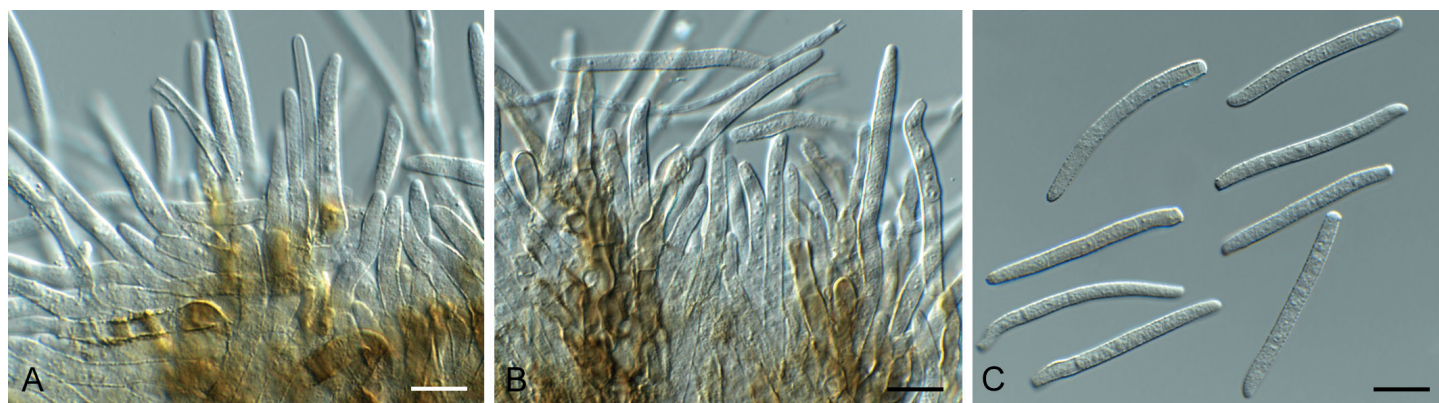


Fig. 48. *Pseudophaeophleospora phormii* (CPC 32742). **A, B.** Conidiogenous cells. **C.** Conidia. Scale bars = 10 µm.

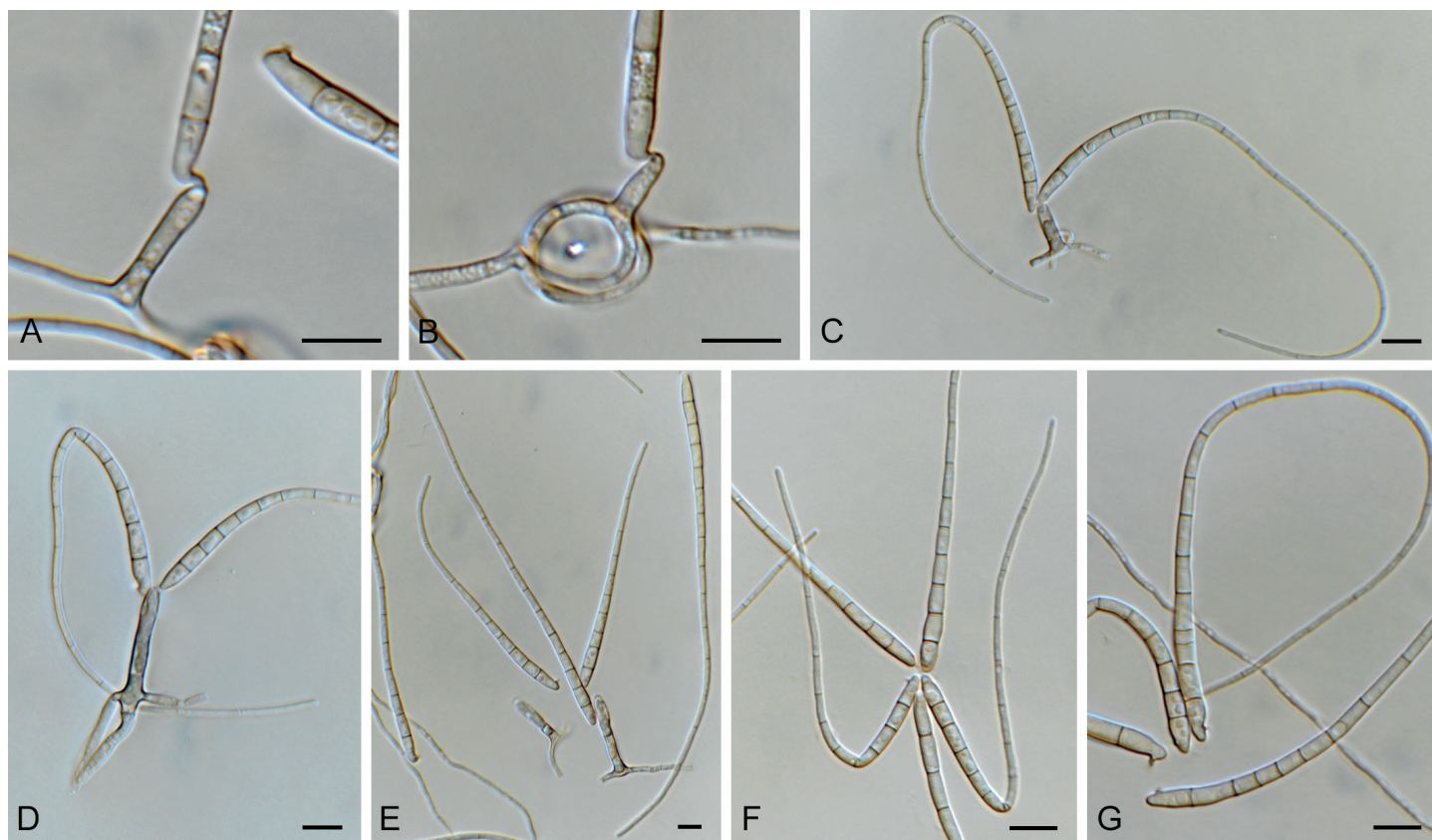


Fig. 49. *Pseudosigmoidea alnicola* (CPC 33776). **A–E.** Conidiogenous cells giving rise to conidia. **F, G.** Conidia. Scale bars = 10 μm .

Macroconidia solitary, septate, guttulate, hyaline, smooth, apex subobtuse, tapering to a truncate base; apical appendages arising from splitting of the conidial sheath, hair-like, flexuous, unbranched, fragile, flexuous, unbranched, mostly absent. *Microconidiogenous cells* hyaline, smooth, subcylindrical to ampulliform, proliferating percurrently. *Microconidia* solitary, aseptate, hyaline, smooth, guttulate, subcylindrical, apex obtuse, base truncate; apical appendages hair-like, flexuous, unbranched, fragile, flexuous, unbranched.

Type genus: *Pseudorobillarda* M. Morelet (1968)

Type species: *Pseudorobillarda phragmitis* (Cunnell) M. Morelet.

Notes: *Pseudorobillarda bolusanthi* was recently introduced by Crous *et al.* (2018b), and placed in the *Pseudorobillardaceae* (*Dothideomycetes*). The family, however, was unpublished, and is therefore formally introduced here.

Pseudosigmoidea alnicola Crous & R.K. Schumach., *sp. nov.* MycoBank MB829346. Fig. 49.

Etymology: Name reflects the host genus *Alnus* from which it was isolated.

Mycelium consisting of pale brown, smooth, 1.5–2 μm diam hyphae, frequently forming hyphal coils, giving rise to solitary, erect conidiophores, subcylindrical, unbranched, pale brown, smooth, 0–1-septate, 10–20 \times 2.5–3 μm . *Conidiogenous cells* integrated, terminal, pale brown, smooth, subcylindrical, 5–15 \times 1.5–3 μm ; apex with one to several denticles-like loci, 0.5–1 \times 1 μm . *Conidia* obclavate, flexuous, multi-septate, pale brown,

smooth-walled, guttulate, apex subobtuse, base obconically truncate, widest at first basal septum, base bluntly rounded, attached to conidiogenous cell via excentric locus which leaves a cylindrical separating cell on the side of the conidium, 1–2 \times 1–1.5 μm , 80–250 \times 3–4 μm , apical region of conidium 1.5–2 μm diam.

Culture characteristics: Colonies spreading, with moderate aerial mycelium and smooth, lobate margin, reaching 25 mm diam after 2 wk at 25 $^{\circ}\text{C}$. On MEA, PDA and OA, surface and reverse umber.

Typus: **Germany**, near Berlin, alder wood, leaf litter of *Alnus glutinosa* (*Betulaceae*), 3 May 2017, R.K. Schumacher, HPC 2100 (**holotype** CBS H-23826, culture ex-type CPC 33776 = CBS 145034).

Notes: *Pseudosigmoidea* (based on *P. cranei*), has rhexolytic conidiogenesis with a separating cell, and long, flexuous, subcylindrical to obclavate, septate, hyaline to pale brown, smooth conidia (Ando & Nakamura 2000). Although the genus is listed as *Ascomycota* “*incertae sedis*”, this study shows that it resides in the *Sympoventuriaceae* (*Venturiales*, *Dothidiomycetes*). *Pseudosigmoidea* is known from two species, *P. cranei* (conidia 26–116.5 \times 1.5–2.5 μm , 3–8-septate) and *P. ibarakiensis* (conidia 68–133 \times 4–8 μm , up to 6-septate; Diene *et al.* 2013), both of which can easily be distinguished from *P. alnicola* based on their conidial morphology.

Based on a megablast search of NCBI’s GenBank nucleotide database, the closest hits using the **ITS** sequence had highest similarity to *Tropospora fumosa* (GenBank DQ351724.1; Identities = 564/585 (96 %), 1 gap (0 %)), *Helicoma monilipes*

(GenBank DQ351723.1; Identities = 556/587 (95 %), 4 gaps (0 %)), and *Pseudosigmoidea ibarakiensis* (GenBank LC146758.1; Identities = 546/577 (95 %), 10 gaps (1 %)). Closest hits using the **LSU** sequence are *Scolecobasidium excentricum* (GenBank MH874174.1; Identities = 854/856 (99 %), no gaps), *Troposporella fumosa* (GenBank MH874121.1; Identities = 850/856 (99 %), no gaps), and *Sympoventuria melaleuca* (GenBank NG_058520.1; Identities = 840/849 (99 %), no gaps).

Pseudoteratosphaeria africana Crous, *sp. nov.* MycoBank MB829347. Fig. 50.

Etymology: Name refers to the continent of Africa where it was collected.

Leaf spots amphigenous, circular, 2–5 mm diam, medium brown, with thin, raised dark brown border. **Ascomata** pseudothecial, predominantly hypophyllous, black, immersed to erumpent, globose, 70–100 µm diam, with apical ostiole; wall of 2–3 layers of brown *textura angularis*. **Asci** paraphysate, fasciculate, bitunicate, sessile, obovoid, straight to slightly curved, 8-spored, 30–35 × 8–11 µm. **Ascospores** bi- to triseriate, overlapping, hyaline, guttulate, thin-walled, straight to slightly curved, obovoid with obtuse ends, widest in middle of apical cell, medianly 1-septate, constricted at septum, tapering towards both ends, but more prominently towards lower end, (11–)12–13(–14) × (2.5–)3–3.5(–4) µm.

Culture characteristics: Colonies erumpent, spreading, with moderate aerial mycelium, folded surface, and smooth, lobate margin, reaching 20–30 mm diam after 2 wk at 25 °C. On MEA, PDA and OA surface and reverse olivaceous grey.

Typus: Angola, Longa River, leaf spot on unidentified host, 6 Nov. 2010, *J. Roux*, HPC 1697 (**holotype** CBS H-23816, culture ex-type CPC 33144 = CBS 144595).

Additional materials examined: Angola, Longa River, leaf spot on unidentified host, 6 Nov. 2010, *J. Roux*, cultures CPC 33145 = CBS 144596, CPC 33072 = CBS 144597.

Notes: *Pseudoteratosphaeria* was introduced by Quaedvlieg *et al.* (2014) to accommodate a genus morphologically similar to *Teratosphaeria*, which lacked any known asexual morphs, and occurred primarily on *Myrtaceae*.

Based on a megablast search of NCBI's GenBank nucleotide

database, the closest hits using the **ITS** sequence of CPC 33072 had highest similarity to *Pseudoteratosphaeria perpendicularis* (GenBank NR_155617.1; Identities = 485/496 (98 %), 1 gap (0 %)), *Pseudoteratosphaeria stramenticola* (as *Mycosphaerella stramenticola*, GenBank DQ632669.1; Identities = 488/500 (98 %), 2 gaps (0 %)), and *Pseudoteratosphaeria gamsii* (as *Teratosphaeria gamsii*, GenBank DQ302959.1; Identities = 481/497 (97 %), 2 gaps (0 %)). The ITS sequences of CPC 33072, 33144 and 33145 are identical. Closest hits using the **LSU** sequence are *Pseudoteratosphaeria perpendicularis* (as *Teratosphaeria perpendicularis*, GenBank JN232443.1; Identities = 859/861 (99 %), no gaps), *Pseudoteratosphaeria ohnowa* (GenBank EU019305.2; Identities = 866/873 (99 %), no gaps), and *Pseudoteratosphaeria flexuosa* (as *Teratosphaeria flexuosa*, GenBank JN232432.1; Identities = 877/885 (99 %), no gaps). The LSU sequences of CPC 33072, 33144 and 33145 are identical. Closest hits using the **actA** sequence had highest similarity to *Pseudoteratosphaeria stramenticola* (GenBank KF903530.1; Identities = 515/541 (95 %), 2 gaps (0 %)), *Pseudoteratosphaeria perpendicularis* (GenBank KF903491.1; Identities = 513/540 (95 %), no gaps), and *Pseudoteratosphaeria gamsii* (GenBank KF903494.1; Identities = 510/540 (94 %), no gaps). The *actA* sequences of CPC 33072, 33144 and 33145 are identical. Closest hits using the **tef1** sequence had highest similarity to *Pseudoteratosphaeria perpendicularis* (GenBank KF903232.1; Identities = 320/347 (92 %), 5 gaps (1 %)), *Pseudoteratosphaeria stramenticola* (GenBank KF903237.1; Identities = 319/354 (90 %), 16 gaps (4 %)), and *Pseudoteratosphaeria gamsii* (GenBank KF903229.1; Identities = 311/352 (88 %), 13 gaps (3 %)). The *tef1* sequences of CPC 33072, 33144 and 33145 are identical. Closest hits using the **tub2** sequence had highest similarity to *Pseudoteratosphaeria ohnowa* (as *Teratosphaeria ohnowa*, GenBank KF442464.1; Identities = 304/338 (90 %), 6 gaps (1 %)), *Pseudoteratosphaeria gamsii* (GenBank KF902933.1; Identities = 221/246 (90 %), 3 gaps (1 %)), and *Pseudoteratosphaeria perpendicularis* (GenBank KF902936.1; Identities = 218/247 (88 %), 5 gaps (2 %)). The *tub2* sequences of CPC 33072 and 33145 are identical; the sequence of CPC 33144 differs at one nucleotide from the others.

Porodiplodia vitis Crous & R.K. Schumach., *sp. nov.* MycoBank MB829349. Fig. 51.

Etymology: Name refers to the host genus *Vitis* from which it was isolated.



Fig. 50. *Pseudoteratosphaeria africana* (CPC 33144). **A.** Leaf spot. **B–E.** Asci and ascospores. Scale bars: A = 5 mm, B–E = 10 µm.

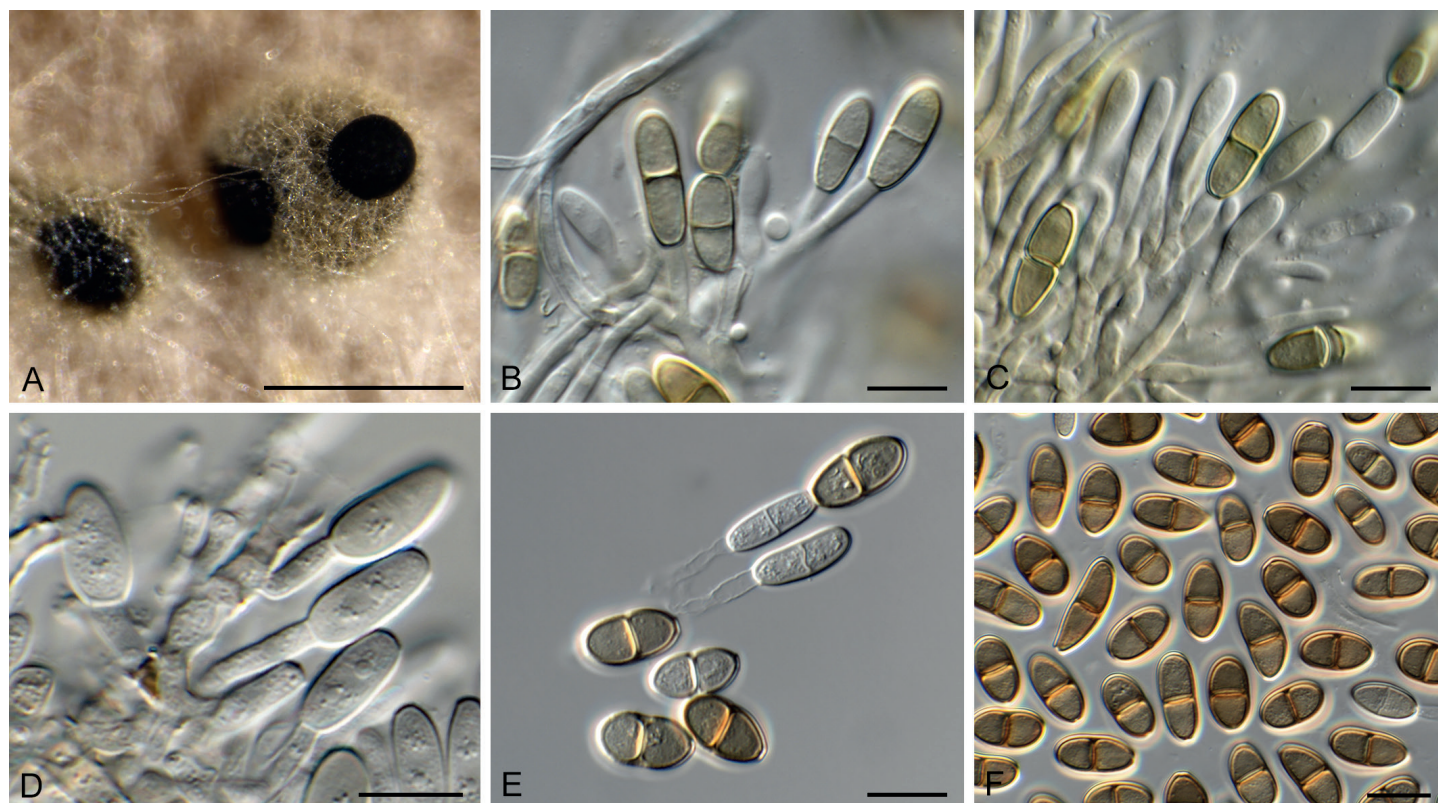


Fig. 51. *Porodiplodia vitis* (CPC 31642). **A.** Conidiomata on OA. **B–E.** Conidiogenous cells giving rise to conidia. **F.** Conidia. Scale bars: A = 300 µm, B–F = 10 µm.

Conidiomata eustromatic, uni- to multilocular, brown, globose, 150–300 µm, aggregated on agar, ostiolate. *Conidiophores* lining inner cavity, subcylindrical, hyaline, smooth, branched, 1–3-septate, 15–20 × 2.5–4 µm, proliferating percurrently near apex. *Paraphyses* intermingled among conidiophores, hyaline, smooth, septate, subcylindrical with obtuse ends, 25–30 × 3–4 µm. *Conidia* in short chains (–3), fusoid-ellipsoid to subcylindrical, medium brown, finely verruculose, guttulate, thick-walled, 1-septate, apex obtuse (at times with central pore), base truncate with central pore, 2 µm diam, (13–)14–16(–19) × (5–)6(–8) µm.

Culture characteristics: Colonies erumpent, spreading, with moderate aerial mycelium and smooth, lobate margin, reaching 35 mm diam after 2 wk at 25 °C. On MEA surface cinnamon to buff, reverse sienna; on PDA surface saffron, reverse cinnamon; on OA surface cinnamon, with diffuse cinnamon pigment.

Typus: USA, New York, Bronx, Van Cortlandt Park, on canes of *Vitis vinifera* (*Vitaceae*), 2016, E. Crenson & R.K. Schumacher, HPC 1372 (**holotype** CBS H-23795, culture ex-type CBS 144634 = CPC 31642).

Notes: *Porodiplodia* was recently established for a genus occurring on leaves of *Livistona australis* in Australia, characterised by having eustromatic conidiomata, and conidia occurring in short chains, with a pore at each end of its conidia (Crous *et al.* 2018c). *Porodiplodia vitis* differs from *P. livistonae* (conidia (14–)15–17(–20) × 5(–6) µm) in having shorter, wider conidia.

Based on a megablast search of NCBI's GenBank nucleotide database, the closest hits using the **ITS** sequence had highest similarity to *Porodiplodia livistonae* (GenBank MH327809.1;

Identities = 533/536 (99 %), no gaps), *Chalara clidemiae* (GenBank NR_145313.1; Identities = 528/547 (97 %), 1 gap (0 %)), and *Mollisia caespiticia* (GenBank KY965813.1; Identities = 506/542 (93 %), 2 gaps (0 %)). Closest hits using the **LSU** sequence are *Porodiplodia livistonae* (GenBank MH327845.1; Identities = 859/859 (100 %), no gaps), *Chalara clidemiae* (GenBank MH878219.1; Identities = 765/772 (99 %), no gaps), and *Chaetochalara africana* (as *Chalara africana*, GenBank FJ176249.1; Identities = 834/849 (98 %), 2 gaps (0 %)). No **tef1** sequences of *Porodiplodia* are available on GenBank for comparison; distant hits using the **tef1** sequence had highest similarity to *Davidhawksworthia ilicicola* (GenBank KU728592.1; Identities = 205/233 (88 %), 7 gaps (3 %)), *Hymenoscyphus menthae* (GenBank KM114512.1; Identities = 203/231 (88 %), 6 gaps (2 %)), and *Fusarium napiforme* (GenBank KM099398.1; Identities = 201/231 (87 %), 4 gaps (1 %)).

Selenodriella fertilis (Piroz. & Hodges) R.F. Castañeda & W.B. Kendr., *Univ. Waterloo Biol. Ser.* **33**: 34. 1990. Fig. 52.

Basionym: *Circinotrichum fertile* Piroz. & Hodges, *Canad. J. Bot.* **51**: 160. 1973.

Conidiophores dimorphic. *Microconidiophores* reduced to conidiogenous cells or with a supporting cell, arising directly from mycelium, hyaline, smooth, subcylindrical, tapering toward denticulate apex, 7–12 × 2.5–3.5 µm. *Macroconidiophores* erect, arising from superficial hyphae, flexuous, branched or not, base with T-cell or rhizoids, subcylindrical, 60–140 × 4–5 µm, 4–10-septate, lateral branches 0–3-septate, 15–60 × 2.5–3 µm. *Conidiogenous cells* pale brown, smooth, subcylindrical to elongated fusoid-ellipsoid, terminal and intercalary, with apical rachis of denticulate loci; denticles 1–2 × 1–1.5 µm, scars somewhat darkened, not thickened nor refractive, 20–30 × 2.5–

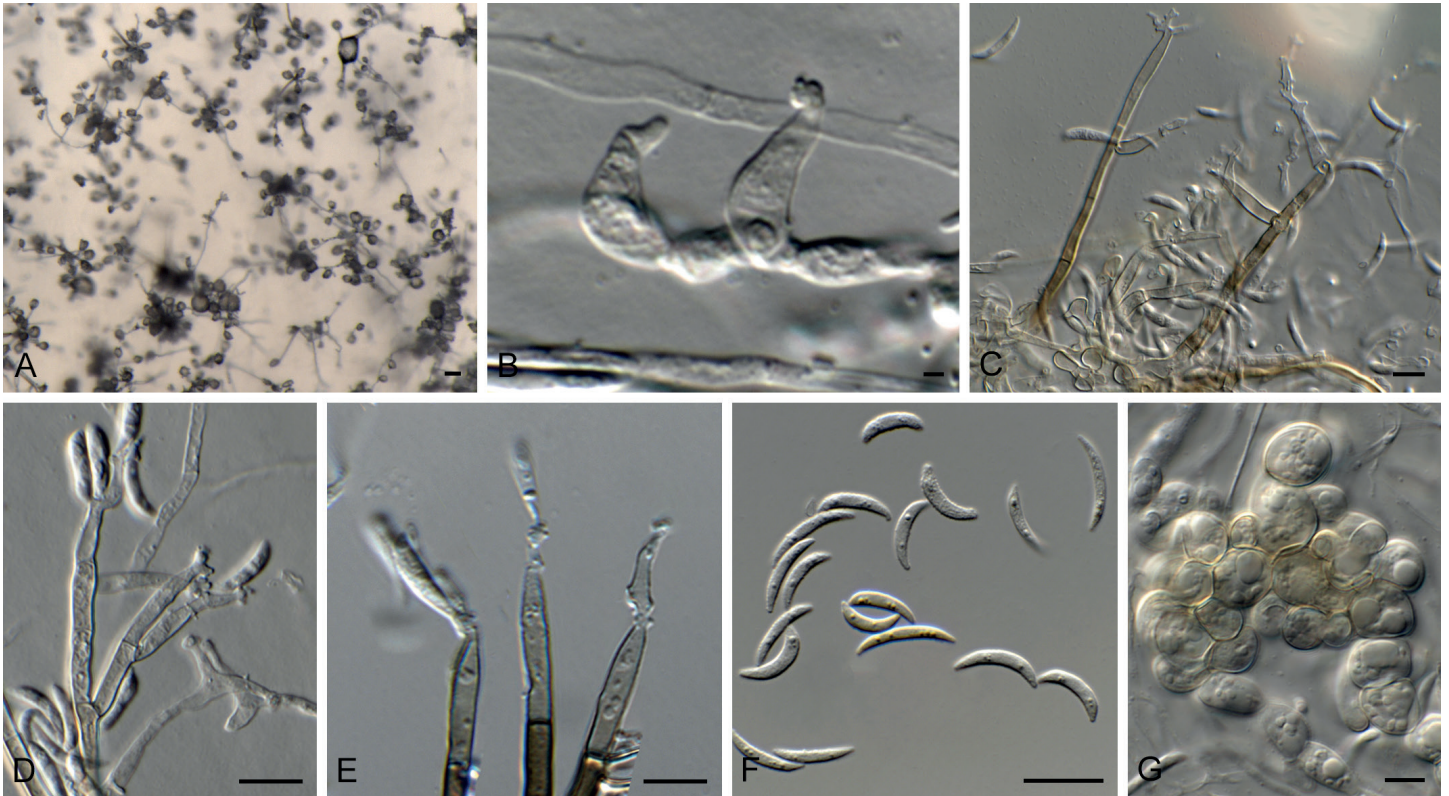


Fig. 52. *Selenodriella fertilis* (CPC 32663). **A.** Colony on SNA. **B.** Conidiogenous cells. **C–E.** Conidiophores. **F.** Conidia. **G.** Chlamydospores. Scale bars: A = 100 μ m, B–G = 10 μ m.

3 μ m. *Conidia* aggregating in mucoid masses, aseptate, fusoid-ellipsoid, prominently curved, apex subobtuse, base truncate, 1 μ m diam, not thickened nor darkened, (9–)12–14(–15) \times 2(–3) μ m. *Chlamydospores* in chains, globose, thin-walled, hyaline, becoming pale brown and forming microsclerotia, 7–12 μ m diam.

Culture characteristics: Colonies flat, spreading, with sparse aerial mycelium, folded surface and smooth, even margin, reaching 35 mm diam after 2 wk at 25 °C. On MEA surface and reverse isabelline to buff; on PDA surface and reverse olivaceous grey; on OA surface olivaceous grey.

Material examined: **Australia**, Victoria, Nowa Nowa, on leaf litter of *Eucalyptus* sp. (*Myrtaceae*), 30 Nov. 2016, P.W. Crous, HPC 1876, culture CPC 32663 = CBS 144589.

Notes: For notes on *Selenodriella*, see Hernández-Restrepo et al. (2016), who confirmed the occurrence of *Selenodriella fertilis* in Australia on *Hakea baxteri*.

Based on a megablast search of NCBI's GenBank nucleotide database, the closest hits using the **ITS** sequence had highest similarity to *Selenodriella fertilis* (GenBank MH861691.1; Identities = 525/526 (99 %), no gaps), *Gyrothrix circinata* (GenBank KJ476968.1; Identities = 477/483 (99 %), 5 gaps (1 %)), and *Selenodriella cubensis* (GenBank NR_154414.1; Identities = 515/522 (99 %), 1 gap (0 %)). Closest hits using the **LSU** sequence are *Selenodriella fertilis* (GenBank KP858992.1; Identities = 849/851 (99 %), 1 gap (0 %)), *Selenodriella cubensis* (GenBank NG_058151.1; Identities = 844/852 (99 %), 1 gap (0 %)), and *Gyrothrix verticiclada* (GenBank KC775726.1; Identities = 800/821 (97 %), 6 gaps (0 %)).

Stagonospora pseudoperfecta Kaz. Tanaka & K. Hiray., *Stud. Mycol.* **82**: 106. 2015. Fig. 53.

Conidiomata globose, brown, 250–300 μ m diam (with papillate neck on host tissue); wall of 2–3 layers of brown *textura angularis*. *Conidiophores* reduced to conidiogenous cells. *Conidiogenous cells* lining the inner cavity, hyaline, smooth, ampulliform to subcylindrical, 5–10 \times 3–5 μ m; proliferating percurrently. *Conidia* solitary, hyaline, smooth, fusoid-ellipsoid, guttulate, 3-septate, apex obtuse, tapering from basal septum to truncate hilum, 2 μ m diam, (13–)20–22(–250 \times (4–)5(–6) μ m).

Culture characteristics: Colonies erumpent, spreading, with abundant, fluffy aerial mycelium covering dish after 2 wk at 25 °C. On MEA, PDA and OA surface smoke grey, and reverse olivaceous grey.

Material examined: **Germany**, near Berlin, on *Typha* sp. (*Typhaceae*), 1 Apr. 2017, R.K. Schumacher, RKS 85 = HPC 2026, culture CPC 33138 = CBS 144607.

Notes: *Stagonospora pseudoperfecta* was described from dead leaves of *Typha latifolia* collected in Japan (Tanaka et al. 2015), and this is the first record of the fungus from Europe.

Based on a megablast search of NCBI's GenBank nucleotide database, the **ITS** sequence was identical to *Stagonospora pseudoperfecta* (GenBank NR_155768.1; Identities = 497/497 (100 %)); and related to *Stagonospora trichophoricola* (GenBank KY750315.1; Identities = 533/538 (99 %), 1 gap (0 %)) and *Stagonospora bicolor* (as *Saccharicola bicolor*, GenBank KT367526.1; Identities = 530/535 (99 %), 1 gap (0 %)). Closest hits using the **LSU** sequence are *Stagonospora pseudoperfecta* (GenBank NG_059399.1; Identities = 797/797 (100 %)),



Fig. 53. *Stagonospora pseudoperfecta* (CPC 33138). **A–C.** Conidiogenous cells. **D.** Conidia. Scale bars = 10 μ m.

Stagonospora forlicesenensis (GenBank NG_059716.1; Identities = 794/797 (99 %), no gaps), and *Stagonospora imperaticola* (GenBank NG_059793.1; Identities = 793/797 (99 %), no gaps). No **tef1** sequences of *Stagonospora pseudoperfecta* are available for comparison on GenBank; distant hits include *Helminthosporium oligosporum* (GenBank KY984449.1; Identities = 304/364 (84 %), 19 gaps (5 %)), *Helminthosporium tiliae* (GenBank KY984456.1; Identities = 304/364 (84 %), 19 gaps (5 %)), and *Corynespora leucadendri* (GenBank KF253110.1; Identities = 313/381 (82 %), 22 gaps (5 %)). No **tub2** sequences of *Stagonospora pseudoperfecta* are available for comparison on GenBank; distant hits include *Stagonospora victoriana* (GenBank MG386166.1; Identities = 331/389 (85 %), 13 gaps (3 %)), *Stagonospora chrysopyla* (GenBank KM033943.1; Identities = 322/387 (83 %), 14 gaps (3 %)), and *Stagonospora cf. paludosa* (GenBank KF252737.1; Identities = 245/296 (83 %), 11 gaps (3 %)).

Sympodiella W.B. Kendr., *Trans. Br. Mycol. Soc.* **41**: 519. 1958. **emend.** Hern.-Restr. & Crous

Mycelium consisting of pale to medium brown, smooth, septate, branched hyphae. *Sympodiella* morph. *Conidiophores* solitary, erect, medium brown, smooth, subcylindrical, straight to flexuous, unbranched, septate, sometimes proliferating

percurrently (in culture). *Conidiogenous cells* terminal, subcylindrical, medium brown, polyblastic, sympodial. *Conidia* aseptate or septate, sometimes constricted at the septa, subcylindrical to acicular, apex obtuse, base truncate, smooth, hyaline to subhyaline. Repetophragma-like *Synasexual morph.* *Conidiophores* solitary, erect, medium brown, smooth, subcylindrical, straight to geniculous-sinuous, unbranched, septate, proliferating percurrently. *Conidiogenous cells* terminal, subcylindrical, straight or flexuous, medium brown, mono- or polyblastic, sometimes sympodial (mainly in culture). *Conidia* solitary, septate, subcylindrical, straight, apex obtuse, sometimes with a dark cap, base truncate, with or without a minute marginal frill, smooth, pale- to medium brown, guttulate; hilum unthickened, not darkened.

Type species: Sympodiella acicola W.B. Kendr.

Notes: We emend *Sympodiella* to include species with a repetophragma-like synasexual morph. A new species is introduced as *S. quercina* and additionally two new combinations are proposed and discussed below.

Sympodiella acicola W.B. Kendr., *Trans. Br. Mycol. Soc.* **41**: 519. 1958. Figs 54–56.

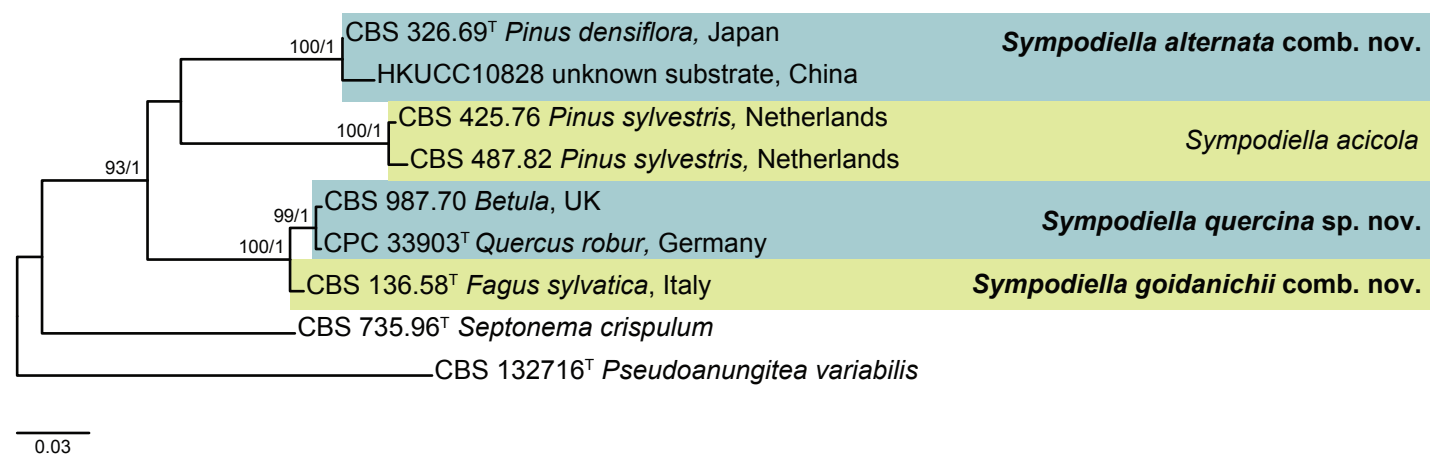
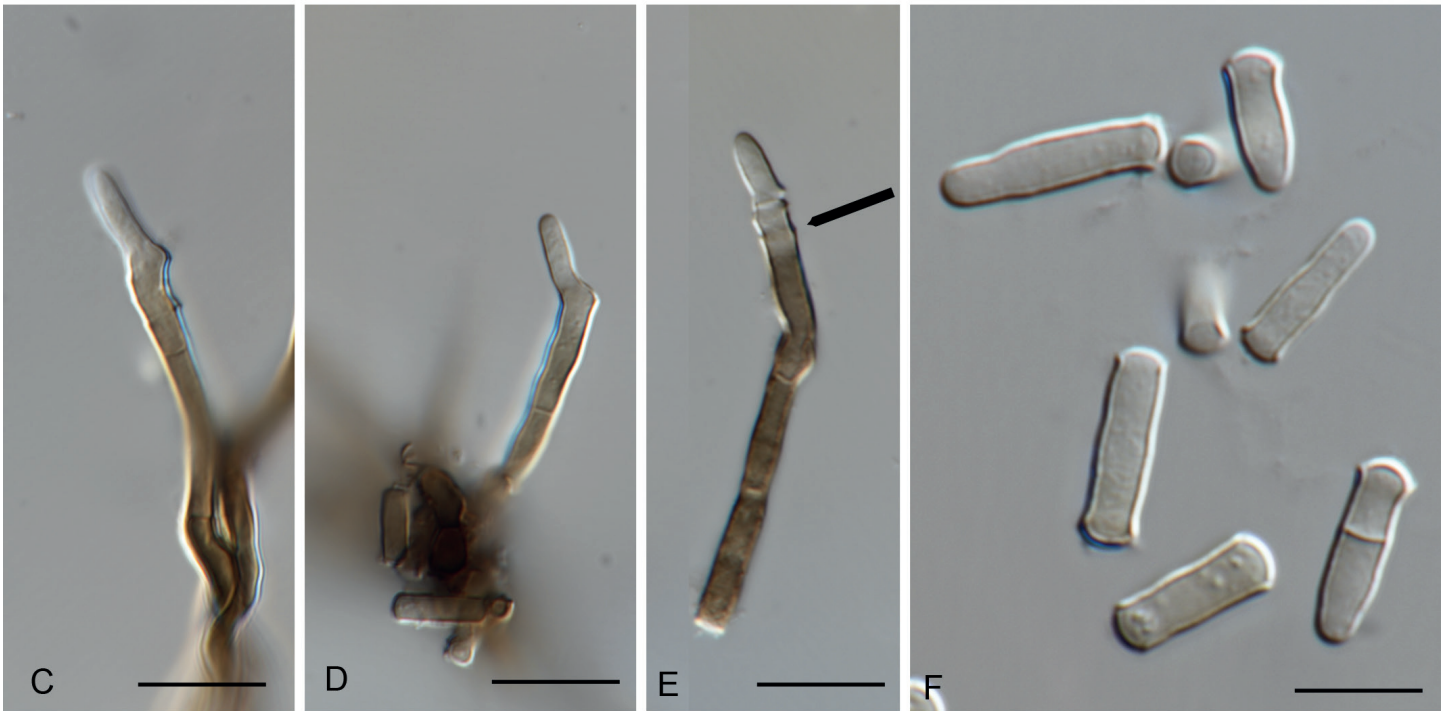
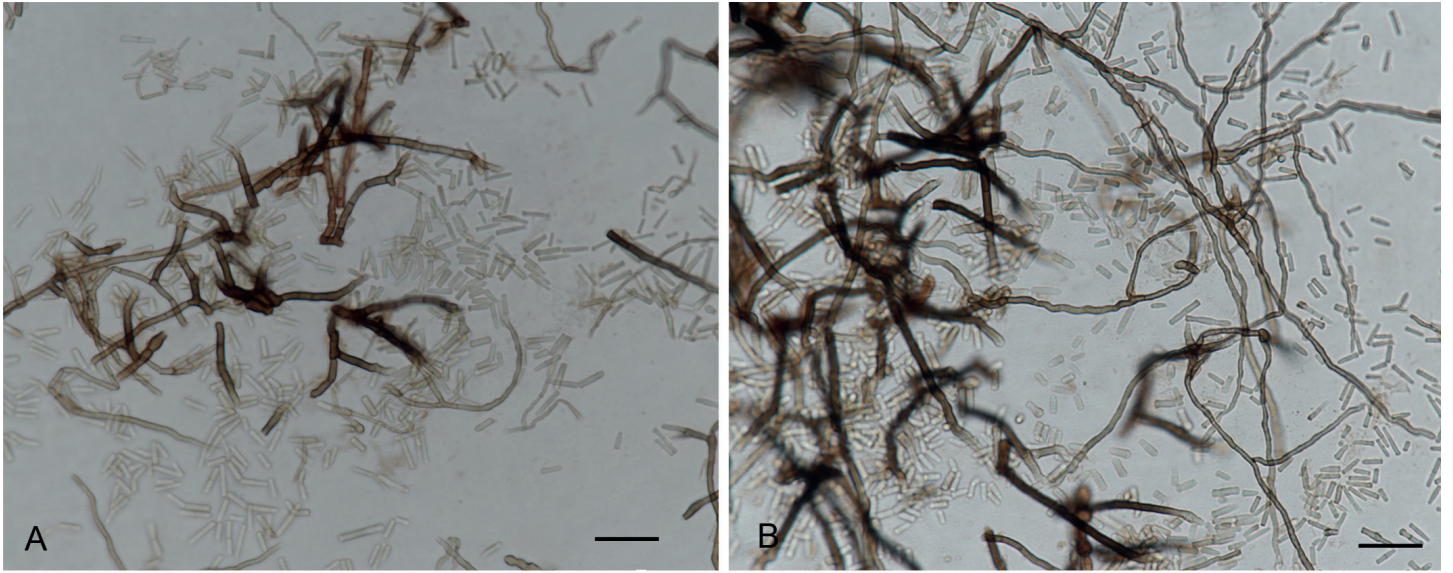


Fig. 54. RAxML phylogenetic tree obtained from a phylogenetic analysis of the *Sympodiella* ITS, LSU, *rpb2* and *tef1* alignment (9 strains including outgroup; 4014 characters analysed: 699 from ITS, 886 from LSU, 921 from *rpb2*, and 1508 from *tef1*). The tree was rooted to *Pseudoanungitea variabilis* CBS 132716 and *Septonema crispulum* CBS 735.96 and the scale bar indicates the number of changes. Bootstrap support values higher than 70 % and Bayesian posterior probabilities higher than 0.95 are shown at the nodes and the species clades are highlighted with coloured boxes. Species names are indicated to the right of the tree. Strain numbers are followed by the substrate/source and country of origin are indicated for each strain.



Fig. 55. *Sympodiella acicola* (CBS H-1620 - *Pinus* needles). **A–L.** *Sympodiella* asexual morph. **A–G.** Conidiophores, conidiogenous cells and conidia. **H–L.** Conidia. **M–V.** Repetophragma-like synsexual morph. **M–S.** Conidiophores and conidia. **T–V.** Conidia. Scale bars = 10 µm.

Fig. 56. *Sympodiella acicola* (CBS 487.82 on OA). **A–E, G, H.** Conidiophores, conidiogenous cells and conidia (arrows showing percurrent proliferations). **F, I–K.** Conidia. Scale bars: A, B = 20 µm, C–K = 10 µm.



Typus: UK, Cheshire, on *Pinus sylvestris* (Pinaceae), 1956, W.B. Kendrick, **holotype** IMI 69967. **Netherlands**, Baarn, De Vuursche, on *Pinus sylvestris*, 12 Apr. 1982, G.S. de Hoog (**epitype** designated here CBS H-1620 MBT385535, ex-epitype culture CBS 487.82).

Synasexual morph repetophragma-like. *Conidiophores* brown, smooth, proliferating percurrently, up to 25 µm long, 2–3.5 µm wide at the base. *Conidiogenous cells* terminal, brown. *Conidia* 3–4(–7)-septate, subcylindrical, straight, apex obtuse, base truncate, with a minute marginal frill, smooth, pale- to medium brown, 13–35 × 3–4 µm.

Notes: Conidia in *S. acicola* have been considered arranged in unbranched chains (Kendrick 1958, Seifert *et al.* 2011). During an examination of the specimen CBS H-1620, some of these conidia resemble phragmoconidia constricted at the septa similar to those described in *Wiesneriomyces*, since they often remain connected together after they separate from the conidiogenous cells. In culture however (CBS 487.82), they are readily deciduous. Furthermore, in a specimen of *Sympodiella acicola* (CBS H-1620) the conidiophores were mixed with a repetophragma-like conidiophores described here as the synasexual morph of *Sympodiella acicola*. Interestingly, in culture (CBS 487.82) we observed some conidiophores with percurrent proliferations and the 1-septate conidia were more abundant than in natural substrate. This species has been reported mainly from *Pinus* spp. (Kendrick 1958, Ellis 1976).

Sympodiella alternata (Tubaki & Saito) Crous & Hern.-Restr., **comb. nov.** MycoBank MB829352. Fig. 57.

Basionym: *Endophragmia alternata* Tubaki & Saito, *Trans. Brit. Mycol. Soc.* **52**: 477. 1969.

Typus: **Japan**, Sendai, on fallen needles of *Pinus densifolia* (Pinaceae), 1966, T. Saitô (**holotype** IFO H-11600, ex-type culture IFO 8933 = CBS 326.69).

Note: *Sympodiella alternata* is only known by the repetophragma-like synasexual morph from Asia (Tubaki & Saitô 1969). During this study we examined the ex-type culture of *Sympodiella alternata* (CBS 326.69). Conidia were similar to those described in the protologue with a dark cap in the apex of the conidia, but they were slightly smaller with less septa (30–36 × 5–6 µm, 5–8-septate vs. (37–)40–46(–70) × 5–6(–7) µm, (7–)8-septate; Tubaki & Saitô 1969). The conidiophores proliferate percurrently and sometimes geniculate conidiophores were observed. This species is known from *Pinus densifolia* from Japan (Tubaki & Saitô 1969) and from an unknown substrate from China (Sheny *et al.* 2006).

Sympodiella goidanichii (Rambelli) Crous & Hern.-Restr., **comb. nov.** MycoBank MB829353.

Basionym: *Ceratosporella goidanichii* Rambelli, *R.C. Secc. Accad. Sci. Ist. Bologna*, sér. 6, **5**: 3. 1958.

Synonyms: *Sporidesmium goidanichii* (Rambelli) S. Hughes, *N.Z. J. Bot.* **17**: 162. 1979.



Fig. 57. *Sympodiella alternata* (CBS 326.69 on OA). **A–C.** Conidiophores with percurrent proliferations. **D, E.** Conidiophores with sympodial proliferations. **F.** Conidiophore with lateral conidia. **G–I.** Conidiophores giving rise to conidia. **J–P.** Conidia. Scale bars = 10 µm.

Repetophragma goidanichii (Rambelli) W.P. Wu, *Fungal Diversity Res. Ser.* **15**: 80. 2005.

Typus: Italy, on cupule of *Fagus sylvatica* (*Fagaceae*), collection date unknown, A. Rambelli, ex-type culture CBS 136.58.

Note: *Sympodiella goidanichii* was described from *Fagus sylvatica* in Italy as *Ceratosporella goidanichii* (Rambelli 1958). Hughes (1979) considered *Ceratosporella goidanichii* and *Endophragma alternata* as conspecific species and include them in *Sporidesmium* due to the successive proliferation of the conidiophores. During his studies the type strain of *Ceratosporella goidanichii* failed to produce conidia and the observations were based on the sporulating culture of *Endophragma alternata* and the descriptions given by Rambelli (1958) and Ellis (1976). Later this species was transferred to *Repetophragma*, because of the percurrent proliferations of the conidiophores and the presence of euseptate conidia (Wu & Zhuang 2005). In our study the ex-type strain of *Ceratosporella goidanichii* (CBS 136.58) remains sterile and the new combination in *Sympodiella* is mainly based on the phylogenetic analysis.

Sympodiella quercina Crous & R.K. Schumach., *sp. nov.* MycoBank MB829351. Figs 58–60.

Etymology: Name refers to the host genus *Quercus* from which it was isolated.

Mycelium consisting of pale to medium brown, smooth, septate, branched, 2.5–3 µm diam hyphae. **Sympodiella-like morph.** **Conidiophores** solitary, erect, medium brown, smooth, subcylindrical, straight to flexuous, unbranched, septate, 48.5–68 × 3–5 µm. **Conidiogenous cells** terminal, subcylindrical, medium brown, polyblastic, sympodial, 15–20 × 3–3.5 µm. **Conidia** septate, subcylindrical to acicular, tapering, apex obtuse, base truncate, smooth, hyaline, 30–74 × 2–3.5 µm, apex 1.5–2.5 µm wide. **Repetophragma-like synasexual morph.** **Conidiophores** solitary, erect, medium brown, smooth, subcylindrical, straight to geniculous-sinuous, unbranched, 2–6-septate, 25–90 × 5–6 µm. **Conidiogenous cells** terminal, subcylindrical, medium brown, 6–17 × 5–6 µm, proliferating percurrently. **Conidia** solitary, subcylindrical, apex obtuse, base truncate, medium brown (end cells frequently subhyaline), smooth, guttulate, straight, (4–)6-septate, (40–)47–55(–65) × (5–)6–6.5(–7) µm; hilum unthickened, not darkened, 5–6.5 µm diam, with minute marginal frill.

Culture characteristics: Colonies erumpent, spreading, with moderate aerial mycelium and smooth, lobate margin, reaching 12 mm diam after 2 wk at 25 °C. On MEA surface umber, reverse chestnut; on PDA surface umber, reverse iron-grey; on OA surface umber.

Typus: Germany, near Berlin, in *Pinus sylvestris* forest, on fallen leaf of *Quercus robur* (*Fagaceae*), 19 Aprs. 2017, H. Schreiber & R.K. Schumacher, HPC 2106 = RKS 94 (**holotype** CBS H-23829, culture ex-type CPC 33903 = CBS 145028).

Additional material examined: UK, Lancashire, on leaf litter of *Betula* sp., 17 Jan. 1968, deposited by J.C. Frankland, CBS 987.70.

Notes: In natural substrate this species has repetophragma-like conidiophores up to 210 µm long with percurrent proliferations

and conidia measuring 32–44 × 5–7 µm, with or without a dark cap in the apex of the conidia. Next to repetophragma-like conidiophores, *Sympodiella* conidiophores were also found, and since the close phylogenetic relationship with *Sympodiella acicola* we also described the synasexual morph. In this species the *Sympodiella* type of conidiophores produce fragile hyaline phragmoconidia similar to those observed in *Cylindrosympodium* (Kendrick & Castañeda 1990) and some species of *Subulispora* (Sutton 1973, Kirk 1985). Additionally, the superficial network of darkly pigmented hyphae described in *S. acicola* (Kendrick 1985) was also observed in *S. quercina*.

An additional strain (CBS 987.70) previously identified as *Repetophragma goidanichii* was phylogenetically related with *S. quercina*. However, the conidial sizes observed in this culture are below the range observed in CPC 33903, and also have more septa (35–50 × 4–7 µm, 6–7(–9)-septate), the dark apical cap was only evident in some of the younger conidia, and conidiophores were not well-developed. The synasexual morph was not observed in any of the cultures of *S. quercina*.

Based on a megablast search of NCBI's GenBank nucleotide database, the closest hits using the **ITS** sequence had highest similarity to *Sporidesmium goidanichii* (GenBank MH860019.1; Identities = 486/489 (99 %), 2 gaps (0 %)), *Septonema crispulum* (GenBank MH862607.1; Identities = 402/445 (90 %), 8 gaps (1 %)), and *Sympodiella acicola* (GenBank KY853468.1; Identities = 432/488 (89 %), 18 gaps (3 %)). Closest hits using the **LSU** sequence are *Repetophragma goidanichii* (GenBank DQ408574.1; Identities = 836/848 (99 %), 1 gap (0 %)), *Sympodiella acicola* (GenBank KY853530.1; Identities = 844/858 (98 %), no gaps), and *Cylindrosympodium lauri* (GenBank EU035414.1; Identities = 836/859 (97 %), 2 gaps (0 %)).

Sympoventuria regnans Crous, *Persoonia* **39**: 425. 2017. Fig. 61.

Mycelium consisting of medium brown, smooth, septate, branched, 1.5–2 µm diam hyphae. **Conidiophores** reduced to conidiogenous cells, or a supporting cell. **Conidiogenous cells** arising directly from hyphae, subcylindrical, medium brown, smooth, 7–18 × 3(–4) µm, with 1(–3) terminal, flat-tipped loci, 1(–1.5) µm diam, thickened and darkened. **Conidia** pale brown, guttulate, smooth-walled, 0(–1)-septate, fusoid-ellipsoid, occurring in chiefly unbranched acropetal chains of up to 10, (10–)13–16(–18) × (2–)3 µm; loci thickened and somewhat darkened, 1(–1.5) µm diam.

Culture characteristics: Colonies flat, spreading, with moderate aerial mycelium and smooth, lobate margin, reaching 10 mm diam after 2 wk at 25 °C. On MEA surface isabelline, reverse umber; on PDA surface umber, reverse dark brick; on OA surface umber.

Material examined: Australia, New South Wales, 31.366346S 151.580038E, Ngulin Nature Reserve, Hell Hole Forest Rd, on leaves of *Eucalyptus pauciflora* (*Myrtaceae*), 13 Jul. 2016, A.J. Carnegie, HPC 1454, culture CPC 31820 = CBS 144605.

Notes: *Sympoventuria* was introduced for a genus of ascomycetes with sympodiella-like asexual morphs occurring on *Eucalyptus* leaf litter in South Africa (Crous *et al.* 2007). *Sympoventuria regnans* is described from leaves of *E. regnans* collected in La Trobe State Forest, Victoria, Australia (Crous *et al.* 2017), and has a similar morphology to the present collection.



Fig. 58. *Sympodiella quercina* (HPC 2106 - *Quercus* leaf). **A–G.** Repetophragma-like synasexual morph. **A–C, E, F.** Conidiophores and conidia. **D.** Network of brown hyphae on the substrate. **G.** Conidia. **H.** Repetophragma-like and *Sympodiella* conidiophores and conidia. **I–M.** *Sympodiella* asexual morph. **I–L.** Conidiophores and conidia. **M.** Conidia. Scale bars **D, E, H, I** = 20 μm , others = 10 μm .

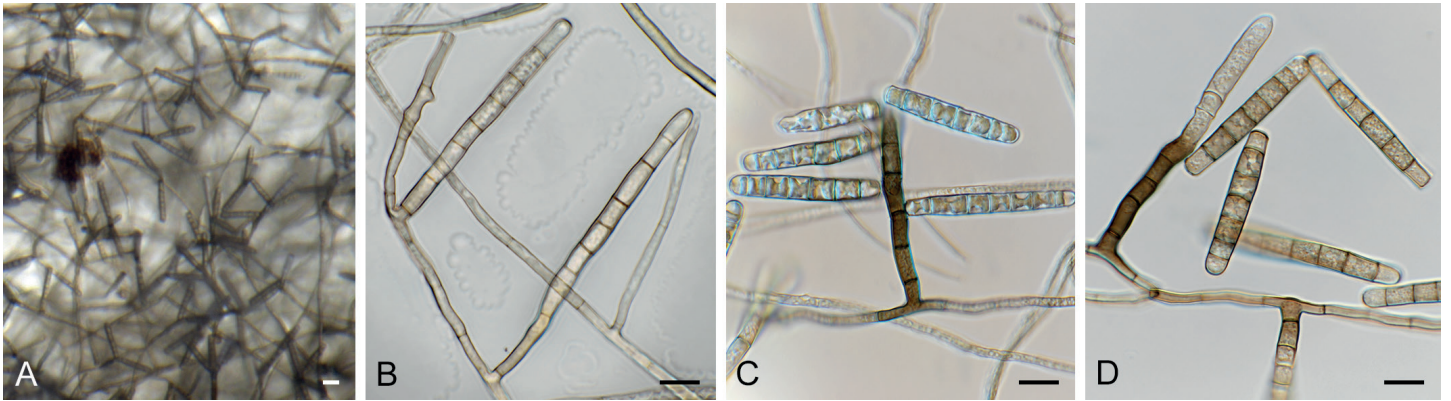


Fig. 59. *Symptodiella quercina* (CPC 33903). A. Colony on SNA. B–D. Conidiophores giving rise to conidia. Scale bars: A = 20 μ m, B–D = 10 μ m.



Fig. 60. *Symptodiella quercina* (CBS 987.70 on SNA). A–D. Conidiophores giving rise to conidia. E, F. Conidiogenous cells. G–K. Conidia. Scale bars = 10 μ m.

Based on a megablast search of NCBI's GenBank nucleotide database, the closest hits using the **ITS** sequence had highest similarity to *Symptoventuria regnans* (GenBank MG386066.1; Identities = 568/569 (99 %), no gaps), *Fusicladium eucalypti* (GenBank HQ599600.1; Identities = 548/573 (96 %), 5 gaps (0 %)), and *Fusicladium eucalypticola* (GenBank NR_145402.1; Identities = 516/538 (96 %), 4 gaps (0 %)). Closest hits using the **LSU** sequence are *Symptoventuria regnans* (GenBank NG_058523.1; Identities = 852/852 (100 %), no gaps), *Fusicladium eucalypticola* (GenBank KX228329.1; Identities = 861/872 (99 %), 1 gap (0 %)), and *Fusicladium eucalypti*

(GenBank HQ599601.1; Identities = 863/877 (98 %), 3 gaps (0 %)). No **tef1** sequences of *Symptoventuria* are available for comparison on GenBank; distant hits include *Pallidocercospora crystallina* (GenBank MF135483.1; Identities = 189/201 (94 %), 3 gaps (1 %)), *Parapallidocercospora thailandica* (as *Mycosphaerella thailandica*, GenBank AY840477.2; Identities = 176/184 (96 %), no gaps), and *Phyllosticta ericarum* (GenBank KR025451.1; Identities = 179/189 (95 %), no gaps). Distant hits using the **tub2** sequence had highest similarity to *Symptoventuria regnans* (GenBank MG386169.1; Identities = 328/373 (88 %), 9 gaps (2 %)), *Didymocyrtis brachylaenae*



Fig. 61. *Sympoventuria regnans* (CPC 31820). A–C. Conidiophores. D. Conidia. Scale bars = 10 μ m.

(GenBank MH327896.1; Identities = 837/946 (88 %), 12 gaps (1 %)), and *Phoma nigrificans* (GenBank AY749030.1; Identities = 836/945 (88 %), 11 gaps (1 %)).

Tubakia suttoniana U. Braun & Crous, *Fungal Syst. Evol.* 1: 90. 2018. Fig. 62.

On SNA: *Pycnothyria* not developing. Central columella developing with aggregated brown, smooth conidiophores. *Conidiophores* tapering toward apex, branched or not, 0–2-septate, 10–30 \times 2.5–3 μ m. *Conidiogenous cells* medium brown, smooth, subcylindrical with apical taper, phialidic, at times with percurrent proliferations, 10–15 \times 2.5–3 μ m. *Conidia* aseptate, solitary, pale brown, smooth, granular, guttulate, ellipsoid, with minute truncate hilum, 1–2 μ m diam, (11–)13–14(–15) \times 7(–8) μ m.

Culture characteristics: Colonies erumpent, spreading in concentric circles, with moderate to profuse aerial mycelium, covering the dish after 2 wk at 25 $^{\circ}$ C. On MEA surface zones of pale olivaceous grey to olivaceous grey, reverse olivaceous grey; on PDA surface zones of olivaceous grey to smoke grey, reverse olivaceous grey; on OA surface olivaceous grey.

Material examined: New Zealand, Auckland, Takanini, Marango PK way, on leaves of *Quercus* sp. (*Fagaceae*), 16 May 2016, R. Thangavel, CBS H-23808, culture CPC 32745 = T16_01981A = CBS 144591.

Notes: *Tubakia suttoniana* is known from branch and stem cankers on *Quercus cerris* in New Zealand (CBS 229.77; Braun et al. 2018), and CPC 32745 represents an additional record from that country.

Based on a megablast search of NCBI's GenBank nucleotide database, the **ITS** sequence was identical to *Tubakia suttoniana* (GenBank MG591919.1; Identities = 605/605 (100 %)); other closest hits included *Tubakia californica* (GenBank MG591847.1; Identities = 602/603 (99 %), 1 gap (0 %)), and *Tubakia melnikiana* (GenBank MG591893.1; Identities = 600/601 (99 %), 1 gap (0 %)). Closest hits using the **LSU** sequence are *Tubakia japonica* (GenBank MG591979.1; Identities = 882/882 (100 %), no gaps), *Tubakia seoraksanensis* (GenBank KP260501.1; Identities = 845/845 (100 %), no gaps), and *Tubakia californica* (GenBank MG591940.1; Identities = 844/844 (100 %), no gaps). Closest hits using the **rpb2** sequence had highest similarity to *Tubakia suttoniana* (GenBank MG976493.1; Identities = 940/941 (99 %), no gaps), *Tubakia californica* (GenBank MG976452.1; Identities = 933/934 (99 %), no gaps), and *Tubakia japonica* (GenBank MG976469.1; Identities = 991/993 (99 %), no gaps). Closest hits using the **tef1** sequence had highest similarity to *Tubakia suttoniana* (GenBank MG592108.1; Identities = 467/467 (100 %), no gaps), *Tubakia* sp. 1 (GenBank MG592101.1; Identities = 550/562 (98 %), no gaps), and *Tubakia japonica* (GenBank MG592075.1; Identities = 550/562 (98 %), no gaps). Closest hits using the **tub2** sequence had highest similarity to *Tubakia suttoniana* (GenBank MG592201.1; Identities = 505/507 (99 %), 1 gap (0 %)), *Tubakia seoraksanensis* (GenBank MG592190.1; Identities = 487/492 (99 %), 1 gap (0 %)), and

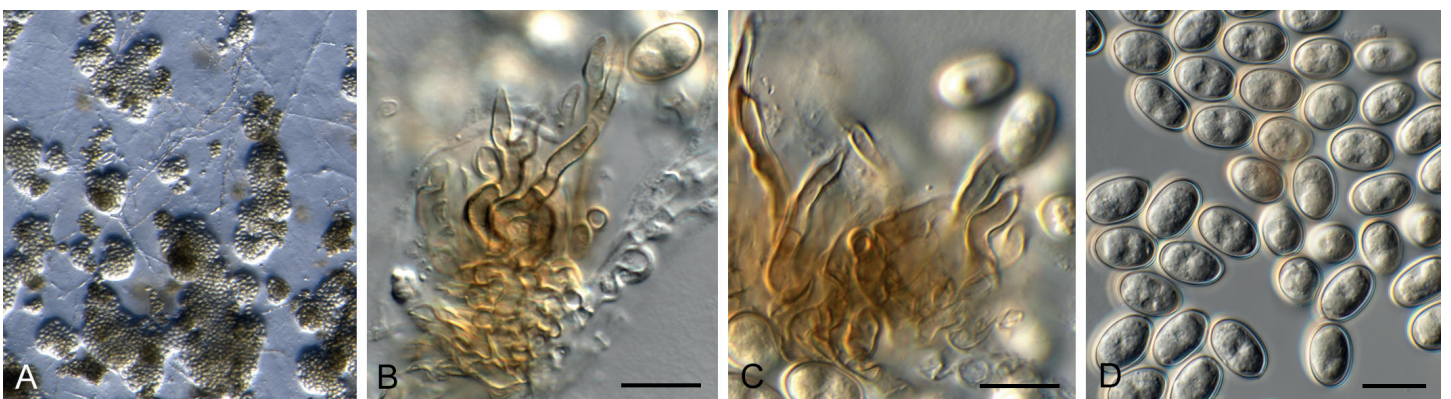


Fig. 62. *Tubakia suttoniana* (CPC 32745). A. Conidiomatal initials developing on SNA. B, C. Conidiogenous cells. D. Conidia. Scale bars = 10 μ m.

Tubakia japonica (GenBank MG592165.1; Identities = 508/515 (99 %), 1 gap (0 %)).

Turquoiseomycetales Crous, **ord. nov.** MycoBank MB829363.

Turquoiseomycetaceae Crous, **fam. nov.** MycoBank MB829461.

Turquoiseomyces Crous, **gen. nov.** MycoBank MB829363.

Etymology: Name refers to the characteristic green-blue discolouration of the host tissue surrounding conidiomata.

Conidiomata solitary to aggregated, dark brown, globose, pycnidial, opening by irregular rupture; wall of 6–8 layers of brown *textura intricata*. **Conidiophores** lining the inner cavity, extensively branched, septate, tightly aggregated, pale green-brown, finely roughened, subcylindrical. **Conidiogenous cells** ampulliform to subcylindrical, pale green-brown, finely roughened, terminal and intercalary, proliferating percurrently. **Conidia** solitary, subcylindrical, guttulate, smooth-walled, medianly 1-septate, apex swollen with mucoid cap, base somewhat tapered, truncate, reflective.

Type species: *Turquoiseomyces eucalypti* Crous.

Turquoiseomyces eucalypti Crous, **sp. nov.** MycoBank MB829364. Fig. 63.

Etymology: Name refers to the host genus *Eucalyptus* from which it was isolated.

Conidiomata solitary to aggregated, dark brown, globose, pycnidial, opening by irregular rupture, 250–350 µm diam; wall of 6–8 layers of brown *textura intricata*. **Conidiophores** lining the inner cavity, extensively branched, septate, tightly aggregated, 10–25 × 3–4 µm, pale green-brown, finely roughened, subcylindrical. **Conidiogenous cells** ampulliform to subcylindrical, pale green-brown, finely roughened, terminal and intercalary, 5–10 × 3–4 µm, proliferating percurrently. **Conidia** solitary, subcylindrical, guttulate, smooth-walled, medianly 1-septate, apex swollen with mucoid cap, base somewhat tapered, truncate, reflective, 1.5–2 µm diam, straight to flexuous, (50–) 55–60(–80) × 3(–4) µm.

Culture characteristics: Colonies erumpent, spreading, surface folded, with sparse aerial mycelium and smooth, lobate margin, reaching 10 mm diam after 2 wk at 25 °C. On MEA surface greenish grey, reverse smoke grey; on PDA surface olivaceous grey, reverse smoke grey; on OA surface iron-grey in centre, buff in outer region.

Typus: **Australia** New South Wales, Cobb Highway, on leaves of *Eucalyptus leptophylla* (Myrtaceae), Aug. 2017, B.A. Summerell, HPC 2220 (**holotype** CBS H-23834, culture ex-type CPC 34399 = CBS 145126).

Notes: This very obvious fungus was first seen on leaves where conidia were surrounded by tissue with a green-blue discolouration, which was different from the normal foliicolous coelomycetes on *Eucalyptus* that generally have structures with shades of brown to black. In culture, it again produced greenish grey colonies on MEA. The present collection is not known from DNA data available in GenBank, and is also distinct morphologically, representing a distinct family and order in *Lecanoromycetes*.

Based on a megablast search of NCBI's GenBank nucleotide database, the closest hits using the **ITS** sequence had highest similarity to *Lecanora subcarnea* (GenBank AY541267.1; Identities = 313/374 (84 %), 25 gaps (6 %)), *Pseudogymnoascus pannorum* var. *pannorum* (GenBank MH866140.1; Identities = 313/374 (84 %), 27 gaps (7 %)), and *Ciliciopodium hyalinum* (GenBank KM231857.1; Identities = 313/374 (84 %), 27 gaps (7 %)). Closest hits using the **LSU** sequence are *Umbilicaria torrefacta* (GenBank JQ740001.1; Identities = 818/886 (92 %), 5 gaps (0 %)), *Umbilicaria muehlenbergii* (GenBank JQ739997.1; Identities = 814/886 (92 %), 4 gaps (0 %)), and *Acarospora anomala* (GenBank LN810758.1; Identities = 813/885 (92 %), 3 gaps (0 %)). No significant hits were obtained when the **tub2** sequence was used in blastn and megablast searches.

Typhicola Crous, **gen. nov.** MycoBank MB829599.

Etymology: Name refers to the genus *Typha* on which it was collected.

Ascomata gregarious along leaf veins, immersed, globose with central ostiole, somewhat papillate to erumpent, black,

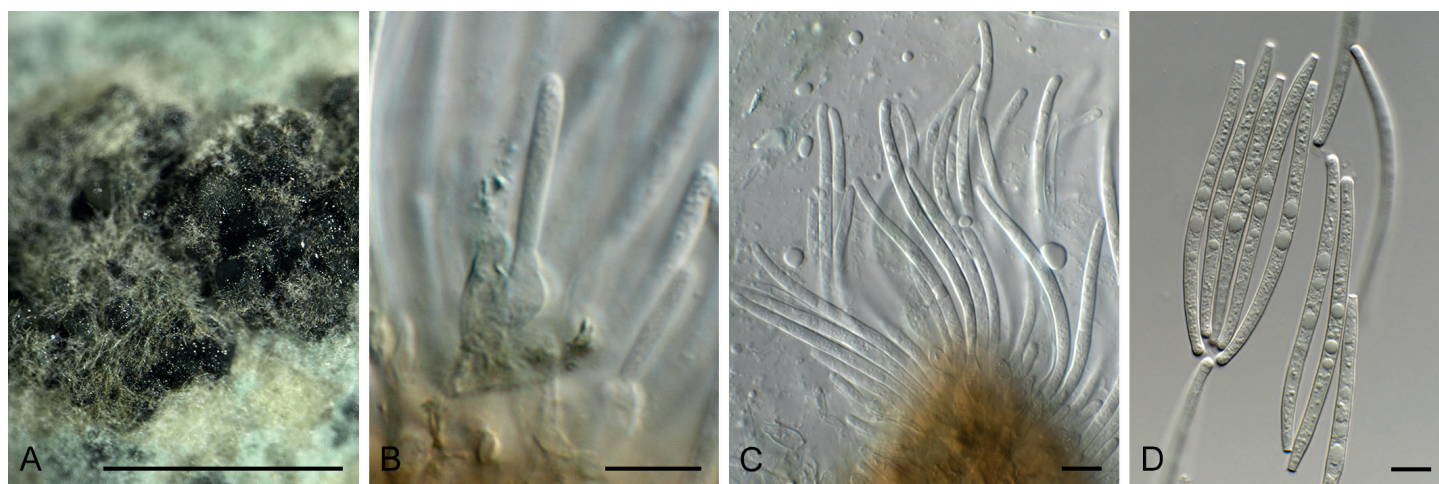


Fig. 63. *Turquoiseomyces eucalypti* (CPC 34399). **A.** Conidiomata in culture on OA (note colour). **B, C.** Conidiogenous cells giving rise to conidia. **D.** Conidia. Scale bars: A = 300 µm, B–D = 10 µm.

soft. *Pseudoparaphyses* numerous, hyaline, smooth, branched with anastomoses, hyphae-like. *Asci* 8-spored, bitunicate, fissitunicate, subcylindrical, with well-developed ocular chamber, thick-walled, short papillate. *Ascospores* ellipsoid, septate, straight to slightly curved, end cells conically rounded, brown, thick-walled, prominently constricted at thick septa, with mucilaginous sheath.

Type species: Typhicola typharum (Desm.) Crous.

Typhicola typharum (Desm.) Crous, **comb. nov.** MycoBank MB829600. Fig. 64.

Basionym: Sphaeria scirpicola var. *typharum* Desm., *Pl. cryptog. Fr.*, ed. 2, nr. 1428. 1848.

Synonym: Juncaceicola typharum (Desm.) Tennakoon *et al.*, *Cryptog. Mycol.* **37**: 151. 2016.

Ascomata on dead leaves, gregarious along leaf veins, immersed, globose with central ostiole, somewhat papillate to erumpent, black, soft, 100–150 µm diam. *Pseudoparaphyses* numerous, hyaline, smooth, branched with anastomoses, hyphae-like, 2–3 µm diam. *Asci* 8-spored, bitunicate, fissitunicate, subcylindrical, with well-developed ocular chamber, 2 µm diam, thick-walled, short papillate, 80–100 × 20–25 µm. *Ascospores* ellipsoid, 3-septate, with central pore in septum, widest in second cell from apex, straight to slightly curved, end cells conically rounded, golden brown, thick-walled (< 0.5 µm), prominently constricted at thick septa, exospore warty, endospore smooth, finely guttulate, with mucilaginous sheath (up to 3 µm diam), covering entire ascospore (when mounted in water), (23–)27–29(–31) × (8–)9–10(–11) µm.

Culture characteristics: Colonies erumpent, spreading, with moderate aerial mycelium and feathery, lobate margin, reaching

45 mm diam after 2 wk at 25 °C. On MEA and PDA surface and reverse olivaceous grey; on OA surface iron-grey.

Typus: France, on leaves of *Typha* sp. (*Typhaceae*), Desm., exsiccata “Plantes Cryptogames de France, ed. 2: no. 1428 (1848)” (**lectotype** designated here in PC, MBT385534). **Germany**, near Berlin, leaf of *Typha* sp. (*Typhaceae*), 1 Apr. 2017, R.K. Schumacher, HPC 2025 = RKS 84 (**epitype** designated here CBS H-23819, MBT385272, culture ex-epitype CPC 33271 = CBS 145043).

Notes: This fungus occurs commonly in Europe, sporulates well in culture, but produced only the sexual morph in the present study. Tennakoon *et al.* (2016) introduced the genus *Juncaceicola* and the combination *J. typharum*, but could not locate any type material of *Sphaeria scirpicola* var. *typharum*, and based their new combination on CBS 296.54 (on *Nardus stricta*, Switzerland), which probably represents an undescribed species of *Juncaceicola*. Although phylogenetically distinct, there is morphologically little to choose between *Typhicola* and *Juncaceicola*, and the two genera are best distinguished based on DNA data.

Based on a megablast search of NCBI’s GenBank nucleotide database, the closest hits using the **ITS** sequence had highest similarity to *Juncaceicola typharum* (as *Leptosphaeria typharum*, GenBank AF439465.1; Identities = 507/518 (98 %), 1 gap (0 %)), *Pleospora typhicola* (GenBank KF636768.1; Identities = 453/486 (93 %), 12 gaps (2 %)), and *Neocamarosporium goegapense* (GenBank KJ869163.1; Identities = 519/587 (88 %), 26 gaps (4 %)). Closest hits using the **LSU** sequence are *Pleospora typhicola* (GenBank KF636774.1; Identities = 848/862 (98 %), 2 gaps (0 %)), *Camarosporidiella robiniicola* (GenBank MF434266.1; Identities = 832/849 (98 %), no gaps), *Camarosporium laburnicola* (GenBank KY497779.1; Identities = 845/863 (98 %), 1 gap

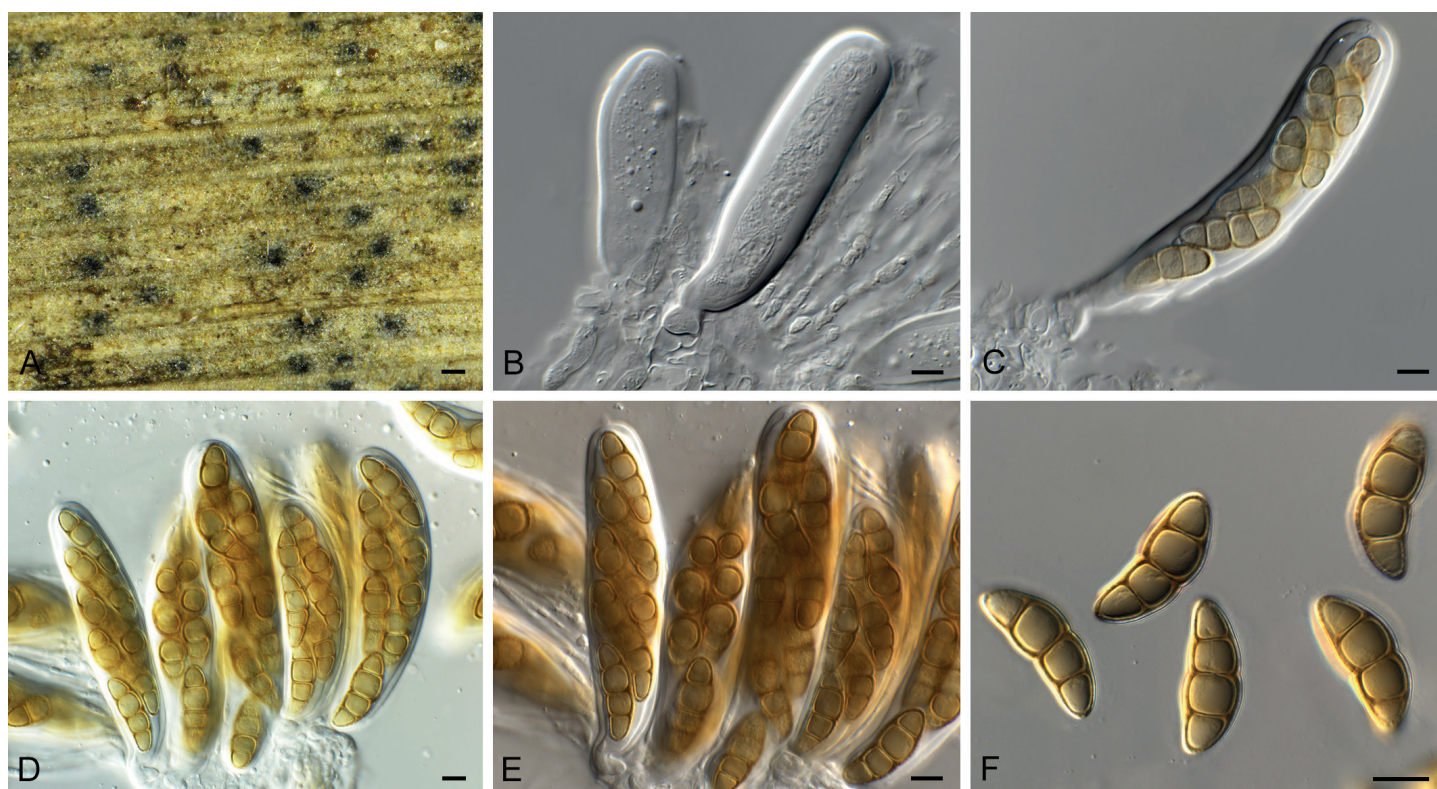


Fig. 64. *Typhicola typharum* (CPC 33271). **A.** Ascomata on host tissue. **B–E.** Asci. **F.** Ascospores. Scale bars: A = 150 µm, B–F = 10 µm.

(0 %)), and *Juncaceicola typharum* (GenBank MH868883.1; Identities = 834/863 (97 %), 3 gaps (0 %)). Distant hits using the *rbp2* sequence had highest similarity to *Pleospora incompta* (GenBank KC584504.1; Identities = 740/867 (85 %), 4 gaps (0 %)), *Comoclathris compressa* (GenBank KC584498.1; Identities = 736/867 (85 %), 4 gaps (0 %)), and *Pleospora typhicola* (GenBank KC584505.1; Identities = 733/865 (85 %), no gaps). Distant hits using the *tef1* sequence had highest similarity to *Juncaceicola typharum* (as *Phaeosphaeria typharum*, GenBank KF253148.1; Identities = 123/131 (94 %), no gaps), *Dendryphion penicillatum* (GenBank AY375371.1; Identities = 261/281 (93 %), 6 gaps (2 %)), *Alternaria ventricosa* (GenBank KY352501.1; Identities = 272/301 (90 %), 5 gaps (1 %)), and *Lasiodiplodia iranensis* (GenBank KU997110.1; Identities = 266/295 (90 %), 4 gaps (1 %)). Distant hits using the *tub2* sequence had highest similarity to *Alternaria solani* (GenBank CP022033.1; Identities = 916/981 (93 %), 9 gaps (0 %)), *Alternaria alternata* (GenBank KJ396337.1; Identities = 905/977 (93 %), 7 gaps (0 %)), and *Alternaria cucumerina* (GenBank HQ413318.1; Identities = 903/977 (92 %), 7 gaps (0 %)).

Wojnowiciella dactylidis (Wijayaw. *et al.*) Hern.-Restr. & Crous, *Sydowia* **68**: 221. 2016. Fig. 65.

Basionym: *Wojnowicia dactylidis* Wijayaw. *et al.*, *Fungal Diversity* **72**: 144. 2015.

Conidiomata erumpent, pycnidial, solitary, globose, papillate, 200–300 µm diam, with 1–2 ostioles; wall of 3–6 layers of brown *textura angularis*. *Microconidiophores* reduced to conidiogenous cells lining the inner cavity, hyaline, smooth, dolliiform to ampulliform, 4–5 × 3–4 µm, phialidic, with periclinal thickening. *Microconidia* solitary, hyaline, smooth, guttulate, aseptate, subcylindrical, apex obtuse, base truncate, (3–)4(–5) × 2 µm.

Culture characteristics: Colonies flat, spreading, with moderate aerial mycelium and smooth, lobate margin, covering dish after 2 wk at 25 °C. On MEA, PDA and OA surface isabelline, reverse isabelline to hazel, with zones of cinnamon.

Material examined: **New Zealand**, Auckland, Grey Lynn, Grey Lynn park, on *Dypsis* sp. (*Arecaceae*), 5 Oct. 2016, R. Thangavel, CBS H-23807, culture T16_03296B = CPC 32741 = CBS 145077.

Notes: *Wojnowiciella dactylidis* was described from *Dactylis glomerata* collected in Italy, and this is the first record from New Zealand. Unfortunately, only the microconidial morph was observed in culture.

Based on a megablast search of NCBI's GenBank nucleotide database, the closest hits using the **ITS** sequence had highest similarity to *Wojnowiciella dactylidis* (GenBank LT990660.1; Identities = 572/572 (100 %), no gaps), *Wojnowiciella cissampeli* (GenBank NR_155972.1; Identities = 568/579 (98 %), 6 gaps (1 %)), and *Wojnowicia rosicola* (GenBank MG828979.1; Identities = 554/568 (98 %), 8 gaps (1 %)). Closest hits using the **LSU** sequence are *Wojnowicia rosicola* (GenBank MG829091.1; Identities = 846/847 (99 %), no gaps), *Wojnowicia italica* (GenBank KX430001.1; Identities = 846/847 (99 %), no gaps), and *Wojnowiciella dactylidis* (GenBank LT990632.1; Identities = 844/845 (99 %), 1 gap (0 %)). Closest hits using the **tef1** sequence had highest similarity to *Wojnowicia italica* (GenBank KX430003.1; Identities = 438/440 (99 %), no gaps), *Wojnowiciella dactylidis* (GenBank LT990613.1; Identities = 423/425 (99 %), no gaps), and *Wojnowiciella cissampeli* (GenBank LT990616.1; Identities = 463/469 (99 %), no gaps). No **tub2** sequences of *Wojnowiciella* or *Wojnowicia* are available for comparison on GenBank; distant hits using the *tub2* sequence had highest similarity to *Fenestella fenestrata* (GenBank MF795893.1; Identities = 247/280 (88 %), 7 gaps (2 %)), *Didymocyrtis banksiae* (GenBank KY979923.1; Identities = 251/284 (88 %), 18 gaps (6 %)), and *Didymocyrtis foliaceiphila* (as *Diederichomyces foliaceiphila*, GenBank KP170700.1; Identities = 246/280 (88 %), 8 gaps (2 %)).

Xenodevriesiaceae Crous, **fam. nov.** MycoBank MB829462.

Xenodevriesia Crous, **gen. nov.** MycoBank MB829365.

Etymology: Name reflects the fact that this is similar to, but distinct from the genus *Devriesia*.

Mycelium consisting of medium brown, smooth, septate, branched hyphae. *Conidiophores* dimorphic. *Microconidiophores* reduced to conidiogenous cells on hyphae, erect, cylindrical, medium brown, smooth with truncate ends, proliferating sympodially. *Macroconidiophores* erect, cylindrical, straight to geniculate-sinuous, medium brown, smooth, unbranched or branched above, septate. *Conidiogenous cells* terminal or lateral on branched conidiophores, medium brown, smooth, cylindrical, proliferating sympodially; loci truncate, inconspicuous, somewhat darkened, not refractive. *Conidia* medium brown, smooth, guttulate, subcylindrical to narrowly obclavate, apex obtuse to truncate, base truncate, occurring in branched chains, septate; hila inconspicuous to somewhat darkened and thickened, not refractive.

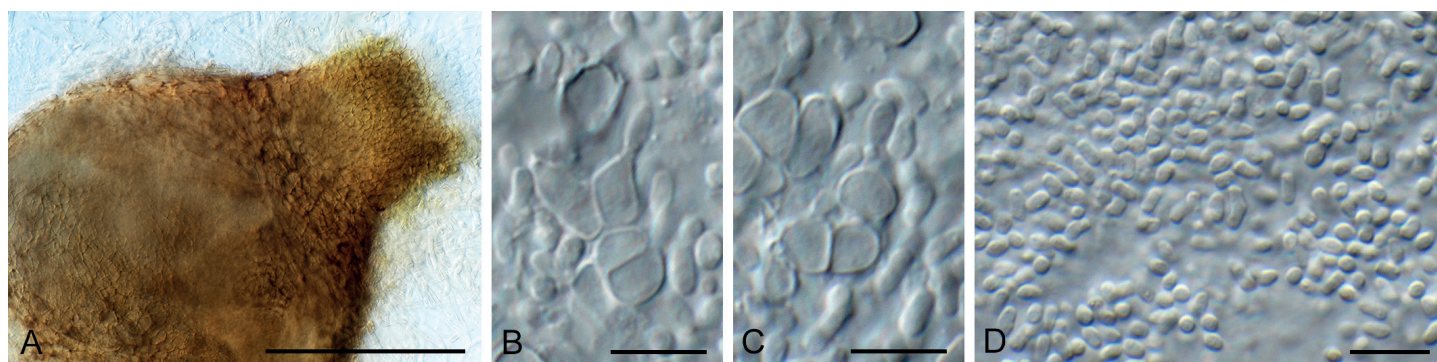


Fig. 65. *Wojnowiciella dactylidis* (CPC 32741). **A.** Conidioma on SNA. **B, C.** Conidiogenous cells. **D.** Conidia. Scale bars: A = 150 µm, B–D = 10 µm.

Type species: Xenodevriesia strelitziicola (Arzanlou & Crous) Crous.

Xenodevriesia strelitziicola (Arzanlou & Crous) Crous, *comb. nov.* MycoBank MB829366.

Basionym: Devriesia strelitziicola Arzanlou & Crous, *Stud. Mycol.* **64**: 38. 2009.

Notes: Devriesia strelitziicola was introduced by Crous *et al.* (2009b) for a fungus that was devriesia-like and pseudocercospora-like in morphology, but which proved to be phylogenetically distinct from both genera. It is morphologically distinct from *Devriesia* in that it does not produce chlamydospores, and from *Pseudocercospora* in that the conidial hila are somewhat darkened and thickened. Phylogenetically, it is also clearly distinct, and represents a new family in *Capnodiales*.

Zasmidium hakeicola Crous, *sp. nov.* MycoBank MB829367. Fig. 66.

Etymology: Name refers to the host genus *Hakea* from which it was isolated.

Mycelium consisting of smooth, pale brown, septate, branched, 2–2.5 µm diam hyphae. *Conidiophores* solitary, erect, geniculous-flexuous, branched or not, subcylindrical,

medium brown, finely verruculose, thick-walled, guttulate, multiseptate, 100–200 × 3–5 µm, arising from superficial hyphae or as a few cells of a weakly developed stroma. *Conidiogenous cells* terminal, at times intercalary, subcylindrical, medium brown, finely verruculose, proliferating sympodially, 25–50 × 5–7 µm; loci prominently thickened and darkened, refractive, 2.5–3 µm diam. *Conidia* solitary, obclavate, apex obtuse, base obconically truncate, verruculose, medium brown, straight, (40–)47–55(–65) × 8(–9) µm; hilum thickened, darkened and refractive, 3–4 µm diam; conidia at times bifurcate, 3(–5)-septate.

Culture characteristics: Colonies erumpent, spreading, with sparse to moderate aerial mycelium and feathery margin, reaching 4 mm diam after 2 wk at 25 °C. On MEA and PDA surface pale olivaceous grey to olivaceous grey, reverse olivaceous grey; on OA surface pale olivaceous grey to olivaceous grey.

Typus: Australia, New South Wales, Australian Botanical Garden Mount Annan, on leaves of *Hakea corymbosa* (*Proteaceae*), 25 Nov. 2016, P.W. Crous, HPC 1722 (**holotype** CBS H-23806, culture ex-type CPC 32703 = CBS 144590).

Notes: A morphologically similar species, *Zasmidium grevilleae* (conidia 3–7(–12)-septate, (30–)50–65(–80) × (5–)6–7 µm), was described from leaves of *Grevillea decurrens* collected in Australia (Crous *et al.* 2009a, Videira *et al.* 2017). The present

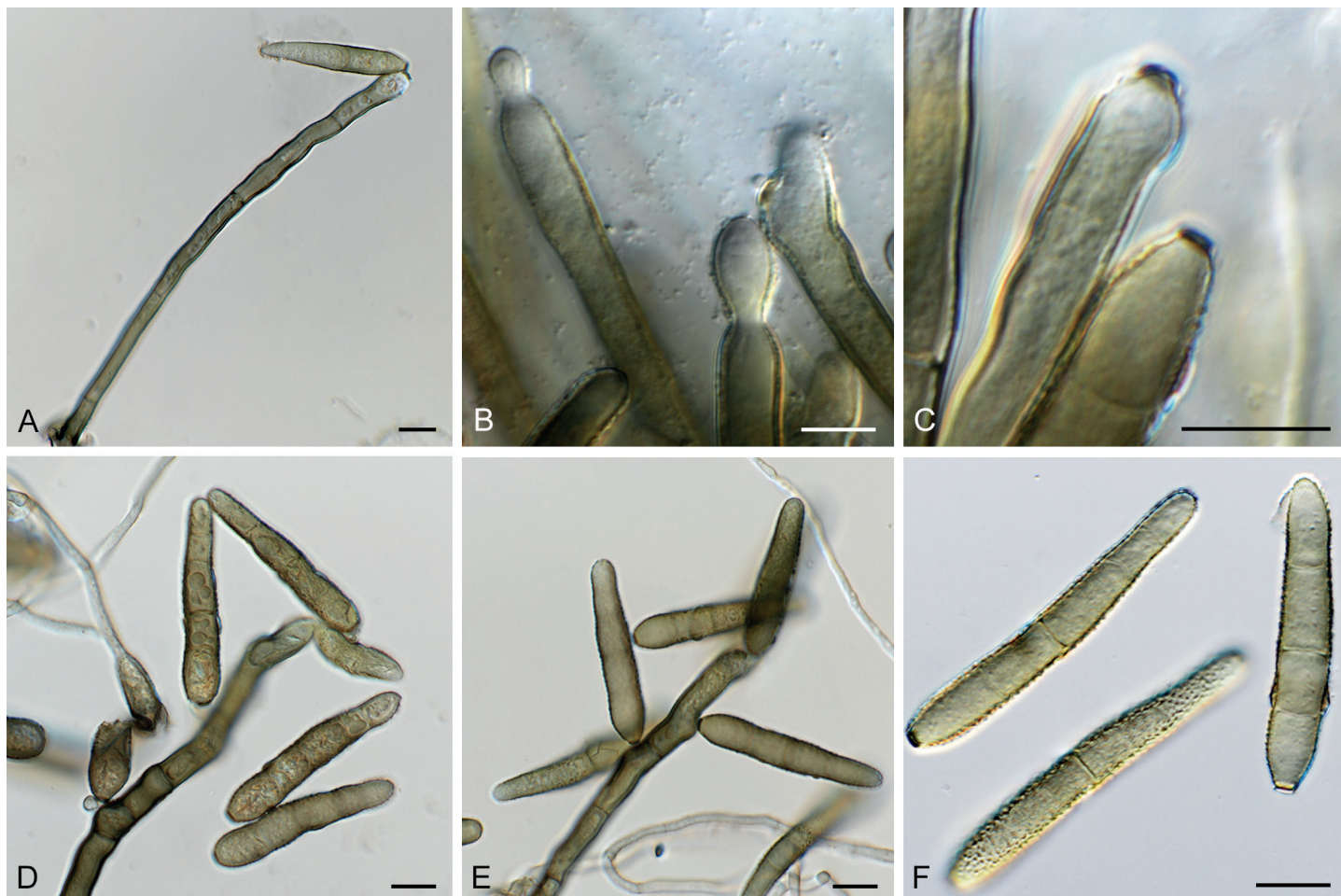


Fig. 66. *Zasmidium hakeicola* (CPC 32703). **A.** Conidiophore giving rise to conidium. **B–E.** Conidiogenous cells and conidial loci. **F.** Conidia. Scale bars = 10 µm.

collection from *Hakea* differs from that species in having shorter, wider conidia, with fewer septa.

Based on a megablast search of NCBI's GenBank nucleotide database, the closest hits using the **ITS** sequence had highest similarity to *Zasmidium grevilleae* (GenBank NR_156522.1; Identities = 533/538 (99 %), 1 gap (0 %)), *Zasmidium proteacearum* (as *Verrucisporota proteacearum*, GenBank FJ839635.1; Identities = 513/539 (95 %), 23 gaps (4 %)), and *Zasmidium velutinum* (as *Periconiella velutina*, GenBank EU041781.1; Identities = 492/545 (90 %), 16 gaps (2 %)). Closest hits using the **LSU** sequence are *Zasmidium proteacearum* (as *Verrucisporota proteacearum*, GenBank FJ839671.2; Identities = 858/860 (99 %), no gaps), *Zasmidium grevilleae* (GenBank MH874876.1; Identities = 857/860 (99%), no gaps), and *Zasmidium biverticillatum* (as *Ramichloridium biverticillatum*, GenBank EU041853.1; Identities = 834/846 (99 %), 2 gaps (0 %)). Closest hits using the **actA** sequence had highest similarity to *Zasmidium proteacearum* (as *Verrucisporota proteacearum*, GenBank KF903478.1; Identities = 433/439 (99 %), 1 gap (0 %)), *Zasmidium citri-griseum* (GenBank KF903676.1; Identities = 392/430 (91 %), 2 gaps (0 %)), and *Parapallidocercospora thailandica* (as *Mycosphaerella thailandica*, GenBank EU514333.1; Identities = 373/410 (91 %), 6 gaps (1 %)). Closest hits using the **rpb2** sequence had highest similarity to *Zasmidium proteacearum* (GenBank MF951721.1; Identities = 677/683 (99 %), no gaps), *Zasmidium grevilleae* (GenBank MF951705.1; Identities = 662/668 (99 %), no gaps), and *Zasmidium musicola* (GenBank MF951717.1; Identities = 663/761 (87 %), no gaps). Closest hits using the **tub2** sequence had highest similarity to *Zasmidium commune* (GenBank KY979928.1; Identities = 721/787 (92 %), no gaps), *Pseudocercospora fijiensis* (GenBank XM_007921924.1; Identities = 702/789 (89 %), no gaps), and *Ramularia collo-cygni* (GenBank JN003648.1; Identities = 701/789 (89 %), no gaps).

Zygosporium pseudogibbum Crous, *Fungal Syst. Evol.* 1: 213. 2018. Fig. 67.

Conidiophores solitary, erect, consisting of 1–2 pale brown basal cells forming a stipe, 8–20 × 3–4 μm, giving rise to a curved, dark brown terminal vesicle, 12–15 × 5–7 μm. *Conidiogenous cells* arranged in a whorl of 3–4 on a terminal vesicle, hyaline, smooth, reniform, 5–6 × 3.5–4 μm. *Vesicle* with single apical cell, 4–6 × 3–4 μm, pale brown, cylindrical, with obtuse apex and prominent collarette. *Conidia* solitary, globose, verruculose, faintly olivaceous, (5–)5.5(–6) μm diam.

Culture characteristics: Colonies flat, spreading, with moderate aerial mycelium, folded surface and even, smooth margin, reaching 25 mm diam after 2 wk at 25 °C. On MEA, PDA and OA surface dirty white, reverse pale luteous.

Material examined: **Australia**, New South Wales, Australian Botanical Garden Mount Annan, on leaves of *Macrozamia miquelii* (*Zamiaceae*), 25 Nov. 2016, P.W. Crous, HPC 1734, CBS H-23580, culture CPC 32120 = CBS 144442.

Notes: *Zygosporium pseudogibbum* (on *Eucalyptus* leaves from Malaysia; Crous *et al.* 2018c) is closely related to *Z. gibbum*, a European taxon (reference isolate, FMR 13130 = CBS 137306; leaf litter Canary Islands; Hernández-Restrepo *et al.* 2017). Morphologically these taxa are very similar and they are thus best distinguished based on their DNA sequences.

Based on a megablast search of NCBI's GenBank nucleotide database, the closest hits using the **ITS** sequence had highest similarity to *Zygosporium mycophilum* (GenBank MH856563.1; Identities = 562/565 (99 %), 2 gaps (0 %)), *Zygosporium pseudogibbum* (GenBank NR_159072.1; Identities = 551/554 (99 %), 2 gaps (0 %)), and *Zygosporium masonii* (GenBank MH860771.1; Identities = 527/567 (93 %), 16 gaps (2 %)).

Closest hits using the **LSU** sequence are *Zygosporium pseudogibbum* (GenBank MH107974.1; Identities = 839/840 (99 %), no gaps), *Atrotorquata spartii* (GenBank KP325443.1; Identities = 845/872 (97 %), 2 gaps (0 %)), and *Lopadostoma fagi* (GenBank KC774577.1; Identities = 829/874 (95 %), 4 gaps (0 %)). The **actA** sequence had highest similarity to *Zygosporium pseudogibbum* (GenBank MH107989.1; Identities = 526/540 (97 %), no gaps); other distant hits include *Nalanthamala psidii* (GenBank KM231245.1; Identities = 346/369 (94 %), no gaps), *Dactylonectria alcacerensis* (GenBank KM231158.1; Identities = 346/369 (94 %), no gaps), and *Dactylonectria novozelandica* (GenBank KM231157.1; Identities = 346/369 (94 %), no gaps). The **tub2** sequence had highest similarity to *Zygosporium pseudogibbum* (GenBank MH108055.1; Identities = 461/475 (97 %), 1 gap (0 %)); other distant hits include *Hypoxylon croceoplum* (GenBank AY951711.1; Identities = 739/798 (93 %), no gaps), *Hypoxylon calileguense* (GenBank KU604579.1; Identities = 739/799 (92 %), no gaps), and *Dicyma funiculosa* (GenBank KU684134.1; Identities = 830/937 (89 %), 11 gaps (1 %)).

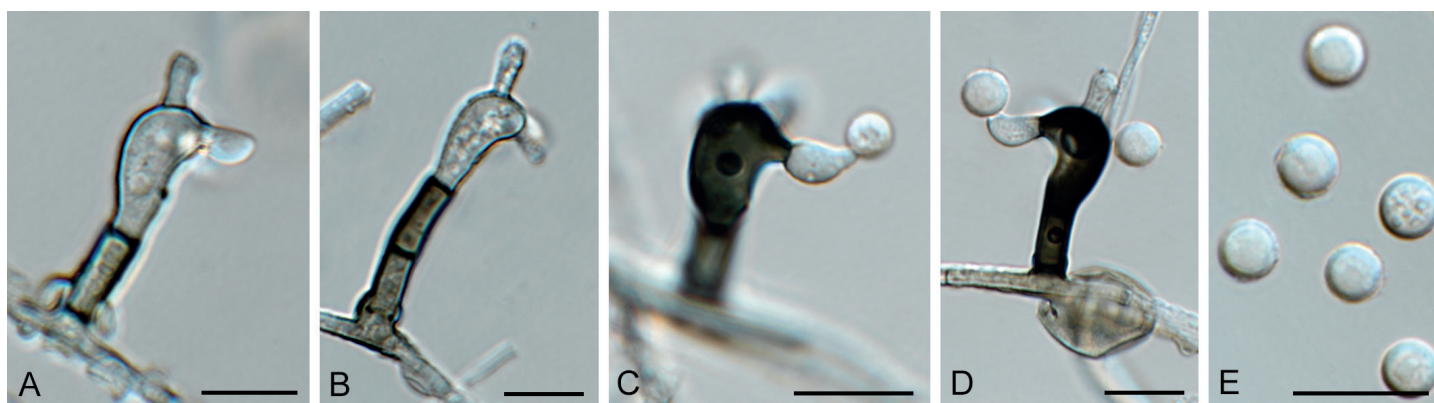


Fig. 67. *Zygosporium pseudogibbum* (CPC 32120). **A–D.** Conidiophores giving rise to conidia. **E.** Conidia. Scale bars = 10 μm.

Addendum: validation of names and typifications

During the course of this study we encountered several names that were invalid based on the International Code of nomenclature for algae, fungi, and plants (see MycoBank and Index Fungorum) due to a variety of reasons. As this has led to problems with new combinations or genera and families subsequently based on these names also being rendered invalid, and thus we decided to validate these names below.

Allelochaeta falcata (B. Sutton) Crous, *Fungal Syst. Evol.* **2**: 288. 2018.

Basionym: *Cryptostictis falcata* B. Sutton, *Mycol. Pap.* **88**: 25. 1963.

Morphological descriptions and illustrations: See Barber *et al.* (2011), Crous *et al.* (2018a).

Typus. **Australia**, Victoria, on *Eucalyptus* sp., 1963, collector unknown (**holotype** Herb IMI 59166); New South Wales, Central Tablelands, ca. 200 metres WSW of 'Coomber' homestead, on Coomber property, ca. 8 km SW of Rylstone, S32°50'04" E149°56'13", alt. 600 ± 10 m, 17 Aug. 2006, R. Johnstone & A.E. Orme, 734259, on *Eucalyptus alligatrix* (**epitype** designated here CBS H-20744, MBT385261, cultures ex-epitype CPC 13578 = CBS 131117).

Notes: *Allelochaeta* was treated by Crous *et al.* (2018a). Unfortunately, the holotype specimen was incorrectly cited and thus the epitype is consequently invalid. This is corrected here.

Arthrocatena Egidi & Selbmann, *gen. nov.* MycoBank MB829384. *Synonym*: *Arthrocatena* Egidi & Selbmann, *Fungal Diversity* **65**: 159. 2014. *Nom. inval.*, Art. 40.7 (Shenzhen).

Etymology: Named after dark, arthric conidia in chains.

Description and illustration: Egidi *et al.* (2014).

Type species: *Arthrocatena tenebrosa* Egidi & Selbmann.

Arthrocatena tenebrosa Egidi & Selbmann, *sp. nov.* MycoBank MB829385.

Synonym: *Arthrocatena tenebrio* Egidi & Selbmann, *Fungal Diversity* **65**: 159. 2014. *Nom. inval.*, Art. 40.7 (Shenzhen).

Etymology: Named after dark, arthric conidia in chains.

Description and illustration: Egidi *et al.* (2014).

Typus: **Italy**, Monte Rosa, Punta Indren, from rock (**holotype** CBS 136100, culture and specimen preserved as metabolically inactive).

Catenulomyces Egidi & de Hoog, *gen. nov.* MycoBank MB829386. *Synonym*: *Catenulomyces* Egidi & de Hoog, *Fungal Diversity* **65**: 154. 2014. *Nom. inval.*, Art. 40.7 (Shenzhen).

Etymology: Named after its conidial chains.

Description and illustration: Egidi *et al.* (2014).

Type species: *Catenulomyces convolutus* Egidi & de Hoog.

Catenulomyces convolutus Egidi & de Hoog, *sp. nov.* MycoBank MB829387.

Synonym: *Catenulomyces convolutus* Egidi & de Hoog, *Fungal Diversity* **65**: 154. 2014. *Nom. inval.*, Art. 40.7 (Shenzhen).

Etymology: Named after the conidial chains and curly shape of conidia.

Description and illustration: Egidi *et al.* (2014).

Typus: **Spain**, La Cabrera, from rock (**holotype** CBS 118609, culture and specimen preserved as metabolically inactive).

Constantinomyces Egidi & Onofri, *gen. nov.* MycoBank MB829388.

Synonym: *Constantinomyces* Egidi & Onofri, *Fungal Diversity* **65**: 155. 2014. *Nom. inval.*, Art. 40.7 (Shenzhen).

Etymology: Genus named after Constantino Ruibal who was one of the first to uncover the stunning diversity of rock-inhabiting fungi.

Description and illustration: Egidi *et al.* (2014).

Type species: *Constantinomyces virgultus* Egidi & Onofri.

Constantinomyces macerans de Hoog & Onofri, *sp. nov.* MycoBank MB829389.

Synonym: *Constantinomyces macerans* de Hoog & Onofri, *Fungal Diversity* **65**: 157. 2014. *Nom. inval.*, Art. 40.7 (Shenzhen).

Etymology: Named after the mere thin hyphal morphology of the fungus.

Description and illustration: Egidi *et al.* (2014).

Typus: **Spain**, Patones, from rock (**holotype** CBS 119304, culture and specimen preserved as metabolically inactive).

Constantinomyces minimus de Hoog & Isola, *sp. nov.* MycoBank MB829390.

Synonym: *Constantinomyces minimus* de Hoog & Isola, *Fungal Diversity* **65**: 157. 2014. *Nom. inval.*, Art. 40.7 (Shenzhen).

Etymology: Named refers to the scant appearance of the fungus.

Description and illustration: Egidi *et al.* (2014).

Typus: **Spain**, La Cabrera, from rock (**holotype** CBS 118766, culture and specimen preserved as metabolically inactive).

Constantinomyces nebulosus Isola & Zucconi, *sp. nov.* MycoBank MB829391.

Synonym: *Constantinomyces nebulosus* Isola & Zucconi, *Fungal Diversity* **65**: 157. 2014. *Nom. inval.*, Art. 40.7 (Shenzhen).

Etymology: The species name refers to the dark and poorly shaped morphology of the fungus.

Description and illustration: Egidi *et al.* (2014).

Typus: Spain, Atazar, from rock (**holotype** CBS 117941, culture and specimen preserved as metabolically inactive).

Constantinomyces virgultus Egidi & Onofri, *sp. nov.* MycoBank MB829392.

Synonym: Constantinomyces virgultus Egidi & Onofri, *Fungal Diversity* **65**: 155. 2014. *Nom. inval.*, Art. 40.7 (Shenzhen).

Etymology: The species' microscopic morphology is shrub-like.

Description and illustration: Egidi *et al.* (2014).

Typus: Spain, Mallorca, from rock (**holotype** CBS 117930, culture and specimen preserved as metabolically inactive).

Exophiala bonariae Isola & Zucconi, *sp. nov.* MycoBank MB829393.

Synonym: Exophiala bonariae Isola & Zucconi, *Fungal Diversity* **76**: 85. 2015 (2016). *Nom. inval.*, Art. 40.7 (Shenzhen).

Etymology: Named after the cemetery of Bonaria, where the type strain was isolated.

Description and illustration: Isola *et al.* (2016).

Typus: Italy, Cagliari, (Zelina Ferri funerary monument) in the cemetery of Bonaria, isolated from marble (**holotype** CBS 139957, culture and specimen preserved as metabolically inactive).

Extremaceae Quaedvl. & Crous, *fam. nov.* MycoBank MB829394. *Synonym: Extremaceae* Quaedvl. & Crous, *Persoonia* **33**: 21. 2014. *Nom. inval.* Art. 32.1(c), see Art. 10.6 (Shenzhen).

Etymology: Named after the genus *Extremus*.

Description and illustration: Quaedvlieg *et al.* (2014).

Type genus: Extremus Quaedvl. & Crous.

Extremus Quaedvl. & Crous, *gen. nov.* MycoBank MB829395.

Synonym: Extremus Quaedvl. & Crous, *Persoonia* **33**: 21. 2014. *Nom. inval.*, Art. 40.7 (Shenzhen).

Etymology: Named after its ecologically extreme, rock-inhabiting habitat.

Description and illustration: Quaedvlieg *et al.* (2014).

Type species: Extremus adstrictus Quaedvl. & Crous.

Extremus adstrictus Quaedvl. & Crous, *sp. nov.* MycoBank MB829396.

Synonyms: Devriesia adstricta Egidi & Onofri, *Fungal Diversity* **65**: 150. 2014. *Nom. inval.*, Art. 40.7 (Shenzhen).

Extremus adstrictus (Egidi & Onofri) Quaedvl. & Crous, *Persoonia* **33**: 22. 2014. *Nom. inval.*, Art. 40.7 (Shenzhen).

Etymology: Named after conidial chains where conidia are densely packed at septa.

Description and illustration: Egidi *et al.* (2014).

Typus: Spain, Mallorca, from rock (**holotype** CBS 118292, culture and specimen preserved as metabolically inactive).

Extremus antarcticus Quaedvl. & Crous, *sp. nov.* MycoBank MB829397.

Synonyms: Devriesia antarctica Selbmann & de Hoog, *Fungal Diversity* **65**: 150. 2014. *Nom. inval.*, Art. 40.7 (Shenzhen).

Extremus antarcticus (Selbmann & de Hoog) Quaedvl. & Crous, *Persoonia* **33**: 22. 2014. *Nom. inval.*, Art. 40.7 (Shenzhen).

Etymology: Named after the geographical origin of the strain.

Description and illustration: Egidi *et al.* (2014).

Typus: Antarctica, Linnaeus Terrace, from rock (**holotype** CBS 136103, culture and specimen preserved as metabolically inactive).

Hyphoconis Egidi & Quaedvl., *gen. nov.* MycoBank MB829398.

Synonym: Hyphoconis Egidi & Quaedvl., *Fungal Diversity* **65**: 153. 2014. *Nom. inval.*, Art. 40.7 (Shenzhen).

Etymology: Named after absence of sporulation.

Description and illustration: Egidi *et al.* (2014).

Type species: Hyphoconis sterilis Egidi & Quaedvl.

Hyphoconis sterilis Egidi & Quaedvl., *sp. nov.* MycoBank MB829399.

Synonym: Hyphoconis sterilis Egidi & Quaedvl., *Fungal Diversity* **65**: 153. 2014. *Nom. inval.*, Art. 40.7 (Shenzhen).

Etymology: Named after poor sporulation by hyphal fragments.

Description and illustration: Egidi *et al.* (2014).

Typus: Spain, Atazar, from rock (**holotype** CBS 118321, culture and specimen preserved as metabolically inactive).

Incertomyces Egidi & Zucconi, *gen. nov.* MycoBank MB829400.

Synonym: Incertomyces Egidi & Zucconi, *Fungal Diversity* **65**: 157. 2014. *Nom. inval.*, Art. 40.7 (Shenzhen).

Etymology: Named after the poor morphological features of the species.

Description and illustration: Egidi *et al.* (2014).

Type species: Incertomyces perditus Egidi & Zucconi.

Incertomyces perditus Egidi & Zucconi, *sp. nov.* MycoBank MB829401.

Synonym: Incertomyces perditus Egidi & Zucconi, *Fungal Diversity* **65**: 157. 2014. *Nom. inval.*, Art. 40.7 (Shenzhen).

Etymology: Named after the poor morphological features of the species.

Description and illustration: Egidi *et al.* (2014).

Typus: Italy, Monte Rosa, from rock (**holotype** CBS 136105, culture and specimen preserved as metabolically inactive).

Knufia karalitana Isola & Onofri, *sp. nov.* MycoBank MB829402.
Synonym: Knufia karalitana Isola & Onofri, *Fungal Diversity* **76**: 88. 2015 (2016). *Nom. inval.*, Art. 40.7 (Shenzhen).

Etymology: Named after the ancient name of Cagliari (Karalis), the city where the strain was isolated.

Description and illustration: Isola et al. (2016).

Typus: Italy, Cagliari, isolated from marble lion in front of the Cathedral of Santa Maria (**holotype** CBS 139720, culture and specimen preserved as metabolically inactive).

Knufia marmoricola Onofri & Zucconi, *sp. nov.* MycoBank MB829403.
Synonym: Knufia marmoricola Onofri & Zucconi, *Fungal Diversity* **76**: 88. 2015 (2016). *Nom. inval.*, Art. 40.7 (Shenzhen).

Etymology: Named after the substratum, from which the type strain was isolated.

Description and illustration: Isola et al. (2016).

Typus: Italy, isolated from travertine of St Peter colonnade (Vatican City State) (**holotype** CBS 139726, culture and specimen preserved as metabolically inactive).

Knufia mediterranea Selbmann & Zucconi, *sp. nov.* MycoBank MB829404.
Synonym: Knufia mediterranea Selbmann & Zucconi, *Fungal Diversity* **76**: 88. 2015 (2016). *Nom. inval.*, Art. 40.7 (Shenzhen).

Etymology: Named after the Mediterranean basin, the site from which the strain was isolated.

Description and illustration: Isola et al. (2016).

Typus: Italy, Cagliari, isolated from Francesca Warzee funerary marble monument, cemetery of Bonaria (**holotype** CBS 139721, culture and specimen preserved as metabolically inactive).

Lapidomyces de Hoog & Stielow, *gen. nov.* MycoBank MB829405.
Synonym: Lapidomyces de Hoog & Stielow, *Fungal Diversity* **65**: 159. 2014. *Nom. inval.*, Art. 40.7 (Shenzhen).

Etymology: Rock-inhabiting fungus.

Description and illustration: Egidi et al. (2014).

Type species: Lapidomyces hispanicus de Hoog & Stielow.

Lapidomyces hispanicus de Hoog & Stielow, *sp. nov.* MycoBank MB829406.
Synonym: Lapidomyces hispanicus de Hoog & Stielow, *Fungal Diversity* **65**: 159. 2014. *Nom. inval.*, Art. 40.7 (Shenzhen).

Etymology: Rock-inhabiting fungus from Spain.

Description and illustration: Egidi et al. (2014).

Typus: Spain, Puebla la Sierra, from rock (**holotype** CBS 118355, culture and specimen preserved as metabolically inactive).

Lithophila Selbmann & Isola, *gen. nov.* MycoBank MB829407.
Synonym: Lithophila Selbmann & Isola, *Fungal Diversity* **76**: 88. 2015 (2016). *Nom. inval.*, Art. 40.7 (Shenzhen).

Etymology: Named after its guttulate cells.

Description and illustration: Isola et al. (2016).

Type species: Lithophila guttulata Selbmann & Isola.

Lithophila guttulata Selbmann & Isola, *sp. nov.* MycoBank MB829408.
Synonym: Lithophila guttulata Selbmann & Isola, *Fungal Diversity* **76**: 90. 2015 (2016). *Nom. inval.*, Art. 40.7 (Shenzhen).

Etymology: Named after its guttulate cells.

Description and illustration: Isola et al. (2016).

Typus: Italy, Vatican City State, isolated from marble stone (cat. 37106) exposed in the Vatican Museums – Cortile della Pigna (**holotype** CBS 139723, culture and specimen preserved as metabolically inactive).

Monticola Selbmann & Egidi, *gen. nov.* MycoBank MB829409.
Synonym: Monticola Selbmann & Egidi, *Fungal Diversity* **65**: 155. 2014. *Nom. inval.*, Art. 40.7 (Shenzhen).

Etymology: Inhabitant of the mountain.

Description and illustration: Egidi et al. (2014).

Type species: Monticola elongata Selbmann & Egidi.

Monticola elongata Selbmann & Egidi, *sp. nov.* MycoBank MB829410.
Synonym: Monticola elongata Selbmann & Egidi, *Fungal Diversity* **65**: 155. 2014. *Nom. inval.*, Art. 40.7 (Shenzhen).

Etymology: Inhabitant of the mountain with elongate conidium-like structures.

Description and illustration: Egidi et al. (2014).

Typus: Italy, Monte Rosa, Stolenberg, from rock (**holotype** CBS 136206, culture and specimen preserved as metabolically inactive).

Meristemomyces Isola & Onofri, *gen. nov.* MycoBank MB829411.
Synonym: Meristemomyces Isola & Onofri, *Fungal Diversity* **65**: 158. 2014. *Nom. inval.*, Art. 40.7 (Shenzhen).

Etymology: Named after the typical meristematic growth of the fungus.

Description and illustration: Egidi et al. (2014).

Type species: Meristemomyces frigidus Isola & Onofri.

Meristemomyces arctostaphyli Crous & M.J. Wingf., *sp. nov.* MycoBank MB829412.

Synonym: *Meristemomyces arctostaphylos* Crous & M.J. Wingf., *Persoonia* 36: 347. 2016. *Nom. inval.* Art 35.1 (Shenzhen).

Etymology: Name refers to *Arctostaphylos*, the plant genus from which this fungus was collected.

Description and illustration: Crous *et al.* (2016).

Typus: **USA**, Utah, near Long Valley, on leaves of *Arctostaphylos patula* (*Ericaceae*), Oct. 2014, M.J. Wingfield (**holotype** CBS H-22600, culture ex-type CPC 25574 = CBS 141290).

Meristemomyces frigidus Isola & Onofri, *sp. nov.* MycoBank MB829413.

Synonym: *Meristemomyces frigidus* Isola & Onofri, *Fungal Diversity* 65: 159. 2014. *Nom. inval.*, Art. 40.7 (Shenzhen).

Etymology: Named after the typical meristematic growth and the cold environment from which the strain was isolated.

Description and illustration: Egidi *et al.* (2014).

Typus: **Himalaya**, Aconcagua, from rock (**holotype** CBS 136109, culture and specimen preserved as metabolically inactive).

Neodevriesia bulbillosa Egidi & Zucconi, *sp. nov.* MycoBank MB829414.

Synonyms: *Devriesia bulbillosa* Egidi & Zucconi, *Fungal Diversity* 65: 148. 2014. *Nom. inval.*, Art. 40.7 (Shenzhen).

Neodevriesia bulbillosa (Egidi & Zucconi) Crous, *Sydowia* 67: 108. 2015. *Nom. inval.*, Art. 40.7 (Shenzhen).

Etymology: Named after large, ellipsoidal multicellular structures present in culture.

Description and illustration: Egidi *et al.* (2014).

Typus: **Spain**, Mallorca, Cala Sant Vicenç (**holotype** CBS 118285, culture and specimen preserved as metabolically inactive).

Neodevriesia modesta Isola & Zucconi, *sp. nov.* MycoBank MB829415.

Synonyms: *Devriesia modesta* Isola & Zucconi, *Fungal Diversity* 65: 148. 2014. *Nom. inval.*, Art. 40.7 (Shenzhen).

Neodevriesia modesta (Isola & Zucconi) Crous, *Sydowia* 67: 108. 2015. *Nom. inval.*, Art. 40.7 (Shenzhen).

Etymology: Named after its scarce exhibition of *Neodevriesia* morphology.

Description and illustration: Egidi *et al.* (2014).

Typus: **Italy**, Viterbo, Vallerano, Grotta del Salvatore (**holotype** CBS 137182, culture and specimen preserved as metabolically inactive).

Neodevriesia sardiniae Isola & de Hoog, *sp. nov.* MycoBank MB829416.

Synonyms: *Devriesia sardiniae* Isola & de Hoog, *Fungal Diversity* 76: 85. 2015 (2016). *Nom. inval.*, Art. 40.7 (Shenzhen).

Neodevriesia sardiniae (Isola & de Hoog) M.M. Wang & L. Cai, *Mycologia* 109: 972. 2017. *Nom. inval.*, Art. 40.7 (Shenzhen).

Etymology: Named after Sardinia, the island where the strain was isolated.

Description and illustration: Isola *et al.* (2016).

Typus: **Italy**, Cagliari, (Frau-Carta funerary monument) in the cemetery of Bonaria, isolated from a marble cross (**holotype** CBS 139724, culture and specimen preserved as metabolically inactive).

Neodevriesia simplex Selbmann & Zucconi, *sp. nov.* MycoBank MB829417.

Synonyms: *Devriesia simplex* Selbmann & Zucconi, *Fungal Diversity* 65: 148. 2014. *Nom. inval.*, Art. 40.7 (Shenzhen).

Neodevriesia simplex (Selbmann & Zucconi) Crous, *Sydowia* 67: 107. 2015. *Nom. inval.*, Art. 40.7 (Shenzhen).

Etymology: Named after simple unbranched chains of aseptate conidia.

Description and illustration: Egidi *et al.* (2014).

Typus: **Italy**, Viterbo, Vallerano, Grotta del Salvatore, from rock (**holotype** CBS 13718, culture and specimen preserved as metabolically inactive).

Oleoguttula Selbmann & de Hoog, *gen. nov.* MycoBank MB829418.

Synonym: *Oleoguttula* Selbmann & de Hoog, *Fungal Diversity* 65: 152. 2014. *Nom. inval.*, Art. 40.7 (Shenzhen).

Etymology: Named after black conidia looking like oil droplets; it is one of the very few sporulating rock-inhabiting fungi.

Description and illustration: Egidi *et al.* (2014).

Type species: *Oleoguttula mirabilis* Selbmann & de Hoog.

Oleoguttula mirabilis Selbmann & de Hoog, *sp. nov.* MycoBank MB829419.

Synonym: *Oleoguttula mirabilis* Selbmann & de Hoog, *Fungal Diversity* 65: 152. 2014. *Nom. inval.*, Art. 40.7 (Shenzhen).

Etymology: Named after black conidia looking like oil droplets; as one of the very few sporulating rock-inhabiting fungi, the morphology is impressive.

Description and illustration: Egidi *et al.* (2014).

Typus: **Antarctica**, Lachman Crags, from rock (**holotype** CBS 136102, culture and specimen preserved as metabolically inactive).

Paradevriesia compacta Crous, *sp. nov.* MycoBank MB829327.

Synonym: *Devriesia compacta* de Hoog & Quaedvl., *Fungal Diversity* 65: 148. 2014. *Nom. inval.*, Art. 40.7 (Shenzhen).

Etymology: Named after densely packed, barrel-shaped conidia.

Description and illustration: Egidi *et al.* (2014).

Typus: **Spain**, Mallorca, Manut II, from rock (**holotype** CBS 118294, culture and specimen preserved as metabolically inactive).

Perusta Egidi & Stielow, *gen. nov.* MycoBank MB829420.
Synonym: *Perusta* Egidi & Stielow, *Fungal Diversity* **65**: 155. 2014. *Nom. inval.*, Art. 40.7 (Shenzhen).

Etymology: Named after the not uniformly burnt-like colour of the colony.

Description and illustration: Egidi *et al.* (2014).

Type species: *Perusta inaequalis* Egidi & Stielow.

Perusta inaequalis Egidi & Stielow, *sp. nov.* MycoBank MB829421.
Synonym: *Perusta inaequalis* Egidi & Stielow, *Fungal Diversity* **65**: 155. 2014. *Nom. inval.*, Art. 40.7 (Shenzhen).

Etymology: Named after the unilaterally inflating conidium-like cells.

Description and illustration: Egidi *et al.* (2014).

Typus: **Spain**, Atazar, from rock (**holotype** CBS 118271, culture and specimen preserved as metabolically inactive).

Petrophila de Hoog & Quaedvl., *gen. nov.* MycoBank MB829422.
Synonym: *Petrophila* de Hoog & Quaedvl., *Fungal Diversity* **65**: 152. 2014. *Nom. inval.*, Art. 40.7 (Shenzhen).

Etymology: Named after the rock substrate it was isolated from.

Description and illustration: Egidi *et al.* (2014).

Type species: *Petrophila incerta* de Hoog & Quaedvl.

Petrophila incerta de Hoog & Quaedvl., *sp. nov.* MycoBank MB829423.
Synonym: *Petrophila incerta* de Hoog & Quaedvl., *Fungal Diversity* **65**: 152. 2014. *Nom. inval.*, Art. 40.7 (Shenzhen).

Etymology: Named after the rock substrate it was isolated from.

Description and illustration: Egidi *et al.* (2014).

Typus: **Spain**, Mallorca, from rock (**holotype** CBS 118608, culture and specimen preserved as metabolically inactive).

Rachicladosporium alpinum Egidi & Zucconi, *sp. nov.* MycoBank MB829424.
Synonym: *Rachicladosporium alpinum* Egidi & Zucconi, *Fungal Diversity* **65**: 159. 2014. *Nom. inval.*, Art. 40.7 (Shenzhen).

Etymology: Named after the mountain chain from which the rock was collected.

Description and illustration: Egidi *et al.* (2014).

Typus: **Italy**, Siusi Alps, from rock (**holotype** CBS 136040, culture and specimen preserved as metabolically inactive).

Rachicladosporium inconspicuum de Hoog & Stielow, *sp. nov.* MycoBank MB829425.
Synonym: *Rachicladosporium inconspicuum* de Hoog & Stielow, *Fungal Diversity* **65**: 162. 2014. *Nom. inval.*, Art. 40.7 (Shenzhen).

Etymology: Name reflects the scarce morphological differentiation observed in the colony.

Description and illustration: Egidi *et al.* (2014).

Typus: **Italy**, Monte Rosa, from rock (**holotype** CBS 136043, culture and specimen preserved as metabolically inactive).

Rachicladosporium mcmurdoi Selbmann & Onofri, *sp. nov.* MycoBank MB829426.
Synonym: *Rachicladosporium mcmurdoi* Selbmann & Onofri, *Fungal Diversity* **65**: 159. 2014. *Nom. inval.*, Art. 40.7 (Shenzhen).

Etymology: Named after the valley from which the rock was collected.

Description and illustration: Egidi *et al.* (2014).

Typus: **Antarctica**, Southern Victoria Land, McMurdo Dry Valleys, Battleship Promontory, from rock (**holotype** CBS 119432, culture and specimen preserved as metabolically inactive).

Rachicladosporium monterosanum Isola & Zucconi, *sp. nov.* MycoBank MB829427.
Synonym: *Rachicladosporium monterosium* Isola & Zucconi, *Fungal Diversity* **65**: 161. 2014. *Nom. inval.*, Art. 40.7 (Shenzhen).

Etymology: Named after the mountain Monte Rosa from which the rock was collected.

Description and illustration: Egidi *et al.* (2014).

Typus: **Italy**, Stolemborg, Monte Rosa, from rock (**holotype** CBS 137178, culture and specimen preserved as metabolically inactive).

Rachicladosporium paucitum Isola & Egidi, *sp. nov.* MycoBank MB829428.
Synonym: *Rachicladosporium paucitum* Isola & Egidi, *Fungal Diversity* **65**: 162. 2014. *Nom. inval.*, Art. 40.7 (Shenzhen).

Etymology: Named after poor sporulation by hyphal fragments.

Description and illustration: Egidi *et al.* (2014).

Typus: **Italy**, Monte Rosa, from rock (**holotype** CBS 136041, culture and specimen preserved as metabolically inactive).

Ramimonilia Stielow & Quaedvl., *gen. nov.* MycoBank MB829429.
Synonym: *Ramimonilia* Stielow & Quaedvl., *Fungal Diversity* **65**: 155. 2014. *Nom. inval.*, Art. 40.7 (Shenzhen).

Etymology: Name reflects the typically chained disposition of hyphae.

Description and illustration: Egidi *et al.* (2014).

Type species: *Ramimonilia apicalis* Stielow & Quaedvl.

Ramimonilia apicalis Stielow & Quaedvl., *sp. nov.* MycoBank MB829430.

Synonym: *Ramimonilia apicalis* Stielow & Quaedvl., *Fungal Diversity* **65**: 155. 2014. *Nom. inval.*, Art. 40.7 (Shenzhen).

Etymology: Name reflects the typical branched hyphae with apical germination.

Description and illustration: Egidi *et al.* (2014).

Typus: **Spain**, Patones, from rock (**holotype** CBS 118327, culture and specimen preserved as metabolically inactive).

Saxophila Selbmann & de Hoog, *gen. nov.* MycoBank MB829431.

Synonym: *Saxophila* Selbmann & de Hoog, *Fungal Diversity* **76**: 90. 2015 (2016). *Nom. inval.*, Art. 40.7 (Shenzhen).

Etymology: Named after the rock substrate where it was isolated.

Description and illustration: Isola *et al.* (2016).

Type species: *Saxophila tyrrhenica* Selbmann & de Hoog.

Saxophila tyrrhenica Selbmann & de Hoog, *sp. nov.* MycoBank MB829432.

Synonym: *Saxophila tyrrhenica* Selbmann & de Hoog, *Fungal Diversity* **76**: 90. 2015 (2016). *Nom. inval.*, Art. 40.7 (Shenzhen).

Etymology: Named after the Tyrrhenian basin, the site from which the strain was isolated.

Description and illustration: Isola *et al.* (2016).

Typus: **Italy**, Cagliari, isolated from little marble angels of an anonymous funerary monument in the cemetery of Bonaria (**holotype** CBS 139725, culture and specimen preserved as metabolically inactive).

Sodiomyces A.A. Grum-Grzhim, Debets & Bilanenko, *gen. nov.* MycoBank MB829354.

Synonym: *Sodiomyces* Grum-Grzhim., Debets & Bilanenko, *Persoonia* **31**: 154. 2013. *Nom. inval.*, Art. 40.1 (Shenzen).

Etymology: From the English soda and Latin *mycetes*, referring to the ability of filamentous fungus grow at high ambient pH and salts.

Description and illustration: Giraldo & Crous (2019).

Types species: *Sodiomyces alkalinus* Grum-Grzhim., Debets & Bilanenko.

Sodiomyces alkalinus Grum-Grzhim., Debets & Bilanenko, *sp. nov.* MycoBank MB829355.

Etymology: From the Latin, *alcalinus* = alkaline.

Description and illustrations: Bilanenko *et al.* (2005) and Grum-Grzhimaylo *et al.* (2013).

Typus: **Mongolia**, Choibalsan area, the soda soil (pH 10.7) on the edge of Shar-Burdiyn lake, 1999, *D. Sorokin* (**holotype** CBS 110278, culture and specimen preserved as metabolically inactive), culture ex-type CBS 110278 = F11 = VKM F-3762.

Sodiomyces alcalophilus (G. Okada) Giraldo López & Crous, *comb. nov.* MycoBank MB829356.

Basionym: *Acremonium alcalophilum* G. Okada, *Trans. Mycol. Soc. Japan* **34**: 173. 1993.

Description and illustrations: Okada *et al.* (1993).

Typus: **Japan**, Kanagawa Pref., Tsukui-gun, near Tsukui Lake, from sludge of pig faeces compost, 9 Dec. 1984, *A. Yoneda* (**holotype** TNS-F-176428, isotype CBS H-5163, ex-isotype culture CBS 114.92 = JCM 7366).

Sodiomyces magadiensis S.A. Bondarenko, Grum-Grzhim., Debets & Bilanenko, *sp. nov.* MycoBank MB829359.

Synonym: *Sodiomyces magadii* S.A. Bondarenko, *et al.*, *Fungal Diversity* **76**: 52. 2015 (2016). *Nom. inval.*, Art. 35.1 (Shenzhen).

Etymology: Name refers to the Magadi Lake in Kenya (Africa), where the fungus was isolated.

Description and illustrations: Grum-Grzhimaylo *et al.* (2016).

Typus: **Kenya**, soda soil (pH 11) at the edge of Magadi Lake, Jan. 2013, *S. Bondarenko* (**holotype** CBS H-21958, culture ex-type MAG2 = CBS 137619 = VKM F-4583).

Sodiomyces tronii S.A. Bondarenko, Grum-Grzhim., Debets & Bilanenko, *sp. nov.* MycoBank MB829361.

Synonym: *Sodiomyces tronii* S.A. Bondarenko, *et al.*, *Fungal Diversity* **76**: 52. 2015 (2016). *Nom. inval.*, Art. 35.1 (Shenzhen)

Etymology: Name refers to the 'trona' salt (carbonate mineral), which is abundant in Magadi Lake in Kenya (Africa), where the fungus was isolated.

Description and illustrations: Grum-Grzhimaylo *et al.* (2016).

Typus: **Kenya**, soda soil (pH 11) at the edge of Magadi Lake, Jan. 2013, *S. Bondarenko* (**holotype** CBS H-21957, culture ex-type MAG1 = CBS 137618 = VKM F-4582).

Notes: Although *Sodiomyces alkalinus* was redescribed in Giraldo & Crous (2019), all species in the genus are invalid. This is due to the fact that the generic name *Sodiomyces* was invalid because it lacked a valid type species. The genus and all species are thus validated here.

Vermiconidia Egidi & Onofri, *gen. nov.* MycoBank MB829433.

Synonym: *Vermiconia* Egidi & Onofri, *Fungal Diversity* **65**: 150. 2014. *Nom. inval.*, Art. 40.7 (Shenzhen).

Etymology: Morphology of conidial chains reminiscent of worms.

Description and illustration: Egidi *et al.* (2014).

Type species: *Vermiconidia foris* Egidi & Onofri.

Vermiconidia antarctica Egidi & Selbmann, *sp. nov.* MycoBank MB829434.

Synonym: *Vermiconia antarctica* Egidi & Selbmann, *Fungal Diversity* **65**: 152. 2014. *Nom. inval.*, Art. 40.7 (Shenzhen).

Etymology: Named after the cold continent the strain was isolated from.

Description and illustration: Egidi *et al.* (2014).

Typus: **Antarctica**, McMurdo Dry Valleys, Battleship Promontory, from rock (**holotype** CBS 136107, culture and specimen preserved as metabolically inactive).

Vermiconidia calcicola de Hoog & Onofri, *sp. nov.* MycoBank MB829435.

Synonym: *Vermiconia calcicola* de Hoog & Onofri, *Fungal Diversity* **76**: 90. 2015 (2016). *Nom. inval.*, Art. 40.7 (Shenzhen).

Etymology: Named after the substrate where the ex-type strain was isolated.

Description and illustration: Isola *et al.* (2016).

Typus: **Italy**, Cagliari, isolated from Giuseppina Ara funerary marble monument in the cemetery of Bonaria (**holotype** CBS 140080, culture and specimen preserved as metabolically inactive).

Vermiconidia foris Egidi & Onofri, *sp. nov.* MycoBank MB829436.

Synonym: *Vermiconia foris* Egidi & Onofri, *Fungal Diversity* **65**: 150. 2014. *Nom. inval.*, Art. 40.7 (Shenzhen).

Etymology: Morphology of propagating cultures reminiscent of extraterrestrial worms.

Description and illustration: Egidi *et al.* (2014).

Typus: **Italy**, Monte Rosa, from rock (**holotype** CBS 136106, culture and specimen preserved as metabolically inactive).

Vermiconidia flagrans Selbmann & Isola, *sp. nov.* MycoBank MB829437.

Synonym: *Vermiconia flagrans* Selbmann & Isola, *Fungal Diversity* **65**: 152. 2014. *Nom. inval.*, Art. 40.7 (Shenzhen).

Etymology: Named after the survival of high summer temperatures prevailing in its natural habitat.

Description and illustration: Egidi *et al.* (2014).

Typus: **Spain**, Mallorca, from rock (**holotype** CBS 118296, culture and specimen preserved as metabolically inactive).

ACKNOWLEDGEMENTS

We are grateful to Arien van Iperen (cultures), Mieke Starink-Willems (DNA isolation, amplification, and sequencing), and Marjan Vermaas (photographic plates) for their technical assistance.

REFERENCES

- Ahmed SA, van de Sande WWJ, Stevens DA, *et al.* (2014). Revision of agents of black-grain eumycetoma in the order *Pleosporales*. *Persoonia* **33**: 141–154.
- Alderman SC, Rao S, Martin R (2010). First report of *Dicyma pulvinata* on *Epichloe typhina* and its potential for control of *E. typhina*. *Plant Health Progress*: doi:10.1094/PHP-2010-0216-01-RS.
- Amaral AL do, Dal Soglio FK, de Carli ML *et al.* (2005). Pathogenic fungi causing symptoms similar to Phaeosphaeria leaf spot of maize in Brazil. *Plant Disease* **89**: 44–49.
- Ando K, Nakamura N (2000). *Pseudosigmaidea*: A new genus for a hyphomycete (ATCC 16660) formerly identified as *Sigmaidea prolifera*. *Journal of General and Applied Microbiology* **46**: 51–57.
- Bakhshi, M, Arzanlou, M, Babai-Ahari, A, *et al.* (2018). Novel primers improve species delimitation in *Cercospora*. *IMA Fungus* **9**: 299–332.
- Barber PA, Crous PW, Groenewald JZ, *et al.* (2011). Reassessing *Vermisporium* (*Amphisphaeriaceae*), a genus of foliar pathogens of eucalypts. *Persoonia* **27**: 90–118.
- Bilanenko E, Sorokin D, Ivanova M (2005). *Heleococcum alkalinum*, a new alkali-tolerant ascomycete from saline soda soils. *Mycotaxon* **91**: 497–507.
- Bills GF, Peláez F (1996). Endophytic isolates of *Creosphaeria sassafras*. *Mycotaxon* **57**: 471–477.
- Braun U, Crous PW, Nakashima C (2015). Cercosporoid fungi (*Mycosphaerellaceae*) 3. Species on monocots (*Poaceae*, true grasses). *IMA Fungus* **6**: 25–97.
- Braun U, Nakashima C, Crous PW, *et al.* (2018). Phylogeny and taxonomy of the genus *Tubakia* s. lat. *Fungal Systematics and Evolution* **1**: 41–99.
- Cheewangkoon R, Groenewald JZ, Verkley GJM, *et al.* (2010). Re-evaluation of *Cryptosporiopsis eucalypti* and *Cryptosporiopsis*-like species occurring on *Eucalyptus*. *Fungal Diversity* **44**: 89–105.
- Chen C, Verkley GJM, Sun G, *et al.* (2016). Redefining common endophytes and plant pathogens in *Neofabraea*, *Pezicula*, and related genera. *Fungal Biology* **120**: 1291–1322.
- Chen Q, Jiang JR, Zhang GZ, *et al.* (2015). Resolving the *Phoma* enigma. *Studies in Mycology* **82**: 137–217.
- Corlett M, MacLachy IA (1987). *Petriella sordida*. *Fungi Canadenses* **313**: 1–2.
- Crous PW (1998). *Mycosphaerella* spp. and their anamorphs associated with leaf spot diseases of *Eucalyptus*. *Mycologia Memoir* **21**: 1–170. APS Press, MN, USA.
- Crous PW, Braun U (1994). *Cercospora* species and similar fungi occurring in South Africa. *Sydowia* **46**: 204–224.
- Crous PW, Braun U, Hunter GC, *et al.* (2013). Phylogenetic lineages in *Pseudocercospora*. *Studies in Mycology* **75**: 37–114.
- Crous PW, Braun U, Wingfield MJ, *et al.* (2009a). Phylogeny and taxonomy of obscure genera of microfungi. *Persoonia* **22**: 139–161.
- Crous PW, Gams W, Stalpers JA, *et al.* (2004). MycoBank: an online initiative to launch mycology into the 21st century. *Studies in Mycology* **50**: 19–22.
- Crous PW, Liu, F, Cai, L, *et al.* (2018a). *Allelochaeta* (*Sporocadaceae*): pigmentation lost and gained. *Fungal Systematics and Evolution* **2**: 273–309.

- Crous PW, Luangsa-ard JJ, Wingfield MJ, *et al.* (2018b). Fungal Planet description sheets: 785–867. *Persoonia* **41**: 238–417.
- Crous PW, Mohammed C, Glen M, *et al.* (2007). *Eucalyptus* microfungi known from culture. 3. *Eucasphaeria* and *Symptoventuria* genera nova, and new species of *Furcaspora*, *Harknessia*, *Heteroconium* and *Phacidiella*. *Fungal Diversity* **25**: 19–36.
- Crous PW, Schoch CL, Hyde KD, *et al.* (2009b). Phylogenetic lineages in the *Capnodiales*. *Studies in Mycology* **64**: 17–47.
- Crous PW, Schumacher RK, Wingfield MJ, *et al.* (2018c). New and interesting fungi. 1. *Fungal Systematics and Evolution* **1**: 169–215.
- Crous PW, Shivas RG, Quaedvlieg W, *et al.* (2014). Fungal Planet Description Sheets: 214–280. *Persoonia* **32**: 184–306.
- Crous PW, Verkley GJM, Groenewald JZ, *et al.* (eds) (2009c). *Fungal Biodiversity*. [CBS Laboratory Manual Series no.1.] Utrecht: Westerdijk Fungal Biodiversity Institute, Utrecht, the Netherlands.
- Crous PW, Wingfield MJ, Burgess TI, *et al.* (2017). Fungal Planet description sheets: 625–715. *Persoonia* **39**: 270–467.
- Crous PW, Wingfield MJ, Le Roux JJ, *et al.* (2015). Fungal Planet Description Sheets: 371–399. *Persoonia* **35**: 264–327.
- Crous PW, Wingfield MJ, Park RF (1991). *Mycosphaerella nubilosa* a synonym of *M. molleriana*. *Mycological Research* **95**: 628–632.
- Crous PW, Wingfield MJ, Richardson DM, *et al.* (2016). Fungal Planet description sheets: 400–468. *Persoonia* **36**: 316–458.
- De Gruyter J, Woudenberg JHC, Aveskamp MM, *et al.* (2010). Systematic reappraisal of species in *Phoma* section *Paraphoma*, *Pyrenochaeta* and *Pleurophoma*. *Mycologia* **102**: 1066–1081.
- De Gruyter J, Woudenberg JHC, Aveskamp MM, *et al.* (2013). Redisposition of *Phoma*-like anamorphs in *Pleosporales*. *Studies in Mycology* **75**: 1–36.
- De Hoog GS (1977). *Rhinochlaetia* and allied genera. *Studies in Mycology* **15**: 1–140.
- Deighton FC (1972). Synonymy of *Hansfordia pulvinata* (Berk. & Curt.) Hughes. *Transactions of the British Mycological Society* **59**: 531–536.
- Diene O, Wang W, Narisawa K (2013). *Pseudosigmoidea ibarakiensis* sp. nov., a dark septate endophytic fungus from a Cedar forest in Ibaraki, Japan. *Microbes and Environments* **28**: 381–387.
- Egidi E, de Hoog GS, Isola D, *et al.* (2014). Phylogeny and taxonomy of meristematic rock-inhabiting black fungi in the *Dothideomycetes* based on multi-locus phylogenies. *Fungal Diversity* **65**: 127–165.
- Ellis MB (1971). *Dematiaceous Hyphomycetes*. Commonwealth Mycological Institute: Kew, England.
- Ellis MB (1976). *More Dematiaceous Hyphomycetes*. Commonwealth Mycological Institute: Kew, England.
- Ellis MB, Ellis JP (1997). *Microfungi on Land Plants - An Identification Handbook*. Richmond Publishing, England.
- Fan XL, Bezerra JDP, Tian CM, *et al.* (2018). Families and genera of diarthalean fungi associated with canker and dieback of tree hosts. *Persoonia* **40**: 119–134.
- Fitzpatrick HM (1942). Revisionary studies in the *Coryneliaceae*. II. The genus *Caliciopsis*. *Mycologia* **34**: 489–514.
- Friebes G (2012). A key to the non-lichenicolous species of the genus *Capronia* (Herpotrichiellaceae). *Ascomycete.org* **4**: 55–64.
- Gao L, Ma Y, Zhao W, *et al.* (2015). Three new species of *Cyphellophora* (*Chaetothyriales*) associated with Sooty Blotch and Flyspeck. *PLOS ONE* **10**: e0136857.
- Gao Y, Liu F, Duan W, *et al.* (2017). *Diaporthe* is paraphyletic. *IMA Fungus* **8**: 153–187.
- Giraldo A, Crous PW (2019). Inside *Plectosphaerellaceae*. *Studies in Mycology* **92**: 227–286.
- Giraldo A, Sutton DA, Samerpitak K, *et al.* (2014). Occurrence of *Ochroconis* and *Verruconis* species in clinical specimens from the United States. *Journal of Clinical Microbiology* **52**: 4189–4201.
- Gomes RR, Glienke C, Videira CIR, *et al.* (2013). *Diaporthe*: a genus of endophytic, saprobic and plant pathogenic fungi. *Persoonia* **31**: 1–41.
- Gonçalves RM, Figueiredo JEF, Pedro ES, *et al.* (2013). Etiology of phaeosphaeria leaf spot disease of maize. *Journal of Plant Pathology* **95**: 559–569.
- Groenewald JZ, Nakashima C, Nishikawa J, *et al.* (2013). Species concepts in *Cercospora*: spotting the weeds among the roses. *Studies in Mycology* **75**: 115–170.
- Grum-Grzhimaylo AA, Debets AJM, van Diepeningen AD (2013). *Sodiomyces alkalinus*, a new holomorphic alkaliphilic ascomycete within the *Plectosphaerellaceae*. *Persoonia* **31**: 147–158.
- Grum-Grzhimaylo AA, Georgieva ML, Bondarenko SA (2016). On the diversity of fungi from soda soils. *Fungal Diversity* **76**: 27–74.
- Guarnaccia V, Crous PW (2017). Emerging citrus diseases in Europe caused by species of *Diaporthe*. *IMA Fungus* **8**: 317–334.
- Guarnaccia V, Groenewald JZ, Li H, *et al.* (2017). First report of *Phyllosticta citricarpa* and description of two new species, *P. paracapitalensis* and *P. paracitricarpa*, from citrus in Europe. *Studies in Mycology* **87**: 161–185.
- Halici MG, Hawksworth DL, Candan M, *et al.* (2010). A new lichenicolous species of *Capronia* (*Ascomycota*, *Herpotrichiellaceae*) with a key to the known lichenicolous species of the genus. *Fungal Diversity* **40**: 37–40.
- Hawksworth DL, Crous PW, Redhead SA, *et al.* (2011). The Amsterdam Declaration on Fungal Nomenclature. *IMA Fungus* **2**: 105–112.
- Hernández-Restrepo M, Gené J, Castañeda-Ruiz RF, *et al.* (2017). Phylogeny of saprobic microfungi from Southern Europe. *Studies in Mycology* **86**: 53–97.
- Hernández-Restrepo M, Groenewald JZ, Crous PW (2015). *Neocordana gen. nov.*, the causal organism of Cordana leaf spot of banana. *Phytotaxa* **205**: 229–238.
- Hernández-Restrepo M, Groenewald JZ, Crous PW (2016). Taxonomic and phylogenetic re-evaluation of *Microdothium*, *Monographella* and *Idriella*. *Persoonia* **36**: 57–82.
- Isola D, Zucconi L, Onofri S, *et al.* (2016). Extremotolerant rock inhabiting black fungi from Italian monumental sites. *Fungal Diversity* **76**: 75–96.
- Jaklitsch WM, Checa J, Blanco MN, *et al.* (2018). A preliminary account of the *Cucurbitariaceae*. *Studies in Mycology* **90**: 71–118.
- Kearse M, Moir R, Wilson A, *et al.* (2012). Geneious Basic: an integrated and extendable desktop software platform for the organization and analysis of sequence data. *Bioinformatics* **28**: 1647–1649.
- Klaubauf S, Tharreau D, Fournier E, *et al.* (2014). Resolving the polyphyletic nature of *Pyricularia* (*Pyriculariaceae*). *Studies in Mycology* **79**: 85–120.
- Lackner M, de Hoog GS (2011). *Parascenedosporium* and its relatives: phylogeny and ecological trends. *IMA Fungus* **2**: 39–48.
- Lombard L, Houbraken J, Decock C, *et al.* (2016). Generic hyperdiversity in *Stachybotriaceae*. *Persoonia* **36**: 156–246.
- Marin-Felix Y, Hernández-Restrepo M, Wingfield MJ, *et al.* (2019). Genera of phytopathogenic fungi: GOPHY 2. *Studies in Mycology* **92**: 47–133.
- Mitchell JK, Taber RA (1986). Factors affecting the biological control of *Cercosporidium* leaf spot of peanuts by *Dicyma pulvinata*. *Phytopathology* **76**: 990–994.
- Okada G, Nimura Y, Sakata T (1993). *Acremonium alcalophilum*, a new alkaliphilic cellulolytic hyphomycete. *Transactions of the Mycological Society of Japan* **34**: 171–185.
- Palm ME (1996). *Kirramyces phormii* comb. nov. from leaves of *Phormium*. *Mycological Research* **100**: 373–376.
- Pascoe IG, McGee (Maher) PA, Smith IW, *et al.* (2018). *Caliciopsis pleomorpha* sp. nov. (*Ascomycota*: *Coryneliales*) causing a severe

- canker disease of *Eucalyptus cladocalyx* and other eucalypt species in Australia. *Fungal Systematics and Evolution* **2**: 45–56.
- Peresse M, Le Picard D (1980). *Hansfordia pulvinata*, mycoparasite destructeur du *Cladosporium fulvum*. *Mycopathologia* **71**: 23–30.
- Phillips AJL, Alves A, Pennycook SR, *et al.* (2008). Resolving the phylogenetic and taxonomic status of dark-spored teleomorph genera in the *Botryosphaeriaceae*. *Persoonia* **21**: 29–55.
- Quaedvlieg W, Binder M, Groenewald JZ, *et al.* (2014). Introducing the Consolidated Species Concept to resolve species in the *Teratosphaeriaceae*. *Persoonia* **33**: 1–40.
- Ramaley, AW (2005). The connection of *Dothidothia aspera* (*Botryosphaeriaceae*) to a hyphomycetous anamorphic fungus, *Thyrostroma negundinis*. *Mycotaxon* **94**: 127–132.
- Rambelli A (1958). Schede Micologiche. Micromiceti della foresta di Campigna. Il Contributo. *Atti della Accademia delle Scienze dell'Istituto di Bologna. Classe di Scienze Fisiche. Rendiconti. Serie 11*, **5**: 1–16.
- Rambelli A (2011). Some Dematiaceous Hyphomycetes from Mediterranean maquis litters. *Flora Mediterranea* **21**: 5–204.
- Rayner RW (1970). *A mycological colour chart*. Commonwealth Mycological Institute and British Mycological Society. Kew, Surrey, UK.
- Réblová M, Hubka V, Thureborn O, *et al.* (2016). From the tunnels into the treetops: new lineages of black yeasts from biofilm in the Stockholm metro system and their relatives among ant-associated fungi in the *Chaetothyriales*. *PLOS ONE* **11**: e0163396.
- Ronquist F, Teslenko M, Van der Mark P, *et al.* (2012). MrBayes 3.2: Efficient Bayesian phylogenetic inference and model choice across a large model space. *Systematic Biology* **61**: 539–542.
- Rossmann AY, Crous PW, Hyde KD, *et al.* (2015). Recommended names for pleomorphic genera in *Dothideomycetes*. *IMA Fungus* **6**: 507–523.
- Samerpitak K, Duarte APM, Attili-Angelis D, *et al.* (2015). A new species of the oligotrophic genus *Ochroconis* (*Symptoventuriaceae*). *Mycological Progress* **14**: 6.
- Seifert KA, Nickerson NL, Corlett M, *et al.* (2004). *Devriesia*, a new hyphomycete genus to accommodate heat-resistant, cladosporium-like fungi. *Canadian Journal of Botany* **82**: 914–926.
- Senanayake IC, Crous PW, Groenewald JZ, *et al.* (2017). Families of *Diaporthales* based on morphological and phylogenetic evidence. *Studies in Mycology* **86**: 217–296.
- Smith H, Wingfield MJ, Crous PW, *et al.* (1996). *Sphaeropsis sapinea* and *Botryosphaeria dothidea* endophytic in *Pinus* spp. and *Eucalyptus* spp. in South Africa. *South African Journal of Botany* **62**: 86–88.
- Summerell BA, Groenewald JZ, Carnegie AJ, *et al.* (2006). *Eucalyptus* microfungi known from culture. 2. *Alysiidiella*, *Fusculina* and *Phlogicylindrium* genera nova, with notes on some other poorly known taxa. *Fungal Diversity* **23**: 323–350.
- Swofford DL (2003). *PAUP*: phylogenetic analysis using parsimony. (*and other methods)*. Version 4.0b10. Sinauer Associates, Sunderland.
- Tanaka K, Hirayama K, Yonezawa H, *et al.* (2015). Revision of the *Massariaceae* (*Pleosporales*, *Dothideomycetes*). *Studies in Mycology* **82**: 75–136.
- Tennakoon DS, Hyde KD, Phookamsak R, *et al.* (2016). Taxonomy and phylogeny of *Juncaceicola* gen. nov. (*Phaeosphaeriaceae*, *Pleosporinae*, *Pleosporales*). *Cryptogamie, Mycologie* **37**: 135–156.
- Thambugala KM, Hyde KD, Tanaka K, *et al.* (2015). Towards a natural classification and backbone tree for *Lophiostomataceae*, *Floricolaceae*, and *Amorosiaceae* fam. nov. *Fungal Diversity* **74**: 199–266.
- Tsui CKM, Sivichai S, Berbee ML (2006). Molecular systematics of *Helicoma*, *Helicomycetes* and *Helicosporium* and their teleomorphs inferred from rDNA sequences. *Mycologia* **98**: 94–104.
- Tubaki K, Saitô T (1969). *Endophragmia alternata* sp. nov. and other hyphomycetes on *Pinus* leaves in Japan. *Transactions of the British Mycological Society* **52**: 477–482.
- Udayanga D, Castlebury LA, Rossmann LA, *et al.* (2014). Insights into the genus *Diaporthe*: phylogenetic species delimitation in the *D. eres* species complex. *Fungal Diversity* **64**: 203–229.
- Untereiner W (1997). Taxonomy of selected members of the ascomycete genus *Capronia* with notes on anamorph-teleomorph connections. *Mycologia* **89**: 120–131.
- Valenzuela-Lopez N, Cano-Lira JF, Guarro J, *et al.* (2018). Coelomycetous *Dothideomycetes* with emphasis on the families *Cucurbitariaceae* and *Didymellaceae*. *Studies in Mycology* **90**: 1–69.
- Van Coller GJ, Denman S, Groenewald JZ, *et al.* (2005). Characterisation and pathogenicity of *Cylindrocladiella* spp. associated with root and cutting rot symptoms of grapevines in nurseries. *Australasian Plant Pathology* **34**: 489–498.
- Videira SIR, Groenewald JZ, Braun U, *et al.* (2016). All that glitters is not *Ramularia*. *Studies in Mycology* **83**: 49–163.
- Videira SIR, Groenewald JZ, Nakashima C, *et al.* (2017). *Mycosphaerellaceae* – chaos or clarity? *Studies in Mycology* **87**: 257–421.
- Wanasinghe DN, Hyde KD, Jeewon R, *et al.* (2017). Phylogenetic revision of *Camarosporium* (*Pleosporinae*, *Dothideomycetes*) and allied genera. *Studies in Mycology* **87**: 207–256.
- Wanasinghe DN, Phukhamsakda C, Hyde KD, *et al.* (2018). Fungal diversity notes 709–839: taxonomic and phylogenetic contributions to fungal taxa with an emphasis on fungi on *Rosaceae*. *Fungal Diversity* **89**: 1–226.
- Wingfield MJ, De Beer ZW, Slippers B, *et al.* (2012). One fungus, one name promotes progressive plant pathology. *Molecular Plant Pathology* **13**: 604–613.
- Wong M-H, Crous PW, Henderson J, *et al.* (2012). *Phyllosticta* species associated with freckle disease of banana. *Fungal Diversity* **56**: 173–187.
- Zhang Z, Schwartz S, Wagner L, *et al.* (2000). A greedy algorithm for aligning DNA sequences. *Journal of Computational Biology* **7**: 203–214.
- Zhou N, Chen Q, Carroll G, *et al.* (2015). Polyphasic characterization of four new plant pathogenic *Phyllosticta* species from China, Japan, and the United States. *Fungal Biology* **119**: 433–446.

doi.org/10.3114/fuse.2019.03.07

Taxonomic revision and multi-locus phylogeny of the North American clade of *Ceratocystis*

L.A. Holland¹, D.P. Lawrence¹, M.T. Nouri², R. Travadon¹, T.C. Harrington³, F.P. Trouillas^{2*}

¹Department of Plant Pathology, University of California, Davis, CA 95616, USA

²Department of Plant Pathology, University of California, Kearney Agricultural Research and Extension Centre, Parlier, CA 93648, USA

³Department of Plant Pathology and Microbiology, Iowa State University, Ames, Iowa 50011, USA

*Corresponding author: flotrouillas@ucdavis.edu

Key words:

almond
Ceratocystidaceae
Ceratocystis canker
new species
taxonomy

Abstract: The North American clade (NAC) of *Ceratocystis* includes pathogenic species that infect a wide range of woody hosts. Previous phylogenetic analyses have suggested that this clade includes cryptic species and a paraphyletic *C. variospora*. In this study, we used morphological data and phylogenetic analyses to characterize NAC taxa, including *Ceratocystis* isolates causing a serious disease of almond trees in California. Phylogenetic analyses based on six gene regions supported two new species of *Ceratocystis*. *Ceratocystis destructans* is introduced as the species causing severe damage to almond trees in California, and it has also been isolated from wounds on *Populus* and *Quercus* in Iowa. It is morphologically similar to *C. tiliae*, a pathogen on *Tilia* and the most recently characterized species in the NAC. *Ceratocystis betulina* collected from *Betula platyphylla* in Japan is also newly described and is the sister taxon to *C. variospora*. Our six-locus phylogenetic analyses and morphological characterization resolved several cryptic species in the NAC.

Effectively published online: 27 February 2019.

INTRODUCTION

The genus *Ceratocystis* (*Sordariomycetes*, *Microascales*, *Ceratocystidaceae*) was proposed in 1890 based on *C. fimbriata*, which was first described as the causal agent of black rot of sweet potato (*Ipomoea batatas*) in the USA (Halsted 1890). The genus now comprises 39 species (Marin-Felix *et al.* 2017, Barnes *et al.* 2018, Liu *et al.* 2018) and consists of a complex of many cryptic and some host-specialized species (Harrington 2000, Oliveira *et al.* 2015a) that cause various wilt and canker diseases on a wide range of economically important crops around the world (Kile 1993, Harrington 2013). Hosts impacted by *Ceratocystis* species include *Coffea arabica* (coffee), *Eucalyptus* spp., *Ficus carica* (fig), *Hevea brasiliensis* (rubber tree), *Mangifera indica* (mango), *Platanus* spp. (sycamore or plane trees), *Populus* spp. (aspen and other poplars), *Prunus* spp. (almond and other stone fruits), *Quercus* spp. (oak) and *Theobroma cacao* (cacao) (Harrington 2000, 2013, de Beer *et al.* 2014). Recently, *Ceratocystis* s. lat. was split into 11 genera (*Ambrosiella*, *Berkeleyomyces*, *Bretziella*, *Ceratocystis*, *Chalaropsis*, *Davidsoniella*, *Endoconidiophora*, *Huntiella*, *Meredithiella*, *Phialophoropsis*, and *Thielaviopsis*) based on morphological observations, namely perithecial and ascospore characters, and to a greater extent based on phylogenetic placement (de Beer *et al.* 2014, 2017, Mayers *et al.* 2015, 2018, Nel *et al.* 2018).

Ceratocystis is morphologically defined as species that produce hat-shaped ascospores from brown to black, globose, unornamented perithecial bases with elongated perithecial necks that terminate as aseptate, divergent, and blunt-tipped ostiolar hyphae (de Beer *et al.* 2014). Long-necked perithecia release sticky masses of ascospores at their terminus (Upadhyay

1981, Seifert *et al.* 1993, Harrington 2013, de Beer *et al.* 2014). The asexual thielaviopsis-like morph, is characterized by phialidic conidial ontogeny producing chains of hyaline, single-celled, cylindrical-shaped conidia, called endoconidia (de Beer *et al.* 2014). Barrel-shaped conidia (doliiform conidia) may also be produced from similar endoconidiophores, and most species produce dark, thick-walled aleurioconidia that facilitate survival in wood or in soil (Harrington 2013, de Beer *et al.* 2014).

Ceratocystis species are mainly wound colonizers and include weak to highly virulent pathogens causing disease on diverse woody plant hosts. However, *Ceratocystis* disease cycles are not well understood due to the diversity of spore types, inoculum sources, and dispersal mechanisms, such as insect vectors, wind, infected planting material, root grafting or mechanical transmission during pruning and harvesting (Harrington 2013). Many *Ceratocystis* species are adapted for insect dispersal by producing sweet-smelling or fruity volatiles that attract insect vectors (Harrington 1993, Kile 1993, Wingfield *et al.* 1993). The sticky ascospore masses adhere to insect bodies where they can be easily vectored from one host to another (Malloch & Blackwell 1993). *Ceratocystis fimbriata* has nonspecific associations with insects such as sap-feeding beetles (*Coleoptera*; *Nitidulidae*), flies (*Diptera*; *Drosophilidae*) and ambrosia beetles (*Coleoptera*; *Curculionidae*) (Kile 1993). In addition to insect dispersal, *Ceratocystis* species that produce aleurioconidia are typically soilborne and can be transported in water (Kile 1993, Harrington 2013).

Currently, phylogenetic hypotheses have placed *Ceratocystis* in four broad geographical clades, the Latin American clade (LAC) (Harrington 2000, Engelbrecht & Harrington 2005), the North American clade (NAC) (Johnson *et al.* 2005), the African

clade (AFC) (Heath *et al.* 2009, Mbenoun *et al.* 2014), and the Asian-Australian clade (AAC) (Johnson *et al.* 2005, Thorpe *et al.* 2005, Li *et al.* 2017).

The LAC is represented by *C. fimbriata* which is the pathogen that causes black rot of sweet potato. This pathogen is native to South and Central America and the Caribbean (Harrington *et al.* 2011) and causes wilt or cankers on coffee, *Eucalyptus* spp., rubber trees, and mango (Harrington 2013). Species in the LAC are considered to be aggressive pathogens responsible for emerging epidemics when introduced to new hosts and locations, such as the recent outbreak of *Ceratocystis* wilt on mango in Oman and Pakistan (Al Adawi *et al.* 2014). Other economically important LAC species include *C. platani*, the causal agent of canker stain on *Platanus* spp. and *C. cacaofunesta*, the causal agent of *Ceratocystis* wilt of *T. cacao* (Engelbrecht & Harrington 2005). In California, *C. platani* from the LAC has caused mortality of California sycamores (*Platanus racemosa* var. *racemosa*) and plane trees in Modesto, California (Perry & McCain 1988), and the pathogen was apparently introduced from the eastern USA (Engelbrecht *et al.* 2005). Most recently, a new *Ceratocystis* species belonging to the LAC, *C. lukuohia*, was identified in Hawai'i and associated with rapid death of 'ōhi'a lehua (*Metrosideros polymorpha*), a devastating disease on an ecologically important native tree species (Barnes *et al.* 2018).

The AFC includes *C. albofundus*, a pathogen of black wattle (*Acacia mearnsii*) in Africa (Wingfield *et al.* 1996). This species is thought to be native to Africa with two genetically isolated populations, in Uganda and South Africa (Barnes *et al.* 2005). The AAC is represented by *C. pirilliformis* (Johnson *et al.* 2005, Thorpe *et al.* 2005), a pathogen discovered on *Eucalyptus nitens* in Australia (Barnes *et al.* 2003). Other species residing in the AAC include *C. changhui* from *Colocasia esculenta* in China (Liu *et al.* 2018) and *C. uchidae* from *C. esculenta* in Hawai'i (Li *et al.* 2017). However, species boundaries within the AAC are unclear and require phylogenetic and taxonomic re-examination (Li *et al.* 2017). Recently, *C. huliohia*, a newly identified species in the AAC, was described together with *C. lukuohia* (LAC), as a second causal agent of rapid death of 'ōhi'a lehua in Hawai'i (Barnes *et al.* 2018).

Morphological features have been used to distinguish isolates from the NAC and LAC, most notably, slightly smaller ascospores in the NAC and the presence of a collar at the base of the neck of the perithecium; this diagnostic feature is absent in members of the LAC (Johnson *et al.* 2005). Within the NAC, *Ceratocystis* species are distinguished from one another based on the presence or absence of conidial stages, host range, isozyme alleles, and DNA-based phylogenetic analyses (Johnson *et al.* 2005, de Beer *et al.* 2014, Oliveira *et al.* 2015a). Yet, the taxonomy and systematics in the NAC needs more rigorous investigation (Johnson *et al.* 2005, Oliveira *et al.* 2015a).

The NAC currently includes five *Ceratocystis* species that have been isolated from various tree hosts, including *Betula*, *Carya*, *Celtis*, *Ostrya*, *Populus*, *Prunus*, *Quercus*, *Tilia*, and *Ulmus* in Europe, Asia, and North America (Johnson *et al.* 2005). Currently, the NAC of *Ceratocystis* is comprised of four strongly supported species including *C. caryae* (*Carya* spp. and other hosts), *C. harringtonii* (synonym *C. populicola*; *Populus* spp.), *C. smalleyi* (*Carya* spp. and an associated bark beetle, *Scolytus quadrispinosus*), *C. tiliae* (*Tilia americana*), and the paraphyletic taxon *C. variospora*. Traditionally, the name *C. variospora* has been used to describe the species infecting oaks (*Quercus* spp.) in the midwestern USA, but it has been isolated from other

hardwood species, and *C. variospora* currently includes the pathogen on *Prunus* spp. in California (Johnson *et al.* 2005). Although isolates of *C. variospora* from oak and *Prunus* differ in their ITS sequences, they could not be distinguished based on morphology nor host association (Johnson *et al.* 2005). A new species within *C. variospora* was recently described as *C. tiliae*, a wound-associated pathogen of basswood (*Tilia americana*) in Nebraska and Iowa (Oliveira *et al.* 2015a). Individual phylogenetic analysis across three loci (LSU, *TEF1*, and *Cerato-platanin*) strongly suggests that *C. variospora* is a paraphyletic taxon as currently defined (Oliveira *et al.* 2015a). Interfertility tests have shown that isolates from the *Quercus* lineage (*C. variospora* s. str.) are only interfertile with each other and not with isolates collected from *Betula*, *Prunus*, or *Tilia* (*C. variospora* s. lat.) (Johnson *et al.* 2005), thus supporting a biological species concept in conjunction with host specialization (Oliveira *et al.* 2015a).

Johnson *et al.* (2005) proposed that the name *C. variospora* should be applied to the *Prunus* pathogen in California. The fungus causes *Ceratocystis* canker of almond (*Prunus dulcis*) (DeVay *et al.* 1960) and infects other stone fruits, including apricot (*P. armeniaca*) and prune (*P. domestica*) (DeVay *et al.* 1962). The fungus is thought to colonize wounds made on the bark of trees during mechanical harvest. This disease is ubiquitous in older almond orchards and has recently become a growing concern for young orchards. Almonds are California's most economically important agricultural crop and over 80 % of the global supply is grown in California. Disease symptoms appear as brown to dark brown, shallow (not extending far beyond the cambium), and sunken, cankers. Canker expansion is rapid during the growing season, eventually girdling infected limbs, causing leaves to wilt and branches to dieback. The use of mechanical shakers has led to bark injuries on the trunks of trees and a high incidence of *Ceratocystis* canker.

The aim of this study was to revisit the taxonomy and phylogeny of *Ceratocystis* isolates recovered from symptomatic almond trees in California. DNA from cultures linked to ex-type and representative specimens for each species in the NAC were obtained and included in a six-gene phylogeny, utilizing portions of 28S (LSU) rDNA, β -tubulin (*TUB2*), translation elongation factor 1-alpha (*TEF1*), mini-chromosome maintenance complex component 7 (*MCM7*), 60S ribosomal protein RPL10 (60S), and *Cerato-platanin* (CP) gene fragments to further resolve cryptic species within the NAC of *Ceratocystis*.

MATERIALS AND METHODS

Collection of isolates

Isolates were collected from symptomatic almond trees throughout the major almond producing regions in the Central Valley of California (Table 1). Frequently, isolates were collected from trees that were damaged by mechanical harvesting at the trunk or near large pruning wounds made on the scaffolding branches. Gummosis delineated the margins of the cankers in most cases. Trees exhibiting gummosis and sunken lesions in the bark were sampled using a hatchet. Fungi were isolated from pieces of inner bark (50 × 50 × 5 mm) from the margins of active cankers; the pieces were surface disinfested in 0.6 % sodium hypochlorite for 2 min, rinsed twice with sterile water and patted dry with a paper towel. The inner bark pieces were incubated

Table 1. *Ceratocystis* species used for phylogenetic analyses in this study. Newly generated sequences appear in **bold**.

Species	Isolate ^a	Host	Geographic origin	Year	Collector	LSU	TUB2	TEF1	GenBank Accession Nos.		
									MCM7	60S	CP ^b
<i>Ceratocystis betulina</i>	C1709/CBS 144246	<i>Betula platyphylla</i>	Japan, Morioko, Iwate	2000	H. Masuya	MG980939	MG980839	MG980743	MG980985	MG980789	MG980889
	C1770	<i>Betula platyphylla</i>	Japan, Morioko, Iwate	2000	H. Masuya	MG980940	MG980840	MG980744	MG980986	MG980790	MG980890
<i>C. caryae</i>	C1829/CBS 114716	<i>Carya cordiformis</i>	Linn Co., Iowa	2001	J.A. Johnson	MG980929	MG980829	MG980733	MG980978	MG980781	MG980879
	C1827/CBS 115168	<i>Carya ovata</i>	Boone Co., Iowa	2001	J.A. Johnson	MG980928	MG980828	MG980732	KM495414	KM495502	MG980878
<i>C. destructans</i>	KARE219	<i>Prunus dulcis</i>	Fresno Co., California	2015	F.P. Trouillas & M.T. Nouri	MG980949	MG980849	MG980753	MG980995	MG980799	MG980899
	KARE230	<i>Prunus dulcis</i>	Fresno Co., California	2015	F.P. Trouillas & M.T. Nouri	MG980951	MG980851	MG980755	MG980997	MG980801	MG980901
	KARE300	<i>Prunus dulcis</i>	Fresno Co., California	2015	F.P. Trouillas & M.T. Nouri	MG980952	MG980852	MG980756	MG980998	MG980802	MG980902
	KARE490	<i>Prunus dulcis</i>	Kern Co., California	2015	F.P. Trouillas & M.T. Nouri	MG980953	MG980853	MG980757	MG980999	MG980803	MG980903
	KARE494	<i>Prunus dulcis</i>	Kern Co., California	2015	F.P. Trouillas & M.T. Nouri	MG980954	MG980854	MG980758	MG981000	MG980804	MG980904
	KARE495	<i>Prunus dulcis</i>	Kern Co., California	2015	F.P. Trouillas & M.T. Nouri	MG980955	MG980855	MG980759	MG981001	MG980805	MG980905
	KARE223	<i>Prunus dulcis</i>	Merced Co., California	2015	F.P. Trouillas & M.T. Nouri	MG980950	MG980850	MG980754	MG980996	MG980800	MG980900
	KARE978	<i>Prunus dulcis</i>	Colusa Co., California	2016	L.A. Holland	MG980956	MG980856	MG980760	MG981002	MG980806	MG980906
	KARE979	<i>Prunus dulcis</i>	Colusa Co., California	2016	L.A. Holland	MG980957	MG980857	MG980761	MG981003	MG980807	MG980907
	KARE994	<i>Prunus dulcis</i>	Colusa Co., California	2016	L.A. Holland	MG980958	MG980858	MG980762	MG981004	MG980808	MG980908
<i>C. destructans</i>	KARE1427	<i>Prunus dulcis</i>	Madera Co., California	2016	L.A. Holland & F.P. Trouillas	MG980959	MG980859	MG980763	MG981005	MG980809	MG980909
	KARE1428/CBS 144247	<i>Prunus dulcis</i>	Madera Co., California	2016	L.A. Holland & F.P. Trouillas	MG980960	MG980860	MG980764	MG981006	MG980810	MG980910
<i>C. destructans</i>	KARE1447	<i>Prunus dulcis</i>	Fresno Co., California	2016	L.A. Holland & F.P. Trouillas	MG980961	MG980861	MG980765	MG981007	MG980811	MG980911
	KARE1448	<i>Prunus dulcis</i>	Fresno Co., California	2016	L.A. Holland & F.P. Trouillas	MG980962	MG980862	MG980766	MG981008	MG980812	MG980912
<i>C. destructans</i>	KARE1609	<i>Prunus dulcis</i>	Merced Co., California	2016	F.P. Trouillas	MG980963	MG980863	MG980767	MG981009	MG980813	MG980913
	KARE1610	<i>Prunus dulcis</i>	Merced Co., California	2016	F.P. Trouillas	MG980964	MG980864	MG980768	MG981010	MG980814	MG980914

Table 1. (Continued).

Species	Isolate ^a	Host	Geographic origin	Year	Collector	LSU	TUB2	TEF1	GenBank Accession Nos.		
									MCM7	60S	CP ^b
	KARE1611	<i>Prunus dulcis</i>	Merced Co., California	2016	F.P. Trouillas	MG980965	MG980865	MG980769	MG981011	MG980815	MG980915
	KARE1612	<i>Prunus dulcis</i>	Merced Co., California	2016	F.P. Trouillas	MG980966	MG980866	MG980770	MG981012	MG980816	MG980916
	KARE1613	<i>Prunus dulcis</i>	Merced Co., California	2016	F.P. Trouillas	MG980967	MG980867	MG980771	MG981013	MG980817	MG980917
	KARE1614	<i>Prunus dulcis</i>	Merced Co., California	2016	F.P. Trouillas	MG980968	MG980868	MG980772	MG981014	MG980818	MG980918
	KARE1622	<i>Prunus dulcis</i>	Merced Co., California	2016	F.P. Trouillas	MG980969	MG980869	MG980773	MG981015	MG980819	MG980919
	KARE1624	<i>Prunus dulcis</i>	Glenn Co., California	2016	F.P. Trouillas	MG980970	MG980870	MG980774	MG981016	MG980820	MG980920
	KARE1627	<i>Prunus dulcis</i>	Glenn Co., California	2016	F.P. Trouillas	MG980971	MG980871	MG980775	MG981017	MG980821	MG980921
	KARE1628	<i>Prunus dulcis</i>	Glenn Co., California	2016	F.P. Trouillas	MG980972	MG980872	MG980776	MG981018	MG980822	MG980922
	C578	<i>Prunus dulcis</i>	California	1989	R. Bostock	MG980945	MG980845	MG980749	MG980991	MG980795	MG980895
	C821	<i>Prunus dulcis</i>	Colusa Co., California	1996	D. Rizzo	MG980948	MG980848	MG980752	MG980994	MG980798	MG980898
	C856	<i>Prunus dulcis</i>	Merced Co., California	1996	T.C. Harrington	MG980946	MG980846	MG980750	MG980992	MG980796	MG980896
	C1822	<i>Prunus dulcis</i>	Stanislaus Co., California	2001	T.C. Harrington	MG980947	MG980847	MG980751	MG980993	MG980797	MG980897
	C1953	<i>Populus</i> sp.	Boone Co., Iowa	2002	J.A. Johnson	MG980942	MG980842	MG980746	MG980988	MG980792	MG980892
	C1956	<i>Quercus macrocarpa</i>	Lucas Co., Iowa	2002	J.A. Johnson	MG980941	MG980841	MG980745	MG980987	MG980791	MG980891
	C1957	<i>Celtis</i> sp.	Lucas Co., Iowa	2002	J.A. Johnson	MG980943	MG980843	MG980747	MG980989	MG980793	MG980893
	C1963	<i>Prunus serotina</i>	Boone Co., Iowa	2002	J.A. Johnson	MG980944	MG980844	MG980748	MG980990	MG980794	MG980894
<i>C. fimbriata</i>	C1476/C1099	<i>Ipomoea batatas</i>	Papua New Guinea	1984	E.H.C. McKenzie & F.M. Quin	MG980927	MG980827	MG980731	MG980977	MG980781	MG980877
<i>C. harringtonii</i>	C685/CBS 115161	<i>Populus tremuloides</i>	Québec, Canada	1993	E. Smalley	MG980932	MG980832	MG980736	MG980980	MG980784	MG980882
	C1485/ATCC 24096	<i>Populus tremuloides</i>	Colorado	1999	T.E. Hinds	MG980933	MG980833	MG980737	MG980981	MG980785	MG980883
	C995/CBS 119.78	<i>Populus</i> sp.	Poland	1978	J. Gremmen	MG980934	MG980834	MG980738	KM495435	KM495523	MG980884
<i>C. smallei</i>	C684/CBS 114724	<i>Carya cordiformis</i>	Wisconsin	1993	E. Smalley	MG980930	MG980830	MG980734	KM495463	KM495553	MG980880
	C682	<i>Carya cordiformis</i>	La Crosse Co., Wisconsin	1986	E. Smalley	MG980931	MG980831	MG980735	MG980979	MG980783	MG980881

Table 1. (Continued).

Species	Isolate ^a	Host	Geographic origin	Year	Collector	GenBank Accession Nos.						
						LSU	TUB2	TEF1	MCM7	60S	CP ^b	
<i>C. tiliae</i>	C2131/CBS 137355	<i>Tilia americana</i>	Story Co., Iowa	2004	T.C. Harrington	MG980975	MG980875	MG980779	MG981021	MG980825	MG980925	
	C2622/CBS 137356	<i>Tilia americana</i>	Douglas Co., Nebraska	2001	T.C. Harrington	MG980973	MG980873	MG980777	MG981019	MG980823	MG980923	
<i>C. variispora</i>	C1954/CBS 137354	<i>Tilia americana</i>	Boone Co., Iowa	2002	J.A. Johnson	MG980974	MG980874	MG980778	MG981020	MG980824	MG980924	
	C1959	<i>Tilia americana</i>	Iowa	2002	J.A. Johnson	MG980976	MG980876	MG980780	MG981022	MG980826	MG980926	
	C1009/CBS 773.73	<i>Quercus ellipsoidalis</i>	Carlton Co., Minnesota	1955/1956	R.N. Campbell	MG980935	MG980835	MG980739	MG980982	MG980786	MG980885	
	C1483/ATCC 12866	<i>Quercus ellipsoidalis</i>	Minnesota	1955/1956	R.N. Campbell	MG980936	MG980836	MG980740	MG980983	MG980787	MG980886	
	C1843/CBS 114715	<i>Quercus alba</i>	Allamakee Co., Iowa	2001	J.A. Johnson	MG980937	MG980837	MG980741	KM495471	KM495561	MG980887	
C1846/CBS 114714	<i>Quercus robur</i>	Marshall Co., Iowa	2001	J.A. Johnson	MG980938	MG980838	MG980742	MG980984	MG980788	MG980888		

^aIsolates in bold represent type specimens. Isolates with the prefix "C" are from the culture collection from T. C. Harrington at Iowa State University, isolates with the prefix "KARE" are from the culture collection at University of California Kearney Agricultural Research and Extension Centre.

^b Cerato-platanin.

bark-side down (cambium-side up) in a moist chamber (metal mesh rack placed over moistened paper towels in clear plastic boxes) at room temperature for one wk in the laboratory under natural photoperiod to promote perithecia formation. Mats of mycelium typical of *Ceratocystis*, namely a white wiry mycelium with black, long-necked perithecia extending from the surface of diseased tissue was observed after 5–6 d. Masses of ascospores exuding from the tips of the perithecia were transferred with a sterilized needle to fresh acidified potato dextrose agar (APDA; 2.6 mL of 25 % [vol/vol] lactic acid per liter of medium) plates followed by hyphal-tip purification to fresh PDA (Potato Dextrose Agar, Difco) filled Petri dishes for additional morphological and phylogenetic analyses. Twenty-six isolates including five cultures linked to ex-type specimens of *Ceratocystis* were obtained from the culture collection of Dr. Thomas C. Harrington, Department of Plant Pathology and Microbiology, Iowa State University, corresponding to isolates lodged at the Westerdijk Fungal Biodiversity Institute (former CBS) and are presented in Table 1.

Phylogenetic analyses

Total genomic DNA was isolated from 24 Californian isolates and an additional 26 NAC isolates from mycelium scraped with a sterile scalpel from the surface of 14-d-old PDA cultures using the DNeasy Plant Kit (Qiagen, Valencia, California), following the manufacturer's instructions. Amplification of translation elongation factor 1- α (*TEF1*) fragments utilized the primer set EFCF1 and EFCF6 (Harrington 2009), β -tubulin (*TUB2*) utilized primers Bt1a and Bt1b (Glass & Donaldson 1995), the 28S (LSU) rDNA region utilized primers LROR and LR7 (Vilgalys & Hester 1990), Cerato-platanin (CP) utilized primers CP-2F and CP-1R (Pazzagli *et al.* 1999, Chen *et al.* 2013), 60S ribosomal protein (60S) utilized primers 60S-506F and 60S-908R (Stielow *et al.* 2015), and the mini-chromosome maintenance complex component 7 (*MCM7*) utilized primers Cer-MCM7F and Cer-MCM7R (de Beer *et al.* 2014). PCR amplification conditions for the *TUB2* and *TEF1* regions were the same as those described by Oliveira *et al.* (2015b); amplification conditions for the cerato-platanin region were the same as those described by Oliveira *et al.* (2015a), and amplification conditions for the LSU region were the same as those described by Vilgalys & Hester (1990). A slightly modified PCR program from de Beer *et al.* (2014) was used for *MCM7* and 60S [initial denaturation (96 °C, 5 min) followed by 35 cycles of denaturation (95 °C, 45 s), annealing (58 °C for *MCM7* and 56 °C for 60S, 45 s), extension (72 °C, 60 s), and a final extension (72 °C, 10 min)]. PCR products were visualized on a 1.5 % agarose gel (120 V for 25 min) to validate presence and size of amplicons, purified *via* Exonuclease I and recombinant Shrimp Alkaline Phosphatase (Affymetrix, Santa Clara, California), and sequenced in both directions *via* BigDye® Terminator v. 3.1 Cycle Sequencing Kit (Thermo Fischer Scientific, Waltham, Massachusetts) on an ABI 3730 Capillary Electrophoresis Genetic Analyzer (College of Biological Sciences Sequencing Facility, University of California, Davis).

Forward and reverse nucleotide sequences were assembled, proofread, and edited in Sequencher v. 5 (Gene Codes Corporation, Ann Arbor, Michigan) and deposited in GenBank (Table 1). Sequences from type and non-type *Ceratocystis* isolates ($n = 5$ and 21, respectively) in the NAC were included for phylogenetic reference (de Beer *et al.* 2014,

Oliveira *et al.* 2015a) (Table 1). Multiple sequence alignments were performed in MEGA v. 6 (Tamura *et al.* 2013) and manually adjusted where necessary in Mesquite v. 3.10 (Maddison & Maddison 2016). Alignments were submitted to TreeBASE under accession number S22454. Concordance among datasets ($P \geq 0.010$) was evaluated with the partition homogeneity test (PHT) conducted in PAUP v. 4.0b162 (Swofford 2002). Datasets were analyzed using two different optimality search criteria, maximum parsimony (MP) and maximum likelihood (ML), in MEGA v. 6 (Tamura *et al.* 2013). For MP analyses, heuristic searches with 1 000 random sequence additions were implemented with the Tree-Bisection-Reconnection algorithm, gaps were treated as missing data. Bootstrap analysis with 1 000 pseudoreplicates was used to estimate branch support. For ML analyses, MEGA was used to infer a model of nucleotide substitution for each dataset, using the Akaike Information Criterion (AIC). ML analysis utilized the Nearest-Neighbor-Interchange heuristic method and branch stability was determined by 1 000 bootstrap pseudoreplicates. Sequences of *Ceratocystis fimbriata* s. str. isolate C1476 from the LAC served as the outgroup taxon in all analyses.

Morphological characterization

Novel fungal species identified during this study were characterized for morphology. Representative isolates (KARE1428, KARE1610, C578, C821, C1709, and C1770) selected based on phylogenetic results were cultured on MEA (2 % Malt Extract Agar; Difco) and PDA. Subculturing was performed by transferring triplicate 5-mm diam mycelial plugs from the colony periphery of a pure culture to the center of fresh Petri dishes filled with MEA and PDA. Cultures were incubated for up to 14 d at room temperature (24 +/- 1 °C) with natural ambient day light and darkness at night (Sep. 2017). Radial growth was measured after 7 d of incubation by taking two measurements at right angles to each other. This experiment was repeated once. Descriptions of colony color (Rayner 1970) and morphology was conducted on day 14. Morphological characterization included measuring the diameter of perithecia and length of ostiolar neck ($n = 30$), length of ostiolar hyphae ($n = 30$), ascospore dimensions ($n = 30$), conidiophores ($n = 10$), dimensions of cylindrical and doliiform conidia ($n = 30$), and aleurioconidia ($n = 30$) at 1000 \times magnification from 14-d-old cultures by mounting and/or squashing perithecia and other structures in a sterile 50 % glycerol solution on glass slides followed by covering with a glass coverslip and observing structures with a Leica DM500B compound microscope (Leica microsystems CMS GmbH, Wetzlar, Germany). No stain was applied in order to preserve the natural pigmentation of the fungal specimens. Morphological measurements are represented by the mean and a range depicting the standard deviation in the center with minima and maxima in parentheses, respectively.

Optimal growth temperature for the representative isolates (KARE1428, KARE1610, C578, C821, C1709, and C1770) was assessed by culturing isolates as described above on MEA and PDA in the dark and incubating them at temperatures ranging from 5 °C to 40 °C in five degree increments for up to 14 d. Radial colony growth was measured as described above every two days and average colony growth rate and average colony diameter were calculated. Three individual colony replicates per isolate were measured for each temperature. This experiment was repeated once.

RESULTS

Collection of isolates

Surveys of almond orchards in California revealed that *Ceratocystis* canker was widespread throughout the Central Valley region where almond trees are grown. Infections produced gummosis at the margin of active cankers (Fig. 1A, B). Internal symptoms in infected trunks or scaffolds included death of cambium and bark tissues as well as diffuse, dark brown discoloration that extended into the primary and secondary xylem (Fig. 1C). Cankers were generally associated with wounds created by mechanical harvesting and pruning equipment on the tree trunks (Fig. 1A, D–F) or main scaffold branches (Fig. 1B). Wounds caused by mechanical harvesters typically ruptured the bark, thus exposing the susceptible cambial tissues. Cankers expanded along the main axis of the tree, sometimes extending into one of the main scaffolds (Fig. 1A). Isolations from 4–15-yr-old trees symptomatic of *Ceratocystis* canker yielded 87 *Ceratocystis* isolates from 20 almond orchards in six California counties.

Phylogenetic analyses

Tests for concordance between datasets using PHT revealed that these data were not significantly inconcordant ($P = 0.10$) and were combined and analyzed as above. For ML analyses, the best-fit model of nucleotide evolution was selected based on the AIC (K2 for 60S and LSU; K2+G for *TEF1*, *TUB2*, *MCM7*, CP, and the combined analysis).

Alignment of the combined sequences (*TEF1*+*TUB2*+CP+60S+*MCM7*+LSU) resulted in a 4905-character dataset, in which 4 432 characters were constant, 198 characters were parsimony-uninformative, and 275 characters were parsimony-informative (6 %). MP analysis generated 8 equally most parsimonious trees of 553 steps and consistency index (CI), retention index (RI), and rescaled consistency index (RC) of 0.8951, 0.9580, and 0.8523, respectively. MP and ML analyses of the combined six-gene dataset revealed seven strongly supported lineages (≥ 91 % / ≥ 99 % MP and ML bootstrap values, respectively) within the NAC (Fig. 2). Of these seven lineages, two represent the newly described species hereinafter identified as *Ceratocystis betulina* sp. nov. and *Ceratocystis destructans* sp. nov. *Ceratocystis betulina* was revealed to be the sister taxon to *C. variospora* s. str., while *C. destructans* includes the almond pathogen and a group of *Ceratocystis* isolates collected from *Populus*, *Celtis* sp., black cherry (*Prunus serotina*), and *Quercus macrocarpa* in Iowa. The branch that included only the California isolates (including a single isolate from *Populus* in Iowa) was strongly supported (91 % / 99 %), but there was only weak support (75 % / < 70 %) for the broader *C. destructans* lineage that included all the Iowa isolates. The *C. destructans* lineage is sister to the recently described species *C. tiliae*. The order of divergence within the NAC was almost fully resolved, thus providing the first strongly supported hypotheses concerning speciation order within the NAC as depicted in Fig. 2. Thus, the six-gene analysis provides strong support not only for species delineation but also for early and late bifurcations of independently evolving lineages within the NAC.

PCR amplification of the *TEF1* locus produced 1 433–1 473 bp fragments and resulted in a 1 473-character dataset, in which 1 351 characters were constant, 39 were parsimony



Fig. 1. Symptoms of *Ceratocystis* canker of almond in California. **A.** Gummosis and canker associated with a large pruning wound on trunk. **B.** Scaffold canker. **C.** Transverse cut of a tree trunk infected with *Ceratocystis* canker and showing dead cambium and bark tissues as revealed by the brown discoloration extending into the primary and secondary xylem. **D–E.** Damaged bark and active *Ceratocystis* cankers developing on the trunk of young almond trees. **F.** Damaged bark and active *Ceratocystis* cankers developing on the trunk of a mature almond tree.

uninformative, and 83 were parsimony informative (6 %). The MP analysis produced eight equally most parsimonious trees of 146 steps and a CI, RI, and RC of 0.8290, 0.9529, and 0.8223, respectively (Fig. 3A). PCR amplification of the *TUB2* locus produced 535–547 bp fragments and resulted in a 547-character dataset, in which 480 characters were constant, 33 were parsimony uninformative, and 34 were parsimony informative (6 %). The MP analysis produced eight equally most parsimonious trees of 76 steps and a CI, RI, and RC of 0.8604, 0.9625, and 0.8870, respectively (Fig. 3B). PCR amplification of the *MCM7* locus produced 628 bp fragments and resulted in a

628-character dataset, in which 570 characters were constant, 20 were parsimony uninformative, and 38 were parsimony informative (6 %). The MP analysis produced 10 equally most parsimonious trees of 68 steps and a CI, RI, and RC of 0.9166, 0.9823, and 0.9254, respectively (Fig. 3C). PCR amplification of the 60S locus produced 415–429 bp fragments and resulted in a 429-character dataset, in which 386 characters were constant, 18 were parsimony uninformative, and 25 were parsimony informative (6 %). The MP analysis produced 10 equally most parsimonious trees of 47 steps and a CI, RI, and RC of 0.9574, 0.9800, and 0.9385, respectively (Fig. 3D). PCR amplification of

Combined Multi-locus Dataset
 TEF1/TUB2/MCM7/60S/Cerato-platanin/LSU
 8 Trees
 568 Steps
 CI = 0.892606
 RI = 0.954781
 RC = 0.852349

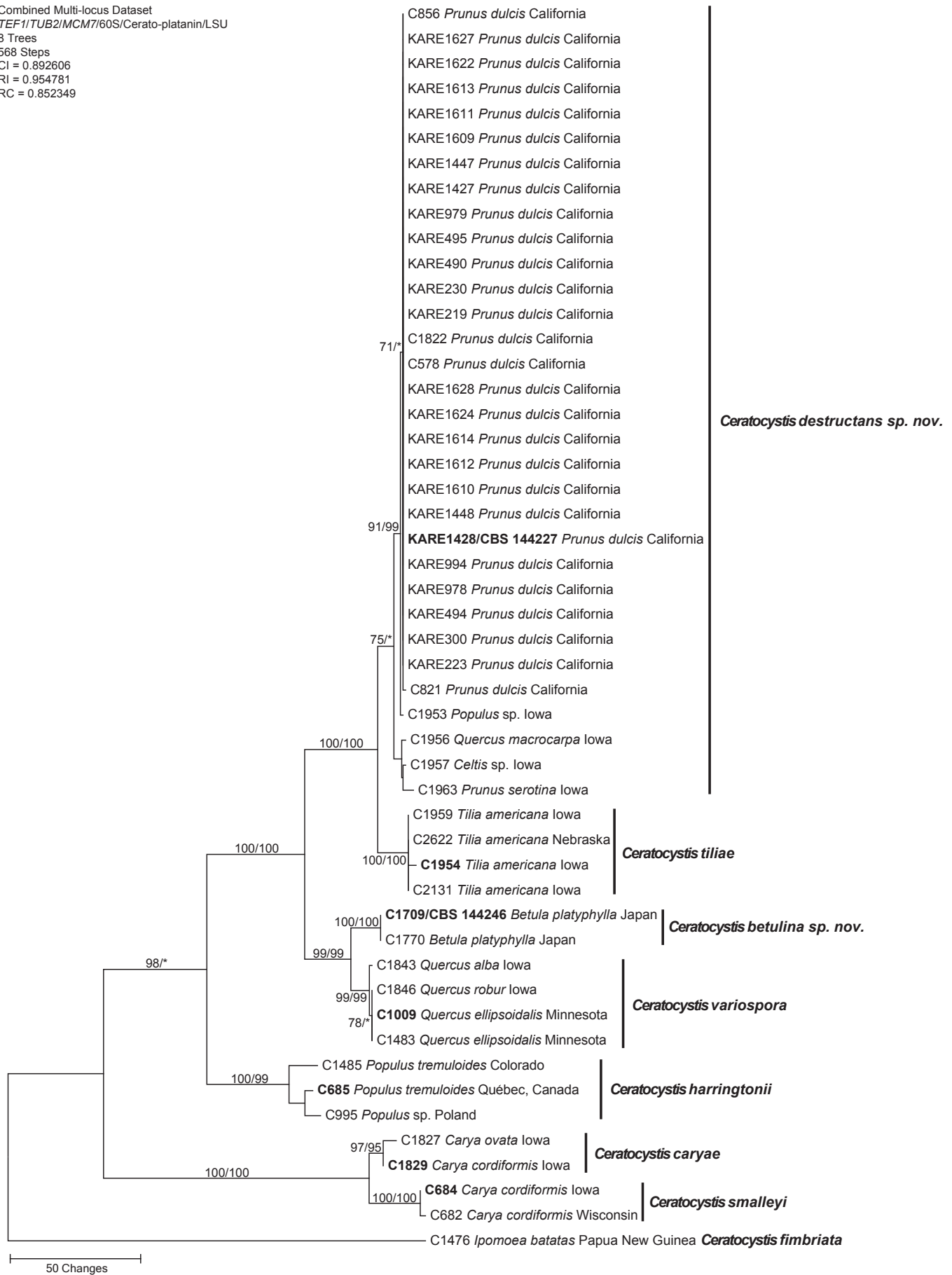


Fig. 2. One of eight equally most parsimonious trees generated from maximum parsimony analysis of the six-gene (*TEF1*+*TUB2*+CP+60S+*MCM7*+LSU) combined dataset. Numbers in front and after the slash represent parsimony and likelihood bootstrap values from 1 000 pseudoreplicates, respectively. Values represented by an asterisk were less than 70 % for the bootstrap analyses. Bar indicates the number of nucleotide changes. Ex-type isolates are in **bold**.

TEF1 Dataset
8 Trees
146 Steps
CI = 0.829060
RI = 0.952941
RC = 0.822397

A

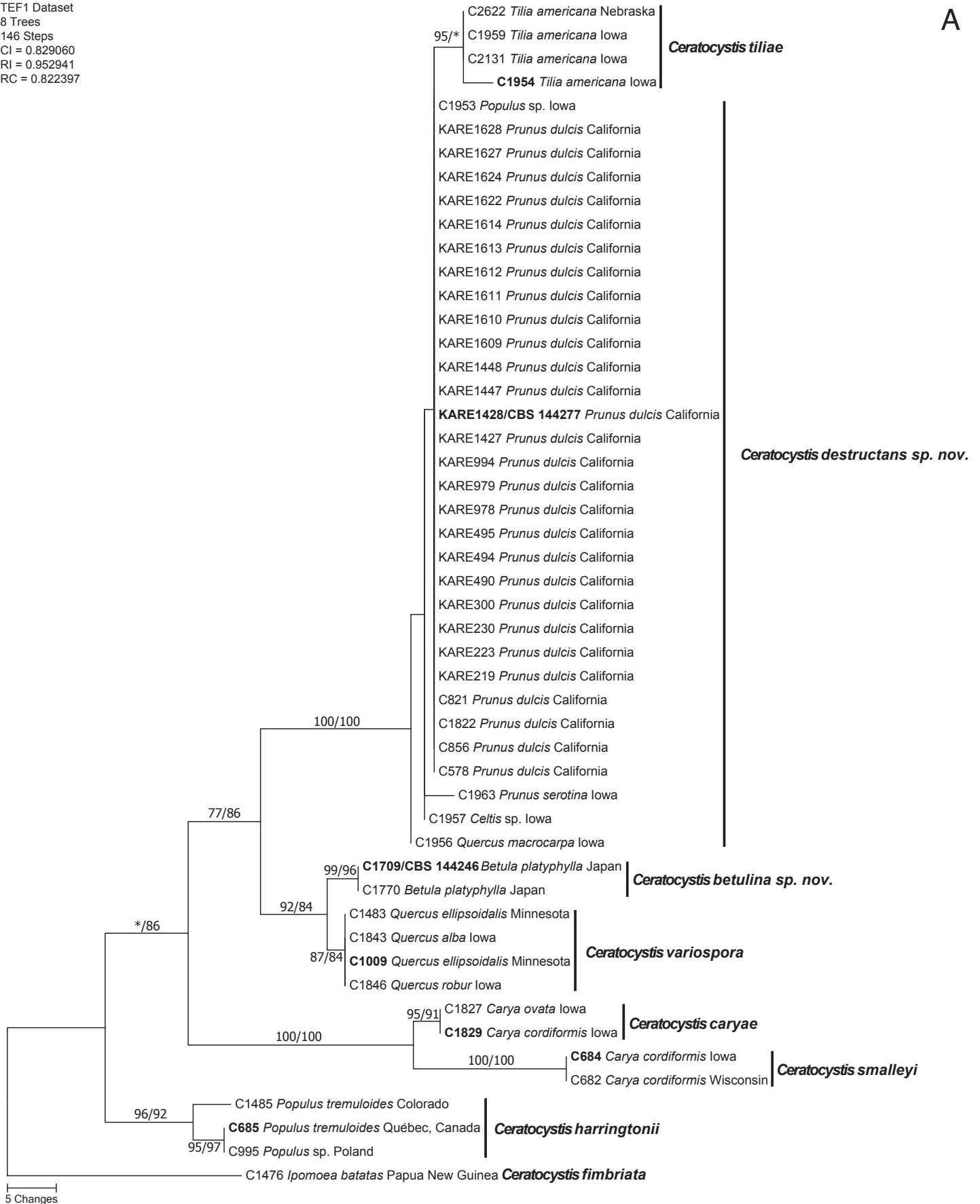


Fig. 3. Equally most parsimonious trees from single-locus analyses. Numbers in front and after the slash represent parsimony and likelihood bootstrap values from 1 000 pseudoreplicates, respectively. Values represented by an asterisk were less than 70 % for the bootstrap analyses. The scale bar indicates the number of nucleotide changes. Ex-type isolates are in **bold**. **A.** One of eight equally most parsimonious trees for the *TEF1* analyses. **B.** One of eight equally most parsimonious trees for the *TUB2* analyses. **C.** One of 10 equally most parsimonious trees for the *MCM7* analyses. **D.** One of 10 equally most parsimonious trees for the 60S analyses. **E.** One of 10 equally most parsimonious trees for the Cerato-platanin analyses. **F.** One of 10 equally most parsimonious trees for the LSU analyses.

TUB2 Dataset
 8 Trees
 76 Steps
 CI = 0.860465
 RI = 0.962500
 RC = 0.887028

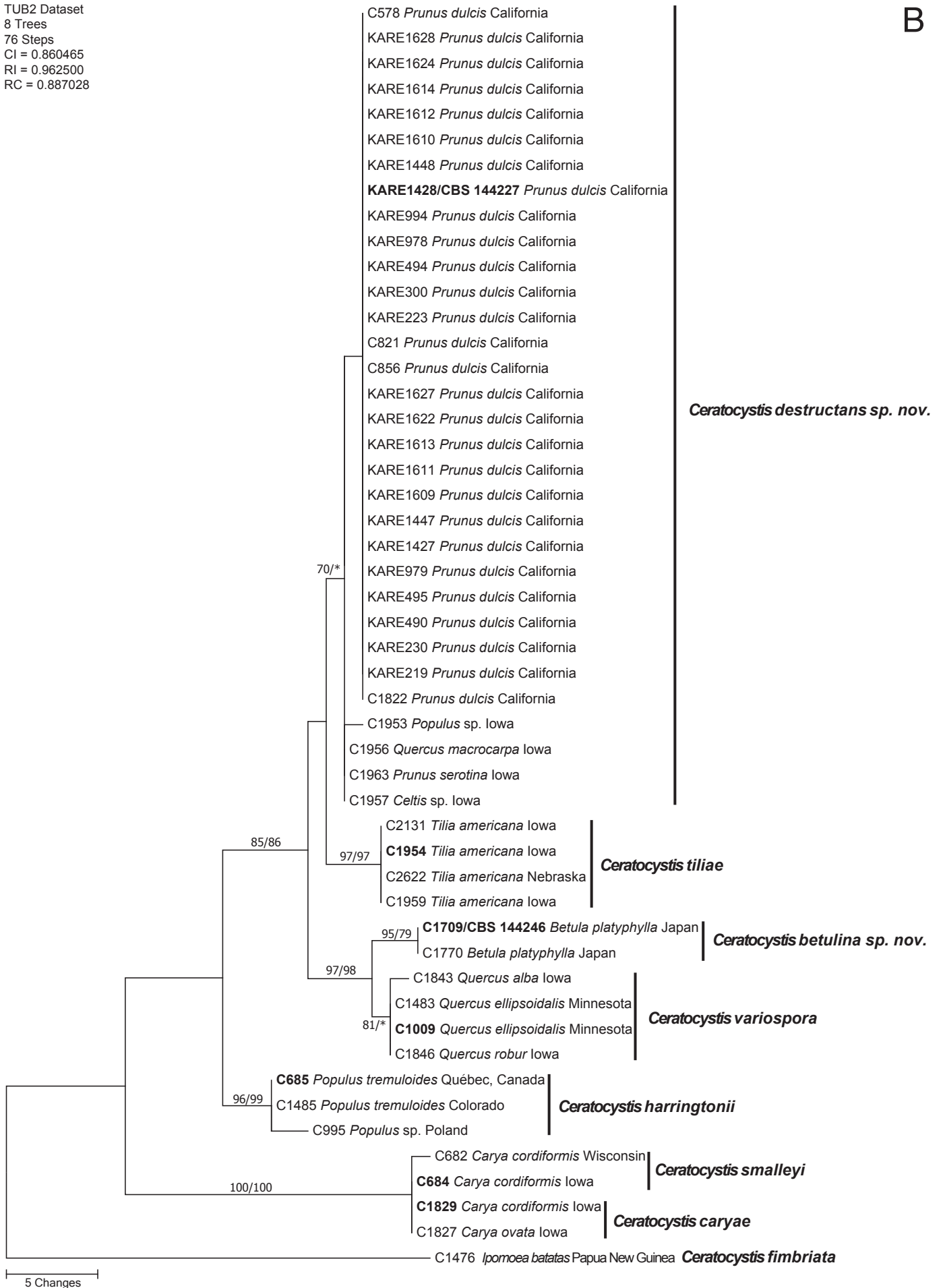


Fig. 3. (Continued).

MCM7 Dataset
 10 Trees
 68 Steps
 CI = 0.916667
 RI = 0.982301
 RC = 0.925481

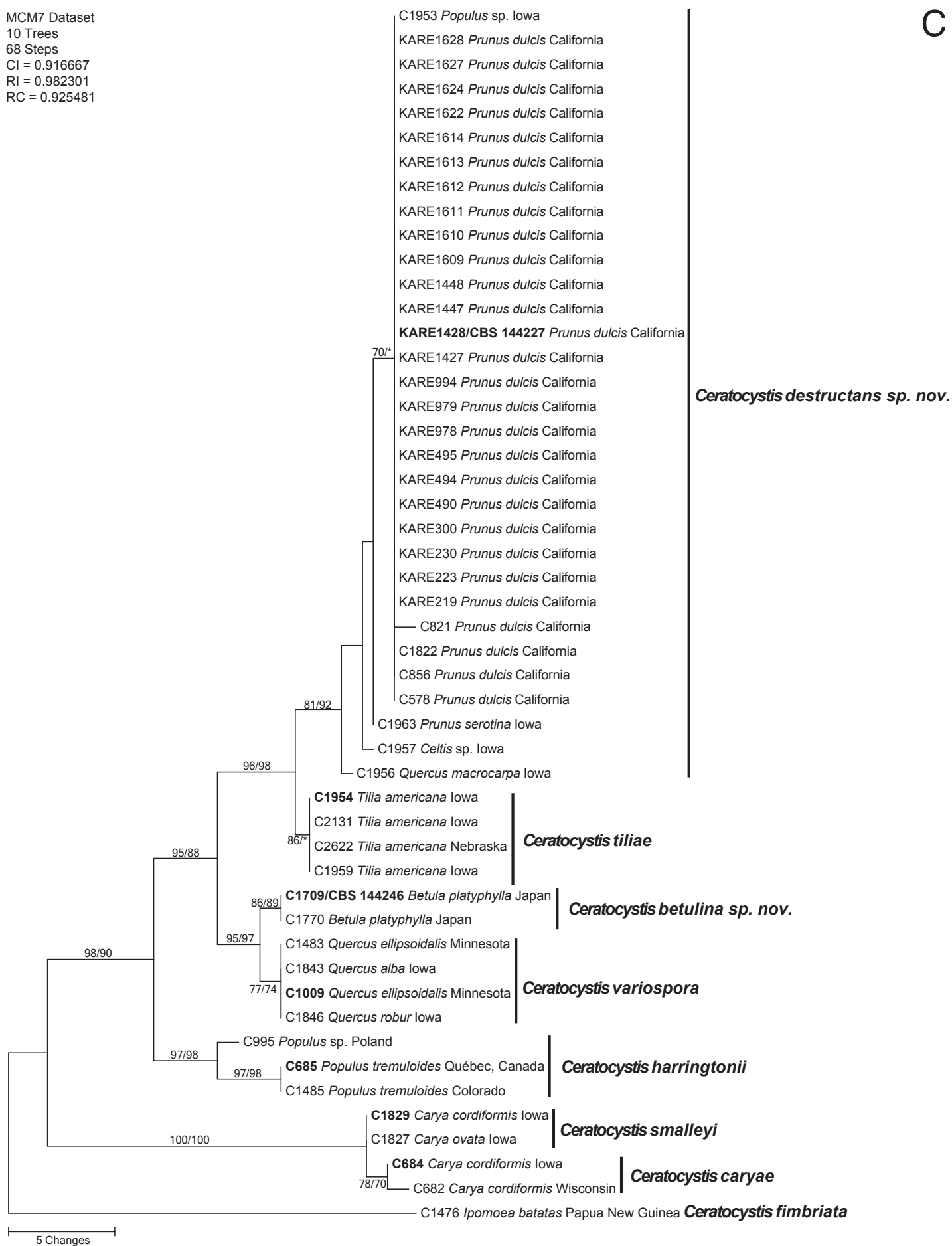


Fig. 3. (Continued).

60S Dataset
 10 Trees
 47 Steps
 CI = 0.957447
 RI = 0.980000
 RC = 0.938573

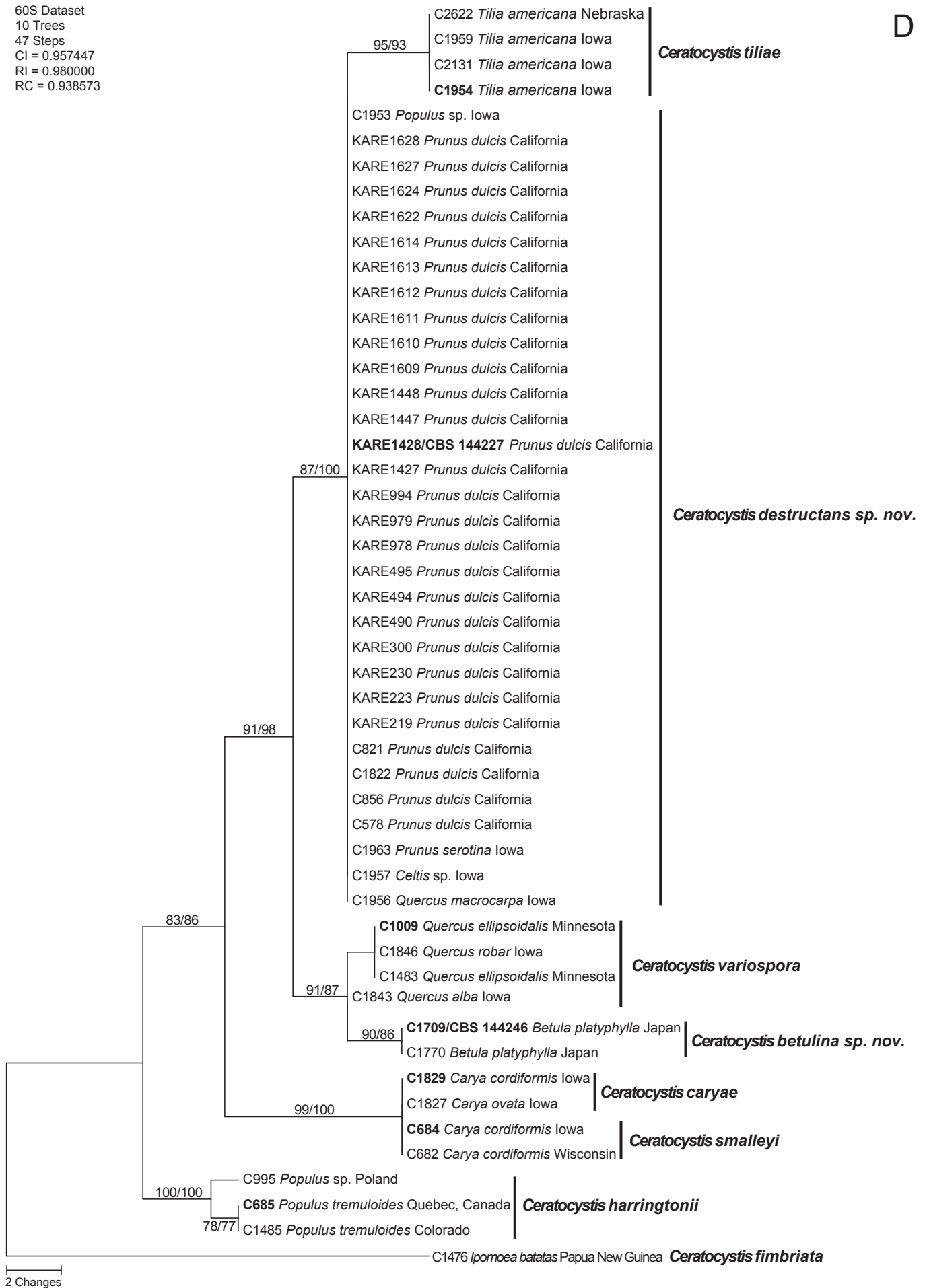


Fig. 3. (Continued).

Cerato-platanin Dataset
 10 Trees
 207 Steps
 CI = 0.860656
 RI = 0.957500
 RC = 0.879513

E

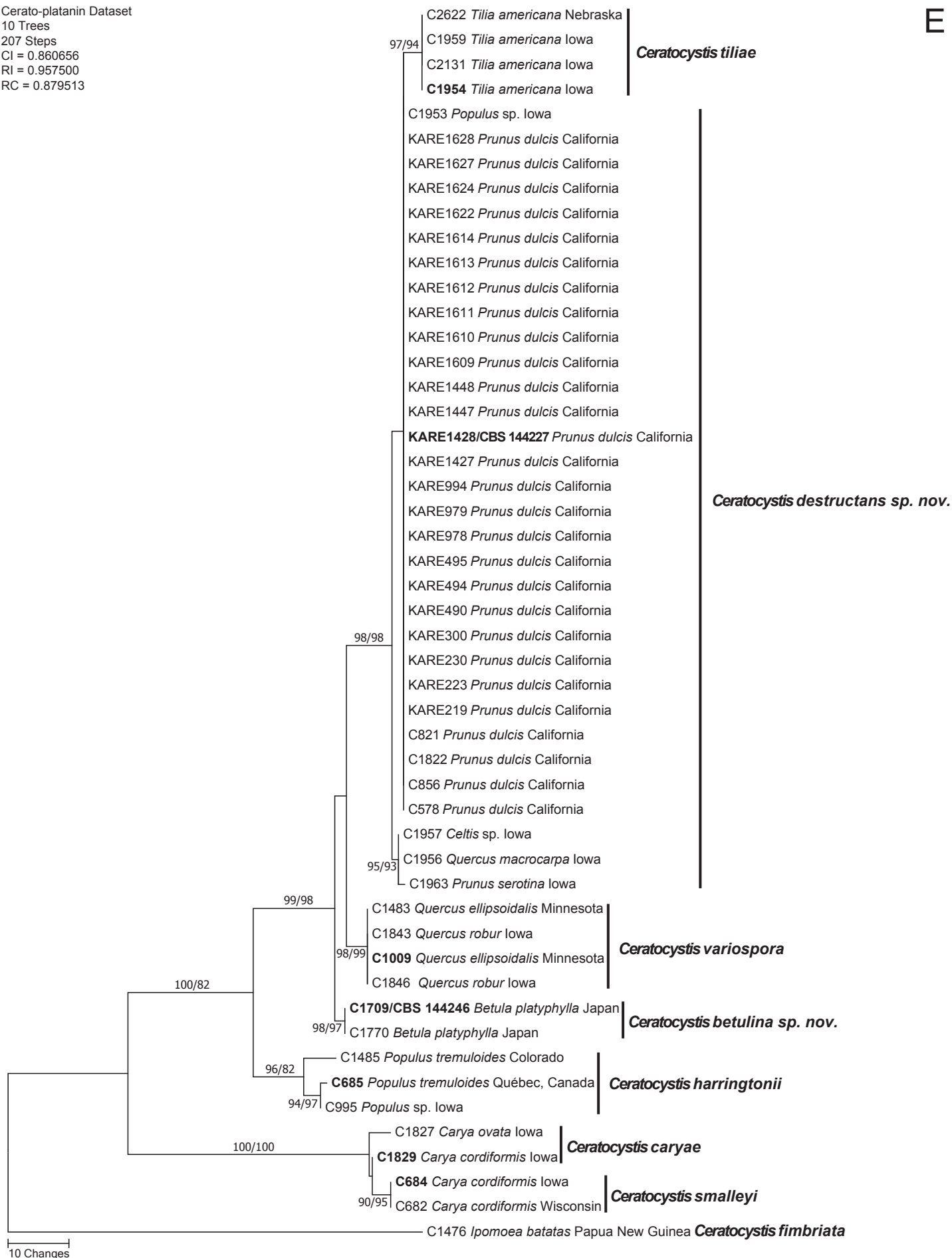


Fig. 3. (Continued).

LSU Dataset
 10 Trees
 13 Steps
 CI = 0.923077
 RI = 0.973684
 RC = 0.893647

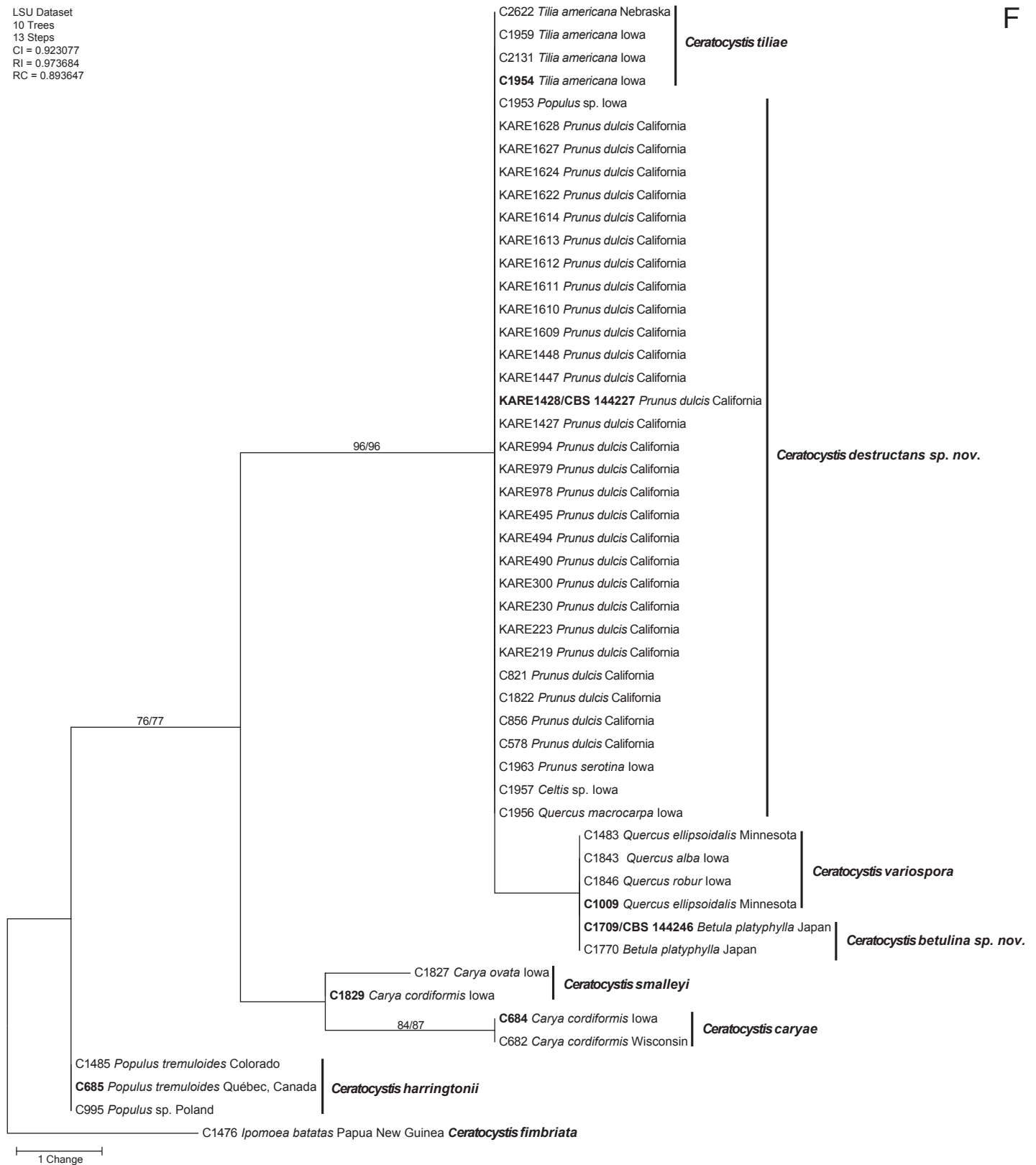


Fig. 3. (Continued).

the Cerato-platanin locus produced 487–498 bp fragments and resulted in a 498-character dataset, in which 327 characters were constant, 85 were parsimony uninformative, and 86 were parsimony informative (17.2 %). The MP analysis produced 10 equally most parsimonious trees of 207 steps and a CI, RI, and RC of 0.8606, 0.9575, and 0.8795 respectively (Fig. 3E). PCR amplification of LSU produced 1 330 bp fragments and resulted in a 1 330-character dataset, in which 1 318 characters were

constant, three were parsimony uninformative, and nine were parsimony informative (1 %). The MP analysis produced 10 equally most parsimonious trees of 13 steps and a CI, RI, and RC of 0.9230, 0.9736, and 0.8936, respectively (Fig. 3F). No single gene fragment was able to confidently recognize all seven lineages within the NAC. Many single gene analyses produced tree topologies that separated most if not all species; however, a lack of support for some phylogenetic positions was realized.

Results strongly suggest that multiple gene regions are required to accurately separate the more recently diverged species *C. tiliae* and *C. destructans*, while earlier diverging members of the NAC (i.e. *C. harringtonii* and *C. smalleyi*) were typically discernible based on fewer loci or even a single locus (i.e. *TEF1*) (Fig. 3A–F). Only the *TEF1* gene region was able to discern the recently diverged *C. caryae* and *C. smalleyi* as separate phylogenetic species, further supporting the use of multiple loci for accurate identification of *Ceratocystis* species in the NAC.

Morphological characterization

Isolates representing *C. betulina* (C1709 and C1770) and *C. destructans* (C578, C821, KARE1428, and KARE1610) were used for morphological characterization (Table 2 and Supplementary Table 1). For *C. betulina* isolates C1709 and C1770, the average colony diameter after 7 d on PDA and MEA at room temperature (24 ± 1 °C) was 27 (PDA)/24.2 (MEA) and 23/22 mm, respectively. For *C. destructans* isolates C578, C821, KARE1428 and KARE1610 the average colony diameter after 7 d on PDA and MEA at room temperature (24 ± 1 °C) was 36/30, 35/32, 40/20.3 and 35/17.3 mm, respectively. In culture, both *C. betulina* and *C. destructans* were slow-growing with even to uneven margins. The colonies of *C. betulina* varied in color from white to grey to olivaceous green. Colonies of *C. destructans* were grey to olivaceous green. *Ceratocystis betulina* isolate C1770 produced few perithecia in culture, and the perithecia often lacked necks or had short necks. Ascospores were not observed for this isolate. Isolates of *C. destructans* produced black ascomata scattered throughout the colony with many perithecia near the colony centre. The ascomatal bases of *C. destructans* isolates ((118–)197(–358) µm) were larger than those produced by isolates of *C. betulina* ((103–)162(–220) µm). The morphological characters that distinguished *C. betulina* from *C. destructans* were the average diameter of the ascomata and lengths of the necks. *Ceratocystis destructans* had larger ascomatal diameters (av. ranging from 163–220 µm among the four isolates) and longer necks (av. ranging from 379–623 µm among the four isolates) compared to smaller ascomata (av. of the two isolates = 149 µm and 175 µm, respectively) and shorter necks (av. of the two isolates = 142 µm and 298 µm, respectively) of *C. betulina*. Cylindrical conidia and thick-walled aleurioconidia were abundant in both species and of similar dimensions. Aleurioconidia of *C. betulina* were often found in short chains compared to *C. destructans*, whose aleurioconidia were found singly or in short chains. Doliiform conidia were abundant in *C. betulina* isolates and sparse or absent in *C. destructans* isolates C578 and C821.

For two isolates of *C. betulina* (C1709 and C1770) and four isolates of *C. destructans* (C578, C821, KARE1428 and KARE1610) the optimal temperature for growth was 25 °C. In general, *Ceratocystis destructans* grew faster than *C. betulina* at 5, 10, 15, 20 and 35 °C on PDA. On the other hand, *C. betulina* isolates grew faster on PDA at the optimal temperature of 25 °C at an average of 3.5 mm/d, while *C. destructans* isolates grew at an average of 3.1 mm/d on PDA at 25 °C. All isolates grew slower on MEA, with an average growth rate of 0.8 mm/d and 1.3 mm/d at 25 °C for *C. destructans* and *C. betulina*, respectively. No growth was observed at 40 °C for any isolates on either growth medium. For both taxa, growth at 5 and 10 °C was reduced, and an abrupt decline was observed at 35 °C, however *C. destructans* (25 mm diam) had almost double the growth of *C. betulina* (15 mm diam) at this temperature after 14 d on PDA. For both taxa ascomatal

production was most abundant when grown at 20 and 25 °C, and no ascomata were produced at 10 and 35 °C.

TAXONOMY

Morphological comparisons coupled with multi-locus phylogenetic analyses (MP and ML) of the combined six-gene dataset identified two distinct and strongly supported lineages for which no apparent species names exists. Thus, we propose the following new species names to properly circumscribe these unique taxa and to further resolve paraphyletic and cryptic taxa in the NAC.

Ceratocystis betulina D.P. Lawr., L.A. Holland & Trouillas, *sp. nov.* MycoBank MB824502. Figs 2, 4.

Etymology: The name refers to the host, *Betula platyphylla*, from which this fungus was isolated.

Typus: **Japan**, Morioko, Iwate, isolated from sporulating fungal mat on a log of *Betula platyphylla*, 22 Sep. 2000, H. Masuya No. C1709 (**holotype** BPI 910648, dried culture; ex-type culture CBS 144246).

Colonies 24.2 mm after 7 d at 25 °C on MEA, slow-growing with uneven margins and copious aerial hyphae. **Hyphae** initially hyaline, smooth, straight, branched, septate, becoming dark with age. **Mycelium** submerged, olivaceous green, aerial mycelium white, producing ascomata in clumps, odor sweet, with banana-like scent. **Ascomata** perithecial, with bases superficially to partially immersed in the substrate, mostly black, globose, (102.5–)124–174(–193) µm diam, unornamented or with undifferentiated hyphae, collar (32–)43–54(–59.5) µm wide at the base of the perithecial neck. **Perithecial necks** black, slender, (144.5–)227.5–368(–438) µm long, (14.5–)16.5–22(–24.5) µm wide at the base, (11.5–)13.5–19.5(–20) µm wide at the apex. **Ostiolar hyphae** hyaline, aseptate, straight to flexuous, 22–55 µm long. **Asci** not seen. **Ascospores** (4.5–)4.5–5(–5.5) × (2.5–)3–3.5(–5) µm with outer sheath forming a hat-shaped brim. **Conidiophores** of three types: endoconidiophores lageniform, hyaline to pale brown, septate, 29–67 µm in length, 3–6.5 µm wide at the base and 3–5 µm wide at the mouth, producing hyaline, concatenated, cylindrical conidia (10–)11–15.5(–19) × (2–)2.5–3(–3) µm; other endoconidiophores shorter, 14–33 µm in length, 3–6 µm wide at the base and 3.5–5.5 µm wide at the mouth, producing hyaline, concatenated, smooth-walled, doliiform conidia (5.5–)6–8(–9.5) × (4.5–)5.5–6(–6.5) µm; and less abundant, simple conidiophores (21.5–)23–30(–30) × (2.5–)3–5(–6) µm, producing smooth- and thick-walled, dark brown, ellipsoid to clavate, aleurioconidia (9–)9.5–10.5(–11) × (7.5–)8–8.5(–8.5) µm either singly or in short chains of 2–3.

Distribution: Morioko, Iwate (Japan).

Additional material examined: **Japan**, Morioko, Iwate, isolated from *Carpophilus sibiricus* from a log of *Betula platyphylla*, 22 Sep. 2000, H. Masuya (C1770).

Notes: *Ceratocystis betulina* was isolated from a log of *Betula platyphylla* located near *Prunus* and *Quercus* trees. Prior to our analyses, isolates C1709 and C1770 were considered to be *C. variospora*. Phylogenetically, *C. betulina* is strongly supported

Table 2. Comparative morphological characteristics of *Ceratocystis fimbriata* and *Ceratocystis platani* (Latin American clade) and *Ceratocystis* species in the North American clade of *Ceratocystis*.

Species	Hosts/Insects	Cultures examined in referenced studies ^a	Perithecia diameter (µm)	Width of collar (µm) at base of perithecial neck	Length of perithecial neck (µm)	Ascospores (µm)	Length of ostiolar hyphae (µm)	Flask-shaped conidiophores (µm)	Cylindrical conidia (µm)	Wide-mouthed conidiophores (µm)	Doliform conidia (µm)	Aleuroconidia (µm)	Reference
<i>Ceratocystis fimbriata</i>	<i>Ipomoea batatas</i>	C1418, C1354, C1476	110–250	Absent	440–770	5.5–7 × 3.5–5	53–136	55–120 × Mouth 3–6 Base 3–8	9–33 × 3–5	Absent	Absent	11–16 × 6.5–12	Engelbrecht & Harrington 2005
<i>Ceratocystis platani</i>	<i>Platanus</i> spp.	C1351, C1317, C1339	175–290	Absent	535–835	4–6.5 × 3–4.5	20–90	55–165 × Mouth 2.5–7.5 Base 3.5–7.5	11–22 × 3–5	35–50 × Mouth 5.5–6.5 Base 4.5–5	6–10 × 3.5–5	10–20 × 6–12	Engelbrecht & Harrington 2005
<i>Ceratocystis destructans</i> ^b	<i>Prunus dulcis</i>	C578, C821, KARE1428 , KARE1610	122–208	44–64	381–626	4–5 × 3–3.5	38–56	33–113 × Mouth 2–3 Base 3–5	12–26 × 2–3	26–69 × Mouth 3–4 Base 5–6	7–11 × 4–6	8–13 × 7–12	This study
<i>Ceratocystis tiliae</i>	<i>Tilia americana</i>	C1954 , C2131, C2622	175–350	50–100	425–915	5–6 × 4–4.5	40–90	80–160 (330) × Mouth 3.5–4.5 Base 4–5.5	15–40 × 3–5.5	50–90 × Mouth 4–6 Base 4.5–5.5	6.5–9 × 4.5–6	7.5–12.5 × 8–11.5	Oliveira et al. 2015
<i>Ceratocystis betulina</i> ^b	<i>Betula platyphylla/</i> <i>Carpophilus sibiricus</i>	C1709 , C1770	103–192	32–60	145–438	4.5–6 × 3–4	22–55	29–67 × Mouth 3–5 Base 2–6.5	10–19 × 2–3	14–33 × Mouth 3–5 Base 3–6	6–9 × 5–7	9–11 × 8–9	This study
<i>Ceratocystis variospora</i>	<i>Quercus alba</i> , <i>Q. ellipsoidalis</i> , <i>Q. robur</i>	C1009 , C1483, C1843, C1846	130–350 (425)	51–80	≤ 830	3.5–6 × 3–5	22–50	52–98 × Mouth 2.5–4.5 Base 4.5–7	6–30 × 2.5–5	32–90 × Mouth 4.5–7.5 Base 4–5.5	5.5–10 × 5–8	6.5–9 × 7.5–14	Johnson et al. 2005
<i>Ceratocystis harringtonii</i> (formerly <i>C. populicola</i>)	<i>Populus tremuloides</i> , <i>Populus hybrid</i>	C89, C685 , C947, C995, C1485	110–275	Present	≤ 665	4.5–6.5 × 3–5	42–75	45–200 × Mouth 3.5–4.5 Base 3.5–7	10–33 × 2–5 (5.5)	17–95 (125) × Mouth 3.5–8.5 Base 3.5–6	6.5–12 × 3.5–5	9–18.5 × 8–17.5	Johnson et al. 2005
<i>Ceratocystis caryae</i>	<i>Carya cordiformis</i> , <i>C. ovata</i> , <i>Ostrya virginiana</i>	C1827, C1829 , C1412, C1413, C1845, C1971	135–340	48–103	≤ 950	4–6 × 3.5–4.5	32–80	42–510 × Mouth 3.2–4.8 Base 3.8–7.5	8.5–27 (43) × 2.5–6	40–100 × Mouth 5.5–8 Base 5–6.5 (7)	6–13.5 (16) × 5.5–9.5	9–21.5 × 8.5–16.5	Johnson et al. 2005
<i>Ceratocystis smalleyi</i>	<i>Carya cordiformis</i> , <i>C. ovata/Scolytus quadrispinosus</i>	C682, C683, C684 , C1410, C1411, C1828, C1839, C1840, C1842, C1844, C1952	100–300 (350)	42–73 (85)	≤ 570	4–6 × 3.5–5	54–101	Absent	Absent	35–105 × Mouth 4–7.5 Base 4–6	7.5–31.5 × 4–7.5	Absent	Johnson et al. 2005

^aType specimen in bold.

^bMeasurements based on the type specimen.



Fig. 4. Morphological characteristics of *Ceratocystis betulina*. **A.** 14-d-old PDA culture. **B.** Close-up of perithecia from 7-d-old culture. **C.** Globose unornamented ascomata base with elongated neck. **D.** Straight to flexuous ostiolar hyphae. **E.** Hat-shaped ascospores from top and side view. **F.** Cylindrical conidia. **G.** Short, barrel-shaped conidia. **H.** Thick-walled aleurioconidia. Scale bars: C = 100 μm ; D = 20 μm ; E = 5 μm ; F–G = 20 μm ; H = 10 μm .

as the sister taxon to *C. variospora*. Morphologically, *C. betulina* is similar to other members in the NAC and cannot be easily distinguished, though it has somewhat smaller perithecia (102.5–149(–192) μm diam, shorter, flask-shaped conidiophores (29–67 μm), shorter, wide-mouth conidiophores (14–33 μm), and smaller aleurioconidia, (9–)10(–11) \times (7.5–)8(–8.5) μm . *Ceratocystis betulina* can be distinguished from *C. variospora* based on slightly smaller cylindrical conidia (10–19 \times 2–3.5 μm for *C. betulina* and 6–30 \times 2.5–5 μm for *C. variospora*) (Table 2; Supplementary Table 1).

Ceratocystis destructans L.A. Holland, D.P. Lawr., & Trouillas, *sp. nov.* MycoBank MB824558. Figs 2, 5.

Etymology: The name refers to this fungus causing destructive cankers in almond.

Typus: **USA**, California, Madera County, 36°52'50.3"N 119°51'25.4"W, isolated from wood canker of *Prunus dulcis*, 19 Jul. 2016, L.A. Holland No. KARE1428 (**holotype** BPI 910649, dried culture; ex-type culture CBS 144247).

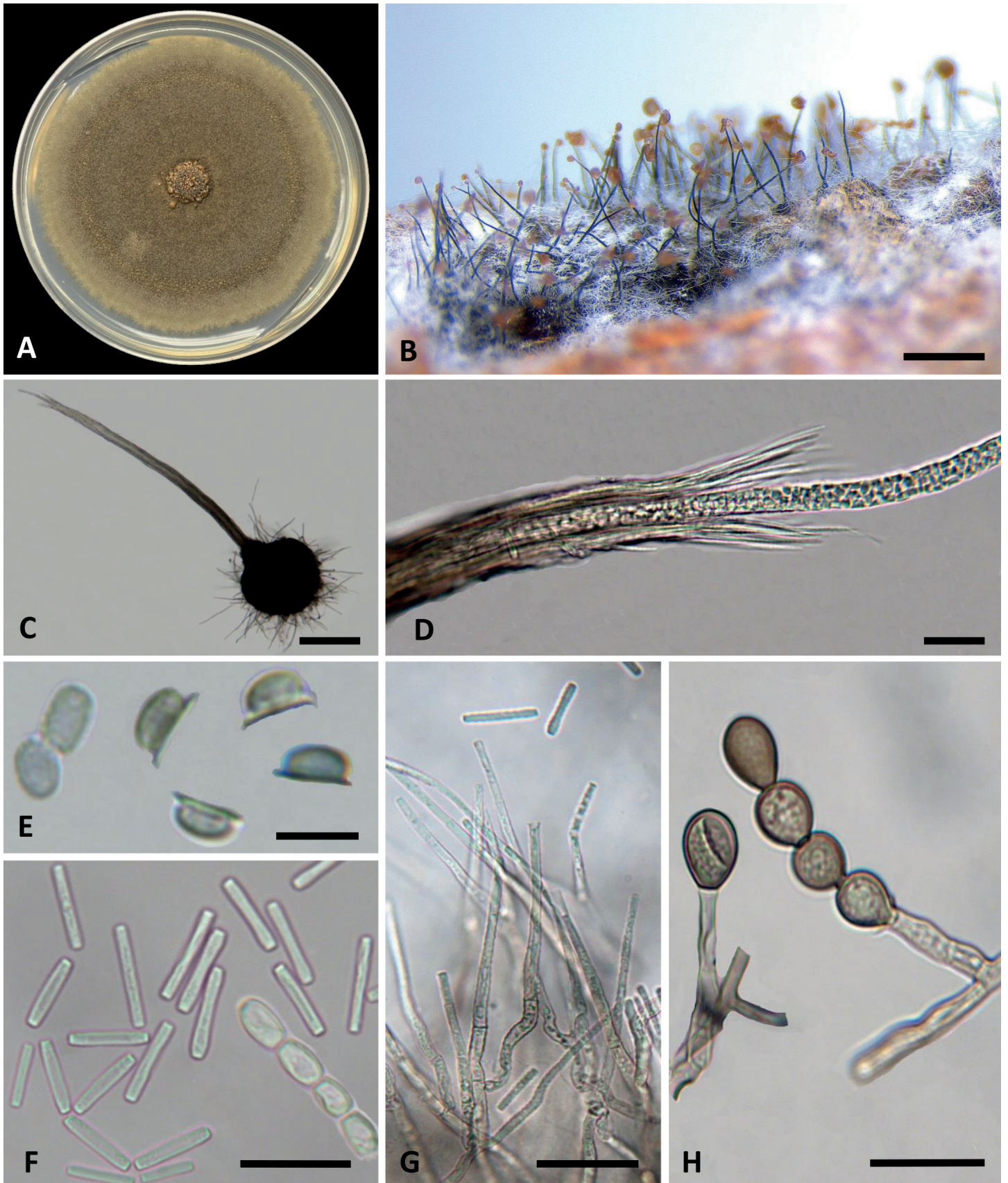


Fig. 5. Morphological characteristics of *Ceratocystis destructans*. **A.** 14-d-old PDA culture. **B.** Close-up of perithecia from 7-d-old culture. **C.** Globose unornamented ascomata base with elongated neck. **D.** Mostly straight ostiolar hyphae. **E.** Hat-shaped ascospores from top and side view. **F.** Cylindrical and short, barrel-shaped conidia. **G.** Flask-shaped conidiophores. **H.** Thick-walled aleurioconidia. Scale bars: B = 500 μ m; C = 100 μ m; D = 25 μ m; E = 5 μ m; F = 25 μ m; G = 20 μ m; H = 25 μ m.

Colonies 20.3 mm after 7 d at 25 °C on MEA, slow-growing with uneven margins and copious aerial hyphae, olivaceous green

to brown, aerial hyphae white, odor sweet, with banana-like scent, ascomata produced in clumps or in concentric rings.

Hyphae initially hyaline, smooth, straight, branched, septate, becoming dark with age. *Ascomata* perithecial, with bases superficially to partially submerged, mostly black, globose, (121.5–)142–184(–208) μm diam, unornamented or with undifferentiated hyphae, collar (44–)47.5–57(–64) μm wide at the base of the perithecial neck. *Perithecial necks* black, slender, (382–)434–573(–626) μm long, (13–)18–23.5(–24.5) μm wide at the base, (11–)12–17(–22) μm wide at the apex. *Ostiolar hyphae* hyaline, aseptate, mostly straight, 38–56 μm long. *Asci* not seen. *Ascospores* (5–)4.5–5(–5) \times (2.5–)3–3.5(–3.5) μm with outer sheath forming a hat-shaped brim. *Conidiophores* of three types: endoconidiophores lageniform, hyaline to pale brown, septate, 34–113 μm in length, 3–5 μm wide at the base and 2–3 μm at the mouth; producing concatenated, hyaline, cylindrical conidia (12–)14.5–20.5(–26) \times (1.5–)2–2.5(–3) μm ; other endoconidiophores less prevalent and shorter, 26–69 μm in length, 3.5–4 μm wide at the base and 4.5–5.5 μm wide at the mouth, producing hyaline, concatenated, smooth-walled, doliiform conidia (7–)8–10(–10.5) \times (4–)4.5–6(–6.5) μm ; and simple conidiophores not as prevalent, (18–)24–41(–45.5) \times (2.5–)3–3.5(–4), producing smooth- and thick-walled, dark brown, clavate, aleurioconidia (7.5–)9–12(–13) \times (7–)8.5–11(–13) μm either singly or in short chains of up to four.

Distribution: California (USA), *Prunus dulcis*; Iowa (USA), *Prunus serotina*, *Populus*, *Celtis* and *Quercus*.

Additional materials examined: USA, California, Colusa County, isolated from bark canker of *P. dulcis*, 1989, *R. Bostock* (C578); California, Colusa County, isolated from stem canker of *P. dulcis*, 24 Feb. 1996, *D. Rizzo* (C821); California, Merced County, isolated from bark canker of *P. dulcis*, 8 Sep. 2016, *F. Trouillas* (KARE1610).

Notes: *Ceratocystis destructans* has been isolated from almond trees throughout the Central Valley Region of California from necrotic inner bark and wood tissues of trees showing sunken cankers and gummosis. *Ceratocystis destructans* is morphologically similar to the sister species *C. tiliae*. However, these species can be distinguished based on average ascospore dimensions, with *C. destructans* having slightly smaller ascospores (4–5 \times 2.5–3.5 μm) than *C. tiliae* (5–6 \times 4–4.5 μm) and smaller ascomata (Table 2; Supplementary Table 1).

DISCUSSION

Morphological and phylogenetic analyses revealed two novel *Ceratocystis* species, *C. betulina* and *C. destructans*, that reside in the North American clade of *Ceratocystis*. The NAC of *Ceratocystis* was established, and the first species delineated by Johnson *et al.* (2005) based on ITS-rDNA phylogeny, electrophoretic phenotypes, interfertility tests, and cross-inoculations experiments. The host-associated lineages included the aspen lineage with *C. harringtonii* (synonym *C. populicola*), the hickory lineage with two species, *C. caryae* and the closely related species *C. smalleyi*, and a third lineage represented by the earlier described *C. variospora* (Davidson 1944), with two well-supported subclades: the ‘oak lineage’ associated with oak (*Quercus*) and birch (*Betula*) and the ‘cherry lineage,’ mainly associated with cherry and almond (*Prunus* spp.), *Populus*, and basswood (*Tilia americana*). Johnson *et al.* (2005) hypothesized that host-associated isolates of *C. variospora* from *Prunus*,

Quercus, and *Tilia* could represent three separate species, respectively, but these intersterile lineages could not be clearly distinguished by phenotypic traits, i.e., morphology or host specialization to *Quercus* vs. *Prunus* spp. Oliveira *et al.* (2015a), using three individual gene analyses (LSU, *TEF1*, and CP), showed that *Ceratocystis* isolates recovered from *Tilia* clustered as a well-supported monophyletic group sister to the cherry lineage of *C. variospora* in the *TEF1* and CP analyses. Not surprising, limited sequence variation failed to identify sublineages within *C. variospora* in the analysis of LSU, the least informative marker in that study and in our study. Inoculation of *Quercus macrocarpa* and *Tilia americana* seedlings demonstrated that only *Tilia*-derived isolates were aggressive on *T. americana*, cultures of the *Tilia* pathogen were distinguished morphologically, and *C. tiliae* was described as new (Oliveira *et al.* 2015a). Like Johnson *et al.* (2005), Oliveira *et al.* (2015a) maintained the name *C. variospora* to accommodate isolates recovered from *Betula*, *Celtis*, *Populus*, *Prunus* and *Quercus*, thus leaving *C. variospora* as a paraphyletic species.

Our individual gene analyses produced similar topologies and support values for species assignments as in de Beer *et al.* (2014) and Oliveira *et al.* (2015a), highlighting the need for combined multi-locus analyses to discriminate closely related species and to estimate species relationships in the NAC. For example, of the six loci tested, only *TEF1* was able to confidently delineate the sister species *C. caryae* and *C. smalleyi*, and all loci except LSU and 60S were able to discern *C. betulina* and *C. variospora* as well-supported sister groups. All loci supported the close relationship of *C. betulina*, *C. variospora*, *C. tiliae*, and *C. destructans*, while *C. harringtonii* and *C. caryae/smalleyi* lineages were more distantly related, in agreement with previous studies (Johnson *et al.* 2005, Oliveira *et al.* 2015a).

The de Beer *et al.* (2014) multi-locus analysis (LSU+MCM7+60S) involving NAC members distinguished the ex-type cultures of *C. caryae* C1829, *C. harringtonii* C685, *C. smalleyi* C684, and *C. variospora* C1009, but they did not examine the intraspecific diversity of the NAC. Analyses with more isolates of the NAC with phylogenetically informative loci such as *TEF1* and CP have revealed greater diversity within the oak and cherry lineages of *C. variospora* (Oliveira *et al.* 2015a) as compared to ITS analyses (Johnson *et al.* 2005). Oliveira *et al.* (2015a) did not perform a multi-locus analysis because they reported a low *P* value (*P* = 0.01) for their three-gene PHT. The topology and support values for our *TEF1* and CP phylograms are very similar to those reported by Oliveira *et al.* (2015a). The results of our PHT (*P* = 0.10) and examination of tree topology and support for phylogenetic species recognition utilizing six loci revealed no significant incongruence amongst loci, and the combined analyses resulted in a more robustly supported inference about species recognition (Taylor *et al.* 2000) and species relationships within the NAC.

The use of multiple phylogenetically informative gene regions has allowed for further taxonomic refinement of species assignments within both the oak and cherry lineages of *C. variospora*. The oak lineage now consists of two robust lineages, which are defined by the species *C. betulina* and *C. variospora*, which was hypothesized by Johnson *et al.* (2005) and is now strongly supported by multi-locus analyses. The former cherry lineage now consists of two strongly supported phylogenetic lineages, *C. tiliae* and *C. destructans*, as predicted by interfertility tests and distinct mycelial phenotypes, namely the former with slower growth and less pigmentation as compared to the latter

(Johnson *et al.* 2005, Oliveira *et al.* 2015a). The phylogenetic position of three isolates (C1956 from *Quercus*, C1957 from *Celtis*, and C1963 from *Prunus*) from Iowa is very close to *C. destructans*, and can be considered this species, but further intersterility testing and phylogenetic analyses would be needed to confidently resolve this small group.

Most *Ceratocystis* species within the NAC are not only supported by multi-locus phylogenetic analyses but also by host specialization, a biological species concept, and in some cases morphological characters. Host specificity through pathogenicity tests has been demonstrated in the aspen (*C. harringtonii*) and hickory lineages (*C. caryae* and *C. smalleyi*) (Johnson *et al.* 2005, Oliveira *et al.* 2015a). Now, with additional locus sampling, the former oak lineage of *C. variospora* consists of two host-associated species, *C. betulina* and *C. variospora*, which have only been isolated from *Betula* and *Quercus*, respectively. A clear pattern of host specialization was not as evident in the oak and cherry lineage cross-inoculations, with one exception. *Ceratocystis tiliae* was more aggressive to *Tilia* than close relatives isolated from *Quercus* and *vice versa* (Oliveira *et al.* 2015a). *Ceratocystis betulina* is represented by isolates from a single *Betula* log, and it is not clear if the log was saprobially colonized or if the fungus was native to Japan. To our knowledge no pathogenicity trials have compared the host associated sister clades *C. betulina* and *C. variospora*, but we predict that some level of host specialization will be realized in this clade as suggested by phylogenetic results. Preliminary pathogenicity trials have shown that isolates of *C. destructans* are highly pathogenic to almond trunks and branches (Holland, unpublished data); however, no cross-inoculation experiments have been performed. *Ceratocystis destructans* appears to have a rather broad geographic and host range, including *Prunus* spp. in California as well as *Celtis*, *Populus*, *Prunus* and *Quercus* in the Midwest of the USA.

Intersterility tests by Johnson *et al.* (2005) revealed that MAT-2 testers from the cherry, oak and *Tilia* lineages of *C. variospora* were only interfertile with MAT-1 testers from the same respective lineages, which are now recognized as *C. destructans*, *C. variospora* and *C. tiliae*. Two MAT-2 testers from almond trees in California (i.e. C578 and C856) were only interfertile with other isolates now defined as *C. destructans*, including other Californian isolates from almond and Iowa isolates from *Populus* and *Quercus*. Furthermore, C1709, the ex-type culture of *C. betulina*, was not interfertile with the MAT-2 testers of these species, nor were MAT-1 strains of *C. harringtonii*, *C. caryae* and *C. smalleyi* interfertile with the MAT-2 testers of *C. destructans*, *C. variospora* and *C. tiliae*. These examples of reproductive isolation support the recognition of biological species, which together with phylogenetic evidence, supports designation of these lineages as distinct taxa.

Morphology in the NAC was similar for all isolates with some unifying features, such as the ability to produce a second endoconidial stage of doliiform conidia from wide-mouth phialides and a distinct collar at the base of the perithecial neck (Johnson *et al.* 2005). Within the NAC, morphological features vary only slightly among the different species. For instance, *C. variospora*, which formerly encompassed what is now identified as *C. tiliae* (Oliveira *et al.* 2015a), *C. destructans* and *C. betulina*, differs morphologically from these species. For example, *C. variospora* possesses larger perithecia (130–350 µm), on average, than *C. destructans* (122–208 µm) and *C. betulina* (103–192 µm). *Ceratocystis variospora* also produces slightly larger

cylindrical endoconidia than *C. betulina*. However, the overall lack of morphological distinction makes it difficult to recognize these species without molecular characterization. *Ceratocystis destructans* and *C. betulina* are similar to other species in the NAC, with a dark green to grey colony color, fruity odor, and both cylindrical and doliiform endoconidia, as well as aleurioconidia (Table 2; Supplementary Table 1). *Ceratocystis caryae* and *C. smalleyi* (hickory lineage) have very similar ITS sequences and allozyme phenotypes, and they appear to be sexually interfertile (Johnson *et al.* 2005), but they differ greatly in morphology and biology. *Ceratocystis smalleyi* lacks cylindrical conidia from flask-shaped phialides and aleurioconidia (Johnson *et al.* 2005).

Several species in the NAC, including *C. caryae*, *C. harringtonii*, *C. tiliae* and *C. variospora*, are most commonly associated with wounded trunks and branches of trees (Johnson *et al.* 2005, Oliveira *et al.* 2015a), suggesting that members of this clade may act primarily as wound colonizers. *Ceratocystis destructans* is proposed as the new name for the causal agent of Ceratocystis canker of almond in California. The disease is common in California almond orchards where the trees have suffered repeated bark injuries during mechanical harvest, and *C. destructans* has been routinely isolated from discolored inner bark of almond trees that have been damaged by mechanical harvesting equipment. *Ceratocystis destructans* can also infect almond trees at wounds caused by pruning, producing branch cankers that result in extensive branch dieback. Several insects have been identified in California almond orchards as potential vectors, including several species of sap-feeding beetles (*Coleoptera*; *Nitidulidae*) and fruit flies (*Diptera*: *Drosophilidae*) (Moller & DeVay 1968). These insects are attracted to the sweet-smelling volatile compounds produced by *Ceratocystis*, and thus the insects may transport infectious spore inoculum from one tree to another. The pathogenicity to almond of *C. destructans* isolates collected for this study was recently investigated. Results showed that this fungus can produce cankers and cause extensive gumming in trunks and branches of almond (Holland *et al.* 2017). The host range of *C. destructans* in California and the occurrence of putative natural inoculum sources in the native vegetation surrounding almond orchards are unknown. Yet, *C. destructans* has been isolated from *Populus* spp. and *Quercus* spp. in the eastern USA. The occurrence in California of *C. destructans* on similar or related plant species should be investigated to better understand the pathogens' biology and putative origin as Ceratocystis canker continues to threaten the almond industry in California.

ACKNOWLEDGEMENTS

We thank the Almond Board of California for the financial support of this research. Hayato Masuya kindly provided *Ceratocystis* isolates from *Betula* logs in Japan.

REFERENCES

- Al Adawi AO, Barnes I, Khan IA, *et al.* (2014). Clonal structure of *Ceratocystis manginecans* populations from mango wilt disease in Oman and Pakistan. *Australasian Plant Pathology* **43**: 393–402.
- Barnes I, Roux J, Wingfield BD, *et al.* (2003). *Ceratocystis pirilliformis*, a new species from *Eucalyptus nitens* in Australia. *Mycologia* **95**: 865–871.

- Barnes I, Nakabonge G, Roux J, *et al.* (2005). Comparison of populations of the wilt pathogen *Ceratocystis albifundus* in South Africa and Uganda. *Plant Pathology* **54**: 189–195.
- Barnes I, Fourie A, Wingfield MJ, *et al.* (2018). New *Ceratocystis* species associated with rapid death of *Metrosideros polymorpha* in Hawai'i. *Persoonia* **40**: 154–181.
- Chen H, Kovalchuck A, Keriö S, *et al.* (2013). Distribution and bioinformatic analysis of the cerato- platanin protein family in *Dikarya*. *Mycologia* **105**: 1479–1488.
- Davidson RW (1944). Two American hardwood species of *Endoconidiophora* described as new. *Mycologia* **36**: 300–306.
- de Beer ZW, Duong TA, Barnes I, *et al.* (2014). Redefining *Ceratocystis* and allied genera. *Studies in Mycology* **79**: 187–219.
- de Beer ZW, Marincowitz S, Duong TA, *et al.* (2017). *Bretziella*, a new genus to accommodate the oak wilt fungus, *Ceratocystis fagacearum* (*Microascales*, *Ascomycota*). *MycKeys* **27**: 1–19.
- DeVay JE, English H, Lukezix FL, *et al.* (1960). Mallet wound canker of almond trees. *California Agriculture* **14**: 8–9.
- DeVay JE, Lukezix FL, English H, *et al.* (1962). *Ceratocystis* canker. *California Agriculture* **16**: 1–3.
- Engelbrecht CJB, Harrington TC (2005). Intersterility, morphology and taxonomy of *Ceratocystis fimbriata* on sweet potato, cacao and sycamore. *Mycologia* **97**: 57–69.
- Glass NL, Donaldson GC (1995). Development of primer sets designed for use with the PCR to amplify conserved genes from filamentous ascomycetes. *Applied and Environmental Microbiology* **6**: 1323–1330.
- Halsted BD (1890). Some fungous diseases of the sweet potato. *Bulletin of the New Jersey Agricultural Experiment Station* **76**: 3–32.
- Harrington TC (1993). Biology and taxonomy of fungi associated with bark beetles. In: *Beetle-pathogen Interactions in Conifer Forests* (Schowalter TD, ed). Academic Press, USA: 37–58.
- Harrington TC (2000). Host specialization and speciation in the American wilt pathogen *Ceratocystis fimbriata*. *Fitopatologia Brasileira* **25** (Suppl): 262–263.
- Harrington TC (2009). The genus *Ceratocystis*: Where does the oak wilt fungus fit? In: *Proceedings of the National Oak Wilt Symposium, 2nd* (Appel DN, Billings RF, eds). USA: 27–41.
- Harrington TC (2013). *Ceratocystis* diseases. In: *Infectious Forest Diseases* (Gonthier P, Nicolotti G, eds). CAB International, England: 230–255.
- Harrington TC, Thorpe DJ, Alfenas AC (2011). Genetic variation and variation in aggressiveness to native and exotic hosts among Brazilian populations of *Ceratocystis fimbriata*. *Phytopathology* **101**: 555–566.
- Heath RN, Wingfield MJ, Wingfield BD, *et al.* (2009). *Ceratocystis* species on *Acacia mearnsii* and *Eucalyptus* spp. in eastern and southern Africa including six new species. *Fungal Diversity* **34**: 41–68.
- Holland LA, Nouri MT, Morris N, *et al.* (2017). Almond Trunk and Scaffold Canker Diseases in California: Diagnosis, Pathogenicity, and Management [Abstract]. American Phytopathological Society Annual Meeting, San Antonio, TX.
- Johnson JA, Harrington TC, Engelbrecht CJB (2005). Phylogeny and taxonomy of the North American clade of the *Ceratocystis fimbriata* complex. *Mycologia* **97**: 1067–1092
- Kile GA (1993). Plant diseases caused by species of *Ceratocystis* sensu stricto and *Chalara*. In: *Ceratocystis and Ophiostoma: Taxonomy, Ecology and Pathogenicity* (Wingfield MJ, Seifert KA, Webber JF, eds). APS Press, USA: 173–183.
- Li Q, Harrington TC, McNew D, *et al.* (2017). *Ceratocystis uchidae*, a new species on *Araceae* in Hawai'i and Fiji. *Mycoscience* **58**: 398–412.
- Liu FF, Barnes I, Roux J, *et al.* (2018). Molecular phylogenetics and microsatellite analysis reveal a new pathogenic *Ceratocystis* species in the Asian-Australian clade. *Plant Pathology* **67**: 1097–1113. <https://doi.org/10.1111/ppa.12820>.
- Maddison WP, Maddison DR (2016). Mesquite: a modular system for evolutionary analysis. Version 3.10 <http://mesquiteproject.org>.
- Malloch D, Blackwell M (1993). Dispersal biology of the ophiostomatoid fungi. In: *Ceratocystis and Ophiostoma: Taxonomy, Ecology and Pathogenicity* (Wingfield MJ, Seifert KA, Webber JF, eds). APS Press, USA: 195–206.
- Marin-Felix Y, Groenewald JZ, Cai L, *et al.* (2017). Genera of phytopathogenic fungi: GOPHY 1. *Studies in Mycology* **86**: 99–216.
- Mayers CG, McNew DL, Harrington TC, *et al.* (2015). Three genera in the *Ceratocystidaceae* are the respective symbionts of three independent lineages of ambrosia beetles with large, complex mycangia. *Fungal Biology* **119**: 1075–1092.
- Mayers CG, Bateman CC, Harrington TC (2018). New *Meredithiella* species from mycangia of *Corthylus* ambrosia beetles suggest genus-level coadaptation but not species-level coevolution. *Mycologia* **110**: 63–78.
- Mbenoun M, Wingfield MJ, Begoude Boyogueno AD, *et al.* (2014). Molecular phylogenetic analyses reveal three new *Ceratocystis* species and provide evidence for geographic differentiation of the genus in Africa. *Mycological Progress* **13**: 219–240.
- Moller WJ, DeVay JE (1968). Insect transmission of *Ceratocystis fimbriata* in deciduous fruit orchards. *Phytopathology* **58**: 1499–1508.
- Nel WJ, Duong TA, Wingfield BD, *et al.* (2018). A new genus and species for the globally important, multihost root pathogen *Thielaviopsis basicola*. *Plant Pathology* **67**: 871–882.
- Oliveira LSS, Harrington TC, Freitas RG, *et al.* (2015a). *Ceratocystis tiliae* sp. nov., a wound pathogen on *Tilia americana*. *Mycologia* **107**: 986–995.
- Oliveira LSS, Harrington TC, Ferreira MA, *et al.* (2015b). Species or genotypes? Reassessment of four recently described species of the *Ceratocystis* wilt pathogen, *Ceratocystis fimbriata*, on *Mangifera indica*. *Phytopathology* **105**: 1229–1244.
- Pazzagli L, Cappugi G, Manao G, *et al.* (1999). Purification, characterization and amino acid sequence of cerato-platanin, a new phytotoxic protein from *Ceratocystis fimbriata* f. sp. *platani*. *Journal of Biological Chemistry* **274**: 24949–24964.
- Perry E, McCain AH (1988). Incidence and management of canker stain in London plane trees in Modesto, California. *Journal of Arboriculture* **14**: 18–19.
- Rayner RW (1970). *A mycological colour chart*. Commonwealth Mycological Institute and British Mycological Society.
- Seifert KA, Wingfield MJ, Kendrick WB (1993). A nomenclator for described species of *Ceratocystis*, *Ophiostoma*, *Ceratocystiopsis*, *Ceratostomella* and *Sphaeronaemella*. In: *Ceratocystis and Ophiostoma: Taxonomy, Ecology and Pathogenicity* (Wingfield MJ, Seifert KA, Webber JF, eds). APS Press, USA: 269–287.
- Stielow JB, Lévesque CA, Seifert KA *et al.* (2015). One fungus, which genes? Development and assessment of universal primers for potential secondary fungal DNA barcodes. *Persoonia* **35**: 242–263.
- Swofford DL (2002). PAUP* 4: phylogenetic analysis using parsimony (*and other methods). Sunderland, Massachusetts: Sinauer Associates.
- Tamura K, Stetcher G, Peterson D, *et al.* (2013). MEGA 6: Molecular Evolutionary Genetics Analysis version 6.0. *Molecular Biology and Evolution* **30**: 2725–2729.
- Taylor JW, Jacobson DJ, Kroken S, *et al.* (2000). Phylogenetic species recognition and species concepts in fungi. *Fungal Genetics and Biology* **31**: 21–32.
- Thorpe DJ, Harrington TC, Uchida JY (2005). Pathogenicity, internal transcribed spacer-rDNA variation, and human dispersal of

Ceratocystis fimbriata on the family *Araceae*. *Phytopathology* **95**: 316–323.

Upadhyay H (1981). *A monograph of Ceratocystis and Ceratocystiopsis*. University of Georgia Press, USA.

Vilgalys R, Hester M (1990). Rapid genetic identification and mapping of enzymatically amplified ribosomal DNA from several *Cryptococcus* species. *Journal of Bacteriology* **174**: 4238–4246.

Wingfield MJ, Seifert KA, Webber JF (1993). *Ophiostoma and Ceratocystis: Taxonomy, Ecology and Pathogenicity*. APS Press, USA.

Wingfield MJ, De Beer C, Visser C, *et al.* (1996). A New *Ceratocystis* species defined using morphological and ribosomal DNA sequence comparisons. *Applied Microbiology* **19**: 191–202.

Supplementary Material: <http://fuse-journal.org/>

Table. S1. Additional specimens of *C. betulina* and *C. destructans* examined.

doi.org/10.3114/fuse.2019.03.08

Epitypification of *Cercospora rautensis*, the causal agent of leaf spot disease on *Securigera varia*, and its first report from Iran

M. Bakhshi*

Department of Botany, Iranian Research Institute of Plant Protection, P.O. Box 19395-1454, Agricultural Research, Education and Extension Organization (AREEO), Tehran, Iran

*Corresponding author: mounesbakhshi@gmail.com

Key words:

Cercospora armoraciae
complex
cercosporoid
leaf spot
Mycosphaerellaceae
new epitype

Abstract: *Cercospora* is a well-studied and important genus of plant pathogenic species responsible for leaf spots on a broad range of plant hosts. The lack of useful morphological traits and the high degree of variation therein complicate species identifications in *Cercospora*. Recent studies have revealed multi-gene DNA sequence data to be highly informative for species identification in *Cercospora*. During the present study, *Cercospora* isolates obtained from Crownvetch (*Securigera varia*) in Iran and Romania were subjected to an eight-gene (ITS, *tef1*, *actA*, *cmdA*, *his3*, *tub2*, *rpb2* and *gapdh*) analysis. By applying a polyphasic approach including morphological characteristics, host data, and molecular analyses, these isolates were identified as *C. rautensis*. To our knowledge, this is the first record of *C. rautensis* from Iran (Asia). In addition, an epitype is designated here for *C. rautensis*.

Effectively published online: 13 March 2019.

INTRODUCTION

Crownvetch (*Securigera varia* ≡ *Coronilla varia*), is a herbaceous, perennial legume with creeping stems belonging in the family *Fabaceae* which is native to the Mediterranean region of Europe, southwest Asia, and northern Africa (Roland 1998). It is an intercropping plant in many orchards in the world, with many benefits, including controlling weeds, decreasing soil erosion, increasing soil enzyme activities, improving the soil micro-ecological environment and, like other *Fabaceae*, it is a nitrogen fixer (Qian *et al.* 2015, Zheng *et al.* 2016). However, this plant may become weedy or invasive in some regions or habitats and may displace desirable vegetation if not properly managed (Randall & Marinelli 1996, Kaufman & Kaufman 2013).

The cosmopolitan genus *Cercospora* is species-rich (2 522 legitimate species names listed in MycoBank, accessed 20 Feb. 2019) that belongs to the family *Mycosphaerellaceae* in the order *Capnodiales*. The genus comprises numerous destructive plant pathogens, for instance *C. apii* on celery (Groenewald *et al.* 2006), *C. beticola* on sugar beet (Weiland & Koch 2004), *C. zonata* on faba beans (Kimber & Paull 2011), *C. zaeae-maydis* and *C. zeina* on maize (Crous *et al.* 2006) and *C. carotae* on carrots (Kushalappa *et al.* 1989). *Cercospora* was established by Fuckel (Fungi Rhen. Exs., no. 117, 1863; as Fresen. ex Fuckel, see Braun & Crous 2016), and *C. apii* was later designated as conserved type of the genus under the International Code of Nomenclature for algae, fungi, and plants, Art. 14.9 (Braun & Crous 2016). The systematics of *Cercospora* has been problematic for a long time, as there are only few distinctive morphological characters useful for species discrimination and since specialised as well as plurivorous species are involved (Crous & Braun 2003, Groenewald *et al.* 2013, Bakhshi *et al.* 2015, 2018). Molecular techniques are commonly used to overcome taxonomic problems posed by the

limitations of morphological characteristics. In this regard, ex-type cultures are essential for the study of *Cercospora*, because the current systematic scheme is based on multilocus phylogeny (Groenewald *et al.* 2013, Nguanhom *et al.* 2015, Soares *et al.* 2015, Bakhshi *et al.* 2015, 2018, Albu *et al.* 2016, Guillin *et al.* 2017, Guatimosim *et al.* 2017) and DNA can rarely be extracted from herbarium samples. Therefore, it is important to typify and epitypify species within this genus to stabilise the names for future studies, and provide connections between specimens assessed through molecular and morphological methods.

In an eight-gene molecular DNA sequence analysis employed for *Cercospora s. str.*, Bakhshi *et al.* (2018) revealed cryptic species within several species complexes. Therefore, besides introducing some new species, epitypes have been designated for some species which were previously regarded as synonyms of other species based on previously published five-gene phylogenies (Groenewald *et al.* 2013, Bakhshi *et al.* 2015, 2018). The objective of the present study was therefore to confirm the taxonomy and DNA phylogeny of the *Cercospora* isolates obtained from *S. varia* from Iran and Romania, which were previously synonymised under *C. armoraciae* based on a five-gene DNA dataset (Groenewald *et al.* 2013, Bakhshi *et al.* 2015).

MATERIAL AND METHODS

Specimens and isolates

Isolates used in this study (Table 1) are maintained in the collection of the Westerdijk Fungal Biodiversity Institute (CBS), Utrecht, The Netherlands, the working collection of Pedro Crous (CPC; housed at Westerdijk Fungal Biodiversity Institute), and the culture collection of Tabriz University (CCTU), Tabriz, Iran.

Table 1. Collection details and GenBank accession numbers of isolates included in this study. Ex-type isolates and newly generated sequences are highlighted in bold.

Species	Culture accession number(s) ¹	Host	Host family	Origin	Collector	GenBank accession numbers ²							
						ITS	<i>tef1</i>	<i>actA</i>	<i>cmdA</i>	<i>his3</i>	<i>tub2</i>	<i>rpb2</i>	<i>gapdh</i>
<i>C. armoraciae</i>	CBS 250.67; CPC 5088 (TYPE)	<i>Armoracia rusticana</i>	Brassicaceae	Romania, Fundulea	O. Constantinescu	JX143545	JX143299	JX143053	JX142807	JX142561	MH496351	–	MH496181
<i>C. bizzoeriana</i>	CCTU 1013	–	–	Iran, East Azerbaijan	M. Torbati	KJ886414	KJ886253	KJ885931	KJ885770	KJ886092	MH496362	MH511855	MH496192
	CCTU 1022; CBS 136028	–	–	Iran, East Azerbaijan	M. Torbati	KJ886415	KJ886254	KJ885932	KJ885771	KJ886093	MH496363	MH511856	MH496193
	CCTU 1127; CBS 136133	<i>Capparis spinosa</i>	Capparidaceae	Iran, Khuzestan	E. Mohammadian	KJ886420	KJ886259	KJ885937	KJ885776	KJ886098	MH496364	MH511857	MH496194
	CCTU 1117; CBS 136132	<i>Lepidium draba</i>	Brassicaceae	Iran, West Azerbaijan	M. Arzanlou	KJ886418	KJ886257	KJ885935	KJ885774	KJ886096	MH496365	MH511858	MH496195
	CCTU 1234	<i>Lepidium draba</i>	Brassicaceae	Iran, West Azerbaijan	M. Arzanlou	KJ886419	KJ886258	KJ885936	KJ885775	KJ886097	MH496366	MH511859	MH496196
	CCTU 1107	–	–	Iran, Zanjan	M. Bakhshi	KJ886417	KJ886256	KJ885934	KJ885773	KJ886095	MH496367	MH511860	MH496197
	CBS 258.67; CPC 5061 (TYPE)	<i>Lepidium draba</i>	Brassicaceae	Romania, Fundulea	O. Constantinescu	JX143546	JX143300	JX143054	JX142808	JX142562	MH496368	–	MH496198
	CBS 540.71; IMI 161110; CPC 5060	<i>Lepidium draba</i>	Brassicaceae	Romania, Hagieni	O. Constantinescu	JX143548	JX143302	JX143056	JX142810	JX142564	MH496369	–	MH496199
	CCTU 1040; CBS 136131	<i>Tanacetum balsamita</i>	Asteraceae	Iran, Zanjan	M. Bakhshi	KJ886416	KJ886255	KJ885933	KJ885772	KJ886094	MH496370	MH511861	MH496200
<i>C. rautensis</i>	CCTU 1190; CBS 136134	<i>Securigera varia</i>	Fabaceae	Iran, West Azerbaijan	M. Arzanlou	KJ886422	KJ886261	KJ885939	KJ885778	KJ886100	MKS31769	MKS564169	MKS531771
	CBS 555.71; IMI 161117; CPC 5082 (TYPE)	<i>Securigera varia</i>	Fabaceae	Romania, Hagieni	O. Constantinescu	JX143550	JX143304	JX143058	JX142812	JX142566	MKS31770	–	MKS531772
<i>C. sorghicola</i>	CCTU 1173; CBS 136448; IRAN 2672C (TYPE)	<i>Sorghum halepense</i>	Poaceae	Iran, Guilan	M. Bakhshi	KJ886525	KJ886364	KJ886042	KJ885881	KJ886203	MH496471	MH511961	MH496301

¹ CBS: Westerdijk Fungal Biodiversity Institute, Utrecht, The Netherlands; CCTU: Culture Collection of Tabriz University, Tabriz, Iran; CPC: Culture collection of Pedro Crous, housed at Westerdijk Fungal Biodiversity Institute; IMI: International Mycological Institute, CAB International, Egham, Surrey, UK; IRAN: Iranian Fungal Culture Collection, Iranian Research Institute of Plant Protection, Tehran, Iran.

² ITS: internal transcribed spacers and intervening 5.8S rDNA; *tef1*: partial translation elongation factor 1-alpha gene; *actA*: partial actin gene; *cmdA*: partial calmodulin gene; *his3*: partial histone H3 gene; *tub2*: partial beta-tubulin gene; *rpb2*: partial DNA-directed RNA polymerase II second largest subunit; *gapdh*: partial glyceraldehyde-3-phosphate dehydrogenase gene.

Dried specimens are preserved in the Fungal Herbarium of the Iranian Research Institute of Plant Protection (IRAN F), Tehran, Iran, and the Westerdijk Fungal Biodiversity Institute (CBS H), Utrecht, The Netherlands.

DNA extraction, PCR amplification and sequencing

DNA samples comprised those previously extracted by Bakhshi *et al.* (2015) and Groenewald *et al.* (2013). Three additional partial nuclear genes were sequenced for each isolate. The primers Gpd1-LM and Gpd2-LM (Myllys *et al.* 2002) were used to amplify part of the glyceraldehyde-3-phosphate dehydrogenase (*gapdh*) gene. Part of the β -tubulin (*tub2*) gene was amplified using the primer set BT-1F and BT-1R (Bakhshi *et al.* 2018), whereas the primer set RPB2-C5F and RPB2-C8R (Bakhshi *et al.* 2018) was used to amplify part of the DNA-directed RNA polymerase II second largest subunit (*rpb2*) gene. All amplification mixtures and conditions were performed in a total volume of 12.5 μ L as described by Bakhshi *et al.* (2018). PCR products were visualised by electrophoresis using a 1.2 % agarose gel, stained with GelRed™ (Biotium, Hayward, CA, USA) and viewed under ultraviolet light. Size estimates were made using a HyperLadder™ I molecular marker (Bioline).

Both strands of the PCR fragments were sequenced using the same primers used for amplification and the BigDye Terminator Cycle Sequencing reaction Kit v. 3.1 (Applied Biosystems, Foster City, CA, USA), following the manufacturer's instructions. Sequencing amplicons were purified through Sephadex G-50 Superfine columns (SigmaAldrich, St Louis, MO, USA) in 96-well MultiScreen HV plates (Millipore, Billerica, MA, USA) and analysed with an ABI Prism 3730xl Automated DNA analyser (Life Technologies Europe BV, Applied Biosystems™, Bleiswijk, The Netherlands) as outlined by the manufacturer.

Phylogenetic analyses

The raw DNA sequences of *tub2*, *rpb2* and *gapdh* were edited using MEGA v. 6 (Tamura *et al.* 2013) and forward and reverse sequences for each isolate were assembled manually to generate consensus sequences. In addition, sequences of isolates from the *C. armoraciae* complex (Groenewald *et al.* 2013, Bakhshi *et al.* 2015, 2018) corresponding to the ITS locus (including ITS1, 5.8S, ITS2), together with parts of seven protein coding genes, *viz.* translation elongation factor 1-alpha (*tef1*), actin (*actA*),

calmodulin (*cmdA*), histone H3 (*his3*), *tub2*, *rpb2* and *gapdh*, were retrieved from the NCBI's GenBank nucleotide database and included in the analyses (Table 1). Sequences were aligned with the MAFFT online interface using default settings (<http://mafft.cbrc.jp/alignment/server/>) (Kato & Standley 2013), and adjusted manually where necessary using MEGA v. 6. Sequences of *C. sorghicola* (CBS 136448 = IRAN 2672C) were used as outgroup.

Phylogenetic analyses were based on Bayesian inference (BI). For this purpose, the best nucleotide substitution model was selected independently for each locus using MrModeltest v. 2.3 (Nylander 2004). The individual alignments of the different loci were subsequently concatenated with Mesquite v. 2.75 (Maddison & Maddison 2011) prior to being subjected to a combined multi-gene analysis. Phylogenetic reconstruction under optimal criteria per partition was performed using Bayesian inference (BI) Markov Chain Monte Carlo (MCMC) algorithm in MrBayes v. 3.2.6 (Ronquist *et al.* 2012). Two simultaneous MCMC analyses, each consisting of four Markov chains, were run from random trees until the average standard deviation of split frequencies reached a value of 0.01, with trees saved every 100 generations and the heating parameter was set to 0.15. The first 25 % of saved trees were discarded as the “burn-in” phase and posterior probabilities (Rannala & Yang 1996) were calculated from the remaining trees. The resulting phylogenetic tree was printed with Geneious v. 5.6.7 (Kearse *et al.* 2012). Newly generated sequences in this study were deposited in NCBI's GenBank nucleotide database (www.ncbi.nlm.nih.gov; Table 1) and alignments and respective phylogenetic trees in TreeBASE, study number 24021 (www.TreeBASE.org).

Morphology

To examine morphological characteristics, diseased leaf tissues were observed under a Nikon® SMZ1500 stereo-microscope and taxonomically informative morphological structures (stromata, conidiophores and conidia) were picked up from lesions with a sterile dissecting needle and mounted on glass slides in clear lactic acid. Structures were examined under a Nikon Eclipse 80i light microscope at ×1000, and 95 % confidence intervals were derived for the 30 measurements with extreme values given in parentheses. High-resolution photographs of microscopic fungal

structures were captured with a Nikon digital sight DS-f1 high definition colour camera mounted on the above-mentioned light microscope and the layout of acquired images and photographic preparations was carried out in Adobe Photoshop CS5. Colony macro-morphology on MEA was determined after 20 d at 25 °C in the dark in duplicate and colony colour was described using the mycological colour charts of Rayner (1970).

Allele group designation

The isolates of this study along with the other isolates from the *C. armoraciae* species complex (Bakhshi *et al.* 2018), including *C. armoraciae s. str.* and *C. bizzozeriana*, were compared using the individual alignments of the eight single loci in MEGA v. 6. Allele groups were established for each locus based on sequence identity, i.e., each sequence with one or more nucleotide difference from the other sequences was regarded as a different allele.

RESULTS AND DISCUSSION

Phylogenetic analyses

The final concatenated alignment contained 12 aligned sequences of the isolates from the *C. armoraciae* species complex (Groenewald *et al.* 2013, Bakhshi *et al.* 2015, 2018) and 4 084 characters including alignment gaps. The gene boundaries were 1–470 bp for ITS, 475–765 bp for *tef1*, 770–956 bp for *actA*, 961–1 208 bp for *cmdA*, 1 213–1 568 bp for *his3*, 1 573–1 982 bp for *tub2*, 1 987–3 215 bp for *rpb2*, and 3 220–4 084 bp for *gapdh*. Four sets of four Ns were used in the alignment to separate adjacent loci and were excluded from the phylogenetic analyses.

Based on the results of MrModeltest, a SYM-gamma model with a gamma distributed rate variation for ITS, a K80-gamma with a gamma distributed rate variation for *tef1*, *actA* and *cmdA*, a HKY+G with gamma-distributed rates for *his3*, a GTR+G model with a gamma distributed rate variation for *tub2* and *rpb2* were applied while *gapdh* required GTR+I+G with inverse gamma distributed rate variation. The ITS, *tef1*, *actA* and *cmdA* partitions had fixed (equal) base frequencies, whereas the remaining partitions (*his3*, *tub2*, *rpb2* and *gapdh*) had dirichlet base frequencies. From this alignment, 4 056 characters were

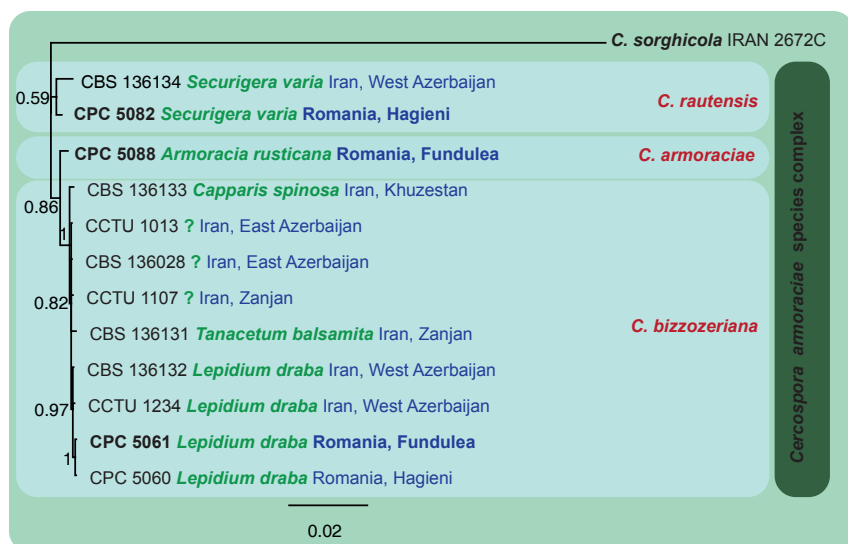


Fig. 1. Consensus phylogram (50 % majority rule) of 850 trees resulting from a Bayesian analysis of the combined eight-gene (ITS, *tef1*, *actA*, *cmdA*, *his3*, *tub2*, *rpb2* and *gapdh*) sequence alignment using MrBayes v. 3.2.6. The scale bar indicates 0.02 expected changes per site. The tree was rooted to *Cercospora sorghicola* (CBS 136448 = IRAN 2672C).

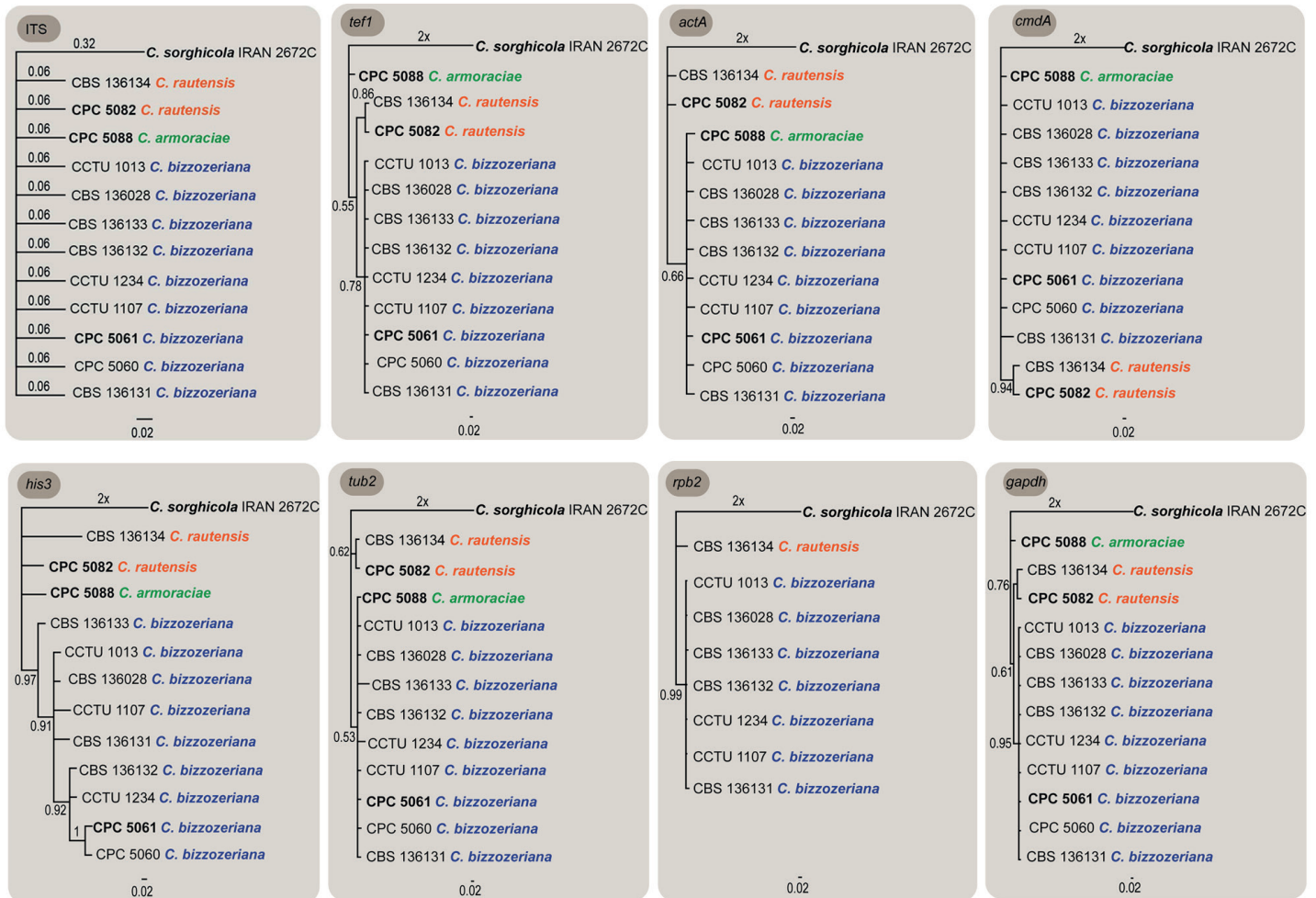


Fig. 2. Bayesian 50 % majority rule consensus trees of the individual gene loci using MrBayes v. 3.2.6. The scale bar indicates 0.02 expected changes per site. The trees were rooted to *Cercospora sorghicola* (CBS 136448 = IRAN 2672C).

used for the Bayesian analysis; these contained 200 unique site patterns (7, 26, 17, 16, 32, 25, 32 and 45 for ITS, *tef1*, *actA*, *cmdA*, *his3*, *tub2*, *rpb2* and *gapdh*, respectively). The Bayesian analysis lasted 565 000 generations and generated a total of 1 132 trees. After discarding the first 25 % of sampled trees for burn-in the phylogenetic tree (50 % majority rule consensus tree) and posterior probabilities were calculated from the remaining 850 trees (Fig. 1).

All genes were also assessed individually using Bayesian analyses under the above-mentioned substitution models, for each data partition (Fig. 2). Based on individual gene tree assessments, the isolates obtained from *Securigera varia* are supported as a clade of its own based on phylogenies derived from the *tef1*, *cmdA*, *tub2*, and *gapdh* alignments (Fig. 2).

Taxonomy

The Consolidated Species Concept (Quaedvlieg *et al.* 2014) accepted in recent revisions of the taxonomy of the genus *Cercospora* (e.g., Groenewald *et al.* 2013, Bakhshi *et al.* 2015, 2018) was employed in this study to distinguish the isolates of the genus *Cercospora* obtained from *Securigera varia*. These isolates were previously recognised as *C. armoraciae* based on the five-gene phylogenetic tree (ITS, *tef1*, *actA*, *cmdA* and *his3*) (Groenewald *et al.* 2013, Bakhshi *et al.* 2015). Recently Bakhshi *et al.* (2018) re-assessed

species of the genus *Cercospora* using a combined approach based on the evaluation of an eight-gene (ITS, *tef1*, *actA*, *cmdA*, *his3*, *tub2*, *rpb2* and *gapdh*) molecular DNA sequence dataset, host, and morphological data. The robust eight-gene phylogeny revealed several novel clades within the existing *Cercospora* species complexes, such as *C. armoraciae*, and the *C. armoraciae* s. lat. isolates were distributed over two clades, *C. armoraciae* s. str. and *C. bizzoeriana* (Bakhshi *et al.* 2018). In this study, the eight-gene phylogeny of the *Cercospora* isolates obtained from *Securigera varia* (as *C. armoraciae* in Groenewald *et al.* 2013, and Bakhshi *et al.* 2015) revealed that the clade comprising these two strains is completely distinct from *C. armoraciae* s. str. and *C. bizzoeriana* (*C. armoraciae* s. lat. complex) clades. Based on a literature survey and morphological similarities, the species name *C. rautensis* was assigned to this clade.

Cercospora rautensis C. Massal., Madonna Verona, Boll. Mus. Civico Verona **3**: 19. 1909. Fig. 3.

Synonyms: *Cercospora coronillae-scorpoidis* Ferraris, Fl. Ital. Cryptog. I, Fungi, Hyphales: 893. 1910.

Cercospora coronillae-variae Lobik, Bolezni Rastenij **17**: 194. 1928.

Description in planta: Leaf spots distinct, circular to irregular, grey-brown, without definite border, 1–5 mm diam. *Mycelium*



Fig. 3. *Cercospora rautensis* (CBS 136134). A–C. Fasciculate conidiophores. D–I. Conidia. Scale bars = 10 μ m.

internal. *Caespituli* amphigenous, brown. *Conidiophores* in moderately dense fascicles (4–25), arising from the upper cells of a well-developed, intraepidermal and substomatal, brown stroma, up to 45 μ m diam; conidiophores pale brown to brown, 0–3-septate, straight to mildly geniculate, flexuous, unbranched, (30–)45–65 \times 4.5–6 μ m, somewhat irregular in width, becoming narrower towards the apex, *Conidiogenous cells* terminal or integrated, brown, smooth, proliferating sympodially, 15–40 \times 3.5–5 μ m, mono-local or multi-local; loci thickened, darkened, refractive, protuberant, mostly apical, sometimes lateral, 2–3.5 μ m diam. *Conidia* solitary, subcylindrical to cylindrical, straight to mildly curved, hyaline, thin-walled, smooth, distinctly 3–9-septate, obtuse at the tip, truncate to obconically truncate at the base, (38–)65–80(–130) \times (4–)4.5–6 μ m; hila thickened, darkened, refractive, 2–3.5 μ m diam.

Typus: Italy, “Nel bosco “delle Raute” presso il paesetto di Cogolo, on *Securigera varia* [= *Coronilla varia*] (*Fabaceae*), Aug., *C. Massalongo* (**holotype** VER, n.v.). Romania, Hagieni, on *S. varia*, 20 Jul. 1970, *O. Constantinescu* (**epitype designated here** CBS H-9861, MBT 385978), ex-epitype culture CBS 555.71 = IMI 161117 = CPC 5082.

Additional material examined: Iran, West Azerbaijan Province, Khoy, Firouragh, on *Securigera varia*, Jul. 2012, *M. Arzanlou* (IRAN 17180F, CCTU 1190 = CBS 136134).

Culture characteristics: Colonies on MEA reaching 60 mm diam after 20 d at 25 $^{\circ}$ C in the dark; flat with smooth, even margins and moderate aerial mycelium; surface olivaceous grey, reverse iron-grey.

Distribution: Italy, Hungary, Lithuania, Poland, Romania, Ukraine (Europe), Russia (European part), Georgia, Pennsylvania (USA) (Crous & Braun 2003, Farr & Rossman 2019) and Iran (Asia) (this study).

Notes: Based on the results of the eight-gene phylogenetic tree, the isolates obtained from *S. varia* from Iran and Romania, previously recognised as *C. armoraciae* based on five-gene phylogenetic tree (Groenewald *et al.* 2013, Bakhshi *et al.* 2015), clustered in a clade, distinct from the ex-type isolate of *C. armoraciae* (CBS 250.67 = CPC 5088) (Fig. 1). Therefore, this species must be regarded as a separate species and appears to be specific to *S. varia*. *Cercospora rautensis* is the only species of *Cercospora* known from *S. varia*. The collection from Iran agrees morphologically well with Chupp’s (1954) description of *C. rautensis* (conidiophores 20–100 \times 3–5 μ m, conidia acicular to cylindrical, straight to mildly curved, 35–100 \times 3–5 μ m, base truncate to obconically truncate, tip subobtuse). It also perfectly agrees with type material of *C. coronillae-variae* (LE 158151), which has been reduced to synonymy with *C. rautensis* (conidiophores 15–65 \times 4–8 μ m, conidia cylindrical, subcylindrical to slightly obclavate, 40–100 \times (3.5–)4–5(–6) μ m, base truncate to somewhat obconically truncate) (examined by Uwe Braun). It is unclear whether Chupp (1954) had seen and examined the type material of *C. rautensis*. A long time ago, U. Braun (pers. commun.) received the information that Massalongo’s types are maintained at VER, but a loan was not possible and is not possible until now. However, as long as the existence of type material of *C. rautensis* at VER must be assumed, neotypification is not justified to solve the issue. Since one European isolate from *S. varia* in Romania (CBS 555.71 =

Table 2. Results from allele group designation per locus for *C. armoraciae*, *C. bizzozzeriana* and *C. rautensis* (*C. armoraciae* s. lat.) isolates.

Species	Culture accession number	Allele group per locus							
		ITS	<i>tef1</i>	<i>actA</i>	<i>cmdA</i>	<i>his3</i>	<i>tub2</i>	<i>rpb2</i>	<i>gapdh</i>
<i>C. armoraciae</i>	CBS 250.67; CPC 5088 (TYPE)	I	I	I	I	I	I	–	I
<i>C. bizzozzeriana</i>	CCTU 1013	I	II	I	I	III	I	I	II
	CCTU 1022; CBS 136028	I	II	I	I	III	I	I	II
	CCTU 1040; CBS 136131	I	III	I	II	VI	I	II	II
	CCTU 1107	I	II	I	I	VII	I	I	II
	CCTU 1117; CBS 136132	I	II	I	I	V	I	I	II
	CCTU 1234	I	II	I	I	V	III	I	II
	CCTU 1127; CBS 136133	I	II	I	I	IV	II	III	II
	CBS 540.71; CPC 5060	I	II	I	I	II	I	–	II
CBS 258.67; CPC 5061 (TYPE)	I	II	I	I	II	I	–	II	
<i>C. rautensis</i>	CCTU 1190; CBS 136134	I	IV	II	III	VIII	IV	IV	III
	CBS 555.71; CPC 5082 (TYPE)	I	IV	II	III	IX	IV	–	IV

IMI 161117 = CPC 5082) (as *C. rautensis* until Jul. 2013; see Groenewald *et al.* 2013) also resides in this clade, I designate it here as epitype for this species, and fix the application of the name *C. rautensis* to this clade.

Allele group designation

The results of allele group designation of the isolates of *C. rautensis* and other isolates in *C. armoraciae* complex are summarised in Table 2. The allele group for the *tef1*, *actA*, *cmdA* and *tub2* sequences for both strains of *C. rautensis* from Iran (CBS 136134) and Romania (CBS 555.71) was similar and also different from the allele group of the *C. armoraciae* and *C. bizzozzeriana* isolates. For ITS, the allele group of these two isolates was the same as *C. armoraciae* and *C. bizzozzeriana* isolates, while for *his3* and *gapdh*, these two isolates had a different allele group which was also distinct from the allele group of the *C. armoraciae* and *C. bizzozzeriana* isolates (Table 2).

CONCLUSIONS

Extensive studies of *Cercospora* and related genera in Iran have generated records of numerous species (Hesami *et al.* 2012, Pirnia *et al.* 2012, Bakhshi *et al.* 2012, 2015, 2018). However, *C. rautensis* has not been detected in Iran before. Therefore, this is the first report of *C. rautensis* infection of Crownvetch in Iran. Since one European isolate was included in this study, I was able to designate an epitype here for this species as well, which was necessary to determine the application of the name *C. rautensis*.

In recent years, two significant advances in the understanding of *Cercospora* have been achieved. First, with the comprehensive molecular examination of *Cercospora* s. str. based on a multi-locus DNA sequence dataset of five genomic loci of the large sampling of species conducted by Groenewald *et al.* (2013), a backbone phylogeny was achieved for *Cercospora*. Second, an eight-gene molecular DNA sequence analysis of *Cercospora* s. str. was conducted by Bakhshi *et al.* (2018), which revealed cryptic species within several species complexes. One important finding of these studies is that it was not always possible to apply North American or European

names to African or Asian strains and *vice versa*. Therefore, type specimens are essential for molecular analyses of *Cercospora* species for correct applications of such species names. Unfortunately, many (epi-)type cultures are lacking for a significant number of *Cercospora* species. These species will have to be recollected from their original hosts and continents from where they were described. These collections are necessary to stabilise the application of the names to facilitate subsequent taxonomic work on *Cercospora*.

ACKNOWLEDGEMENTS

The Iran National Science Foundation (INSF) and the Research Deputy of the Iranian Research Institute of Plant Protection, Agricultural Research, Education and Extension Organization (AREEO) are acknowledged for financial support. Prof. dr Uwe Braun (Martin Luther University, Halle, Germany) is thanked for his helpful advice concerning typification of *Cercospora rautensis* and his valuable comments on the manuscript.

REFERENCES

- Albu S, Schneider R, Price P, *et al.* (2016). *Cercospora* cf. *flagellaris* and *Cercospora* cf. *sigesbeckiae* are associated with *Cercospora* leaf blight and purple seed stain on soybean in North America. *Phytopathology* **106**: 1376–85.
- Bakhshi M, Arzanlou M, Babai-Ahari A (2012). Comprehensive checklist of Cercosporoid fungi from Iran. *Plant Pathology and Quarantine* **2**: 44–55.
- Bakhshi M, Arzanlou M, Babai-ahari A, *et al.* (2015). Application of the consolidated species concept to *Cercospora* spp. from Iran. *Persoonia* **34**: 65–86.
- Bakhshi M, Arzanlou M, Babai-ahari A, *et al.* (2018). Novel primers improve species delimitation in *Cercospora*. *IMA Fungus* **9**: 299–332.
- Braun U, Crous PW (2016). (2415) Proposal to conserve the name *Cercospora* (Ascomycota: Mycosphaerellaceae) with a conserved type. *Taxon* **65**: 185.
- Chupp C (1954). *A Monograph of the Fungus Genus Cercospora*. Ithaca, New York.

- Crous PW, Braun U (2003). *Mycosphaerella* and its anamorphs: 1. Names published in *Cercospora* and *Passalora*. *CBS Biodiversity Series* **1**: 1–571.
- Crous PW, Groenewald JZ, Groenewald M, *et al.* (2006). Species of *Cercospora* associated with grey leaf spot of maize. *Studies in Mycology* **55**: 189–197.
- Farr DF, Rossmann AY (2019). Fungal Databases, U.S. National Fungus Collections, ARS, USDA. Available online at <https://nt.ars-grin.gov/fungaldatabases>
- Groenewald JZ, Nakashima C, Nishikawa J, *et al.* (2013). Species concepts in *Cercospora*: spotting the weeds among the roses. *Studies in Mycology* **75**: 115–170.
- Groenewald M, Groenewald JZ, Braun U, *et al.* (2006). Host range of *Cercospora apii* and *C. beticola* and description of *C. apiicola*, a novel species from celery. *Mycologia* **98**: 275–285.
- Guatimosim E, Schwartsburd PB, Barreto RW, *et al.* (2017). Novel fungi from an ancient niche: cercosporoid and related sexual morphs on ferns. *Persoonia* **37**: 106–41.
- Guillin EA, de Oliveira LO, Grijalba PE, *et al.* (2017). Genetic entanglement between *Cercospora* species associating soybean purple seed stain. *Mycological Progress* **16**: 593–603.
- Hesami S, Khodaparast S, Zare R (2012). New reports on *Cercospora* and *Pseudocercospora* from Guilan province. *Rostaniha* **13**: 95–100.
- Katoh K, Standley DM (2013). MAFFT multiple sequence alignment software version 7: improvements in performance and usability. *Molecular Biology and Evolution* **30**: 772–780.
- Kaufman SR, Kaufman W (2013). Invasive plants: guide to identification and the impacts and control of common North American species. Stackpole Books.
- Kearse M, Moir R, Wilson A, *et al.* (2012). Geneious Basic: an integrated and extendable desktop software platform for the organization and analysis of sequence data. *Bioinformatics* **28**: 1647–1649.
- Kimber RBE, Paull JG (2011). Identification and genetics of resistance to *Cercospora* leaf spot (*Cercospora zonata*) in faba bean (*Vicia faba*). *Euphytica* **177**: 419–429.
- Kushalappa AC, Boivin G, Brodeur L (1989). Forecasting incidence thresholds of *Cercospora* blight in carrots to initiate fungicide application. *Plant Disease* **73**: 979–983.
- Maddison WP, Maddison DR (2011). Mesquite: a modular system for evolutionary analysis. Version 2.75. <http://mesquiteproject.org>.
- Myllys L, Stenroos S, Thell A (2002). New genes for phylogenetic studies of lichenized fungi: glyceraldehyde-3-phosphate dehydrogenase and beta-tubulin genes. *Lichenologist* **34**: 237–246.
- Nguanhom J, Cheewangkoon R, Groenewald JZ, *et al.* (2015). Taxonomy and phylogeny of *Cercospora* spp. from Northern Thailand. *Phytotaxa* **233**: 27–48.
- Nylander JAA (2004). *MrModeltest. Version 2.0*. Program distributed by the author. Evolutionary Biology Centre, Uppsala University, Uppsala, Sweden.
- Pirnia M, Zare R, Zamanizadeh HR, *et al.* (2012). New records of cercosporoid hyphomycetes from Iran. *Mycotaxon* **120**: 157–169.
- Qian X, Gu J, Pan HJ, *et al.* (2015). Effects of living mulches on the soil nutrient contents, enzyme activities, and bacterial community diversities of apple orchard soils. *European Journal of Soil Biology* **70**: 23–30.
- Quaedvlieg W, Binder M, Groenewald JZ, *et al.* (2014). Introducing the Consolidated Species Concept to resolve species in the *Teratosphaeriaceae*. *Persoonia* **33**: 1–40.
- Randall JM, Marinelli J (1996). Invasive plants: weeds of the global garden (Vol. 149). Brooklyn Botanic Garden.
- Rannala B, Yang Z (1996). Probability distribution of molecular evolutionary trees: a new method of phylogenetic inference. *Journal of Molecular Evolution* **43**: 304–311.
- Rayner RW (1970). A Mycological Colour Chart. Kew, UK: Commonwealth Mycological Institute.
- Roland AE (1998). *Roland's Flora of Nova Scotia, 3rd edition*. Nimbus Publishing Ltd. and Nova Scotia Museum, Halifax, Nova Scotia.
- Ronquist F, Teslenko M, van der Mark P, *et al.* (2012). MrBayes 3.2: efficient Bayesian phylogenetic inference and model choice across a large model space. *Systematic Biology* **61**: 539–542.
- Soares APG, Guillin EA, Borges LL, *et al.* (2015). More *Cercospora* species infect soybeans across the Americas than meets the eye. *PloS One* **10**: e0133495.
- Tamura K, Stecher G, Peterson D, *et al.* (2013). MEGA6: Molecular Evolutionary Genetics Analysis Version 6.0. *Molecular Biology and Evolution* **30**: 2725–2729.
- Weiland J, Koch G (2004). Sugarbeet leaf spot disease (*Cercospora beticola* Sacc.). *Molecular Plant Pathology* **5**: 157–166.
- Zheng W, Li Y, Gong Q, *et al.* (2017). Improving yield and water use efficiency of apple trees through intercrop-mulch of crown vetch (*Coronilla varia* L.) combined with different fertilizer treatments in the Loess Plateau. *Spanish Journal of Agricultural Research* **14**: 1207.

doi.org/10.3114/fuse.2019.03.09

Blastacervulus metrosideri sp. nov. leaf spot on *Metrosideros excelsa* in New Zealand

P.R. Johnston¹*, D. Park¹

¹Manaaki Whenua Landcare Research, Private Bag 92170, Auckland 1142, New Zealand

*Corresponding author: johnstonp@landcareresearch.co.nz

Key words:

Alysidiella
Asterinaceae
Aulographina eucalypti
chocolate spot
pohutukawa

Abstract: A leaf-spotting fungal pathogen common on *Metrosideros excelsa* in New Zealand is described here as *Blastacervulus metrosideri* sp. nov. It has previously been identified in the New Zealand literature as *Leptomelanconium* sp. and as *Staninwardia breviuscula*. The choice of genus for this new species is supported by a phylogeny based on ITS and LSU sequences. It is phylogenetically close to several morphologically similar *Eucalyptus* leaf spotting pathogens.

Effectively published online: 15 March 2019.

INTRODUCTION

A leaf-spotting fungus common on *Metrosideros excelsa* (pohutukawa, *Myrtaceae*) in New Zealand is morphologically similar to a number of leaf-spotting fungi on another myrtaceous host, *Eucalyptus*. These fungi on *Eucalyptus* leaves have been placed in a range of genera, including *Alysidiella*, *Blastacervulus*, and *Staninwardia* (Swart 1988, Sutton 1971, Summerell *et al.* 2006, Cheewangkoon *et al.* 2012), and collectively the diseases they cause on *Eucalyptus* have sometimes been referred to as chocolate spot (e.g. Cheewangkoon *et al.* 2012; Crous *et al.* 2016).

Cheewangkoon *et al.* (2012) presented a phylogeny that resolves a clade of closely-related species of *Eucalyptus* chocolate-spot leaf pathogens that they refer to the genera *Blastacervulus*, *Alysidiella* and *Aulographina*. These taxa form a well-resolved clade, and were placed in the *Asterinaceae* by Giraldo *et al.* (2017). Species in the genera *Alysidiella* and *Blastacervulus* have a similar morphology. They share acervular conidiomata with dry, powdery masses of conidia, the 0–3-septate conidia having thick, verruculate, brown to pale brown walls, base truncate, the conidiogenous cells with a broad conidiogenous locus, sometimes with annellate thickenings. The species accepted by Summerell *et al.* (2006) and Cheewangkoon *et al.* (2012) were distinguished genetically and by differences in conidial size. Crous (2016) later described another genetically similar *Eucalyptus* leaf spotting pathogen as *Blastacervulus eucalyptorum*. *Aulographina* was represented by DNA sequences from the culture CPC 12986 that Cheewangkoon *et al.* (2012) and Giraldo *et al.* (2017) accepted as *A. eucalypti*. *Aulographina eucalypti* differs morphologically from the other chocolate spot pathogens treated by Cheewangkoon *et al.* (2012) in forming a sexual morph and a putatively spermatial asexual morph (Swart 1988, Wall & Keane 1984), and in lacking the acervular conidial morph so distinctive of the other species in this clade. Although the sexual morph of *A. eucalypti* is morphologically typical of *Asterinaceae*, the lack of an acervular asexual morph means that

it would be useful to confirm its genetic characterisation with additional specimens.

Staninwardia was first described by Sutton (1971), based on *S. breviuscula*, a *Eucalyptus*-associated fungus from Mauritius that is morphologically similar to the chocolate spot pathogens. Summerell *et al.* (2006) described a second species, *S. suttonii*, on *Eucalyptus* from Australia. Based on DNA sequencing from an ex-type culture of *S. suttonii*, Quaedvlieg *et al.* (2014) place *Staninwardia* in their new family *Extremaceae* (*Capnodiales*), genetically distant from the chocolate spot species of *Alysidiella* and *Blastacervulus* treated by Summerell *et al.* (2006) and Cheewangkoon *et al.* (2012). Another species with similar morphology and associated with similar symptoms on *Eucalyptus* was described by Sutton (1974) as *Leptomelanconium australiense*. Crous *et al.* (2009) recombined it as *Teratosphaeria australiensis*, and Taylor *et al.* (2012) selected an epitype for this species, which again proved to be genetically distant to the chocolate spot species of Cheewangkoon *et al.* (2012).

The New Zealand *Metrosideros* leaf-spotting pathogen was identified tentatively as *Leptomelanconium* sp. by McKenzie *et al.* (1999) and as *Staninwardia breviuscula* by Gadgil & Dick (2006). A record of *S. breviuscula* on *Metrosideros umbellata* may represent the same fungus (Bain 2007), although because of the host difference, this should be confirmed genetically. Based on DNA sequences from a recently obtained culture of the *Metrosideros* pathogen, we describe it here as a new species of *Blastacervulus*.

MATERIALS AND METHODS

Conidia from the fresh collection subsequently dried and stored as fungarium specimen PDD 108694 were suspended in streptomycin solution and streaked across a water agar plate. After 24 h germinating conidia were removed and transferred to 2 % Difco potato dextrose agar (PDA) plates. The cultures had a consistent macromorphological appearance and one was

later selected and stored as ICMP 21883. DNA was extracted from mycelium from this culture, and ITS and LSU sequences generated following the methods of Johnston & Park (2013). The sequences were aligned with *Alysidiella*, *Blastacervulus* and *Aulographina* ITS and LSU sequences from Cheewangkoon *et al.* (2012), *Blastacervulus eucalyptorum* from Crous *et al.* (2016), *B. eucalypti* from Cheewangkoon *et al.* (2009) and additional *Asterinaceae* LSU sequences selected from sister clades in the Giraldo *et al.* (2017) phylogeny, with *Venturia populina* as the outgroup (Table 1). For taxa with both ITS and LSU sequences available, the sequences were concatenated, an alignment carried out using MAFFT v. 1.3.7 as implemented in Geneious R10 (Kearse *et al.* 2012), and a ML phylogenetic tree generated using PhyML v. 3.2.2 (Guindon *et al.* 2010) with the GTR model as implemented in Geneious R10, with support values estimated using 1 000 bootstrap replicates.

Dried specimens were rehydrated using 3% KOH, conidia and conidiogenous cells examined in 3% KOH in squash mounts, and the excised acervuli sectioned at about 10 µm thickness using a freezing microtome and the sections mounted in lactic acid.

RESULTS

Based on the taxa and genes sampled, there is no clear genetic difference that can be used to distinguish *Alysidiella* from *Blastacervulus* (Fig. 1). Based on published descriptions, species in the two genera are also very similar morphologically (Swart 1988, Summerell *et al.* 2006, Crous *et al.* 2016). We have chosen to refer our new species to the older genus *Blastacervulus*.

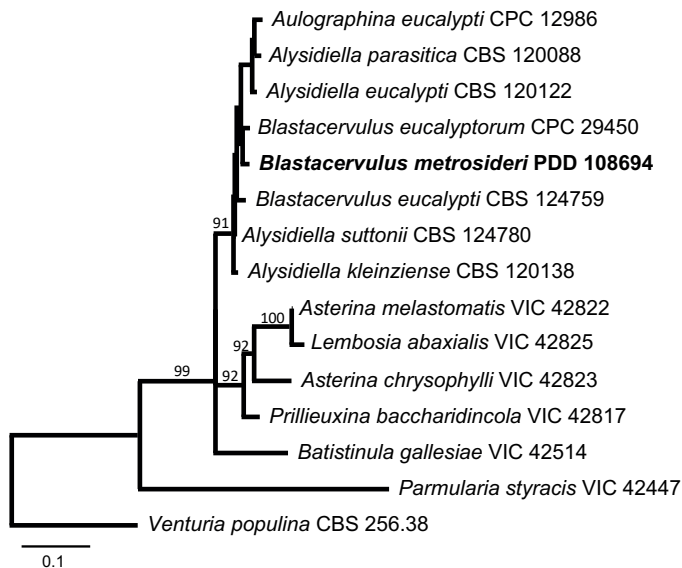


Fig. 1. PhyML maximum likelihood tree based on concatenated ITS and LSU sequences. Bootstrap support values are provided where greater than 90%. The novel species described here is indicated in bold text.

Blastacervulus metrosideri P.R. Johnst. sp. nov.

Mycobank MB829588. Fig. 2.

Etymology: Refers to the host plant.

Diagnosis: Differs from the type species *Blastacervulus eucalypti* in host preference and conidial size and shape.

Typus: **New Zealand**, Auckland, Glen Innes, Auckland University Tamaki Campus, on living leaves of *Metrosideros excelsa* (*Myrtaceae*), 5 Oct. 2017, P.R. Johnston (**holotype** PDD 108694; ex-type culture ICMP 21883).

Leaf spots on upper surface of living leaves, initially red-brown with narrow yellow margin, becoming darker, almost black with age, round, up to 4 mm diam. Discolouration of the spots sometimes extending through to the lower leaf surface. Apart from the cells associated with the acervuli, fungal tissue is sparse within the leaf, forming a narrow plate of hyaline, thin-walled hyphae about 3–5 µm diam between the cuticle and epidermis. Little or no fungal hyphae is present more deeply in the leaf. The colour of the spots is associated with deposition of tannins or other compounds within the intact epidermal and palisade cells of the host. **Acervuli** develop within the spots on the upper leaf surface, 0.1–0.3 mm diam, upper wall black, breaking open irregularly to expose the black, powdery conidial mass. In vertical section acervuli develop between the cuticle and the epidermal cells, with the upper and lower walls comprising 2–3 rows of angular cells 4–7(–10) µm diam. **Conidiogenous cells** line the inside of both the upper and lower walls, solitary, 6–8 × 4–5 µm, cylindrical, conidiogenous locus broad, apical, often with several thickened and slightly flaring annellations. **Conidia** cylindrical, base truncate, apex broadly rounded, 1–3(–9)-septate, 1-septate 8–10 µm long, 2-septate 10–14 (–18) µm long, 3-septate 13–16 (–19) µm long, 4-septate 16–19 µm long, 9-septate up to 33 µm long × 3.5–6 µm wide, walls thickened, dark brown, finely verruculate.

Culture characteristics: Cultures on PDA about 15–25 mm diam after 20 wk. Margin of colony uneven, surface black, convoluted, lumpy and cracked, finely felted, brown pigment diffusing into agar. Cells in the mycelium near the edge of the colony starting to become swollen and to develop thick and dark walls, cells in the older parts of the colony almost all short, broad-cylindric, with walls thick, dark, smooth, hyphae partly disarticulating.

Additional materials examined: **New Zealand**, Auckland, Leigh, on *Metrosideros excelsa*, 30 Mar. 1924, E.G. Bollard, (PDD 43314); Te Henga, on *M. excelsa*, 25 Mar. 1949, J.M. Dingley (PDD 15909); Titirangi Beach, on *M. excelsa*, 3 Dec. 1963, F.J. Morton & J.D. Read (PDD 30158); Langholm, on *M. excelsa*, 3 Dec. 1963, F.J. Morton & J.D. Read (PDD 30159); Auckland City, Mt Albert Rd, on *M. excelsa*, Feb. 1994, P.R. Johnston (PDD 64252); Glen Innes, Auckland University Tamaki Campus, on *M. excelsa*, 5 Oct. 2016, P.R. Johnston (PDD 108727); Glen Innes, Colin Maiden Park, on *M. excelsa*, 23 Jan. 2019, P.R. Johnston (PDD 116628); Coromandel: Port Charles, between wharf and Big Sandy Bay, on *M. excelsa*, 26 Mar. 1989, P.R. Johnston (PDD 55197); Port Charles, on *M. excelsa*, 28 Mar. 1993, P.R. Johnston (PDD 62168); Port Charles, Little Sandy Bay, on *M. excelsa*, Nov. 1993, P.R. Johnston & E.M. Gibellini (PDD 64249); Port Charles, Big Sandy Bay, on *M. excelsa*, 29 Dec. 1993, P.R. Johnston & E.M. Gibellini (PDD 64236); Port Charles, Big Sandy Bay, on *M. excelsa*, 24 Oct. 1994, P.R. Johnston & E.M. Gibellini (PDD 64251); Northland: Bay of Islands, Black Rocks off Moturoa, north west islet of Crater Rim group, on *M. excelsa*, 23 Jan. 1990, R.E. Beever (PDD 56841); Westland: Hokitika, Hokitika Hospital, on *M. umbellata* cultivated plant, 22 May 2007, B.H. Doherty (NZFS 5422).

Notes: Symptoms that match those associated with *Blastacervulus metrosideri* are very common on *Metrosideros excelsa* wherever it grows in New Zealand. The literature cited in

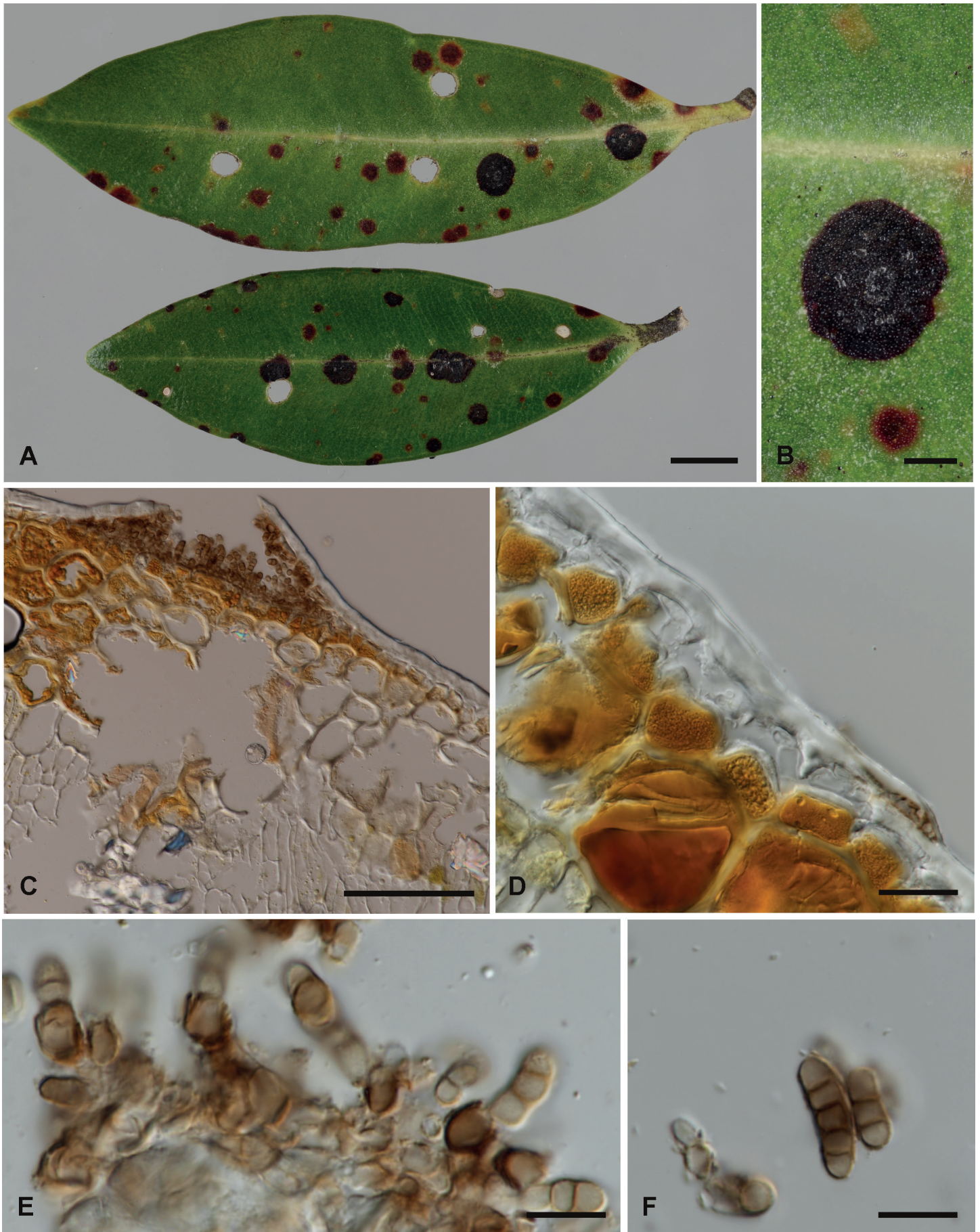


Fig. 2. *Blastacervulus metrosideri*. **A.** Immature and mature spots on *Metrosideros excelsa* leaf. **B.** Detail of one of the mature spots, with several individual erumpent acervuli. **C.** Acervulus in vertical section. **D.** Leaf in vertical section with incipient acervulus, apart from the dark-walled cells of the acervulus, fungal tissue restricted to a single layer of hyaline cells beneath the cuticle. **E.** Conidiogenous cells. **F.** Conidiogenous cell and released conidia. A, B, E, F — PDD 116628; C, D — PDD 108694. Scale bars: A = 5 mm; B = 1 mm; C = 100 μ m; D = 20 μ m; E, F = 10 μ m.

Table 1. Specimens and GenBank accession numbers of sequences used for the phylogeny in Fig. 1.

Species	Voucher	Country, Collector	Host	Reference	ITS	LSU
<i>Alysiidiella eucalypti</i>	CBS 120122	Uruguay, M.J. Wingfield	<i>Eucalyptus dunnii</i>	Crous <i>et al.</i> (2006)	DQ885893	DQ885893
<i>Alysiidiella kleinzii</i>	CBS 120138	South Africa, Z.A. Pretorius	<i>Eucalyptus</i> sp.	Crous <i>et al.</i> (2007a)	EF110616	EF110616
<i>Alysiidiella parasitica</i>	CBS 120088	South Africa, P.W. Crous	<i>Eucalyptus</i> sp.	Crous <i>et al.</i> (2007a)	DQ923525	DQ923525
<i>Alysiidiella suttonii</i>	CBS 124780	Cyprus, A. van Iperen	<i>Eucalyptus</i> sp.	Cheewangkoon <i>et al.</i> (2012)	HM628774	HM628777
<i>Asterina chrysophylli</i>	VIC 42823	Brazil, A.L. Firmino	<i>Henriettea succosa</i>	Guatimosim <i>et al.</i> (2015)	—	KP143738
<i>Asterina melastomatis</i>	VIC 42822	Brazil, A.L. Firmino	<i>Miconia</i> sp.	Guatimosim <i>et al.</i> (2015)	—	KP143739
<i>Aulographina eucalypti</i>	CPC 12986	Australia, A. Carnegie	<i>Eucalyptus cloeziana</i>	Cheewangkoon <i>et al.</i> (2012)	HM535599	HM535600
<i>Batistinula galleisiae</i>	VIC 42514	Brazil, A.L. Firmino <i>et al.</i>	<i>Caesalpinia echinata</i>	Guatimosim <i>et al.</i> (2015)	—	KP143736
<i>Blastacervulus eucalypti</i>	CBS 124759	Australia, B.A. Summerell	<i>Eucalyptus robertsonii</i>	Cheewangkoon <i>et al.</i> (2009)	GQ303271	GQ303302
<i>Blastacervulus eucalyptorum</i>	CPC 29450	Australia, P.W. Crous	<i>Eucalyptus decipiens</i>	Crous <i>et al.</i> (2013)	KY173390	KY173484
<i>Blastacervulus metrosideri</i>	ICMP 21883	New Zealand, P.R. Johnston	<i>Metrosideros excelsa</i>	This paper	MK547091	MK547100
<i>Lembosia abaxialis</i>	VIC 42825	Brazil, A.L. Firmino	<i>Miconia jucunda</i>	Guatimosim <i>et al.</i> (2015)	—	KP143737
<i>Parmularia styracis</i>	VIC 42447	Brazil, R.W. Barreto	<i>Styrax ferrugineus</i>	Guatimosim <i>et al.</i> (2015)	—	KP143728
<i>Prillieuxina baccharidinicola</i>	VIC 42817	Brazil, O.L. Pereira	<i>Baccharis</i> sp.	Guatimosim <i>et al.</i> (2015)	—	KP143735
<i>Venturia populina</i>	CBS 256.38, IMI 163996	Italy, E.J.H. Nijhaf	<i>Populus x canadensis</i>	Crous <i>et al.</i> (2007b), Schoch <i>et al.</i> (2009)	EU035467	GU323212

the Introduction shows that *Eucalyptus* has several superficially similar leaf-spotting fungi, and more intensive study of the *M. excelsa* associated fungi may reveal a greater diversity of species than currently recognised. For example, *Teratosphaeria* spp. were commonly detected from environmental DNA sequences from *M. excelsa* leaves (unpubl. data), and the symptoms caused by *Teratosphaeria australiensis* are similar to those associated with *B. metrosideri* (Sutton 1974, as *Leptomelanconium australiense*; Taylor *et al.* 2012). Commonly, the blastacervulus-like spots seen in the field are sterile, making a definitive identification based on morphology impossible.

The single, small specimen on *Metrosideros umbellata* (NZFS 5422) has markedly paler spots than those on *M. excelsa* and its acervuli are smaller. Microscopically, this specimen appears to match those from *M. excelsa*. Additional specimens are needed to determine whether the macroscopic differences are consistent, and DNA sequences from a specimen on *M. umbellata* would confirm whether *M. metrosideri* occurs on more than one species of *Metrosideros*.

The holotype specimen was selected because a culture and DNA sequences were derived from it, but this specimen is not large. To examine the morphology, particularly nice specimens include PDD 30158 and PDD 116628.

ACKNOWLEDGEMENTS

The New Zealand Department of Conservation are thanked for providing permits to allow the collection of the fungi reported here.

The curator of the SCION National Forest Mycological Herbarium kindly provided specimen NZFS 5422 on loan. This research was supported through the Manaaki Whenua – Landcare Research Characterising Land Biota Portfolio with funding from the Science and Innovation Group of the New Zealand Ministry of Business, Innovation and Employment.

REFERENCES

- Bain J (2007). New records. *Forest Health News* **173**: 2.
- Cheewangkoon R, Groenewald JZ, Summerell BA, *et al.* (2009). *Myrtaceae*, a cache of fungal biodiversity. *Persoonia* **23**: 55–85.
- Cheewangkoon R, Groenewald JZ, Hyde KD, *et al.* (2012). Chocolate spot disease of *Eucalyptus*. *Mycological Progress* **11**: 61–69.
- Crous PW, Groenewald JZ, Wingfield MJ (2006). *Heteroconium eucalypti*. Fungal Planet, no. 10. Westerdijk Fungal Biodiversity Institute, Utrecht, the Netherlands.
- Crous PW, Mohammed C, Glen M, *et al.* (2007a). *Eucalyptus* microfungi known from culture. 3. *Eucasphaeria* and *Sympoventuria* genera nova, and new species of *Furcasporea*, *Harknessia*, *Heteroconium* and *Phacidiella*. *Fungal Diversity* **25**: 19–36.
- Crous PW, Schubert K, Braun U, *et al.* (2007b). Opportunistic, human-pathogenic species in the *Herpotrichiellaceae* are phenotypically similar to saprobic or phytopathogenic species in the *Venturiaceae*. *Studies in Mycology* **58**: 185–217.
- Crous PW, Summerell BA, Carnegie AJ, *et al.* (2009) Unravelling *Mycosphaerella*: do you believe in genera? *Persoonia* **23**: 99–118
- Crous PW, Wingfield MJ, Guarro J, *et al.* (2013.) Fungal Planet description sheets: 154–213. *Persoonia* **31**: 188–296.

- Crous PW, Wingfield MJ, Burgess TI, *et al.* (2016). Fungal Planet description sheets: 469–557. *Persoonia* **37**: 218–403.
- Gadgil D, Dick MA (2006). Fungi silvicolae novazelandiae 6. *New Zealand Journal of Forestry Science* **36**: 3–10.
- Guatimosim E, Firmino AL, Bezerra JL, *et al.* (2015). Towards a phylogenetic reappraisal of *Parmulariaceae* and *Asterinaceae* (*Dothideomycetes*). *Persoonia* **35**: 230–241.
- Guindon S, Dufayard JF, Lefort V, *et al.* (2010). New algorithms and methods to estimate maximum-likelihood phylogenies: assessing the performance of PhyML 3.0. *Systematic Biology* **59**: 307–321.
- Johnston PR, Park D (2013). The phylogenetic position of *Lanzia berggrenii* and its sister species. *Mycosystema* **32**: 366–385.
- Kearse M, Moir R, Wilson A, *et al.* (2012). Geneious Basic: an integrated and extendable desktop software platform for the organization and analysis of sequence data. *Bioinformatics* **28**: 1647–1649.
- Quaedvlieg W, Binder M, Groenewald JZ, *et al.* (2014). Introducing the Consolidated Species Concept to resolve species in the *Teratosphaeriaceae*. *Persoonia* **33**: 1–40.
- Schoch CL, Crous PW, Groenewald JZ, *et al.* (2009). A class-wide phylogenetic assessment of *Dothideomycetes*. *Studies in Mycology* **64**: 1–15.
- Summerell BA, Groenewald JZ, Carnegie AJ, *et al.* (2006). *Eucalyptus* microfungi known from culture. 2. *Alysidiella*, *Fusculina* and *Phlogicylindrium* genera nova, with notes on some other poorly known taxa. *Fungal Diversity* **23**: 323–350.
- Sutton BC (1971). *Staninwardia* gen. nov. (*Melanconiales*) on *Eucalyptus*. *Transactions of the British Mycological Society* **57**: 539–542.
- Sutton BC (1974). Miscellaneous Colelomycetes on *Eucalyptus*. *Nova Hedwigia* **25**: 161–172.
- Swart HJ (1988). Australian leaf-inhabiting fungi XXVI. Some noteworthy coelomycetes on *Eucalyptus*. *Transactions of the British Mycological Society* **90**: 279–291.
- Taylor K, Andjic V, Barber PA, *et al.* (2012). New species of *Teratosphaeria* associated with leaf diseases on *Corymbia calophylla* (Marri). *Mycological Progress* **11**: 159–169.
- Wall E, Keane PJ (1984). Leaf spot of *Eucalyptus* caused by *Aulographina eucalypti*. *Transactions of the British Mycological Society* **82**: 257–273.

doi.org/10.3114/fuse.2019.03.10

Revisiting *Salisapiliaceae*

R.M. Bennett^{1,2}, M. Thines^{1,2,3*}

¹Senckenberg Biodiversity and Climate Research Centre (SBik-F), Senckenberganlage 25, 60325 Frankfurt am Main, Germany

²Department of Biological Sciences, Institute of Ecology, Evolution and Diversity, Goethe University Frankfurt am Main, Max-von-Laue-Str. 9, 60438, Frankfurt am Main, Germany

³Integrative Fungal Research Cluster (IPF), Georg-Voight-Str. 14-16, 60325 Frankfurt am Main, Germany

*Corresponding author: m.thines@thines-lab.eu

Key words:

Estuarine oomycetes
Halophytophthora
mangroves
new taxa
phylogeny
Salisapilia

Abstract: Of the diverse lineages of the Phylum *Oomycota*, saprotrophic oomycetes from the salt marsh and mangrove habitats are still understudied, despite their ecological importance. *Salisapiliaceae*, a monophyletic and monogeneric taxon of the marine and estuarine oomycetes, was introduced to accommodate species with a protruding hyaline apical plug, small hyphal diameter and lack of vesicle formation during zoospore release. At the time of description of *Salisapilia*, only few species of *Halophytophthora*, an ecologically similar, phylogenetically heterogeneous genus from which *Salisapilia* was segregated, were included. In this study, a revision of the genus *Salisapilia* is presented, and five new combinations (*S. bahamensis*, *S. elongata*, *S. epistomia*, *S. masteri*, and *S. mycoparasitica*) and one new species (*S. coffeyi*) are proposed. Further, the species description of *S. nakagirii* is emended for some exceptional morphological and developmental characteristics. A key to the genus *Salisapilia* is provided and its generic circumscription and character evolution in cultivable *Peronosporales* are discussed.

Effectively published online: 22 March 2019.

INTRODUCTION

The Phylum *Oomycota* is a monophyletic group of fungal-like eukaryotes of the Kingdom *Straminipila* (Beakes & Thines 2017). Members of this group are saprotrophs, pathogens, or parasites of various plant and animal species in both aquatic and terrestrial environments. Habitats in which oomycetes seem to play a major role are the mangrove and salt marshes (Marano *et al.* 2016). Fallen senescent leaves of mangrove and salt marsh plants have proven to be rich in oomycete decomposers, which were originally subsumed as estuarine or marine *Phytophthora* (Fell & Master 1975, Pegg & Alcorn 1982, Nakagiri *et al.* 1989). Based on their environmental preference, they were later assigned to a morphologically diverse genus of their own, *Halophytophthora* (Ho & Jong 1990).

Halophytophthora was found to be polyphyletic on the basis of phylogenetic studies (Hulvey *et al.* 2010, Lara & Belbahri 2011). Based on recent phylogenetic analyses, there are only five known species of the *Halophytophthora s. str.*, namely *H. vesicula* (the type species of the genus), *H. avicenniae*, *H. batemanensis*, *H. polymorphica* (Hulvey *et al.* 2010, Lara & Belbahri 2011, Nigrelli & Thines 2013, Marano *et al.* 2014, Thines 2014), and the freshwater isolate, *H. fluviatilis* (Yang & Hong 2014) – the only known congener to date which was isolated from a freshwater biome. A few species of *Halophytophthora* were transferred to *Phytopythium* (*Phytopythium kandeliae*, basionym: *H. kandeliae*) (Thines 2014), and *Salispina* (*Salispina lobata*, basionym: *Phytophthora spinosa* var. *lobata*, and *Salispina spinosa*, basionym: *Phytophthora spinosa* var. *spinosa*) (Li *et al.* 2016); whereas some species were either

associated with *Phytophthora* or *Salisapilia*, or are forming separate lineages (Li *et al.* 2016, Marano *et al.* 2014, Jung *et al.* 2017).

The genus *Salisapilia*, which type species, *Salisapilia sapeloensis*, was isolated from *Spartina alterniflora*, was described based on the following features contrasting to *Halophytophthora*: a small hyphal diameter, the formation of an apical or protruding hyaline plug, the absence of an evanescent or persistent vesicle during zoospore release, and homothallism. However, *Salisapilia nakagirii*, a homothallic species described by Hulvey *et al.* (2010), did not develop sporangia under the cultivation conditions applied, so the description of this species was based only on the morphology of gametangia and its phylogenetic placement within *Salisapiliaceae*. However, Hulvey *et al.* (2010) included only a small fraction of the species described in *Halophytophthora* in their dataset. Thus, it cannot be ruled out that several lineages not strongly supported as nested within *Halophytophthora* (Lara & Belbahri 2011) represent members of the genus *Salisapilia*. It was the aim of this study to close this knowledge gap by detailed phylogenetic and morphological analyses.

MATERIALS AND METHODS

Acquisition of strains and sporulation

Ex-type strains of *Halophytophthora* and *Salisapilia* were either acquired from NBRC in Japan or the Westerdijk Fungal Biodiversity Institute (formerly CBS-KNAW) in the Netherlands. Strains were

cultivated and maintained on clarified-vegetable juice agar (VJA) (Medium No. 15 NBRC, using Alnatura Gemüsesaft or Campbell V8 Juice) (<http://www.nite.go.jp/en/nbrc/cultures/media/culture-list-e.html>) with or without antibiotics: Nystatin (500 mg/mL), as well as Rifampicin (30 mg/mL) or Streptomycin (0.5 mg/mL).

All strains used in this study were tested for sporulation in saline solution at 0, 10, 20 and 30 promille (w/v) from 3–7-d-old cultures in 60 mm Petri plates. Plates were incubated in the dark at room temperature for 18–24 h or until sporangia were formed. Morphological characteristics were observed using a Motic AE31 trinocular inverted microscope (Motic, Wetzlar, Germany) and photos were taken using a Canon Digital Camera EOS 500D (Canon, Tokyo, Japan). Isolates were also grown on agarised media: Potato Carrot Agar (PCA), Peptone Yeast Glucose Agar (PYGA) and Potato Dextrose Agar (PDA) at room temperature (~20–25 °C) (Crous *et al.* 2009).

DNA extraction, PCR, and phylogenetic reconstruction

Cultures were grown on VJA plates at room temperature in a dark compartment. After 7–10 d, mycelia were harvested and subjected to DNA extraction following the method outlined in Bennett *et al.* (2017a). Extracted genomic DNA for all samples was amplified by PCR for the internal transcribed spacers (ITS), and the large nuclear ribosomal subunit (LSU). The primers ITS1-O (Bachofer 2004) and LR0 (Moncalvo *et al.* 1995) were used for the ITS region, while LR0R (Moncalvo *et al.* 1995) and LR6-O (Riethmüller *et al.* 2002) were used for the LSU region.

The 25 µL PCR reaction mixes contained 1× PCR Buffer, 0.2 mM dNTPs, 2.0 mM MgCl₂, 0.8 µg bovine serum albumin, 0.4 µM of each primer, 0.5 U *Taq* polymerase and 10–50 ng of DNA. Cycling conditions for the ITS included an initial denaturation at 94 °C for 4 min, followed by 36 cycles of denaturation at 94 °C for 40 s, annealing at 55 °C for 20 s, and elongation at 72 °C for 60 s; and a final elongation at 72 °C for 4 min. For the LSU region, initial denaturation was set at 95 °C for 2 min, followed by 35 cycles of denaturation at 95 °C for 20 s, annealing at 53 °C for 20 s, and elongation at 72 °C for 2 min; and a final elongation at 72 °C for 7 min. All amplification reactions were carried out in an Eppendorf Mastercycler Pro equipped with a vapoprotect lid (Eppendorf AG, Hamburg, Germany).

PCR amplicons were sequenced by the laboratory centre of the Senckenberg Biodiversity and Climate Research Centre (SBIK-F, Frankfurt am Main, Germany) using the primer used in PCR. Sequences were analysed, assembled into contigs, and edited using Geneious v. 5.0.4 (Biomatters Ltd., USA). Edited contigs in FASTA format and ex-type sequences from the NCBI (<https://www.ncbi.nlm.nih.gov/nucleotide>) and the *Phytophthora* database (<http://www.phytophthoradb.org/>) (Table S1) were uploaded to the TrEase webserver (<http://www.thines-lab.senckenberg.de/trease/>) for multiple sequence alignment using MAFFT, version 7 (Katoh *et al.* 2002). A primary phylogenetic tree computation using Minimum Evolution (ME) was generated using FastTree, version 1 (Price *et al.* 2009) as implemented on the TrEase webserver following the Generalized Time-Reversible (GTR) algorithm and 1 000 bootstrap replicates. Maximum Likelihood (ML) inference was done as the secondary tree using the FastTree, version 2 (Price *et al.* 2010) with the GTR algorithm model and 1 000 bootstrap replicates. A third phylogenetic reconstruction was done using Bayesian Inference (BI) as implemented in the TrEase webserver using MrBayes,

version 3.2 (Ronquist *et al.* 2012). For Bayesian analysis the 6-GTR substitution model was used and 1 M generations were run, with trees sampled at every 10 000th generation, discarding the first 30 % of the sampled trees to ensure sampling always reached the stationary phase. After checking that there were no supported conflicts between the datasets, alignments of each locus were concatenated into a single alignment file using SequenceMatrix (Vaidya *et al.* 2010) and phylogenetic trees of concatenated alignments were generated following the above-mentioned protocols. Phylogenetic trees were viewed using MEGA v. 6 or 7 (Tamura *et al.* 2013).

Ancestral state reconstruction for papilla and hyaline apical plug

The ancestral state reconstruction of the papilla and the hyaline apical plug was done using observed or recorded characteristics for *Halophytophthora* (Anastasiou & Churchland 1969, Gerretson-Cornel & Simpson 1984), *Salisapilia* (Table 1), and other members of *Peronosporaceae* (e.g. *Phytophthora*, *Phytopythium*, and *Pythium*) (van der Plaats-Niterink 1981, de Cock *et al.* 1987, Paul 1987, Erwin & Ribeiro 1996, Paul *et al.* 1999, Paul 2000, Nechwatal & Oßwald 2003, Uzuhashi *et al.* 2010, Kroon *et al.* 2012, de Cock *et al.* 2015). The traits were mapped on the Bayesian phylogeny of the concatenated dataset using Mesquite v. 3.2, and the likelihood ancestral reconstruction algorithm (Maddison & Maddison 2018) was run using the following character data: (0) Papilla (P) forming an apical plug (AP); (1) P not forming an AP; (2) Semi-papilla (SP) forming an AP; (3) SP not forming an AP; (4) Non-papillate; and, “?” when sporangial germination was neither reported nor observed.

RESULTS

Phylogenetic reconstructions

According to the phylogeny based on concatenated sequences of ITS and LSU in this study (Fig. 1), strains *Halophytophthora bahamensis* NBRC 32556 (Fig. 2), the strain NBRC 32557 (Fig. 4), which was named as *H. bahamensis*, but is not conspecific with the ex-type strain, *H. elongata* NBRC 100786 (Fig. 3), *H. epistomia* NBRC 32617 (Fig. 5), *H. masteri* NBRC 32604 (Fig. 6), and *H. mycoparasitica* NBRC 32966 (= NBRC 32967) (Fig. 7) clustered with other members of the *Salisapiliaceae* with strong to maximum support (Fig. 1). Further, these strains were distinct from *S. nakagirii* LT6456 (= CBS 127947) (Fig. 8), *S. sapeloensis* LT6440 (= CBS 127946) (Fig. 9), and *S. tartarea* CBS 208.95 (Fig. 10).

Morphology

Halophytophthora bahamensis NBRC 32556 (Fig. 2E–F), *H. elongata* NBRC 100786 (Fig. 4C–D), *H. epistomia* NBRC 32617 (Fig. 5E–F), *H. masteri* NBRC 32604 (Fig. 6C–D), and *H. mycoparasitica* NBRC 32966 (= NBRC 32967) (Fig. 7E–F), were all forming a distinct hyaline apical plug at the apex of the discharge tube similar to *S. sapeloensis* CBS 127946 (Fig. 9E) and *S. tartarea* CBS 208.95 (Fig. 10E–F). The apical hyaline plug was indistinct in *S. nakagirii* CBS 127947 (Fig. 8F–G). The shape of sporangia varied among species. The mode of zoospore release was either directly through a discharge tube or by the formation

Table 1. Morphological comparison of *Salisapilia* spp. Measurements for sporangia are given as (min.–)average_{minus}_SD–SD–average_{plus}_SD(–max.).

Structure	<i>S. sapeloensis</i> (Hulvey <i>et al.</i> 2010)	<i>S. coffeyi</i> (This study)	<i>S. bahamensis</i> (Fell & Master 1975)	<i>S. elongata</i> (Ho <i>et al.</i> 2003)	<i>S. epistomia</i> (Fell & Master 1975, Ho <i>et al.</i> 1990 ^a)	<i>S. nakagirii</i> (Hulvey <i>et al.</i> 2010, This study ^b)	<i>S. masteri</i> (Nakagiri <i>et al.</i> 1994)	<i>S. mycoparasitica</i> (Fell & Master 1975)	<i>S. tartarea</i> (Nakagiri <i>et al.</i> 1994)
Hyphal diam (µm)	1–2	1–3	1–3	3–9	2–4	1–2	2–10	2–9	1–3(–9)
Septa	Occurs at maturity	Occurs at maturity	Occurs at maturity	Occurs at maturity	Occurs at maturity	Occurs at maturity	Occurs at maturity	Develop numerous septa with age	Non-septate, or septate with age
Branching pattern	Branched or unbranched	Branched or unbranched	Branching, rare	Unbranched	Branching, rare	Branched or unbranched	Branched or unbranched	Branched or unbranched	Unbranched or branched
Sporangiogenic hyphae	Undifferentiated to vegetative hyphae	Undifferentiated to vegetative hyphae	Undifferentiated to vegetative hyphae	Undifferentiated to vegetative hyphae	Undifferentiated to vegetative hyphae	Undifferentiated to vegetative hyphae	Undifferentiated to vegetative hyphae	Undifferentiated to vegetative hyphae	Undifferentiated to vegetative hyphae
Sporangia Size (µm)	34–97 (av. 59)	44.05–107.33 × 6.51–16.92 (av. 74.01 × 10.32)	26–119 × 19–43 (av. 61 × 28) 39–97 × 14–31 (av. 68 × 23)	115–530 × 32–64	43–184 × 56–107 (av. 127.6 × 63.3)	81.5–205.25 × 32.25–113 (av. 136.88 × 66.43) ^b	26–92 × 18–91 (av. 64 × 62.6)	26–131 × 14–111 (av. 82 × 61)	20–104 × 18–96 (av. 55.6 × 47.6)
Discharge tube size (µm)	6–18	4.81–13 × 2.58–3.94 (av. 9.07 × 3.12)	3–7	-	10–51 × 9–10	6.18–18.02 × 4.3–8.7 (av. 11.95 × 6.63) ^b	5–28 × 6–10	Av. 22, tapering	10–22 × 4–8
Apical plug size (µm)	3–8, protruding	~1–3	1–2 (width)	10 × 5.6	14–90 × 9–10	Indistinct ^b	5–24 × 5–14	5–15 × 3–10	11–29 × 5–8
Surface	Smooth, partly rough	Smooth	Smooth	Smooth	Smooth	Non-smooth ^b	Smooth	Denticulate, few spines	Smooth
Vacuole	Absent	Present	Present	Absent	Absent	Absent ^b	Absent	Absent	Absent
Basal plug	Present in some, hyaline	Present, hyaline	Present, hyaline	Present, hyaline	Present, hyaline	Present, hyaline ^b	Present, hyaline	Present, hyaline	Present, hyaline
Detachment	Non-caducous	Non-caducous	Non-caducous	Non-caducous	Non-caducous	Non-caducous ^b	Non-caducous	Non-caducous	Non-caducous
Shape	Ovoid, obpyriform	Bursiform to often narrowly bursiform, obpyriform to narrowly-elongate and obclavate; Setiform appendages, absent	Highly variable, bursiform, multi-lobed, obclavate, obpyriform; Setiform appendages, present, aseptate to septate	Obovoid, obclavate, bursiform, cylindrical, elongated	Lageniform, obpyriform	Ovoid, globose, obpyriform ^b	Spherical, ovoid, obpyriform	Obnapiform	Spherical, ovoid to obpyriform

Table 1. (Continued).

Structure	<i>S. sapeloensis</i> (Hulvey <i>et al.</i> 2010)	<i>S. coffeyi</i> (This study)	<i>S. bahamensis</i> (Fell & Master 1975)	<i>S. elongata</i> (Ho <i>et al.</i> 2003)	<i>S. epistomia</i> (Fell & Master 1975, Ho <i>et al.</i> 1990 ^a)	<i>S. nakagirii</i> (Hulvey <i>et al.</i> 2010, This study ^b)	<i>S. masteri</i> (Nakagiri <i>et al.</i> 1994)	<i>S. mycoparasitica</i> (Fell & Master 1975)	<i>S. tartarea</i> (Nakagiri <i>et al.</i> 1994)
Zoospore release	Zoospores exit through the discharge tube after ejection of the apical plug	Zoospores exit through the discharge tube after ejection of the apical plug	Zoospores exit through the discharge tube after ejection of the apical plug	Zoospores exit through the discharge tube after ejection of the apical plug	Zoospores exit through the discharge tube after ejection of the apical plug	Zoospores are released in a vase-like discharge vesicle ^b	The apical plug is extruded, and a tubular vesicle is ejected. Zoospores exit through the opening	Zoospores exit through the discharge tube after ejection of the apical plug. Plug evanesces rapidly.	Zoospores exit through the discharge tube after ejection of the apical plug
Vesicle	Absent	Absent	Absent	Present, tubular	Absent	Present, vase-like ^b	Present, tubular	Absent	Absent
Oogonia									
Size (µm)	35–60, 49	Not observed	Not observed	Not observed	34–40, 37 ^a	33–48, 39	Not observed	Not observed	33–66
Surface	Smooth				Smooth ^a	Smooth			Smooth
Shape	Spherical, ovoid				Spherical ^a	Spherical			Spherical, tapered base
Oospore	Plerotic	Not observed	Not observed	Not observed	Plerotic ^a	Plerotic	Not observed	Not observed	Aplerotic
Size (µm)	28–56, 48				- ^a	28–44			24–62
Wall (µm)	2–9				4–5 ^a	1–7			3–10
Antheridia	Paragynous	Not observed	Not observed	Not observed	Paragynous ^a	Paragynous	Not observed	Not observed	Diclinous, paragynous
Size (µm)	2–9				6–24 × 2–8, 12–6 ^a	3–10			4–10
Shape	Simple, lobed or branched				- ^a	Club-shaped, lobed			Partly enwraps oogonia

- no data provided.

^a Data from Ho *et al.* (1990).

^b Characteristics of *S. nakagirii* observed in this study.

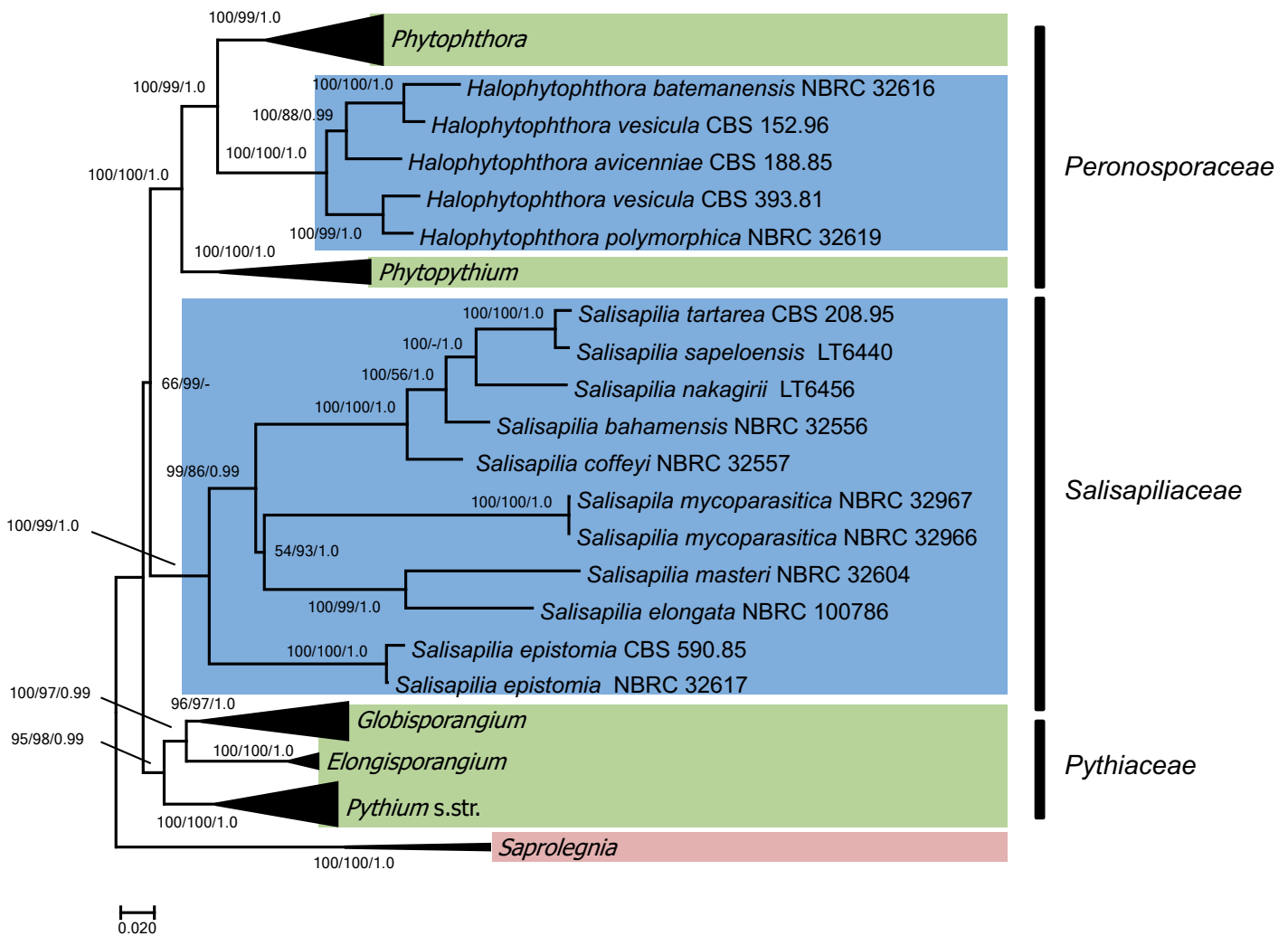


Fig. 1. Phylogenetic tree based on concatenated ITS and LSU alignments based on Minimum Evolution (ME) inference, with bootstrap support values from ME and Maximum Likelihood, as well as posterior probabilities from Bayesian Inference, in the respective order. (-) indicates support below 50 % (bootstrap) or 0.8 (posterior probability), or alternating but not strongly supported topology (support below 70 % bootstrap or 0.9 posterior probability). The scale bar indicates the number of nucleotide substitutions per site.

of an evanescent vesicle. A summary of the morphology of *Salisapilia* spp. is presented in Table 1.

The shape of sporangia of NBRC 32557 (Fig. 3E–H) was different from the ex-type culture of *H. bahamensis* (NBRC 32556) to which it had been assigned. The sporangia of the ex-type culture were bursiform, obclavate, obpyriform to highly variable and multi-lobed; whereas strain NBRC 32557 has narrowly bursiform, obpyriform to narrowly-elongated and obclavate sporangia. Variation of the shape of the sporangium was pronounced for *H. bahamensis* NBRC 32556, and some sporangia bore two discharge tubes. In contrast, NBRC 32557 always formed a single discharge tube and its sporangial shape was more stable. The strain NBRC 32557 releases its zoospore after extrusion of the small hyaline apical plug from the discharge tube. Zoospores are released directly out from the discharge pore and a vesicle was absent. After the sporangia had released zoospores, an umbonate or elevated basal plug was observed. Gametangia and chlamydospores were not observed for the strain NBRC 32557.

The ancestral trait reconstruction (Fig. 11) of the papilla and hyaline apical plug suggested that papillate and semi-papillate sporangia were putatively derived from non-papillate sporangia. Further, a sporangium with papilla forming a discharge tube and

a hyaline apical plug appeared to be a synapomorphic trait for *Salisapilia*.

Taxonomy

Based on the presented phylogenetic and morphological analyses of the different taxa included in this study, the genus *Salisapilia* contains several additional species previously treated as members of *Halophytophthora*. As a consequence, five new combinations (i.e. *S. bahamensis*, *S. elongata*, *S. epistomia*, *S. masteri*, and *S. mycoparasitica*) and a new species (*S. coffeyi*) for the genus *Salisapilia* are introduced here. Measurements for sporangia are given as (min.–)average_minus_SD–SD–average_plus_SD(–max.).

Salisapilia Hulvey *et al.*, *Persoonia* **25**: 112 (2010), *emend.* MycoBank MB517465.

Colonies on VJ agar stellate, indistinct, petalloid; *aerial hyphae* limited; *vegetative hyphae* with regular branching, septae occur at maturity; *hyphal swellings* present, shape variable; *sporangia* produced in saline water, shape obpyriform, ovate, obovate, elongate to irregular; *proliferation* often external; *dehiscence* or

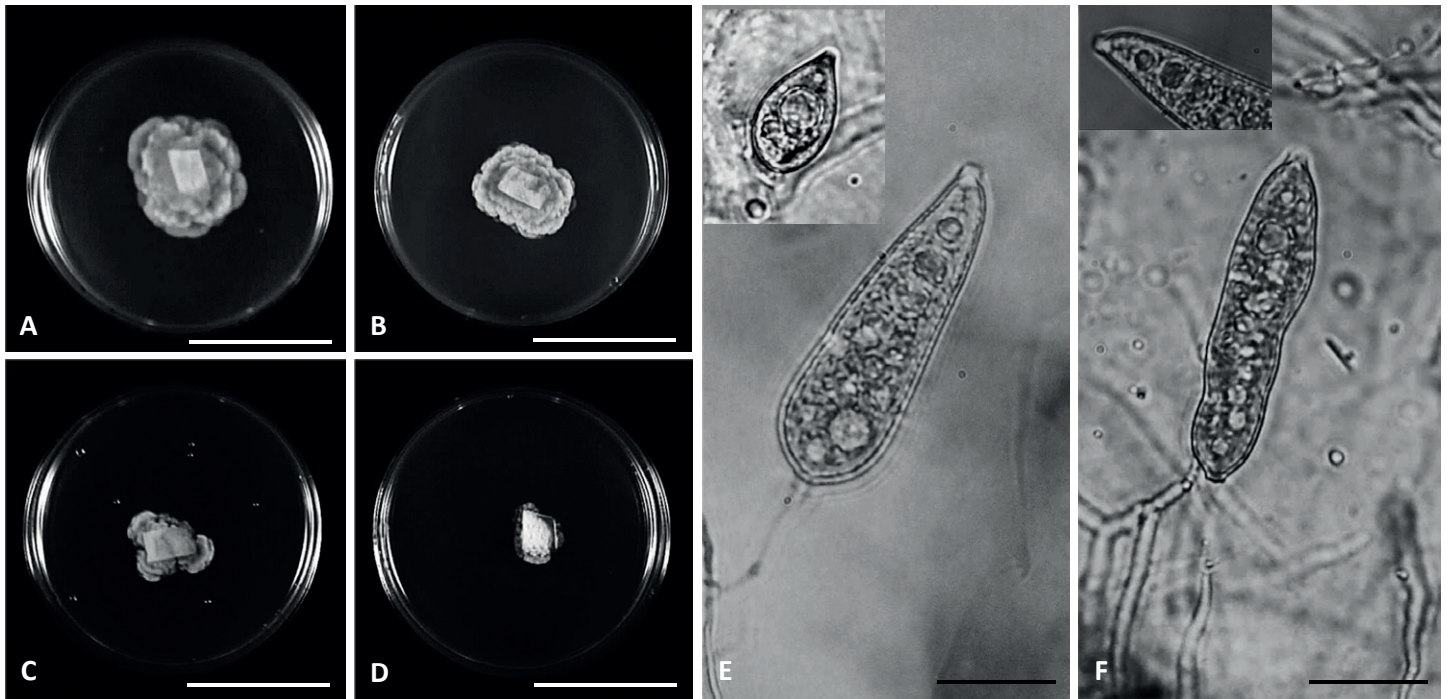


Fig. 2. *Salisapilia bahamensis* NBRC 32256. Colony patterns on **A.** Vegetable juice agar. **B.** Potato carrot agar. **C.** Peptone yeast glucose agar. **D.** Potato dextrose agar. **E, F.** Mature, vacuolated sporangia, (inset figure, sporangium showing hyaline apical plug). Scale bars: A–D. = 30 mm, E, F. = 20 μ m.

discharge tube present, usually with a hyaline plug at the apex; *zoospore release* occurs after dehiscence of the hyaline plug at the apex of the discharge tube, or zoospores exit directly from the discharge pore or through an evanescent tubular to vase-like vesicle; *gametangia* observed for some species; *antheridial attachment* paragynous, declinuous; *oogonia* smooth-walled; *oospores* spherical to ovoid, terminal or intercalary.

Type species: *Salisapilia sapeloensis* Hulvey *et al.*

Synopsis of species included in *Salisapilia*

Salisapilia bahamensis (Fell & Master) R. Bennett & Thines, *comb. nov.* MycoBank MB823448. Fig. 2.

Basionym: *Phytophthora bahamensis* Fell & Master, *Canad. J. Bot.* **53**: 2913. 1975. MB320472.

Synonym: *Halophytophthora bahamensis* (Fell & Master) Ho & Jong, *Mycotaxon* **36**: 381. 1990. MB126014.

Typus: **Holotype** ATCC 28296, cultures ex-type = CBS 586.85 = IMI 330182 = NBRC 32556, voucher ex ex-type strain NBRC3256 = USTH 014147, University of Santo Tomas Herbarium, Manila, Philippines.

Distribution: Bahamas, Philippines.

Salisapilia coffeyi R. Bennett & Thines, *sp. nov.* MycoBank MB823342. Fig. 3.

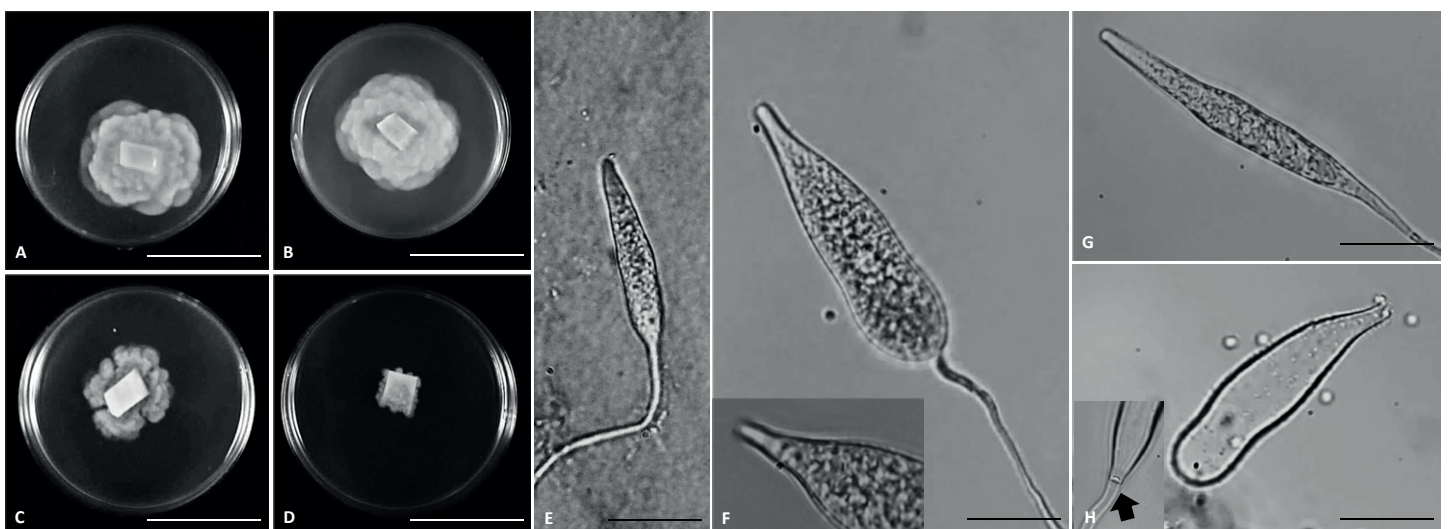


Fig. 3. *Salisapilia coffeyi* NBRC 32557. Colony patterns on **A.** Vegetable juice agar. **B.** Potato carrot agar. **C.** Peptone yeast glucose agar. **D.** Potato dextrose agar. **E.** Immature sporangium. **F, G.** Mature sporangia, (inset figure) sporangium showing hyaline apical plug. **H.** Empty sporangium; inset, elevated or umbonate basal plug. Scale bars: A–D = 30 mm, E–H = 20 μ m.

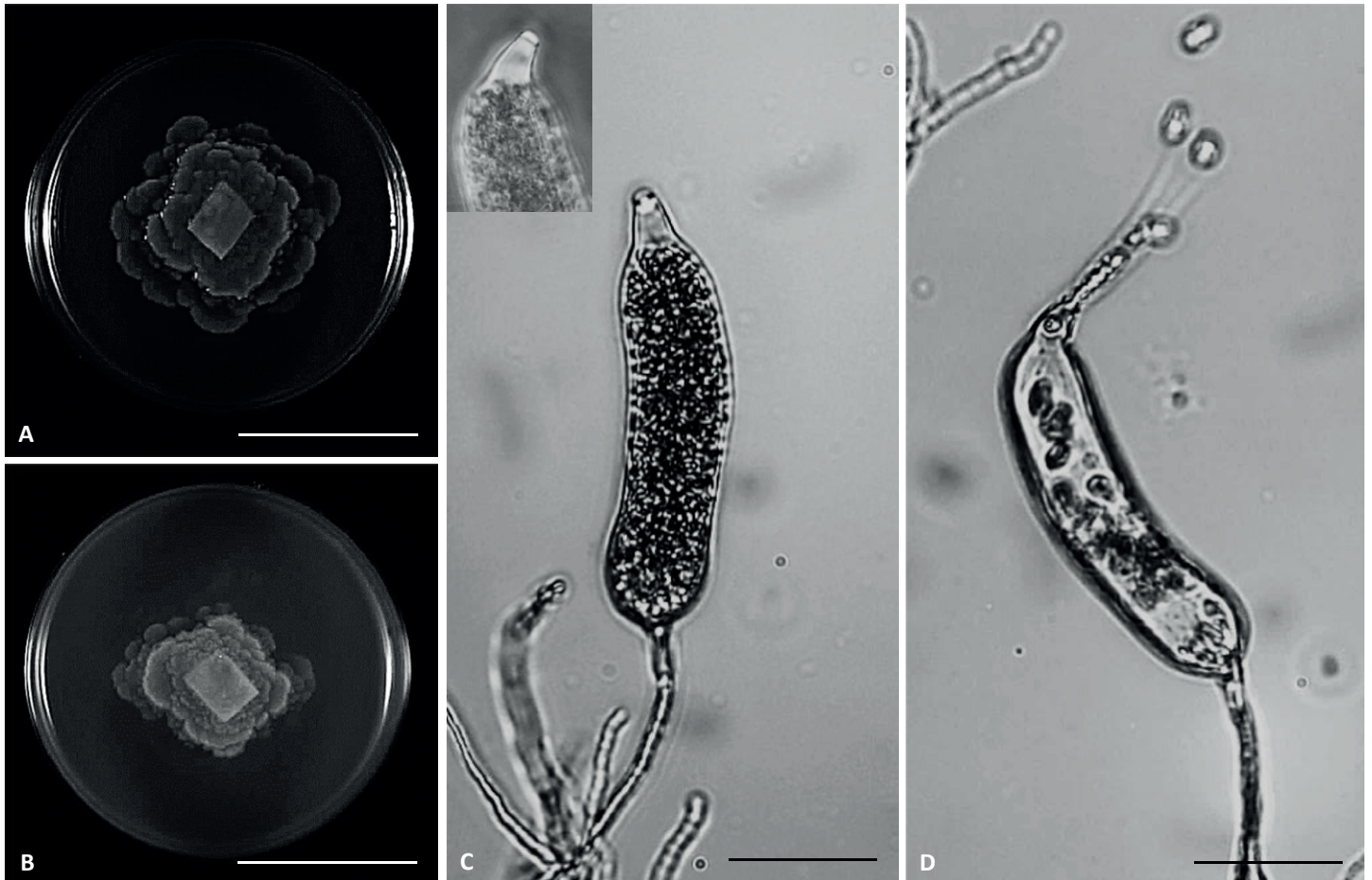


Fig. 4. *Salisapilia elongata* NBRC 100786. Colony patterns on **A.** Vegetable juice agar. **B.** Potato carrot agar. **C.** Mature sporangium; hyaline apical plug (inset). **D.** Mature sporangium releasing zoospores through a tubular vesicle. Scale bars: A, B = 30 mm, C, D. = 20 μ m.

Etymology: Dedicated to Michael Coffey for his contributions to the study of cultivable oomycetes.

Colony pattern on vegetable juice agar and potato carrot agar petaloid to rosette-like; **vegetative hyphae** highly branched, with septae at maturity; **sporangiogenic hyphae** undifferentiated from vegetative hyphae, bearing a single sporangium; **sporangia** smooth and thin-walled, with vacuoles, non-deciduous, (25.5–) 44–74–107(–126) \times (4–)6.5–10.5–17(–19.5) μ m, bursiform, narrowly bursiform, obpyriform to narrowly-elongate and obclavate, mostly with a tapering apex; **dehiscence tube** present; 5–13 \times 2.5–4 μ m; **dehiscence plug** present, hyaline, 1–3 μ m in diameter; **basal plug** present, hyaline, raised to umbonate; **proliferation** external; **zoospore release** directly through the dehiscence tube after ejection of the dehiscence plug; **vesicle** not observed; **chlamydospores** not observed; **gametangia** not observed.

Typus: **Bahamas**, Conception Island, isolated from decaying leaf of *Rhizophora mangle*, Oct. 1972, J.W. Fell & I.M. Master (**holotype** USTH 014149, ex-type culture NBRC 32557, GenBank: ITS, MF979510; LSU, MF979503).

Salisapilia elongata (Ho & Chang) R. Bennett & Thines, **comb. nov.** MycoBank MB823450. Fig. 4.

Basionym: *Halophytophthora elongata* Ho & Chang, *Mycotaxon* **85**: 417. 2003. MB372647.

Typus: **Holotype** 17II2001, Y.M. Ju, Institute of Botany, Academia Sinica, Taipei, Taiwan, cultures ex-type BCRC 33983 = NBRC 100786.

Distribution: Taiwan, Philippines.

Salisapilia epistomia (Fell & Master) R. Bennett & Thines, **comb. nov.** MycoBank MB823449. Fig. 5.

Basionym: *Phytophthora epistomium* Fell & Master, *Canad. J. Bot.* **53**: 2913. 1975. MB320475.

Synonym: *Halophytophthora epistomia* (Fell & Master) Ho & Jong, *Abstracts IMC-4*, Regensburg, 1990. MB126016.

Typus: **Holotype** ATCC 28293, cultures ex-type IMI 330183 = CBS 590.85 = NBRC 32617, voucher ex ex-type strain NBRC32617 = USTH 014147, University of Santo Tomas Herbarium, Manila, Philippines.

Distribution: USA.

Salisapilia masteri (Nakagiri & Newell) R. Bennett & Thines, **comb. nov.** MycoBank MB823447. Fig. 6.

Basionym: *Halophytophthora masteri* Nakagiri & Newell, *Mycoscience* **35**: 227. 1994. MB363473.

Typus: **Holotype** NBRC H-12169, NITE Biological Resource Center, Japan, cultures ex-type IFO 32604 = ATCC 96906 = CBS 207.95 = NBRC 32604.

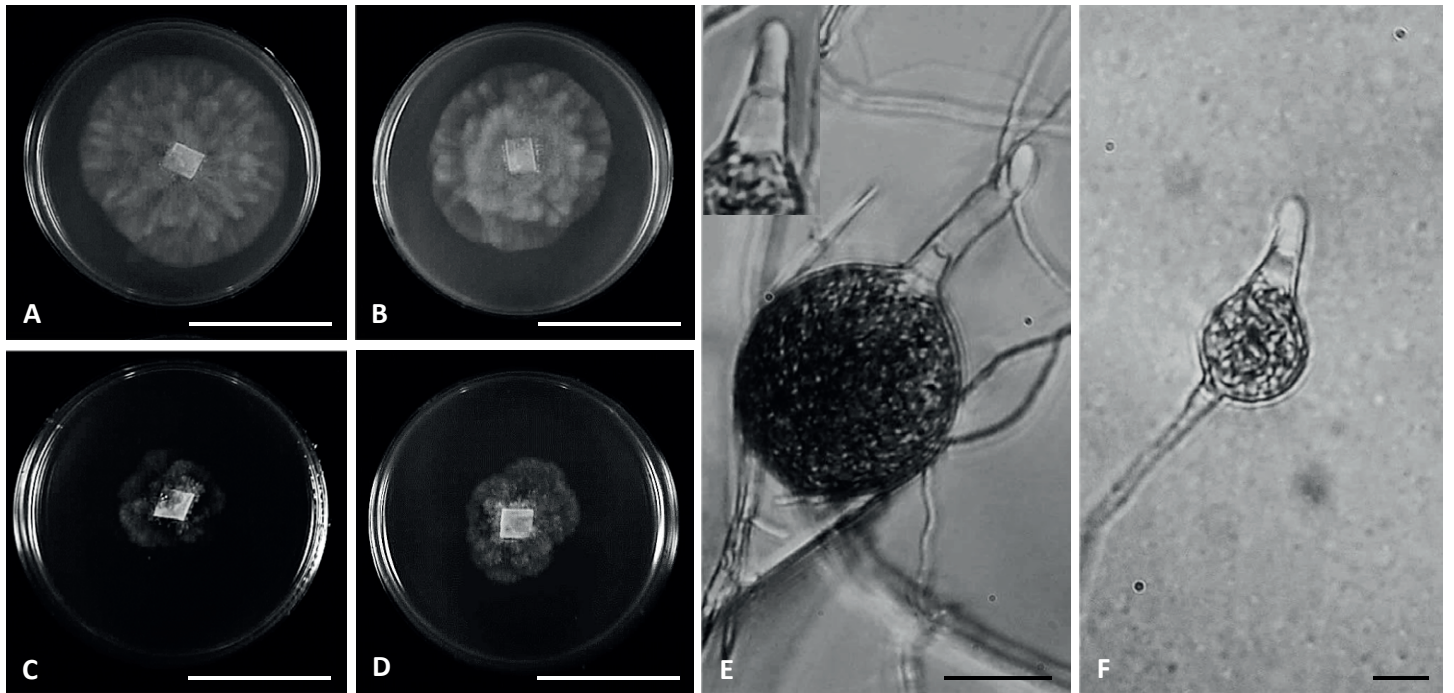


Fig. 5. *Salisapilia epistomia* NBRC 32617. Colony patterns on A. Vegetable juice agar. B. Potato carrot agar. C. Peptone yeast glucose agar. D. Potato dextrose agar. E–F. Mature sporangia; hyaline apical plug (inset, Fig. 4E). Scale bars: A–D. = 30 mm, E, F. = 20 μ m.

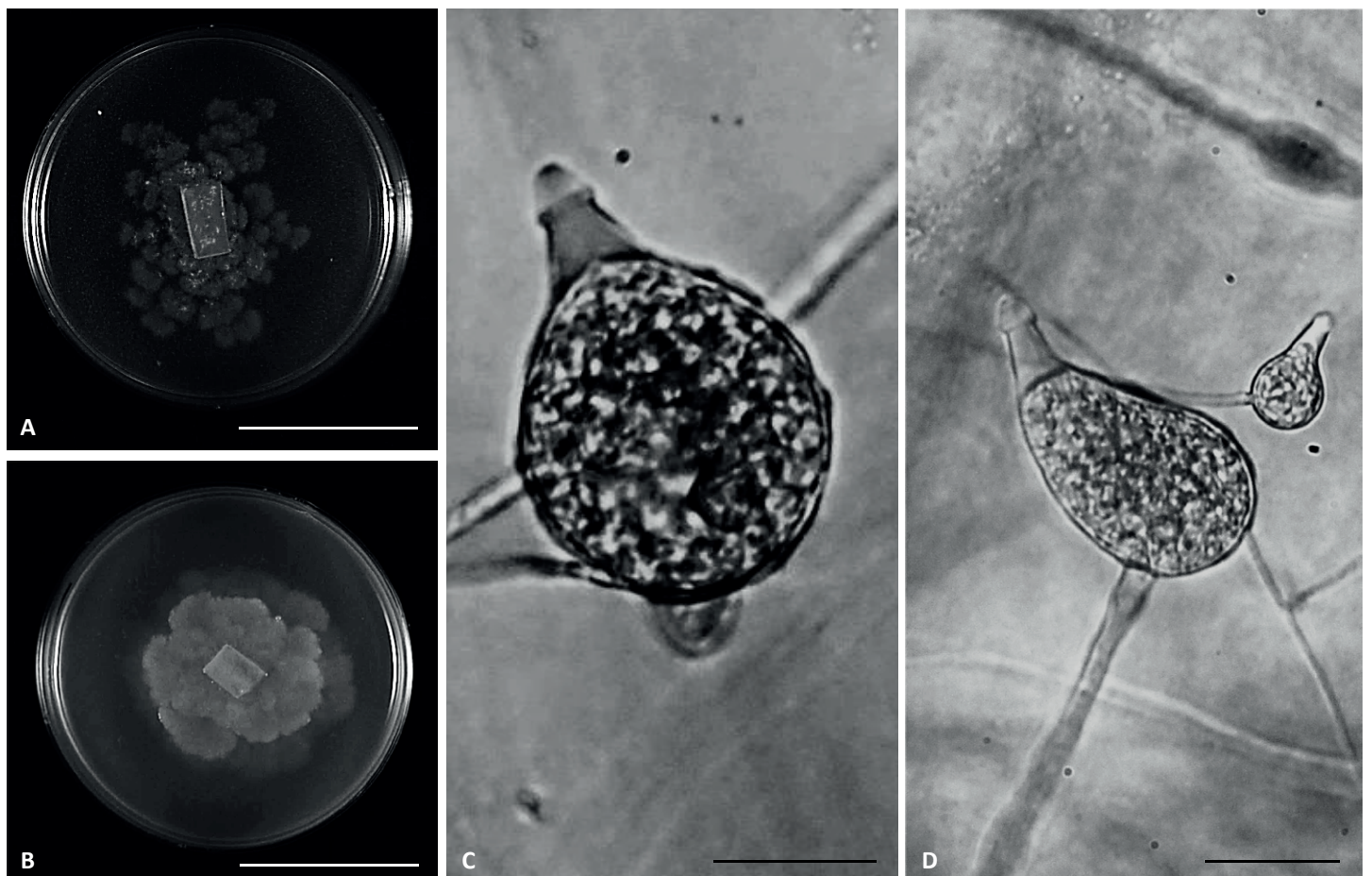


Fig. 6. *Salisapilia masteri* NBRC 32604. Colony patterns on A. Vegetable juice agar. B. Potato carrot agar. C, D. Mature sporangia. Scale bars: A, B = 30 mm, C, D = 20 μ m.

Distribution: Bahamas.

Salisapilia mycoparasitica (Fell & Master) R. Bennett & Thines, *comb. nov.* MycoBank MB824539. Fig. 7.

Basionym: *Phytophthora mycoparasitica* Fell & Master, *Canad. J. Bot.* **53**: 2916. 1975. MB320485.

Synonym: *Halophytophthora mycoparasitica* (Fell & Master) Ho & Jong, *Mycotaxon* **36**: 381. 1990. MB126017.

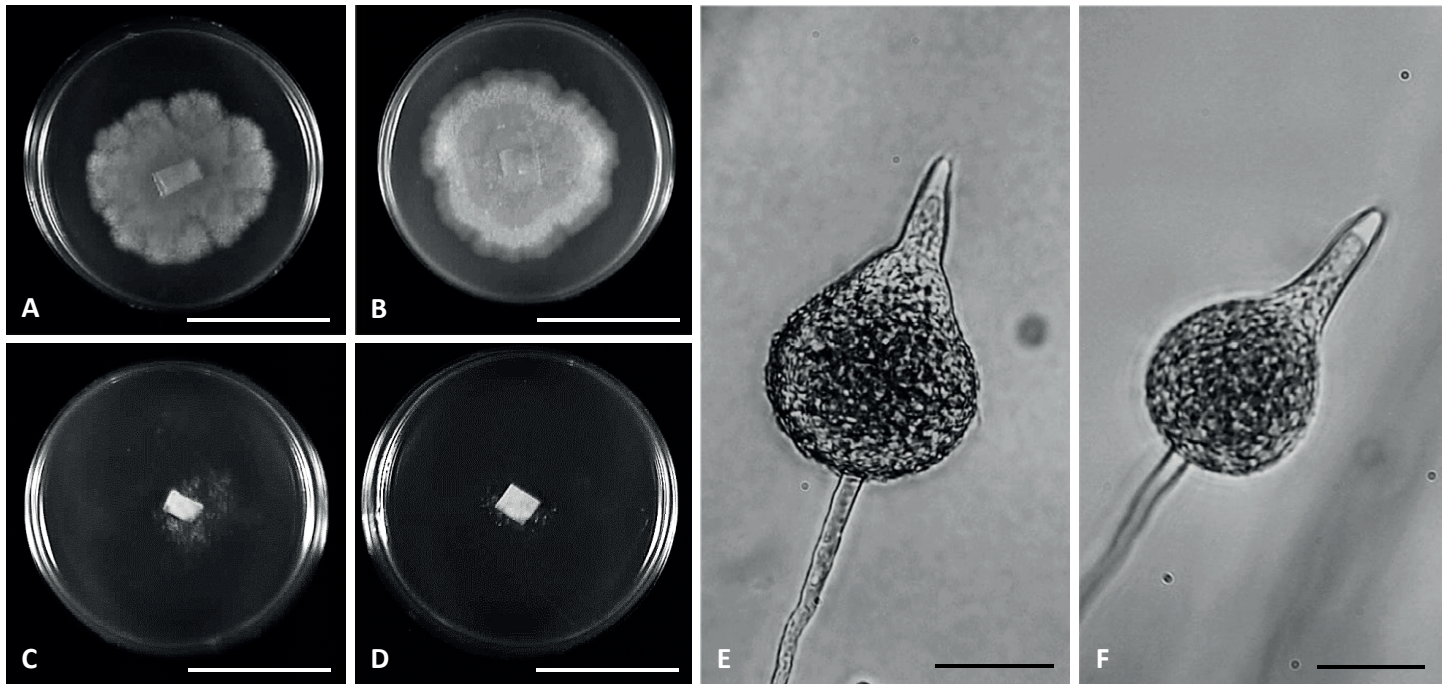


Fig. 7. *Salisapilia mycoparasitica* NBRC 32966. Colony patterns on **A.** Vegetable juice agar. **B.** Potato carrot agar. **C.** Peptone yeast glucose agar. **D.** Potato dextrose agar. **E, F.** Mature sporangia. Scale bars: A–D = 30 mm, E–F = 20 μ m.

Typus: **Holotype** ATCC 28292 (discarded), (**lectotype** designated here fig. 16, *Canad. J. Bot.* **53**: 2918 (1975), MBT386266; **epitype** designated here NBRC H-12221, MBT386249, ex-epitype culture NBRC 32966, NITE Bioresource Centre, Japan).

Other materials examined: NBRC 32967, NITE Bioresource Centre, Tokyo Japan.

Distribution: Malaysia, Japan.

Notes: The designated type, ATCC 28292, is no longer available, and no additional specimen was deposited in any recognised fungarium at the time *Phytophthora mycoparasitica* was proposed. Since neither inactive nor living material appears to

remain from the collection of Fell & Master (1975), fig. 16 from that publication is designated as the **lectotype**, the specimen NBRC H-12221 is designated as the **epitype** and NBRC 32996 (NBRC, Japan) as the **ex-epitype culture**.

Salisapilia nakagirii Hulvey *et al.*, *Persoonia* **25**: 113. 2010, **emend.** MycoBank MB517466. Fig. 8.

Typus: **Holotype** CBS H-20478, Westerdijk Fungal Biodiversity Institute, Utrecht, the Netherlands, ex-type cultures CBS 127947 = NBRC 108757 = LT6456.

Distribution: USA.

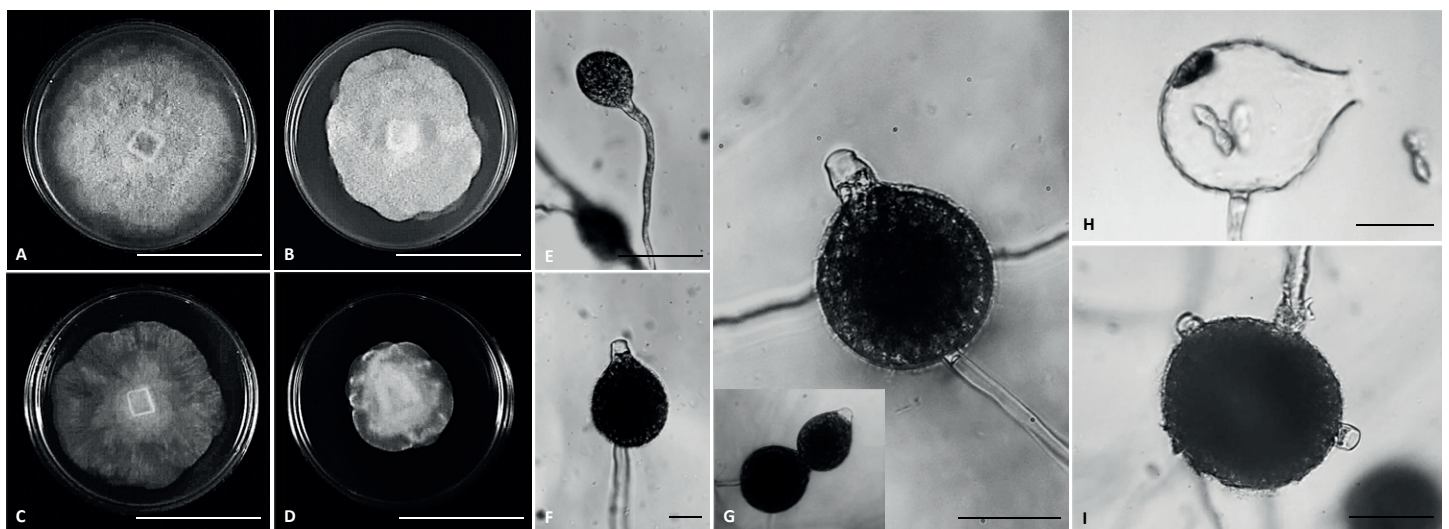


Fig. 8. *Salisapilia nakagirii* CBS 127947. Colony patterns on **A.** Vegetable juice agar. **B.** Potato carrot agar. **C.** Peptone yeast glucose agar. **D.** Potato dextrose agar. **E.** Immature sporangium. **F–I.** Mature sporangia, (inset figure) modified shape of a sporangium. **H.** Empty sporangium. **I.** Mature sporangium with two discharge tubes. Scale bars: A–D = 30 mm, E–I = 20 μ m.

Colony pattern on Vegetable juice agar and potato carrot agar indistinct; stellate to rosette-like on peptone yeast agar; *hyphae* branched with *septa* at maturity; *sporangia* ovoid, globose to obpyriform, (26–)81.5–137–205(–231) × (11.5–)32–66.5–113(–133.5) μm; *dehiscence tube* present, filled with non-sporogenous protoplasmic mass, size 6–18.0 × 4.5–8.5 μm; *hyaline apical plug* indistinct; *sporangial wall* wrinkled in some sporangia; *basal plug* present in few sporangia; *proliferation* external; *zoospore release* through an evanescent vesicle; *vesicle* vase-shaped; *gametangia* present; *antheridia* diclinous, paragynous, club-shaped or lobed, 3–10 μm in length; *oogonia* hyaline, spherical, 33–48 μm; *oospores* 28–44 μm, hyaline, with a uniformly refractile ooplast vacuole; wall 1–7 μm.

Salisapilia sapeloensis Hulvey *et al.*, *Persoonia* **25**: 113. 2010. MycoBank MB517467. Fig. 9.

Typus: Holotype CBS H-20477, Westerdijk Fungal Biodiversity Institute, Utrecht, the Netherlands, ex-type cultures NBRC 108756 = LT6440 = CBS 127946.

Distribution: USA.

Salisapilia tartarea (Nakagiri & Newell) Hulvey, Nigrelli, Telle, Lamour & Thines, *comb. nov.* MycoBank MB517468. Fig. 10.

Basionym: *Halophytophthora tartarea* Nakagiri & Newell, *Mycoscience* **35**: 224. 1994. MB363474.

Synonym: *Salisapilia tartarea* (Nakagiri & S.Y. Newell) Hulvey *et al.*, *Persoonia* **25**: 114. 2010. Nom. inval., Art. 41.5 (Melbourne).

Typus: Holotype NBRC H-12168, NITE Biological Resource Center, Japan, ex-type cultures NBRC 32606 = ATCC 96905 = CBS 208.95.

Distribution: USA.

Note: Invalidly proposed in *Persoonia* **25**: 114 (2010), as the date of publication of the basionym was omitted.

DISCUSSION

Estuarine and saltmarsh oomycetes are a diverse group of heterokonts that recently received much attention. Members of this ecological group are in the genera *Halophytophthora* (Ho & Jong 1990), *Phytophythium* (Bala *et al.* 2010), *Salisapilia* (Hulvey *et al.* 2010), *Salispina* (Li *et al.* 2016), and *Calycofera* (Bennett *et al.* 2017b). Of these taxa, *Halophytophthora* and *Salisapilia* were regarded to be in need of taxonomic revision (Nigrelli & Thines 2013, Marano *et al.* 2014, Beakes & Thines 2017), and the latter genus was resolved in this study.

Members of the monogeneric *Salisapiliaceae* are characterised by a small hyphal diameter, a protruding hyaline apical plug, and the absence of a vesicle during zoospore release (Hulvey *et al.* 2010). However, the sporangia of *S. nakagirii* CBS 127947 were reported to release zoospores into a semi-persistent vesicle and that the typical hyaline apical plug was absent (Marano *et al.* 2014). These observations are largely confirmed in this study, demonstrating that *S. nakagirii* has an exceptional mode of sporulation, even though we classify the vesicle as evanescent, as the structure is not readily observable sometime after zoospore release. Marano *et al.* (2014) reached the conclusion that *S. nakagirii* is papillate; however, it appears that the discharge tube is rather filled with some non-sporogenous mass, which is protoplasmic of origin, and its distalmost part is probably homologous to the apical plug observed in other species of *Salisapilia*, giving the impression of a papilla (Gerretson-Cornell & Simpson 1984).

Hulvey *et al.* (2010) suggested that the intricacies of zoospore release might be of phylogenetic relevance and, thus, useful for resolving some systematic complexities of saprotrophic oomycetes. However, the example of *S. nakagirii*,

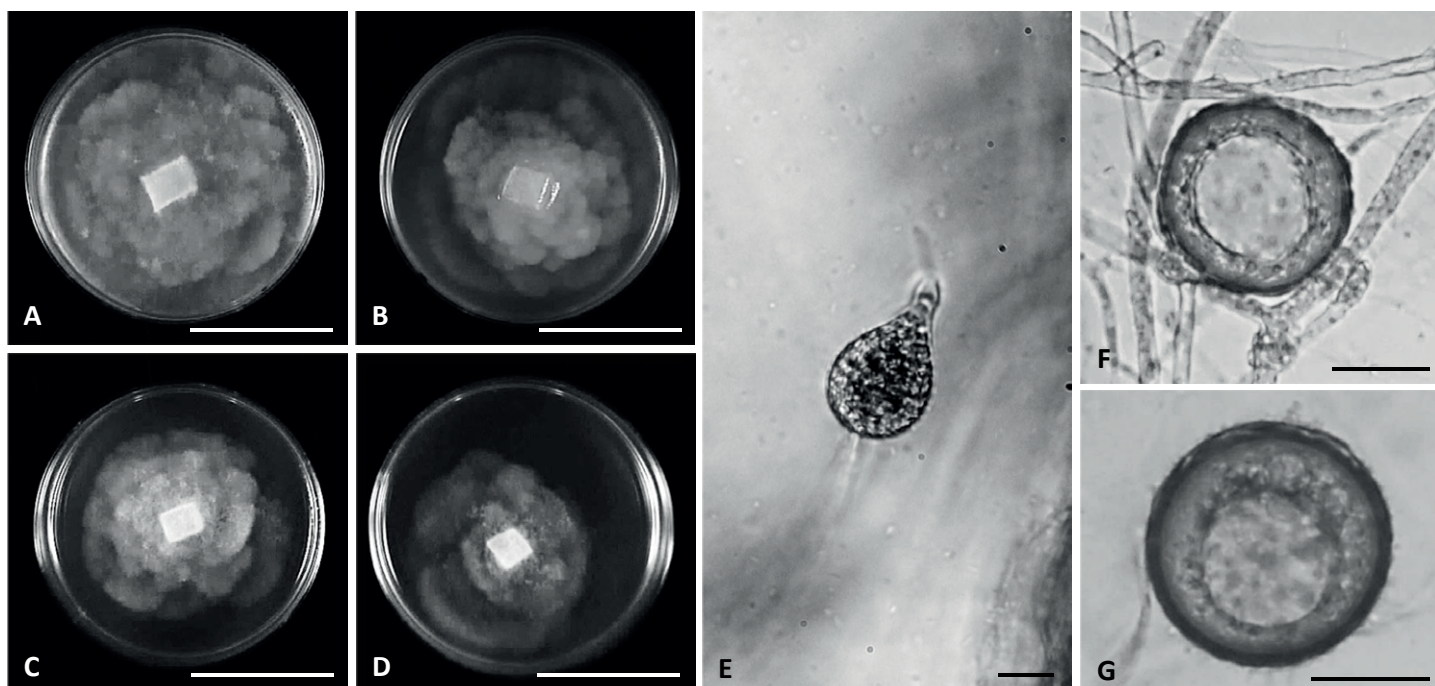


Fig. 9. *Salisapilia sapeloensis* CBS 127946. Colony patterns on **A.** Vegetable juice agar. **B.** Potato carrot agar. **C.** Peptone yeast glucose agar. **D.** Potato dextrose agar. **E.** Mature sporangium. **F, G.** Oogonia. Scale bars: A–D = 30 mm, E–G = 20 μm.

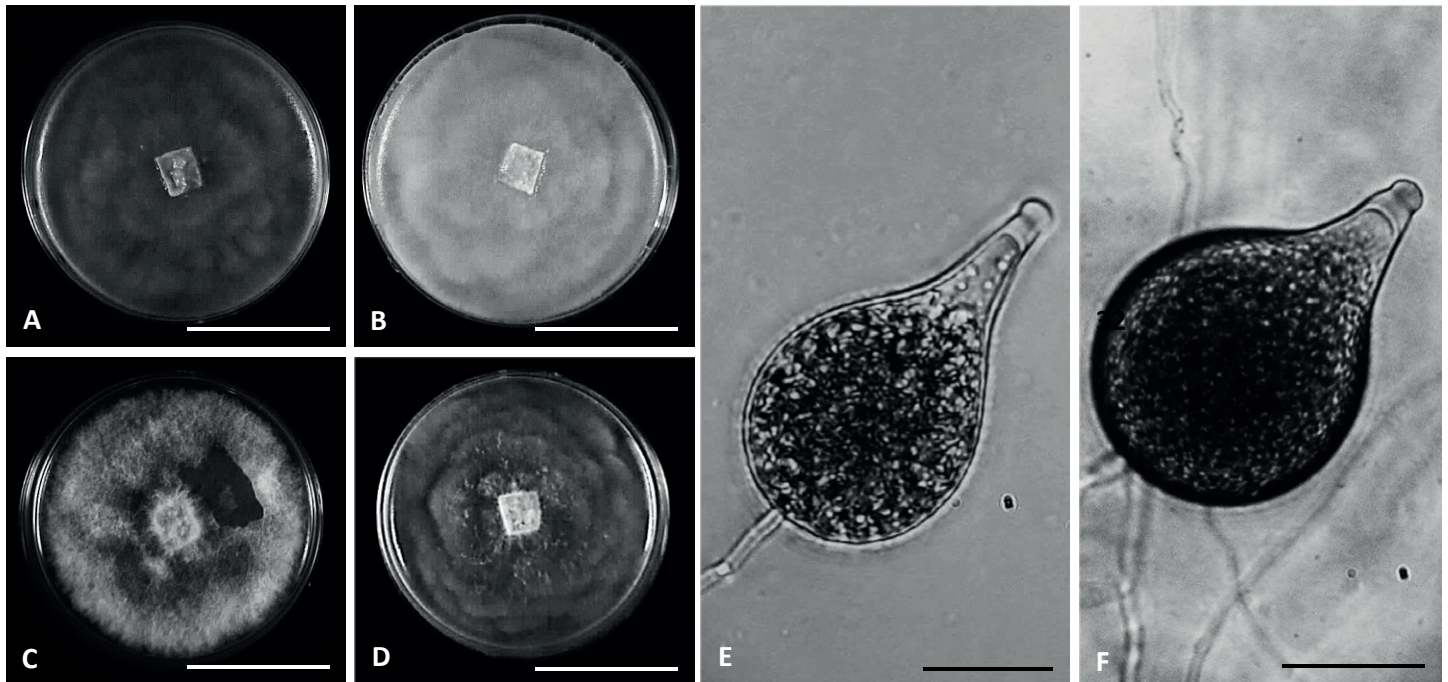


Fig. 10. *Salisapilia tartarea* CBS 208.95. Colony patterns on **A.** Vegetable juice agar. **B.** Potato carrot agar. **C.** Peptone yeast glucose agar. **D.** Potato dextrose agar. **E, F.** Mature sporangia. Scale bars: A–D = 30 mm, E, F = 20 μ m.

in line with observations on other species of saprotrophic or hemibiotrophic *Peronosporales*, demonstrates the necessity to combine morphological and ontogenetic data with molecular phylogenetics, as the process of zoospore release might be variable within genera (Gisi *et al.* 1979, Gerretson-Cornell & Simpson 1984, Bala *et al.* 2010, de Cock *et al.* 2015). Difficulty in finding clade specific-synapomorphies is common in saprotrophic and hemibiotrophic oomycetes. A good example of this is the paraphyletic genus *Phytophthora*, where the classification by Waterhouse (1963) or Stamps *et al.* (1990) does not reflect natural groupings resolved by multigene-phylogenies (Cooke *et al.* 2000, Kroon *et al.* 2004, Blair *et al.* 2008, Runge *et al.* 2011). *Halophytophthora elongata* (Ho *et al.* 2003) and *H. masteri* (Nakagiri *et al.* 1994) formed elongated to tubular-shaped, discharge-tube-like vesicles, similar to the vase-like vesicle of *S. nakagirii* prior to zoospore release.

While the absence of a vesicle does not seem to be a characteristic useful for delineating *Salisapilia*, the hyaline apical plug is a feature that seems to be of more diagnostic value. It is a usually readily observable cone-like structure nested at and eventually protruding from the apex of the discharge tube. Prior to zoospore release, the hyaline plug is ejected or detached from the discharge tube (Nakagiri *et al.* 1994, Ho *et al.* 2003) giving way for the release of zoospores. The only species in which this feature does not manifest is *S. nakagirii*. However, variation

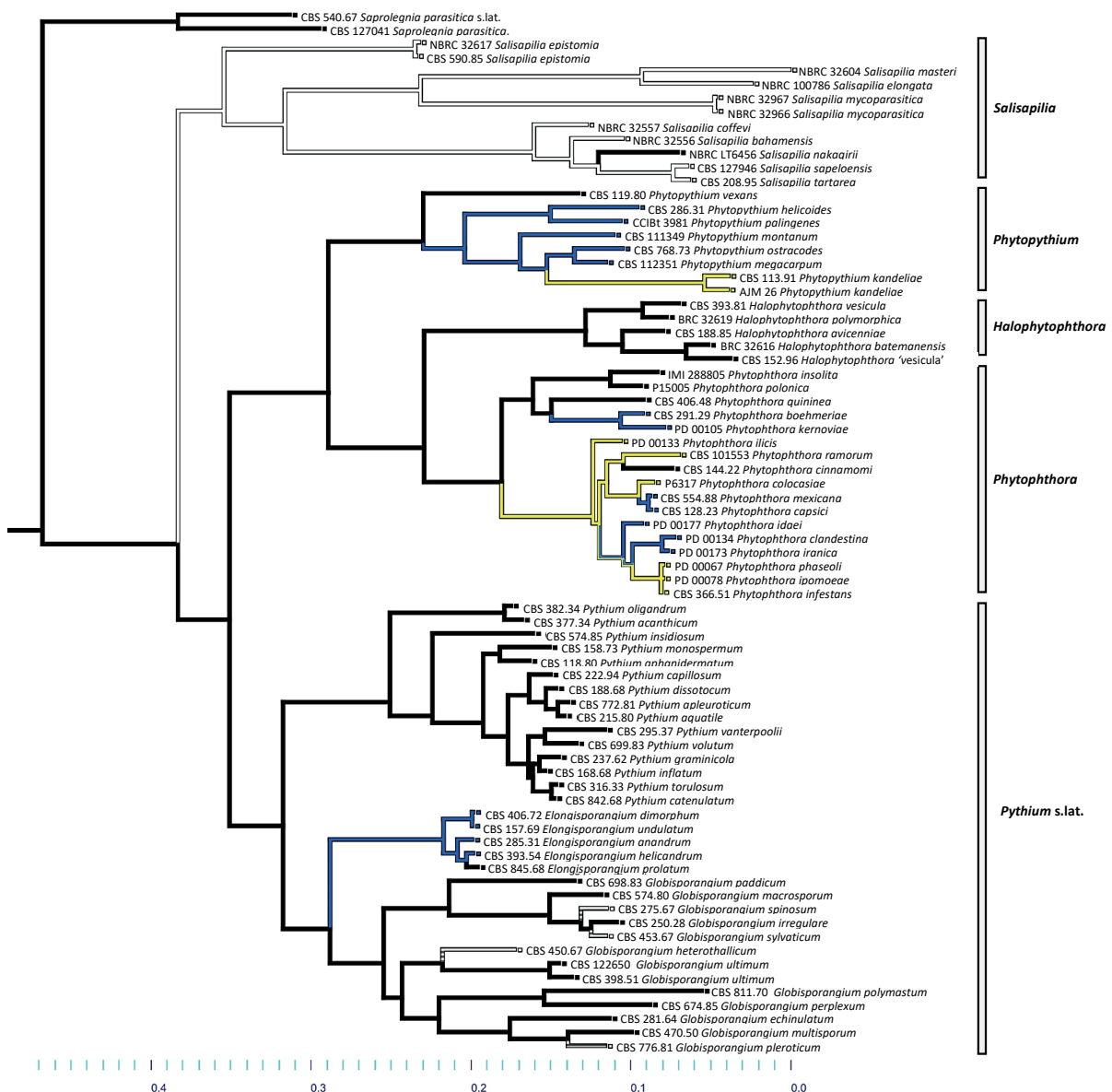
in size of the hyaline apical plug is present among members of *Salisapilia* (Table 1). Based on the ancestral trait reconstruction analysis, it was observed that non-papillate sporangia appear as an ancestral trait to papillate and semi-papillate sporangia (Yang *et al.* 2017). In the present ancestral state reconstruction (Fig. 11), the absence of the hyaline apical plug seems to be a derived feature in *S. nakagirii*, and otherwise appears to be an exclusive synapomorphy for the genus *Salisapilia*.

Phylogenetically, *Salisapiliaceae* is a well-supported clade that appears to be a sister group to *Peronosporaceae* and *Pythiaceae* (Hulvey *et al.* 2010, this study). Hulvey *et al.* (2010) suggested that *H. bahamensis*, *H. epistomia*, *H. exoprolfiera*, and *H. operculata* might belong to the genus *Salisapilia*, but as no sequence data were available at that time to support this, Hulvey *et al.* (2010) refrained from proposing new combinations for any of these taxa. Of these species, *Halophytophthora operculata* was recently transferred to the genus *Calycofera* (Bennett *et al.* 2017b), which was inferred to be the sister taxon to *Phytophthora*. Jung *et al.* (2017) suggested that *H. epistomia* might need to be accommodated in a genus of its own, but in the present study, it could be demonstrated that the morphology of *H. epistomia* fits well to the emended diagnosis of *Salisapilia*. Thus, it was combined into that genus instead of erecting a new one.

Key to the species of *Salisapilia*

- | | |
|---|----------------------------|
| 1. Sporangia non-papillate; hyaline plug absent | <i>S. nakagirii</i> |
| 1. Sporangia papillate; hyaline plug present | 2 |
| 2. Zoospore release through an evanescent vesicle | 3 |
| 2. Zoospore release directly through the discharge tube | 4 |

- 3. Dehiscence tube ragged appearance, with collar-like folds;
sporangium shape ovoid, obpyriform, spherical *S. masteri*
- 3. Dehiscence tube smooth with cone-like plug; sporangium shape, mainly elongated, bursiform,
cylindrical-elongated *S. elongata*
- 4. Sporangia vacuolated 5
- 4. Sporangia non-vacuolated 6
- 5. Sporangium shape bursiform; multi-lobed with aseptate or septate
setiform appendages *S. bahamensis*
- 5. Sporangium shape narrowly bursiform, obpyriform, elongate to obclavate;
single-lobed, setiform appendages absent *S. coffeyi*
- 6. Sexual structures absent; sporangium surface denticulate with few spines *S. mycoparasitica*
- 6. Sexual structures present, homothallic; sporangium surface smooth, spines absent 7
- 7. Oospores aplerotic *S. tartarea*
- 7. Oospores plerotic 8
- 8. Hyaline apical plug protruding through the discharge tube, 3–8 µm long;
sporangium shape ovoid to obpyriform *S. sapeloensis*
- 8. Hyaline apical plug nested at the discharge tube, 14–90 µm long;
sporangium shape langeniform to obpyriform *S. epistomia*



ACKNOWLEDGEMENTS

RMB was funded by the Katholischer Akademischer Ausländer Dienst (KAAD), Goethe University, and partly by the Studienstiftung für mykologische Systematik und Ökologie. Sampling and export permits in the Philippines were granted by the Biodiversity Management Bureau, DENR through the collaborative efforts of the Integrative Fungal Research Cluster (LOEWE-IPF) and UST Collection of Microbial Strains. Research support was provided by the LOEWE initiative of the government in the framework of the excellence cluster for Integrative Fungal Research (IPF) and the LOEWE Centre for Translational Biodiversity Genomics (TBG).

REFERENCES

- Anastasiou CJ, Churchland LM (1969). Fungi on decaying leaves in marine habitats. *Canadian Journal of Botany* **47**: 251–257.
- Bachofer M (2004). *Molekularbiologische Populationsstudien an Plasmopara halstedii, dem Falschen Mehltau der Sonnenblume*. PhD thesis, University of Hohenheim, Germany.
- Bala K, Robideau GP, Lévesque CA, et al. (2010). *Phytophythium* Abad, de Cock, Bala, Robideau, Lodhi and Lévesque, *gen. nov.* and *Phytophythium sindhum* Lodhi, Shahzad and Lévesque, *sp. nov.* *Persoonia* **24**: 136–137.
- Beakes GW, Thines M (2017). *Hyphochytriomycota* and *Oomycota*. In: *Handbook of the Protists* (JM Archibald, AGB Simpson, C Slamovits, eds). Springer International Publishing, Germany: 435–505.
- Bennett RM, Dedeles GR, Thines M (2017a). *Phytophthora elongata* (*Peronosporaceae*) is present as an estuarine species in Philippine mangroves. *Mycosphere* **8**: 959–967.
- Bennett RM, de Cock AWAM, Lévesque CA, et al. (2017b). *Calycofera* gen. nov., an estuarine sister taxon to *Phytophythium*, *Peronosporaceae*. *Mycological Progress* **16**: 947–954.
- Blair JE, Coffey MD, Park SY, et al. (2008). A multi-locus phylogeny for *Phytophthora* utilizing markers derived from complete genome sequences. *Fungal Genetics and Biology* **45**: 266–277.
- Cooke DEL, Drenth A, Duncan JM, et al. (2000). A molecular phylogeny of *Phytophthora* and related Oomycetes. *Fungal Genetics and Biology* **30**: 17–32.
- Crous PW, Verkley GJM, Groenewald JZ, et al. (2009). *Fungal Biodiversity. CBS Laboratory Manual* **1**: 1–269. Centraalbureau voor Schimmelcultures, Utrecht, The Netherlands.
- de Cock AW, Mendoza L, Padhye AA, et al. (1987). *Pythium insidiosum* sp. nov., the etiologic agent of pythiosis. *Journal of Clinical Microbiology* **25**: 344–349.
- de Cock AWAM, Lodhi AM, Rintoul TL, et al. (2015). *Phytophythium*: molecular phylogeny and systematics. *Persoonia* **34**: 25–39.
- Erwin DC, Ribeiro OK (1996). *Phytophthora Diseases Worldwide*. American Phytopathological Society Press. Minnesota, USA.
- Fell JW, Master IM (1975). Phycomycetes (*Phytophthora* spp. nov. and *Pythium* sp. nov.) associated with degrading mangrove (*Rhizophora mangle*) leaves. *Canadian Journal of Botany* **53**: 2908–2922.
- Gerretson-Cornell L, Simpson J (1984). Three new marine *Phytophthora* species from New South Wales. *Mycotaxon* **19**: 453–470.
- Gisi U, Hemmes DE, Zentmyer GA (1979). Origin and significance of the discharge vesicle in *Phytophthora*. *Experimental Mycology* **3**: 321–339.
- Ho HH, Chang HS, Huang SH (2003). *Halophytophthora elongata*, a new marine species from Taiwan. *Mycotaxon* **85**: 417–422.
- Ho HH, Hsieh SY, Chang HS (1990). *Halophytophthora epistomium* from mangrove habitats in Taiwan. *Mycologia* **82**: 659–662.
- Ho HH, Jong SC (1990). *Halophytophthora* gen. nov., a new member of the family *Pythiaceae*. *Mycotaxon* **36**: 377–382.
- Hulvey J, Telle S, Nigrelli L, et al. (2010). *Salisapiliaceae* – a new family of oomycetes from marsh grass litter of southeastern North America. *Persoonia* **25**: 109–116.
- Jung T, Scanu B, Bakonyi J, et al. (2017). *Nothophytophthora* gen. nov., a new sister genus of *Phytophthora* from natural and semi-natural ecosystems. *Persoonia* **39**: 143–174.
- Katoh K, Misawa K, Kuma K, et al. (2002). MAFFT: a novel method for rapid multiple sequence alignment based on fast fourier transform. *Nucleic Acid Research* **30**: 3059–3066.
- Kroon LPNM, Bakker FT, van den Bosch GB, et al. (2004). Phylogenetic analysis of *Phytophthora* species based on mitochondrial and nuclear DNA sequences. *Fungal Genetics and Biology* **41**: 766–782.
- Kroon LP, Brouwer H, de Cock AW, et al. (2012). The genus *Phytophthora* anno 2012. *Phytopathology* **102**: 348–364.
- Lara E, Belbahri L (2011). SSU rRNA reveals major trends in oomycete evolution. *Fungal Diversity* **49**: 93–100.
- Li GJ, Hyde KD, Zhao RL, et al. (2016). Fungal diversity notes 253–366: taxonomic and phylogenetic contributions to fungal taxa. *Fungal Diversity* **78**: 1–237.
- Maddison WP, Maddison DR (2018). *Mesquite: a modular system for evolutionary analysis*. <http://mesquiteproject.org>.
- Marano AV, Jesus AL, de Souza JI, et al. (2016). Ecological roles of saprotrophic *Peronosporales* (*Oomycetes*, *Straminipila*) in natural environments. *Fungal Ecology* **19**: 77–88.
- Marano AV, Jesus AL, Pires-Zottarelli CLA, et al. (2014). Phylogenetic relationships of *Pythiales* and *Peronosporales* (*Oomycetes*, *Straminipila*) within the “peronosporalean galaxy”. In: *Freshwater fungi and fungal-like organisms*. (EBG Jones, KD Hyde, KL Pang, eds). Walter de Gruyter, Germany: 177–199.
- Moncalvo JM, Wang HH, Hseu RS (1995). Phylogenetic relationships in *Ganoderma* inferred from the internal transcribed spacers and 25S ribosomal DNA sequences. *Mycologia* **87**: 223–238.
- Nakagiri A, Newell SY, Ito T (1994). Two new *Halophytophthora* species, *H. tartarea* and *H. masteri*, from intertidal decomposing leaves in saltmarsh and mangrove regions. *Mycoscience* **35**: 223–232.
- Nakagiri A, Tokumasu S, Araki H, et al. (1989). Succession of fungi in decaying mangrove leaves in Japan. In: *Recent Advances in Microbial Ecology* (T Hattori, Y Ishida, Y Moruyama, et al., eds). Japan Scientific Society Press, Japan: 297–301.
- Nechwatal J, Oßwald WF (2003). *Pythium montanum* sp. nov., a new species from a spruce stand in the Bavarian Alps. *Mycological Progress* **2**: 73–80.
- Nigrelli L, Thines M (2013). Tropical oomycetes in the German Bight – climate warming or overlooked diversity? *Fungal Ecology* **6**: 152–160.
- Paul B (1987). A new species of *Pythium* with filamentous sporangia from Algeria. *Transactions of the British Mycological Society* **89**: 195–198.

Fig. 11. Ancestral trait reconstruction of the papilla and hyaline apical plug for *Elongisporangium*, *Globisporangium*, *Halophytophthora*, *Phytophthora*, *Phytophythium*, *Pythium*, and *Salisapilia*. White-coloured branches represent lineages with papillate sporangia bearing a hyaline apical plug; blue – papillate sporangia with no hyaline apical plug; yellow – semi-papillate sporangia with no hyaline apical plug; black – non-papillate sporangia. The scale corresponds to species divergence relative to nucleotide substitution rates based on the Bayesian phylogenetic inference.

- Paul B (2000). ITS1 region of the rDNA of *Pythium megacarpum* sp. nov., its taxonomy and its comparison with selected species. *FEMS Microbiology Letters* **186**: 229–233.
- Paul B, Galland D, Masih I (1999). *Pythium prolatum* isolated from soil in the Burgundy region: a new record for Europe. *FEMS Microbiology Letters* **173**: 69–75.
- Pegg KG, Alcorn JL (1982). *Phytophthora operculata* sp. nov., a new marine fungus. *Mycotaxon* **15**: 99–102.
- Price MN, Dehal PS, Arkin AP (2009). FastTree: computing large minimum evolution trees with profiles instead of a distance matrix. *Molecular Biology and Evolution* **26**: 1641–1650.
- Price MN, Dehal PS, Arkin AP (2010). FastTree 2 – Approximately Maximum-Likelihood trees for large alignments. *PLoS ONE* **5**: e9490.
- Riethmüller A, Voglmayr H, Göker M, et al. (2002). Phylogenetic relationships of the downy mildews (*Peronosporales*) and related groups based on nuclear large ribosomal DNA sequences. *Mycologia* **84**: 834–849.
- Ronquist F, Teslenko M, van der Mark P, et al. (2012). MrBayes 3.2: efficient Bayesian phylogenetic inference and model choice across a large model spaces. *Systematic Biology* **61**: 539–542.
- Runge F, Telle S, Ploch S, et al. (2011). The inclusion of downy mildews in a multi-locus-dataset and its reanalysis reveals a high degree of paraphyly in *Phytophthora*. *IMA Fungus* **2**: 163–171.
- Stamps SJ, Waterhouse GM, Newhook FJ, et al. (1990). Revised tabular key to the species of *Phytophthora*. *CMI Mycological Papers* **162**: 1–28.
- Tamura K, Stecher G, Peterson D, et al. (2013). MEGA6: molecular evolutionary genetics analysis version 6.0. *Molecular Biology and Evolution* **30**: 2725–2729.
- Thines M (2014). Phylogeny and evolution of plant pathogenic oomycetes – a global overview. *European Journal of Plant Pathology* **138**: 431–447.
- Uzuhashi S, Tojo M, Kakishima M (2010). Phylogeny of the genus *Pythium* and description of new genera. *Mycoscience* **51**: 337–365.
- Vaidya G, Lohman DJ, Meier R (2010). SequenceMatrix: concatenation software for the fast assembly of multi-gene datasets with character set and codon information. *Cladistics* **27**: 171–180.
- van der Plaats-Niterink AJ (1981). Monograph of the genus *Pythium*. *Studies in Mycology* **21**: 1–244.
- Waterhouse GM (1963). Key to the species *Phytophthora* de Bary. *CMI Mycological Papers* **92**: 1–22.
- Yang X, Hong C (2014). *Halophytophthora fluviatis* sp. nov. from freshwater in Virginia. *FEMS Microbiology Letters* **352**: 230–237.
- Yang X, Tyler BM, Hong C (2017). An expanded phylogeny for the genus *Phytophthora*. *IMA Fungus* **8**: 355–384.

Supplementary Material: <http://fuse-journal.org/>

Table S1. GenBank numbers of sequences used in this study.

Fig. S1. Phylogenetic tree based on ITS sequences. The primary phylogenetic tree was inferred using Minimum Evolution (ME), with bootstrap support values from ME and Maximum Likelihood, and posterior probabilities from Bayesian Inference, in the respective order. (-) indicates unsupported alternating topology or bootstrap value and posterior probability of $\leq 50 / 0.8$, respectively. The scale bar indicates the number of nucleotide substitutions per site.

Fig. S2. Phylogenetic tree based on LSU sequences. The primary phylogenetic tree was inferred using Minimum Evolution (ME), with bootstrap support values from ME and Maximum Likelihood, and posterior probabilities from Bayesian Inference, in the respective order. (-) indicates unsupported alternating topology or bootstrap value and posterior probability of $\leq 50 / 0.8$, respectively. The scale bar indicates the number of nucleotide substitutions per site.

Fungal Systematics and Evolution (ISSN: 2589-3823, E-ISSN: 2589-3831)

About Fungal Systematics and Evolution

Fungal Systematics and Evolution has an OPEN ACCESS publishing policy. All manuscripts will undergo peer review before acceptance, and will be published as quickly as possible following acceptance. There are no page charges or length restrictions, or fees for colour plates. The official journal language is English. All content submitted to Fungal Systematics and Evolution is checked for plagiarism.

Fungal Systematics and Evolution is licensed under a Creative Commons Attribution-NonCommercial-ShareAlike 4.0 International License

For more information and ordering of other books and publications, see www.westerdijkinstituut.nl and www.fuse-org.com.

About the Westerdijk Fungal Biodiversity Institute

The Westerdijk Fungal Biodiversity Institute is the largest expertise centre for microfungi in the world. Our renowned researchers dedicate themselves to enriching and expanding our Fungal Biobank. We explore the fungal kingdom to gain a better understanding of their fungal characteristics and their potential applications, especially in the fields of industry, agriculture and healthcare.

The Westerdijk Fungal Biodiversity Institute is part of the Royal Netherlands Academy of Arts and Sciences (KNAW).

Explore - study - preserve
